NM1 - ___35______

Part 36

MAJOR MODIFICATION Application

3C of 5

July 30, 2019

Permit Application

FOR MODIFICATION

Lea Land Landfill
OCD Facility Permit No.: NM-1-0035
Lea County, New Mexico

VOLUME III:
ENGINEERING DESIGN AND CALCULATIONS

Submitted To:

New Mexico Energy, Minerals, and Natural Resources Department
Oil Conservation Division
1220 South St. Francis Drive
Santa Fe, NM 87505
505.476.3440

Prepared For:

Lea Land LLC
1300 W. Main St.
Oklahoma City, OK 73106
405.236.4257

Prepared By:

Gordon Environmental/PSC
333 Rio Rancho Blvd, Suite 400
Rio Rancho, NM 87124
505.867.6990

June 2019

Gordon/PSC Project #: 01041618.00

ATTACHMENT III.5.B

SHARMA, HARI D. AND SANGEETA P. LEWIS. 1994.
WASTE CONTAINMENT SYSTEMS, WASTE STABILIZATION AND LANDFILLS: DESIGN AND EVALUATION.
NEW YORK: JOHN WILEY AND SONS

WASTE CONTAINMENT SYSTEMS, WASTE STABILIZATION, AND LANDFILLS: DESIGN AND EVALUATION

HARI D. SHARMA, PH.D., P.E.
Chief Engineer and Director
EMCON Associates
San Jose, California

SANGEETA P. LEWIS, P.E.
Project Manager
CH_2M Hill
Oakland, California

A Wiley-Interscience Publication
JOHN WILEY & SONS, INC.
New York / Chichester / Toronto / Brisbane / Singapore

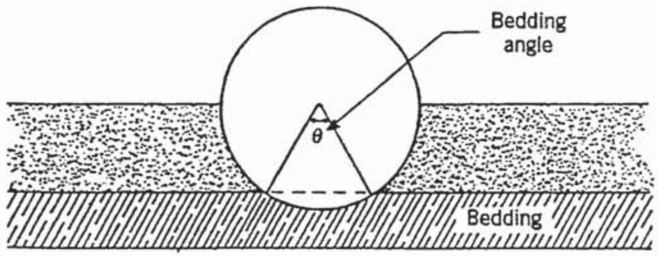

Figure 9.29 Bedding angle. (From Moser, 1990.)

approximately 1.5 times greater than the load determined using Marston's equation. The bedding constant is dependent on the bedding angle, as depicted in Figure 9.29. Values for the bedding constant are given in Table 9.12.

In the preceding paragraphs on soil stiffness we discussed the modulus of passive resistance of the soil, *e*, and noted that the units for *e* were not dimensionally correct. The Iowa formula was therefore modified and the following equation is known as the modified Iowa formula:

$$\Delta X \simeq \Delta Y = \frac{D_L K\, W_C r^3}{EI + 0.061\, E' r^3} \tag{9.34}$$

where $E' = er$. E' is known as the modulus of soil reaction. Methods for establishing this value were given in the preceding soil stiffness paragraphs. Actual deflections may be estimated using the modified Iowa formula by assuming that horizontal and vertical deflections are equal.

WATKINS' RING STABILITY EQUATION. Deflection may also be calculated using Watkins' (1989) ring stability equation. The ring stability equation is based on assuming incipient collapse of the pipe; however, it is important to note that incipient collapse does not mean imminent collapse. Rather, it refers to a condition of possible col-

TABLE 9.12 Values of Bedding Constant, *K*

Bedding Angle (deg)	K
0	0.110
30	0.108
45	0.105
60	0.102
90	0.096
120	0.090
180	0.083

Source: Moser (1990).

ATTACHMENT III.5.C

WASHINGTON STATE DEPARTMENT OF ECOLOGY. 1987.
SOLID WASTE LANDFILL DESIGN MANUAL.
WASHINGTON: WDOE

TABLE OF CONTENTS

Page

4C.1 COLLECTION PIPE MATERIALS 4C-1
    4C.1.1 Pipe Perforations 4C-3

4C.2 STRUCTURAL REQUIREMENTS 4C-4
    4C.2.1 Loading Conditions 4C-4
    4C.2.2 Refuse and Earth Loads 4C-6
    4C.2.3 Superimposed Loads 4C-13
    4C.2.4 Design Safety Factor 4C-18

4C.3 RIGID PIPE DESIGN 4C-19
    4C.3.1 Classes of Bedding and Bedding Factors 4C-19
    4C.3.2 Selection of Pipe Strength 4C-23

4C.4 FLEXIBLE PIPE DESIGN 4C-23
    4C.4.1 General Approach 4C-23
    4C.4.2 Selection of Plastic Pipe 4C-25
    4C.4.3 Selection of Other Flexible Pipes 4C-26
    4C.4.4 Bedding Material 4C-26

LIST OF FIGURES

Page

4C.1 Installation Conditions 4C-5

4C.2 Trench Condition-Values of Load Coefficient Cus (Trench Uniform Surcharge) 4C-8

4C.3 Trench Condition-Values of Load Coefficient Cd (Backfill)........ 4C-10

4C.4 Diagram for Load Coefficient Cc for Positive Projecting Pipes 4C-11

4C.5 Diagrams for Load Coefficient Cn for Negative Projecting and Induced Trench Pipes 4C-14

4C.6 Trench Beddings: Circular Pipe 4C-20

4C.7 Positive Projecting Embankment Beddings: Circular Pipe 4C-21

LIST OF TABLES

Page

4C.1 Maximum Value of Ku' for Typical Backfill Soils 4C-8

4C.2 Recommended Design Values of rsd (Positive Projecting Embankment *Conditions)* 4C-12

4C.3 Values of Load Coefficients, Cs, for Concentrated and Distributed Superimposed Loads Vertically Centered over Sever Pipe 4C-16

4C.4 Superimposed Concentrated Load Impact Factors, F 4C-17

4C.5 Equipment Loads 4C-17

4C.6 Values of N for Circular Pipe 4C-22

4C.7 Values of X for Circular Pipe 4C-22

4C.8 Values of Bedding Constant, *K*b 4C-25

APPENDIX 4C

COLLECTION PIPE MATERIALS AND STRUCTURAL REQUIREMENTS

4C.1 COLLECTION PIPE MATERIALS

Pipe that may be suitable for leachate collection systems is manufactured -to meet nationally recognized product specifications. Some materials are moire appropriate than others for use in a leachate collection system and the various types of pipe should be evaluated carefully. Various factors -to consider are:

- Intended use (type of leachate)
- Flow requirements
- Scour or abrasion conditions
- Corrosion conditions
- Product characteristics
- Physical properties
- Installation requirements
- Handling requirements
- Cost effectiveness

No single pipe product will provide optimum capability in every characteristic for all leachate collection system design conditions. Specific application requirements should be evaluated prior to selecting pipe materials.

Pipe materials for leachate collection applications fall within the two commonly accepted classifications of rigid pipe and flexible pipe. Rigid pipe materials derive a substantial part of their basic earth load carrying capacity from the structural strength inherent in the rigid pipe wall, while flexible pipe materials derive load carrying capacity from the interaction of the flexible pipe and the embedment soils. Products commonly available within these two classes are:

1. Rigid Pipe
    a. Asbestos-cement pipe (ACP)
    b. Cast iron pipe (CIP)
    C. Concrete pipe (CP)
    d. Vitrified clay pipe (VCP)

2. Flexible Pipe
    a. Ductile iron pipe (DIP)
    b. Steel pipe (SP)
    c. Thermoplastic pipe
        - Acrylonitrile-butadiene-styrene (ABS)
        - ABS composite
        - Polyethylene (PE)
        - Polyvinyl chlorine (PVC) d. Thermoset plastic pipe
        - Reinforced plastic mortar (RPM)

- Reinforced thermosetting resin (RTR)

Within the rigid pipe classification, the suitability of cast iron arid concrete pipe for leachate collection systems is limited by the difficulty of incorporating perforations in the pipe walls and their susceptibility to corrosion by acidic leachates. The use of asbestos-cement pipe is limited by its low beam strength. It is also susceptible to attack by acidic leachates. Vitrified clay pipe can be perforated and is highly resistant to chemical corrosion, but its relatively low beam strength limits the fill height that can be placed over it. For these reasons, rigid pipes have very limited use potential in leachate collection systems.

As a group, flexible pipes offer good potential for use in leachate collection systems. Within the flexible pipe group, however, only certain products are suitable. Ductile iron and steel pipe have little application for leachate collection systems primarily because of their susceptibility to attack by acidic leachates. Also, although ductile iron pipe has high load bearing capacity, incorporating perforations in the pipe walls is difficult. Thermoplastic and thermoset plastic pipe are more suitable products for leachate collection systems.

Thermoplastic materials are characterized by their ability to be repeatedly softened by heating and hardened by cooling through a temperature range characteristic for each plastic. Materials suitable for use in leachate collection systems include ABS pipe, ABS composite pipe, PE pipe, and PVC pipe. All of these materials are subject to attack by certain organic chemicals, so compatibility with the leachate must be considered in this selection. ABS is generally not as resistant to acids as PVC and neither of these two materials has good resistance to concentrated ketones and esters. Pipes manufactured from any of these materials are subject to excessive deflection when improperly bedded and haunched, so proper design and construction are important. With the exception of PVC pipe, these pipes are also subject to environmental stress cracking. Thermoplastic pipe product design should be based on long-term data.

Thermoset plastic materials, cured by heat or other means, are substantially infusible and insoluble. The two categories of thermoset plastic materials suitable for leachate collection systems include RPM pipe and RTR pipe. RPM pipe is manufactured containing reinforcements, such as fiberglass, arid aggregates, such as sand, embedded in or surrounded by cured thermosetting resin. RTR pipe is manufactured using a number of methods including centrifugal casting, pressure laminating, and filament winding. In general, the product contains fibrous reinforcement materials, such as fiberglass, embedded in or surrounded by cured thermosetting resin. Pipes manufactured from both of these materials are subject to strain corrosion in some environments, attack by certain organic chemicals, and excessive deflection when improperly bedded and haunched. Therefore, leachate compatibility arid proper design and construction are important when thermoset plastic pipe is used in leachate collection systems.

4C.1.1 Pipe Perforations

By nature of their intended use, leachate collection lines must be perforated. The size and spacing of the openings sho ld be determined based on hydraulic considerations. The effects of the perforations should be considered in the structural design of the leachate collection pipes.

4C.1.1.1 Size and Spacing

A leachate collection line, to function correctly, must be capable of accepting all the leachate flowing to it through the gravel drainage layer. After the pipe is sized to handle the flow, the size and spacing of the perforations should be selected. The rate of flow into the leachate collection pipes through the perforations is dependent on several factors, including the hydraulic conductivity of the gravel material around the pipe and the head loss due to convergence of flow to the perforations in the pipe.

W.T. Moody, as cited in U.S * Department of the Interior (1978) determined the theoretical relationship among the above factors and concluded that increasing the hydraulic conductivity of the gravel envelope around the pipe was a more effective method for increasing the rate~of flow into the pipe than increasing the size of the openings. Therefore, the selection of the size and spacing of the perforations should be based on: consideration of standard perforated pipe commonly available from manufacturer; bedding and backfill requirements for the particular installation; and effects on pipe strength. For a given rate of leachate inflow and a perforated pipe, the minimum required hydraulic conductivity of the gravel envelope around the pipe can be determined using a procedure similar to that presented in U.S. Department of the Interior (1978).

4C.1.1.2 Effects on Load Capacity

The various design procedures for rigid and flexible pipes and the various pipe performance limits are based on solid wall pipe. Pacey, et al., as cited in Dietzler (1984) has suggested that the effect of perforations could be compensated by arbitrarily increasing the earth load on the pipe. Data presented in Dietzler (1984) indicated the inclusion of typical perforations in'the lover quarters of 6-inch ABS and PVC pipe has little influence on pipe stiffness and deflection versus load performance. Others have stated there are indications that perforations will reduce the effective length of pipe available to carry loads and resist deflection suggest taking the effect of perforations into account by increasing the load in proportion to the reduction in the effective length. This later method appears to be an adequately conservative approach. If Lp equals the cumulative length of the perforations per unit length of the pipe, L, then thelactual load on the pipe should be increased as follows:

$$\text{Design Load} = \text{Actual Load} \times \frac{L}{L-Lp} \qquad (4C\text{-}1)$$

Methods to determine the actual load are discussed in the following sections.

4C.2 STRUCTURAL REQUIREMENTS

Leachate collection systems installed underneath a landfill must be designed to withstand the anticipated height and weight of refuse to be placed over them. It is not uncommon to find heights in excess of 100 feet. Appropriately, leachate collection systems must be designed for vertical pressure acting at the base of the landfill, considering the height of the landfill and the weighted average density of the refuse, daily cover, final cover system, and any superimposed loads during the life of the landfill. Perimeter collection systems that generally lie outside the landfill should be designed for the earth loads acting on them along with any superimposed loads.

The supporting strength of a leachate collection pipe is a function of installation conditions as well as the strength of the pipe itself. Structural analysis and design of the collection system are problems of soilstructure interaction. This section presents general procedures for determining the structural requirements of the pipes in a leachate collection system. Detailed discussions concerning structural design of pipelines may be found in ASCE and WPCF (1982). The design procedure for the selection of pipe strength consists of the following:

- Determination of loading condition
- Determination of refuse and earth loads
- Determination of superimposed loads
- Selection of bedding and determination of bedding factor
- Application of factor of safety
- Selection of pipe strength

4C.2.1 Loading Conditions

The load transmitted to a pipe is largely dependent on the type of installation. The common types of installation conditions are shown in Figure 4C.1 and include trench, positive projecting embankment, negative projecting embankment, and induced trench. Jacked or tunneled is also an installation condition, but has little application for leachate collection systems. The difficulty in controlling the placement of the embankment material greatly limits the potential use of the induced trench condition for leachate collection systems.

Trench installation* conditions are defined as those in which the pipe is installed in a relatively narrow trench cut in undisturbed ground and covered with backfill to the original ground surface. Embankment conditions are defined as those in which the pipe is covered above the original ground surface or in which a trench in undisturbed soil is so wide that wall friction does not affect the load on the pipe. The embankment classification is further subdivided into positive projecting and negative projecting classification. Pipe is positive projecting when its top is above the adjacent original ground surface. Negative projecting pipe is installed with its top below the adjacent original ground surface in a trench that is narrow with respect to the pipe and depth of cover.

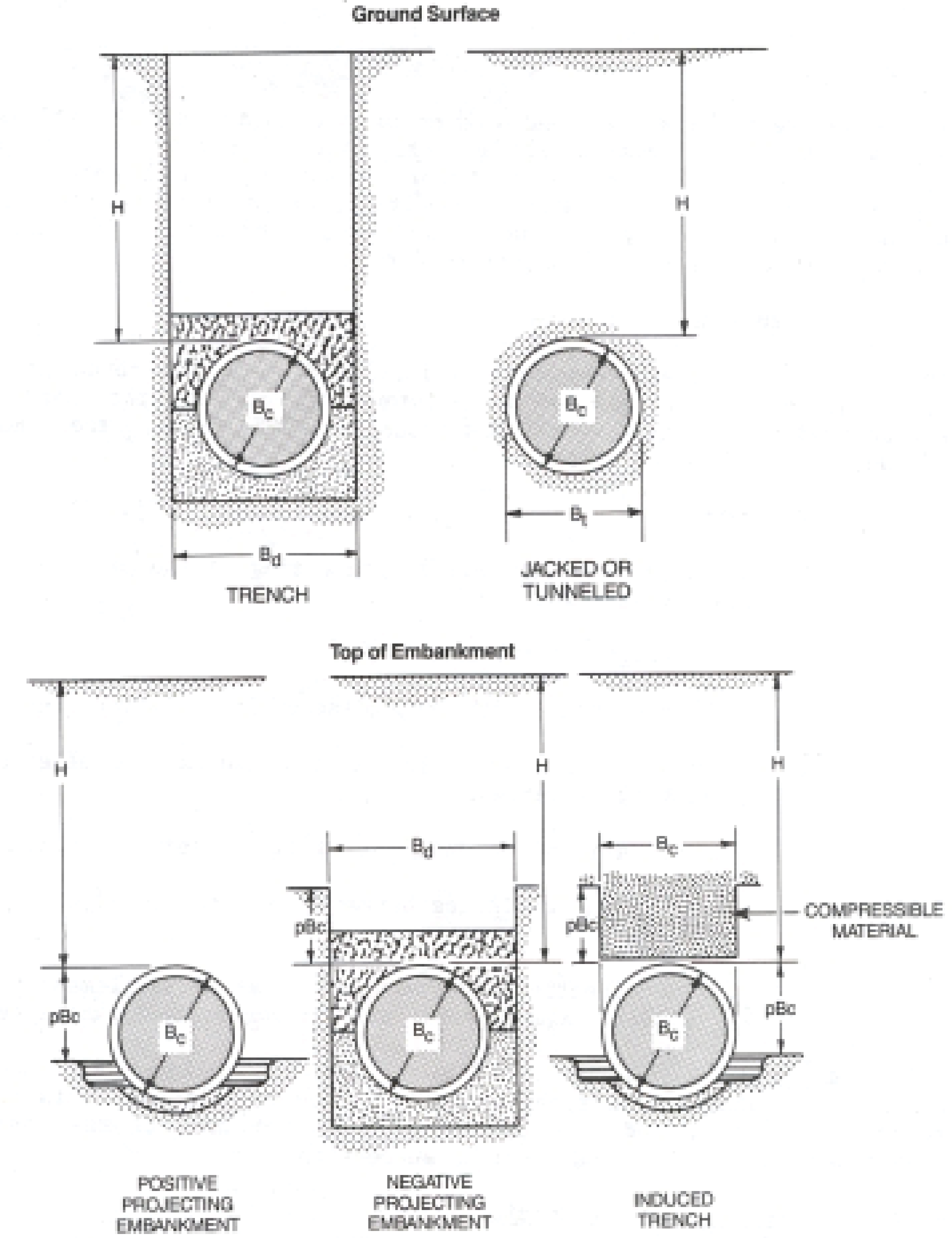

Adapted From: American Concrete Pipe Association, 1980

Figure 4C.1
Installation Conditions

Both the trench condition and either of the embankment conditions may be appropriate in the design of leachate collection systems. A perimeter collection system may be designed for either the trench condition or the negative projecting embankment condition, depending on trench width. Leachate collection systems underneath the landfill would generally be designed for one of the embankment conditions.

4C.2.2 Refuse and Earth Loads

The methods for determining the vertical load on buried conduits caused by soil forces were developed by Marston for all of the most commonly encountered construction conditions (ASCE and WPCF, 1982). The general form of the Marston equation is:

$$W = CWB2 \qquad (4C\text{-}2)$$

where: W = Vertical load per unit length acting on the pipe because of gravity soil loads

v = Unit weight of the soil

B = Trench or pipe width, depending on installation conditions

C = Dimensionless coefficient that measures the effects of the following variables:

- The ratio of the height of fill to width of trench or pipe
- The shearing forces between interior and adjacent soil prisms
- The direction and amount of relative settlement between interior and adjacent soil prisms for embankment conditions

While the general form of the Marston equation includes all the factors necessary to analyze all types of installation conditions, it is convenient to write a specialized form of the equation for each of the installation conditions described in the previous subsection.

4C.2.2.1 Loads for Trench Conditions

In the trench condition, the load on the pipe is caused by both the waste fill and the trench backfill (U.S. EPA, 1983). These two components of the total vertical pressure on the pipe are computed separately and then added to obtain the total vertical pressure acting on the top of the pipe.

The waste fill is assumed to develop a uniform surcharge pressure, Of, at the base of the fill. The magnitude of Qf is given by the expression:

$$Q_f = (w_f)(H_f) \qquad (4C\text{-}3)$$

where: Q_f = Vertical pressure at the base of the waste fill (lbs/sq ft)

w_f = Weighted average density of the waste fill including refuse, intermediate cover, and final cover system (lbs/cu ft)

H_f = Height of waste fill including cover (ft)

The weighted average density of the waste fill, w_f is computed as follows:

$$w_f = \frac{(w_r)(H_r) + (w_i)(T) + (w_c)(T_c)}{H_f} \qquad (4C\text{-}4)$$

where: w_r = Average in-place wet density of the refuse (lbs/cu ft)

H_r = Height of refuse excluding cover layers (ft)

w_i = Wet density of intermediate cover (lbs/cu ft)

T_i = Total thickness of intermediate cover layers (ft)

w_c = Wet density of the final cover system (lbs/cu ft)

T_c = Thickness of the final cover system (ft)

$H_f = H_r + T_i + T_c$

The value of the vertical pressure at the top of the pipe due to the waste fill, Pvf (in lbs/sq ft), is determined from the following:

$$Pvf = ({}^{Q}f)({}^{C}us) \qquad (4C\text{-}5)$$

where: Cus = Dimensionless load coefficient that is a function of the ratio of the depth of the trench, H (measured from the original ground surface to the top of the pipe) to the trench width, B_d, and of the friction between the backfill and the sides of the trench.

The load coefficient, C_{us}, may be calculated from the following equation or obtained from Figure 4C.2:

$${}^{C}us = e^{-2KU'(H/Bd)} \qquad (4C\text{-}6)$$

where: e = Base of natural logarithms
K = Rankine's ratio of lateral pressure to vertical pressure
u'= Coefficient of friction between backfill material and the sides of the trench

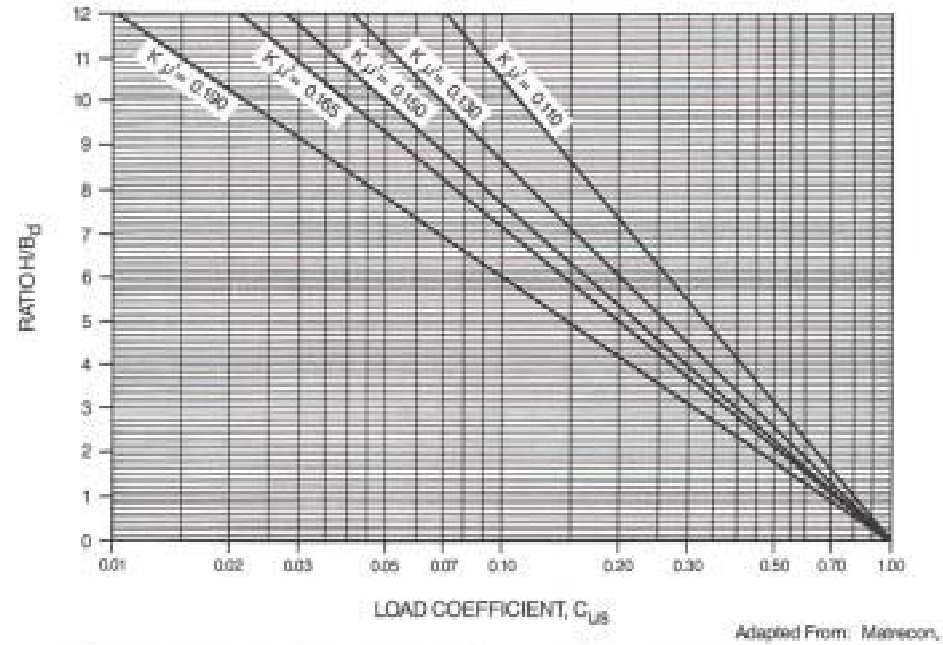

Adapted From: Matrecon, Inc., 1983

Figure 4C.2
Trench Condition—Values of Load Coefficient C_{us} (Trench Uniform Surcharge)

H = Depth of trench from original ground surface to top of pipe (f t)

B_d = Width of trench at top of pipe (ft)

The product of Ku' is characteristic for a given combination of backfills in natural, undisturbed soil. Maximum values of Kul for typical soils are listed in Table 4C.1.

Table 4C.1. Maximum Value of Kul for Typical Backfill Soils

Type of Soil	Maximum Value of Ku'
Granular Materials Without Cohesion	0.19
Sand and Gravel	0.165
Saturated Topsoil	0.150
Clay	0.130
Saturated Clay	0.110

Source: U.S. EPA (1983)

The value of the vertical pressure at the top of the pipe due to the trench backfill is determined from the following equation developed by Marston (see U.S. EPA, 1983):

$$Pvt = (Bd)(w)(Cd) \qquad (4C\text{-}7)$$

where:

Pvt = Value of the vertical pressure at. the top of the pipe (lbs/sq ft)

W = Unit weight of trench backfill (lbs/cu ft)

C_d = Dimensionless load coefficient which is a function of the ratio of the depth of the trench, H, to the trench width, B_d, and of the friction between the backfill and the sides of the trench

The load coefficient, C_d, may be computed from the following equation or obtained from Figure 4C.3:

$$C_d = \frac{1\text{-}e\text{-}2Ku'(H/B_d)}{2Ku'} \qquad (4C\text{-}8)$$

in which the terms are as previously defined.

The total vertical pressure at the top of the pipe, Pv, is equal to:

$$Pv = P_{vf} + P_{vt} \qquad (4C\text{-}9)$$

$$P_v = (Q_f)(C_{us})+(B)(w)(C_d) \qquad (4C\text{-}10)$$

Based on Marston's formula, the load on a rigid pipe in the trench condition would be:

$$we = P_vB_d \qquad (4C\text{-}11)$$

or:

$$w_c = (B_d)(Q_f)(C_{us}) + (B_d)^2 (w)(C_d) \qquad (4C\text{-}12)$$

where: w_c = Force per unit length of pipe (lb/ft)

For flexible pipe in the trench condition, the load as given by Marston's formula would be:

$$w_c = P_vB_c \qquad (4C\text{-}13)$$

or:

$$w_c = (B)(Q_f)(C_{us}) + (B_d)(w)(C_d)(B_c) \qquad (4C\text{-}14)$$

where: B_c = Outside diameter of pipe (ft)

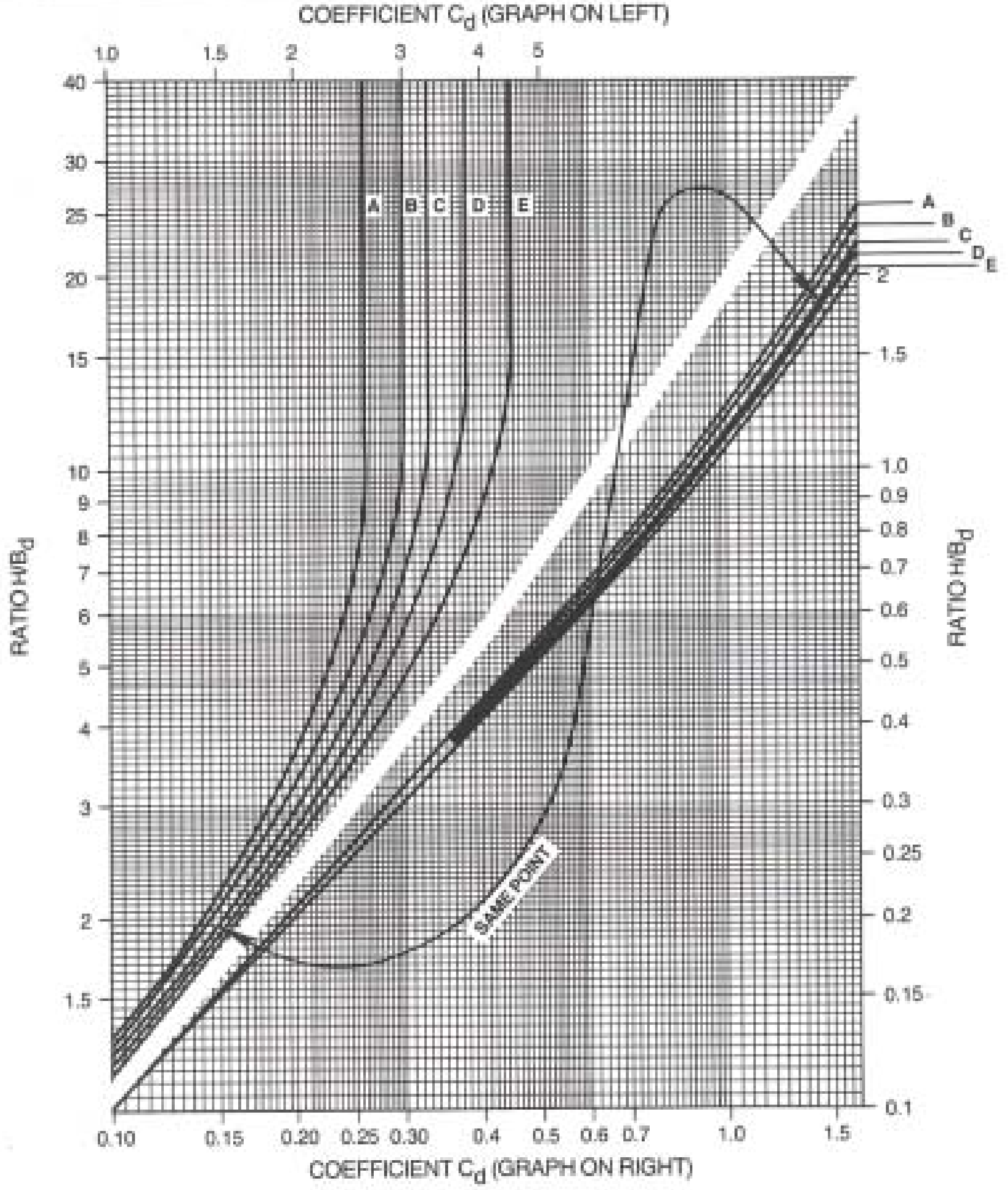

A-C_d for $K\mu'$ = 0.19, for Granular Materials Without Cohesion

B-C_d for $K\mu'$ = 0.165 Maximum for Sand and Gravel

C-C_d for $K\mu'$ = 0.150 Maximum for Saturated Top Soil

D-C_d for $K\mu'$ = 0.130 Maximum Ordinary for Clay

E-C_d for $K\mu'$ = 0.110 Maximum for Saturated Clay

Adapted From: Matrecon, Inc., 1983

Figure 4C.3
Trench Condition—Values of Load Coefficient C_d (Backfill)

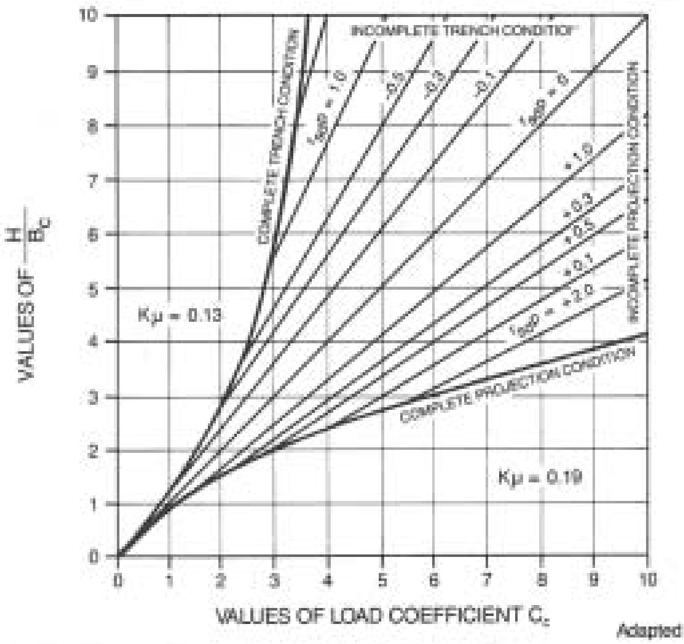

Adapted From: ASCE and WPCF, 1982

Figure 4C.4
Diagram for Load Coefficient C_c for Positive Projecting Pipes

This formula is applicable to flexible pipes only if the backfill material at the sides of the pipe is compacted so that it will deform under vertical load less than the pipe itself will deform. In this condition, the side fills between the sides of the pipe and the sides of the trench may be expected to carry their proportional share of the total load. If this condition does not exist, then the loads are determined as described below for the embankment conditions.

4C.2.2.2 Loads for Positive Protecting Embankment Conditions

Marston's formula for the fill load on a pipe in the positive projecting embankment condition is:

$$W_c = C_c{}^{w}fB_c{}^{2} \qquad (4C\text{-}15)$$

where: W_c = Load on the pipe (lbs/ft)

w_f = Weighted average density of the waste fill (lbs/cu ft)

B_c = Outside width of pipe (ft)

C_c = Load coefficient

A complete discussion of this load coefficient may be found in the Concrete Pipe Design Manual developed by the American Concrete Pipe Association (1980)' and Gravity Sanitary Sever Design and Construction published by the ASCE and WPCF (1982). Values of Cc may be obtained from Figure 4C.4.

Table 4C.2. Recommended Design Values of rsd (Positive , Projecting Embankment Conditions).

Type of Pipe	Soil Conditions	Settlement Ratio, r_{sd}
Rigid	Rock or unyielding foundation	+1.0
Rigid	Ordinary foundation	+0.5 to +0.8
Rigid	Yielding foundation	0 to +0.5
Rigid	Negative projecting installation	-0.3 to -0.5
Flexible	Poorly compacted side fills	-0.4 to 0
Flexible	Well compacted side fills	0

Source: ASCB and WPCF, 1982, p. 178

The fill load on a pipe installed in a positive projecting embankment condition is influenced by the product of the settlement ratio (r_{sd}) and the projecting ratio (p'). The settlement ratio is the relationship between the pipe deflection and the relative settlement between the prism of fill directly above the pipe and the adjacent material. Design values of the settlement ratio is the vertical distance the pipe projects above the original ground divided by the outside vertical height of the pipe, and can be determined when the size and elevation of pipe has been established.

In the last three cases shown in Table 4C.2, the settlement ratio may be conservatively assumed to be zero which results in designing for the weight of the prism of material directly above the pipe. In such cases, C_c is equal to H/B_c and Marston's formula for the prism load becomes:

$$W_c = (H)(w_f)(B_c) \qquad (4C\text{-}16)$$

where: W_c = Load on pipe (lbs/ft)

H = Height of the fill above the pipe (ft)

w_f = Weighted average density of the waste fill, including gravel backfill above the pipe, refuse, intermediate cover, and final cover system (lbs/cu ft)

B_c = Outside diameter of the pipe (ft)

The load on the pipe is also influenced by the coefficient of internal friction of the embankment material. ASCE and WPCF (1982) recommends the following values of the product Ku for use in Figure 4C.4.

For a positive settlement ratio: $K_u = 0.19$
For a negative settlement ratio: $K_u = 0.13$

4C.2.2.3 Loads for Negative Projecting Embankment and Induced Trench Conditions

The formula for the fill load on a negative projecting pipe is:

$$W_c = C_n^{wB}d^2 \qquad (4C\text{-}17)$$

where: W_c = Load on the pipe (lbs/ft)

w = Density of fill above pipe (lbs/cu ft)

B_d = Width of trench (ft)

C_n = Load coefficient

In the case of induced trench pipe, B_c is substituted for B_d in the preceding equation. B_c is the outside diameter of the sever pipe which is assumed to be the width of the trench.

A complete discussion of the load coefficient, C_n, may be found in American Concrete Pipe Association (1980) and ASCE and WPCE (1982). Values of C_n may be obtained from Figure 4C.5.

As in the case of the positive projecting embankment condition, the fill load is influenced by the product of the settlement ratio (r_{sd}) and the projection ratio (p'). The settlement ratio for the negative projecting embankment condition is the quotient obtained by taking the difference between the settlement of the firm ground surface and the settlement of the plane in the trench backfill which was originally level with the ground surface and dividing this difference by the compression of the column of material in trench. Values for the negative projecting settlement ratio range from -0.1 for P' = 0.5' to -1.0 for P' = 2.0' for rigid pipe (American Concrete Pipe Association, 1980, p. 162). Induced trench settlement ratios range from -0.3 to 05 (ASCE and WPCF, 1982). The projection ratio for this condition, p' is equal to the vertical distance from the firm ground surface down to the top of the pipe, divided by the width of the trench, B_d.

4C.2.3 Superimposed Loads

Leachate collection pipes in a landfill may be subjected to two types of superimposed loads: concentrated loads and distributed loads. Loads of pipes caused by these loadings can be determined by application of the Boussinesq equations (ASCE and WPCF, 1982).

4C.2.3.1 Concentrated Loads

The formula for load caused by a superimposed concentrated load, such as a

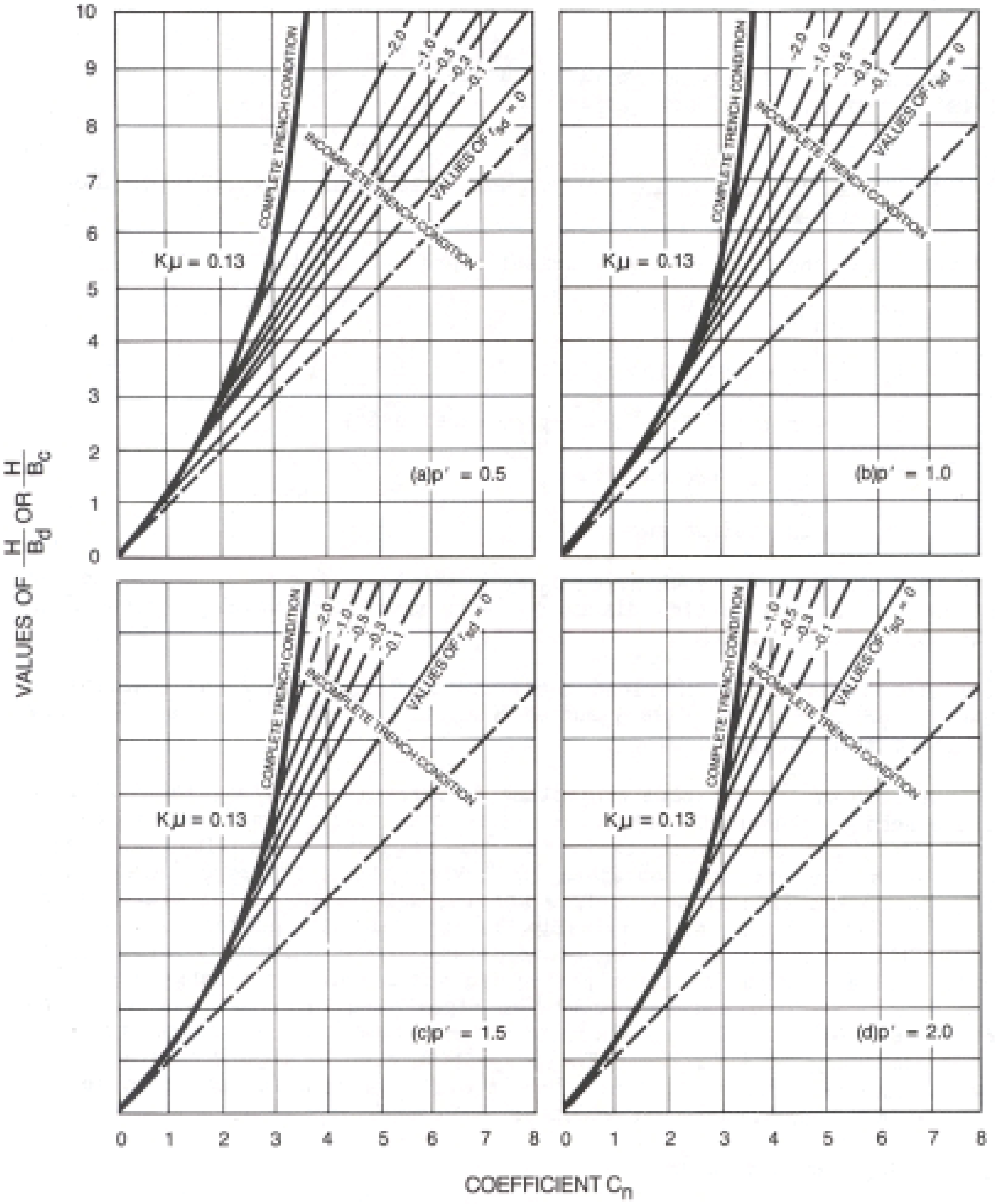

Adapted From: ASCE and WPCF, 1982

Figure 4C.5
Diagrams for Load Coefficient C_n for Negative Projecting and Induced Trench Pipes

wheel load during construction, is given the following form (ASCE and WPCF, 1982):

$$W_{sc} = \frac{PF}{C_S L} \qquad (4C\text{-}18)$$

where: W_{sc} = Load on pipe (lbs/ft)

P = Concentrated load (lbs)

F = Impact factor

L = Effective length of pipe (ft)

C_s = Load coefficient

The load coefficient, C_s, is a function of $B_c/2H$ and $L/2H$, in which B_c is the outside diameter of the pipe and H is the height of fill from the top of the pipe to the ground surface. Table 4C.3 lists values of the load coefficients for concentrated and distributed superimposed loads centered over the pipe.

The effective length, L, is the length over which the average load caused by surface wheels produces nearly the same stress in the pipe wall as does the actual load which varies in intensity from point to point. ASCE and WPCF (1982) recommends using an effective length equal to 3 feet for pipes greater than 3 feet long and using the actual length of pipes shorter than 3 feet.

The impact factor, F, reflects the influence of dynamic loads caused by traffic at ground surface. The impact factors recommended by AASHTO are listed in Table 4C.4 (American Concrete Pipe Association, 1980).

Various equipment loads that may occur during construction are listed in Table 4C.5.

Loads on pipes resulting from concentrated loads during construction may be greater than the loads caused by the refuse placed in the landfill. It is important that both construction loads and long-term loads be considered in determining the maximum load expected on pipes.

4C.2.3.2 Distributed Loads

Superimposed loads distributed over an area of considerable extent such as a truck load during construction may be determined from the following equation (ASCE and WPCF, 1982):

$$W_{sd} = CspFBc \qquad (4C\text{-}19)$$

where: W_{sd} = Load on pipe (lbs/ft)

p = Intensity of distributed load (lbs/sq ft)

F = Impact factor

Table 4C.3. Values of Load Coefficients, C_s, for Concentrated and Distributed Superimposed Loads Vertically Centered over Sewer Pipe.

$\frac{D}{2H}$ or $\frac{B_c}{2H}$	$\frac{M}{2H}$ or $\frac{L}{2H}$													
	0.1	0.2	0.3	0.4	0.5	0.6	0.7	0.8	0.9	1.0	1.2	1.5	2.0	5.0
0.1	0.019	0.037	0.053	0.065	0.079	0.089	0.097	0.103	0.108	0.112	0.117	0.121	0.124	0.128
0.2	0.037	0.072	0.103	0.131	0.155	0.174	0.189	0.202	0.211	0.219	0.229	0.238	0.244	0.248
0.3	0.053	0.103	0.149	0.190	0.224	0.252	0.274	0.292	0.306	0.318	0.333	0.345	0.355	0.360
0.4	0.067	0.131	0.190	0.241	0.284	0.320	0.349	0.373	0.391	0.405	0.425	0.440	0.454	0.460
0.5	0.079	0.155	0.224	0.284	0.336	0.379	0.414	0.441	0.463	0.481	0.505	0.525	0.540	0.548
0.6	0.089	0.174	0.252	0.320	0.379	0.428	0.467	0.499	0.524	0.544	0.572	0.596	0.613	0.624
0.7	0.097	0.189	0.274	0.349	0.414	0.467	0.511	0.546	0.584	0.597	0.628	0.650	0.674	0.688
0.8	0.103	0.202	0.292	0.373	0.441	0.499	0.546	0.584	0.615	0.639	0.674	0.703	0.725	0.740
0.9	0.108	0.211	0.306	0.391	0.463	0.524	0.574	0.615	0.647	0.673	0.711	0.742	0.766	0.784
1.0	0.112	0.219	0.318	0.405	0.481	0.544	0.597	0.639	0.673	0.701	0.740	0.774	0.800	0.816
1.2	0.117	0.229	0.333	0.425	0.505	0.572	0.628	0.674	0.711	0.740	0.783	0.820	0.849	0.868
1.5	0.121	0.238	0.345	0.440	0.525	0.596	0.650	0.703	0.742	0.774	0.820	0.861	0.894	0.916
2.0	0.124	0.244	0.355	0.454	0.540	0.613	0.674	0.725	0.766	0.800	0.849	0.894	0.930	0.956

Bc = Outside diameter of pipe (ft)

Cs = Load coefficient

Table 4C.4 Superimposed Concentrated Load Impact Factors, F.

Height of Cover	Impact Factor
0 - 1.0 ft.	1.3
1.1 - 2.0 ft.	1.2
2.1 - 2.9 ft.	1.1
3.0 ft. and greater	1.0

Table 4C.5 Equipment Loads

Equipment	Operating Weight (lbs)	Ground Contact	Track or Wheel Load (lbs)
Caterpillar D-6	32,850	181101 9.011	16,425 Track Load
Caterpillar D-8	81,950	2211x 1016.5	40,975 Track Load
Scrapers, loaded 21/31 cu yd capacity (631 D)	168,410	Wheel load	45,470 Drive Wheel Load
Compactor Caterpillar 825-C	71,429	81 Width Coverage	35,715 Roller Load

Adapted From: Caterpillar Performance Handbook, 1984

The load coefficient, Cs, is a function of D/2H and M/2H, in which H is the height from the top of the pipe to the ground surface and D and M are the width and length, respectively, or the area over which the distributed load acts. Table 4C.3 lists the values of the load coefficients for loads centered over the pipe. A method for determining the loads on the pipe from offset uniform loads may be found in ASCE and WPCF, 1982. A typical offset uniform. load would be the waste fill placed inside and adjacent to a perimeter leachate collection system.

4C.2.4 Design Safety Factor

The factor of safety for a pipe is defined as the ratio of the maximum performance limit to the design or service performance limit. The selection of a suitable safety factor is an essential part of the structural design of leachate collection pipes. The factor of safety should be related either to an allowable working stress or to a pre-established ultimate failure condition. Factors of safety compensate for poor construction practice or for inadequate inspection. Properly established design performance values and adequate factors of safety must be realized in installation and operation to provide reasonable assurance of long-term leachate collection system performance.

The relationship between safety factors and design performance values is similar for rigid and flexible pipes. However, there are differences in the design requirements for each type of pipe and these affect the form of the safety factor associated with each.

4C.2.4.1 Rigid Pipe

Design performance limits for rigid pipes are expressed in terms of strength under load. Testing is generally used to determine the service strength for rigid pipe. Strengths of rigid pipe are measured in terms of 1) the ultimate three-edge bearing strength, and 2) the ultimate and 0.01-inch crack, three-edge bearing strengths for reinforced concrete pipe. A safety factor of 1.0 should be applied to the specified minimum ultimate three-edge bearing strength to determine the working strength for other rigid pipes (ASCE and WPCF, 1982). Common practice is to use a factor of safety of 1.25 for the ultimate load of reinforced concrete pipe, and up to 1.50 for vitrified clay.

4C.2.4.2 Flexible Pipe

Design performance limits for flexible pipes are most commonly expressed in terms of deflection. The design limit varies with different pipe materials and the pipe manufacturing process. Flexible pipes must be able to deflect without experiencing cracking, liner failure, or other distress; and they should be designed with a reasonable factor of safety.

Manufacturers should be consulted on the value of the deflection limits for various types of flexible pipes. The PVC pipe manufacturers suggest limiting the deflection of buried PVC pipe to 7-1/2 percent. This strain is one-fourth the minimum strain level at which cracking and reverse curvature reportedly occurs when subjecting PVC pipe to testing in accordance with ASTSM D 2412. To maintain this same factor of safety (FS-4.0) with ABS pipe, the allowable strain for ABS pipe should be limited to 5-1/2 percent. The high safety factor of 4.0 is intended to compensate for the long-term effects of creep of the plastic. Dietzler (1984) suggests that deflections of ABS and PVC pipe should be limited to one-third the deflection at which reverse curvature of splitting occurs in ASTM D 2412, including a deflection lag factor.

4C.3 RIGID PIPE DESIGN

For reasons previously indicatedt rigid pipes have limited use potential in leachate collection systems. In situations where they are used, their structural design should follow the recognized procedures for the various rigid pipe products available. The design of rigid pipe systems relates to the product's performance limit, expressed in terms of strength of the installed pipe. When determining field strength of rigid pipes, it is convenient to classify the *installation conditions* as either trench or embankment. For each of these conditions, bedding classes and corresponding bedding factors have been developed for use in determining and the required pipe strength.

4C-3-1 Classes of Bedding and Bedding Factors

4C.3-1.1 Trench Beddings

Four general classes of bedding for installation of rigid pipes in a trench condition are illustrated in Figure 4C.6. The bedding factor for each of the classes of pipe bedding are also listed in Figure 4C.6. Because leachate collection pipes are normally installed with granular material *surrounding* the pipe, the appropriate bedding class is usually Class B with a bedding factor of 1.9.

4C.3.1.2 Embankment Beddings

Four general classes of bedding for the installation of rigid pipes in a positive projecting embankment condition are illustrated in Figure 4C.7. Most leachate collection lines installed in a positive projecting embankment condition would have Class B or C bedding, depending on the projection ratio, p, of the actual installation. For pipe installed in a positive projecting embankment condition, active lateral pressure is exerted against the sides of the pipe. The bedding factor, Lf, for this type of installation is computed by the equation:

$$Lf \qquad \frac{A}{N-xq} \qquad (4C-20)$$

where: A Pipe shape factor

N A parameter that is a function of the bedding class

x A parameter dependent on the area over which lateral pressure effectively acts

q Ratio of total lateral pressure to total vertical load on the pipe

For circular pipe, A has a value of 1.431. Values of N for various classes of bedding are given in Table 4C.6. Values of x are listed in Table 4C.7.

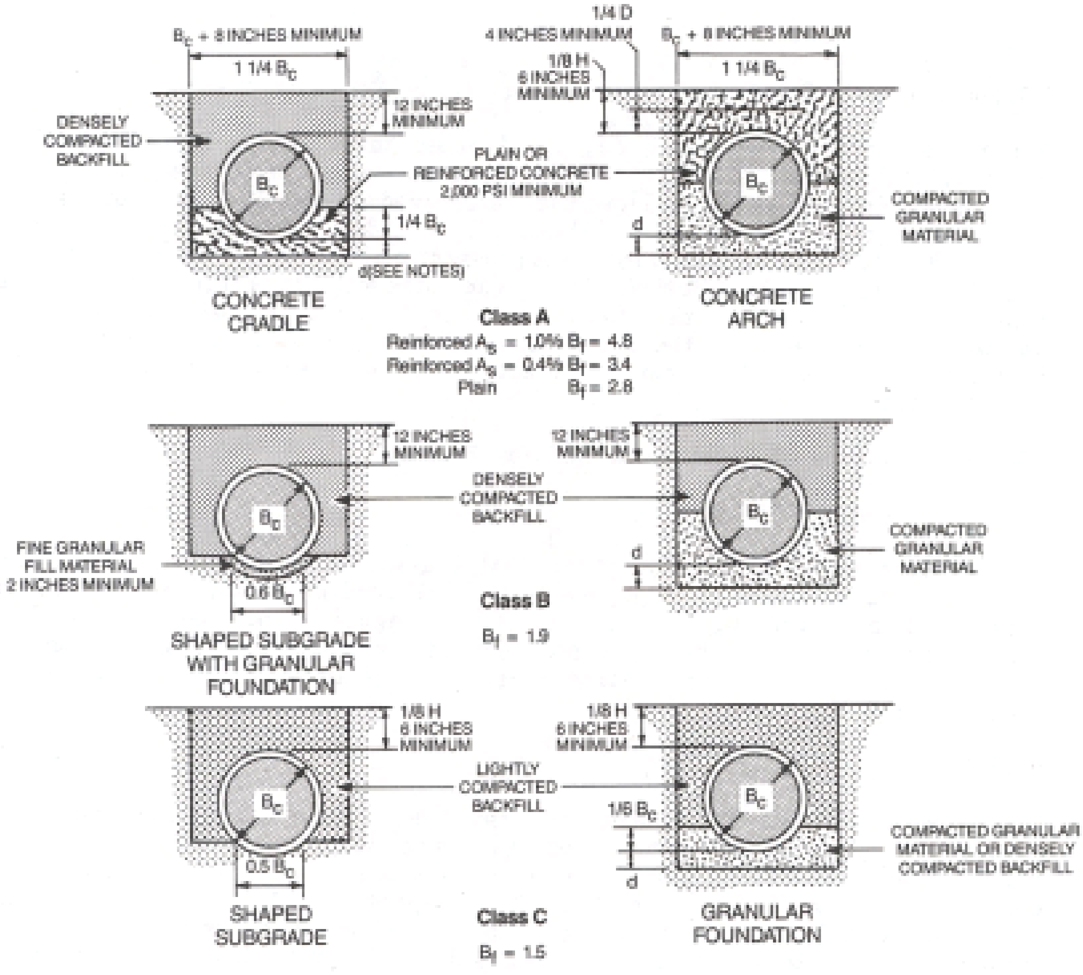

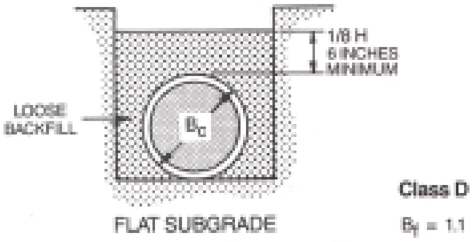

Depth of Bedding Material Below Pipe

D	d(Minimum)
27 Inches and Smaller	3 Inches
30 Inches to 60 Inches	4 Inches
66 Inches and Larger	6 Inches

Adapted From: American Concrete Pipe Association, 1980

Figure 4C.6
Trench Beddings:
Circular Pipe

B_c = Outside Diameter
H = Backfill Cover Above Top of Pipe
d = Depth of Bedding Material Below Pipe
D = Inside Diameter
A_s = Area of Transverse Steel in the Cradle of Arch Expressed as a Percentage of Area of Concrete at Invert or Crown

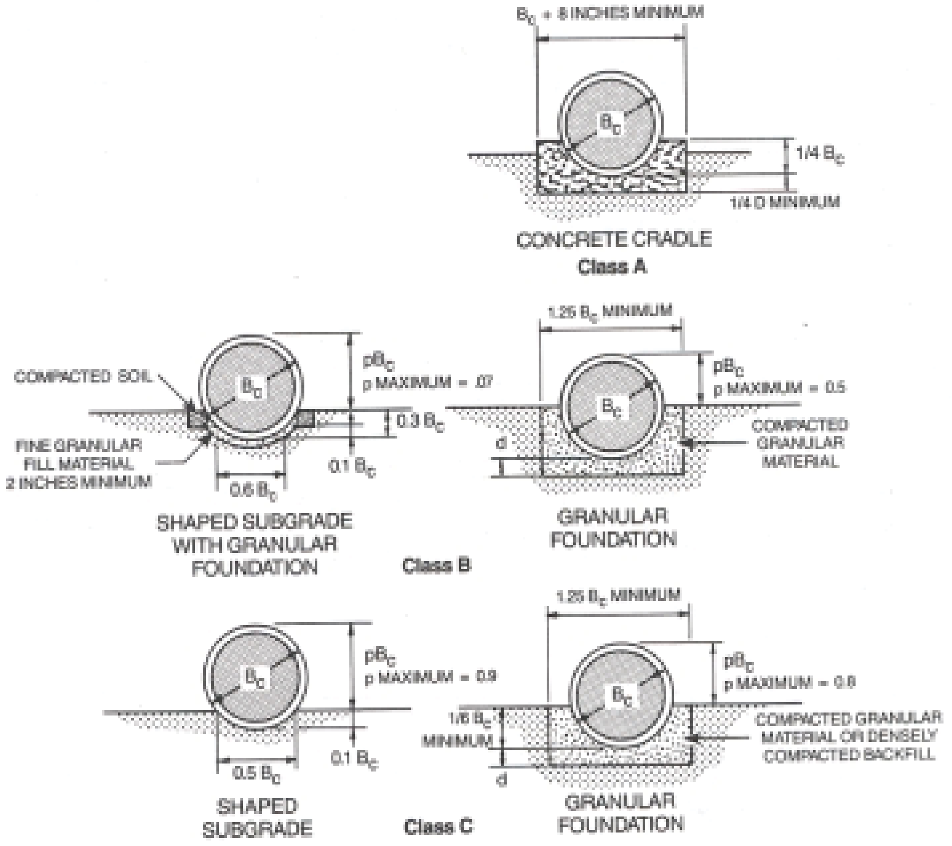

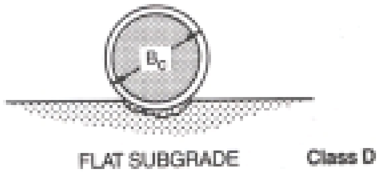

Depth of Bedding Material Below Pipe

D	d(Minimum)
27 Inches and Smaller	3 Inches
30 Inches to 60 Inches	4 Inches
66 Inches and Larger	6 Inches

Adapted From: American Concrete Pipe Association, 1980

B_c = Outside Diameter
H = Backfill Cover Above Top of Pipe
D = Inside Diameter
d = Depth of Bedding Material Below Pipe

Figure 4C.7
Positive Projecting Embankment Beddings: Circular Pipe

Table 4C.6 Values of N for Circular Pipe

Class of Bedding	N
A (reinforced cradle)	0.421 to 0.505
Aa (unreinforced cradle)	0.505 to 0.636
B	0.707
C	0.840
D	1.310

Adapted from: ASCE and WPCF (1982)

The projection ratio, m, in Table 4C.7 refers to the fraction of the vertical pipe diameter over which lateral pressure is effective. For pressure acting on the top half of the pipe above the horizontal diameter, m equals 0.5. Values for q may be estimated by the formula:

$$q \qquad \frac{mk}{C_c}\left[\frac{H}{B_c}+\frac{m}{2}\right] \tag{4C-21}$$

where: k Ratio of unit lateral pressure to unit vertical pressure (Rankine's ratio)

A value of k equal to 0.33 usually be sufficiently accurate. Values of C_c may be found in Figure 4C.4.

Table 4C.7 Values of x for Circular Pipe

Fraction of Pipe Subjected to Lateral Pressure, m	Class A Bedding	Other Than Class A Bedding
0	0.150	0
0.3	0.743	0.217
0.5	0.856	0.423
0.7	0.811	0.594
0.9	0.678	0.655
1.0	0.638	0.638

Adapted from: ASCE and WPCF (1982)

The classes of bedding for rigid pipes installed in a negative projecting embankment condition are the same as those for the trench condition. The trench condition bedding factors listed in Figure 4C.6 should be used for negative projecting embankment installations. For leachate collection lines, this would generally be Class B bedding and a bedding factor of 1.9.

4C.3.2 Selection of Pipe Strength

The design strength of rigid pipes is commonly related to a three-edge bearing strength measured at the manufacturing plant in accordance with recognized national testing standards. For pipes installed under specified conditions of bedding and backfilling, the required three-edge bearing strength for a given class of bedding and design load can be determined from the following:

$$\text{Required Three Edge Bearing Strength (lb/ft)} = \frac{\text{Design Load (lb/ft) x Factor of Safety}}{\text{Bedding Factor}}$$

The strength of reinforced concrete pipe at either the 0.01-inch crack or ultimate load divided by the internal diameter of the pipe is defined as the D-load strength. The D-load concept provides strength classification of pipe independent of pipe diameter. The required three-edge -bearing strength of reinforced concrete pipe expressed as D-load is determined by the following equation:

$$\text{D-Load (lbs)} = \frac{\text{Design Load (lbs/ft) x Safety Factor}}{\text{Bedding Factor x Diameter (ft)}}$$

The above equations are applicable to rigid pipes installed in both trench conditions and embankment conditions. After determining the design load, the selection of the pipe strength involves applying the appropriate safety factor and bedding factor for the installation conditions in either of the above equations.

4C.4 FT BLE PIPE DESIGN

4C.4.1 General Approach

Flexible pipes derive the majority of their load supporting ability from the passive resistance of the soil in side fills as the pipe deflects under load. Because of this resistance, it is important ' to examine the interaction between the bedding or fill material and the pipe, rather than simply studying pipe characteristics. The extent to which flexible pipe deflects as installed is most commonly used as a basis for design since it reflects this interaction. The approximate long-term deflection of flexible pipe in place can be calculated using the Modified Iowa Formula developed by Spangler and Watkins (ASCE and WPCF, 1982):

$$Y = \frac{D_l K_b W_c r^3}{EI + 0.061\, E' r^3} \qquad (4C\text{-}22)$$

where: Y = Vertical deflection (inches), assumed to approximately equal horizontal deflection

D_l = Deflection lag factor
K_b = Bedding constant
W_c = Load (lbs/inch)
r = Mean radius of pipe (inches)
E = Modulus of tensile elasticity (lbs/sq in)
I = Moment of inertia per length (in0n)
E' = Modulus of soil reaction (lbs/sq in)

The above equation can be rewritten to express pipe deflection as a decimal fraction of the pipe outside diameter, Bc, and relate it to the vertical stress on the pipe, Pv, as follows:

$$\frac{W_C}{B_c} = P_v = \frac{Y(EI + 0.061\ E'n^3)}{B_c(D_l K_b r^3)} \qquad (4C\text{-}23)$$

Pipe manufacturers may establish limits for pipe deflection or vertical stress on the pipe (P_v). Maximum vertical stress is often referred to as critical buckling pressure.

The deflection lag factor, D^1, compensates ' for time consolidation of the bedding, which may permit flexible pipes to continue to deform after installation. Long-term deflection will be greater with low degrees of compaction of the bedding in the side fills compared to higher degrees of compaction. Values recommended for this factor range from 1.25 to 1.50 (ASCE and WPCF, 1982), although values over 2.5 have been recorded in dry soil. A deflection lag factor of 2.0 may be realistic for design of leachate collection pipes if weathering and/or softening of the bedding material is likely to occur over the life of the landfill or if the bedding material is rounded or may be placed with minimal compaction (Dietzler, 1984).

Values for the bedding constant, Kb, are listed in Table 4C.8. Spangler's data suggested a Kb value of 0.10 for pipe embedded in native soil with no bedding and a Kb value of 0.083 for pipe embedded in gravel up to the spring line. The installation of leachate collection pipes is more closely represented by the latter case, and a Kb value of 0.083 should therefore be used in lieu of actual field data.

Table 4C.8. Values of Bedding Constant, Kb-

Bedding Angle (Degrees)	K_b
0	0.110
30	0.108
45	0.105
60	0.102
90	0.096
120	0.090
180	0.083

Source: ASCE and WPCF (1982)

Values for the soil reaction modulus, El, range from 0 to 3,000, depending on the soil type of the bedding material and relative degree of compaction (ASCE and WPCF, 1982). The use of a high value for El is not realistic for leachate collection pipes in many localites (Dietzler, 1984). In a situation where a rounded river gravel will be used for the bedding material and a high degree of compaction may be unobtainable in the bedding around the leachate collection pipe, aa realistic value for E, of 400 may be appropriate (Dietzler, 1984).

The first term in the denominator (EI) of the Modified Iowa Formula is the stiffness factor and reflects the influence of the inherent stiffness of the pipe on deflection. The second term, 0.061 Eld, reflects the influence of the passive pressure on the side of the pipe. With flexible pipes, the second term is normally predominant.

After the allowable strain level in the pipe has been determined, the design procedure for flexible pipes is to perform a trial and adjustment analysis to find a class of pipe that will result in deflections less than the established limit. There are slight variations in the procedure for the various types of flexible pipe.

4C.4.2 Selection of Plastic Pipe

The standard test to determine pipe stiffness or the load deflection characteristic of plastic pipe is the parallel-plate loading test conducted in accordance with ASTM D 2412. The test determines the pipe stiffness, PS, at a prescribed deflection, Y, which for convenience in testing is arbitrarily set at 5 percent. The pipe stiffness is defined as the value obtained by dividing the load per unit length, F, by the resulting deflection at the prescribed percentage deflection:

$$PS = \frac{F}{Y} \qquad (4C\text{-}.24)$$

The stiffness factor, SF, in the Modified Iowa Formula is related to the pipe stiffness by the following expression:

$$SF = EI = 0.149r3(PS) \qquad (4C\text{-}25)$$

in which the terms are as previously defined.

For circular plastic pipes, the approximate deflection based on pipe stiffness can be determined by using the following simplified version of the Modified Iowa Formula:

$$Y = \frac{D_1 K_b W_c}{0.149(PS) + 0.061\,E'} \qquad (4C\text{-}26)$$

The pipe stiffness for the various plastic pipe materials and diameters of pipe may be obtained from the manufacturer or may be determined by tests performed in accordance with ASTM D 2412.

4C.4.3 Selection of Other Flexible Pipes

Flexible pipes of material other than plastic, such as ductile iron and corrugated metal, have little potential for general use in leachate collection systems for reasons previously discussed. However, if they are found suitable for a specific installation, their structural design should follow recognized procedures for the particular flexible pipe being considered. Procedures for designing ductile iron and corrugated metal pipes are described in ASCE and WPCF (1982). Manufacturers of the specific products should also be consulted.

4C.4.4 Bedding Material

Bedding provides a: contact between a pipe and the foundation on which it rests. The total load that a pipe will support depends on the width of the contact area and the quality of the contact between the pipe and the bedding material. The influence of the bedding on the supporting strength of the pipe is a factor that must be considered in the design of a leachate collection pipe. This section discusses bedding material considerations. More detailed requirements are given in previous sections of this Appendix.

An important consideration in selecting a material for bedding is positive contact between the bed and the pipe. A well-graded crush stone or a well-graded gravel are suitable bedding materials based on supporting strength considerations, and both are more suitable than a uniformly graded pea gravel (ASCE and WPCF, 1982). Larger particle sizes give greater stability; however, the maximum size and shape of the bedding material should be related to the pipe material and the recommendations of the manufacturer. For small pipes, the maximum size of the bedding material should be limited to about 10 percent of the pipe diameter and, in general, well-graded crush stone or gravel ranging in size from 3/4 inch to the No. 4 sieve will provide the most satisfactory pipe bedding (ASCE and WPCF, 1982).

In addition to providing support, bedding for leachate collection pipes must allow unrestricted flow of leachate through the bedding into the perforated leachate collection pipes. The bedding material must also be resistant to attack from the leachate. Redundancy in the design of leachate collection systems is important to minimize the effects of failures when they occur. One of the primary ways to provide redundancy is to design the bedding to meet drainage requirements through the gravel layer alone if flow through the pipe is restricted (Bass, 1984).

A well-graded material with 100 percent passing the 1-1/2 inch clear, square screen openings and not more than 5 percent passing the No. 50 U.S. Standard Series sieve is recommended for drainage purposes (U.S. Department of the Interior, 1978). To determine whether the material is well-graded, the coefficient of uniformity which describes the slope of the gradation curve must be greater than 4 for gravels and greater than 6 for sands. In addition, the coefficient of curvature that describes the shape of the curve must be between 1 and 3 for both gravels and sands. These coefficients are defined as follows:

$$\text{Coefficient of uniformity, } C_u, \quad = \frac{D60}{D_{10}} \qquad (4C\text{-}27)$$

and

$$\text{Coefficient of curvature, } C_c, \quad = \frac{(D30)_2}{(D_{10})(D_{60})} \qquad (4C\text{-}28)$$

where: D_{10}, D_{30}, and D — Diameter of particles in millimeters passing the 10, 30, and 60 percent points, respectively, on the base material gradation curve.

Based on the above criteria for supporting strength and drainage, a bedding material for leachate collection pipes should be well-graded gravel with the following properties:

Gradation:	100% passing 1-1/2" sieve 5% maximum passing No. 50 sieve
C_u:	4.0 or greater
C_c:	1.0 to 3.0

The actual bedding material should be selected within these limits after consideration of the pipe material, availability of bedding material, and its resistance to leachate attack.

ATTACHMENT III.5.D

POLY PIPE INDUSTRIES, INC. 2008.

DESIGN AND ENGINEERING GUIDE FOR POLYETHYLENE PIPING.

WWW.PLASTICPIPE.ORG

PolyPipe®

Design and Engineering Guide for Polyethylene Piping

Table A-2 (cont'd)
PIPE WEIGHTS AND DIMENSIONS *(IPS)*
PE3608 *(BLACK)*

OD			**SDR**	**Nominal ID**		**Minimum Wall**		**Weight**	
Nominal	**Actual**							**lb. per**	**kg. per**
in.	**in.**	**mm.**		**in.**	**mm.**	**in.**	**mm.**	**foot**	**meter**
			7	2.44	61.98	0.500	12.70	2.047	3.047
			7.3	2.48	63.08	0.479	12.18	1.978	2.943
			9	2.68	67.96	0.389	9.88	1.656	2.464
			9.3	2.70	68.63	0.376	9.56	1.609	2.395
			11	2.83	71.77	0.318	8.08	1.387	2.065
3	3.500	88.90	11.5	2.85	72.51	0.304	7.73	1.333	1.984
			13.5	2.95	74.94	0.259	6.59	1.153	1.716
			15.5	3.02	76.74	0.226	5.74	1.015	1.511
			17	3.06	77.81	0.206	5.23	0.932	1.386
			21	3.15	79.93	0.167	4.23	0.764	1.136
			26	3.21	81.65	0.135	3.42	0.623	0.927
			7	3.14	79.68	0.643	16.33	3.384	5.037
			7.3	3.19	81.11	0.616	15.66	3.269	4.865
			9	3.44	87.38	0.500	12.70	2.737	4.073
			9.3	3.47	88.24	0.484	12.29	2.660	3.958
			11	3.63	92.27	0.409	10.39	2.294	3.413
4	4.500	114.30	11.5	3.67	93.23	0.391	9.94	2.204	3.280
			13.5	3.79	96.35	0.333	8.47	1.906	2.836
			15.5	3.88	98.67	0.290	7.37	1.678	2.497
			17	3.94	100.05	0.265	6.72	1.540	2.292
			21	4.05	102.76	0.214	5.44	1.262	1.879
			26	4.13	104.98	0.173	4.40	1.030	1.533
			32.5	4.21	106.84	0.138	3.52	0.831	1.237
			7	3.88	98.51	0.795	20.19	5.172	7.697
			7.3	3.95	100.27	0.762	19.36	4.996	7.435
			9	4.25	108.02	0.618	15.70	4.182	6.224
			9.3	4.29	109.09	0.598	15.19	4.065	6.049
			11	4.49	114.07	0.506	12.85	3.505	5.216
5	5.563	141.30	11.5	4.54	115.25	0.484	12.29	3.368	5.012
			13.5	4.69	119.11	0.412	10.47	2.912	4.334
			15.5	4.80	121.97	0.359	9.12	2.564	3.816
			17	4.87	123.68	0.327	8.31	2.353	3.502
			21	5.00	127.04	0.265	6.73	1.929	2.871
			26	5.11	129.78	0.214	5.43	1.574	2.343
			32.5	5.20	132.08	0.171	4.35	1.270	1.890
			7	4.62	117.31	0.946	24.04	7.336	10.917
			7.3	4.70	119.41	0.908	23.05	7.086	10.545
			9	5.06	128.64	0.736	18.70	5.932	8.827
			9.3	5.11	129.92	0.712	18.09	5.765	8.579
			11	5.35	135.84	0.602	15.30	4.971	7.398
6	6.625	168.28	11.5	5.40	137.25	0.576	14.63	4.777	7.109
			13.5	5.58	141.85	0.491	12.46	4.130	6.147
			15.5	5.72	145.26	0.427	10.86	3.637	5.413
			17	5.80	147.29	0.390	9.90	3.338	4.967
			21	5.96	151.29	0.315	8.01	2.736	4.072
			26	6.08	154.55	0.255	6.47	2.233	3.322
			32.5	6.19	157.30	0.204	5.18	1.801	2.680

See ASTM D3035, F714 and AWWA C-901/906 for OD and wall thickness tolerances.
Weights are calculated in accordance with PPI TR-7.

EARTHLOADING

PolyPipe®, due to its flexibility, will deflect when it is buried. The degree of deflection will depend upon the soil conditions, burial conditions, trench width, and the depth of burial. The degree of deflection of the pipe is limited by the soil around its periphery, especially in the lateral direction. When the soil compacts around the pipe, there is a supportive effect from the soil itself, and as compaction occurs, there is soil friction and cohesion over the pipe that reduces the direct load on the pipe.

PolyPipe®, as do other flexible conduits, depends on the surrounding soil for support, and has to be considered as one component in a pipe/soil system. The presence of the soil arch and the support derived from the lateral movement limitations are highly beneficial to the efficiency of the system. Therefore, the flexibility of **PolyPipe®** is the major reason for these advantages. As has been stated, the durability of polyethylene is the reason for its resistance to high levels of mechanical abuse, and this is no less true for buried systems where forced deflections may occur due to subsidence, washout and settlement.

External loading analysis must be conducted to determine the application's feasibility. There are two loading calculations necessary when designing or engineering below ground applications of **PolyPipe®.** These calculations are ring deflection and wall buckling. Wall crushing, calculated using the allowable compressive strength of the PE material, is usually not critical when using solid wall **PolyPipe®,** as ring deflection and wall buckling are predominant parameters.

RING DEFLECTION

PolyPipe®, when buried in loose soil conditions, will exhibit the tendency to deflect, called ring deflection. Listed below are the recommended maximum allowable design limits for ring deflection of **PolyPipe®** for the different available Dimension Ratios (DR).

Table C-1
Design Limits for Ring Deflection

DR	Safe Deflection, % of Diameter
32.5	8.0
26	7.0
21	6.0
17	5.0

Figure C-1

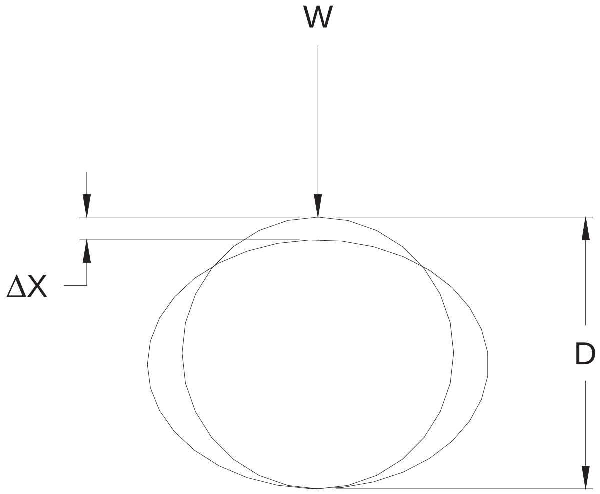

PolyPipe®, due to its inherent physical properties of flexibility, resilience and toughness can withstand significant deflection without failure. It can be flattened without causing a fracture of the pipe wall. However, this condition is unacceptable as far as service is concerned. A deflection of 15% would be acceptable for a butt fused polyethylene system, although a reduction in flow would be noted. It would also be difficult to utilize conventional cleaning equipment with this severity of deflection. Ring deflection resulting in hydraulic flow area reductions should be taken into account when engineering the flow characteristics. Refer to Table C-2 for the percentage of area reduction based on percent of ring deflection.

Table C-2
AREA REDUCTION DUE TO RING DEFLECTION

Ring Deflection, %	Area Reduction, %
2	0.04
4	0.16
5	0.25
6	0.36
8	0.64
10	1.00
12	1.44
14	1.96
15	2.25
16	2.56

In calculating the soil load placed on a buried pipe, the designer must be able to calculate to some degree of accuracy the type and condition of the backfill material. Saturated clay would be more difficult to place and adequately compact than would coarse granular material that would not stick together. It is important in the pipe/soil system that the backfill material utilized for haunching and initial backfill (see Installation, Section F, for explanation of terminology) be granular and non-cohesive, free of debris, organic matter, frozen earth and rocks larger than 1½ inch in diameter. This material can be described as Class I or II of ASTM D2321 "Angular ¼ to 1½ inch Graded Stone, Slag, Cinders, Crushed Shells and Stone or Sands and Gravel Containing Small Percentages of Fines, Generally Granular and Non-Cohesive, Wet or Dry." This material can easily be worked into the pipe haunch, and compacted in approximately 4-6 inch lifts.

To determine the ring deflection of externally loaded **PolyPipe®**, you must first determine the earthload in pounds per linear inch of pipe by use of the following modified Marston formula[5]:

$$W = \frac{C_d \cdot \rho \cdot B_d \cdot D}{144} \tag{17}$$

Where W = Earthload per unit length of pipe, lbs/in
C_d = Trench Coefficient, (dimensionless) (See Figure C-2)
ρ = Soil density, lbs/ft^3
D = Outside diameter, inches
B_d = Trench width at top of pipe, feet

---

[5] Moser, A.P. Buried Pipe Design. 2nd Edition. New York: McGraw-Hill, 2001.

Table C-3
CLASSIFICATION OF BACKFILL MATERIAL
PER ASTM D2321*

Class	Comments
Class I - Angular graded stone, ¼" to 1½", including a number of fill materials that have regional significance such as coral, slag, cinders, crushed stone, crushed gravel and crushed shells.	100 - 200 pounds per cubic foot. Pipe sizes less than 10" should limit maximum particle size to ½" to ¾" for ease of placement.
Class II - Coarse sands and gravel with maximum particle size of 1½", including variously graded sands and gravel containing small percentages of fines, generally granular and non-cohesive, wet or dry.	110 - 130 pounds per cubic foot. Pipe sizes less than 10" should limit maximum particle size to ½" to ¾" inch for ease of placement.
Class III - Fine sand and clay gravel, including fine sands, sand-clay mixtures, and gravel-clay mixtures.	140 - 150 pounds per cubic foot.
Class IV - Silt, silty clays, and clays, including inorganic clays and silts of medium to high plasticity and liquid limits.	150 - 180 pounds per cubic foot.
Class V - Includes organic soils as well as soils containing frozen earth, debris, rocks larger than 1½" in diameter, and other foreign materials.	Not recommended for backfill except in the final backfill zone.

* For further classification of soils the designer may want to review ASTM D2487, "Standard Test Method for Classification of Soil for Engineering Purposes."

Figure C-2
TRENCH COEFFICIENT, C_d
DEPENDENT ON SOIL TYPE AND DITCH CONFIGURATION

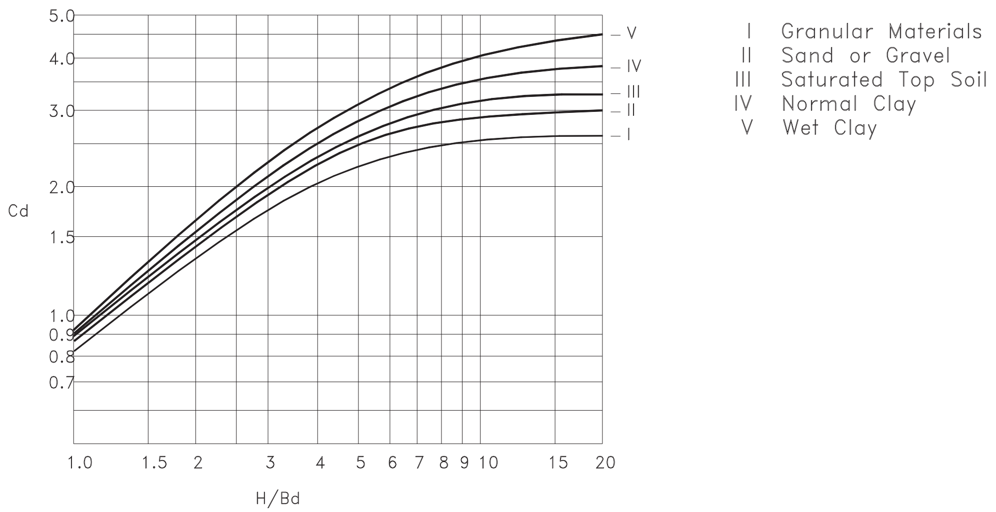

In general practice, the trench width can be kept to a minimum of six inches per side greater than the pipe diameter itself. Although this may seem narrow in comparison to trenching of conventional materials, it must be noted that **PolyPipe®** can be pre-assembled above ground and later placed into the trench. The trench width should be maintained as narrow as possible as the soil loading on the pipe is a relationship of the trench width.

The linear deflection of the pipe can be calculated from the following modified Spangler equation[6]:

$$\Delta x = \frac{D_l \cdot K \cdot W}{\left(\frac{2E}{3(DR-1)^3}\right) + 0.061E'} \tag{18}$$

Where Δx = Horizontal deflection or change in diameter, inches
D_l = Deflection lag factor, **PolyPipe®** recommends 1.0 (dimensionless)
K = Bedding constant, **PolyPipe®** recommends 0.1 (dimensionless)
W = Earthload, lbs/inch (See Equation (17))
E = Modulus of elasticity of pipe, 30,000 psi
E' = Soil modulus, psi
DR = Dimension ratio, (dimensionless)

** For further values of K see reference.*

The percent deflection can be calculated by use of the following formula[6]:

$$d = \frac{\Delta x}{D} \cdot 100 \tag{19}$$

Where d = Percent deflection, %
Δx = Horizontal deflection, inches (See Equation (*18*))
D = Outside diameter, inches

Table C-4
TYPICAL SOIL MODULUS VALUES (PSI)

Type of Soil	**Depth of Cover**		**Standard AASHTO relative compaction**			
	ft	m	85%	90%	95%	100%
Fine-grained soils with less than 25% sand content (CL, ML, CL-ML)	0-5	0-1.5	500	700	1000	1500
	5-10	1.5-3.1	600	1000	1400	2000
	10-15	3.0-4.6	700	1200	1600	2300
	15-20	4.6-6.1	800	1300	1800	2600
Coarse-grained soils with fines (SM., SC)	0-5	0-1.5	600	1000	1200	1900
	5-10	1.5-3.0	900	1400	1800	2700
	10-15	3.0-4.6	1000	1500	2100	3200
	15-20	4.6-6.1	1100	1600	2400	3700
Coarse-grained soils with little or no fines (SP, SW, GP, GW)	0-5	0-1.5	700	1000	1600	2500
	5-10	1.5-3.0	1000	1500	2200	3300
	10-15	3.0-4.6	1050	1600	2400	3600
	15-20	4.6-6.1	1100	1700	2500	3800

---

[6] Plastics Pipe Institute. Underground Installation of Polyethylene Pipe, 1996.

Values of modulus of soil reaction, E' (psi) based on depth of cover, type of soil, and relative compaction. Soil type symbols are from the United Classifications System. Source: Hartley, James D. and Duncan, James M., "E' and its Variation with Depth," Journal of Transportation, Division of ASCE, Sept. 1987.

WALL BUCKLING

PolyPipe®, when buried in dense soil conditions and subjected to excessive external loading, will exhibit the tendency of wall buckling. As seen in Figure C-3, wall buckling is a longitudinal wrinkle that usually occurs between the 10:00 and 2:00 positions. Wall buckling should become a design consideration when the total vertical load exceeds the critical buckling stress of **PolyPipe®.**

Figure C-3

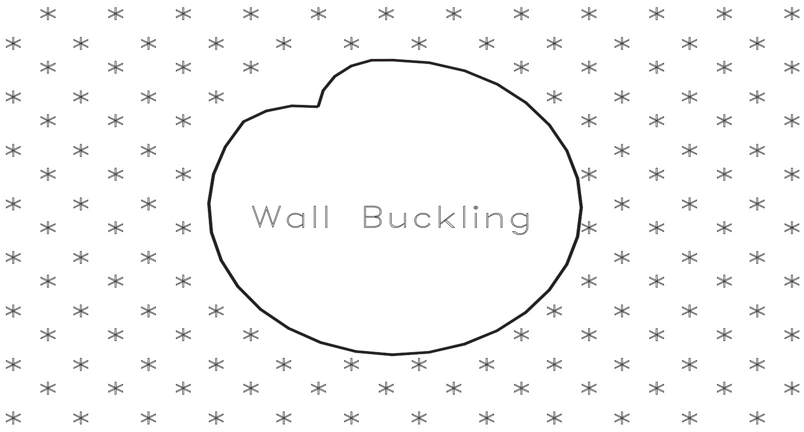

Vertical loading can be determined by the summation of the calculated dead load (load resulting from backfill overburden and static surface loads) and live load (loads resulting from cars, trucks, trains, etc.).

BACKFILL LOAD[1]

$$P_b = \frac{\rho_{soil} \cdot H}{144} \tag{20}$$

Where P_b = Backfill load, psi
ρ_{soil} = Backfill density, lbs/ft^3
H = Height of backfill above pipe, feet

SURFACE LOAD

Surface loads are those forces exerted by permanent structures in close proximity to buried **PolyPipe®.** These loads can be buildings, storage tanks, or other structures of significant weight that could add to the backfill loading. The force exerted on **PolyPipe®** by structural surface loads can be approximated by use of the following Boussinesq[17] formulation:

$$P_s = \frac{3Lz^3}{144 \cdot 2\pi R^5} \tag{21}$$

Where P_s = Surface load on pipe, psi
L = Static surface load, lbs.
z = Vertical distance from top of pipe to surface load level, feet
R = Straight line distance from the top of pipe to surface load, feet

Where,

---

[1] Nayyar, Mohinder L. Ed. Piping Handbook. 6th Edition. New York: McGraw-Hill, Inc., 1992.

[17] Chen, W. F., Liew, Richard L. Y. The Civil Engineering Handbook. New York: CRC Press, 2003. 2nd Edition.

$$R = \sqrt{x^2 + y^2 + z^2} \tag{22}$$

Where x = Horizontal distance from surface load, feet (Refer to Figure C-4)
y = Horizontal distance from surface load, feet (Refer to Figure C-4)
z = Vertical distance from top of pipe to surface load level, feet (Refer to Figure C-4)

Figure C-4
RESULTANT SURFACE LOAD

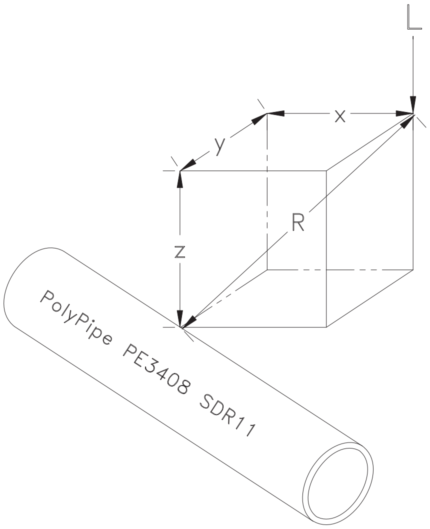

LIVE LOAD

Live loading can be determined by extracting the load from Figure C-5 for H20 highway loading or from Figure C-6 for Cooper E-80 loading or by estimating, using available analytical techniques.

Figure C-5
H20 HIGHWAY LOADING

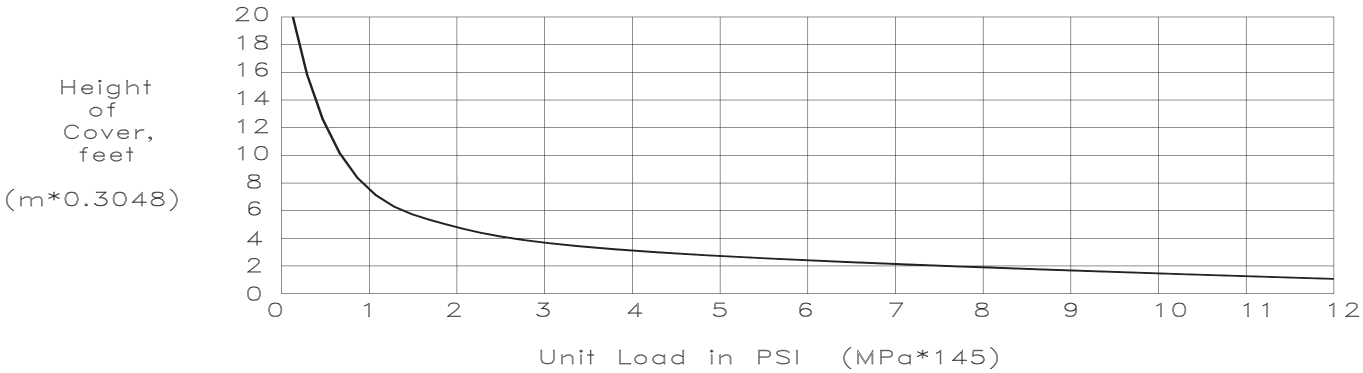

***Note:** The H20 live load assumes two 16,000 lb. loads applied to two 18" x 20" areas, one located over the point in question, and the other located at a distance of 72" away. In this manner, a truckload of 20 tons is simulated.*

Source: American Iron and Steel Institute, Washington, DC

Figure C-6
COOPER E-80

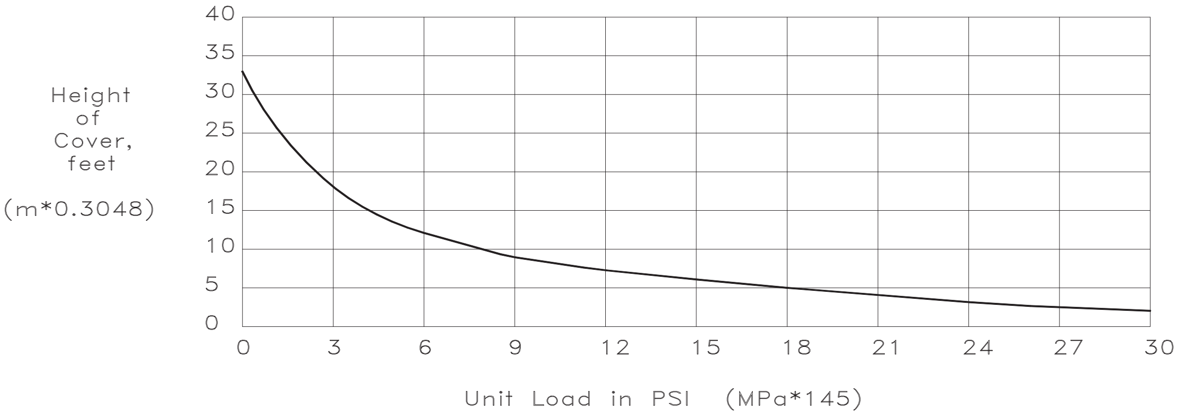

Note: *The Cooper E-80 live load assumes 80,000 pounds applied to three 2' x 6' areas on 5' centers, such as might be encountered through live loading from a locomotive with three 80,000 pounds axle loads.*

Source: American Iron and Steel Institute, Washington, DC

TOTAL EXTERNAL LOADING

Total Load = Live Load + Backfill Load + Surface Load

$$P_t = P_l + P_b + P_s \tag{23}$$

Once the external loading on buried **PolyPipe**® has been determined, it will be necessary to calculate the critical buckling stress for contained **PolyPipe**® to determine if the pipe can withstand the external loading. The external loading capacity, or critical buckling stress, can be determined by the use of the following Von Mises formula:

$$P_{cb} = \frac{1}{SF} \cdot \left(\frac{2.67 \cdot R_w \cdot B \cdot E_s \cdot E}{DR^3} \right)^{1/2} \tag{24}$$

Where P_{cb} = Critical buckling stress, psi
SF = Safety factor, **PolyPipe**® recommends SF=2
R_w = Water buoyancy factor, (dimensionless)
B = Empirical Coefficient of Elastic Support, (dimensionless)
E_s = Soil modulus, (See Table C-4)
E = Pipe modulus of elasticity, psi
DR = Dimension Ratio

Where,

$$R_w = 1 - \left(0.33 \cdot \frac{H_w}{H} \right) \tag{25}$$

H_w = Height of water table above pipe, feet
H = Height of soil cover above pipe, feet

Note: *H_w must be less than H*

and,

$$B = \frac{1}{1 + 4 \cdot e^{-0.065 \cdot H}} \tag{26}$$

Where e = 2.718
H = Height of soil cover above pipe, feet

If the total external loading, Equation (23), is less than the critical buckling stress ($P_t < P_{cb}$), then the application should be considered safe. However, if this is not the case ($P_t > P_{cb}$), then the required parameters can be determined for a safe application from the following variations of the above equation:

$$DR = \left(\frac{2.67 \cdot R_w \cdot B \cdot E_s \cdot E}{SF^2 \cdot P_{cb}^2} \right) \tag{27}$$

or

$$E_s = \frac{P_{cb}^2 \cdot SF^2 \cdot DR^3}{2.67 \cdot R_w \cdot B \cdot E} \tag{28}$$

ATTACHMENT III.5.E

DRISCOPIPE, INC. 2008.

POLYETHYLENE PIPING SYSTEMS MANUAL

www.driscopipe.com

DRISCOPIPE®

Polyethylene Piping Systems Manual

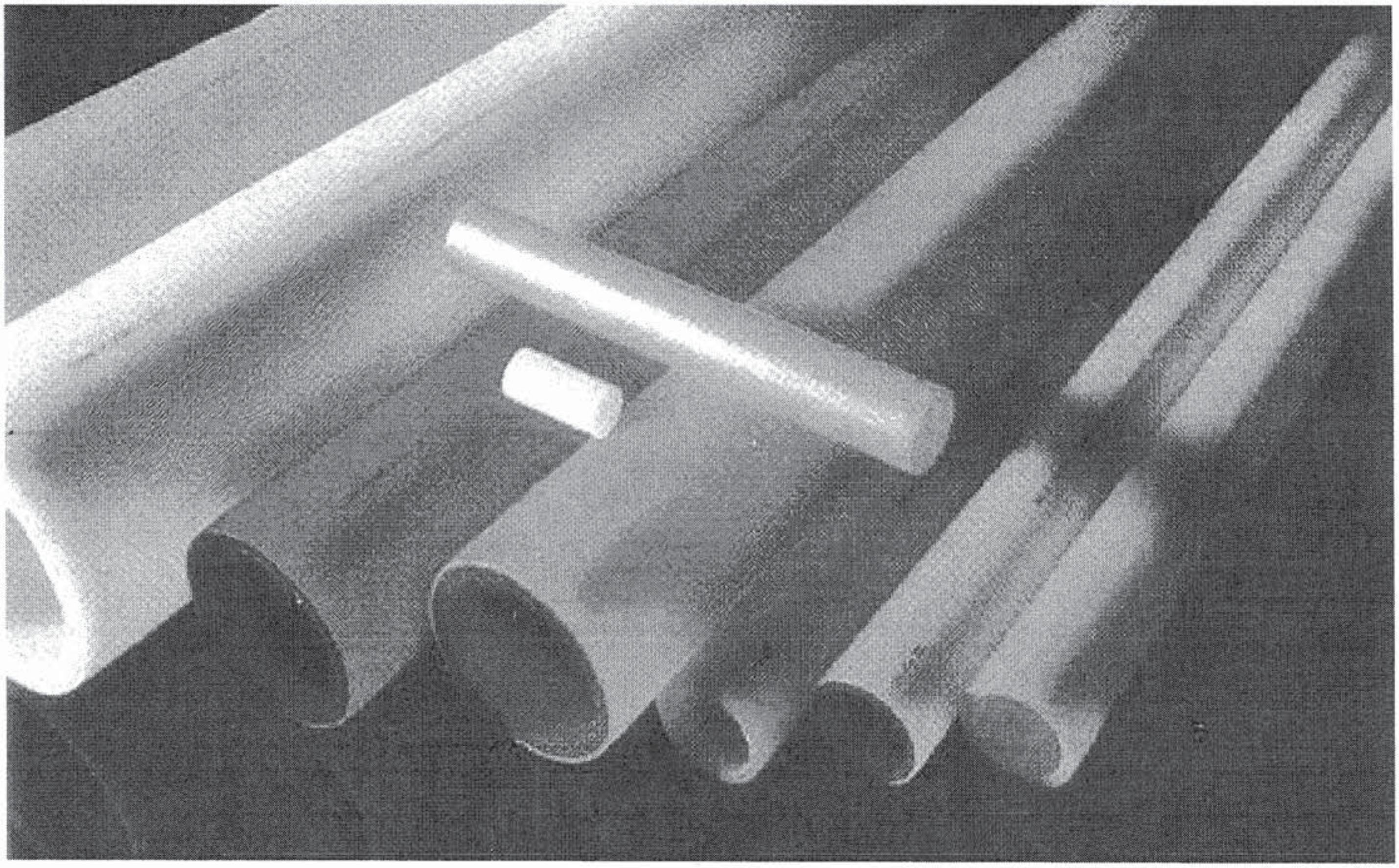

Innovative Supplier of Quality Piping Systems.

PHILLIPS 66

FIGURE 6: COOPER E-80 LIVE LOADING

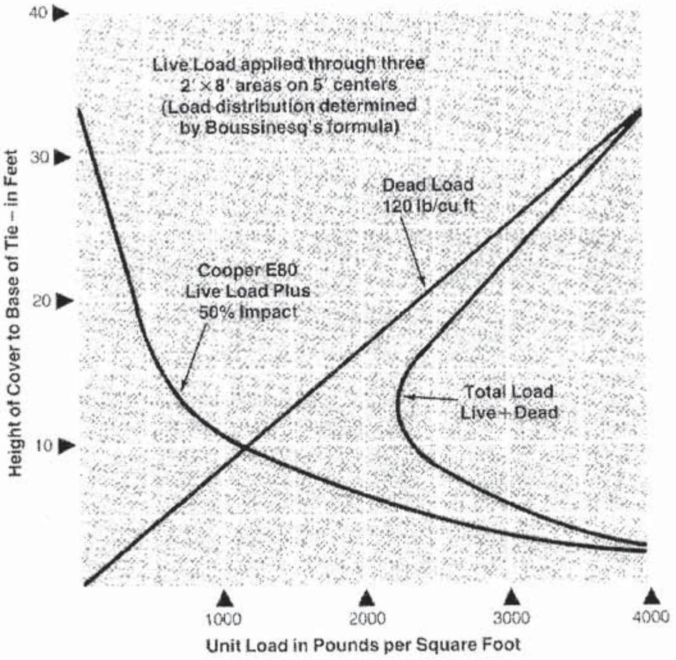

Note: Cooper E-80 live load assumes 80,000 pounds applied to three 2' x 8' areas on 5' centers such as might be encountered through live loading from a locomotive with three 80,000 pound axle loads.

Source: American Iron and Steel Institute, Washington, DC

APPARENT EXTERNAL PRESSURE DUE TO INTERNAL VACUUM, P_I Vacuum generates a compressive hoop stress in the wall of a pipe and acts to collapse the pipeline. Under vacuum conditions, the value of P_I is positive. P_I is added to the other two external pressure components, P_S and P_L, to obtain the total external pressure, P_T, acting on the pipe. An internal vacuum generates pressure equal to the absolute value of the vacuum. The maximum apparent external pressure due to a vacuum inside the pipe is 14.7 psi (2,117 psf).

BURIAL DESIGN GUIDELINES

The design engineer must select the proper pipe DR and specify the backfill conditions to obtain the desired performance of the "pipe-soil" system.

DESIGN BY WALL CRUSHING Wall crushing occurs when external vertical pressure causes the compressive stress in the pipe wall to exceed the long-term compressive strength of the pipe material. To design for wall crushing, the following check should be made:

$$S_A = \frac{(SDR-1)}{2} P_T$$

Where:

S_A = Actual compressive stress, psi
SDR = Standard Dimension Ratio
P_T = Total external pressure on the top of the pipe, psi

Safety Factor = 1500 psi /S_A (where 1500 psi is the compressive yield strength of Driscopipe HDPE pipe)

DESIGN BY WALL BUCKLING Local wall buckling is a longitudinal wrinkling of the pipe wall. Buckling can occur over the long term in non-pressurized pipe if the total external soil pressure, P_T, exceeds the pipe-soil system's critical buckling pressure, P_{cb}. Although wall buckling is seldom the limiting factor in the design of a Driscopipe system, a check of non-pressurized pipelines can be made according to the following steps to insure $P_T < P_{cb}$. All pipe diameters with the same DR in the same burial situation have the same critical collapse and critical buckling endurance.

1. Calculate or estimate the total soil pressure, P_T, at the top of the pipe.

2. Calculate the stress, S_a, in the pipe wall:

$$S_a = \frac{(SDR-1)P_T}{2}$$

3. Based upon the stress S_a and the estimated time duration of non-pressurization, find the value of the pipe's modulus of elasticity, E, in psi (approximate value for E is 35,000 psi).

4. Calculate the pipes hydrostatic, critical-collapse differential pressure, P_c

$$P_c = \frac{2E\left(t/D\right)^3\left(D_{MIN}/D_{MAX}\right)^3}{\left(1-\mu^2\right)} \quad \text{or} \quad P_c = \frac{2.32(E)}{SDR^3}$$

Where:
$(D_{MIN}/D_{MAX}) = 0.95$
μ = Poission's Ratio = 0.45 for polyethylene pipe
E = stress and time dependent tensile modulus of elasticity, psi
E = 35,000 psi (approximate)
D = Outside Diameter, in.
t = thickness, in.

5 Calculate the soil modulus, E', by plotting the total external soil pressure, P_T, against a specified soil density to derive the soil strain as shown in the example problem below Figure 7.

6. Calculate the critical buckling pressure at the top of the pipe by the formula:

$$P_{cb} = 0.8\sqrt{(E')(P_c)}$$

Where:
P_{cb} = Critical buckling soil pressure at the top of the pipe, psi
E' = Soil Modulus, psi
P_c = Hydrostatic critical-collapse differential pressure, psi

7. Calculate the Safety Factor: SF = P_{cb}/ P_T .

8. The above procedures can be reversed to calculate the minimum pipe DR required for a given soil pressure and an estimated soil density.

In a direct burial pressurized pipeline, the internal pressure is usually great enough to exceed the external critical-buckling soil pressure. When a pressurized line is to be shut down for a period, wall buckling should be examined.

ATTACHMENT III.5.F

CHEVRON PHILLIPS CHEMICAL COMPANY, LP. 2003.

PERFORMANCE PIPE ENGINEERING MANUAL.

BULLETIN: PP 900

DriscoPlex™ 2000 SPIROLITE® pipe is manufactured to ASTM F 894, which states that profile pipe designed for 7.5% deflection will perform satisfactorily when installed in accordance with ASTM D 2321. Deflection is measured at least 30 days after installation.

Manufacturing processes for DriscoPlex™ 2000 SPIROLITE® and DriscoPlex™ OD controlled pipe differ. Deflection limitations for OD controlled pipe are controlled by long-term material strain.

Ring Bending Strain

As pipe deflects, bending strains occur in the pipe wall. For an elliptically deformed pipe, the pipe wall ring bending strain, ε, can be related to deflection:

$$\varepsilon = f_D \frac{\Delta X}{D_M} \frac{2C}{D_M} \tag{7-39}$$

Where

ε = wall strain
f_D = deformation shape factor
ΔX = deflection, in
D_M = mean diameter, in
C = distance from outer fiber to wall centroid, in

For DriscoPlex™ 2000 SPIROLITE® pipe

$$C = h - z \tag{7-40}$$

For DriscoPlex™ OD Controlled pipe

$$C = 0.5(1.06\,t) \tag{7-41}$$

Where

h = pipe wall height, in
z = pipe wall centroid, in
t = pipe minimum wall thickness, in

For elliptical deformation, $f_D = 4.28$. However, buried pipe rarely has a perfectly elliptical shape. Irregular deformation can occur from installation forces such as compaction variation alongside the pipe. To account for the non-elliptical shape many designers use $f_D = 6.0$.

Lytton and Chua report that for high performance polyethylene materials such as those used by Performance Pipe, 4.2% ring bending strain is a conservative value for non-pressure pipe. Jansen reports that high performance polyethylene material at an 8% strain level has a life expectancy of at least 50 years.

When designing non-pressure heavy wall OD controlled pipe (DR less than 17), and high RSC (above 200) DriscoPlex™ 2000 SPIROLITE® pipe, the ring bending strain at the predicted deflection should be calculated and compared to the allowable strain.

In pressure pipe, the combined stress from deflection and internal pressure should not exceed the material's long-term design stress rating. Combined stresses are incorporated into Table 7-9 values, which presumes deflected pipe at full pressure. At reduced pressure, greater deflection is allowable.

ATTACHMENT III.5.G

LEACHATE COLLECTION PIPE DESIGN CALCULATIONS – 6” SDR 13.5

ATTACHMENT III.5.G - Leachate Collection Pipe Design Calculations
6" SDR 13.5

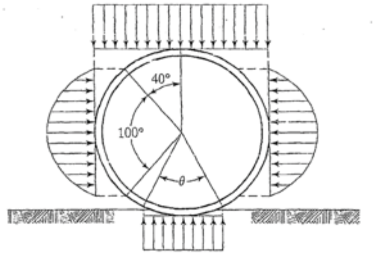

Assumed Pressure Distribution on Flexible Pipe

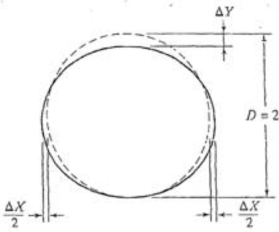

Pipe Deflection Under Pressure

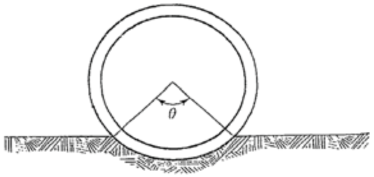

Pipe Bedding Angle

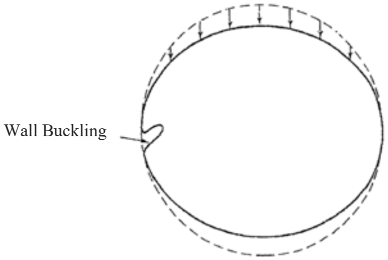

Material	H (ft)	γ (lb/ft^3)	Pressure (lb/ft^2)
Vegetative (Erosion) Layer	0.5	102.0	51.0
Barrier (Infiltration) Layer	2.5	102.0	255.0
Intermediate Cover Soil	1.0	102.0	102.0
Waste	205.0	74.0	15,170.0
Protective Soil Layer	2.0	102.0	204.0
Drainage Aggregate	1.0	130.0	130.0
Design Load (P_T) =	$\Sigma\gamma_i \bullet H_i$	=	15,912.0

P_T = 110.50 psi

D_O =	6.625	in
SDR =	13.500	
t =	0.491	in
D =	6.134	in
r =	3.067	in
I =	0.010	in^3
n =	9.000	
d =	0.500	in
K =	0.083	
D_L =	1.500	

Ring Deflection:

Modified Iowa Formula is used to calculated horizontal pipe deflection

$$\Delta X = \frac{D_L \bullet K \bullet W_C \bullet r^3}{E \bullet I + 0.061E' \bullet r^3} \qquad (9.16)^1$$

Where:

ΔX =	Horizontal deflection of the pipe	**0.748**	in
D_L =	Deflection lag factor	1.50	
K =	Bedding constant	0.083	
W_C =	Vertical load per unit length of perforated pipe	1,171.30	lbs/in
	$W_C = (\Sigma\gamma_i \bullet H_i) \bullet D_o = P_{TP} \bullet D_o$ $(9.17)^1$	14,055.60	lbs/ft
P_{TP} =	Design load on perforated pipe	176.80	psi
	$P_{TP} = \frac{\Sigma\gamma_i \bullet H_i}{[1-((n \bullet d)/12)]}$ $(9.23)^1$		
D_o =	Outside diameter of the pipe	6.625	in
γ_i =	Unit weight of material i		
H_i =	Thickness of material i		
d =	Diameter of perforated hole	0.500	in
n =	Number of perforated holes per foot	9.0	
E =	Elastic modulus of the pipe material	35,000	psi
I =	Moment of inertia of the pipe wall per unit length	0.0099	in^4/in
	$I = t^3/12$		
t =	Thickness of pipe	0.491	in
E′ =	Soil reaction modulus	3,000	psi
r =	Mean radius of the pipe, $r = (D_O - t)/2$	3.067	in
SDR =	Standard Dimension Ratio	13.5	

Pipe Wall Ring Bending Strain:

$$\varepsilon = f_D \bullet \frac{\Delta X}{D} \bullet \frac{2C}{D} \qquad (7\text{-}39)^2 \qquad \mathbf{6.2}\ \%$$

Where:

ε =	Wall strain	0.062	
f_D =	Deformation shape factor	6.0	
ΔX =	Horizontal and vertical deflection of the pipe	0.748	in
D =	Mean diameter of the pipe		
	$D = D_O - t$ $(9.20)^1$	6.134	in
C =	Distance from outer fiber to wall centroid		
	$C = 0.5(1.06t)$ $(7\text{-}41)^2$	0.260	in
$\varepsilon_{critical}$ =	Critical wall strain	8.0	%

$$FS = \frac{\varepsilon_{critical}}{\varepsilon} \qquad \mathbf{1.29}$$

References:

[1] “Geotechnical Aspects of Landfill Design and Construction”, Xuede Qian, Robert M. Koerner, Donald H. Gray, Prentice Hall, 2002.

[2] Chevron Phillips, “Bulletin: PP 900”, Book 2 – Chapter 7, p. 112, 2003

ATTACHMENT III.5.G - Leachate Collection Pipe Design Calculations
6" SDR 13.5

Wall Buckling:

$$P_C = \frac{2.32E}{SDR^3}$$ (p. 43)[3]

Where:

P_C =	Critical-collapse differential pressure	33.00	psi
E =	Elastic modulus of the pipe material	35,000	psi
SDR =	Standard Dimension Ratio	13.5	
P_{CB} =	Critical buckling pressure	**251.73**	psi
	$P_{CB} = 0.8(E' \cdot P_C)^{0.5}$ (p. 43)[3]		
E′ =	Soil reaction modulus	3,000	psi
$FS = \frac{P_{CB}}{P_{TP}}$		**1.42**	
P_{TP} =	Design load on perforated pipe	176.80	psi

Wall Crushing:

$$S_A = \frac{(SDR - 1)}{2} \cdot P_{TP}$$ (p. 42)[3]

Where:

S_A =	Actual compressive stress	1105	psi
SDR =	Standard Dimension Ratio	13.5	
P_{TP} =	Design load on perforated pipe	176.80	psi
$FS = \frac{\text{Compressive Yield Strength}}{S_A}$		**1.36**	
Compressive yield strength =		1,500	psi

Equipment Loading:

CAT 627 Scraper Specs (Caterpillar Performance Handbook, Edition 2

• Tractor Weight =	48,061	lbs
• Scraper Weight =	33,399	lbs
• Soil Load (20 cy) =	48,000	lbs
• Total weight =	129,460	lbs
• Max weight per tire (assumes 49% of the total weight acts on the rear tires and 51% of the weight acts on the front tires) L_{tire} =	33,012	lbs
• Tire width (approximately) =	18	in
• Tire contact length (approximately) =	4	in
• Tire contact area =	72	in^2

$$W_{SD} = C_S \cdot p \cdot F \cdot B_C$$ (4C-19)[4]

Where:

W_{SD} =	Load on pipe	1951.404	lb/ft
		162.62	lb/in
C_S =	Load coefficient	0.053	
p =	Intensity of distributed load p = Ltire/D • M	66,691	lb/ft^2
F =	Impact factor	1.0	
B_C =	Outside diameter of the pipe	0.55	ft
H =	Height from the top of the pipe to the ground surfac	3.00	ft
D =	Width over which the distributed load acts	1.50	ft
M =	Length over which the distributed load acts	0.33	ft
D/2H =		0.25	
M/2H =		0.055	
$FS = \frac{W_C}{W_{SD}}$		**7.20**	
W_C =	Vertical load per unit length of pipe	1,171.30	lbs/in

References:

[3] "Polyethylene Piping Systems Manual", Driscopipe, Inc., 2008

[4] WDOE Landfill Design Manual, 1987

Lea Land LLC Surface Waste Management Facility
Application for Permit Modification
Volume III: Engineering Design and Calculations
Section 6: Geosynthetics Application and Compatibility Documentation

June 2019

TABLE OF CONTENTS

Section No. **Title** **Page**

1.0 INTRODUCTION III.6-1
  1.1 Site Location III.6-1
  1.2 Facility Description III.6-1
2.0 SUMMARY III.6-2

LIST OF TABLES

Table No. **Title** **Page**

III.6.1 GEOSYNTHETIC APPLICATIONS AND COMPATIBILITY DOCUMENTATION III.6-4

LIST OF ATTACHMENTS

Attachment No. **Title**

III.6.A HDPE GEOMEMBRANES REFERENCE DOCUMENTATION
III.6.B GEOTEXTILE REFERENCE DOCUMENTATION
III.6.C GEONET REFERENCE DOCUMENTATION
III.6.D GEOSYNTHETIC CLAY LINER (GCL) REFERENCE DOCUMENTATION
III.6.E HDPE PIPE REFERENCE DOCUMENTATION

1.0 INTRODUCTION

Lea Land LLC (the Facility) is an existing Surface Waste Management Facility (SWMF) providing oil field waste solids (OFWS) disposal services. The existing Lea Land SWMF is subject to regulation under the New Mexico Oil and Gas Rules, specifically 19.15.9.711 and 19.15.36 NMAC, administered by the Oil Conservation Division (OCD) of the NM Energy, Minerals, and Natural Resources Department (NMEMNRD). This document is a component of the “Application for Permit Modification” that proposes continued operations of the existing approved waste disposal unit; lateral and vertical expansion of the landfill via the construction of new double-lined cells; and the addition of waste processing capabilities. The proposed Facility is designed in compliance with 19.15.36 NMAC, and will be constructed and operated in compliance with a Surface Waste Management Facility Permit issued by the OCD. The Facility is owned by, and will be constructed and operated by, Lea Land LLC.

The Lea Land SWMF is one of the most recently designed facilities to meet the new more stringent standards that, for instance, mandate double liners and leak detection for land disposal. The new services that Lea Land will provide needed resources to fill an existing void in the market for technologies that exceed current OCD requirements.

1.1 Site Location

The Lea Land site is located approximately 27 miles northeast of Carlsbad, straddling US Highway 62-180 (Highway 62) in Lea County, NM. The Lea Land site is comprised of a 642-acre ± tract of land encompassing Section 32, Township 20 South, Range 32 East, Lea County, NM. Site access is currently provided on the south side of US Highway 62. The coordinates for the approximate center of the Lea Land site are Latitude 32°31’46.77” and Longitude -103°47’18.25”.

1.2 Facility Description

The Lea Land SWMF comprises approximately 463 acres ± of the 642-acre ± site, and will include two main components: an oil field waste Processing Area and an oil field waste solids Landfill, as well as related infrastructure (i.e., access, waste receiving, stormwater management, etc.). Oil field wastes are delivered to the Lea Land SWMF from oil and gas exploration and production operations in southeastern NM and west Texas. The Permit Plans (**Attachment III.1.A**) identify the locations of the Processing Area and Landfill Disposal facilities. The proposed facilities are detailed in **Table II.1.2** (**Volume II.1**), and are anticipated to be developed in four primary phases as described in **Table II.1.3** (**Volume II.1**).

2.0 SUMMARY

19.15.36.14 NMAC Specific requirements applicable to Landfills:

D. Liner specifications and requirements.

(1) General requirements.

(a) Geomembrane liner specifications. Geomembrane liners shall consist of a 30-mil flexible PVC or 60-mil HDPE liner, or an equivalent liner approved by the division. Geomembrane liners shall have a hydraulic conductivity no greater than 1 x 10-9 cm/sec. Geomembrane liners shall be composed of impervious, geosynthetic material that is resistant to petroleum hydrocarbons, salts and acidic and alkaline solutions. Liners shall also be resistant to ultraviolet light, or the operator shall make provisions to protect the material from sunlight. Liner compatibility shall comply with EPA SW-846 method 9090A.

19.15.36.17 NMAC Specific requirements applicable to evaporation, storage, treatment, and skimmer ponds:

B. Construction, standards.

(3) Liner specifications. Liners shall consist of a 30-mil flexible PVC or 60-mil HDPE liner, or an equivalent liner approved by the division. Synthetic (geomembrane) liners shall have a hydraulic conductivity no greater than 1 x 10^{-9} cm/sec. Geomembrane liners shall be composed of an impervious, synthetic material that is resistant to petroleum hydrocarbons, salts and acidic and alkaline solutions. Liner materials shall be resistant to ultraviolet light, or the operator shall make provisions to protect the material from sunlight. Liner compatibility shall comply with EPA SW-846 method 9090A.

Geosynthetics have a proven track record in a variety of civil engineering applications, primarily over the past 30 years. Fluid Containment design provides a unique opportunity to incorporate a range of engineered materials that exceed the equivalent performance of soils.

EPA SW-846 Method 9090A (July 1992 and subsequent revisions; the latest being June 2005) references ASTM methods for the majority of the physical properties of geosynthetics. Subsequent to the publication of EPA Method 9090A, the Geosynthetic Research Institute (GRI) published GRI-GM13 "*Test Methods, Test Properties and Testing Frequency for High Density Polyethylene (HDPE) Smooth and Textured Geomembranes"* (Revision 11: 12/14/12). Although this specification is not mandatory, the geosynthetics manufacturing industry has used this specification in the manufacturing of geosynthetics; and have used the noted ASTM methods for determining the adequacy of the geosynthetic physical properties for its intended use in landfills.

Compatibility testing of membrane liners has been completed by geosynthetic manufacturers in accordance with EPA method 9090A (July 1992) and subsequent updates. Additionally, the EPA promulgated the Methods Innovation Rule in the June 2005. This Rule provides greater flexibility by allowing the use of alternate test procedures other than SW-846 that are considered “appropriate” as long as they fall within EPA’s mission to safeguard human health and the environment, and meet the goals, data quality objectives, and quality control parameters of the project.

The design of the Lea Land SWMF includes several examples of geosynthetics and plastics deployed for their superior characteristics, usually applied in conjunction with soil layers:

- Geomembranes (flexible membrane liners) provided as barrier layer in the primary and secondary liner system (**Attachment III.6.A**).
- Geotextiles serving as cushioning layers and as filters to maintain flow (**Attachment III.6.B**).
- Geonets deployed as drainage layers and in leak detection systems (**Attachment III.6.C**).
- Geosynthetic clay liners (GCLs) employed as secondary composite layers for liners (**Attachment III.6.D**).
- The use of HDPE (High Density Polyethylene) piping systems (**Attachment III.6.E**).

Geosynthetics are selected in the design process for their performance characteristics in the project’s environmental setting. These materials must be able to withstand the physical forces that they will experience, as documented in this section. **Attachment III.6.A** includes recent research results that indicate the functional longevity of HDPE liners in similar installations is in the hundreds of years.

This section provides demonstrations, as required by 19.15.36.14.D.1 and 19.15.36.17.B NMAC that the geosynthetic components are compatible with the materials to be contained within the cells and ponds. The attached compatibility documentation includes published reports and test results; and is further endorsed by industry experience and proven installations by the design engineer. For the performance criteria of both soil and geosynthetic components to be achieved, they must be constructed in strict accordance with the **Permit Plans** (**Volume III.1**) and the Liner Construction Quality Assurance (CQA) Plan, (**Volume II.7**) of this Application for Permit.

Table III.6.1 provides an index of compatibility data provided for each of the prescribed geosynthetic materials and their function in the engineering design.

TABLE III.6.1 - Geosynthetic Applications and Compatibility Documentation

MATERIAL	FUNCTION	ATTACHED REFERENCE DOCUMENTATION	
HDPE Geomembrane	Primary and secondary barrier layer for landfill liner	III.6.A	*Geomembrane Lifetime Prediction: Unexposed and Exposed Conditions - GRI*
			Cold Temperature and Free-Thaw Cycling Behavior of Geomembranes and Their Seams
			Chemical Compatibility of Poly-Flex Liners
			Chemical Resistance Table Low Density and High Density Polyethylene
			NSC, Contaminant Solutions for Industrial Waste; HDPE Geomembrane
			Liner Longevity Article: Geosynthetics Magazine, Oct/Nov 2008
Geotextile *(upper & lower component of geocomposite)*	Filter layer around leachate collection piping	III.6.B	*Amoco Technical Note No. 7, Chemical Resistance of Amoco Polypropylene Geotextiles*
			Amoco Technical Note No. 14, Geotextile Polymers for Waste Applications
Geonet *(middle component of geocomposite)*	Drainage layer between primary and secondary liner	III.6.C	*GSE TenDrain 275 mil Geocomposite*
			Evaluation on Stress Cracking Resistance of Various HDPE Drainage Geonets
GCL	Secondary layer in composite liner	III.6.D	*The Effects of Leachate on the Hydraulic Conductivity of Bentomat*
			Bench-scale Hydraulic Conductivity Tests of Bentonitic Blanket Materials for Liner and Cover Systems (Thesis by Paula Estornell)
HDPE Pipe	Solid and slotted piping, leachate collection system and GCCS	III.6.E	*Chemical Resistance of Plastics and Elastomers Used in Pipeline Construction*
			Driscopipe Engineering Characteristics
			Plexco Chemical Resistance Information

Acronyms used:
GCL: Geosynthetic Clay Liner
FML: Flexible Membrane Liner
GSE: Gundle Schlegel Environmental
HDPE: High Density Polyethylene
NSC: National Seal Company

ATTACHMENT III.6.A

HDPE GEOMEMBRANES REFERENCE DOCUMENTATION

Geosynthetic Institute
475 Kedron Avenue
Folsom, PA 19033-1208 USA
TEL (610) 522-8440
FAX (610) 522-8441

GRI White Paper #6

- on -

Geomembrane Lifetime Prediction:
Unexposed and Exposed Conditions

by

Robert M. Koerner, Y. Grace Hsuan and George R. Koerner
Geosynthetic Institute
475 Kedron Avenue
Folsom, PA 19033 USA

Phone (610) 522-8440
Fax (610) 522-8441

E-mails:
robert.koerner@coe.drexel.edu
grace.hsuan@coe.drexel.edu
gkoerner@dca.net

Original: June 7, 2005

Updated: February 8, 2011

Geomembrane Lifetime Prediction: Unexposed and Exposed Conditions

1.0 Introduction

Without any hesitation the most frequently asked question we have had over the past thirty years' is "how long will a particular geomembrane last".* The two-part answer to the question, largely depends on whether the geomembrane is covered in a timely manner or left exposed to the site-specific environment. Before starting, however, recognize that the answer to either covered or exposed geomembrane lifetime prediction is neither easy, nor quick, to obtain. Further complicating the answer is the fact that all geomembranes are formulated materials consisting of (at the minimum), (i) the resin from which the name derives, (ii) carbon black or colorants, (iii) short-term processing stabilizers, and (iv) long-term antioxidants. If the formulation changes (particularly the additives), the predicted lifetime will also change. See Table 1 for the most common types of geomembranes and their approximate formulations.

Table 1 - Types of commonly used geomembranes and their approximate formulations (based on weight percentage)

Type	Resin	Plasticizer	Fillers	Carbon Black	Additives
HDPE	95-98	0	0	2-3	0.25-1
LLDPE	94-96	0	0	2-3	0.25-3
fPP	85-98	0	0-13	2-4	0.25-2
PVC	50-70	25-35	0-10	2-5	2-5
CSPE	40-60	0	40-50	5-10	5-15
EPDM	25-30	0	20-40	20-40	1-5

HDPE = high density polyethylene
LLDPE = linear low density polyethylene
fPP = flexible polypropylene
PVC = polyvinyl chloride (plasticized)
CSPE = chlorsulfonated polyethylene
EPDM = ethylene propylene diene terpolymer

---

* More recently, the same question has arisen but focused on geotextiles, geogrids, geopipe, turf reinforcement mats, fibers of GCLs, etc. This White Paper, however, is focused completely on geomembranes due to the tremendous time and expense of providing such information for all types of geosynthetics.

The possible variations being obvious, one must also address the degradation mechanisms which might occur. They are as follows accompanied by some generalized commentary.

- Ultraviolet Light - This occurs only when the geosynthetic is exposed; it will be the focus of the second part of this communication.
- Oxidation - This occurs in all polymers and is the major mechanism in polyolefins (polyethylene and polypropylene) under all conditions.
- Ozone - This occurs in all polymers that are exposed to the environment. The site-specific environment is critical in this regard.
- Hydrolysis - This is the primary mechanism in polyesters and polyamides.
- Chemical - Can occur in all polymers and can vary from water (least aggressive) to organic solvents (most aggressive).
- Radioactivity - This is not a factor unless the geomembrane is exposed to radioactive materials of sufficiently high intensity to cause chain scission, e.g., high level radioactive waste materials.
- Biological - This is generally not a factor unless biologically sensitive additives (such as low molecular weight plasticizers) are included in the formulation.
- Stress State – This is a complicating factor which is site-specific and should be appropriately modeled in the incubation process but, for long-term testing, is very difficult and expensive to acheive.
- Temperature - Clearly, the higher the temperature the more rapid the degradation of all of the above mechanisms; temperature is critical to lifetime and furthermore is the key to

time-temperature-superposition which is the basis of the laboratory incubation methods which will be followed.

2.0 Lifetime Prediction: Unexposed Conditions

Lifetime prediction studies at GRI began at Drexel University under U. S. EPA contract from 1991 to 1997 and was continued under GSI consortium funding until ca. 2002. Focus to date has been on HDPE geomembranes placed beneath solid waste landfills due to its common use in this particular challenging application. Incubation of the coupons has been in landfill simulation cells (see Figure 1) maintained at 85, 75, 65 and 55°C. The specific conditions within these cells are oxidation beneath, chemical (water) from above, and the equivalent of 50 m of solid waste mobilizing compressive stress. Results have been forthcoming over the years insofar as three distinct lifetime stages; see Figure 2.

Stage A - Antioxidant Depletion Time

Stage B - Induction Time to the Onset of Degradation

Stage C - Time to Reach 50% Degradation (i.e., the Halflife)

2.1 Stage A - Antioxidant Depletion Time

The dual purposes of antioxidants are to (i) prevent polymer degradation during processing, and (ii) prevent oxidation reactions from taking place during Stage A of service life, respectively. Obviously, there can only be a given amount of antioxidants in any formulation. Once the antioxidants are depleted, additional oxygen diffusing into the geomembrane will begin to attack the polymer chains, leading to subsequent stages as shown in Figure 2. The duration of the antioxidant depletion stage depends on both the type and amount of the various antioxidants, i.e., the precise formulation.

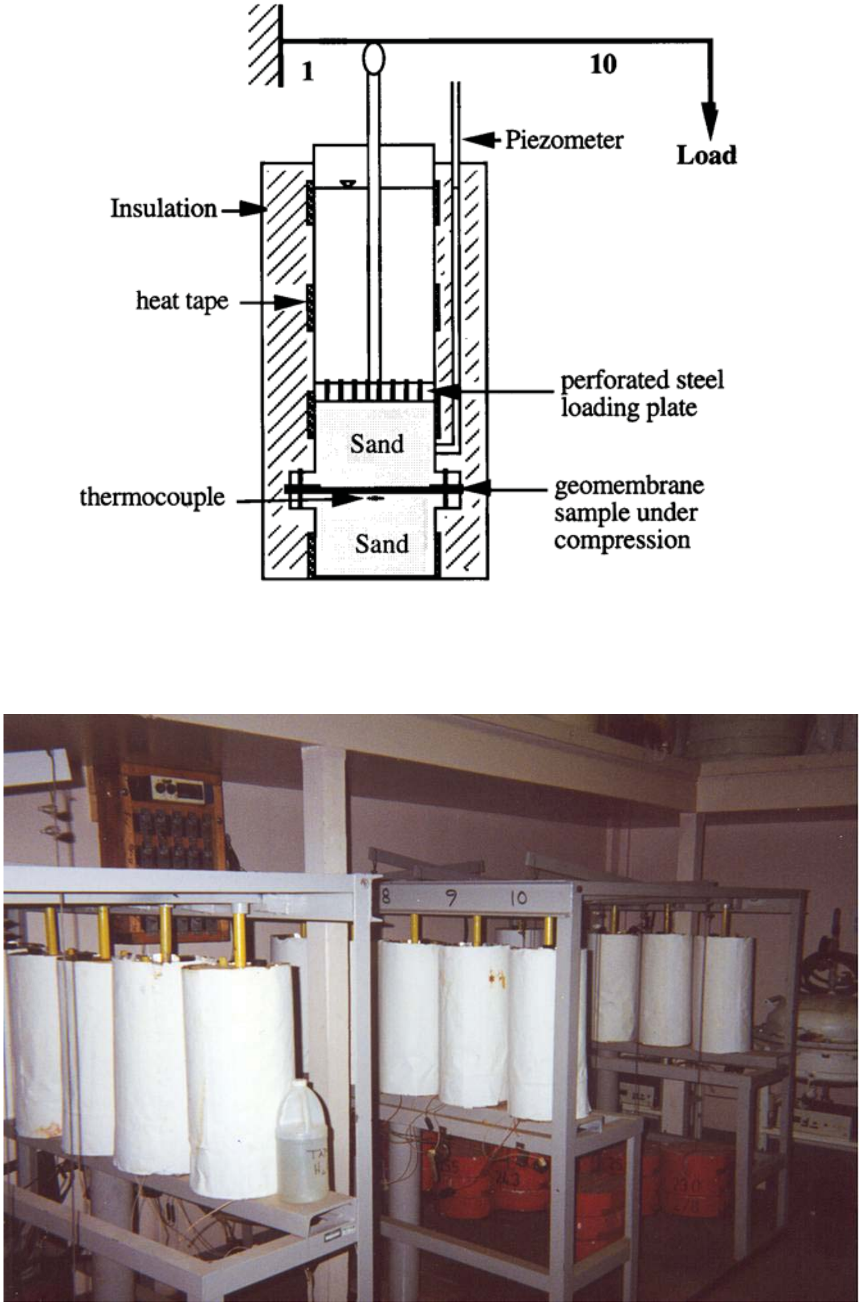

Figure 1. Incubation schematic and photograph of multiple cells maintained at various constant temperatures.

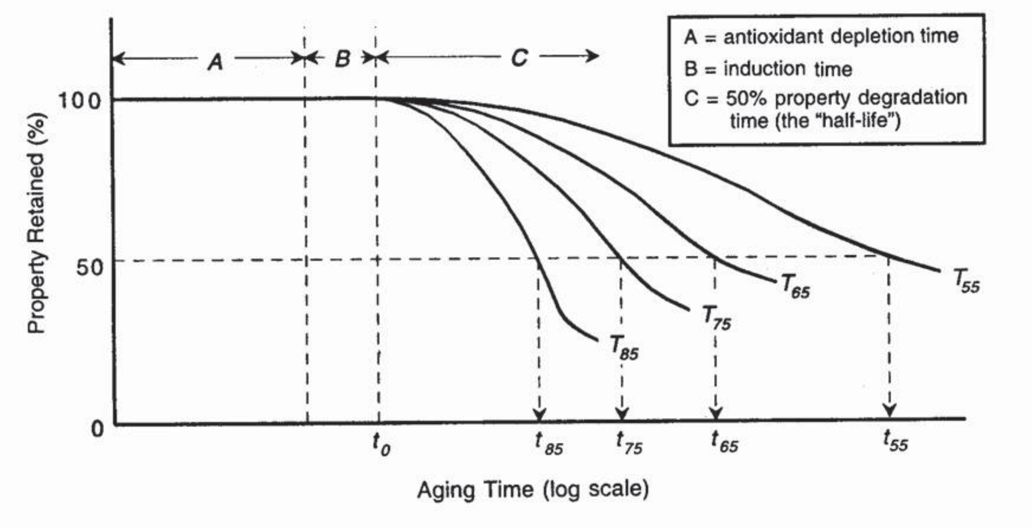

Figure 2. Three individual stages in the aging of most geomembranes.

The depletion of antioxidants is the consequence of two processes: (i) chemical reactions with the oxygen diffusing into the geomembrane, and (ii) physical loss of antioxidants from the geomembrane. The chemical process involves two main functions; the scavenging of free radicals converting them into stable molecules, and the reaction with unstable hydroperoxide (ROOH) forming a more stable substance. Regarding physical loss, the process involves the distribution of antioxidants in the geomembrane and their volatility and extractability to the site-specific environment.

Hence, the rate of depletion of antioxidants is related to the type and amount of antioxidants, the service temperature, and the nature of the site-specific environment. See Hsuan and Koerner (1998) for additional details.

2.2 Stage B - Induction Time to Onset of Degradation

In a pure polyolefin resin, i.e., one without carbon black and antioxidants, oxidation occurs extremely slowly at the beginning, often at an immeasurable rate. Eventually, oxidation occurs more rapidly. The reaction eventually decelerates and once again becomes very slow.

This progression is illustrated by the S-shaped curve of Figure 3(a). The initial portion of the curve (before measurable degradation takes place) is called the induction period (or induction time) of the polymer. In the induction period, the polymer reacts with oxygen forming hydroperoxide (ROOH), as indicated in Equations (1)-(3). However, the amount of ROOH in this stage is very small and the hydroperoxide does not further decompose into other free radicals which inhibits the onset of the acceleration stage.

In a stabilized polymer such as one with antioxidants, the accelerated oxidation stage takes an even longer time to be reached. The antioxidants create an additional depletion time stage prior to the onset of the induction time, as shown in Figure 3(b).

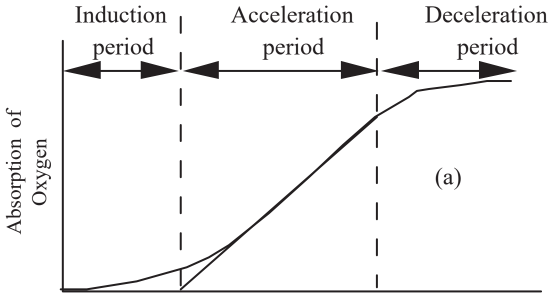

(a) Pure unstabilized polyethylene

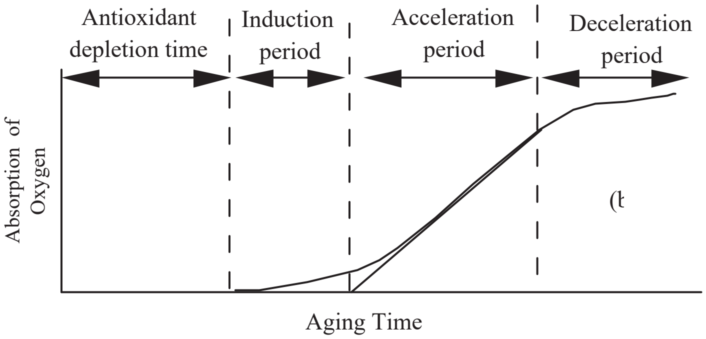

(b) Stabilized polyethylene

Figure 3. Curves illustrating various stages of oxidation.

$$RH \rightarrow R\bullet + H\bullet \qquad (1)$$

(aided by energy or catalyst residues in the polymer)

$$R\bullet + O2 \rightarrow ROO\bullet \qquad (2)$$

$$ROO\bullet + RH \rightarrow ROOH + R\bullet \qquad (3)$$

In the above, RH represents the polyethylene polymer chains; and the symbol "•" represents free radicals, which are highly reactive molecules.

2.3 Stage C - Time to Reach 50% Degradation (Halflife)

As oxidation continues, additional ROOH molecules are being formed. Once the concentration of ROOH reaches a critical level, decomposition of ROOH begins, leading to a substantial increase in the amount of free radicals, as indicated in Equations (4) to (6). The additional free radicals rapidly attack other polymer chains, resulting in an accelerated chain reaction, signifying the end of the induction period, Rapopport and Zaikov (1986). This indicates that the concentration of ROOH has a critical control on the duration of the induction period.

$$ROOH \rightarrow RO\bullet\ OH\bullet \text{ (aided by energy)} \qquad (4)$$

$$RO\bullet + RH \rightarrow ROH + R\bullet \qquad (5)$$

$$OH\bullet + RH \rightarrow H2O + R\bullet \qquad (6)$$

A series of oxidation reactions produces a substantial amount of free radical polymer chains (R•), called alkyl radicals, which can proceed to further reactions leading to either cross-linking or chain scission in the polymer. As the degradation of polymer continues, the physical and mechanical properties of the polymer start to change. The most noticeable change in physical properties is the melt index, since it relates to the molecular weight of the polymer. As for mechanical properties, both tensile break stress (strength) and break strain (elongation) decrease.

Ultimately, the degradation becomes so severe that all tensile properties start to change (tear, puncture, burst, etc.) and the engineering performance is jeopardized. This signifies the end of the so-called "service life" of the geomembrane.

Although quite arbitrary, the limit of service life of polymeric materials is often selected as a 50% reduction in a specific design property. This is commonly referred to as the halflife time, or simply the "halflife". It should be noted that even at halflife, the material still exists and can function, albeit at a decreased performance level with a factor-of-safety lower than the initial design value.

2.4 Summary of Lifetime Research-to-Date

Stage A, that of antioxidant depletion for HDPE geomembranes as required in the GRI-GM13 Specification, has been well established by our own research and corroborated by others, e.g., Sangram and Rowe (2004). The GRI data for standard and high pressure Oxidative Induction Time (OIT) is given in Table 2. The values are quite close to one another. Also, as expected, the lifetime is strongly dependent on the service temperature; with the higher the temperature the shorter the lifetime.

Table 2 - Lifetime prediction of HDPE (nonexposed) at various field temperatures

In Service Temperature (°C)	Stage "A" (years)			Stage "B" (years)	Stage "C" (years)	Total Prediction* (years)
	Standard OIT	High Press. OIT	Average OIT			
20	200	215	208	30	208	446
25	135	144	140	25	100	265
30	95	98	97	20	49	166
35	65	67	66	15	25	106
40	45	47	46	10	13	69

*Total = Stage A (average) + Stage B + Stage C

Stage "B", that of induction time, has been obtained by comparing 30-year old polyethylene water and milk containers (containing no long-term antioxidants) with currently produced containers. The data shows that degradation is just beginning to occur as evidenced by slight changes in break strength and elongation, but not in yield strength and elongation. The lifetime for this stage is also given in Table 2.

Stage “C”, the time for 50% change of mechanical properties is given in Table 2 as well. The data depends on the activation energy, or slope of the Arrhenius curve, which is very sensitive to material and experimental techniques. The data is from Gedde, et al. (1994) which is typical of the HDPE resin used for gas pipelines and is similar to Martin and Gardner (1983).

Summarizing Stages A, B, and C, it is seen in Table 2 that the halflife of covered HDPE geomembranes (formulated according to the current GRI-GM13 Specification) is estimated to be 449-years at 20°C. This, of course, brings into question the actual temperature for a covered geomembrane such as beneath a solid waste landfill. Figure 4 presents multiple thermocouple monitoring data of a municipal waste landfill liner in Pennsylvania for over 10-years, Koerner and Koerner (2005). Note that for 6-years the temperature was approximately 20°C. At that time and for the subsequent 4-years the temperature increased to approximately 30°C. Thus, the halflife of this geomembrane is predicted to be from 166 to 446 years within this temperature range. The site is still being monitored, see Koerner and Koerner (2005).

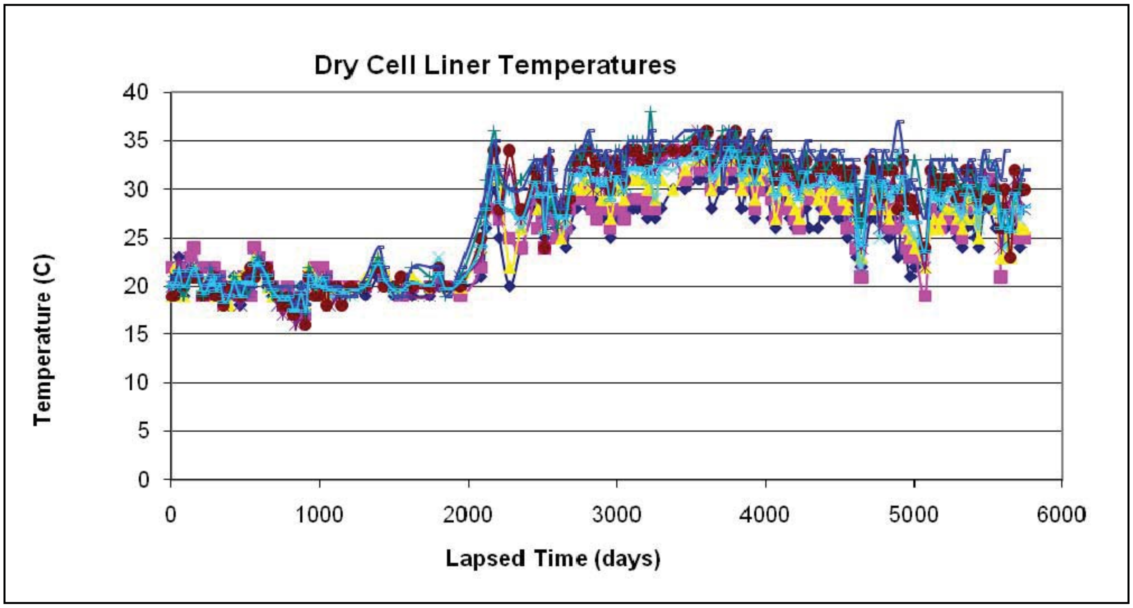

Figure 4. Long-term monitoring of an HDPE liner beneath a municipal solid waste landfill in Pennsylvania.

2.5 Lifetime of Other Covered Geomembranes

By virtue of its widespread use as liners for solid waste landfills, HDPE is by far the widest studied type of geomembrane. Note that in most countries (other than the U.S.), HDPE is the required geomembrane type for solid waste containment. Some commentary on other-than HDPE geomembranes (recall Table 1) follows:

2.5.1 Linear Low Density Polyethylene (LLDPE) geomembranes

The nature of the LLDPE resin and its formulation is very similar to HDPE. The fundamental difference is that LLDPE is a lower density, hence lower crystallinity, than HDPE; e.g., 10% versus 50%. This has the effect of allowing oxygen to diffuse into the polymer structure quicker, and likely decreases Stages A and C. How much is uncertain since no data is available, but it is felt that the lifetime of LLDPE will be somewhat reduced with respect to HDPE.

2.5.2 Plasticizer migration in PVC geomembranes

Since PVC geomembranes necessarily have plasticizers in their formulations so as to provide flexibility, the migration behavior must be addressed for this material. In PVC the plasticizer bonds to the resin and the strength of this bonding versus liquid-to-resin bonding is significant. One of the key parameters of a stable long-lasting plasticizer is its molecular weight. The higher the molecular weight of the plasticizer in a PVC formulation, the more durable will be the material. Conversely, low molecular weight plasticizers have resulted in field failures even under covered conditions. See Miller, et al. (1991), Hammon, et al. (1993), and Giroud and Tisinger (1994) for more detail in this regard. At present there is a considerable difference (and cost) between PVC geomembranes made in North America versus Europe. This will be apparent in the exposed study of durability in the second part of this White Paper.

2.5.3 Crosslinking in EPDM and CSPE geomembrnaes

The EPDM geomembranes mentioned in Table 1 are crosslinked thermoset materials. The oxidation degradation of EPDM takes place in either ethylene or propylene fraction of the co-polymer via free radical reactions, as expressed in Figure 5, which are described similarly by Equations (4) to (6).

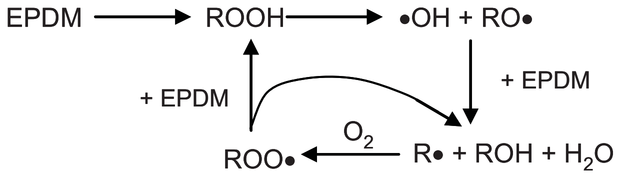

Figure 5. Oxidative degradation of crosslinked EPDM geomembranes, (Wang and Qu, 2003).

For CSPE geomembranes, the degradation mechanism is dehydrochlorination by losing chlorine and generating carbon-carbon double bonds in the main polymer chain, as shown in Figure 6.

The carbon-carbon double bonds become the preferred sites for further thermodegradation or cross-linking in the polymer, leading to eventual brittleness of the geomembrane.

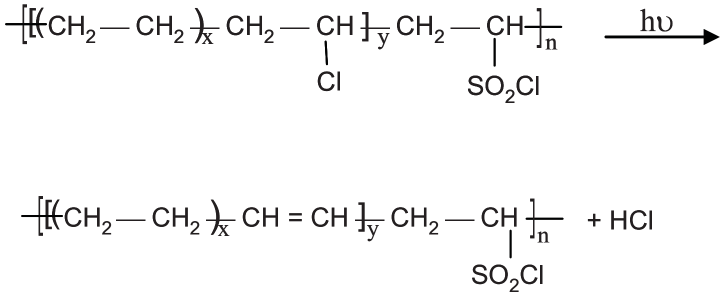

$$\left[\left[(CH_2-CH_2)_x\, CH_2-\underset{\displaystyle Cl}{\underset{|}{CH}}\right]_y CH_2-\underset{\displaystyle SO_2Cl}{\underset{|}{CH}}\right]_n \xrightarrow{h\upsilon}$$

$$\left[\left[(CH_2-CH_2)_x\, CH=CH\right]_y CH_2-\underset{\displaystyle SO_2Cl}{\underset{|}{CH}}\right]_n + HCl$$

Figure 6. Dechlorination degradation of crosslinked CSPE geomembranes (Chailan, et al., 1995).

Neither EPDM nor CSPE has had a focused laboratory study of the type described for HDPE reported in the open literature. Most of lifetime data for these geomembranes is antidotal by virtue of actual field performance. Under covered conditions, as being considered in this section, there have been no reported failures by either of these thermoset polymers to our knowledge.

3.0 Lifetime Prediction: Exposed Conditions

Lifetime prediction of exposed geomembranes have taken two very different pathways; (i) prediction from anecdotal feedback and field performance, and (ii) from laboratory weathering device predictions.

3.1 Field Performance

There is a large body of anecdotal information available on field feedback of exposed geomembranes. It comes form two quite different sources, i.e., dams in Europe and flat roofs in the USA.

Regarding exposed geomembranes in dams in Europe, the original trials were using 2.0 mm thick polyisobutylene bonded directly to the face of the dam. There were numerous problems encountered as described by Scuero (1990). Similar experiences followed using PVC geomembranes. In 1980, a geocomposite was first used at Lago Nero which had a 200 g/m^2 nonwoven geotextile bonded to the PVC geomembrane. This proved quite successful and led to the now-accepted strategy of requiring drainage behind the geomembrane. In addition to thick nonwoven geotextiles, geonets, and geonet composites have been successful. Currently over 50 concrete and masonry dams have been rehabilitated in this manner and are proving successful for over 30-years of service life. The particular type of PVC plasticized geomembranes used for these dams is proving to be quite durable. Tests by the dam owners on residual properties show only nominal changes in properties, Cazzuffi (1998). As indicated in Miller, et al. (1991) and Hammond, et al. (1993), however, different PVC materials and formulations result in very different behavior; the choice of plasticizer and the material's thickness both being of paramount importance. An excellent overview of field performance is recently available in which 250 dams which have been waterproofed by geomembranes is available from ICOLD (2010).

Regarding exposed geomembranes in flat roofs, past practice in the USA is almost all with EPDM and CSPE and, more recently, with fPP. Manufacturers of these geomembranes regularly warranty their products for 20-years and such warrants appear to be justified. EPDM and CSPE, being thermoset or elastomeric polymers, can be used in dams without the necessity of having seams by using vertical attachments spaced at 2 to 4 m centers, see Scuero and Vaschetti (1996). Conversely, fPP can be seamed by a number of thermal fusion methods. All of these geomembrane types have good conformability to rough substrates as is typical of concrete and masonry dam rehabilitation. It appears as though experiences (both positive and negative) with geomembranes in flat roofs should be transferred to all types of waterproofing in civil engineering applications.

3.2 Laboratory Weatherometer Predictions

For an accelerated simulation of direct ultraviolet light, high temperature, and moisture using a laboratory weatherometer one usually considers a worst-case situation which is the solar maximum condition. This condition consists of global, noon sunlight, on the summer solstice, at normal incidence. It should be recognized that the UV-A range is the target spectrum for a laboratory device to simulate the naturally occurring phenomenon, see Hsuan and Koerner (1993), and Suits and Hsuan (2001).

The Xenon Arc weathering device (ASTM D4355) was introduced in Germany in 1954. There are two important features; the type of filters and the irradiance settings. Using a quartz inner and borosilicate outer filter (quartz/boro) results in excessive low frequency wavelength degradation. The more common borosilicate inner and outer filters (boro/boro) shows a good correlation with solar maximum conditions, although there is an excess of energy below 300 nm wavelength. Irradiance settings are important adjustments in shifting the response although they do not eliminate the portion of the spectrum below 300 nm frequency. Nevertheless, the Xenon Arc device is commonly used method for exposed lifetime prediction of all types of geosynthetics.

UV Fluorescent devices (ASTM D7238) are an alternative type of accelerated laboratory test device which became available in the early 1970's. They reproduce the ultraviolet portion of the sunlight spectrum but not the full spectrum as in Xenon Arc weatherometers. Earlier FS-40 and UVB-313 lamps give reasonable short wavelength output in comparison to solar maximum. The UVA-340 lamp was introduced in 1987 and its response is seen to reproduce ultraviolet light quite well. This device (as well as other types of weatherometers) can handle elevated temperature and programmed moisture on the test specimens.

Research at the Geosynthetic Institute (GSI) has actively pursued both Xenon and UV Fluorescent devices on a wide range of geomembranes. Table 3 gives the geomembranes that were incubated and the number of hours of exposure as of 12 July 2005.

Table 5 - Details of the GSI laboratory exposed weatherometer study on various types of geomembranes

Geomembrane Type	Thickness (mm)	UV Fluorescent Exposure*	Xenon Exposure*	Comment
1. HDPE (GM13)	1.50	8000 hrs.	6600 hrs.	Basis of GRI-GM13 Spec
2. LLDPE (GM17)	1.00	8000	6600	Basis of GRI-GM-17 Spec
3. PVC (No. Amer.)	0.75	8000	6600	Low Mol. Wt. Plasticizer
4. PVC (Europe)	2.50	7500	6600	High Mol. Wt. Plasticizer
5. fPP (BuRec)	1.00	2745**	4416**	Field Failure at 26 mos.
6. fPP-R (Texas)	0.91	100	100	Field Failure at 8 years
7. fPP (No. Amer.)	1.00	7500	6600	Expected Good Performance

*As of 12 July 2005 exposure is ongoing
**Light time to reach halflife of break and elongation

3.3 Laboratory Weatherometer Acceleration Factors

The key to validation of any laboratory study is to correlate results to actual field performance. For the nonexposed geomembranes of Section 2 such correlations will take hundreds of years for properly formulated products. For the exposed geomembranes of Section 3, however, the lifetimes are significantly shorter and such correlations are possible. In particular, Geomembrane #5 (flexible polypropylene) of Table 3 was an admittedly poor geomembrane formulation which failed in 26 months of exposure at El Paso, Texas, USA. The reporting of this failure is available in the literature, Comer, et al. (1998). Note that for both UV Fluorescent and Xenon Arc laboratory incubation of this material, failure (halflife to 50% reduction in strength and elongation) occurred at 2745 and 4416 hours, respectively. The comparative analysis of laboratory and field for this case history allows for the obtaining of acceleration factors for the two incubation devices.

3.3.1 Comparison between field and UV Fluorescent weathering

The light source used in the UV fluorescent weathering device is UVA with wavelengths from 295-400 nm. In addition, the intensity of the radiation is controlled by the Solar Eye irradiance control system. The UV energy output throughout the test is 68.25 W/m^2.

The time of exposure to reach 50% elongation at break was as follows:

= 2745 hr. of light
= 9,882,000 seconds
Total energy in MJ/m^2 = 68.25 W/m^2 × 9,882,000
= 674.4 MJ/m^2

The field site was located at El Paso, Texas. The UVA radiation energy (295-400 nm) at this site is estimated based on data collected by the South Florida Testing Lab in Arizona (which is a similar atmospheric location). For 26 months of exposure, the accumulated UV radiation energy is 724 MJ/m^2 which is very close to that generated from the UV fluorescent weatherometer. Therefore, direct comparison of the exposure time between field and UV fluorescent is acceptable.

Field time vs. Fluorescent UV light time: **Thus, the acceleration factor is 6.8.**
= 26 Months = 3.8 Months

3.3.2 Comparison between field and Xenon Arc weathering

The light source of the Xenon Arc weathering device simulates almost the entire sunlight spectrum from 250 to 800 nm. Depending of the age of the light source and filter, the solar energy ranges from 340.2 to 695.4 W/m^2, with the average value being 517.8 W/m^2.

The time of exposure to reach 50% elongation at break

= 4416 hr. of light
= 15,897,600 seconds
Total energy in MJ/m^2 = 517.8 W/m^2 × 15,897,600
= 8232 MJ/m^2

The solar energy in the field is again estimated based on data collected by the South Florida Testing Lab in Arizona. For 26 months of exposure, the accumulated solar energy (295-800 nm) is 15,800 MJ/m^2, which is much higher than that from the UV Fluorescent device. Therefore, direct comparison of halflives obtained from the field and Xenon Arc device is not anticipated to be very accurate. However, for illustration purposes the acceleration factor based on Xenon Arc device would be as follows:

Field vs. Xenon Arc : **Thus, the acceleration factor is 4.3.**
= 26 Months = 6.1 Months

The resulting conclusion of this comparison of weathering devices is that the UV Fluorescent device is certainly reasonable to use for long-term incubations. When considering the low cost of the device, its low maintenance, its inexpensive bulbs, and ease of repair it (the UV Fluorescent device) will be used exclusively by GSI for long-term incubation studies.

3.3.3 Update of exposed lifetime predictions

There are presently (2011) four field failures of flexible polypropylene geomembranes and using unexposed archived samples from these sites their responses in laboratory UV Fluorescent devices per ASTM D7328 at 70°C are shown in Figure 5. From this information we deduce that the average correlation factor is approximately *1200 light hours ≃ one-year in a hot climate.* This value will be used accordingly for other geomembranes.

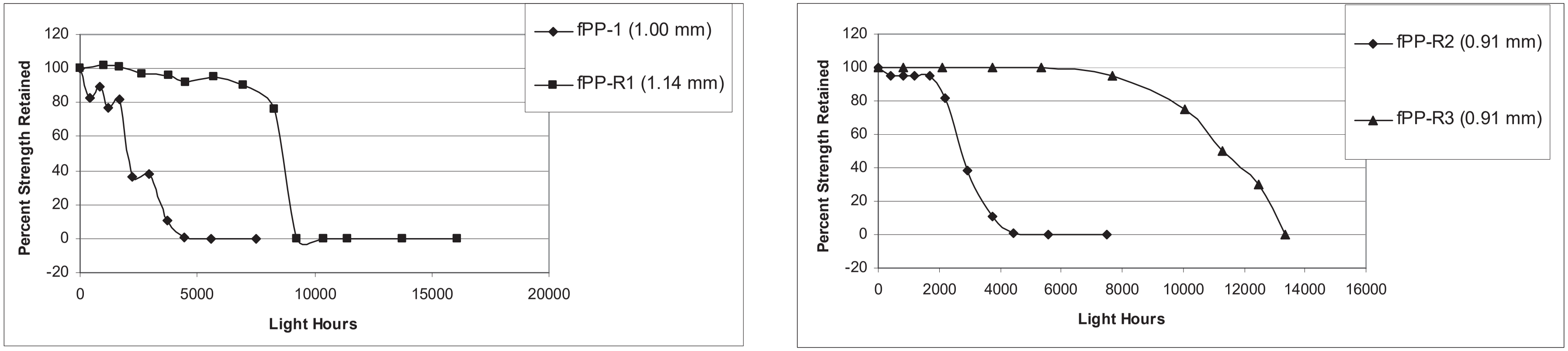

(a) Two Sites in West Texas

(b) Two Sites in So. Calif.

Lab-to-Field Correlation Factors
(ASTM D7238 @ 70°C)

Method	Thickness (mm)	Field (yrs.)	Location	Lab (lt. hr.)	Factor (lt. hrs./1.0 yr.)
fPP-1	1.00	$\simeq 2$	W. Texas	1800	900
fPP-R1	1.14	$\simeq 8$	W. Texas	8200	1025
fPP-R2	0.91	$\simeq 2$	So. Calif.	2500	1250
fPP-R3	0.91	$\simeq 8$	So. Calif.	11200	1400
					1140*

*Use 1200 lt. hr. = 1.0 year in hot climates

Figure 5. Four field failures of fPP and fPP-R exposed geomembranes.

Exposure of a number of different types of geomembranes in laboratory UV Fluorescent devices per ASTM D7238 at 70°C has been ongoing for the six years (between 2005 and 2011) since this White Paper was first released. Included are the following geomembranes:

- Two black 1.0 mm (4.0 mil) unreinforced flexible polypropylene geomembranes formulated per GRI-GM18 Specification; see Figure 6a.
- Two black unreinforced polyethylene geomembranes, one 1.5 mm (60 mil) high density per GRI-GM13 Specification and the other 1.0 mm (40 mil) linear low density per GRI-GM17 Specification; see Figure 6b.
- One 1.0 (40 mil) black ethylene polypropylene diene terpolymer geomembrane per GRI-GM21 Specification; see Figure 6c.
- Two polyvinyl chloride geomembranes, one black 1.0 mm (40 mil) formulated in North America and the other grey 1.5 mm (60 mil) formulated in Europe; see Figure 6d.

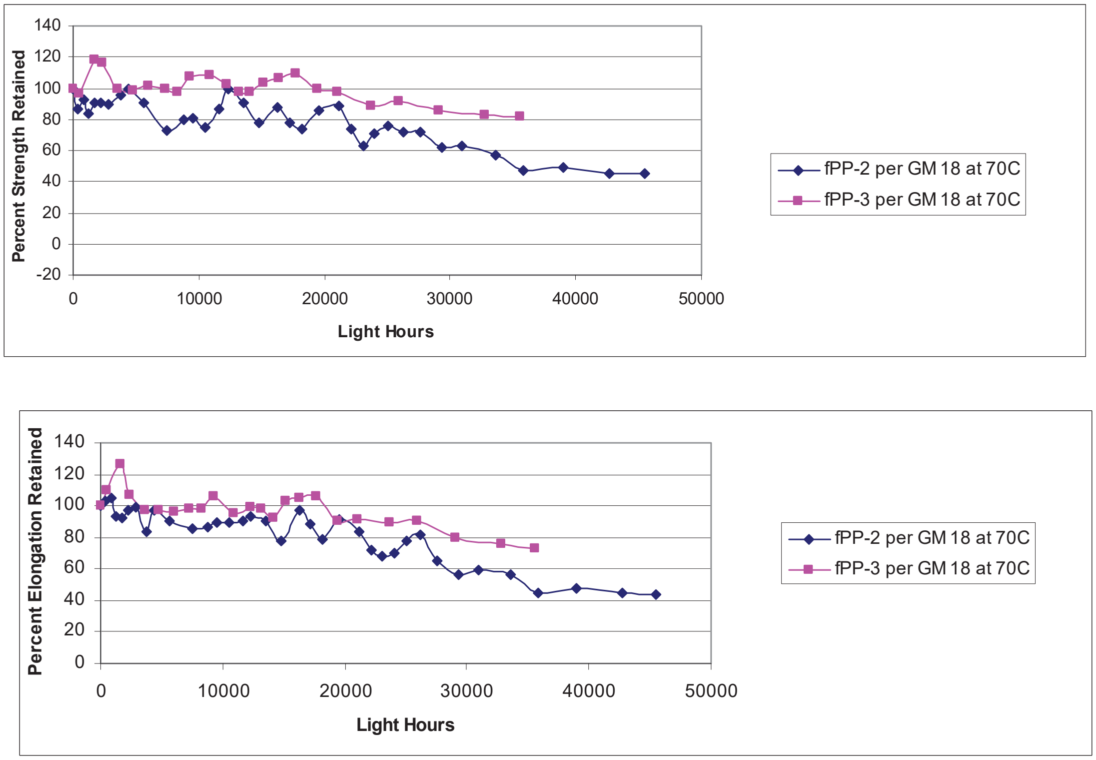

Figure 6a. Flexible polyethylene (fPP) geomembrane behavior.

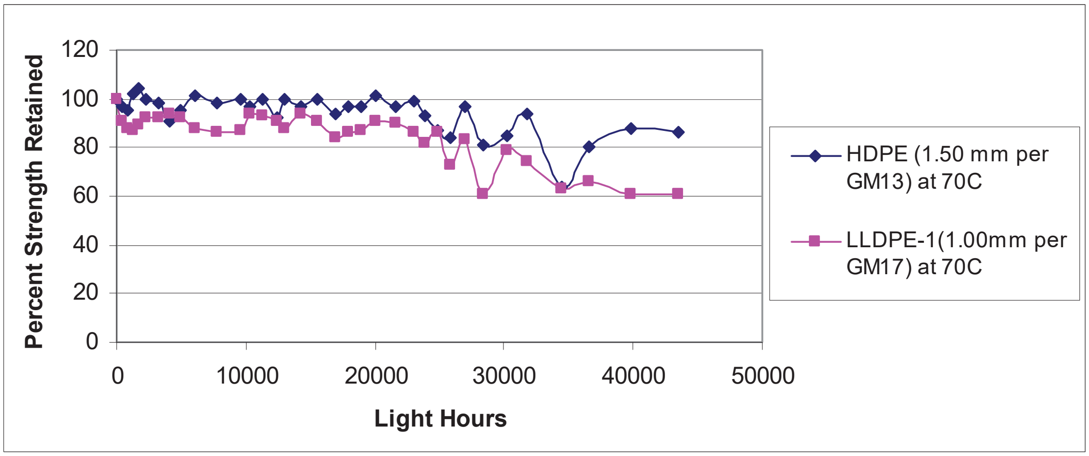

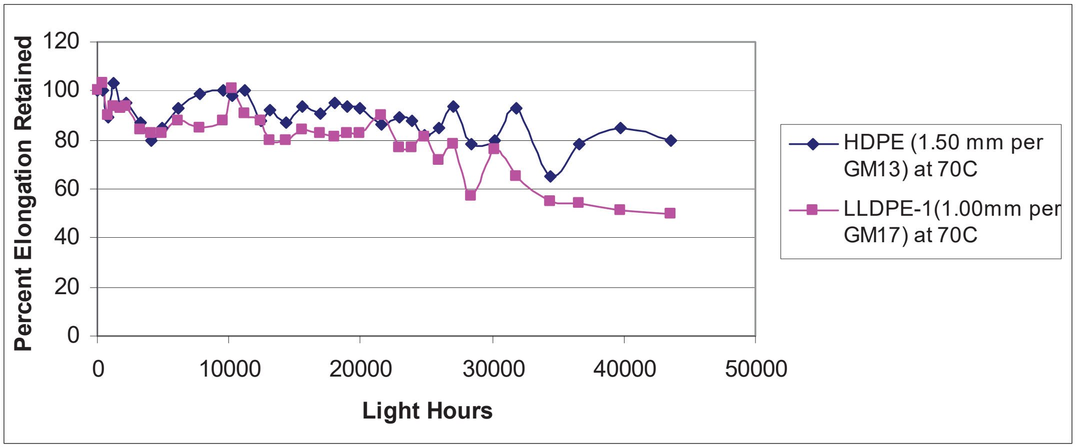

Figure 6b. Polyethylene (HDPE and LLDPE) geomembrane behavior.

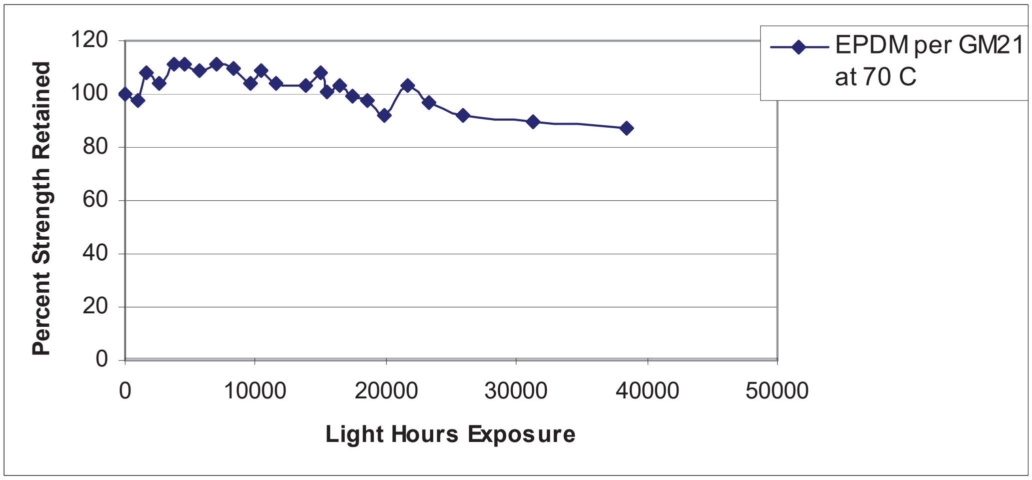

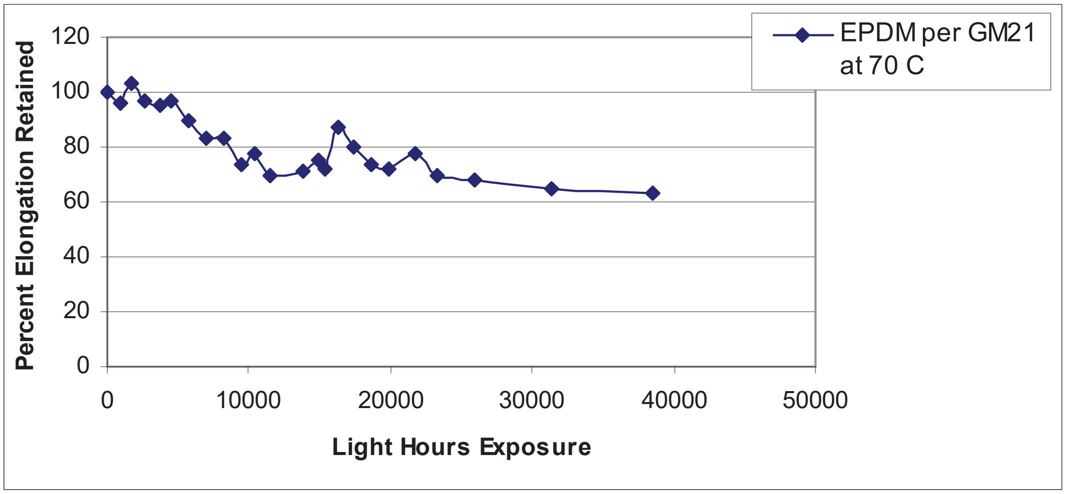

Figure 6c. Ethylene polypropylene diene terpolymer (EPDM) geomembrane.

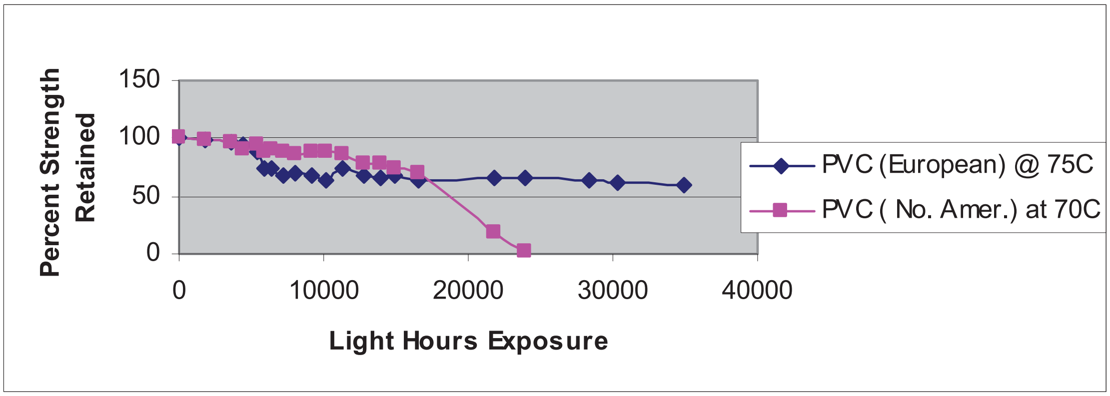

Figure 6d. Polyvinyl chloride (PVC) geomembranes.

From the response curves of the various geomembranes shown in Figure 6a-d, the 50% reduction value in strength or elongation (usually elongation) was taken as being the “halflife”. This value is customarily used by the polymer industry as being the materials lifetime prediction value. We have done likewise to develop Table 6 which is our predicted values for the designated exposed geomembrane lifetimes to date.

Table 6 – Exposed lifetime prediction results of selected geomembranes to date

Type	Specification	Prediction Lifetime in a Dry and Arid Climate
HDPE	GRI-GM13	> 36 years (ongoing)
LLDPE	GRI-GM17	≃ 36 years (halflife)
EPDM	GRI-GM21	> 27 years (ongoing)
fPP-2	GRI-GM18	≃ 30 years (halflife)
fPP-3	GRI-GM18	> 27 years (ongoing)
PVC-N.A.	(see FGI)	≃ 18 years (halflife)
PVC-Eur.	proprietary	> 32 years (ongoing)

4.0 Conclusions and Recommendations

This White Paper is bifurcated into two very different parts; covered (or buried) lifetime prediction of HDPE geomembranes and exposed (to the atmosphere) lifetime prediction of a number of geomembrane types. In the covered geomembrane study we chose the geomembrane type which has had the majority of usage, that being HDPE as typically used in waste containment applications. Invariably whether used in landfill liner or cover applications *the geomembrane is covered.* After ten-years of research Table 2 (repeated here) was developed which is the conclusion of the covered geomembrane research program. Here it is seen that HDPE decreases its predicted lifetime (as measured by its halflife) from 446-years at 20°C, to 69-years at 40°C. Other geomembrane types (LLDPE, fPP, EPDM and PVC) have had essentially no focused effort on their covered lifetime prediction of the type described herein. That said, all are candidates for additional research in this regard.

Table 2 - Lifetime prediction of HDPE (nonexposed) at various field temperatures

In Service Temperature (°C)	Stage "A" (years)			Stage "B" (years)	Stage "C" (years)	Total Prediction* (years)
	Standard OIT	High Press. OIT	Average OIT			
20	200	215	208	30	208	446
25	135	144	140	25	100	265
30	95	98	97	20	49	166
35	65	67	66	15	25	106
40	45	47	46	10	13	69

*Total = Stage A (average) + Stage B + Stage C

Exposed geomembrane lifetime was addressed from the perspective of field performance which is very unequivocal. Experience in Europe, mainly with relatively thick PVC containing high molecular weight plasticizers, has given 25-years of service and the geomembranes are still in use. Experience in the USA with exposed geomembranes on flat roofs, mainly with EPDM and CSPE, has given 20^+-years of service. The newest geomembrane type in such applications is fPP which currently carries similar warranties.

Rather than using the intricate laboratory setups of Figure 1 which are necessary for covered geomembranes, exposed geomembrane lifetime can be addressed by using accelerating laboratory weathering devices. Here it was shown that the UV fluorescent device (per ASTM D7238 settings) versus the Xenon Arc device (per ASTM D 4355) is equally if not slightly more intense in its degradation capabilities. As a result, all further incubation has been using the UV fluorescent devices per D7238 at 70°C.

Archived flexible polypropylene geomembranes at four field failure sites resulted in a correlation factor of 1200 light hours equaling one-year performance in a hot climate. Using this value on the incubation behavior of seven commonly used geomembranes has resulted in the following conclusions (recall Figure 6 and Table 6);

- HDPE geomembranes (per GRI-GM13) are predicted to have lifetimes greater than 36-years; testing is ongoing.
- LLDPE geomembranes (per GRI-GM17) are predicted to have lifetimes of approximately 36-years.
- EPDM geomembranes (per GRI-GM21) are predicted to have lifetimes of greater than 27-years; testing is ongoing.
- fPP geomembranes (per GRI-GM18) are predicted to have lifetimes of approximately 30-years.
- PVC geomembranes are very dependent on their plascitizer types and amounts, and probably thicknesses as well. The North American formulation has a lifetime of approximately 18-years, while the European formulation is still ongoing after 32-years.

Regarding continued and future recommendations with respect to lifetime prediction, GSI is currently providing the following:

(i) Continuing the exposed lifetime incubations of HDPE, EPDM and PVC (European) geomembranes at 70°C.

(ii) Beginning the exposed lifetime incubations of HDPE, LLDPE, fPP, EPDM and both PVC's at 60°C and 80°C incubations.

(iii) With data from these three incubation temperatures (60, 70 and 80°C), time-temperature-superposition plots followed by Arrhenius modeling will eventually provide information such as Table 2 for covered geomembranes. This is our ultimate goal.

(iv) Parallel lifetime studies are ongoing at GSI for four types of geogrids and three types of turf reinforcement mats at 60, 70 and 80°C.

(v) GSI does not plan to duplicate the covered geomembrane study to other than the HDPE provided herein. In this regard, the time and expense that would be necessary is prohibitive.

(vi) The above said, GSI is always interested in field lifetime behavior of geomembranes (and other geosynthetics as well) whether covered or exposed.

Acknowledgements

The financial assistance of the U. S. Environmental Protection Agency for the covered HDPE lifetime study and the member organizations of the Geosynthetic Institute and its related institutes for research, information, education, accreditation and certification is sincerely appreciated. Their identification and contact member information is available on the Institute's web site at <<geosynthetic-institute.org>>.

References

Cazzuffi, D., "Long-Term Performance of Exposed Geomembranes on Dams in the Italian Alps," Proc. 6th Intl. Conf. on Geosynthetics, IFAI, 1998, pp. 1107-1114.

Chailan, J.-F., Boiteux, C., Chauchard, J., Pinel, B. and Seytre, G., "Effect of Thermal Degradation on the Viscoelastic and Dielectric Properties of Chlorosulfonated Polyethylene (CSPE) Compounds," Journal of Polymer Degradation and Stability, Vol. 48, 1995, pp. 61-65.

Comer, A. I., Hsuan, Y. G. and Konrath, L., "The Performance of Flexible Polypropylene Geomembranes in Covered and Exposed Environments," 6th International Conference on Geosynthetics, Atlanta, Georgia, USA, March, 1998, pp. 359-364.

Gedde, U. W., Viebke, J., Leijstrom, H. and Ifwarson, M., "Long-Term Properties of Hot-Water Polyolefin Pipes - A Review," Polymer Engineering and Science, Vol. 34, No. 24, 1994, pp. 1773-1787.

Giroud, J.-P. and Tisinger, L. G., "The Influence of Plasticizers on the Performance of PVC Geomembranes," PVC GRI-17 Conference, IFAI, Roseville, MN, 1994, pp. 169-196.

Hammon, M., Hsuan, G., Levin, S. B. and Mackey, R. E., "The Re-examination of a Nine-Year-Old PVC Geomembrane Used in a Top Cap Application," 31st Annual SWANA Conference, San Jose, CA, 1993, pp. 93-108.

Hsuan, Y. G. and Guan, Z., “Evaluation of the Oxidation Behavior of Polyethylene Geomembranes Using Oxidative Induction Time Tests,” ASTM STP 1326, Riga and Patterson, Eds., ASTM, 1997, pp. 138-149.

Hsuan, Y. G. and Koerner, R. M., “Can Outdoor Degradation be Predicted by Laboratory Acceleration Weathering?,” GFR, November, 1993, pp. 12-16.

Hsuan, Y. G. and Koerner, R. M., “Antioxidant Depletion Lifetime in High Density Polyethylene Geomembranes,” Jour. Geotech. and Geoenviron. Engr., ASCE, Vol. 124, No. 6, 1998, pp. 532-541.

ICOLD (2010), “Geomembrane Sealing Systems for Dams: Design Principles and Return of Experience,” Intl. Committee on Large Dams, Bulletin 135, Paris, France.

Koerner, G. R. and Koerner. R. M., “In-Situ Temperature Monitoring of Geomembranes,” Proc. GRI-18 Conf. at GeoFrontiers, Austin, TX, 2005, 6 pgs.

Martin, J. R. and Gardner, R. J. (1983), “Use of Plastics in Corrosion Resistant Instrumentation,” 1983 Plastics Seminar, NACE, October 24-27.

Miller, L. V., Koerner, R. M., Dewyea, J. and Mackey, R. E., “Evaluation of a 30 mil PVC Liner and Leachate Collection System,” Proc. 29th Annual GRCDA/SWANA Conf., Cincinnati, OH, 1991.

Müeller, W. and Jakob, I., “Oxidative Resistance of High-Density Polyethylene Geomembranes,” Jour. Polymer Degradation and Stability,” Elsevier Publ. Co., No. 79, 2003, pp. 161-172.

Rapoport, N. Y. and Zaikov, G. E., “Kinetics and Mechanisms of the Oxidation of Stressed Polymer,” Developments in Polymer Stabilization—4, G. Scott, Ed., Applied Science Publishers Ltd., London, U.K., 1986, pp. 207-258.

Sangam, H. P. and Rowe, R. K., “Effects of Exposure Conditions on the Depletion of Antioxidants from HDPE Geomembranes”, Canadian Geotechnical Journal, Vol. 39, 2002, pp. 1221-1230.

Scuero, A., “The Use of Geocomposites for the Rehabilitation of Concrete Dams,” Proc. 4th Intl. Conf. on Geosynthetics, The Hague, Balkema Publ. Co., 1990, pg. 474.

Scuero, A. M. and Vaschetti, G. L., “Geomembranes for Masonry and Concrete Dams: State-of-the-Art Report,” Proc. Geosynthetics Applications, Design and Construction, M. B. deGroot, et al., Eds., A. A. Balkema, 1996, pp. 889-898.

Suits, L. D. and Hsuan, Y. G., “Assessing the Photo Degradation of Geosynthetics by Outdoor Exposure and Laboratory Weatherometers,” Proc. GRI-15 Conference, Hot Topics in Geosynthetics II, GII Publ., Folsom, PA, 2001, pp. 267-279.

Wang, W. and Qu, B., “Photo and Thermo-Oxidative Degradation of Photocrosslinked Ethylene-Propylene-Diene Terpolymer,” Journal of Polymer Degradation and Stability, Vol. 81, 2003, pp. 531-537.

Geosynthetic Institute
475 Kedron Avenue
Folsom, PA 19033-1208 USA
TEL (610) 522-8440
FAX (610) 522-8441

GSI White Paper #28

"Cold Temperature and Free-Thaw Cycling Behavior of Geomembranes and Their Seams"

by

Y. (Grace) Hsuan, Ph.D.
Professor of Civil, Architectural and
Environmental Engineering
Drexel University
215-895-2785
ghsuan@coe.drexel.edu

Robert M. Koerner, Ph.D., P.E., NAE
Director Emeritus – Geosynthetic Institute
Director Emeritus – Geosynthetic Institute
610-522-8440
robert.koerner@coe.drexel.edu

Alice I. Comer, P.E.
Project Manager
Formally With U. S. Bureau of Reclamation
Denver, Colorado

June 17, 2013

"Cold Temperature and Free-Thaw Cycling Behavior of Geomembranes and Their Seams"

Introduction

It is common knowledge that materials in general, and polymeric materials in particular, will somewhat soften and increase in flexibility under high temperatures and will conversely somewhat harden and decrease in flexibility under cold temperatures. While there are indeed circumstances where high ambient temperatures are important, this white paper focuses entirely on cold ambient temperatures. Even further, it addresses cold temperature behavior of the various geomembranes by themselves and, most importantly, the freeze-thaw cycling behavior of a large number of geomembrane sheets and their seams.

The stimulus for writing the white paper is the myriad questions that regularly come to GSI as to the potential negative effects on the tensile strength of geomembranes and their seams under cold temperature and cyclic freeze-thaw field conditions. As will be seen, the primary source for the information to be presented herein is a joint U.S. EPA/U.S. BuRec study conducted by Alice Comer and Grace Hsuan in 1996. Other companion technical information will also be presented.

Cold Temperature Behavior of Geomembranes

A report by Thornton and Blackall (1976) appears to be the first in describing Canadian experiences with geomembranes in cold regions. Subsequently, Rollin, et al. (1984) conducted a laboratory study on 21 types of geomembranes at temperatures down to - 35°C. They found increasing tensile strength with decreasing temperature. Richards, et al. (1985) did similar studies which also resulted in an increase in strength and a decrease in elongation with decreasing temperatures. They evaluated PVC, CPE and HDPE geomembranes and presented the stress-versus-strain curves at +23°C, -7°C and -26°C temperatures; see Figures 1a, 1b, and

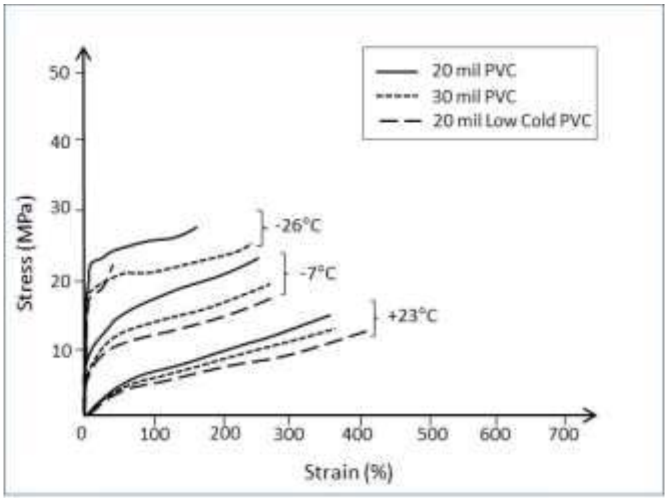

(a) Tensile test results for PVC geomembranes

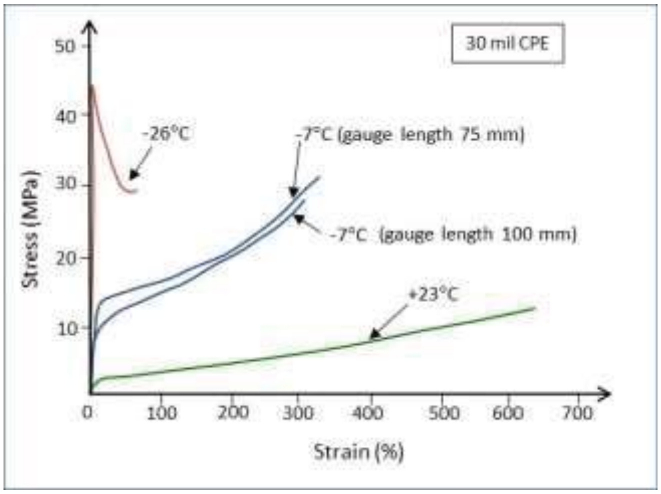

(b) Tensile test results for CPE geomembranes

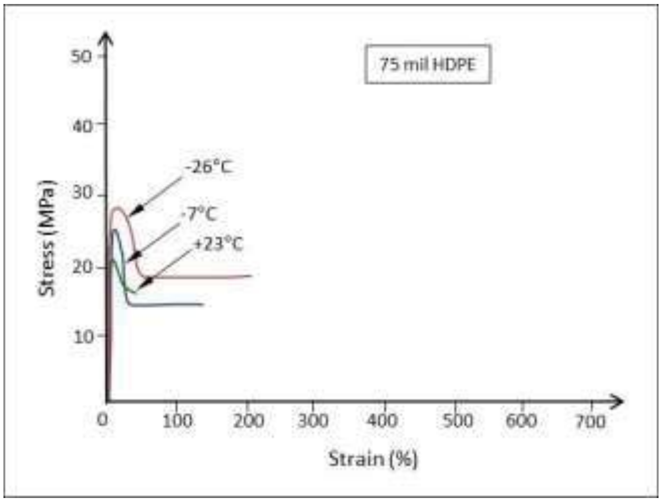

(c) Tensile test results for HDPE geomembranes

Figure 1 – Stress-versus-strain behavior of three geomembrane types under progressively colder testing environments, Richards, et al. (1985)

1c. Here one can readily observe how the sets of curves transition from relatively ductile behavior at +23°C, to relatively brittle behavior at -26°C, with the intermediate behavior at -7°C. There are a few outliers, but the trends are undeniable. This general behavior was confirmed by Peggs, et al. (1990) and Giroud, et al. (1993), the latter working with both smooth and textured HDPE geomembranes.

While this type of thermal behavior is of interest, such information for a specific type of geomembrane must be obtained by performing or commissioning individual tests so as to obtain actual design information. Such individual testing is required due to the uniqueness of each polymer type and its specific formulation. Additives such as plasticizers, fillers, antioxidants, carbon black, colorants, etc., can influence the results to varying degrees. Even the resins themselves have behavioral differences at different temperatures. For example, the glass transition temperature of propylene is -7°C, below which the polymer is glassy and above which it is characterized as rubbery. In such a case the tensile properties are greatly influenced, as well as the material's creep and stress relaxation behavior.

There are other aspects of cold temperatures on geomembranes that go beyond the scope of this white paper. In particular are cases of impact shuttering failures in cold climates and installation concerns such as frozen subgrade, bridging, snow and ice removal and worker discomfort, Burns, et al. (1990).

Freeze-Thaw Cycling of Geomembrane Sheets and Seams

Budiman (1994) reported on both cold temperature behavior but also appears to be the first to include freeze-thaw cycling for up to 150 repetitions. He focused entirely on HDPE sheet (of different thicknesses) but not on seams. There was no degradation observed during his tests but he suggested that more cycles would be appropriate. At approximately the same time a much larger freeze-thaw study was ongoing. The final report by Comer and Hsuan was released by the U.S. Bureau of Reclamation in 1996. Related papers leading up to this final report are Hsuan, et al. (1993), Comer, et al. (1995), and Hsuan, et al. (1997). Their combined study involved 19 different geomembrane sheet materials and 31 different seam types. Furthermore, seven different resin types were evaluated. The resin types were the following:

- polyvinyl chloride (PVC)
- linear low density polyethylene (LLDPE)
- high density polyethylene (HDPE)
- flexible polypropylene (fPP)
- chlorosulfonated polyethylene (CSPE)
- fully crosslinked elastomeric alloy (FCEA)

All except FCEA are currently available, however, changes in additives and formulations have occurred and will likely to do so in the future. The entire study was conducted in four discrete parts although the fourth part was focused on induced tensile stress and stress relaxation and is not the specific purpose of this white paper. See Table 1 for the relevant three parts of their study.

Table 1 – Experimental Design of Different Parts of Comer and Hsuan (1996) Study

Part	Cyclic Temperature Range	Maximum Cycles	Incubation Condition	Tensile Test Temperature
I	+20°C to -20°C	200	relaxed	+20°C
II	+20°C to -20°C	200	relaxed	-20°C
III	+30°C to -20°C	500	constrained	+20°C

Part I consisted of 19 sheet materials and 27 seams. They underwent freeze-thaw cycles at +20°C for 8 hours and then -20°C for 16 hours. Tensile tests were then conducted at +20°C after 1, 5, 10, 20 50, 100 and 200 cycles.

Part II consisted of 6 sheet materials and 13 seams. They also underwent freeze-thaw cycling at +20°C for 8 hours and then -20°C for 16 hours. Different in this regard was that tensile tests were then conducted at -20°C after 1, 5, 10, 20, 50, 100 and 200 cycles. The -20°C tests were conducted in an environmental chamber (both specimens and their grips) cooled by liquid nitrogen and set at -20°C temperature.

Part III consisted of the same set of 19 sheet materials and 27 seams as in Part I but were now tensioned at a constant strain during the freeze-thaw cycling. The rack used for the tensioning is shown in Figure 2a and the assembly within the environmental chamber is shown in Figure 2b. After the targeted number of freeze-thaw cycles at +20°C for 8 hours and -20°C for 16 hours, specimens were removed and tested at +20°C after 1, 10, 50, 100, 200 and 500 cycles.

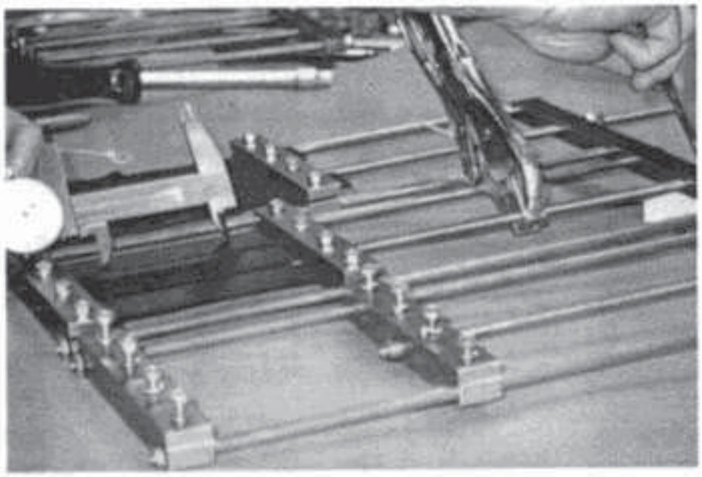

(a) Method of applying tensile load to test specimens in Part III tests

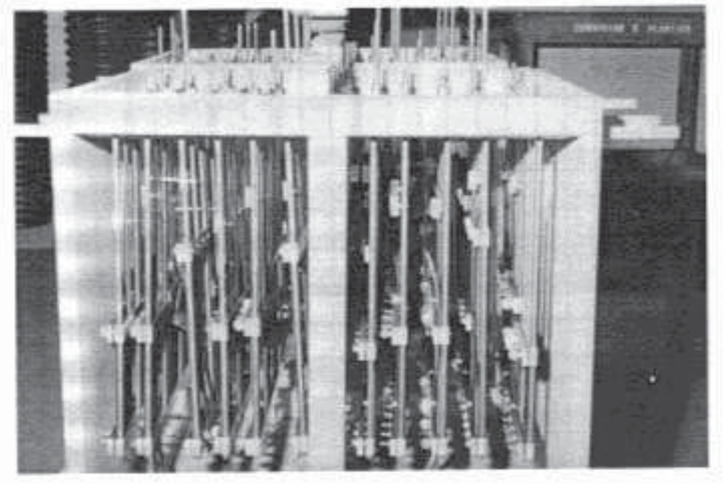

(b) Geomembrane racks in holding frame used in Part III series

Figure 2 – Method used for tensioning samples during incubation; Comer and Hsuan (1996)

Rather than showing the graphic results of the above freeze-thaw cycling study (it is available in full in the Comer and Hsuan report by the Bureau of Reclamation and the related papers by these authors) only the concluding comments will be reproduced here. They follow verbatim from the report.

<u>Part I – Results on 200 Freeze-Thaw Cycles Tested at +20°C</u>

- Tensile tests on geomembrane sheets: "The results show no change in either the peak strength or peak elongation of any of the tested materials".
- Shear tests on the geomembrane seams: "The results show no change in shear strength of any of the tested seam materials".
- Peel tests on the geomembrane seams: "The results show no change in peel strength of any of the tested seam materials.

Part II – Results on 200 Freeze-Thaw Cycles Tested at -20°C

- Tensile tests on geomembrane sheets: "The results show no change in either the peak strength or peak elongation of any of the tested materials".
- Shear tests on the geomembrane seams: "The results show no change in shear strength of any of the tested seam materials".
- Peel tests on the geomembrane seams: "The results show no change in peel strength of any of the tested seam materials.

Part III – Results on 500 Freeze-Thaw Cycles Tested at +20°C in a Constrained Condition

- Tensile tests on geomembrane sheets: "The results show no change in either the peak strength or peak elongation of any of the tested materials".
- Shear tests on the geomembrane seams: "The results show no change in shear strength of any of the tested seam materials".
- Peel tests on the geomembrane seams: "The results show no change in peel strength of any of the tested seam materials.

Conclusion and Recommendations

This two-part white paper focused initially on the cold temperature tensile behavior of the stress- versus-strain curves of several different types of geomembranes. As expected, the colder the temperature the more brittle, hence less ductile, were the response curves. Geomembranes made from PVC, CPE and HDPE were illustrated in this regard. The recommendation reached for this part of the white paper is that if a formulation-specific geomembrane under site-specific conditions is to be evaluated for its stress-versus-strain response, actual tests must be commissioned accordingly. The literature can only give general trends in this regard.

The second (and more important) part of this white paper focused entirely on freeze-thaw behavior of geomembranes and their different seam types. The U.S. Bureau of Reclamation report is extremely revealing in this regard. *The conclusion that the authors reached is that there is simply "no change" in tensile behavior of geomembrane sheets or their seams after freeze-thaw cycling.* It is felt that this conclusion in the context of their study is so impressive that it has essentially "closed the door" to further research on this specific topic. The essential question often raised in this regard, i.e., "will freeze-thaw conditions affect geomembrane sheets or their seam behavior," is answered with a resounding "NO".

References

Budiman, J. (1994), "Effects of Temperature on Physical Behavior of Geomembranes," Proc. 5th Intl. Conf. on Geosynthetics, Singapore, SEAC-IGS Publication, pp. 1093-1100.

Burns, D. E. and Pierce, S. V. (1990), "Technical Note on Cold Weather Installation of HDPE," Jour. Geotextiles and Geomembranes, Vol. 9, Nos. 4-6, pp. 457-459.

Comer, A. I. and Hsuan, Y. G. (1996), "Freeze-Thaw Cycling and Cold Temperature Effects on Geomembrane Sheets and Seams," U. S. Bureau of Reclamation Report R-96-03, March, 136 pgs.

Comer, A. I., Sculli, M. L. and Hsuan, Y. G. (1995), "Effects of Freeze-Thaw Cycling on Geomembrane Sheets and Their Seams," Proc. of Geosynthetics '95, Nashville, TN, pp. 853-866.

Giroud, J. P., Soderman, K. L. and Monroe, M. (1993), "Mechanical Design of Geomembrane Applications," Proc. of Geosynthetics '93, Vancouver, Canada, pp. 1455-1468.

Hsuan, Y. G., Sculli, M. L. and Comer, A. I. (1997), "Effects of Freeze-Thaw Cycling on Geomembranes Sheets and Their Seams – Part II Cold Temperature Tensile Behavior and

Thermal Induced Cyclic Stress," Geosynthetics '97 Conference Proceedings, Long Beach, CA, published by IFAI, pp. 201-216.

Hsuan, Y. G., Sculli, M. L. and Koerner, R. M. (1993), "Effects of Freeze-Thaw Cycling on Geomembranes and Their Seams," Proc. GRI-7 Conference on Geosynthetic Liner Systems: Innovations, Concerns and Designs, IFAI, Rosewell, IN, pp. 209-224.

Koerner, R. M. (20120, Designing With Geosynthetics, 6th Edition, Xlibris Publ. Co., 914 pgs.

Lord, Jr., A.E., Soong, T. Y. and Koerner, R. M. (1995), "Relaxation Behavior of Thermally-Induced Stress in HDPE Geomembranes," Geosynthetics International, Vol. 2, No. 3, pp. 626-634.

Peggs, I. D., Carlson, D. S. and Peggs, S. J. (1990), "Understanding and Preventing 'Shattering' Failures of Polyethylene Geomembranes," Geotextiles, Geomembranes and Related Products, Rotterdam, Balkema.

Richards, E. A., Scott, J. D. and Chalaturnyk (1985), "Cold Temperature Properties of Geomembranes," Proc. 2nd Conf. on Geotextiles and Geomembranes, Canadian Geotechnical Society, Edmonton, Alberta, pp. 121-132.

Rollin, A. L., Lafleur, J., Marcotte, M., Dascal, O. and Akber, Z. (1984), "Selection Criteria for the Use of Geomembranes in Dams and Dykes in Northern Climate," Proc. of the Intl. Conf. on Geomembranes, Denver, CO, pp. 493-499.

Thornton, D. E. and Blackall, P. (1976), "Field Evaluation of Plastic Film Liners for Petroleum Storage Areas in the Mackenzie Delta," Canadian Environmental Protection Service, Economic and Technical Review Report EPA-3-76-13.

CHEMICAL COMPATIBILITY OF POLY-FLEX LINERS

Chemical compatibility or resistance as applied to geomembranes is a relative term. Actually compatibility would mean that one material will dissolve in the other such as alcohol in water or grease in gasoline. An example of incompatibility would be oil and water. In liners it is undesirable to have the chemicals dissolve in the liner hence the term compatibility is the reverse of what is normally meant in the chemical industry. In the strictest sense and from a laboratory prospective, chemical compatibility, as the term applies to this industry, would imply that the chemical has no effect on the liner. On the other hand, from an engineering prospective, chemical compatibility means that a liner will survive the exposure to a given chemical even though the chemical could have some effect on the performance of the liner, but not enough to cause failure. Therefore, one must understand and define chemical compatibility for a specific project.

Generally polyethylene will be effected by chemicals in one of three ways.

1. No effect—This means that the chemical in question and the polyethylene do not interact. The polyethylene does not gain (lose) weight, swell, and the physical properties are not significantly altered.
2. Oxidizes (cross linking)—Chemicals classed as oxidizing agents will cause the polyethylene molecules to cross link and cause irreversible changes to the physical properties of the liner. Basically it makes the liner brittle.
3. Plasticizes—Chemicals in this classification are soluble in the polyethylene structure. They do not change the structure of the polyethylene itself but will act as a plasticizer. In doing so, the liner will experience weight gain of 3-15%, may swell by up to 10%, and will have measurable changes in physical properties (i.e. the tensile strength at yield may decrease by up to 20%). Even under these conditions the liner will maintain its integrity and will not be breached by liquids, provided the liner has not been subjected to any stress. These effects are reversible once the chemicals are removed and the liner has time to dry out.

Aside from the effect that chemicals have on a liner is the issue of vapor permeation through the liner. Vapor permeation is molecular diffusion of chemicals through the liner. Vapor transmission for a given chemical is dependent primarily on liner type, contact time, chemical solubility, temperature, thickness, and concentration gradient, but not on hydraulic head or pressure. Transmission through the liner can occur in as little as 1-2 days. Normally, a small amount of chemical is transmitted. Generally HDPE has the lowest permeation rate of the liners that are commercially available.

As stated above chemical compatibility is a relative term. For example, the use of HDPE as a primary containment of chlorinated hydrocarbons at a concentration of 100% may not be recommended, but it may be acceptable at 0.1% concentration for a limited time period or may be acceptable for secondary containment. Factors that go into assessment of chemical compatibility are type of chemical(s), concentration, temperature and the type of application. No hard and fast rules are available to make decisions on chemical compatibility. Even the EPA 9090 test is just a method to generate data so that an opinion on chemical compatibility can be more reliably reached.

A simplified table on chemical resistance is provided to act as a screening process for chemical containment applications.

Poly-Flex, Inc. • 2000 W. Marshall Dr. • Grand Prairie, TX 75051 U.S.A. • 888-765-9359

CHEMICAL RESISTANCE INFORMATION

CHEMICAL CLASS	CHEMICAL EFFECT	PRIMARY CONTAINMENT (LONG TERM CONTACT) HDPE	PRIMARY CONTAINMENT (LONG TERM CONTACT) LLDPE	SECONDARY CONTAINMENT (SHORT TERM CONTACT) HDPE	SECONDARY CONTAINMENT (SHORT TERM CONTACT) LLDPE
CARBOXYLIC ACID	1				
- Unsubstituted (e.g. Acetic acid)		B	C	A	C
- Substituted (e.g. Lactic acid)		A	B	A	A
- Aromatic (e.g. Benzoic acid)		A	B	A	A
ALDEHYDES	3				
- Aliphatic (e.g. Acetaldehyde)		B	C	B	C
- Hetrocyclic (e.g. Furfural)		C	C	B	C
AMINE	3				
- Primary (e.g. Ethylamine)		B	C	B	C
- Secondary (e.g. Diethylamine)		C	C	B	C
- Aromatic (e.g. Aniline)		B	C	B	C
CYANIDES (e.g. Sodium Cyanide)	1	A	A	A	A
ESTER (e.g. Ethyl acetate)	3	B	C	B	C
ETHER (e.g. Ethyl ether)		C	C	B	C
HYDROCARBONS	3				
- Aliphatic (e.g. Hexane)		C	C	B	C
- Aromatic (e.g. Benzene)		C	C	B	C
- Mixed (e.g. Crude oil)		C	C	B	C
HALOGENATED HYDROCARBONS	3				
- Aliphatic (e.g. Dichloroethane) +A4		C	C	B	C
- Aromatic (e.g. Chlorobenzene)		C	C	B	C
ALCOHOLS	1				
- Aliphatic (e.g. Ethyl alcohol)		A	A	A	A
- Aromatic (e.g. Phenol)		A	C	A	B
INORGANIC ACID					
- Non-Oxidizers (e.g. Hydrocloric acid)	1	A	A	A	A
- Oxidizers (e.g. Nitric Acid)	2	C	C	B	C
INORGANIC BASES (e.g. Sodium hydroxide)	1	A	A	A	A
SALTS (e.g. Calcium chloride)	1	A	A	A	A
METALS (e.g. Cadmium)	1	A	A	A	A
KETONES (e.g. Methyl ethyl ketone)	3	C	C	B	C
OXIDIZERS (e.g. Hydrogen Peroxide)	2	C	C	C	C

Chemical effect (see discussion on Chemical Resistance)

1. No Effect--Most chemicals of this class have no or minor effect.
2. Oxidizer--Chemicals of this class will cause irreversible degradaton.

3. Plasticizer--Chemicals of this class will cause a reversible change in physical properties.

Chart Rating

A. Most chemicals of this class have little or no effect on the liner.
   Recommended regardless of concentration or temperature (below 150° F).

B. Chemicals of this class will effect the liner to various degrees.
   Recommendations are based on the specific chemical, concentration and temperature.
   Consult with Poly-Flex, Inc.

C. Chemicals of this class at high concentrations will have significant effect on the physical properties of the liner.
   Generally not recommended but may be acceptable at low concentrations and with special design considerations.
   Consult with Poly-Flex, Inc.

This data is provided for informational purposes only and is not intended as a warranty or guarantee. Poly-Flex, Inc. assumes no responsibility in connection with the use of this data. Consult with Poly-Flex, Inc. for specific chemical resistance information and liner selection.

Poly-Flex, Inc. • 2000 W. Marshall Dr. • Grand Prairie, TX 75051 U.S.A. • 888-765-9359

CHEMICAL COMPATIBILITY OF POLY-FLEX LINERS

Chemical compatibility or resistance, as applied to geomembranes, is a relative term. Actual compatibility would mean that one material dissolves in the other such as alcohol in water or grease in gasoline. An example of incompatibility would be oil and water. In liners it is undesirable to have the chemicals dissolve in the liner, hence the term compatibility is the reverse of what is normally meant in the chemical industry. In the strictest sense and from a laboratory perspective, chemical compatibility, as the term applies to this industry, would imply that the chemical has no effect on the liner. On the other hand, from an engineering perspective, chemical compatibility means that a liner survives the exposure to a given chemical even though the chemical could have some effect on the performance of the liner, but not enough to cause failure. Therefore, one must understand and define chemical compatibility for a specific project.

Generally polyethylene is effected by chemicals in one of three ways.

1. No effect—This means that the chemical in question and the polyethylene do not interact. The polyethylene does not gain (lose) weight or swell, and the physical properties are not significantly altered.
2. Oxidizes (cross linking)—Chemicals classed as oxidizing agents cause the polyethylene molecules to cross link and cause irreversible changes to the physical properties of the liner. Basically they make the liner brittle.
3. Plasticizes—Chemicals in this classification are soluble in the polyethylene structure. They do not change the structure of the polyethylene itself but act as a plasticizer. In doing so, the liner experiences weight gain of 3-15%, may swell by up to 10%, and has measurable changes in physical properties (e.g. the tensile strength at yield may decrease by up to 20%). Even under these conditions the liner maintains its integrity and is not breached by liquids, provided the liner has not been subjected to any stress. These effects are reversible once the chemicals are removed and the liner has time to dry out.

Aside from the effect that chemicals have on a liner is the issue of vapor permeation through the liner. Vapor permeation is molecular diffusion of chemicals through the liner. Vapor transmission for a given chemical is dependent primarily on liner type, contact time, chemical solubility, temperature, thickness, and concentration gradient, but not on hydraulic head or pressure. Transmission through the liner can occur in as little as 1-2 days. Normally, a small amount of chemical is transmitted. Generally HDPE has the lowest permeation rate of the liners that are commercially available.

As stated above chemical compatibility is a relative term. For example, the use of HDPE as a primary containment of chlorinated hydrocarbons at a concentration of 100% may not be recommended, but it may be acceptable at 0.1% concentration for a limited time period or may be acceptable for secondary containment. Factors that go into assessment of chemical compatibility are type of chemical(s), concentration, temperature and the type of application. No hard and fast rules are available to make decisions on chemical compatibility. Even the EPA 9090 test is just a method to generate data so that an opinion on chemical compatibility can be more reliably reached.

A simplified table on chemical resistance is provided to act as a screening process for chemical containment applications.

CHEMICAL RESISTANCE INFORMATION

CHEMICAL CLASS	CHEMICAL EFFECT	PRIMARY CONTAINMENT (LONG TERM CONTACT)		SECONDARY CONTAINMENT (SHORT TERM CONTACT)	
		HDPE	LLDPE	HDPE	LLDPE
CARBOXYLIC ACID	1				
- Unsubstituted (e.g. Acetic acid)		B	C	A	C
- Substituted (e.g. Lactic acid)		A	B	A	A
- Aromatic (e.g. Benzoic Acid)		A	B	A	A
ALDEHYDES	3				
- Aliphatic (e.g. Acetaldehyde)		B	C	B	C
- Hetrocyclic (e.g. Furfural)		C	C	B	C
AMINE	3				
- Primary (e.g. Ethylamine)		B	C	B	C
- Secondary (e.g. Diethylamine)		C	C	B	C
- Aromatic (e.g. Aniline)		B	C	B	C
CYANIDES (e.g. Sodium Cyanide)	1	A	A	A	A
ESTER (e.g. Ethyl acetate)	3	B	C	B	C
ETHER (e.g. Ethyl ether)		C	C	B	C
HYDROCARBONS	3				
- Aliphatic (e.g. Hexane)		C	C	B	C
- Aromatic (e.g. Benzene)		C	C	B	C
- Mixed (e.g. Crude oil)		C	C	B	C
HALOGENATED HYDROCARBONS	3				
- Aliphatic (e.g. Dichloroethane) +A4		C	C	B	C
- Aromatic (e.g. Chlorobenzene)		C	C	B	C
ALCOHOLS	1				
- Aliphatic (e.g. Ethyl alcohol)		A	A	A	A
- Aromatic (e.g. Phenol)		A	C	A	B
INORGANIC ACID					
- Non-oxidizers (e.g. Hydrochloric acid)	1	A	A	A	A
- Oxidizers (e.g. Nitric Acid)	2	C	C	B	C
INORGANIC BASES (e.g. Sodium hydroxide)	1	A	A	A	A
SALTS (e.g. Calcium chloride)	1	A	A	A	A
METALS (e.g. Cadmium)	1	A	A	A	A
KETONES (e.g. Methyl ethyl ketone)	3	C	C	B	C
OXIDIZERS (e.g. Hydrogen peroxide)	2	C	C	C	C

Chemical Effect (see discussion on Chemical Resistance)

1. No Effect—Most chemicals of this class have no or minor effect.
2. Oxidizer—Chemicals of this class will cause irreversible degradation.
3. Plasticizer—Chemicals of this class will cause a reversible change in physical properties.

Chart Rating

A. Most chemicals of this class have little or no effect on the liner.
Recommended regardless of concentration or temperature (below 150° F).

B. Chemicals of this class will affect the liner to various degrees.
Recommendations are based on the specific chemical, concentration and temperature.
Consult with Poly-Flex, Inc.

C. Chemicals of this class at high concentrations will have significant effect on the physical properties of the liner.
Generally not recommended but may be acceptable at low concentrations and with special design considerations.
Consult with Poly-Flex, Inc.

The data in this table is provided for informational purposes only and is not intended as a warranty or guarantee. Poly-Flex, Inc. assumes no responsibility in connection with the use of this data. Consult with Poly-Flex, Inc. for specific chemical resistance information and liner selection.

Chemicals Resistance Table Low Density and High Density Polyethylene

INTRODUCTION

The table in this document summarises the data given in a number of chemical resistance tables at present in use in various countries, derived from both practical experience and test results.

Source: ISO/TR 7472, 7474; Carlowitz: "Kunststofftabellen-3. Auflage".

The table contains an evaluation of the chemical resistance of a number of fluids judged to be either aggressive or not towards low and high density polyethylene. This evaluation is based on values obtained by immersion of low and high density polyethylene test specimens in the fluid concerned at 20 and 60°C and atmospheric pressure, followed in certain cases by the determination of tensile characteristics.

A subsequent classification will be established with respect to a restricted number of fluids deemed to be technically or commercially more important, using equipment which permits testing under pressure and the determination of the ìcoefficient of chemical resistanceî for each fluid. These tests will thus furnish more complete indications on the use of low and high density polyethylene products for the transport of stated fluids, including their use under pressure.

SCOPE AND FIELD APPLICATION

This document establishes a provisional classification of the chemical resistance of low and high density polyethylene with respect to about 300 fluids. It is intended to provide general guidelines on the possible utilisation of low and high density polyethylene:

- at temperatures up to 20 och 60°C
- in the absence of internal pressure and external mechanical stress
  (for example flexural stresses, stresses due to thrust, rolling loads etc).

DEFINITIONS, SYMBOLS AND ABBREVIATIONS

The criteria of classification, definitions, symbols and abbreviations adopted in this document are as follows:

S = Satisfactory

The chemical resistance of low or high density polyethylene exposed to the action of a fluid is classified as "satisfactory" when the results of test are acknowledged to be ìsatisfactoryî by the majority of the countries participating in the evaluation.

L = Limited

The chemical resistance of low or high density polyethylene exposed to the action of a fluid is classified as "limited" when the results of tests are acknowledged to be "limited" by the majority of the countries participating in the evaluation.

Also classified as "limited" are the resistance to the action of chemical fluids for which judgements "S" and "NS" or "L" are pronounced to an equal extent.

NS = Not satisfactory

The chemical resistance of low or high density polyethylene exposed to the action of a fluid is classified as "not satisfactory" when the results of tests are acknowledged to be "not satisfactory" by the majority of the countries participating in the evaluation.

Also classified as "not satisfactory" are materials for which judgements "L" and "NS" are pronounced to an equal extent.

Sat.sol	Saturated aqueous solution, prepared at 20°C
Sol	Aqueous solution at a concentration higher than 10 %, but not saturated
Dil.sol	Dilute aqueous solution at a concentration equel to or lower than 10 %
Work.sol	Aqueous solution having the usual concentration for industrial use

Solution concentrations reported in the text are expressed as a percentage by mass.
The aqueous solutions of sparingly soluble chemicals are considered, as far as chemical action towards low or high density polyethylene is concerned, as saturated solutions.

In general, common chemical names are used in this document.

The table is made as a first guideline for user of polyethylene. If a chemical compound is not to be found or if there is an uncertainty on the chemical resistance in an application, please contact Borealis for advise and proposal on testing.

Chemical resistance of low density and high density polyethylene, not subjected to mechanical stress, to various fluids at 20 and 60°C

Chemical or product	Concentration	LD	°C	HD	°C
		20	60	20	60
Acetaldehyde	100 %	L	NS	S	L
Acetanilide	–			S	S
Acetic acid	10 %	S	S	S	S
Acetic acid	60 %	S	L	S	S
Acetic acid, glacial	Greater than 96 %	L	NS	S	L
Acetic anhydride	100 %	L	NS	S	L
Acetone	100 %	L	NS	L	L
Acrylnitrile	–	S	S	S	S
Acetylsilicacid	–	S	S	S	S
Adipic acid	Sat.sol	S	S	S	S
After shave	–	NS	NS	NS	NS
Aliphatic hydocarbons	–	L	NS	L	L
Allyl acetate	–	S	L	S	L
Allyl alcohol	100 %	L	NS	–	–
Allyl alcohol	96 %	–	–	S	S
Allyl chloride	–	L	NS	L	NS
Aluminium chloride	Sat.sol	S	S	S	S
Aluminium fluoride	Sat.sol	S	S	S	S
Aluminium hydroxide	Sat.sol	S	S	S	S
Aluminium nitrate	Sat.sol	S	S	S	S
Aluminium oxychloride	Sat.sol	S	S	S	S
Al/potassium sulphate	Sat.sol	S	S	S	S
Aluminium sulphate	Sat.sol	S	S	S	S
Alums	Sol	S	S	S	S
Aminobenzoic acid	–	S	S	S	S
Ammonia, dry gas	100 %	S	S	S	S
Ammonia, liquid	100 %	L	L	S	S
Ammonia, aqueous	Dil.sol	S	S	S	S
Ammonium acetate	–	S	S	S	S
Ammonium carbonate	Sat.sol	S	S	S	S
Ammonium chloride	Sat.sol	S	S	S	S
Ammonium fluoride	Sol	S	–	S	S
Ammonium hexafluorosilicate	Sat.sol	S	S	S	S
Ammonium hydrogen carbonate	Sat.sol	S	S	S	S
Ammonium hydroxide	10 %	S	S	S	S
Ammonium hydroxide	30 %	S	S	S	S

Chemical or product	Concentration	LD	°C	HD	°C
		20	60	20	60
Ammonium metaphosphate	Sat.sol	S	S	S	S
Ammonium nitrate	Sat.sol	S	S	S	S
Ammonium oxalate	Sat.sol	S	S	S	S
Ammonium phosphate	Sat.sol	S	S	S	S
Ammonium persulphate	Sat.sol	S	S	S	S
Ammonium sulphate	Sat.sol	S	S	S	S
Ammonium sulphide	Sol	S	S	S	S
Ammonium thiocyanate	Sat.sol	S	S	S	S
Amyl acetate	100 %	NS	NS	L	L
Amyl alcohol	100 %	L	L	S	L
Amyl chloride	100 %	NS	NS	–	–
Amyl phthalate	–	L	L	S	L
Aniline	100 %	NS	NS	S	L
Anilinchlorohydrate	–	L	–	–	–
Antimony (III) chloride	90 %	–	–	S	S
Antimony (III) chloride	Sat.sol	S	S	S	S
Antimony trichloride	Sol	S	S	S	S
Apple juice	Sol	–	–	S	L
Aqua regia	$HCl/HNO_3 = 3/1$	NS	NS	NS	NS
Aromaitic hydrocarbons	–	NS	NS	NS	NS
Arsenic acid	Sat.sol	S	S	S	S
Asorbic acid	10 %	S	S	S	S
Barium bromide	Sat.sol	S	S	S	S
Barium carbonate	Sat.sol	S	S	S	S
Barium chloride	Sat.sol	S	S	S	S
Barium hydroxide	Sat.sol	S	S	S	S
Barium sulphate	Sat.sol	S	S	S	S
Barium sulphide	Sat.sol	S	S	S	S
Beer	–	S	S	S	S
Benzaldehyde	100 %	L	NS	S	L
Benzene	100 %	NS	NS	L	L
Benzoic acid	Sat.sol	S	S	S	S
Benzoylchloride	–	S	L	S	L
Benzyl alcohol	–	S	L	S	S
Benzylsulphonic acid	10 %	S	S	S	S
Bismuth carbonate	Sat.sol	S	S	S	S
Bitumen	–	S	L	S	S
Bleach lye	10 %	S	S	S	S

Chemical or product	Concentration	LD	°C	HD	°C
		20	60	20	60
Borax	Sat.sol	S	S	S	S
Boric acid	Sat.sol	S	S	S	S
Boron trifluoride	–	L	NS	L	NS
Brake fluid	–	L	NS	L	NS
Brine	–	S	S	S	S
Bromine, dry gas	100 %	NS	NS	NS	NS
Bromine, liquid	100 %	NS	NS	NS	NS
Bromoform	100 %	NS	NS	NS	NS
Butandiol	10 %	S	S	S	S
Butandiol	60 %	S	S	S	S
Butandiol	100 %	S	S	S	S
Butane, gas	100 %	–	–	S	S
Butanol	100 %	S	L	S	S
Butter	–	S	S	S	S
Butyl acetate	100 %	S	L	S	L
Butyl alcohol	100 %	S	S	S	S
Butyl chloride	–	S	–	S	–
Butylene glycol	10 %	S	S	S	S
Butylene glycol	60 %	S	S	S	S
Butylene glycol	100 %	S	S	S	S
Butyraldehyde	–	–	–	S	L
Butyric acid	100 %	L	L	S	L
Calcium arsenate	–	S	S	S	S
Calcium benzoate	–	S	S	S	S
Calcium bisulphide	–	S	S	S	S
Calcium bromate	10 %	S	S	S	S
Calcium bromide	Sat.sol	S	S	S	S
Calcium carbonate	Sat.sol	S	S	S	S
Calcium chlorate	Sat.sol	S	S	S	S
Calcium chloride	Sat.sol	S	S	S	S
Calcium chromate	40 %	S	S	S	S
Calcium cyanide	–	S	S	S	S
Calcium hydrosulphide	Sol	S	S	S	S
Calcium hydroxide	Sat.sol	S	S	S	S
Calcium hypochlorite	Sol	S	S	S	S
Calcium nitrate	Sat.sol	S	S	S	S
Calcium oxide	Sat.sol	S	S	S	S
Calcium perchlorate	1 %	S	–	S	S

Chemical or product	Concentration	LD	°C	HD	°C
		20	60	20	60
Calcium permanganate	20 %	S	S	S	S
Calcium persulphate	Sol	S	S	S	S
Calcium sulphate	Sat.sol	S	S	S	S
Calcium sulphide	Dil.sol	–	–	L	L
Camphor oil	–	NS	NS	L	L
Carbon dioxide, dry gas	100 %	–	–	S	S
Carbon dioxide, wet	–	S	S	S	S
Carbon disulphide	100 %	NS	NS	L	NS
Carbon monoxide	100 %	S	S	S	S
Carbon tetrachloride	100 %	NS	NS	L	NS
Carbonic acid		S	S	S	S
Castor oil	Sol	S	S	S	S
Chlorine, water	2 % Sat.sol	L	L	S	S
Chlorine, aqueous	Sat.sol	NS	NS	L	NS
Chlorine, dry gas	100 %	NS	NS	L	NS
Chloroacetic acid	Sol	–	–	S	S
Chlorobenzene	100 %	NS	NS	NS	NS
Chloroethanol	100 %	S	S	S	S
Chloroform	100 %	NS	NS	NS	NS
Chloromethane, gas	100 %	L	–	L	–
Chlorosulphonic acid	100 %	NS	NS	NS	NS
Chloropropene	–	NS	–	L	–
Chrome alum	Sol	S	S	S	S
Chromic acid	Sat.sol	S	S	–	–
Chromic acid	20 %	–	–	S	L
Chromic acid	50 %	–	–	S	L
Chromium VI oxide	Sat.sol	S	S	S	S
Cider	–	S	S	S	S
Citric acid	Sat.sol	S	S	S	S
Citric acid	10 %	S	S	S	S
Citric acid	25 %	S	S	S	S
Coconut oil alcoholic	–	S	S	S	S
Coffee	–	S	S	S	S
Copper (II) chloride	Sat.sol	S	S	S	S
Copper cyanide	Sat.sol	S	S	S	S
Copper (II) fluoride	Sat.sol	S	S	S	S
Copper (II) fluoride	2 %	S	S	S	S
Copper (II) nitrate	Sat.sol	S	S	S	S
Copper (II) sulphate	Sat.sol	S	S	S	S

Chemical or product	Concentration	LD °C 20	LD °C 60	HD °C 20	HD °C 60
Corn oil	–	S	S	S	S
Cottonseed oil	–	S	S	S	S
Cresylic acid	Sat.sol	–	–	L	–
Crotonaldehyde	Sat.sol	L	–	–	–
Cyclanone	–	S	S	S	S
Cyclohexane	–	NS	NS	NS	NS
Cyclohexanol	Sat.sol	L	NS	–	–
Cyclohexanol	100 %	–	–	S	S
Cyclohexanone	100 %	NS	NS	S	L
Decahydronaphthalene	100 %	L	NS	S	L
Decane	–	NS	NS	L	NS
Decalin	100 %	–	–	S	L
Detergents, synthetic	–	S	S	S	S
Developers (photographic)	Work.conc	–	–	S	S
Dextrin	Sol	S	S	S	S
Dextrose	Sol	S	S	S	S
Diacetone alcohol	–	L	L	L	L
Diazo salts	–	S	S	S	S
Dibutyl amine	–	NS	NS	L	NS
Dibuthyl ether	–	NS	NS	L	–
Dibutylphthalate	–	L	L	S	L
Dichlorobenzene	–	NS	NS	NS	NS
Dichloroethylene	–	NS	NS	NS	NS
Dichloropropylene	–	NS	NS	NS	NS
Diesel oil	–	S	NS	S	L
Diethyl ether	100 %	NS	NS	L	–
Diethyl ketone	–	L	NS	L	L
Diethylene glycol	–	S	S	S	S
Diglycolic acid	–	S	S	S	S
Diisobutylketone	100 %	S	L	S	L
Dimethyl amine	100 %	NS	NS	–	–
Dimethyl formamid	–	S	L	S	S
Dioctyl phthalate	100 %	L	NS	S	L
Dioxan	100 %	–	–	S	S
Dipentene	–	NS	NS	NS	NS
Disodium phosphate	–	S	S	S	S
Drano, plumbing cleaner	–	S	S	S	S

Chemical or product	Concentration	LD	°C	HD	°C
		20	60	20	60
Emulsions, photographic	–	S	S	S	S
Ethandiol	100 %	S	S	S	S
Ethanol	40 %	S	L	S	L
Ethanol	96 %	L	L	–	–
Ethyl acetate	100 %	L	NS	S	NS
Ethyl acrylate	100 %	NS	NS	L	NS
Ethyl alcohol	35 %	S	S	S	S
Ethyl alcohol	100 %	S	S	S	S
Ethyl benzene	–	NS	NS	NS	NS
Ethyl chloride	100 %	NS	NS	NS	NS
Ethylene chloride	100 %	NS	NS	NS	NS
Ethylene diamine	100 %	S	L	S	S
Ethyl ether	–	NS	NS	NS	NS
Ethylene glycol	100 %	S	S	S	S
Ethyl mercaptan	–	NS	NS	NS	NS
Ferric chloride	Sat.sol	S	S	S	S
Ferric nitrate	Sat.sol	S	S	S	S
Ferric sulphate	Sat.sol	S	S	S	S
Ferrous chloride	Sat.sol	S	S	S	S
Ferrous sulphate	Sat.sol	S	S	S	S
Fish solubles	Sol	S	S	S	S
Fluoboric acid	–	S	S	S	S
Fluorine gas	100 %	L	NS	NS	NS
Fluorine gas, dry	100 %	NS	NS	NS	NS
Fluorine gas, wet	100 %	NS	NS	NS	NS
Fluorosilic acid	Conc	S	L	S	L
Fluorosilic acid	40 %	S	S	S	S
Formaldehyde	40 %	S	S	S	S
Formic acid	40 %	S	S	S	S
Formic acid	98 to 100 %	S	S	S	S
Fructose	Sat.sol	S	S	S	S
Fruit pulps	Sol	S	S	S	S
Furfural	100 %	NS	NS	NS	NS
Furfuryl alcohol	100 %	L	NS	S	L
Gallic acid	Sat.sol	S	S	S	S
Gasoline, petrol	–	L	NS	L	L
Gelatine	–	S	S	S	S

Chemical or product	Concentration	LD	°C	HD	°C
		20	60	20	60
Glucose	Sat.sol	S	S	S	S
Glycerine	100 %	S	S	S	S
Glycerol	100 %	S	S	S	S
Glycolic acid	30 %	S	L	–	–
Glycolic acid	Sol	–	–	S	S
n-Heptane	100 %	NS	NS	L	NS
Hexachlorobenzene	–	S	S	S	L
Hexachlorophene	–	NS	NS	L	L
Hexamethylenetriamine	40 %	S	–	S	–
Hexane	–	S	L	S	L
Hexanol, tertiary	–	S	S	S	S
Hydrobromic acid	50 %	S	S	S	S
Hydrobromic acid	Up to 100 %	S	S	S	S
Hydrochloric acid	Up to 36 %	S	S	S	S
Hydrochloric acid	Conc	S	S	S	S
Hydrochlorous acid	Conc	S	S	S	S
Hydrocyanic acid	10 %	S	S	S	S
Hydrocyanic acid	Sat.sol	S	S	S	S
Hydrofluoric acid	40 %	S	S	S	S
Hydrofluoric acid	60 %	S	L	S	L
Hydrogen	100 %	S	S	S	S
Hydrogen chloride	Dry gas	S	S	S	S
Hydrogen peroxide	30 %	S	L	S	S
Hydrogen peroxide	90 %	S	NS	S	NS
Hydrogen sulphide gas	100 %	S	S	S	S
Hydroquinone	Sat.sol	S	S	–	–
Hydroxylamine	up to 12 %	S	S	S	S
Inks	–	S	S	S	S
Iodine (in potassium sol)	–	L	NS	NS	NS
Iodine (in alcohol)	–	NS	NS	NS	NS
Iron (II) chloride	Sat.sol	S	S	S	S
Iron (II) sulphate	Sat.sol	S	S	S	S
Iron (III) chloride	Sat.sol	S	S	S	S
Iron (III) nitrate	Sol	S	S	S	S
Iron (III) sulphate	Sat.sol	S	S	S	S
Iso octane	100 %	S	NS	S	L
Iso pentane	–	NS	NS	NS	NS

Chemical or product	Concentration	LD	°C	HD	°C
		20	60	20	60
Isopropanol	–	S	S	S	S
Isopropyl amine	–	NS	NS	NS	NS
Isopropyl ether	100 %	L	NS	S	NS
Kerosene	–	NS	NS	NS	NS
Lactic acid	10 %	S	S	S	S
Lactic acid	28 %	S	S	S	S
Lactic acid	up to 100 %	S	S	S	S
Latex	–	S	S	S	S
Lead acetate	Dil.sol	S	S	S	S
Lead acetate	Sat.sol	S	S	S	S
Lead arsenate	–	S	S	S	S
Lubricating oil	–	S	S	S	S
Lysol	–	NS	NS	L	NS
Magnesium carbonate	Sat.sol	S	S	S	S
Magnesium chloride	Sat.sol	S	S	S	S
Magnesium hydroxide	Sat.sol	S	S	S	S
Magnesium nitrate	Sat.sol	S	S	S	S
Magnesium sulphate	Sat.sol	S	S	S	S
Maleic acid	Sat.sol	S	S	S	S
Mercury	–	S	S	S	S
Mercury (I) nitrate	Sol	S	S	S	S
Mercury (II) chloride	Sat.sol	S	S	S	S
Mecury (II) cyanide	Sat.sol	S	S	S	S
Mercury	100 %	S	S	S	S
Methanol	100 %	S	L	S	S
Methyl alcohol	100 %	S	L	S	S
Methyl benzoic acid	Sat.sol	NS	NS	L	–
Methyl bromide	100 %	NS	NS	NS	NS
Methyl chloride	100 %	NS	NS	NS	NS
Methylcyclohexane	–	L	NS	L	NS
Methyl ethyl ketone	100 %	–	–	S	L
Methylene chloride	–	NS	NS	NS	NS
Methoxybutanol	100 %	S	L	S	L
Milk	–	S	S	S	S
Milk of Magnesia	–	S	L	S	L
Mineral oils	–	L	NS	S	L

Chemical or product	**Concentration**	**LD**	**°C**	**HD**	**°C**
		20	**60**	**20**	**60**
Molasses	Work.conc	S	S	S	S
Motor oil	–	S	L	S	S
Naphtha	–	L	NS	L	NS
Naphtahalene	–	NS	NS	L	–
Nickel chloride	Sat.sol	S	S	S	S
Nickel nitrate	Sat.sol	S	S	S	S
Nickel sulphate	Sat.sol	S	S	S	–
Nicotine	Dil.sol	S	S	S	S
Nicotinic acid	Dil.sol	L	L	S	–
Nitric acid	25 %	S	S	S	S
Nitric acid	50 %	S	L	S	L
Nitric acid	70 %	S	L	S	L
Nitric acid	95 %	NS	NS	NS	NS
Nitric acid	100 %	NS	NS	NS	NS
Nitrobenzene	100 %	NS	NS	NS	NS
Nitroethane	100 %	S	NS	S	NS
Nitromethane	100 %	S	–	S	–
Nitrotoluene	–	NS	NS	NS	NS
n-Octane	–	S	S	S	S
Octyl alcohol	–	S	NS	S	NS
Oil and fats		L	NS	S	L
Oleic acid	100 %	L	NS	S	S
Oleum (H2SO4 + 10 % SO3)		NS	NS	NS	NS
Oleum (H2SO4 + 50 % SO3)		NS	NS	NS	NS
Olive oil	–	S	NS	S	NS
Orthophosphoric acid	50 %	S	S	S	S
Orthophosphoric acid	95 %	S	L	S	L
Oxalic acid	Sat.sol	S	S	S	S
Oxygen	100 %	S	–	S	L
Ozone	100 %	NS	NS	L	NS
Paraffin oil	–	S	L	S	S
n-Pentane	–	NS	NS	NS	NS
Pentane-2	–	NS	NS	NS	NS
Perchloric acid	20 %	S	S	S	S
Perchloric acid	50 %	S	L	S	L
Perchloric acid	70 %	S	NS	S	NS

Chemical or product	**Concentration**	**LD**	**°C**	**HD**	**°C**
		20	60	20	60
Perchloroethylene	–	NS	NS	NS	NS
Phenol	Sol	L	NS	S	S
Phosphine	100 %	S	S	S	S
Phosphoric acid	up to 25 %	S	S	S	S
Phosphoric acid	25 to 50 %	S	S	S	S
Phosphoric (III) chloride	100 %	S	L	S	L
Phosphorous (II) chloride	100 %	–	–	S	L
Phosphorous pentoxide	100 %	S	S	S	S
Phosphorous trichloride	100 %	S	L	S	L
Photographic solutions	–	S	S	S	S
Phtalic acid	50 %	S	S	S	S
Picric acid	Sat.sol	S	L	S	–
Plating solutions	–	S	S	S	S
Potassium acetate	–	S	S	S	S
Potassium aluminium sulphate	Sat.sol	S	S	S	S
Potassium benzoate	–	S	S	S	S
Potassium bicarbonate	Sat.sol	S	S	S	S
Potassium borate	Sat.sol	S	S	S	S
Potassium bromate	Sat.sol	S	S	S	S
Potassium bromide	Sat.sol	S	S	S	S
Potassium carbonate	Sat.sol	S	S	S	S
Potassium chlorate	Sat.sol	S	S	S	S
Potassium chloride	Sat.sol	S	S	S	S
Potassium chromate	Sat.sol	S	S	S	S
Potassium cyanide	Sol	S	S	S	S
Potassium dichromate	Sat.sol	S	S	S	S
Potassium fluoride	Sat.sol	S	S	S	S
Potassium hexacyanoferrate (III)	Sat.sol	S	S	S	S
Potassium hexacyanoferrate (II)	Sat.sol	S	S	S	S
Potassium hexafluorosilicate	Sat.sol	S	S	S	S
Potassium hydrogen carbonate	Sat.sol	S	S	S	S
Potassium hydrogen sulphate	Sat.sol	S	S	S	S
Potassium hydrogen sulphide	Sol	–	–	S	S
Potassium hydroxide	10 %	S	S	S	S
Potassium hydroxide	Sol	S	S	S	S
Potassium hypochlorite	Sol	S	L	S	L
Potassium iodate	10 %	S	S	S	S
Potassium iodide	Sat.sol	S	S	S	S
Potassium nitrate	Sat.sol	S	S	S	S

Chemical or product	Concentration	LD	°C	HD	°C
		20	60	20	60
Potassium orthophosphate	Sat.sol	S	S	S	S
Potassium oxalate	Sat.sol	S	S	S	S
Potassium perchlorate	Sat.sol	S	S	S	S
Potassium permanganate	20 %	S	S	S	S
Potassium persulphate	Sat.sol	S	S	S	S
Potassium phosphate	Sat.sol	S	S	S	S
Potassium sulphate	Sat.sol	S	S	S	S
Potassium sulphide	Sol	S	S	S	S
Potassium sulphite	Sat.sol	S	S	–	–
Potassium thiocyanate	Sat.sol	S	S	S	S
Potassium thiosulphate	Sat.sol	S	S	S	S
Propargul alcohol	–	S	S	S	S
n-Propyl alcohol	–	S	S	S	S
Propionic acid	50 %	–	–	S	S
Propionic acid	100 %	–	–	S	L
Propylene dichloride	100 %	NS	NS	NS	NS
Propylene glycol	–	S	S	S	S
Pyridine	100 %	–	–	S	L
Quinol (hydroquinone)	Sat.sol	S	S	S	S
Resorcinol	Sat.sol	S	S	S	S
Salicylic acid	Sat.sol	S	S	S	S
Sea water	–	S	S	S	S
Selenic acid	–	S	S	S	S
Silicon oil	–	S	S	S	S
Silver acetate	Sat.sol	S	S	S	S
Silver cyanide	Sat.sol	S	S	S	S
Silver nitrate	Sat.sol	S	S	–	–
Soap solution	100 %	S	S	S	S
Sodium acetate	Sat.sol	S	S	–	–
Sodium antimonate	Sat.sol	S	S	S	S
Sodium arsenite	Sat.sol	S	S	S	S
Sodium benzoate	Sat.sol	S	S	S	S
Sodium bicarbonate	Sat.sol	S	S	S	S
Sodium bisulphate	Sat.sol	S	S	S	S
Sodium bisulphite	Sat.sol	S	S	S	S
Sodium borate	–	S	S	S	S
Sodium bromide	Sat.sol	S	S	S	S
Sodium carbonate	Sat.sol	S	S	S	S

Chemical or product	Concentration	LD	°C	HD	°C
		20	60	20	60
Sodium chlorate	Sat.sol	S	S	S	S
Sodium chloride	Sat.sol	S	S	S	S
Sodium chlorite	Sat.sol	L	–	–	–
Sodium cyanide	Sat.sol	S	S	S	S
Sodium dichromate	Sat.sol	S	S	S	S
Sodium fluoride	Sat.sol	S	S	S	S
Sodium hexacyanoferrate (III)	Sat.sol	–	–	S	S
Sodium hexacyanoferrate (II)	Sat.sol	–	–	S	S
Sodium hexafluorosilicate	Sat.sol	S	S	S	S
Sodium hydrogen carbonate	Sat.sol	S	S	S	S
Sodium hydrogen sulphate	Sat.sol	S	S	S	S
Sodium hydrogen sulphite	Sol	S	S	S	S
Sodium hydroxide	40 %	S	S	S	S
Sodium hydroxide	Sol	–	–	S	S
Sodium hypochloride	–	L	NS	S	S
Sodium hypochlorite	15 %	–	–	S	S
	available Cl	–	–	S	S
Sodium iodate	10 %	S	S	S	S
Sodium iodide	Sat.sol	S	S	S	S
Sodium nitrate	Sat.sol	S	S	S	S
Sodium nitrite	Sat.sol	S	S	S	S
Sodium ortophosphate	Sat.sol	S	S	S	S
Sodium oxalate	Sat.sol	S	S	S	S
Sodium phosphate	Sat.sol	S	S	S	S
Sodium silicate	Sol	S	S	S	S
Sodium sulphate	Sat.sol	S	S	S	S
Sodium sulphide	Sat.sol	S	S	S	S
Sodium sulphite	Sat.sol	S	S	S	S
Sodium thiocyanate	Sat.sol	S	S	S	S
Stannic chloride	Sat.sol	S	S	S	S
Stannous chloride	Sat.sol	S	S	S	S
Starch solution	Sat.sol	S	S	S	S
Stearic acid	Sat.sol	S	L	S	–
Styrene	Sol	L	NS	L	NS
Sulphur dioxide, dry	100 %	S	S	S	S
Sulphur trioxide	100 %	NS	NS	NS	NS
Sulphur acid	10 to 50 %	S	S	S	S
Sulphuric acid	10 %	S	S	S	S
Sulphuric acid	50 %	S	S	S	S

Chemical or product	**Concentration**	**LD**	**°C**	**HD**	**°C**
		20	**60**	**20**	**60**
Sulphuric acid	70 %	S	L	S	L
Sulphuric acid	80 %	S	NS	S	NS
Sulphuric acid	98 %	L	NS	S	NS
Sulphuric acid	Fuming	NS	NS	NS	NS
Sulphurous acid	30 %	S	S	S	S
Sulphurous acid	Sol	S	S	S	S
Tallow	–	S	L	S	L
Tannic acid	Sol	S	S	S	S
Tartaric acid	Sat.sol	S	S	S	S
Tartaric acid	Sol	–	–	S	S
Tetrachloroethylene	100 %	NS	NS	NS	NS
Tetrachloromethane	100 %	NS	NS	L	NS
Tetradecane		NS	NS	NS	NS
Tetrahydrofuran	–	NS	NS	NS	NS
Tetrahydronaphthalene	100 %	L	NS	S	L
Thionyl chloride	100 %	NS	NS	NS	NS
Tin (II) chloride	Sat.sol	S	S	S	S
Tin (IV) chloride	Sol	S	S	S	S
Tin (IV) chloride	Sat.sol	–	–	S	S
Titanium tetrachloride	Sat.sol	NS	NS	NS	NS
Toluene	100 %	NS	NS	L	NS
Tribromomethane	–	NS	NS	NS	NS
Trichloroacetaldehyde	–	S	–	S	–
Trichlorobenzene	–	NS	NS	–	–
Trichloroethylene	100 %	NS	NS	NS	NS
Triethanolamine	100 %	S	–	S	–
Triethanolamine	Sol	–	–	S	L
Triethylene glycol	–	S	S	S	S
Trisodium phosphate	Sat.sol	S	S	–	–
Turpentine	–	NS	NS	NS	NS
Urea	up to 30 %	S	S	S	S
Urea	Sol	S	S	S	S
Urine	-	S	S	S	S
Vanilla extract	–	S	S	S	S
Vaseline	–	S	L	S	S
Vegetables oils		S	L	S	S
Vinegar		S	S	S	S
Water		S	S	S	S
Wetting agents	–	S	S	S	S
Wines and spirits		S	S	S	S
Chemical or product	**Concentration**	**LD**	**°C**	**HD**	**°C**
		20	60	20	60

Xylene	100 %	NS	NS	L	NS
Yeast	Sol	S	S	S	S
Zinc bromide	Sat.sol	S	S	S	S
Zinc carbonate	Sat.sol	–	–	S	S
Zinc chloride	Sat.sol	S	S	S	S
Zinc oxide	Sat.sol	S	S	S	S
Zinc stearate	–	S	S	S	S
Zinc sulphate	Sat.sol	S	S	S	S
o-Zylene		NS	NS	NS	NS
p-Zylene	–	NS	NS	NS	NS

CONTAINMENT SOLUTIONS FOR INDUSTRIAL WASTE

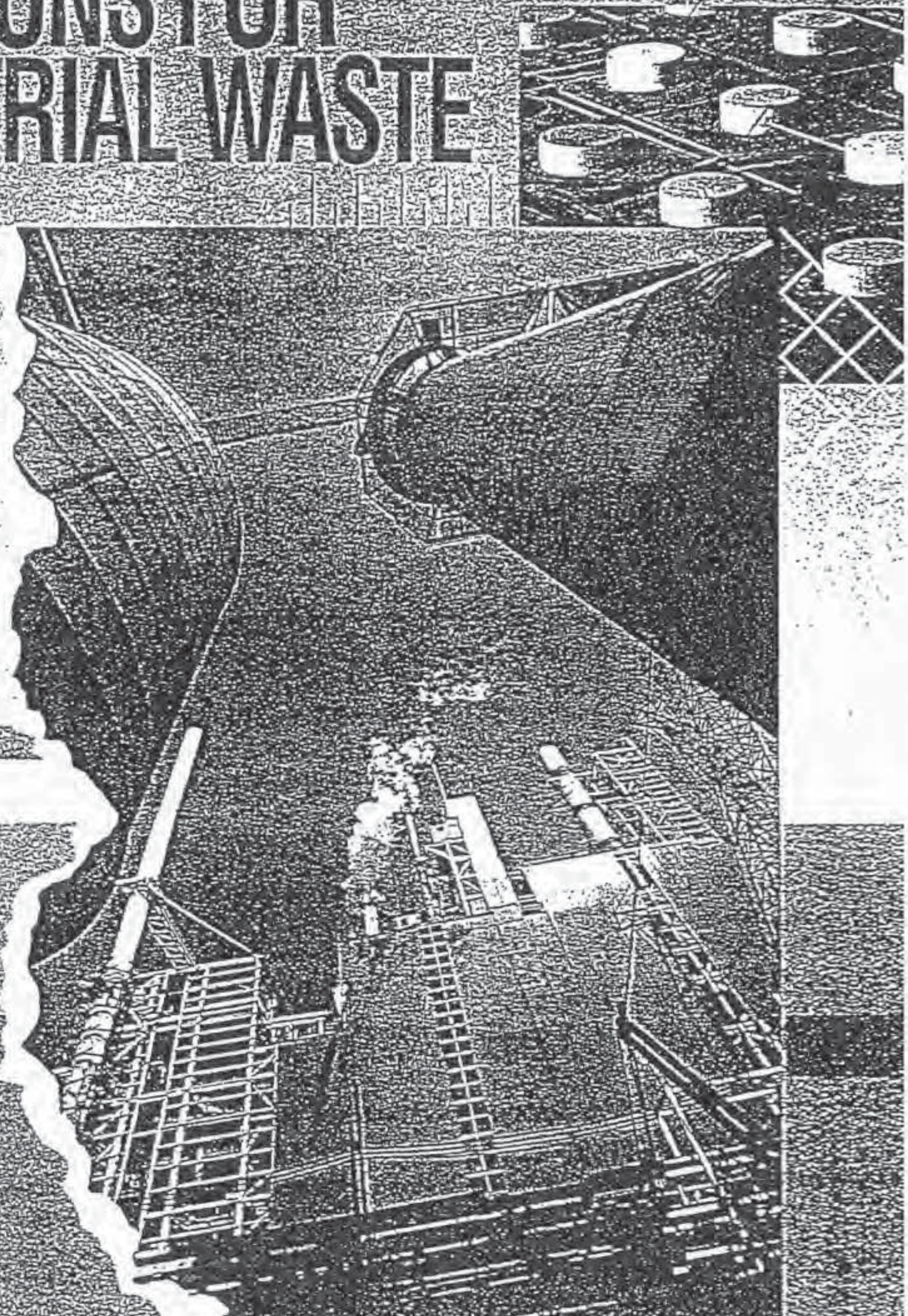

- Dike raising
- Sludge caps
- Sludge ponds
- Secondary containment
- Landfill linings
- Landfill caps
- Floating covers

NSC

NSC

HIGH DENSITY POLYETHYLENE (HDPE) GEOMEMBRANE

Over the past five years, the geomembrane industry has experienced numerous changes. Factors such as the increased concern for the environment; new products in the marketplace; and the push for tighter governmental control over the environment have all played a significant role in revolutionizing the geosynthetic industry.

Today, the most widely used geomembrane in the waste management industry is High Density Polyethylene (HDPE). HDPE offers superior performance by maintaining the highest standards of durability.

FEATURES AND BENEFITS

National Seal Company's HDPE geomembrane is manufactured on a computer controlled, flat sheet extruder using virgin, first quality, high molecular weight polyethylene. This process guarantees a material thickness of ±5% from target, the most stringent quality control available in the industry. NSC also guarantees the minimum average thickness of our liner will be greater than or equal to the nominal thickness. HDPE is available in 40 (1.0mm), 50 (1.25mm), 60 (1.5mm), 80 (2.0mm), and 100 (2.5mm) mil thicknesses.

Chemical Resistance - Often the chemical resistance of the liner is the most critical aspect of the design process. HDPE is the most chemically resistant of all geomembranes. Typical landfill leachates pose no threat to a liner made of HDPE.

Low Permeability - The low permeability of HDPE provides assurance that groundwater will not penetrate the liner; rainwater will not infiltrate a cap; and methane gas will not migrate away from the gas venting system.

Ultraviolet Resistance - HDPE has excellent resistance to ultraviolet degradation. NSC adds carbon black which provides UV protection. Plasticizers are never used in NSC's geomembranes so there is never a concern about volatilization of the plasticizer which can be caused by UV exposure.

APPLICATIONS:

Landfill (primary and secondary containment)
Landfill caps
Lagoon liners
Pond liners
Floating covers
Secondary containment for above ground storage tanks
Retention ponds for mining applications
Wastewater treatment facilities
Potable water reservoirs
Tank linings
Canal linings
Heap leach pads

HDPE GEOMEMBRANE
PHYSICAL PROPERTIES

60 mil

The properties on this page are not part of NSC's Manufacturing Quality Control program and are not included on the material certifications. Seam testing is the responsibility of the installer and/or CQA personnel.

PROPERTIES	METHOD	UNITS	MINIMUM[1]	TYPICAL
Multi-Axial Tensile Elongation	GRI, GM-4	percent	20.0	28.0
Critical Cone Height	GRI, GM-3, NSC mod.	cm	1.0	1.5
Wide Width Tensile	ASTM D 4885			
Stress at Yield		psi	2000	2110
Strain at Yield		%	15.0	20.0
Brittleness Temp. by Impact[2]	ASTM D 746	°C	-75	<-90
Coef. of Linear Thermal Exp.[2]	ASTM D 696	$°C^{-1}$	1.5×10^{-4}	1.2×10^{-4}
ESCR, Bent Strip	ASTM D 1693	hours	1500	>10,000
Hydrostatic Resistance	ASTM D 751	psi	450	510
Modulus of Elasticity	ASTM D 638	psi	80,000	135,000
Ozone Resistance	ASTM D 1149, 168 hrs	P/F	P	P
Permeability[2]	ASTM E 96	cm/sec · Pa	2.3×10^{-14}	8.1×10^{-15}
Puncture Resistance	FTMS 101, method 2065	ppi	1300	1700
		lbs	78	105
Soil Burial Resistance[2]	ASTM D 3083, NSF mod.	% change	10	0
Tensile Impact	ASTM D 1822	ft lbs/in^2	250	420
Volatile Loss[2]	ASTM D 1203, A	percent	0.10	0.06
Water Absorption[2]	ASTM D 570, 23°C	percent	0.10	0.04
Water Vapor Transmission[2]	ASTM E 96	$g/day \cdot m^2$	0.024	0.009

SEAM PROPERTIES	METHOD	UNITS	MINIMUM[1]	TYPICAL
Shear Strength	ASTM D 4437, NSF mod.	psi	2000	2700
		ppi	120	166
Peel Strength (hot wedge fusion)	ASTM D 4437, NSF mod.	psi	1500	1870
		ppi	90	115
Peel Strength (fillet extrusion)	ASTM D 4437, NSF mod.	psi	1300	1590
		ppi	78	98

STANDARD ROLL DIMENSIONS

Length	1110 feet	Area	16,650 ft^2
Width	15 feet	Weight	5,000 lbs

NSC reserves the right to update the information contained herein in accordance with technological advances in the material properties.

6H-0893

NSC
NATIONAL SEAL COMPANY
1245 Corporate Blvd. • Suite 300
Aurora, IL 60504
(708) 898-1161 • (800) 323-3820
Fax (708) 898-3461

HDPE GEOMEMBRANE
QUALITY CONTROL SPECIFICATIONS

60 mil

National Seal Company's High Density Polyethylene (HDPE) Geomembranes are produced from virgin, first quality, high molecular weight resins and are manufactured specifically for containment in hydraulic structures. NSC HDPE geomembranes have been formulated to be chemically resistant, free of leachable additives and resistant to ultraviolet degradation.

The following properties are tested as a part of NSC's quality control program. Certified test results for properties on this page are available upon request. Refer to NSC's Quality Control Manual for exact test methods and frequencies.

All properties meet or exceed NSF Standard Number 54.

RESIN PROPERTIES	METHOD	UNITS	MINIMUM[1]	TYPICAL
Melt Flow Index[2]	ASTM D 1238	g/10 min	0.50	0.25
Oxidative Induction Time	ASTM D 3895, Al pan, 200°C, 1 atm O_2	minutes	100	120

SHEET PROPERTIES	METHOD	UNITS	MINIMUM[1]	TYPICAL
Thickness	ASTM D 751, NSF mod.			
Average		mils	60.0	61.5
Individual		mils	57.0	59.7
Density	ASTM D 1505	g/cm^3	0.940	0.948
Carbon Black Content	ASTM D 1603	percent	2.0-3.0	2.35
Carbon Black Dispersion	ASTM D 3015, NSF mod.	rating	A1, A2, B1	A1
Tensile Properties	ASTM D 638			
Stress at Yield		psi	2200	2550
		ppi	132	157
Stress at Break		psi	3800	4850
		ppi	228	298
Strain at Yield	1.3" gage length (NSF)	percent	13.0	16.9
Strain at Break	2.0" gage or extensometer	percent	700	890
	2.5" gage length (NSF)	percent	560	710
Dimensional Stability[2]	ASTM D 1204, NSF mod.	percent	1.5	0.4
Tear Resistance	ASTM D 1004	ppi	750	860
		lbs	45	53
Puncture Resistance	ASTM D 4833	ppi	1800	2130
		lbs	108	131
Constant Load ESCR, Single Point	GRI, GM-5a	hours	200	>400

[1] This value represents the minimum acceptable test value for a roll as tested according to NSC's Manufacturing Quality Control Manual. Individual test specimen values are not addressed in this specification except thickness.

[2] Indicates Maximum Value

NSC

NATIONAL SEAL COMPANY
1245 Corporate Blvd. • Suite 300
Aurora, IL 60504
(708) 898-1161 • (800) 323-3820
Fax: (708) 898-3461

How long will my liner last?

| What is the remaining service life of my HDPE geomembrane?

By Ian D. Peggs, P.E., P.Eng., Ph.D.

Introduction

In his keynote lecture at the GeoAmericas-2008 conference last March, Dr. Robert Koerner (et al., 2008) of the Geosynthetic Institute (GSI) reported the ongoing Geosynthetic Research Institute (GRI) work to make the first real stab at assessing the service lives of high-density polyethylene (HDPE), linear low-density polyethylene (LLDPE), reinforced PE, ethylene propylene diene terpolymer (EPDM), and flexible polypropylene (fPP) exposed geomembranes.

The selected environment simulated that of Texas, USA, in sunny ambient temperatures between ~7°C (45°F) and 35°C (95°F). Of course, an exposed black HDPE geomembrane in the sun will achieve much higher temperatures, probably in excess of 80°C (176°F).

I do not know what the temperature would be at 150-300mm above the liner (for those still specifying this parameter), but it is quite immaterial. The only temperature of concern is the actual geomembrane temperature.

The lifetimes are shown in **Table 1**, but it must be recognized that these data are for specific manufactured products with specific formulations. The "greater than" notation indicates that laboratory exposures (incubations) are still on-going, not that some samples have failed after the indicated time period. The PE-R-1 material is a thin LLDPE, so it might be expected to be the first to reach the defined end of life; the half-life—the time to loss of 50% of uniaxial tensile properties.

It is interesting to note that HDPE-1 and LLDPE-1 are proceeding apace, but it would be expected that the LLDPE-1 would reach its half-life earlier than HDPE-1. However, this does not automatically follow. With adequate additive formulations, perhaps LLDPE could be left exposed and demonstrate more weathering resistance than some HDPEs. This demonstrates the fact that all PEs, whether HD or LLD, are not identical—they can have different long-term performances dependent on the PE resin used and the formulation of the stabilizer package. However, such differences are not evident in the conventional mechanical properties such as tensile strength/elongation, puncture and tear resistances, and so on.

The two fPPs are performing well. However, there had also been an fPP-1, one of the first PP geomembranes that did not perform well. This was due to a totally inappropriate stabilizer formulation. That particular product lasted 1.5 years in service. In

Final Inspection continued on page 44

Type	Specification	Predicted Lifetime in Texas, USA
HDPE-1	GRI-GM13	>28 years (Incubation ongoing)
LLDPEE-1	GRI-GM17	>28 years (Incubation ongoing)
EPDM-1	GRI-GM21	>20 years (Incubation ongoing)
PE-R-1	GRI-GM22	≈17 years (reached halflife)
fPP-2	GRI-GM18 (temp. susp.)	>27 years (Incubation ongoing)
fPP-3	GRI-GM18 (temp. susp.)	>17 years (Incubation ongoing)

Table 1 | Estimated exposed geomembrane lifetimes

| Ian Peggs is president of I-CORP International Inc. and is a member of *Geosynthetics* magazine's Editorial Advisory Committee.

Final Inspection continued from page 56

the QUV weatherometer, it lasted 1,800 light hours at 70°C (158°F). Therefore, the lab/field correlation is that 1,000 QUV light hours is equivalent to a 0.83yr service life under those specific environmental conditions.

At another location in Texas, Koerner/GRI found 1,000hr of QUV exposure was equivalent to 1.1 year actual field exposure. Consequently, for Texas exposures GRI is using a correlation of 1000hr QUV exposure as equivalent to lyr of in-service exposure. Clearly, the correlation would be different in less sunny and colder environments.

The failed fPP-1 liner was replaced with a correctly stabilized fPP that, subsequently, performed well.

While estimated correlations might be made for other locations using historical weather station sunshine and temperature data, there is no question that the best remaining lifetime assessments will be obtained using samples removed from the field installation of interest.

A lifetime in excess of 28yr, demonstrated for a recently-made HDPE geomembrane, is comparable to the present actual service periods of as long as 30-35yr. However, actual lifetimes of as low as ~15yr have also been experienced.

Do service lifetimes now exceeding 30yr mean that we might expect to see another round of stress cracking failures as exposed liners finally oxidize sufficiently on the surface to initiate stress cracking?

This would be frustrating after resolving the early 1980s problems with stress cracking failures at welds and stone protrusions when the liners contracted at low temperatures, but it is the way end-of-life will become apparent. And will that be soon or in another 5-20 years? It would be useful to know.

So how can we evaluate the condition of our exposed liners in a simple and practical manner to ensure they will continue to provide adequate service lifetimes and to get sufficient warning of impending expiration?

For each installation, a baseline needs to be established, and changes from that baseline need to be monitored.

A liner lifetime evaluation program

Rather than be taken by surprise when a liner fails or simply expires, it should be possible to monitor the condition of the liner to obtain a few years of notice for impending expiration. One can then plan for a timely replacement without the potential for accidental environmental damage and undesirable publicity. A program of periodic liner-condition assessment is proposed.

... it should be possible to monitor the condition of the liner to obtain a few years of notice for impending expiration.

For baseline data, it would be useful to have some archive material to test, but that is not usually available. Manufacturers often discard retained samples after about 5 years. Perhaps facility owners should be encouraged to keep retained samples at room temperature and out of sunlight. The next best thing is to use material from the anchor trench or elsewhere that has not experienced extremes in temperature and that has not been exposed to UV radiation or to expansion/contraction stresses.

Less satisfactory options are to use the original NSF 54 specifications, the manufacturer's specifications, or the GRI-GM13 specifications at the appropriate time of liner manufacturing. The concern with using these specifications is that while aged material may meet them, there is no indication of whether the measured values have significantly decreased from the actual as-manufactured values that generally significantly exceed the specification.

A final option for the baseline would be to use the values at the time of the first liner assessment.

The first liner condition assessment would consist of a site visit during which a general visual examination would be done together with a mechanical probing of the edges of welds. A visual examination would include the black/gray shades of different panels that might indicate low carbon contents.

A closer examination should be done using a loupe (small magnifier) on suspect areas such as wrinkle peaks, the tops and edges of multiple extrusion weld beads, and the apex-down creases of round die-manufactured sheet.

The last detail is significant because the combination of oxidizing surface and exposed surface tension when the liner contracts at low temperatures and the crease is pulled flat can be one of the first locations to crack. The apex-up creases do not fail at the same time because the oxidized exposed surface is under compression (or less tension) when the crease is flattened out.

Appropriate samples for detailed laboratory testing will be removed.

It may be appropriate to do a water lance electrical integrity survey on the exposed sideslopes, but this would only be effective on single liners, and on double liners with a composite primary liner, a conductive geomembrane, or a geocomposite with a conductive geotextile on top.

A sampling and testing regime

A liner lifetime evaluation program should be simple, meaningful, and cost-effective.

While it will initially require expert polymer materials science/engineering input to analyze the test data and to define the critical parameters, it should ultimately be possible to use an expert system to automatically make predictions using the input test data.

Small samples will be taken from deep in the anchor trench and from appropriate

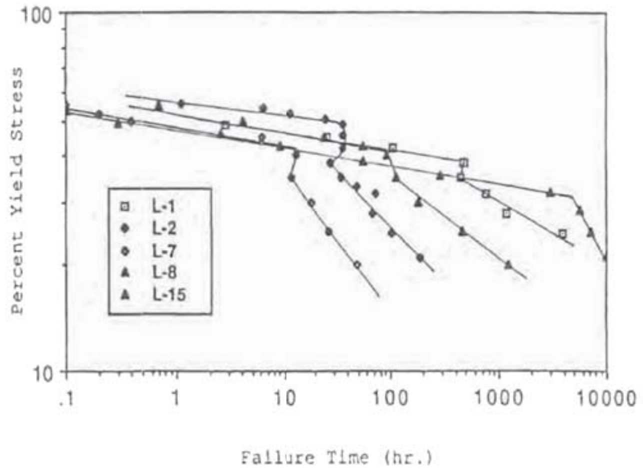

Figure 1 | Standard stress rupture curves for five HDPE geomembranes (Hsuan, et al. 1992)

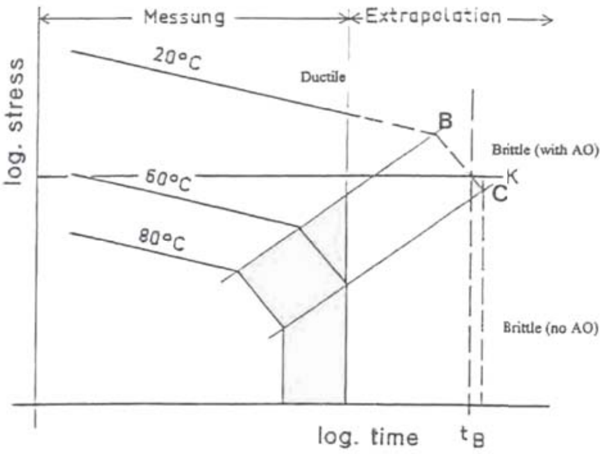

Figure 2 | Stress rupture curves showing third stage (Brittle no AO) oxidized limit. (Gaube, et al. 1985)

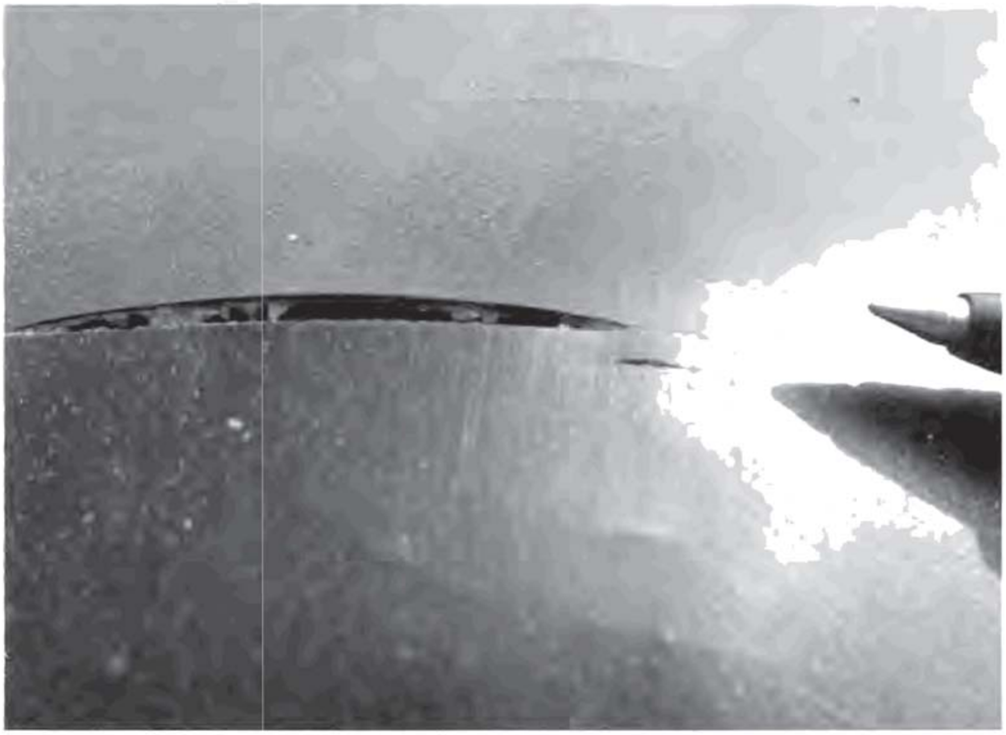

Figure 3 | Stress crack initiated by extruder die line at stone protrusion

exposed locations. Potential sites for future sample removal by the facility owner for future testing will be identified and marked by the expert during the first site visit.

The baseline sample(s) will be tested as follows:

- Single-point stress cracking resistance (SCR) on a molded plaque by ASTM D5397
- High-pressure oxidative induction time (HP-OIT) by ASTM D5885
- Fourier transform infrared spectroscopy (FTIR-ATR) on upper surface to determine carbonyl index (CI) on nonarchive samples only
- Oven aging/HP-OIT (GRI-GM13)
- UV resistance/HP-OIT (GRI-GM13)

The exposed samples will be tested as follows:

- Carbon content (ASTM D1603)
- Carbon dispersion (ASTM D5596)
- Single-point SCR on molded plaque (ASTM D5397)
- Light microscopy of exposed surface, through-thickness cross sections, and thin microsections (~15 µm thick) as necessary
- HP-OIT on 0.5-mm-thick exposed surface layers from basic sheet and from sheet at edge of extruded weld bead (ASTM D5885), preferably at a double-weld bead
- FTIR-ATR on exposed surface to determine CI
- Oven aging/HP-OIT on 0.5mm surface layer (GRI-GM13)
- UV resistance/HP-OIT on 0.5 mm surface layer (GRI-GM13)

Carbon content is done to ensure adequate basic UV protection. Carbon dispersion is done to ensure uniform surface UV protection and to evaluate agglomerates that might act as initiation sites for stress cracking.

HP-OIT is used to assess the remaining amount of stabilizer additives, both in the liner panels and in the sheet adjacent to an extrusion weld. Most stress cracking is observed at the edges of extrusion weld beads in the lower sheet, so it is important to monitor this location.

While standard OIT (ASTM D3895 at 200°C) better assesses the relevant stabilizers effective at processing (melting) and welding temperatures, the relevant changes in effective stabilizer content during continued service, including in the weld zone, will be provided by measurement of HP-OIT. There will be no future high temperature transient where knowledge of S-OIT will be useful. It is expected that the liner adjacent to the weld bead will be more deficient in stabilizer than the panel itself. Therefore, S-OIT is not considered in this program.

Note that HP-OIT is measured on a thin surface layer because the surface layer may be oxidized while the body of the geomembrane may not. If material from the full thickness of the geomembrane is used it could show a significant value of OIT, implying that there is still stabilizer present and that oxidation is far from occurring. However, the surface layer could be fully oxidized with stress cracks already initiated and propagating. A crack will then propagate more easily through unoxidized material than would initiation and propagation occur in unoxidized material.

The fact that the HP-OIT meets a certain specification value in the as-manufactured condition provides no guarantee that thermo- and photo-oxidation protection will be provided for a long time. Stabilizers might be consumed quickly or slowly while providing protection. They may also be consumed quickly to begin with, then more slowly, or vice versa.

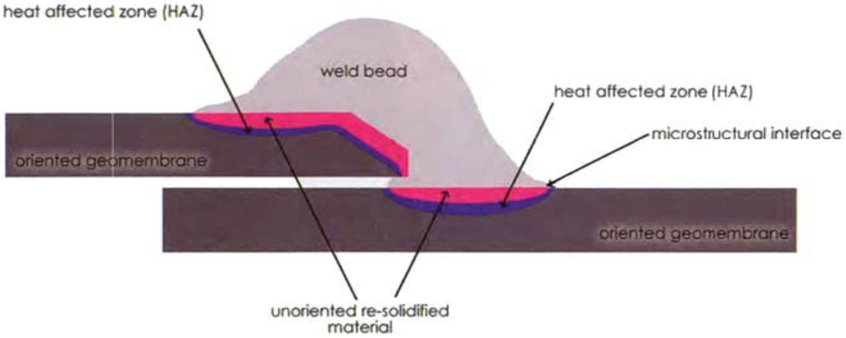

Figure 4 | Schematic of microstructure at extrusion weld

Hence, the need for continuing oven (thermal) aging and UV resistance tests. These two parameters, assessed by measuring retained HP- OIT, are critical to the assessment of remaining service life.

Oven (thermal) aging and UV resistance tests performed in this program will provide an extremely valuable data base that relates laboratory testing to in-service performance and that will further aid in more accurately projecting in-service performance from laboratory testing results.

Special considerations

Because we do not know, by OIT measurements alone, whether the surface layer is or is not oxidized (unless OIT is zero), and since we do not yet know at what level of OIT loss there might be an oxidized surface layer (the database has not yet been generated), FTIR directly on the surface of the geomembrane is performed using the attenuated total reflectance (ATR) technique to deny or confirm the presence of oxidation products (carbonyl groups).

Following the practice of Broutman, et al. (1989) and Duvall (2002) on HDPE pipes, if the ratio of the carbonyl peak at wave number 1760 cm-1 and the C-H stretching (PE) peak at wave number 1410 cm -1 is more than 0.10, there is a sufficiently oxidized surface layer that stress cracking might be initiated. For those familiar with the two slope stress rupture curve (**Figure 1**) where the brittle stress cracking region is the steeper segment below the knee, there is a third vertical part of the curve (**Figure 2**) where the material is fully oxidized and fracture occurs at the slightest stress. This is what will happen at the end of service life. But first note the times to initiation of stress cracking (the knees in the curves) in **Figure 1**—they range from ~10/hr to ~5,000/hr—clearly confirming that all HDPEs are not the same. Some are far more durable than others.

At the end of service life, at some level of OIT, there will be a critically oxidized surface layer that when stressed, such as at low temperatures by an upwards protruding stone, or by flexing due to wind uplift, will initiate a stress crack on the surface that will propagate downward through the geomembrane, as shown by the crack in **Figure 3**.

This crack, initiated at a stress concentrating surface die mark, occurred when the liner contracted at low temperatures, and tightened over an upwardly protruding stone. The straight morphology of the crack, and the ductile break at the bottom surface as the stress in the remaining ligament rose above the knee in the stress rupture curve, are typical of a stress crack. Note the shorter stress cracks initiated along other nearby die marks.

Stress cracks are preferentially initiated along the edges of welds because the adjacent geomembrane has been more depleted of stabilizers during the high temperature welding process. Thus, under further oxidizing service conditions, it will become the first location to

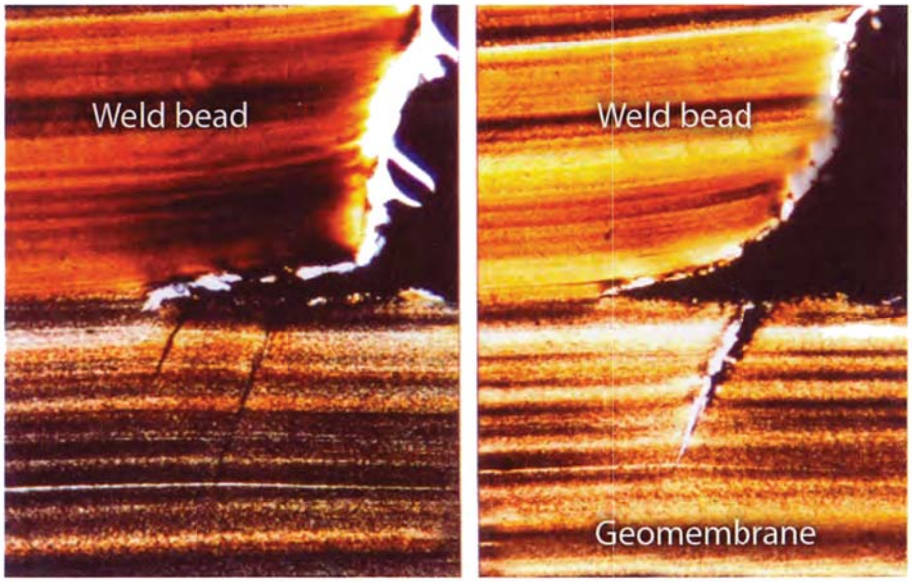

Figure 5 | Typical off-normal angle of precursor crazes (left) and stress crack (right) at edge of extrusion weld.

Type	Specification	Predicted Lifetime in Texas, USA
Side wall exposed	54	5
Side wall concrete side	81	71
Lower launder exposed	16	3
Lower launder concrete side	145	1

Table 2 | S-OIT values on solution and concrete liner surfaces (Peggs, 2008).

be oxidized to the critical level at which stress cracks will be initiated under any applied stress. In addition, the geometrical notches at grinding gouges and at the edges of the bead increase local stresses to critical levels for SC to occur.

I also believe that an internal microstructural flaw exists between the originally oriented geomembrane structure and the pool of more isotropic melted and resolidified material at the edge of the weld zone, as shown schematically in **Figure 4**. Most stress cracks occur at an off-normal angle at the edge of the weld bead that may be related to the angle of this molten-pool to oriented-structure interface (**Figure 5**). It is also known that stress increases the extraction of stabilizers from polyolefin materials.

With all of these agencies acting synergistically, it is not surprising that stress cracking often first occurs adjacent to extrusion welds.

Looking ahead

With the first field assessment test results available to us, and the extent of changes from the baseline sample known, removal of a second set of samples by the facility owner (at locations previously identified and marked by the initial surveyor), will be planned for a future time, probably in 2 or 3 years.

Why 2 or 3 years? In an extreme chemical environment, extensive reductions in S-OIT of studded HDPE concrete protection liners in mine solvent extraction facilities using kerosene/aromatic hydrocarbon/sulfuric acid process solutions at 55°C (131°F) have been observed on the solution and concrete sides of the liner (**Table 2**) within 1 year (Peggs 2008). But it is unlikely that such rapid decreases will be observed in air-exposed material.

With this second set of field samples, and with three sets of data points, practically reliable extrapolations of remaining lifetime can start to be made.

It is expected that a few years of notice for impending failures will be possible.

The key point to note in making these condition assessments is that, while all HDPE geomembranes have very similar conventional index properties, they can have widely variable photo-oxidation, thermal-oxidation, and stress-cracking resistances. Therefore, some HDPEs are more durable than others.

Thus, while one HDPE geomembrane manufactured in 1990 failed after 15 years in 2005, another HDPE geomembrane made in 1990 from a different HDPE resin (or more correctly a medium-density polyethylene [MDPE] resin), and with a better stabilizer additive package, could still have a remaining lifetime of 5, 20, or 30 years.

So, keep a close eye on those exposed liners and we'll learn a great deal more about liner performance and get notice of the end of service lifetime. And if owners can retain some archive material from new installations, so much the better.

References

Broutman L.J., Duvall, D.E., So, P.K. (1989). "Fractographic Study of a Polyethylene Sewer Pipe Failure." SPE Antec, pp 1599-1602.

Duvall, D.E. (2002). "Analyses of Large Diameter Polyethylene Piping Failures." Proceedings of the Society of Plastics Engineers, 60th Annual Technical Conference.

Gaube, E., Gebler, H., Müller, W., and Gondro, C. (1985). "Creep Rupture Strength and Aging of HDPE Pipes 30 Years Experience in Testing of Pipes." Kunststoffe 74 7, pp 412-415.

Koerner, R.M., Hsuan, Y.G., Koerner, G. (2008). "Freshwater and Geosynthetics: A Perfect Marriage." Keynote Lecture at GeoAmericas 2008, IFAI, Roseville, Minn., USA.

Hsuan, Y.G., Koerner, R.M., Lord, A.E., Jr., (1992). "The Notched Constant Tensile Load (NCTL) Test to Evaluate Stress Cracking Resistance." 6th GRI Seminar, MQC/MQA and CQC/CQA of Geosynthetics, Folsom, Pa., USA, pp 244-256.

Peggs, I.D., (2008). "The Performance of Concrete Protection liners in Mine SX/EW Mixers and Settlers: The Need for Chemical Resistance Testing." Proceedings of GeoAmericas 2008, IFAI, Roseville, Minn., USA.

ATTACHMENT III.6.B

GEOTEXTILES REFERENCE DOCUMENTATION

Technical
Note No. 7

Chemical Resistance of Amoco Polypropylene Geotextiles

Amoco woven and nonwoven geotextiles are manufactured from polypropylene with ultra violet stabilizing additives. The excellent chemical resistance of Amoco polypropylene geotextiles is one of the qualities which has established Amoco as a leading producer of geotextiles for use in the waste containment industry. This technical note addresses the chemical resistance of polypropylene with a focus on recent testing programs which have clearly demonstrated the durability of Amoco fabrics in a variety of chemical environments.

Are polypropylene geotextiles durable in the chemical environment of landfill leachates?

Yes. Of the polymers used to manufacture geotextiles, polypropylene exhibits the greatest resistance to chemical attack. In fact, polypropylene is the polymer of choice for such commonly used products as landfill liners, synthetic grass for athletic fields, outdoor carpeting, battery cases, bleach bottles, antifreeze jugs, washing machine agitators, and thousands of other commonly used items that are routinely exposed to chemical environments. Polypropylene is stable within a pH range of 2 to 13, making one of the most stable polymers.

Polypropylene geotextiles have been found to be durable in a wide range of chemical environments (Bell, et. al., 1980; Haxo, 1978, 1983; Pucetas, et.al., 1991; Tisinger, et. al., 1989). Research has found both woven and nonwoven polypropylene geotextiles to be non-biodegradable and resistant to commonly encountered soil-bound chemicals, landfill achates, mildew, and insects.

How is the chemical resistance of polypropylene geotextiles determined?

Numerous laboratory test programs have subjected polypropylene to severe chemical environments such as solutions of organic solvents, oils, organic acids, and inorganic acids. The laboratory tests are generally performed in accordance with ASTM D 543, "Standard Test Method for Resistance of Plastics to Chemical Reagents." These test programs have found polypropylene to exhibit superb chemical resistance.

In the ASTM D 543 procedure, the specimens are immersed in a concentrated chemical solution at a specified temperature for a specified exposure period. This test method exposes the polypropylene to etremely harsh conditions which are considerably more severe than those encountered in most civil engineering applications.

The chemical compatibility of geotextiles with leachates is determined by EPA Test Method 9090 (EPA 9090), *"Compatibility Test for Wastes and Membrane Liners."* This was the laboratory method used in the Amoco geotextile test programs reported in this technical note. Geotextile samples are immersed in a constant temperature leachate bath for four months. At the end of each month samples of the fabric are removed and subjected to physical testing. Changes in properties may indicate chemically imposed degradation.

Have Amoco geotextiles been proven to be chemically resistant?

Four laboratory testing programs have been performed to evaluate the chemical compatibility of Amoco geotextiles with landfill leachates. The tests exposed both Amoco woven and nonwoven products to hazardous and municipal waste leachates.

In all testing programs there was no indication of geotextile degradation due to exposure to landfill leachates. The test results are summarized in the remainder of this technical note.

Hazardous waste leachate

A laboratory testing program was performed in 1989 to evaluate the chemical compatibility of Amoco geotextiles with a hazardous waste leachate. The program included EPA 9090 testing of 4 oz/yd^2 and 8 oz/yd^2 nonwoven specimens. The testing exposed the geotextiles to leachate in both the laboratory and in a leachate collection sump at a hazardous waste landfill.

Test evaluation incorporated detailed microstructural analyses which are not typically incorporated into chemical resistance testing programs. Methods included differential scanning calorimetry, thermal gravimetric analysis, and infrared spectrophotometry. These analyses were performed to identify any changes in the microstructure of the geotextile due to immersion in the leachate.

The results of this testing program found the geotextile microstructure remained intact, stable, and unchanged (Tisinger, et. al., 1989).

Municipal waste leachate

The chemical resistance of Amoco geotextiles to municipal solid waste leachate was evaluated in three laboratory testing programs. The first program, completed in 1990, included EPA 9090 testing of 16 oz/yd^2 nonwoven geotextile specimens. The second test program, performed in 1992, tested specimens of 8 oz/yd^2 nonwoven geotextile. The third program, completed in 1993, evaluated the chemical resistance of a high strength woven geotextile. The testing programs evaluated changes in physical properties of the specimens, including specimen dimensions, thickness, grab tensile strength and elongation, puncture resistance, burst strength, and tear strength. In all cases there were no measurable changes in physical properties of the specimens after exposure to the leachate.

Are the results of these tests applicable to Amoco geotextiles which have not been similarly tested?

Yes. All Amoco geotextiles are equally resistant to chemical degradation because they are all manufactured using the same polymer and additives. This conclusion is supported by the test results, which demonstrated no difference in chemical resistance for different types of Amoco geotextiles. The information in this technical note, therefore, is considered to be applicable to all Amoco geotextiles regardless of weight, thickness, or strength.

References

Bell, J.R., et. al., "*Evaluation of Test Methods and Use Criteria for Geotechnical Fabrics in Highway Applications,*" Federal Highway Administration, FHWA/RD-80-021, 1980, 202 p.

EPA Method 9090, "Compatibility Test for Wastes and Membrane Liners,"
Test Methods for Evaluating Solid Waste, Physical/Chemical Methods, US Environmental Protection Agency, EPA 530/SW-846, 1988.

Haxo, R.S., "Chemical Resistance of Lining Materials with Different Waste Fluids," *Proceedings of the Colloque sur l'Etanche'ite' Superficielle des Bassins, Barrages* et Canaux, Paris, France, 1983, pp. 13-20.

Haxo, R.S., "Interaction of Selected Lining Materials with Various Hazardous Wastes," *Proceedings of the Fourth Annual Research Symposium on Land Disposal of Hazardous Wastes,* EPA-600/9-78-016, Southwest Research Institute, US Environmental Protection Agency, Solid and Hazardous Waste Research Division, San Antonio, TX, 1978, pp. 256-273.

Pucetas, R.C., Verschoor, K.L., Allen, S.R., and Sprague, C.J., "The Chemical Resistance of Geotextiles to be Used in Secondary Containment Systems for Underground Storage Tanks," *Geosynthetics '91 Conference Proceedings,* Atlanta, GA, published by the Industrial Fabrics Association International,
St. Paul, MN, 1991, pp. 311-314.

Tisinger, L.G. and Dudzik, B.E., "An Evaluation of Chemical Resistance Test Results of Nonwoven, Needle-Punched Polypropylene Geotextile Exposed to Hazardous Waste Landfill Leachate," *Sardinia '89 2nd International Landfill Symposium,* 1989.

Amoco Fabrics and Fibers Company
260 The Bluffs
Austell, GA 30168
770-984-4444 800-445-7732
770-944-4584 · fax
email address: geotextiles@bp.com
http://geotextile.com
Part of the BP Amoco Group

Code 94-007/3,000/12-97

Technical Note No. 14

AMOCO GEOTEXTILES

Amoco Fabrics and Fibers Company

Geotextile Polymers for Waste Applications

What types of polymers are used to manufacture geotextiles?

Virtually all geotextile fibers are made from either polypropylene or polyester polymers.

Are these polymers used in a 100% pure form?

The manufacture of geosynthetics usually includes the addition of stabilizers and other additives that are blended with the base polymer. The additives constitute a minor fraction of the polymer mixture.

Additives are used primarily to counteract the effects of oxidation, to which many synthetic polymers are sensitive. Oxidation can cause a reduction in material properties such as strength and elasticity. The main sources of oxidation are heat/temperature (thermal oxidation) and ultra violet (UV) radiation from sunlight (photo-oxidation). Manufacturers of geosynthetics add a variety of proprietary additives during production to make the polymers more stable against thermal and UV degradation (see Amoco Technical Note No. 9).

Should the designer specify polypropylene or polyester for geotextiles to be used in waste applications?

The type of polymer used in the fabrication of the geotextile is not a relevant design parameter. The specifications should be developed to focus on the required physical properties of the geotextile relative to strength, hydraulic performance, and chemical compatibility and durability. These elements are addressed in detail in the Amoco Waste-Related Geotextile Guide Specifications.

Does the type of base polymer affect the chemical resistance of geotextiles used in landfills?

Geotextiles in landfills are exposed to leachates, which are generally dilute solutions of chemicals. The geotextile must be resistant to degrading in this chemical environment. Chemical resistance of geotextiles to leachates is evaluated in the laboratory using EPA Test Method 9090 (EPA 9090). The results of such testing on polypropylene and polyester have proved both polymers to be relatively inert and durable in various chemical environments of hazardous and nonhazardous waste landfills (refer to Amoco Technical Note No. 7).

Of the polymers used to manufacture geotextiles, polypropylene exhibits the greatest resistance to chemical attack. Polypropylene is inert to most chemicals except for some highly concentrated solvents. Geotextiles are not expected to be exposed to such solvents in waste applications, where the associated leachates typically contain only trace to very low concentrations of solvent constituents.

Polyester exhibits comparable chemical compatibility. However, unlike polypropylene, polyester is subject to hydrolysis in aqueous environments such as landfill leachates. Hydrolysis is a process in which water-based solvents or water alone causes the polymer chains to break. This can result in a reduction in the mechanical properties of the polymer. Despite this characteristic, the results of EPA 9090 testing on polyester do not show an impact from hydrolysis.

What effect does polymer type have on the UV resistance of geotextiles used in landfills?

There are only slight differences in the UV stability of various geotextile polymers. From a construction perspective, these differences have no impact on the selection of geotextiles for landfill applications. Regardless of the polymer type, it is important to limit exposure of the geotextile to potentially damaging UV radiation.

In landfill applications, geotextiles are usually covered by soil layers and waste soon after construction. Their exposure to UV radiation therefore generally occurs only during construction. Regardless of polymer type, exposure of the fabrics to sunlight during installation should be limited in accordance with the project specifications (see Amoco Waste-Related Geotextile Guide Specifications).

On some landfill side slopes, the geotextile might be left exposed for an extended time before being covered with soil. In these cases, the geotextile must be protected from UV radiation by alternative methods, regardless of whether the fabric is manufactured of polypropylene or polyester. Alternatives include covering the geotextile with a sacrificial geotextile layer or opaque plastic sheet. The sacrificial layer would be removed prior to placing soil cover.

Has the performance of Amoco geotextiles in landfill applications been verified?

Yes. In fact, the excellent chemical resistance of Amoco polypropylene geotextiles is one of the qualities that has established Amoco as a leading supplier of fabrics to the waste containment industry.

Laboratory testing programs have been performed specifically to evaluate the chemical compatibility of Amoco polypropylene geotextiles with landfill leachates. In all test cases there were no measurable changes in the physical properties of the Amoco geotextiles after exposure to leachates. Also, unlike polyester, polypropylene does not undergo hydrolysis. Amoco Technical Note No. 7 provides detailed information regarding the chemical compatibility test conditions, procedures, and results.

References

Amoco Fabrics and Fibers Company, *Technical Note No. 7, Chemical Resistance of Amoco Polypropylene Geotextiles.*

Amoco Fabrics and Fibers Company, *Technical Note No. 9, Ultra Violet Light Degradation.*

Amoco Fabrics and Fibers Company, *Technical Note No. 12, Staple Fiber and Continuous Filament Polypropylene Geotextiles: A Comparison.*

Amoco Fabrics and Fibers Company, *Waste-Related Geotextile Guide Specifications.*

EPA Method 9090, "Compatibility Test for Wastes and Membrane Liners," *Test Methods for Evaluating Solid Waste, Physical/Chemical Methods, Environmental Protection Agency,* EPA 530/SW-846, 1988.

GeoSyntec Consultants, Correspondence to Amoco Fabrics and Fibers Company, Atlanta, GA, July 1993.

Amoco Fabrics and Fibers Company 900 Circle 75 Parkway, Suite 550 Atlanta, Georgia 30339 (770) 984-4444
FAX: (770) 956-2430

Code 94-014/3000/12-97

ATTACHMENT III.6.C

GEONET REFERENCE DOCUMENTATION

PRODUCT DATA SHEET

GSE TenDrain 275 mil Geocomposite

GSE TenDrain geocomposite consists of a 275 mil thick GSE TenDrain geonet heat-laminated on one or both sides with a GSE nonwoven needle-punched geotextile. TenDrain 275 is comprised of a tri-planar structure consisting of middle ribs that provide direct channelized flow, with diagonally placed top and bottom ribs. The geotextile is available in mass per unit area range of 6 oz/yd^2 to 16 oz/yd^2. TenDrain 275 geocomposite provides high transmissivity under high and low loads.

[*]

AT THE CORE:
A 275 mil thick TenDrain geonet heat-laminated on one or both sides with a nonwoven needlepunched geotextile.

Product Specifications

Tested Property	Test Method	Frequency	Minimum Average Roll Value(1)	
Geocomposite			**6 oz/yd^2**	**8 oz/yd^2**
Transmissivity(2), gal/min/ft, (m^2/sec) Double-Sided Composite	ASTM D 4716	1/540,000 ft^2	24.2 (5x10^{-3})	24.2 (5x10^{-3})
Ply Adhesion, lb/in	ASTM D 7005	1/50,000 ft^2	0.5	0.5
Geonet Core(1,3) – GSE TenDrain				
Geonet Core Thickness, mi	ASTM D 5199	1/50,000 ft^2	275	275
Density, g/cm^3	ASTM D 1505	1/50,000 ft^2	0.94	0.94
Tensile Strength (MD), lb/in	ASTM D 7179	1/50,000 ft^2	75	75
Carbon Black Content, %	ASTM D 4218	1/50,000 ft^2	2.0	2.0
Creep Reduction Factor(4)	GRI-GC8	per formulation	1.2	1.2
Compressive Strength, psf	ASTM D 6364	1/540,000 ft^2	60,000	60,000
Geotextile(1,3)				
Mass per Unit Area, oz/yd^2	ASTM D 5261	1/90,000 ft^2	6	8
Grab Tensile Strength, lb	ASTM D 4632	1/90,000 ft^2	160	220
Grab Elongation	ASTM D 4632	1/90,000 ft^2	50%	50%
CBR Puncture Strength, lb	ASTM D 6241	1/90,000 ft^2	435	575
Trapezoidal Tear Strength, lb	ASTM D 4533	1/90,000 ft^2	65	90
AOS, US sieve(1), (mm)	ASTM D 4751	1/540,000 ft^2	70 (0.212)	80 (0.180)
Permittivity, sec^{-1}	ASTM D 4491	1/540,000 ft^2	1.5	1.3
Water Flow Rate, gpm/ft^2	ASTM D 4491	1/540,000 ft^2	110	95
UV Resistance, % retained	ASTM D 4355 (after 500 hours)	per formulation	70	70
NOMINAL ROLL DIMENSIONS(5)				
Roll Width, ft			12.75	12.75
Roll Length, ft	Double-Sided Composite		200	200
Roll Area, ft^2	Double-Sided Composite		2,550	2,550

NOTES:

- (1) All geotextile properties are minimum average roll values except AOS which is maximum average roll value and UV resistance is typical value. Geonet core thickness is minimum average value.
- (2) Gradient of 0.02, normal load of 7,000 psf, boundary condition: plate/sand/geocomposite/geomembrane/plate, water at 70°F for 1 hour.
- (3) Component properties prior to lamination.
- (4) 10,000 hour creep test under 10,000 psf at 70°F temperature.
- (5) Roll widths and lengths have a tolerance of ±1%.

GSE is a leading manufacturer and marketer of geosynthetic lining products and services. We've built a reputation of reliability through our dedication to providing consistency of product, price and protection to our global customers.

Our commitment to innovation, our focus on quality and our industry expertise allow us the flexibility to collaborate with our clients to develop a custom, purpose-fit solution.

[DURABILITY RUNS DEEP] For more information on this product and others, please visit us at GSEworld.com, call 800.435.2008 or contact your local sales office.

GSE ENVIRONMENTAL™

Proceedings of the 4th Asian Regional Conference on Geosynthetics
June 17 - 20, 2008 Shanghai, China

EVALUATION ON STRESS CRACKING RESISTANCES OF VARIOUS HDPE DRAINAGE GEONETS

M.S. Mok[1], E. Blond[2], J. Mlynarek[3] and H. Y. Jeon[4]

ABSTRACT: Specimens from each geonet were placed under various compressive loads in a vessel containing a solution of 10% surface-active agent and 90% water at a temperature of 50°C. Then the surface morphology study of the specimen was performed after 500 hours test duration. The results show that all of these geonets did not appear any kind of stress cracking in the condition of 400 kPa, which is a typical landfill's loading condition. However, in the case of bi-planar geonet there were some deposits on the surface of geonet's strand and it is expected that this phenomena is due to the results of chemical clogging. On the other hand, in the case of the tri-planar and circular type bi-planar geonets, it maintained very clean flow channels until the end of the test. For high normal pressure some environmental stress cracks were detected for the circular type bi-planar geonet. The results show that the resistance to the environmental stress cracking is related to its polymer density, crystallinity and also rigidity not its mechanical properties.

KEYWORDS: geonet, compressive loads, surface morphology, stress cracking, chemical clogging, flow channels

INTRODUCTION

Land filling, by all indications, will continue to be the predominant method of solid waste disposal. As the use of high density polyethylene (HDPE) geonets increase in landfill applications, it is required to evaluate their long-term properties in several chemical conditions. (Ward and Brown 1990; Carlson 1993)

Typically, the high crystallinity of polyethylene geonets provides an excellent chemical resistance to harsh chemical leachate, however can be problematic with regard to environmental stress cracking. (Qian and Brown 1993; Thomas 1998) Under low stresses in the circumstance of room temperature polyethylenes will fracture by slow crack growth. This mode of failure limits the lifetime of polyethylenes used in critical applications as drainage materials, lining under landfills. (Lagaron, Pastor, Kip 1999; Bobsein 1999)

Geomembranes and geonets are used as a barrier and drainage component in this system, respectively. With addition of carbon black which is an anti-oxidation material HDPE geomembranes and geonets are normally used in hazardous landfill system as a barrier and drainage respectively.

Many researchers and a lot of work about environmental stress cracking resistance for the geomembranes were done and many beneficial reports have already been published. (Peggs and Kannien 1995; Thomas and Deschepper 1993) However a few research results on the environmental stress cracking resistance for the geonet drainage material were performed. Therefore, in this study the resistance to environmental stress cracking (ESCR) was examined mainly in morphological issues for various geonets (bi-planar, tri-planar and circular type of bi-planar geonet) under condition of various normal pressures.

SPECIMEN & TEST METHODS

Total three types of geonets were test in this study. Sample A has 5.6 mm mean value of thickness and two layers which means bi-planar geonet. The cross sectional shape of strand of Sample A is more likely to a square. Sample B has average of 8.6 mm thickness and has 3 layers (tri-planar). Sample C is also bi-planar geonet however has circular type cross sectional shape and thicker than sample A. The raw material of all these samples is high density polyethylene (HDPE). Typical specifications of the samples are provided in Table 1.

Fig. 1 shows these samples. Short-term compressive deformation test was performed using the procedures set forth in Standard Test Method for Determining Short-term Compression Behavior of Geosynthetics (ASTM

---

[1] Researcher, CTT Group/SAGEOS, Saint-Hyacinthe, Quebec, CANADA, Email: munsungmok@gmail.com
[2] Director, CTT Group/SAGEOS, Saint-Hyacinthe, Quebec, CANADA, Email: eblond@gcttg.com
[3] CEO, CTT Group/SAGEOS, Saint-Hyacinthe, Quebec, CANADA, Email: jmlynarek@gcttg.com
[4] Professor, Division of Nano-Systems Engineering, Inha University, Incheon, KOREA, Email: hyjeon@inha.ac.kr

D6364) to evaluate basic mechanical properties of samples. Specimen is positioned between two rigid steel platens and compressed at a constant rate of 1.0 mm/min. To control an accurate temperature of specimen of 23°C heating platens were manufactured and its heating is 14°C/min. Also special test equipment for ESCR under compression was manufactured and this equipment is shown Fig. 2.

The specimens were immersed in a solution of 90% water and 10% I-gepal CO630 at a temperature of 50°C. The solution level was checked daily and de-ionized water used to keep the bath at a constant level.

And the solution was replaced every 2 weeks. 200, 400 and 700 kPa for sample A, 600, 1,000 and 1,200 kPa for sample B and 400, 600 and 800 kPa for C of load were subjected as compressive load using 6:1 arm lever loading system within considering their compressive strengths.

The immersion duration was 500 hours and during and after the test apparent observation and microscopic morphology was evaluated for the specimen.

Table 1 Typical specification of the samples

Property	Test method	Unit	Sample		
			A	B	C
Thickness	ASTM D5199	mm	5.6	8.6	8.2
Mass per unit area	ASTM D5261	g/m^2	920	1700	2300
Carbon black	ASTM D4218	%	2.3	2.2	2.3
Density	ASTM D1505	g/cm^3	0.942	0.944	0.940
Crystallinity	ASTM D2910	%	56	55	61

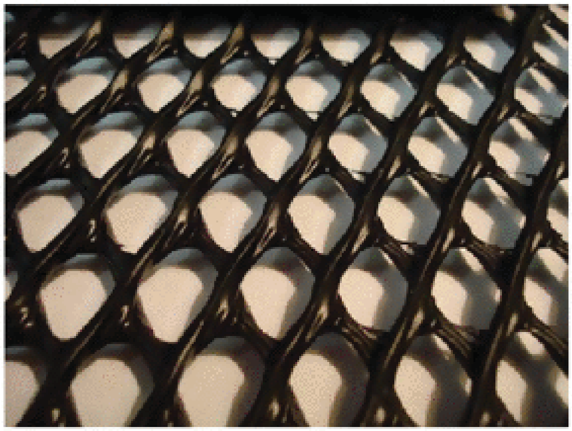

(a) Sample A

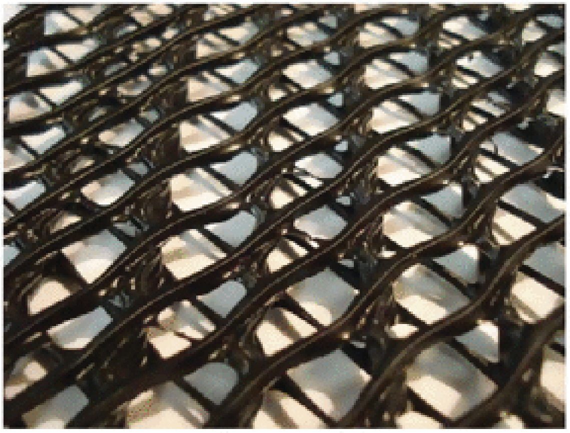

(b) Sample B

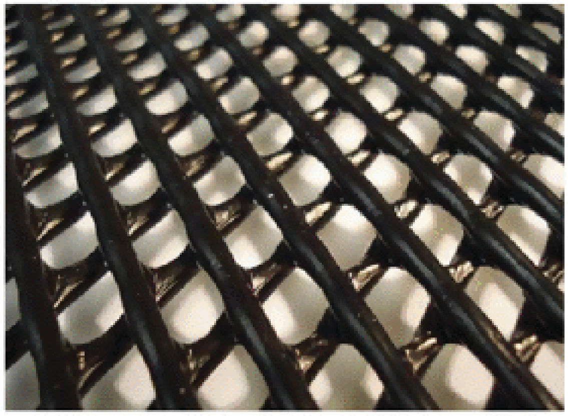

(c) Sample C

Fig. 2 Compressive environmental stress cracking test equipment

RESULTS & DISCUSSION

Considering the compressive strength and strain properties, the sample C has the stiffest behavior in these three Samples. Initial 5% elastic modulus is much higher than other samples. From this behavior of Sample C it is expected that sample C has rigid structure and has high crystallinity of over 60%. Table 1 confirms this phenomenon. In the other hand Sample A and C have more flexible behavior and low initial elastic modulus.

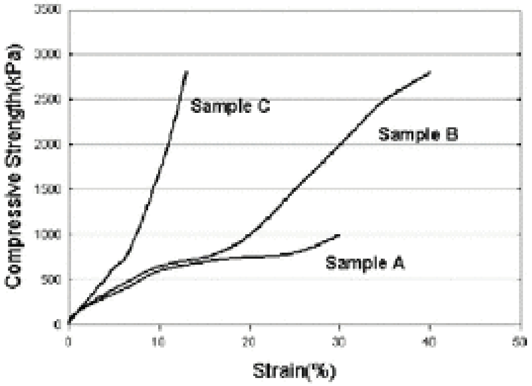

Fig. 3 Short-term compression test results

Figs. 4—9 exhibit the results of apparent observations and microscopic morphologies. Some kind of chemical clogging due to the I-gepal solution is expected for the Sample A because of its flow channel and thickness. This chemical clogging for the Sample A was confirmed by the apparent observation. Fig. 4 shows the results of apparent observations for Sample A. In this figure many deposits on the surface of the specimens were detected during and end of the test and it seems that these deposits which were induced from the chemical solution may occur clogging and therefore affect geonet's in-plane flow capacity. Also there is no chemical clogging on the surface of the specimen for Sample B and this fact was confirmed by apparent observation (Fig. 5).

Considering flowing pattern of the I-gepal solution through out the specimen, the I-gepal has zig-zag flow pattern and this courses some frictions with strands of sample A, therefore the chance of clogging is higher than the Sample B which has straight flow pattern. Also thin thickness compared to other samples can increase chance of any clogging. For the Sample C, the initial creep deformation was very low which means the initial modulus is higher than the other samples and therefore high modulus indicate more rigid than others. High rigidity has brittle failure pattern rather than ductile failure and this can induce a stress crack during the compressive creep test. Also it seems that the chemical act a stress cracking accelerator.

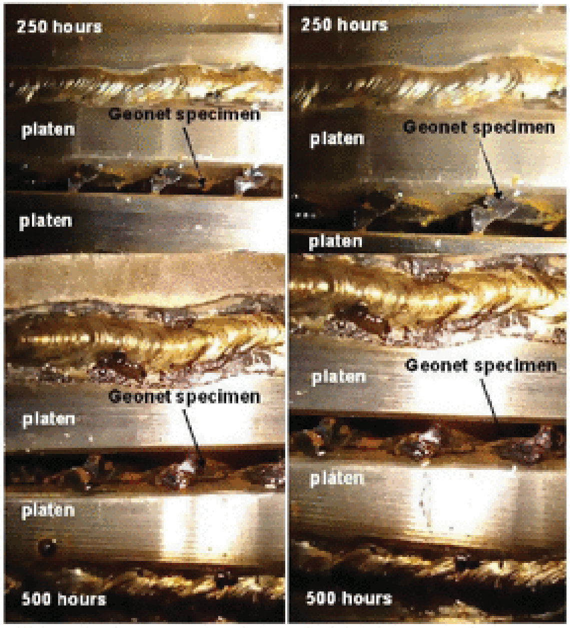

Fig. 4 Apparent observation during and end of the test for sample A (200kPa)

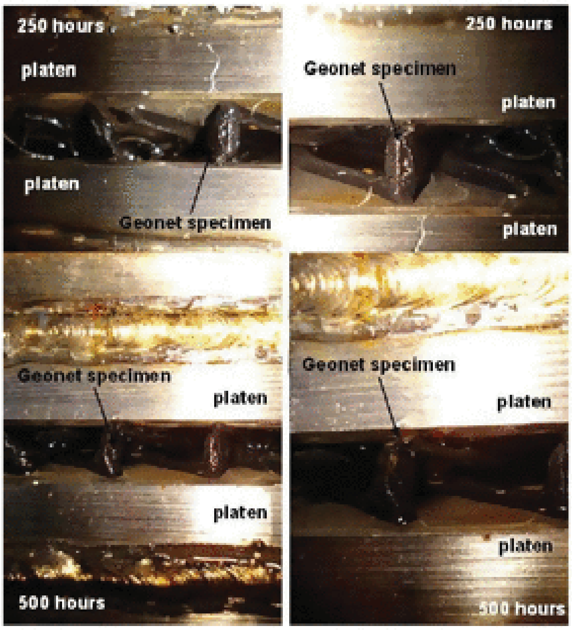

Fig. 5 Apparent observation during and end of the test for sample B (700 kPa)

Figs. 6—9 confirm this environmental stress cracking phenomenon. From these exhibitions it is clear that Sample A and Sample B which have relatively more flexible HDPE strand than Sample C didn't experience any kind of environmental stress cracking. For the Sample C which is more rigid and has high crystallinity (Table 1) likely has to chance of stress cracking. The microscopic morphologies indicate that the extent of environmental stress cracking observed in the Sample C is related to its flexibility and crystallinity. And from the morphologies it seems that the stress cracks occurred at the junction point of the strands first and then propagate to strands with increasing normal pressure.

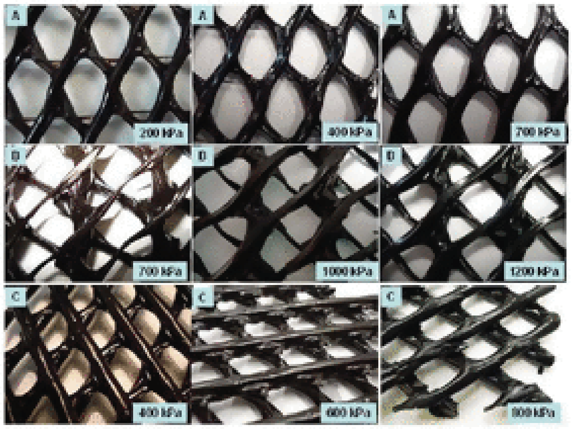

Fig. 6 Apparent observations end of the test for samples under various normal pressures

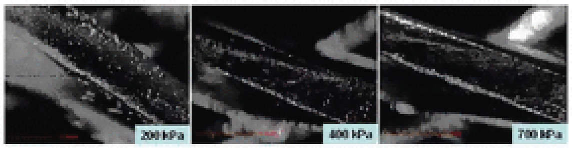

Fig. 7 Microscopic morphologies of Sample A after the test for various normal pressures

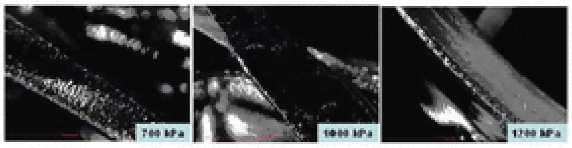

Fig. 8 Microscopic morphologies of Sample B after the test for various normal pressures

Fig. 9 Microscopic morphologies of Sample C after the test for various normal pressures

CONCLUSIONS

In this study long-term (500 hours) environmental stress cracking resistance for various geonets under various normal pressures were evaluated. The conclusions are as follows:

1. ESCR property is one of the most critical parameters for evaluating long-term chemical resistance of HDPE geonets which used in hazardous landfill systems.
2. Traditional bi-planar geonets which have square type strand and tri-planar geonet have very strong chemical and stress cracking resistance even high normal pressure.
3. Cylindrical type bi-planar geonets is more rigid material than other samples and it is very week to environmental stress cracking with increasing normal pressure

REFERENCES

Bobsein RL (1999) factors influencing SP-NCTL test results, Proceedings of the 13th GRI Seminar: 46-57

Carlson, DS, etc. (1993) laboratory evaluation of HDPE geomembrane seams, Geosyntheitcs 93, Vancouver, Canada: 1543

Lagaron JM, Pastor JM, Kip BJ (1999) Polymer 40: 1629-1636

Peggs ID, Kannien MF (1995) Geosynthetics International 2(1)

Qian R, Lu X, Brown N (1993) Polymer 34(22)

Thomas, RW (1998) evaluating the stress crack resistance of HDPE seams, 6th International Conference on Geosynthetics

Thomas RW, Deschepper BW (1993) stress crack testing of unnotched HDPE geomembrane and seams, Proceedings of the 7th GRI seminar Dec. 14-15

Ward AL, Lu X, Brown N (1990) Polymer Engineering and Science, Sep 30(18)

ATTACHMENT III.6.D

GEOSYNTHETIC CLAY LINER REFERENCE DOCUMENTATION

geosynthetic clay liners • geosynthetic clay liners • geosynthetic clay liners

CETCO
LINING TECHNOLOGIES

Laboratory Data Reports

THE EFFECTS OF LEACHATE ON THE HYDRAULIC CONDUCTIVITY OF BENTOMAT®

Compatibility testing was performed to determine the effects of solid waste landfill leachate on the permeability of Bentomat over a prescribed time period. Testing was performed in accordance with United States Environmental Protection Agency (USEPA) Method 9100, as provided in SW846.

Hydration of specimens was conducted using de-aired tap water for approximately 48 hours. Saturation was also conducted using de-aired tap water until a minimum B value of 0.95 was achieved. Following hydration and saturation, baseline hydraulic conductivity was performed using water. After the baseline hydraulic conductivity was established, the permeant was switched to leachate. Testing continued for an additional 30 days to allow a sufficient number of pore volumes to permeate the specimen to establish a hydraulic conductivity with leachate.

Results show that the hydraulic conductivity of Bentomat was unaffected when permeated with this leachate.

TR-101A
Revised 12/00

TR-101A

FINAL REPORT

LABORATORY TESTING OF BENTOMAT

Prepared for

American Colloid Company
One North Arlington
1500 West Shure Drive
Arlington Heights, Illinois 60004-1434

Prepared by

GeoSyntec Consultants
Geomechanics and Environmental Laboratory
1600 Oakbrook Drive, Suite 565
Norcross, Georgia 30093

GeoSyntec Consultants Project Number: GL1614

31 July 1991

2. TEST PROCEDURES

2.1 Task 1: EPA 9100 Compatibility Testing

Compatibility testing on the Bentomat was performed to measure the effect of leachate on the hydraulic conductivity of the mat product over a prescribed period of time. Testing was performed in accordance with the United States Environmental Protection Agency (USEPA) Method 9100 SW-846, Revision 1, 1987. The test conditions for Task 1 were as follows:

- Testing was conducted using flexible-wall triaxial permeameters, as shown in Photograph 2.1-1.
- Three replicate samples of the Bentomat were tested.
- Each sample was trimmed to a diameter of 2.8 in. (70 mm) and assembled in the following test configuration (from bottom to top): porous stone/filter paper/sand layer/Bentomat/sand layer/filter paper/porous stone.
- Hydration and saturation of the samples using de-aired tap water was conducted at an effective stress of 2.0 psi (14 kPa) for a time period of approximately 48 hours. Saturation was defined as a minimum Skempton's B-parameter of 0.95.
- Consolidation of the saturated test samples was performed at an effective stress of 5.0 psi (35 kPa). Pore-water displacement was monitored until primary consolidation was complete.
- To determine the baseline hydraulic conductivity, the samples were permeated using de-aired tap water. The average hydraulic gradient used for baseline permeation was approximately 50. For this testing program, initial hydration and saturation was

conducted using de-aired tap water. Hydration with leachate may or may not yield different results.

- After establishing the baseline hydraulic conductivity, the permeant was switched to the leachate. Because of the slow permeation rates and the objective to increase the volume of leachate in contact with the Bentomat, the sand layer was replaced on all samples by an Amoco 4516 geotextile after approximately three weeks of testing. Permeation of the samples with the leachate continued for an additional 30 days. The hydraulic conductivity of the sample was monitored and reported daily during this period.

- Permeation of the test specimens with the leachate was initially conducted at an average hydraulic gradient of approximately 50. In order to increase flow through the Bentomat during the prescribed time period, the average hydraulic gradient was increased to approximately 160.

- Because the final hydrated thickness of the Bentomat is unknown until the completion of testing and for comparison of the test data, the hydraulic conductivity was calculated using 0.4 in. (1.0 cm) for the Bentomat. These values were used in all calculations of hydraulic conductivity in Tasks 1 through 7.

TABLE 3.1-1

EPA 9100 COMPATIBILITY TESTING
BENTOMAT SPECIMEN CONDITIONS

American Colloid Company

Parameters	Specimen No. 1		Specimen No. 2		Specimen No. 3	
	Initial	Final	Initial	Final	Initial	Final
Thickness, in.	0.29	0.39	0.33	0.43	0.28	0.36
Diameter, in.	3.01	3.14	3.19	3.30	3.11	3.18
[1]Dry Mass, g	30.8	24.4	38.3	31.4	34.4	26.1
[2]Mass/Area, lb/ft^2	1.37	1.00	1.54	1.16	1.44	1.05
Water Content, %	18.8	170.1	15.7	169.4	10.9	167.4

Notes:

[1] The dry mass includes the dry weight of the bentonite and the geotextiles bonded to the specimen.

[2] The mass/area is determined using the dry mass of the material normalized with respect to the cross-sectional area of the test specimen before drying.

EPA 9100 COMPATIBILITY TESTING
BENTOMAT SAMPLE #EL005

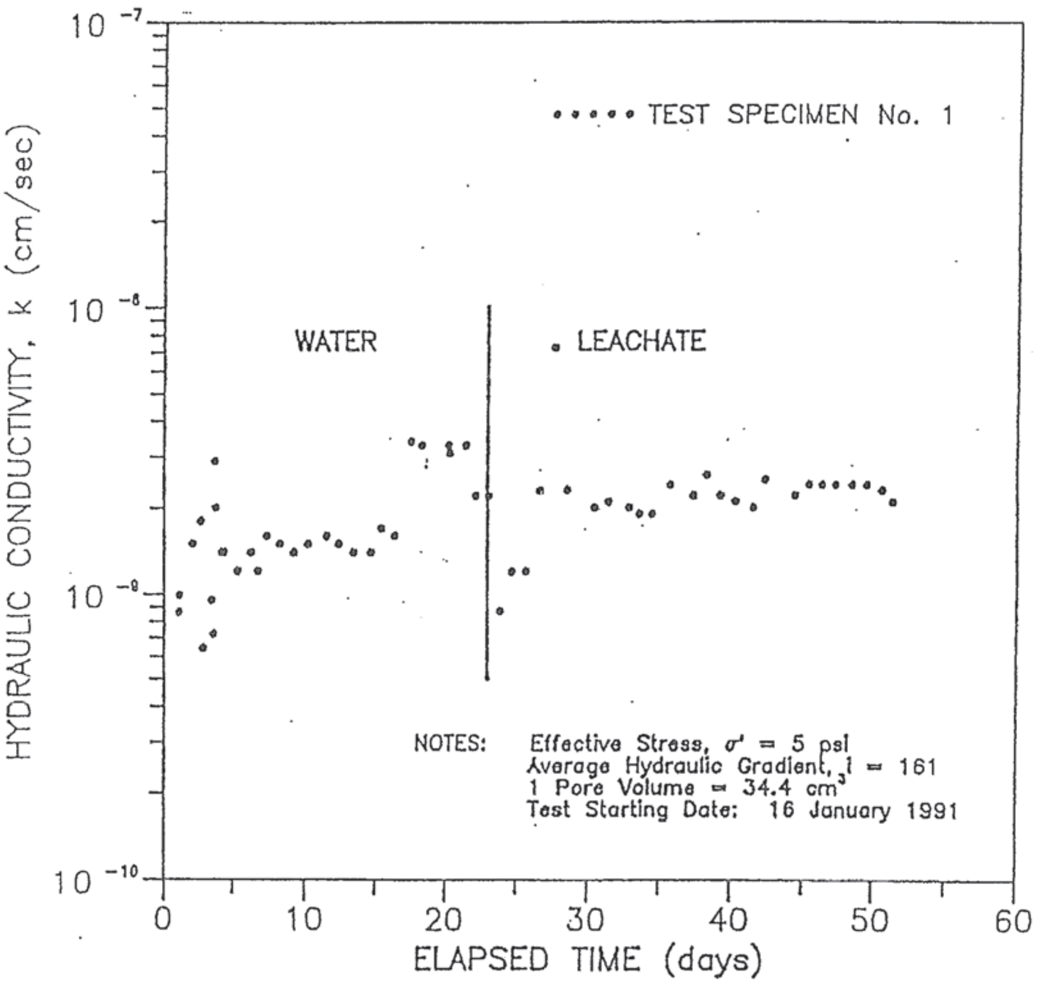

NOTES: Effective Stress, σ' = 5 psi
Average Hydraulic Gradient, i = 161
1 Pore Volume = 34.4 cm^3
Test Starting Date: 16 January 1991

GeoSyntec Consultants
GEOMECHANICS AND ENVIRONMENTAL LABORATORY

FIGURE NO.	3.1-1
PROJECT NO.	GL1614
DOCUMENT NO.	GEL91066
PAGE NO.	

EPA 9100 COMPATIBILITY TESTING
BENTOMAT SAMPLE #EL005

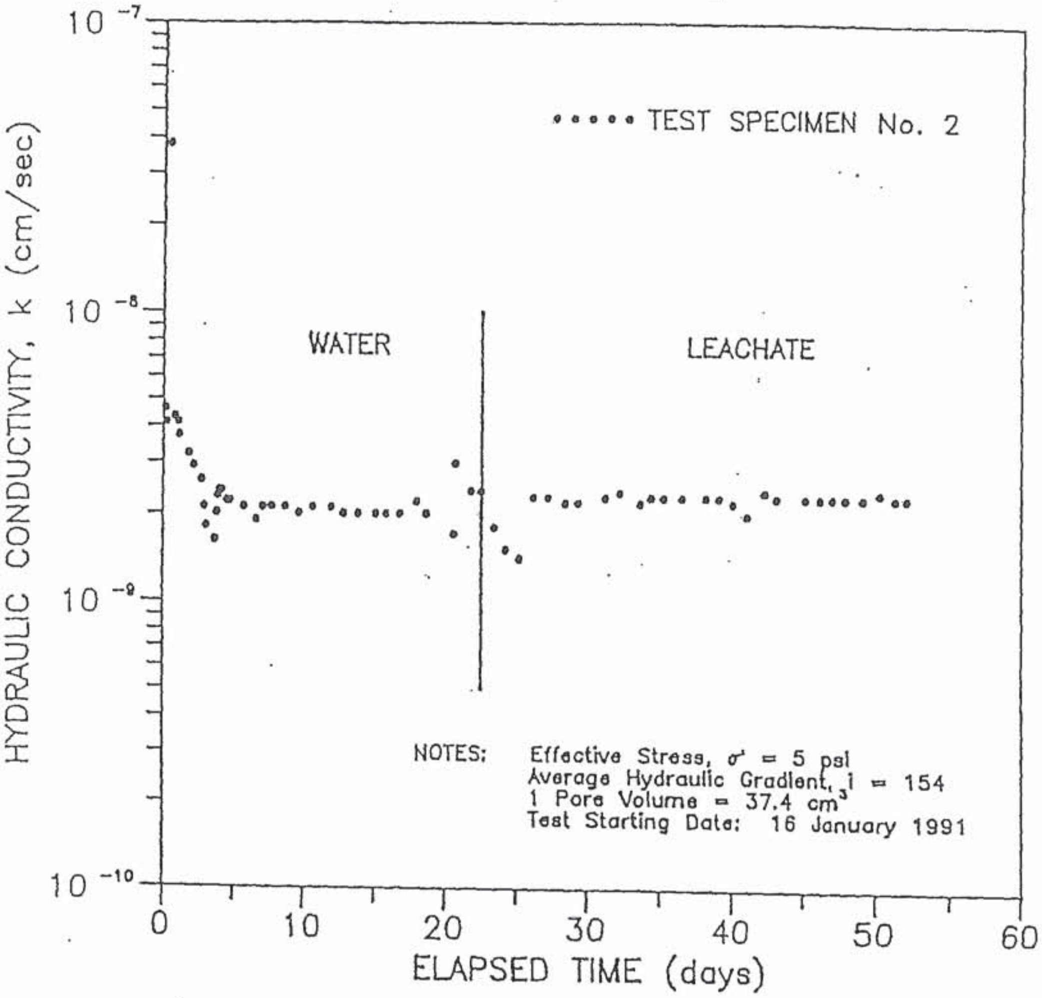

NOTES: Effective Stress, σ' = 5 psi
Average Hydraulic Gradient, i = 154
1 Pore Volume = 37.4 cm^3
Test Starting Date: 16 January 1991

GeoSyntec Consultants
GEOMECHANICS AND ENVIRONMENTAL LABORATORY

FIGURE NO.	3.1-2
PROJECT NO.	GL1614
DOCUMENT NO.	GEL91066
PAGE NO.	

EPA 9100 COMPATIBILITY TESTING
BENTOMAT SAMPLE #EL005

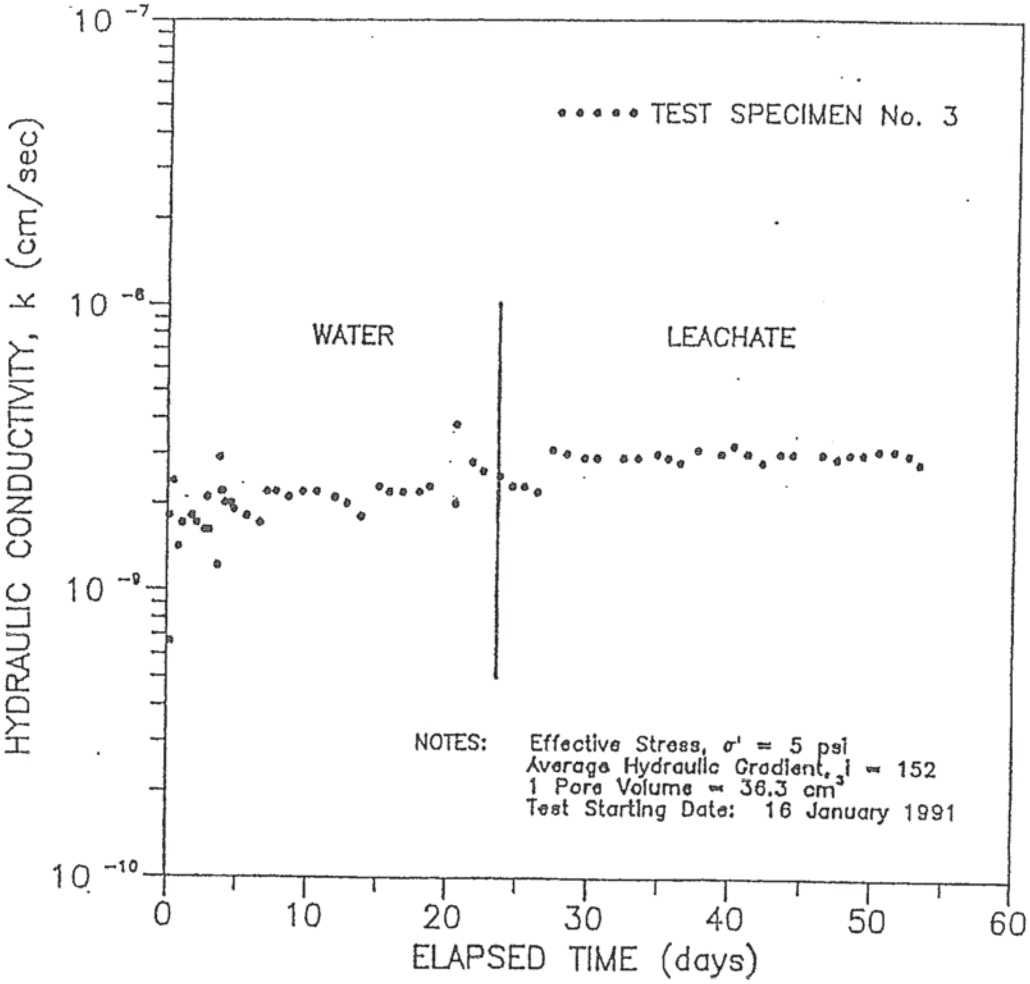

NOTES: Effective Stress, σ' = 5 psi
Average Hydraulic Gradient, i = 152
1 Pore Volume = 36.3 cm^3
Test Starting Date: 16 January 1991

GeoSyntec Consultants

FIGURE NO.	3.1-3
PROJECT NO.	GL1614
DOCUMENT NO.	GFL91066

EPA 9100 COMPATIBILITY TESTING
BENTOMAT SAMPLE #EL005

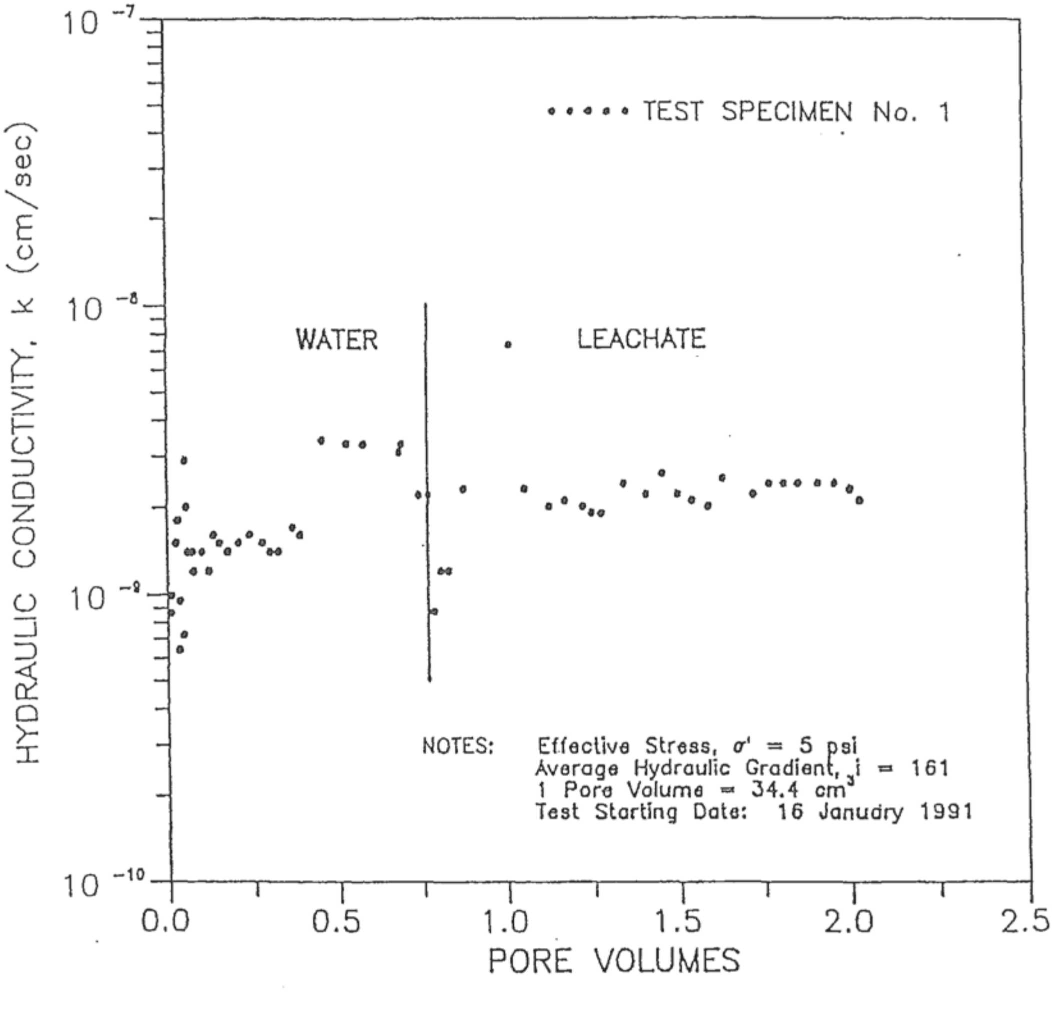

NOTES: Effective Stress, $\sigma' = 5$ psi
Average Hydraulic Gradient, i = 161
1 Pore Volume = 34.4 cm^3
Test Starting Date: 16 January 1991

GEOSYNTEC CONSULTANTS
GEOMECHANICS AND ENVIRONMENTAL LABORATORY

FIGURE NO. 3.1-4
PROJECT NO. GL1614
DOCUMENT NO. GEL91066
PAGE NO.

EPA 9100 COMPATIBILITY TESTING
BENTOMAT SAMPLE #EL005

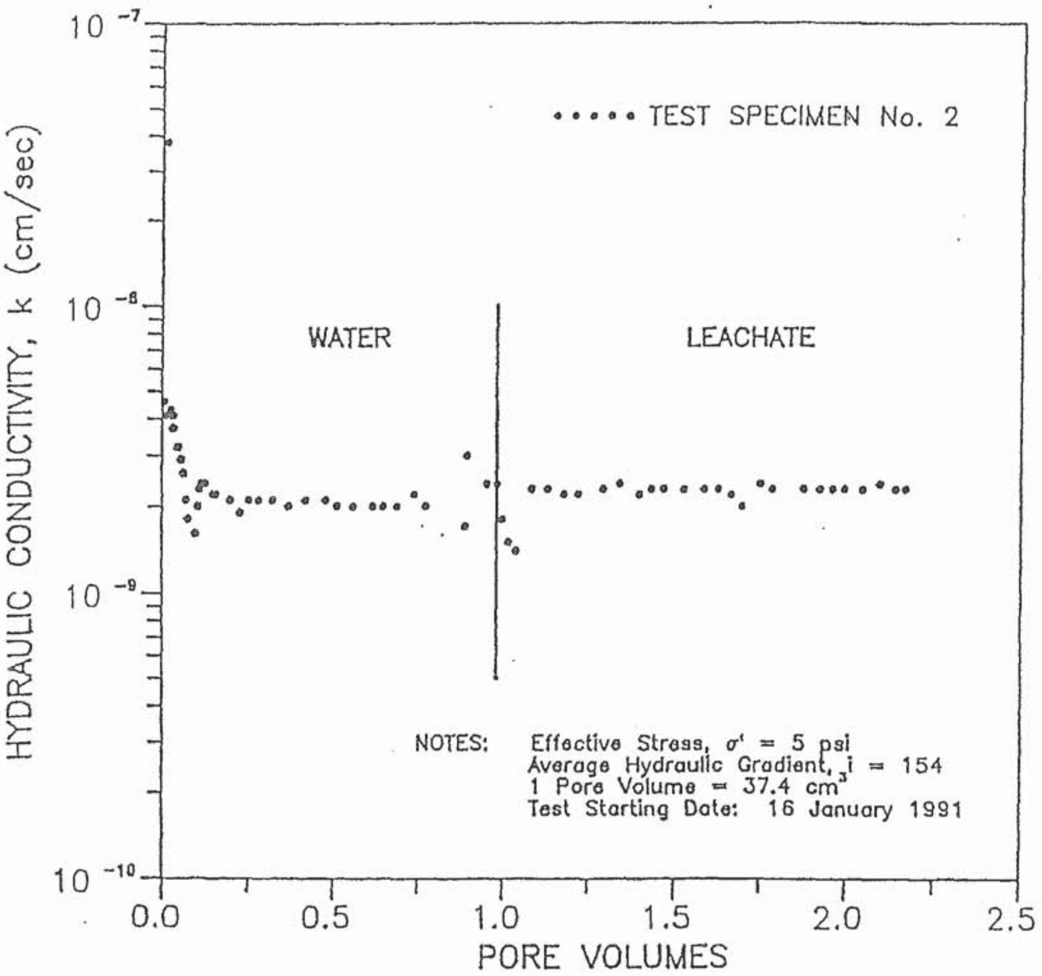

NOTES: Effective Stress, $\sigma' = 5$ psi
Average Hydraulic Gradient, $i = 154$
1 Pore Volume = 37.4 cm^3
Test Starting Date: 16 January 1991

GeoSyntec Consultants
GEOMECHANICS AND ENVIRONMENTAL LABORATORY

FIGURE NO.	3.1-5
PROJECT NO.	GL1614
DOCUMENT NO.	GEL91066
PAGE NO.	

EPA 9100 COMPATIBILITY TESTING
BENTOMAT SAMPLE #EL005

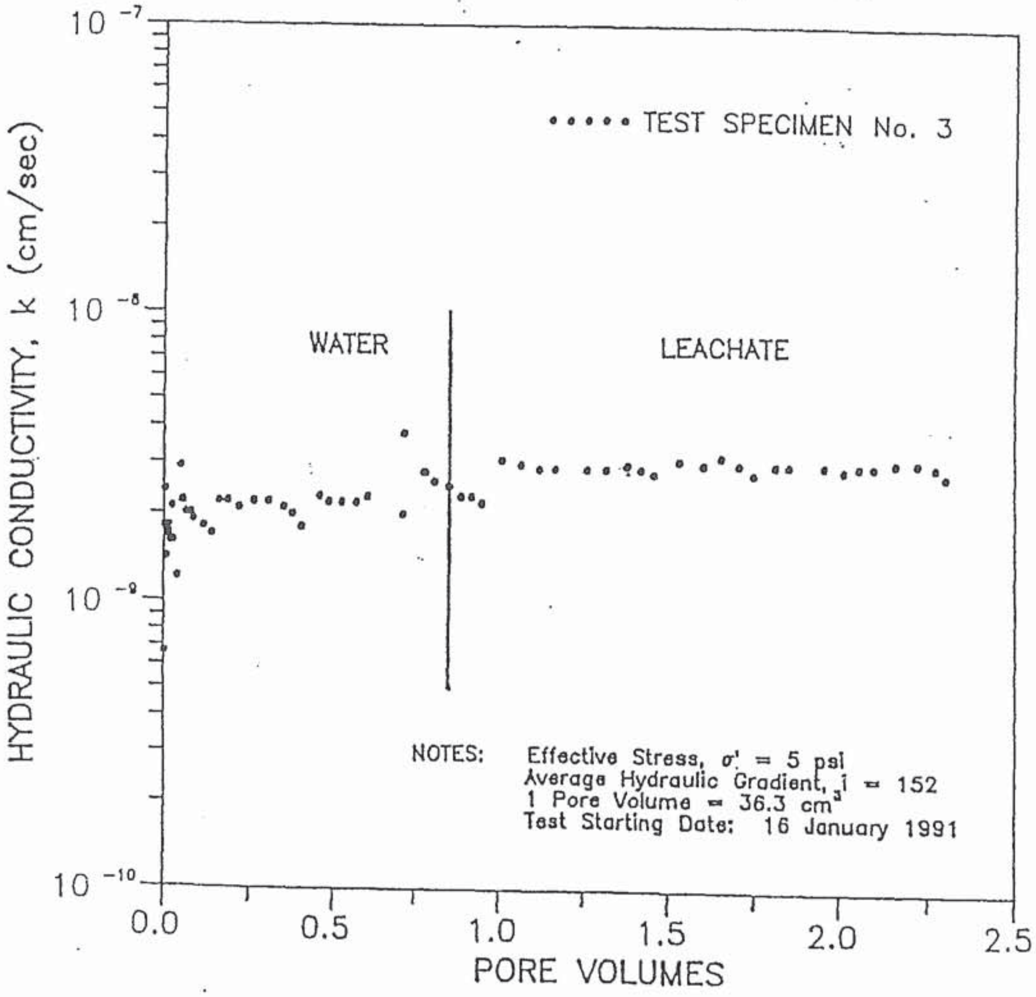

GEOSYNTEC CONSULTANTS
GEOMECHANICS AND ENVIRONMENTAL LABORATORY

FIGURE NO.	3.1-6
PROJECT NO.	GL1614
DOCUMENT NO.	GEL91066
PAGE NO.	

3.1 Task 1: EPA 9100 Compatibility Testing

3.1.1 Test Results

The physical conditions of the three Bentomat specimens, measured before and after the tests, are summarized in Table 3.1-1. Graphical presentations of the hydraulic conductivity as a function of elapsed time are presented in Figures 3.1-1, 2, and 3. Graphical presentations of the hydraulic conductivity as a function of the volume of liquid passed through the specimens (i.e., pore volumes) are presented in Figures 3.1-4, 5, and 6.

3.1.2 Observations

Because of the low hydraulic conductivity of the bentonite mat, and in order to maximize the volume of leachate through the mat, the sand layer in each test was replaced by an Amoco 4516 geotextile during that test. This generally occurred shortly before the permeant was switched from water to leachate. In many cases the data indicated erratic behavior for a short time after the switch, but the hydraulic conductivities eventually became consistent.

All specimens were initially permeated at a hydraulic gradient of 50. The resulting hydraulic conductivity measurements were somewhat variable. The hydraulic gradient was subsequently increased to 160 after approximately five days of testing. The test results tended to stabilize after the gradient increase. The average hydraulic gradients that were used for the remainder of each test after the initial increase gradient is indicated on each figure.

In all cases, the data presented in the tables show that each specimen swelled in thickness and in diameter, and that each specimen experienced an apparent loss of mass. The effluent water however, was not visibly cloudy in any of the tests.

In each figure, a transition from water to leachate is indicated. The variability in the test results near this transition is likely the result of disturbance due to leachate injection and removal of the sand layer. Within a short period of time, the test results stabilized.

BENCH-SCALE HYDRAULIC CONDUCTIVITY TESTS OF BENTONITIC BLANKET MATERIALS FOR LINER AND COVER SYSTEMS

by

PAULA ESTORNELL, B.S.C.E.

THESIS

Presented to the Faculty of the Graduate School of
The University of Texas at Austin
in Partial Fulfillment
of the Degree of
MASTER OF SCIENCE IN ENGINEERING

THE UNIVERSITY OF TEXAS AT AUSTIN
August, 1991

aid in maintaining a 6- to 9-in-wide overlap during installation.

2.1.2 Available Laboratory Test Data of the Hydraulic Properties of Bentomat®

2.1.2.1 Bentomat® Permeation with Water

J & L Testing Company (1990) conducted flexible-wall hydraulic conductivity tests on 6-in (150-mm) diameter samples of Bentomat® containing either untreated granular bentonite ("CS" grade) or high-contaminant-resistant bentonite ("SS" grade). Test conditions and results are summarized in Table 2.2. The duration of the tests was not reported. Figure 2.2 presents the relationship between hydraulic conductivity and maximum effective stress. Hydraulic conductivities ranged from 6 x 10^{-10} cm/s to 6 x 10^{-9} cm/s.

2.1.2.2 Bentomat® Permeation with Chemical Leachates

GeoSyntec Consultants (1991a) performed compatibility tests on Bentomat® in flexible-wall permeameters in order to measure the effect of landfill leachate on the alternative barrier material. Three 2.8-in (70-mm) diameter replicate samples were permeated first with de-aired water (under an effective stress of 2.0 psi (14 kPa) and a hydraulic gradient of about 50) and then with leachate (under an effective stress of

Table 2.2 Summary of Results of Hydraulic Conductivity Tests on Bentomat® (J&L Testing Company, 1990)

	Stress (psi)				Hydraulic Conductivity (cm/s)
Grade of Bentonite	Cell	Headwater	Tailwater	Maximum Effective	
High-Contaminant-Resistant ("SS")	50	42.2	41.8	8.2	2.1×10^{-9}
	50	44.6	39.4	10.6	7.5×10^{-10}
	50	47.2	36.8	13.2	5.8×10^{-10}
Untreated Granular Bentonite ("CS")	50	42.2	41.8	8.2	5.6×10^{-9}
	50	44.6	39.4	10.6	1.1×10^{-9}
	50	47.2	36.8	13.2	9.8×10^{-10}

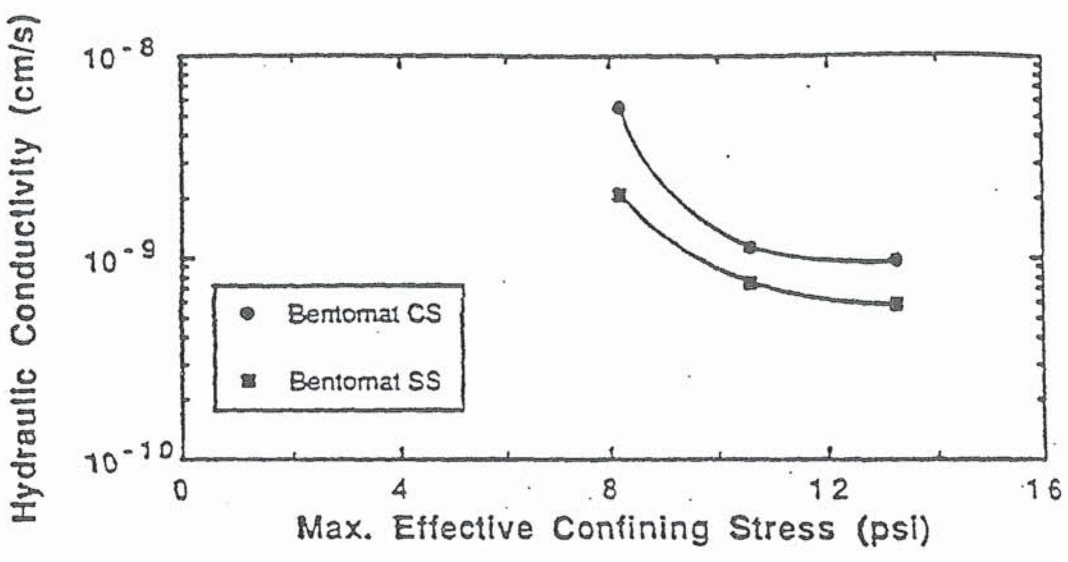

Fig. 2.2 Results of Flexible-Wall Hydraulic Conductivity Tests on Bentomat® (J&L Testing Company, 1990)

5.0 psi (35 kPa) and an average hydraulic gradient of approximately 160). The steady-state hydraulic conductivity, after two months of testing and 2.3 pore volumes of flow, was approximately 2 x 10^{-9} cm/s using the de-aired water and approximately 2.5 x 10^{-9} cm/s using the landfill leachate. The results seem to indicate that Bentomat® samples that have been hydrated first with de-aired water will have very little increase in hydraulic conductivity after the introduction of landfill leachate.

2.1.2.3 Effects of Desiccation on Bentomat®

GeoSyntec Consultants (1991a) conducted a flexible-wall hydraulic conductivity test on a 2.8-in (70-mm) sample of Bentomat® that had undergone 4 desiccation cycles. Each cycle involved first permeating the sample with de-aired water (using an effective stress of 5.0 psi (34 kPa) and an average hydraulic gradient of approximately 25) then desiccating the sample for two weeks in a 40°C (104°F) oven. This procedure was repeated 4 times. The steady-state hydraulic conductivity, measured after each cycle, ranged sporadically between 1 x 10^{-9} cm/s and 3 x 10^{-9} cm/s. The results show little effect of desiccation on the hydraulic conductivity of Bentomat®.

2.2.2 Available Laboratory Test Data on the Hydraulic Properties of Claymax®

2.2.2.1 Claymax® Permeation with Water

Literature published by the James Clem Corporation lists 2 x 10^{-10} cm/s as the hydraulic conductivity of Claymax® permeated with de-aired water. A summary of published measurements of the hydraulic conductivity of Claymax® to water is given in Table 2.4. Results are plotted in Fig. 2.5 in terms of hydraulic conductivity versus effective confining stress. The results show that the hydraulic conductivity to water varies from just under about 1 x 10^{-8} cm/s at low effective stress to just above 1 x 10^{-10} cm/s at high effective stress.

2.2.2.2 Claymax® Permeation with Various Liquid and Chemical Leachates

The information available concerning hydraulic conductivity of Claymax® permeated with liquids other than water is summarized in Table 2.5. All of the test specimens that were hydrated with water and then permeated with chemicals maintained a hydraulic conductivity $\leq$ 1 x 10^{-8} cm/s, even for compounds such as diesel fuel and heptane that would normally be very aggressive to soil liner materials. Brown, Thomas, and Green (1984), for example, found that the

Table 2.4 Results of Hydraulic Conductivity Tests on Claymax® Permeated with Water

Source of Information	Permeameter	Backpressure Saturation?	Permeant Water	Diameter of Sample (in.)	Effective Stress (psi)	Hydraulic Conductivity (cm/s)
Clem Corp. Literature	- -	- -	Deaired Water	- -	- -	2×10^{-10}
Chen-Northern (1988)	Flex. Wall	Yes	- -	2.5	3.5	2×10^{-9}
GeoServices (1988a)	Flex. Wall	Yes	Deaired Tap Water	2.8	29	4×10^{-10}
GeoServices (1989c)	Flex. Wall	Yes	Deaired Tap Water	2.8	30	8×10^{-10}
GeoServices (1989c)	Flex. Wall	Yes	Deaired Tap Water	2.8	30	8×10^{-10}
GeoServices (1989c)	Flex. Wall	Yes	Deaired Tap Water	2.8	30	3×10^{-10}
GeoServices (1989c)	Flex. Wall	Yes	Deaired Tap Water	2.8	30	7×10^{-10}
Shan (1990)	Flex. Wall	No	Distilled Water	4.0	2	2×10^{-9}
Shan (1990)	Flex. Wall	No	Tap Water	4.0	2	2×10^{-9}
Shan (1990)	Flex. Wall	No	Distilled Water	4.0	5	1×10^{-9}
Shan (1990)	Flex. Wall	No	Tap Water	4.0	5	8×10^{-10}
Shan (1990)	Flex. Wall	No	Distilled Water	4.0	10	6×10^{-10}
Shan (1990)	Flex. Wall	No	Distilled Water	4.0	20	3×10^{-10}
Shan (Unpub.)	Flex. Wall	Yes	Tap Water	12	2	2×10^{-9}
GeoServices (1990b)	Flex. Wall	Yes	Deaired Water	- -	30	3×10^{-10}
GeoSyntec (1990a)	Flex. Wall	Yes	Deaired Water	- -	1.0	2×10^{-9}
GeoSyntec (1990a)	Flex. Wall	Yes	Deaired Water	- -	1.5	4×10^{-9}

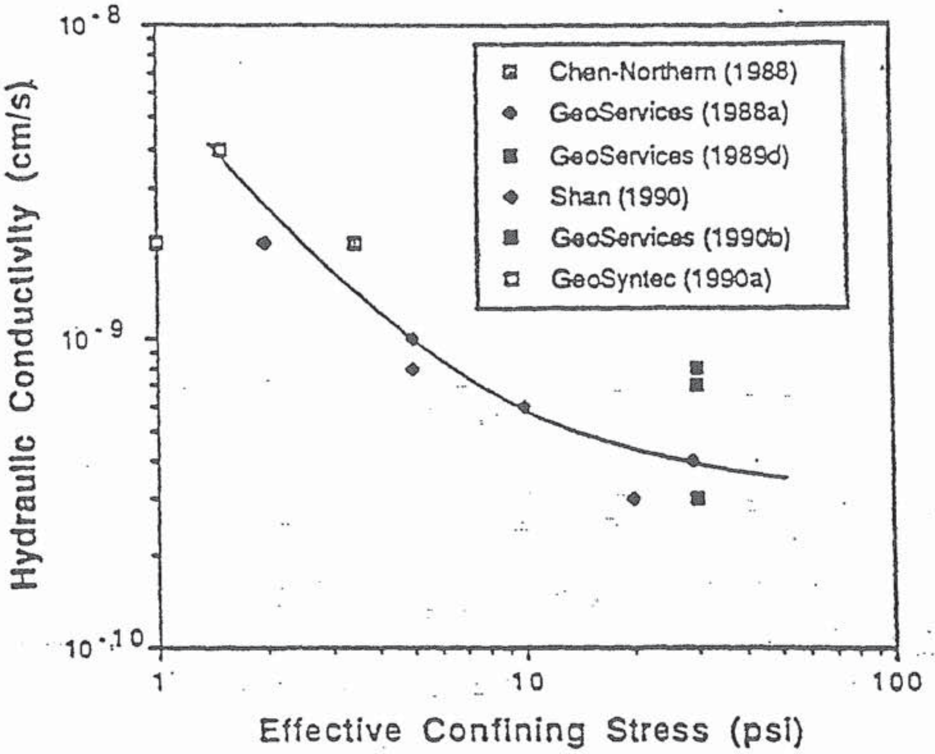

Fig. 2.5 Results of Hydraulic Conductivity Tests on Claymax® Permeated with Water

Table 2.5 Hydraulic Conductivity of Claymax® Permeated with Various Liquids

Source of Information	Permeant Liquid	Hydration Liquid	Pore Volumes of Flow	Effective Stress (psi)	Hydraulic Conductivity (cm/s)
STS Consultants (1988b)	Sewage Leachate	Sewage Leachate	- -	- -	8×10^{-10}
STS Consultants (1988c)	Paper Pulp Sludge	Paper Pulp Sludge	- -	- -	2×10^{-10}
GeoServices (1988b)	Simulated Seawater	Simulated Seawater	- -	30	2×10^{-10}
STS Consultants (1989a)	Landfill Leachate	Landfill Leachate	- -	- -	4×10^{-10}
STS Consultants (1989b)	Ash-Fill Leachate	Ash-Fill Leachate	- -	- -	1×10^{-10}
GeoServices (1989c)	Diesel Fuel	Water	1.5	30	9×10^{-10}
GeoServices (1989c)	Jet Fuel	Water	2.5	30	9×10^{-10}
GeoServices (1989c)	Unleaded Gasoline	Water	1.6	30	3×10^{-10}
Shan (1990)	50% (Vol) Methanol	Water	2.2	5	9×10^{-10}
Shan (1990)	Heptane	Water	0.2	5	1×10^{-10}
Shan (1990)	Sulfiric Acid	Water	3.1	5	6×10^{-11}
Shan (1990)	0.01 N $CaSO_4$	Water	2.2	5	1×10^{-9}
Shan (1990)	0.5 N $CaCl_2$	Water	24	5	8×10^{-9}
Shan (Unpublished)	50% (Vol) Methanol	50% Methanol	4	5	5×10^{-6}
Shan (Unpublished)	Methanol	Methanol	5.4	5	3×10^{-5}
Shan (Unpublished)	Heptane	Heptane	4.3	5	5×10^{-5}
GeoServices (1990a)	Methyl Tertiary Butyl Ether	Deaired Water	1.6	30	7×10^{-10}
Klohn Leonoff (1990)	Solution from Goldmine	Solution from Goldmine	1.8	17.4	2×10^{-10}
GeoSyntec (1991b)	Landfill Leachate	Deaired Water	1.7	5	3×10^{-9}

hydraulic conductivity of a compacted, micaceous soil was 1 to 4 orders of magnitude higher to kerosene, diesel fuel, and gasoline than it was to water. The inconsistency of results reported in Table 2.5 to the research conducted by Brown and his co-workers may be related to either a small cumulative pore volumes of flow in the tests on Claymax® or application of a high compressive stress to the test specimens. The cumulative pore volumes of flow of permeant liquid was not reported in many of the test referenced in Table 2.5; in many cases, there was probably an insufficient quantity of flow to determine the full effects of the permeant liquids. In some tests, a large effective confining stress was used. Broderick and Daniel (1990) found that one compacted clay was vulnerable to significant alterations in hydraulic conductivity when compressive stresses were ≤ 5 - 10 psi (34 - 69 kPa) but did not undergo an increase in hydraulic conductivity when the specimens were permeated with compressive stresses larger than 5 to 10 psi (34 to 69 kPa). Brown and his co-workers applied no compressive stress to their test specimens.

Tests on specimens of Claymax® that were hydrated with the same liquid as the eventual permeant liquid (rather than water) showed mixed results. For leachates, a paper pulp sludge, and simulated seawater, the hydraulic conductivity was found to be < 1 x 10^{-9} cm/s. However, the significance of these results is questionable because the duration of the tests was short, the cumulative pore volumes of flow was not reported, and the applied compressive stress was not reported. In as-yet unpublished tests by Shan, markedly different results were obtained when Claymax® was not prehydrated with water. Shan found that when dry Claymax® was permeated directly with a 50% mixture of water and methanol, with pure methanol, or with heptane, the bentonite did not hydrate even after several pore volumes of flow, and the hydraulic conductivity did not drop below 1 x 10^{-6} cm/s. Shan used a compressive stress of 5 psi (34 kPa). Thus, with concentrated organic liquids, the conditions of hydration appear to play an important role in determining the ability of the bentonitic blanket to resist the deleterious action of organic chemicals. The bentonite appears to be more chemically resistant if hydrated with fresh water before exposure to concentrated organic chemicals.

2.2.2.3 Effects of Desiccation on Claymax®

The effects of desiccation were investigated by GeoServices (1989d). Three hydrated samples of Claymax® were placed in a temperature- and humidity-controlled chamber. The chambers operated on a timed cycle to simulate day and night conditions. The temperature and humidity during thick HDPE geomebrane, was the material tested during this study.

2.3.2 Available Laboratory Test Data of the Hydraulic Properties of Paraseal and Gundseal

2.3.2.1 Paraseal Permeation with Water

Pittsburgh Testing Laboratory (1985) conducted a hydraulic conductivity test on a 2.5-in (64-mm) diameter sample of Paraseal. A 15-ft (4.6-m) head of water was applied to the sample, which was soaked for 5 days prior to permeation. A single, falling-head test was performed, which yielded a hydraulic conductivity reported to be 4 x 10^{-10} cm/s. Further details of the test procedures are not available. However, because the direction of flow was apparently through the HDPE membrane, the test may have provided a measure of sidewall leakage rather than flow through the material.

2.3.2.2 Gundseal Permeation with Chemical Leachates

The hydraulic conductivity of Gundseal permeated with landfill leachate was measured by GeoSyntec Consultants (1991c). A grid of 0.12-in (3-mm) diameter holes on 0.3 in (0.75 cm) centers were drilled into the Gundseal test samples in order to effectively test the bentonite portion of the Gundseal product. Three 2.8-in (70-mm) diameter samples were placed in flexible-wall permeameters and subjected to an effective stress of 5.0 psi (35 kPa). The test specimens were permeated, first with de-aired water then with leachate. The average hydraulic gradient applied during permeation with de-aired water was 50. The hydraulic gradient was increased to 230 during permeation with the leachate in order to increase flow through the Gundseal. The average hydraulic conductivity of the punctured Gundseal specimens was 1 x 10^{-9} cm/s for both the de-aired water and the leachate after approximately 1.2 pore volumes of flow. The hydraulic conductivity of the prehydrated bentonite appeared unaffected by the introduction of the leachate.

2.3.2.3 Effects of Desiccation on Gundseal

GeoSyntec Consultants (1991c) measured the hydraulic conductivity of a sample of Gundseal that had undergone 4 desiccation cycles. The 2.8-in (70-mm) diameter sample was punctured with small holes in the same grid pattern as the samples described previously. The test sample was permeated with de-aired water in a flexible-wall permeameter under an effective stress of 5.0 psi (34 kPa) and an average hydraulic gradient of 215 in order to determine hydraulic conductivity. The sample was removed from the permeameter, subjected to a 0.4 psi (3 kPa) confining stress, and placed in an oven for two

2.5 Summary of Hydraulic Properties of Bentomat®, Claymax®, and Paraseal/Gundseal

Table 2.10 is an abridged summary of the hydraulic conductivity data of Bentomat®, Claymax®, and Paraseal/Gundseal. The table includes results from tests conducted by GeoSyntec (1991a,b,c), GeoSyntec (1990b), and Shan (1990). Results from hydraulic conductivity tests conducted by other laboratories have not been included in Table 2.10 in order to present the information in a simplified and consise form.

Table 2.10 Summary of Hydraulic Conductivity Tests on Bentomat®, Claymax®, and Paraseal/Gundseal

	Bentomat®			Claymax®			Paraseal/Gundseal		
Sample	Reference	Effective Stress (psi)	Hydraulic Conductivity (cm/s)	Reference	Effective Stress (psi)	Hydraulic Conductivity (cm/s)	Reference	Effective Stress (psi)	Hydraulic Conductivity (cm/s)
Sample Permeated with Deaired Water	GeoSyntec (1991a)	2.0	2.0×10^{-9}	GeoSyntec (1991b)	2.0	1.8×10^{-9}	GeoSyntec (1991c)	5.0	1×10^{-9}
☆ Sample Permeated with Landfill Leachate	GeoSyntec (1991a)	5.0	2.5×10^{-9}	GeoSyntec (1991b)	5.0	2.6×10^{-9}	GeoSyntec (1991c)	5.0	1×10^{-9}
Dislocated Sample	GeoSyntec (1991a)	5.0	1.0×10^{-9} to 3.0×10^{-9}	Shan (1990)	2.0	2.0×10^{-9}	GeoSyntec (1991c)	8.0	5.0×10^{-10} to 2.0×10^{-9}
Freeze-Thaw Sample	GeoSyntec (1991a)	6.0	1.0×10^{-9} to 6.0×10^{-9}	Shan (1990)	2.0	2.2×10^{-9}	GeoSyntec (1991c)	- -	1.0×10^{-9}
Damaged Sample									
1-in diameter hole	GeoSyntec (1991a)	- -	1.3×10^{-4}	Shan (1990)(1)	2.0	5.0×10^{-9}	GeoSyntec (1991c)	- -	1.0×10^{-3}
2-in diameter hole		- -	1.7×10^{-4}		- -	- -		- -	1.0×10^{-3}
3-in long slit		- -	3.0×10^{-5}		- -	- -		- -	1.0×10^{-3}
Composite Sample	GeoSyntec (1991a)	- -	3.0×10^{-9}	Shan (1990)	2.0	4.0×10^{-9}	GeoSyntec (1991c)	- -	2.0×10^{-9}
Overlapped Seam Sample	GeoSyntec (1991a)	- -	6.0×10^{-7} to 2.0×10^{-5}	GeoSyntec (1990b)	1.0	2.0×10^{-9}	GeoSyntec (1991c)	- -	5.0×10^{-8}

(1) The damaged Claymax® sample tested by Shan (1990) was punctured with 3 - 1 inch diameter holes.

Report

Project

HYDRAULIC CONDUCTIVITY AND
COMPATIBILITY TESTING OF CLAYMAX
BALTIMORE COUNTY LANDFILL PROJECT
TOWNSON, MARYLAND

Client

CLEM ENVIRONMENTAL CORPORATION
444 NORTH MICHIGAN AVENUE, SUITE 1610
CHICAGO, IL 60611

Project # 25868-XH

Date MAY 11, 1989

STS Consultants Ltd.
Consulting Engineers
111 Pfingsten Road

HYDRAULIC CONDUCTIVITY AND COMPATIBILITY TESTING OF CLAYMAX
BALTIMORE COUNTY LANDFILL PROJECT
TOWNSON, MARYLAND

SCOPE OF SERVICES

STS was to perform two hydraulic conductivity tests on sections of Claymax liner material in conjunction with a six inch sand layer utilizing leachates as the hydration medium and the permeants. The Claymax specimens were supplied to STS by Clem Environmental and the leachate specimens were obtained from L.A. Solamen. Inc. All testing materials were delivered to our Northbrook Testing Facility.

Test Equipment

The equipment used in the compatibility study was a triaxial compression permeameter. This equipment incorporates the use of a flexible membrane, preventing sidewall seepage. back pressure to facilitate specimen saturation small diameter burettes making measurement of small volumes of collected permeant possible and the system is closed preventing the permeant from being exposed to the surrounding air.

Specimen Construction

Each of the specimens, utilized throughout the testing program, consisted of an approximately six inch cylindrical column of silica sand on top of which a circular section of Claymax was placed. The orientation of the Claymax to the sand provided for permeant flow initiated through the sand followed by the Claymax section. The directional flow of the permeant. is similar to those conditions found in the field applications.

Once the specimens were assembled, a flexible rubber membrane was used to encase the specimens while sealed in the triaxial permeameter chamber.

Test Procedures

After its initial construction and placement in a triaxial compression permeameter each of the specimens is backpressure saturated. To aide in specimen saturation, carbon dioxide gas was allowed to flow freely through the test specimen, inundating the voids in the sand and dry Claymax. The use of this carbon dioxide gas has been accepted as a procedure to aide in specimen saturation. The carbon dioxide gas will go into solution more readily than normal atmospheric air. Once it was determined that the carbon dioxide gas had completely inundated the voids of the test specimen, the permeants were allowed to free flow through the test specimen first saturating the silica sand and then the Claymax section. For this study, the leachates were utilized both as a set hydrating medium and as the actual permeant for the hydraulic conductivity determination.

Two leachates were used during the study. The first was labeled Parkton Landfill and the second labeled as Eastern Sanitary Landfill. It is the understanding of STS Consultants that the two leachates were a municipal landfill leachate and contained such things as heavy metals, phenals, cyanide, copper, phosphorus and other substances.

Once the leachate had fully hydrated the test specimen, the specimen was allowed to stand for a 24 hour hydration period. Following the hydration period, the backpressure saturation techniques were implemented to complete the saturation procedures. This was accomplished by simultaneously increasing the cell and back pressures in increments while maintaining a pressure differential of 0.125 kilograms per square centimeter (KSC). Pressures were incrimentally increased until obtaining testing pressures of 4.125 KSC cell pressure and 4.00 KSC back pressure.

Specimen saturation was considered complete when a Skempton's Pore Pressure B-parameter of 0.95 or greater was obtained. The "B" parameter is simply a ratio of an increase in pore water pressure to a simultaneous increase in confining pressure. When full specimen saturation was determined, permeant flow was initiated through the bottom of the test specimen, allowed to flow through the top of the test specimen and collect in a calibrated burette.. The test was performed utilizing two separate gradients. The initial gradient consisted of an application of a hydraulic head of one foot. The second gradient was applied as a hydraulic head equivalent to 35 feet.

During the entire test, permeant volume versus time measurements were recorded and the hydraulic conductivity of the test specimen at the two gradients was determined. The test was allowed to continue until it had been determined that a minimum of three pore volumes of pore fluid had passed through the test specimen. Once this had occurred and steady state flow had been established. the test was terminated.

Laboratory Test Results

As a result of the testing as outlined above, the Claymax section utilizing the Parkton Landfill Leachate, as the permeant, obtained hydraulic conductivity values of 2×10^{-10} centimeters per second (cm/sec) for a hydraulic head of one foot and 4×10^{-10} cm/sec for a hydraulic head of 35 feet. The Claymax section exposed to the Eastern Sanitary Landfill leachate obtain hydraulic conductivity values of 3 x 10 -10 cm/sec utilizing a hydraulic head of 1 foot and 4×10^{-10} cm/sec utilizing a hydraulic head of 35 feet. A summary of specific specimen characteristics and final hydraulic conductivity values is attached to this report.

STS Consultants Ltd.

STS PROJECT NO. 25868-XH

PROJECT Baltimore County
Landfill Project

DATE 4-24-89

SUMMARY OF HYDRAULIC CONDUCTIVITY TESTS

Permeant	Parkton Landfill	Eastern Sanitary Landfill
Sample No.	1	2
Classification	Claymax with 6" Silica Sand	Claymax with 6" Silica Sand
v Unit ght (pcf)	51.6	62.5
Water Content (%)	Dry	Dry
Diameter (cm)	7.028	7.026
Length (cm)	0.568	0.616
Saturation B Value	0.97	0.99
Hydraulic Conductivity k (cm/sec)	1 ft. 2×10^{-10} 35 ft. 4×10^{-10}	1 ft. 3×10^{-10} 35 ft. 4×10^{-10}

Rev: 12/87

Dennis F. Rasmussen
County Executive

BALTIMORE COUNTY
WASTEWATER MONITORING AND ANALYSIS DIVISION
INDUSTRIAL DISCHARGE CONTROL PROGRAM

SAMPLING/ANALYSIS FORM

Sample No.: 9 01110

Industry Name: EASTERN SANITARY LANDFILL Facility No.:

Address: Days Cove Road

Telephone: Requested by: P. Phillips

Sampling Site Location: Leachate pit

Special Instructions: STD 5, metals, Total alkalinity & Chlorides

FIELD

Date and Time of Sampling: Start 1/18/89 10:20 a.m. Finish

Sampled by: P. Phillips, T.E. Ryan

Type of Sample: Grab

Sampler Settings: N/A

Sample Characteristics: 1 quart: dark gray; 1 quart: dark brown

Preservatives Added: Cooled with ice

Comments and Observations:

Delivered to Lab by: PP, TER Date: 1/18/89 Time: 11:50 a.m.

LABORATORY

Sample received by: WP Date: 1/18/89 Time: 11:50 a.m.

Characteristics of Note:

(Origin of Seed: Polyseed)

ANALYTICAL RESULTS

Code	BDL	Parameter	Conc. (mg/L)	Code	BDL	Parameter	Conc. (mg/L)
		pH	6.3	3011	0.05	Ni (Nickel)	BDL
		BOD	122 mg/L	3015	0.01	Zn (Zinc)	0.05 mg/L
		COD	148 mg/L	3130		Phenols	
		TSS	125 mg/L	3013	0.01	Silver	BDL
5012		FOG - A&V					
5013		FOG - Petr		*		GRAB pH	
2026		P(Phosphorus)	2.52 mg/L				
3006	0.01	Cd(Cadmium)	BDL			Total Fe	3.88 mg/L
3007	0.05	Cr(Chromium)	BDL			Total alkalinity	350 mg/L
3008	0.02	Cu(Copper)	0.04 mg/L			Chloride	80 mg/L
4		Cn(Cyanide)					
3009	0.10	Pb (Lead)	0.36 mg/L				

Dennis F. Rasmusson
County Executive

BALTIMORE COUNTY
WASTEWATER MONITORING AND ANALYSIS DIVISION
INDUSTRIAL DISCHARGE CONTROL PROGRAM

Rev: 12/87

SAMPLING/ANALYSIS FORM

Sample No.: 9 02104

Industry Name: PARKTON

Facility No.:

Address:

Telephone:

Requested by: R. Much

Sampling Site Location: Cell 03

Special Instructions: pH, BOD, COD, TSS, Alkalinity, Chloride, Metals

FIELD

Date and Time of Sampling: Start 2/9/89 Finish

Sampled by: R. Much, B. Kramer

Type of Sample: Grab

Sampler Settings:

Sample Characteristics:

Preservatives Added:

Comments and Observations:

Delivered to Lab by: BK, RM Date: 2/9/89 Time: 2:20 P.M.

LABORATORY

Sample received by: WP Date: 2/9/89 Time: 2:20 P.M.

Characteristics of Note:

(Origin of Seed: Polyseed)

ANALYTICAL RESULTS

ode	BDL	Parameter	Conc. (mg/L)	Code	BDL	Parameter	Conc. (mg/L)
		pH	6.1	3011	0.05	Ni (Nickel)	1.44 mg/L
		BOD	38,888 mg/L	3015	0.01	Zn (Zinc)	5.45 mg/
		COD	60,831 mg/L	3130		Phenols	
		TSS	691 mg/L	3013	0.01	Silver	0.03 mg/L
012		FOG - A&V					
013		FOG - Petr		*		GRAB pH	
026		P(Phosphorus)	Interference				
006	0.01	Cd(Cadmium)	0.10 mg/L			Total Fe	736.00 mg/L
007	0.05	Cr(Chromium)	0.22 mg/L			Total alkalinity	15,000 mg/L
008	0.02	Cu(Copper)	0.17 mg/L			Chloride	1,500 mg/L
002		Cn(Cyanide)					
009	0.10	Pb (Lead)	0.60 mg/L				

ATTACHMENT III.6.E

HDPE PIPE REFERENCE DOCUMENTATION

Chemical Resistance of Plastics and Elastomers Used in Pipeline Construction

1. Introduction

It is now inconceivable to construct pipelines without the use of plastics. Pipes made from plastics are used not only for drinking water, water for general use and waste water, but also for the conveyance of aggressive liquids and gases. Expensive pipe materials such as lined metal, ceramic or glass, have been largely superseded by plastic pipes. It is, however, important that the most suitable plastic material is selected for each application. This "Chemical Resistance List" serves as a useful guide in this respect. The list is periodically revised to include the latest findings. It contains all plastics and elastomers in the George Fischer product range which can come into direct contact with the media.

The information is based on experiments, immersion and, when available, on data from tests which include temperature and pressure as stress factors. The results achieved in immersion experiments cannot be applied without reservation to pipes under stress, i.e. internal pressure, as the factor "stress corrosion cracking" is not taken into consideration. In certain cases it can be of advantage to test the suitability under the planned working conditions. The tests referred to have been carried out partly by George Fischer and partly by the International Standardization Organization (ISO) or national standards organizations.

Pure chemicals were used for the tests. If a mixture of chemicals is to be conveyed in practice this may affect the chemical resistance of the plastic. It is possible in special cases to carry out appropriate tests with the specific mixture. Suitable test equipment is available at George Fischer for this purpose, which we regard as part of our service to the customer. It goes without saying that we are willing to give individual advice at any time. In this connection it is worth mentioning that George Fischer already possesses information concerning the behavior towards plastics of a number of chemicals or mixtures of chemicals which are not yet included in this list. The "Chemical Resistance List" gives valuable assistance in the planning of plastic pipelines. Please refer to the following instructions, which are important for the application and evaluation of this list.

2. Instructions for the Use of the Chemical Resistance List

2.1 General

As stated in the introduction, the "Chemical Resistance List" is only intended as a guide. Changes in the composition of the medium or special working conditions could lead to deviations. If there is any doubt, it is advisable to test the behavior of the material under the specific working conditions, by means of a pilot installation. No guarantees can be given in respect of the information contained in this booklet. The data shown is based upon information available at the time of printing, but it may, however, be revised from time to time in the light of subsequent research and experience.

2.2 Classification

The customary classifications: **resistant, conditionally resistant** and **not recommended** are depicted by the signs: +, O, and –, which allow simple presentation and application. These classifications are defined as:

Resistant: +
Within the acceptable limits of pressure and temperature the material is unaffected or only insignificantly affected.

Conditionally Resistant: O
The medium can attack the material or cause swelling. Restrictions must be made in regard to pressure and/or temperature, taking the expected service life into account. The service life of the installation can be noticeably shortened. Further consultation with George Fischer is recommended.

Not recommended: –
The material cannot be used with the medium at all, or only under special conditions.

(Courtesy George Fischer Engineering Handbook)

2.3 Pipe Joints

2.3.1 Solvent Cement Joints (PVC)

Solvent cement joints made with standard PVC cement and primer systems are generally as resistant as the PVC material itself. The following chemicals are, however, an exception:

- Sulphuric acid H_2SO_4 in concentrations above 70 percent
- Hydrochloric acid HCl in concentrations above 25 percent
- Nitric acid HNO_3 in concentrations above 20 percent

Hydrofluoric acid in any concentration
In conjunction with the above media the solvent cement joining is classified as "conditionally resistant". Previously recommended solvent cement (Dytex, by Henkel, Germany) used for pipe and fittings to carry concentrated acids, can no longer be brought into the United States because of its methylene chloride solvent system being classified as a carcinogen. There is no known domestically available substitute. Special consideration should be given to the possible attack of the cemented joints by these concentrated acids.

2.3.2 Fusion Joints

In the case of PE, PP, and PVDF (SYGEF®) heat fusion joints have practically the same chemical resistance as the respective material. In conjunction with media which could cause stress cracking, the fused joints can be subjected to an increased risk due to residual stress from the joining process.

2.4 Sealing Materials

Depending upon the working conditions and the stress involved, the life span of the sealing materials can differ from that of the pipeline material. Seals in PTFE, which are not included in this list, are resistant to all the chemicals indicated. The greater permeability of PTFE should, however, be considered. Under certain working conditions, for example when conveying highly aggressive media such as hydrochloric acid, this material characteristic must be taken into account.

2.5 General Summary and Limits of Application

The following table includes all the materials contained in the George Fischer product range, and their abbreviations. The summary gives preliminary information regarding the general behavior of the materials and the temperature limits.

2.6 Standards

This list has been compiled with reference to the following ISO standards:
ISO/TR 7473
Unplasticized polyvinyl chloride pipes and fittings – Chemical resistance with respect to fluids.
ISO/TR 7474
High density polyethylene pipes and fittings – Chemical resistance with respect to fluids to be conveyed.
ISO/TR 7471
Polypropylene (PP) pipes and fittings – Chemical resistance with respect to fluids.
ISO TR 10358
Plastic pipes and fittings – Combined chemical resistance classification table.
DVS 2205 Part I
Calculations for thermoplastic containers and appliances.
DIN 8080 Supplement 1 «Pipes of chlorinated polyvinyl chloride (PVC-C), PVC-C 250 – Chemical Resistance».

(Courtesy George Fischer Engineering Handbook)

Material	Abbreviation	Remarks	Maximum Permissible Temperature (Water) °C	
			Constant	Short Term
Polyvinyl Chloride	PVC	Resistant to most solutions of acids, alkalis and salts and to organic compounds miscible with water. Not resistant to aromatic and chlorinated hydrocarbons	60°	60°
Chlorinated Polyvinyl Chloride	CPVC	Can be used similarly to PVC but at higher temperatures. Consult factory for specific applications.	90°	110°
High-density Polyethylene	PE 50	Resistant to hydrous solutions of acids, alkalis and salts as well as to a large number of organic solvents. Unsuitable for concentrated oxidizing acids.	60°	80°
Polypropylene, heat stabilized	PP	Chemical resistance similar to that of PE but suitable for higher temperatures	90°	110°
Polyvinylidene Fluoride	PVDF (SYGEF®)	Resistant to acids, solutions of salts, aliphatic, aromatic and chlorinated hydrocarbons, alcohols and halogens. Conditionally suitable for ketones, esters, organic bases and alkaline solutions	140°	150°
Polybutylene-1	PB	Similar to PE 50, but can be used up to 90°C	90°	100°
Polyoxymethylene	POM	Resistant to most solvents and hydrous alkalis. Unsuitable for acids	60°	80°
Polytetrafluoroethylene (e.g. Teflon®)	PTFE	Resistant to all chemicals in this list	250°	300°
Nitrile Rubber	NBR	Good resistance to oil and petrol. Unsuitable for oxidizing media	90°	120°
Butyl Rubber Ethylene Propylene Rubber	IIR EPDM	Good resistance to ozone and weather. Especially suitable for aggressive chemicals. Unsuitable for oils and fats	90°	120°
Chloroprene Rubber (e.g. Neoprene®)	CR	Chemical resistance very similar to that of PVC-U and between that of Nitrile and Butyl Rubber	80°	110°
Fluorine Rubber (e.g. Viton®)	FPM	Has best chemical resistance to solvents of all elastomers	150°	200°
Chlorine Sulphonyl Polyethylene (e.g. Hypalon®)	CSM	Chemical resistance similar to that of EPDM	100°	140°

®Registered trade name

The abbreviations listed below are found throughout the listings and have the following definition:

Q/E (Quellung/Erweichung) = swelling/softening
D/P (Diffusion/Permeation) = diffusion/permeation
SpRB (Spannungsrissbildung) = environmental stress cracking

(Courtesy George Fischer Engineering Handbook)

Aggressive Media					Chemical Resistance											
Medium	Formula	Boiling point °C	Concentration	Temperature °C	PVC	CPVC	ABS	PE	PP-H	PVDF (SYGEF)		EPDM	FPM	NBR	CR	CSM
Acetaldehyde	CH_3-CHO (C_2H_4O)	21	technically pure	20	-	-	-	+	O	-		+	O	-	-	O
				40				O	-			O	-			-
				60								-				
				80												
				100												
				120												
				140												
Acetaldehyde			40%, aqueous solution	20	O	-	-	+	+	-		+	+	-	+	+
				40	-			+	+			+	+		+	+
				60				O	+			+	O		O	+
				80					O			+	-		-	+
				100					-							
				120												
				140												
Acetic acid (SpRB)	CH_3COOH	118	technically pure, glacial	20	O	-	-	+	+	+		O	-	-	O	O
				40	-			+	+	O						
				60				O	O	-						
				80					-							
				100												
				120												
				140												
Acetic acid (SpRB)	CH_3COOH		10%, aqueous	20	+	+	+	+	+	+		+	O	+	+	O
				40	+	+	+	+	+	+		+	-	O	+	-
				60	O	+	O	+	+	+		O			O	
				80		+			+	+						
				100					+	+						
				120						+						
				140												
Acetic acid (SpRB)			50%, aqueous	20	+	+	-	+	+	+		+	O	-	O	O
				40	+			+	+	+						
				60	O			+	+	+						
				80						O						
				100						O						
				120												
				140												
Acetic acid (SpRB)	CH_3COOH		60%	20	+	-	-	+	+	+		+				
				40												
				60												
				80												
				100												
				120												
				140												
Acetic acid (SpRB)		118	98%	20	-	-	-	+	+	+		O	-			
				40												
				60												
				80												
				100												
				120												
				140												
Acetic acid anhydride (SpRB)	$(CH_3\text{-}CO)_2O$	139	technically pure	20	-	-	-	+	+	-		O	-	-	-	+
				40				O	O							
				60												
				80												
				100												
				120												
				140												

(Courtesy George Fischer Engineering Handbook)

Aggressive Media					Chemical Resistance											
Medium	Formula	Boiling point °C	Concentration	Temperature °C	PVC	CPVC	ABS	PE	PP-H	PVDF (SYGEF)		EPDM	FPM	NBR	CR	CSM
Acetic acid isobutyl ester	$(CH_2)_2\text{-}CH\text{-}(CH_2)_2\text{-}CO_2H$		technically pure	20						-						
				40												
				60												
				80												
				100												
				120												
				140												
Acetone	$CH_3\text{-}CO\text{-}CH_3$	56	technically pure	20	-	-	-	+	+	-		+	-	-	-	O
				40				+	+			+				O
				60				+	+			+				O
				80												
				100												
				120												
				140												
Acetone			up to 10%, aqueous	20	-	-	O	+	+	O		+	O	-	+	O
				40				+	+	O		+	O		O	O
				60				+	+	O		+	-		-	O
				80												
				100												
				120												
				140												
Acetonitrile	CH_3CN	81.6	100%	20	-	-	-			-						
				40												
				60												
				80												
				100												
				120												
				140												
Acetophenone	$CH_3\text{-}CO\text{-}C_6H_5$		100 %	20	-	-	-			-		+	-	-	-	
				40												
				60												
				80												
				100												
				120												
				140												
Acrylic acid methyl ester	$CH_2{=}CHCOOCH_3$	80.3	technically pure	20	-	-	-			+		O				
				40												
				60												
				80												
				100												
				120												
				140												
Acrylic ester	$CH_2{=}CH\text{-}COO\ CH_2CH_3$	100	technically pure	20	-	-	-		-	-		O	-	-	O	+
				40												
				60												
				80												
				100												
				120												
				140												
Acrylonitrile	$CH_2{=}CH\text{-}CN$	77	technically pure	20	-	-	-	+	+	-		+	O	-	+	O
				40				+	O			+	O		+	O
				60				+				O	-		+	-
				80												
				100												
				120												
				140												

(Courtesy George Fischer Engineering Handbook)

Aggressive Media					Chemical Resistance										
Medium	Formula	Boiling point °C	Concentration	Temperature °C	PVC	CPVC	ABS	PE	PP-H	PVDF (SYGEF)	EPDM	FPM	NBR	CR	CSM
Adipic acid	$HOOC\text{-}(CH_2)_4\text{-}COOH$	Fp 153	saturated, aqueous	20	+	+	-	+	+	+	+	+	+	+	+
				40	+	+		+	+		+	+	+	+	+
				60	-	+		+	+		+	+	+	+	+
				80		+			+						
				100											
				120											
				140											
Alum	see Potassium/ aluminium sulphate														
Alcoholic spirits (Gin, Whisky,etc.)			approx. 40% ethyl alcohol	20	+	O	-	+	+	+	+	+	+	+	+
				40											
				60											
				80											
				100											
				120											
				140											
Allyl alcohol	$H_2C{=}CH\text{-}CH_2\text{-}OH$	97	96%	20	O	O	-	+	+		O	O	+	O	+
				40	-			+	+		O	-	+	-	+
				60				+	+		O		+		+
				80							-		+		-
				100											
				120											
				140											
Aluminium chloride	$AlCl_3$		10%, aqueous	20	+	+	+	+	+	+	+	+	+	+	+
				40	+	+	+	+	+	+	+	+	+	+	+
				60	+	+	+	+	+	+	+	+	O	+	+
				80		+				+	+	+			+
				100						+	+	+			
				120						+					
				140											
Aluminium chloride	$AlCl_3$	115	saturated	20	+	+	+	+	+	+	+	+	+	+	+
				40	+	+	+	+	+	+	+	+	+	+	+
				60	+	+	+	+	+	+	+	+	+	+	+
				80		+			+	+		+	O	+	+
				100					O	+		+	-		+
				120						+					
				140											
Aluminium fluoride	AlF_3		saturated	20		+				+					
				40		+				+					
				60		+				+					
				80						+					
				100											
				120											
				140											
Aluminium hydroxide	$Al(OH)_3$		Suspension	20		+					+				
				40		+					+				
				60		+					+				
				80		+									
				100											
				120											
				140											
Aluminium nitrate	$Al(NO_3)_3$		saturated	20		+				+	+				
				40		+				+	+				
				60		+				+	+				
				80		+									
				100											
				120											
				140											

(Courtesy George Fischer Engineering Handbook)

Aggressive Media					Chemical Resistance											
Medium	Formula	Boiling point °C	Concentration	Temperature °C	PVC	CPVC	ABS	PE	PP-H	PVDF (SYGEF)		EPDM	FPM	NBR	CR	CSM
Aluminium sulphate	$Al_2(SO_4)_3$		10%, aqueous	20	+	+	+	+	+	+		+	+	+	+	+
				40	+	+	+	+	+	+		+	+	+	+	+
				60	O	+	+	+	+	+		+	+	+	+	+
				80		+			+	+			+			O
				100					+	+						
				120						+						
				140												
Aluminium sulphate			cold saturated, aqueous	20	+	+	+	+	+	+		+	+	+	+	+
				40	+	+	+	+	+	+		+	+	+	+	+
				60	+	+	+	+	+	+		+	+	+	+	O
				80		+			+	+			+			O
				100						+						
				120						+						
				140												
Ammonia (SpRB)	NH_3	-33	gaseous, technically pure	20	+	-	-	+	+	+		+	+	+	+	+
				40	+			+	+	+			O			
				60	+			+	+	O						
				80						O						
				100						O						
				120												
				140												
Ammonium acetate	CH_3COONH_4		aqueous, all	20	+	+	O	+	+	+		+	+	+	+	+
				40	+	+		+	+	+		+	+	O	+	+
				60	O	+		+	+	+		+	+		O	
				80		+			+	+		O				
				100					+	+						
				120												
				140												
Ammonium aluminium sulfate				20						+						
				40						+						
				60						+						
				80						+						
				100						+						
				120												
				140												
Ammonium bromide				20						+						
				40						+						
				60						+						
				80												
				100												
				120												
				140												
Ammonium carbonate	$(NH_4)_2CO_3$		50%, aqueous	20	+	+	+	+	+	+		+	+	+	+	+
				40	+	+	+	+	+	+		+	+	+	+	+
				60	O	+	+	+	+	+		+	+	+	+	+
				80		+			+	+		+	+			+
				100					+	+						
				120						+						
				140												
Ammonium chloride	NH_4Cl	115	aqueous, cold saturated	20	+	+	+	+	+	+		+	+	+	+	+
				40	+	+	+	+	+	+		+	+	+	+	+
				60	O	+	+	+	+	+		+	+	+	+	+
				80		+			+	+		+	+		+	+
				100					+	+		+	+			+
				120						+			+			
				140												

(Courtesy George Fischer Engineering Handbook)

Aggressive Media					Chemical Resistance											
Medium	Formula	Boiling point °C	Concentration	Temperature °C	PVC	CPVC	ABS	PE	PP-H	PVDF (SYGEF)		EPDM	FPM	NBR	CR	CSM
Ammonium citrate				20	+					+						
				40	+					+						
				60	+					+						
				80						+						
				100						+						
				120												
				140												
Ammonium dicromate	$(NH_4)_2 Cr_2 O_7$		saturated	20		+										
				40		+										
				60		+										
				80		+										
				100												
				120												
				140												
Ammonium dihydrogenphosphate				20	+			+	+							
				40	+			+	+							
				60	+			+	+							
				80					+							
				100												
				120												
				140												
Ammonium fluoride	NH_4F			20	+	+		+	+	+						
				40	+			+	+	+						
				60	+			+	+	+						
				80					+	+						
				100						+						
				120												
				140												
Ammonium formiate				20						+						
				40						+						
				60						+						
				80						+						
				100						+						
				120												
				140												
Ammonium hexafluorosilicate				20						+						
				40						+						
				60						+						
				80						+						
				100						+						
				120												
				140												
Ammonium hydrogen fluoride	NH_4HF_2		50%, aqueous	20	+	+		+	+	+		+	+			
				40	+	+		+	+	+						
				60	O	+		+	+	+						
				80												
				100												
				120												
				140												
Ammonium hydrogencarbonate				20	+			+	+							
				40	+			+	+							
				60	+			+	+							
				80					+							
				100												
				120												
				140												

(Courtesy George Fischer Engineering Handbook)

Aggressive Media					Chemical Resistance											
Medium	Formula	Boiling point °C	Concentration	Temperature °C	PVC	CPVC	ABS	PE	PP-H	PVDF (SYGEF)		EPDM	FPM	NBR	CR	CSM
Ammonium hydrogenphosphate				20	+			+	+							
				40	+			+	+							
				60	+			+	+							
				80					+							
				100												
				120												
				140												
Ammonium hydrogensulfite				20						+						
				40						+						
				60						+						
				80						+						
				100						+						
				120												
				140												
Ammonium hydroxide	NH_4OH		aqueous, cold saturated	20	+	-	+		+	-		+	-	+	+	+
				40	+		+		+			+		O	+	+
				60	O		O		+			O		O	+	O
				80											O	-
				100												
				120												
				140												
Ammonium nitrate	NH_4NO_3	112	aqueous, saturated	20	+	+	+	+	+	+		+	+	+	+	+
				40	+	+	+	+	+	+		+	+	+	+	+
				60	+	+	+	O	+	+		+	+	O		O
				80		+			O	+			+			
				100						+						
				120						+						
				140												
Ammonium oxalate	$H_4NOOC\text{-}COONH_4$			20						+		+				
				40						+						
				60						+						
				80						+						
				100						+						
				120												
				140												
Ammonium persulphate	$(NH_4)_2S_2O_8$			20		+				+						
				40		+				+						
				60		+				+						
				80		+				+						
				100						+						
				120												
				140												
Ammonium phosphate	$(NH_4)_3PO_4$		saturated	20	+	+	+	+	+	+		+	+	+	+	+
				40	+	+	+	+	+	+		+	+	+	+	+
				60	+	+	+	+	+	+			+	O	+	O
				80					+	+			+			
				100						+			+			
				120												
				140												
Ammonium sulphate	$(NH_4)_2SO_4$		aqueous, saturated	20	+	+	+	+	+	+		+	+	+	+	+
				40	+	+	+	+	+	+		+	+	+	+	+
				60	+	+	+	+	+	+		+	+	O	+	O
				80		+			+	+		+	+			
				100					+	+			+			
				120						+						
				140												

(Courtesy George Fischer Engineering Handbook)

Aggressive Media					Chemical Resistance											
Medium	Formula	Boiling point °C	Concentration	Temperature °C	PVC	CPVC	ABS	PE	PP-H	PVDF (SYGEF)		EPDM	FPM	NBR	CR	CSM
Ammonium sulphide	$(NH_4)_2S$		aqueous, all	20	+	O	+	+	+	+		+	+	+	+	+
				40	+	O	+	+	+	+		+	O	+	+	+
				60	O	O	+	+	+	+		+	-	+	+	+
				80		-			+							
				100												
				120												
				140												
Ammonium tetrafluoroborate				20						+						
				40						+						
				60						+						
				80						+						
				100						+						
				120												
				140												
Ammonium thiocyanate	NH_4SCN		saturated	20		+				+						
				40		+				+						
				60		+				+						
				80		+										
				100												
				120												
				140												
Amyl acetate	$CH_3(CH_2)_4\text{-}COOCH_3$	141	technically pure	20	-	-	-	+	O	+		O	-	-	-	-
				40				+	O	O						
				60				+	-	O						
				80												
				100												
				120												
				140												
Amyl alcohol (SpRB)	$CH_3(CH_2)_3\text{-}CH_2\text{-}OH$	137	technically pure	20	+	+	-	+	+	+		+	O	+	+	O
				40	+	+		+	+	+		+		+	+	
				60	O	+		+	+	+		+		+	+	
				80					+	+						
				100						+						
				120						O						
				140												
Aniline	$C_6H_5NH_2$	182	technically pure	20	-	-	-	O	O	+		-	O	-	-	-
				40						O			O			
				60						-			O			
				80												
				100												
				120												
				140												
Aniline hydrochloride	C_6H_7N+HCl	245	aqueous, saturated	20	+	+	-	+	+	+		+	O	O	-	+
				40	O	+		+	+			+	-	-		+
				60				O	O			+				+
				80												O
				100												
				120												
				140												
Antimony thiocyanate				20						+						
				40						+						
				60						+						
				80						+						
				100						+						
				120												
				140												

(Courtesy George Fischer Engineering Handbook)

Aggressive Media					Chemical Resistance										
Medium	Formula	Boiling point °C	Concentration	Temperature °C	PVC	CPVC	ABS	PE	PP-H	PVDF (SYGEF)	EPDM	FPM	NBR	CR	CSM
Antimony trichloride (SpRB)	$SbCl_3$		90%, aqueous	20	+	+	-	+	+	+	+	+	-	+	+
				40	+			+	+	+					
				60				+	+	+					
				80											
				100											
				120											
				140											
Aqua regia (SpRB)	HNO_3+HCl			20	+	+	-	-	-	O	-	O	-	-	O
				40	O										
				60											
				80											
				100											
				120											
				140											
Arsenic acid	H_3AsO_4		80%, aqueous	20	+	+	+	+	+	+	+	+	+	+	+
				40	+	+	+	+	+	+	+	+	+	+	+
				60	O	+	+	+	+	+	+	+	+	+	+
				80		+			+	+	+	+	O	+	+
				100						+		+			
				120						+					
				140											
Barium carbonate	$BaCO_3$			20	+	+	+	+	+	+	+	+	+	+	+
				40	+	+		+	+	+	+	+	+		
				60	+	+		+	+	+	+				
				80		+			+						
				100											
				120											
				140											
Barium chloride	$BaCl_2$		saturated	20	+	+	+	+	+	+	+	+	+	+	+
				40	+	+		+	+	+	+	+	+		
				60	+	+		+	+	+	+	+			
				80		+			+	+		+			
				100						+					
				120											
				140											
Barium hydroxide	$Ba(OH)_2$	102	aqueous, saturated	20	+	+	+	+	+	-	+	+	+	+	+
				40	+	+	+	+	+		+		+	+	O
				60	O	+	+	+	+		+		+	+	
				80		+			+		+				
				100											
				120											
				140											
Barium salts			aqueous, all	20	+	+	+	+	+	+	+	+	+	+	+
				40	+	+	+	+	+	+	+	+	+	+	+
				60	+	+	+	+	+	+	+	+	+	+	+
				80		+			+	+	+	+			
				100						+					
				120											
				140											
Barium sulfate	$BaSO_4$			20	+			+	+	+	+				
				40	+			+	+	+	+				
				60	+			+	+	+	+				
				80					+	+					
				100						+					
				120											
				140											

(Courtesy George Fischer Engineering Handbook)

Aggressive Media					Chemical Resistance											
Medium	Formula	Boiling point °C	Concentration	Temperature °C	PVC	CPVC	ABS	PE	PP-H	PVDF (SYGEF)		EPDM	FPM	NBR	CR	CSM
Barium sulfide	BaS		suspension	20	+	+		+	+	+		+				
				40	+	+		+	+	+		+				
				60	+	+		+	+	+		+				
				80		+			+	+						
				100						+						
				120												
				140												
Battery acid	see Sulphuric acid 40%															
Beef tallow emulsion, sulphonated (Sp&B)			usual commercial	20	+	o	+	+	+	+		-	+	+	+	+
				40						+						
				60						+						
				80												
				100												
				120												
				140												
Beer			usual commercial	20	+	+	+	+	+	+			+	+	+	+
				40	+	+	+	+	+	+						
				60	+	+	+	+	+	+						
				80		+				+						
				100												
				120												
				140												
Benzaldehyde	C_6H_5-CHO	180	saturated, aqueous	20	-	-	-	+	+	+		+	+	O	-	-
				40				+		O		+	+			
				60				+		-		+	+			
				80												
				100												
				120												
				140												
Benzene	C_6H_6	80	technically pure	20	-	-	-	O	O	+		-	+	O	-	-
				40				O	-	O						
				60						-						
				80												
				100												
				120												
				140												
Benzenesulfonic acid	$C_6H_5SO_3H$		technically pure	20						+			+			
				40						+			+			
				60						+						
				80						+						
				100						+						
				120												
				140												
Benzoic acid	C_6H_5-COOH	Fp.*, 122	aqueous, all	20	+	+	+	+	+	+		+	+	-	-	-
				40	+	+	+	+	+	+		+	+			
				60	O	+		+	+	+			+			
				80		O			+	+			+			
				100					+	+			O			
				120						+						
				140												
Benzoyl chloride	$C_6H_5CHCl_2$		technically pure	20						+						
				40						+						
				60						+						
				80						O						
				100						-						
				120												
				140												

(Courtesy George Fischer Engineering Handbook)

Aggressive Media					Chemical Resistance											
Medium	Formula	Boiling point °C	Concentration	Temperature °C	PVC	CPVC	ABS	PE	PP-H	PVDF (SYGEF)		EPDM	FPM	NBR	CR	CSM
Benzyl alcohol (SpRB)	$C_6H_5\text{-}CH_2\text{-}OH$	206	technically pure	20	O	-	-	+	+	+		-	+	-	+	O
				40				+	+	+					+	
				60				O	O	O					+	
				80						-						
				100												
				120												
				140												
Beryllium chloride				20						+						
				40						+						
				60						+						
				80												
				100												
				120												
				140												
Beryllium sulfate				20						+			+			
				40						+			+			
				60						+			+			
				80						+						
				100						+						
				120												
				140												
Borax	$Na_2B_4O_7$		aqueous, all	20	+	+	+	+	+	+		+	+	+	+	+
				40	+	+	+	+	+	+		+	+	+	+	+
				60	O	+		+	+	+		+	+	+	+	O
				80		+			+	+		+	+			
				100					+	+						
				120												
				140												
Boric acid	H_3BO_3		all, aqueous	20	+	+	+	+	+	+		+	+	+	+	+
				40	+	+	+	+	+	+		+	+	+	+	+
				60	O	+	+	+	+	+		+	+	+	+	+
				80		+			+	+		+	+			
				100					+	+			+			
				120						+						
				140												
Brine, containing chlorine				20	+	+	-	+	O	+		O	+	O	O	O
				40	+	+				+						
				60	+	+				O						
				80												
				100												
				120												
				140												
Brombenzene	C_6H_5Br			20	-	-				+			+			
				40												
				60												
				80												
				100												
				120												
				140												
Bromine, liquid	Br_2	59	technically pure	20	-	-	-	-	-	+		-	+	-	-	-
				40						+						
				60						+						
				80						+						
				100						O						
				120												
				140												

(Courtesy George Fischer Engineering Handbook)

Aggressive Media					Chemical Resistance											
Medium	Formula	Boiling point °C	Concentration	Temperature °C	PVC	CPVC	ABS	PE	PP-H	PVDF (SYGEF)		EPDM	FPM	NBR	CR	CSM
Bromine, vapours	Br_2		high	20	-	-	-	-	-	+		-	+	-	-	-
				40						+						
				60						+						
				80						+						
				100						O						
				120												
				140												
Bromine water	$Br.H_2O$		saturated, aqueous	20	+	o	-	-	-	+		-	+	-	-	-
				40						+						
				60						+						
				80						+						
				100												
				120												
				140												
Butadiene (Q/E)	$H_2C=CH-CH=CH_2$	-4	technically pure	20	+	+	-	+	+	+		-	O	-	+	+
				40					+	+					+	O
				60					+	+					O	-
				80						+						
				100						+						
				120												
				140												
Butane	C_4H_{10}	0	technically pure	20	+	+	+	+	+	+		-	+	+	+	+
				40												
				60												
				80												
				100												
				120												
				140												
Butanediol (SpRB)	$HO-(CH_2)_4-OH$	230	aqueous, 10%	20	+	+	-	+	+			+	+	+	O	+
				40	O	+		+	+			+	+	+	-	+
				60				+	+			+	+	+		+
				80												
				100												
				120												
				140												
Butanol (SpRB)	C_4H_9OH	117	technically pure	20	+	+	-	+	+	+		+	+	+	+	+
				40	+	+		+	+	+		+	O	+	+	+
				60	O	+		+	O	+		+	-	+	O	+
				80		O			-	+						
				100						O						
				120												
				140												
Butyl acetate	$CH_3COOCH_2CH_2CH_2CH_3$	126	technically pure	20	-	-	-	+	O	+		+	O	-	O	O
				40						O		-	-		-	-
				60						-						
				80												
				100												
				120												
				140												
Butyl phenol, p-tertiary	$(CH_3)_3C-C_6H_4-OH$	237	technically pure	20	O	O	-	O	+	+		-	O	-	-	-
				40	-	-				+						
				60						+						
				80						+						
				100												
				120												
				140												

(Courtesy George Fischer Engineering Handbook)

Aggressive Media					Chemical Resistance											
Medium	Formula	Boiling point °C	Concentration	Temperature °C	PVC	CPVC	ABS	PE	PP-H	PVDF (SYGEF)		EPDM	FPM	NBR	CR	CSM
Butylene glycol (SpRB)	$HO\text{-}CH_2\text{-}CH{=}CH\text{-}CH_2\text{-}OH$	235	technically pure	20	+	+	+	+	+	+		+	+	-	+	O
				40	+	+	+	+	+	+		+	+		+	
				60	O	+	+	+	+	+		+	O		+	
				80						+						
				100												
				120												
				140												
Butylene liquid	C_4H_8	51	technically pure	20	+			-	-	+		O	+	+	+	O
				40												
				60												
				80												
				100												
				120												
				140												
Butyric acid (SpRB)	$CH_3\text{-}CH_2\text{-}CH_2\text{-}COOH$	163	technically pure	20	+	+	-	+	+	+		O	O	-	O	O
				40				+		+						
				60				O		+						
				80						+						
				100						O						
				120												
				140												
Cadmium bromide	$CdBr_2$			20	+	+		+	+			+	+			
				40	+	+		+	+			+	+			
				60	+	+		+	+			+	+			
				80		+							+			
				100												
				120												
				140												
Cadmium chloride	$CdCl_2$			20	+	+		+	+			+	+			
				40	+	+		+	+			+	+			
				60	+	+		+	+			+	+			
				80					+							
				100												
				120												
				140												
Cadmium cyanide	Cd(CN)2			20	+			+	+							
				40	+			+	+							
				60	+			+	+							
				80					+							
				100												
				120												
				140												
Cadmium sulfate	$CdSO_4$			20	+	+		+	+			+	+			
				40	+	+		+	+			+	+			
				60	+	+		+	+			+	+			
				80		+			+				+			
				100												
				120												
				140												
Calcium acetate	$(CH_3COO)_2Ca$		saturated	20	+	+	+	+	+	+		+	+			
				40	+	+		+	+	+		+				
				60		+		+	+	+		+				
				80		+										
				100												
				120												
				140												

(Courtesy George Fischer Engineering Handbook)

Aggressive Media					Chemical Resistance											
Medium	Formula	Boiling point °C	Concentration	Temperature °C	PVC	CPVC	ABS	PE	PP-H	PVDF (SYGEF)		EPDM	FPM	NBR	CR	CSM
Calcium bisulphite	$Ca(HSO_3)_2$		cold saturated, aqueous	20	+	+	+			+		+	+	-	O	+
				40		+	+			+			+			
				60		+				+			+			
				80		+				+			+			
				100						+			+			
				120						+						
				140												
Calcium carbonate	$CaCO_3$			20	+	+		+	+	+		+	+			
				40	+	+		+	+	+		+	+			
				60	+	+		+	+	+		+	+			
				80		+			+	+		+	+			
				100						+						
				120												
				140												
Calcium chlorate	$Ca(ClO_3)_2$			20	+	+		+	+	+						
				40	+	+		+	+	+						
				60	+	+		+	+	+						
				80		+										
				100												
				120												
				140												
Calcium chloride	$CaCl_2$	125	saturated, aqueous, all	20	+	+	+	+	+	+		+	+	+	+	+
				40	+	+	+	+	+	+		+	+	+	+	+
				60	O	+		+	+	+		+	+	+	+	+
				80		+			+	+		+	+	O	O	+
				100					+	+		O	+			+
				120						+						
				140												
Calcium fluoride	Caf_2			20	+			+	+				+			
				40	+			+	+				+			
				60	+			+	+				+			
				80					+							
				100												
				120												
				140												
Calcium hydrogencarbonate				20						+		+	+			
				40						+		+	+			
				60						+		+	+			
				80						+		+	+			
				100						+			+			
				120												
				140												
Calcium hydrogensulfide	$Ca(SH)_2$			20		+				+		+				
				40		+				+		+				
				60		+				+		+				
				80		+				+						
				100						+						
				120												
				140												
Calcium hydrosulfite	$Ca(HSO_3)_2$		saturated	20						+						
				40						+						
				60						+						
				80						+						
				100						+						
				120												
				140												

(Courtesy George Fischer Engineering Handbook)

Aggressive Media					Chemical Resistance											
Medium	Formula	Boiling point °C	Concentration	Temperature °C	PVC	CPVC	ABS	PE	PP-H	PVDF (SYGEF)		EPDM	FPM	NBR	CR	CSM
Calcium hydroxide	$Ca(OH)_2$	100	saturated, aqueous	20	+	+	+	+	+	O		+	+	+	+	+
				40	+	+	+	+	+	-		+	+	+	+	+
				60	+	+	+	+	+			+	+	O	+	+
				80		+			+			+	+			+
				100									+			+
				120												
				140												
Calcium nitrate	$Ca(NO_3)_2$	115	50%, aqueous	20	+	+	+	+	+	+		+	+	+	+	+
				40	+	+	+	+	+	+		+	+	+	+	+
				60		+		+	+	+		+	+			+
				80		+				+			+			
				100						+						
				120												
				140												
Calcium phosphate	$Ca(H_2PO_4)_2$ $CaHPO_4$ $Ca_3(PO_4)_2$			20						+						
				40						+						
				60						+						
				80						+						
				100						+						
				120												
				140												
Calcium sulfide	Cas			20	+				+			+				
				40	+				+							
				60	+				+							
				80					+							
				100												
				120												
				140												
Calcium sulphate	$CaSO_4$		suspensions	20	+	+				+		+				
				40	+	+				+		+				
				60	+	+				+		+				
				80		+				+						
				100						+						
				120												
				140												
Calcium sulphite	$Ca(HSO_3)_2$		aqueous, cold saturated	20	+			+	+			+				
				40	+			+	+							
				60	+			+	+							
				80					+							
				100												
				120												
				140												
Calcium tungstate				20						+						
				40						+						
				60						+						
				80												
				100												
				120												
				140												
Calciumbromide	$CaBr_2$			20	+	+		+	+			+	+			
				40	+	+		+	+			+	+			
				60	+	+		+	+			+	+			
				80		+			+							
				100												
				120												
				140												

(Courtesy George Fischer Engineering Handbook)

Aggressive Media					Chemical Resistance											
Medium	Formula	Boiling point °C	Concentration	Temperature °C	PVC	CPVC	ABS	PE	PP-H	PVDF (SYGEF)		EPDM	FPM	NBR	CR	CSM
Calciumlactate	$(CH_3COO)_2Ca$		saturated	20				+	+	+		+				
				40				+	+	+		+				
				60				+	+	+		+				
				80					+	+						
				100						+						
				120												
				140												
Caprolactam	$C_6H_{11}NO$			20		-										
				40												
				60												
				80												
				100												
				120												
				140												
Caprolactone	$C_6H_{10}O_2$			20		-										
				40												
				60												
				80												
				100												
				120												
				140												
Carbon dioxide -carbonic acid	CO_2		technically pure, anhydrous	20	+	+	+	+	+	+		+	+	+	+	+
				40	+	+	+	+	+	+		+	+	+	+	+
				60	+	+	+	+	+	+			+	+	+	+
				80		+			+	+			+			+
				100						+						
				120												
				140												
Carbon disulphide	CS_2	46	technically pure	20	-	-	-	O	O	+			+	-	-	-
				40												
				60												
				80												
				100												
				120												
				140												
Carbon tetrachloride	CCl_4	77	technically pure	20	-	-	-	-	-	+		-	+	-	-	-
				40												
				60												
				80												
				100												
				120												
				140												
Carbonic acid				20	+	+		+	+	+		+	+			
				40	+	+		+	+	+		+	+			
				60	+	+		+	+	+		+	+			
				80		+			+	+		+	+			
				100						+			+			
				120												
				140												
Caro's acid	see Peroxomonosulfuric acid															
Casein				20						+						
				40						+						
				60						+						
				80												
				100												
				120												
				140												

(Courtesy George Fischer Engineering Handbook)

Aggressive Media					Chemical Resistance											
Medium	Formula	Boiling point °C	Concentration	Temperature °C	PVC	CPVC	ABS	PE	PP-H	PVDF (SYGEF)		EPDM	FPM	NBR	CR	CSM
Cäsium chloride	ClCs			20						+						
				40						+						
				60						+						
				80												
				100												
				120												
				140												
Cäsiumhydroxide	CsOH			20						+						
				40						+						
				60						+						
				80												
				100												
				120												
				140												
Caustic potash solution (potassium hydroxide)	KOH	131	50%, aqueous	20	+	+	+	+	+	-		+	-	O	-	+
				40	+	+	+	+	+			+		-		O
				60	O	+	+	+	+			+				O
				80		+			+			O				-
				100					+							
				120												
				140												
Caustic soda solution	NaOH		50%, aqueous	20	+	+	+	+	+	O		+	-	O	-	+
				40	+	+		+	+			+		-		O
				60		+		+	+			+				-
				80					+							
				100												
				120												
				140												
Cerium (III) -chloride	$CeCl_3$			20						+						
				40						+						
				60						+						
				80												
				100												
				120												
				140												
Chloral hydrate	CCl_3-$CH(OH)_2$	98	technically pure	20	-		-	+	O	-		O	O	-	O	+
				40				+								
				60				+	-							
				80												
				100												
				120												
				140												
Chloric acid (SpRB)	$HClO_3$		10%, aqueous	20	+	+	-	+	-	+		+	-	-	-	+
				40	+	+		+		+		+				+
				60	O	+						+				+
				80												
				100												
				120												
				140												
Chloric acid (SpRB)	$HClO_3$		20%, aqueous	20	+	+	-	O	-	+		+	-	-	-	+
				40	+	+						+				+
				60	O	+										
				80												
				100												
				120												
				140												

(Courtesy George Fischer Engineering Handbook)

Aggressive Media					Chemical Resistance											
Medium	Formula	Boiling point °C	Concentration	Temperature °C	PVC	CPVC	ABS	PE	PP-H	PVDF (SYGEF)		EPDM	FPM	NBR	CR	CSM
Chlorosulphonic acid	$ClSO_3H$	158	technically pure	20	O	-	-	-	-	O		-	-	-	-	-
				40						-						
				60												
				80												
				100												
				120												
				140												
Chrome alum (chromium potassium sulphate)	$KCr(SO_4)2$		cold saturated, aqueous	20	+	+	+	+	+	+		+	+	+	+	+
				40	+	+	+	+	+	+		+	+	+	+	+
				60	+	+		+	+			+	+	+	+	+
				80								+	+			
				100									+			
				120												
				140												
Chromic acid (SpRB)	CrO_3+H_2O		up to 50%, aqueous	20	O	+	-	O	O	+		O	+	-	-	O
				40	O	O		-	-	+		O	+			O
				60	-	O				+		O	+			O
				80		-				+						
				100						O						
				120						O						
				140												
Chromic acid (SpRB)			all, aqueous	20	O	O	-	O	O	+			+	-	-	O
				40						+			+			O
				60						+			O			O
				80						O						
				100						O						
				120												
				140												
Chromic acid + sulphuric acid + water (SpRB)	CrO_3 H_2SO_4 H_2O		50 g 15 g 35 g	20	+	+	-	-	-	+		O	+	-	-	O
				40	+	+				+		O	+			O
				60	O	+				+			+			
				80		O				O						
				100												
				120												
				140												
Chromium (II) -chloride				20	+					+						
				40	+					+						
				60	+					+						
				80						+						
				100						+						
				120												
				140												
Chromium (II) -fluoride	CrF_3			20						+						
				40						+						
				60						+						
				80												
				100												
				120												
				140												
Chromium (III) -chloride	$CrCl_3$			20	+					+						
				40	+					+						
				60	+					+						
				80						+						
				100						+						
				120												
				140												

(Courtesy George Fischer Engineering Handbook)

Aggressive Media					Chemical Resistance											
Medium	Formula	Boiling point °C	Concentration	Temperature °C	PVC	CPVC	ABS	PE	PP-H	PVDF (SYGEF)		EPDM	FPM	NBR	CR	CSM
Chlorine	Cl_2		moist, 97%, gaseous	20	-	-	-	-	-	-		-	+	-	-	O
				40												
				60												
				80												
				100												
				120												
				140												
Chlorine	Cl_2		anhydrous, technically pure	20	-	-	-	O	-	+		O	+	-	-	O
				40				O		+						
				60				-		+						
				80						+						
				100						O						
				120												
				140												
Chlorine	Cl_2		liquid, technically pure	20	-	-	-	-	-	+		-	O	-	-	-
				40												
				60												
				80												
				100												
				120												
				140												
Chlorine water (SpRB)	Cl_2 H_2O		saturated	20	+	+	O	O	O	O		O	O	-	O	-
				40	+	+		O								
				60	O	O										
				80		-										
				100												
				120												
				140												
Chloroacetic acid, mono (SpRB)	$ClCH_2COOH$		50%, aqueous	20	+	-	-	+	+	+		O	-	-	-	O
				40	+			+	+	O						
				60				+	+	-						
				80												
				100												
				120												
				140												
Chloroacetic acid, mono (SpRB)	$ClCH_2COOH$	188	technically pure	20	+	-	-	+	+	-		O	-	-	-	O
				40	+			+	+							
				60	O			+	+							
				80												
				100												
				120												
				140												
Chlorobenzene	C_6H_5Cl	132	technically pure	20	-	-	-	O	+	+		-	-	-	-	O
				40						+						
				60						O						
				80						-						
				100												
				120												
				140												
Chloroethanol	$ClCH_2$-CH_2OH	129	technically pure	20	-		-	+	+	+		O	-	+	-	O
				40				+	+	O						
				60				+	+	O						
				80						-						
				100												
				120												
				140												

(Courtesy George Fischer Engineering Handbook)

Aggressive Media					Chemical Resistance										
Medium	Formula	Boiling point °C	Concentration	Temperature °C	PVC	CPVC	ABS	PE	PP-H	PVDF (SYGEF)	EPDM	FPM	NBR	CR	CSM
Chromium (III) -nitrate	$Cr(NO_3)_3$			20	+					+					
				40	+					+					
				60	+					+					
				80						+					
				100						+					
				120											
				140											
Chromium (III) -sulfate	$Cr_2(SO_4)_3$			20	+					+					
				40	+					+					
				60	+					+					
				80						+					
				100						+					
				120											
				140											
Cider				20	+	+	+	+	+	+	+	+	+	+	+
				40			+			+					
				60						+					
				80											
				100											
				120											
				140											
Citric acid		Fp. *153	10%, aqueous	20	+	+	+	+	+	+	+	+	+	+	+
				40	+	+	+	+	+	+	+	+	+	+	+
				60	O	+	+	+	+	+	+	+	O	+	+
				80					+	+					
				100					+	+					
				120											
				140											
Citric acid				20	+			+	+						
				40	+			+	+						
				60				+	+						
				80					+						
				100											
				120											
				140											
Citric acid up to 10 %				20						+					
				40						+					
				60						+					
				80											
				100											
				120											
				140											
Coal gas, benzene free				20	+	+	+	+	+	+		+	+	O	+
				40											
				60											
				80											
				100											
				120											
				140											
Coconut fat alcohol (SpRB)			technically pure	20	+	-	-	+	+	+		+	+	+	+
				40	+			O	+	+		+	+	O	O
				60	O				O	+		+	+		
				80											
				100											
				120											
				140											

(Courtesy George Fischer Engineering Handbook)

Aggressive Media					Chemical Resistance											
Medium	Formula	Boiling point °C	Concentration	Temperature °C	PVC	CPVC	ABS	PE	PP-H	PVDF (SYGEF)		EPDM	FPM	NBR	CR	CSM
Compressedair, containing oil (SpRB)				20	-	-	-	+	O	+		-	+	+	+	+
				40				+		+						
				60						+						
				80												
				100												
				120												
				140												
Copper salts	CuCl, $CuCl_2$, CuF_2, $Cu(NO_3)_2$, $CuSO_4$, $Cu(CN)_2$		all, aqueous	20	+	+	+	+	+	+		+	+	+	+	+
				40	+	+	+	+	+	+		+	+	+	+	+
				60	O	+	+	+	+	+			+	O	+	O
				80		+			+	+			+			
				100						+						
				120												
				140												
Corn oil (SpRB)			technically pure	20	O	O	O	+	+	+			+	+	O	+
				40		O		+	+	+			+	+	-	+
				60				O	O	+			+	+		O
				80						+						
				100												
				120												
				140												
Cresol	HO-C_6H_4-CH_3		cold saturated, aqueous	20	O	-	-	+	+	+			+	O	-	O
				40				+	+	+			+	O		
				60						+						
				80						O						
				100												
				120												
				140												
Crotonic aldehyde	CH_3-CH=CH-CHO	102	technically pure	20	-	-	-	+	+	+		+	+	+	+	+
				40						O						
				60						-						
				80												
				100												
				120												
				140												
Cyclohexone (Q/E)	C_6H_{12}	81	technically pure	20	-	-	-	+	+	+		-	+	+	-	-
				40				+		+						
				60				+		+						
				80						+						
				100												
				120												
				140												
Cyclohexanol (SpRB)	$C_6H_{12}O$	161	technically pure	20	+	+	-	+	+	+		-	+	O	+	+
				40	+	+		+	+	+						
				60	+	+		+	O	O						
				80		O				O						
				100						-						
				120												
				140												
Cyclohexanone	$C_6H_{10}O$	155	technically pure	20	-	-	-	+	+	+		O	-	-	-	-
				40				O	O	O						
				60				O	O	-						
				80												
				100												
				120												
				140												

(Courtesy George Fischer Engineering Handbook)

Aggressive Media					Chemical Resistance											
Medium	Formula	Boiling point °C	Concentration	Temperature °C	PVC	CPVC	ABS	PE	PP-H	PVDF (SYGEF)		EPDM	FPM	NBR	CR	CSM
Densodrine W				20	+	+	O			+			+	+	+	
				40	+	+										
				60	+	+										
				80												
				100												
				120												
				140												
Detergents (SpRB)	see washing powder		for usual washing lathers													
Dextrine	$(C_6H_{10}O_5)_n$		usual commercial	20	+	+	+	+	+	+		+	+	+	+	+
				40	+	+	+	+		+		+	+	+	+	+
				60	+	+	+	+		+		+	+	+	+	+
				80		+				+						
				100						+						
				120						+						
				140												
Dextrose	siehe Glucose			20	+	+	+	+	+	+		+	+			
				40	+	+		+	+	+		+	+			
				60	+	+		+	+	+		+	+			
				80		+			+	+		+	+			
				100						+			+			
				120												
				140												
Dibuttyl ether	$C_4H_9OC_4H_9$	142	technically pure	20	-	-	-	O	O			-	+	+	-	O
				40									+	O		O
				60				-	-				O	-		O
				80												
				100												
				120												
				140												
Dibutyl phthalate	$C_6H_4(COOC_4H_9)_2$	340	technically pure	20	-	-	-	+	+	+		O	O	-	-	-
				40				O	O	+						
				60				O	O	O						
				80												
				100												
				120												
				140												
Dibutyl sebacate	$C_8H_{16}(COOC_4H_9)_2$	344	technically pure	20	-	-	-	+	+	+		+	+	-	-	-
				40												
				60												
				80												
				100												
				120												
				140												
Dichlorbenzol	$C_6H_4Cl_2$	180	technically pure	20	-	-	-									
				40												
				60												
				80												
				100												
				120												
				140												
Dichloroacetic acid	$Cl_2CHCOOH$	194	technically pure	20	+	-	-	+	+	+		+	O	-	O	+
				40	+			+	+	+		+	-		-	O
				60	O			O	O	O		+				-
				80						-						
				100												
				120												
				140												

(Courtesy George Fischer Engineering Handbook)

Aggressive Media					Chemical Resistance											
Medium	Formula	Boiling point °C	Concentration	Temperature °C	PVC	CPVC	ABS	PE	PP-H	PVDF (SYGEF)		EPDM	FPM	NBR	CR	CSM
Dichloroacetic acid (SpRB)	$Cl_2CHCOOH$		50%, aqueous	20	+	-	-	+	+	+		+	O	-	+	+
				40	+			+	+	+		+	O		O	+
				60	O			+	+	+		+	-		-	O
				80						O						
				100						-						
				120												
				140												
Dichloroacetic acid methyl ester	$Cl_2CHCOOCH_3$	143	technically pure	20	-	-	-	+	+	O		+	-	-	-	+
				40				+	+			+				+
				60				+	+			O				O
				80												
				100												
				120												
				140												
Dichlorcethan	Ethylene chloride															
Dichloroethylene	ClCH=CHCl	60	technically pure	20	-	-	-	-	O	+		-	O	-	-	-
				40						+						
				60												
				80												
				100												
				120												
				140												
Dichloromethane				20	-	-	-									
				40												
				60												
				80												
				100												
				120												
				140												
Diesel oil (SpRB, Q/E)				20	+	+	O	+	O	+		-	+	+	O	O
				40	+	+				+			+	+		-
				60				O		+						
				80						+						
				100						+						
				120						+						
				140												
Diethyl ether				20	-	-	-									
				40												
				60												
				80												
				100												
				120												
				140												
Diethylamine	$(C_2H_5)_2NH$	56	technically pure	20	O	-	-	+	+	+		O	-	-	-	-
				40						O						
				60						-						
				80												
				100												
				120												
				140												
Diethylene glycol butyl ether				20	-	-	-									
				40												
				60												
				80												
				100												
				120												
				140												

(Courtesy George Fischer Engineering Handbook)

Aggressive Media					Chemical Resistance											
Medium	Formula	Boiling point °C	Concentration	Temperature °C	PVC	CPVC	ABS	PE	PP-H	PVDF (SYGEF)		EPDM	FPM	NBR	CR	CSM
Diglycolic acid (SpRB)	HOOC-CH_2-O-CH_2-COOH	Fp*., 148	30%, aqueous	20	+	+	+	+	+	+		+	O	+	+	O
				40	+	+		+	+							
				60	O	+		+	+							
				80												
				100												
				120												
				140												
Di-isobutyl ketone	$[(CH_3)2CHCH_2]_2CO$	124	technically pure	20	-	-	-	+	+	+		O	-	-	-	-
				40						+						
				60				-	-	O						
				80												
				100												
				120												
				140												
Dimethyl formamide	$(CH_3)_2CHNO$	153	technically pure	20	-	-	-	+	+	-		O	-	O	+	+
				40				+	+							
				60				O	+							
				80												
				100												
				120												
				140												
Dimethylamine	$(CH_3)_2NH$	7	technically pure	20	O	-	-	+	+	O		O	-	-	-	-
				40						-						
				60				O								
				80												
				100												
				120												
				140												
Dimethylphthalate (DMP)	$C_6H_4(CH_3)_2$			20	-	-	-									
				40												
				60												
				80												
				100												
				120												
				140												
Dinonylphthalate (DNP)			technically pure	20	-	-	-	O	+			O	+	-	-	-
				40												
				60												
				80												
				100												
				120												
				140												
Dioctylephthalate (SpRB) (DOP)			technically pure	20	-	-	-	O	+			O	+	-	-	-
				40												
				60					-							
				80												
				100												
				120												
				140												
Dioxane	$C_4H_8O_2$	101	technically pure	20	-	-	-	+	O	-			-	O	-	-
				40				+	O							
				60				+	O							
				80					-							
				100												
				120												
				140												
Drinking water	see water															

(Courtesy George Fischer Engineering Handbook)

Aggressive Media					Chemical Resistance											
Medium	Formula	Boiling point °C	Concentration	Temperature °C	PVC	CPVC	ABS	PE	PP-H	PVDF (SYGEF)		EPDM	FPM	NBR	CR	CSM
Ethanolamine	see Annino ethanol															
Ethyl acetate	$CH_3COOCH_2-CH_3$	77	technically pure	20	-	-	-	+	+	O		+	-	-	-	-
				40				O	O							
				60				O	O							
				80												
				100												
				120												
				140												
Ethyl alcohol + acetic acid (fermentation mixture)			technically pure	20	+	O	-	+	+	+		O	O	O	+	+
				40	+			+		+		O	O	O	+	+
				60	O			+		+			O		+	+
				80						O						
				100												
				120												
				140												
Ethyl alcohol (Ethnol) (SpRB)	CH_3-CH_2-OH	78	technically pure, 96%	20	+	O	-	+	+	+		+	O	O	+	+
				40	+			+	+	O		+	O			
				60	O			+	+	-		+	O			
				80					+							
				100												
				120												
				140												
Ethyl benzene	$C_6H_5-CH_2CH_3$	136	technically pure	20	-	-	-	O	O	O		-	+	-	-	-
				40												
				60					-							
				80												
				100												
				120												
				140												
Ethyl chloride	CH_3-CH_2Cl	12	technically pure	20	-	-	-	O	O	O		-	O	-	-	-
				40												
				60												
				80												
				100												
				120												
				140												
Ethyl ether	$CH_3CH_2-O-CH_2CH_3$	35	technically pure	20	-	-	-	+	O	+		-	-	-	-	-
				40												
				60												
				80												
				100												
				120												
				140												
Ethylenchloride (1,2-Dichloroethane)				20	-	-	-									
				40												
				60												
				80												
				100												
				120												
				140												
Ethylene chloride	$ClCH_2-CH_2Cl$	83	technically pure	20	-	-	-	O	O	+		-	+	O	O	-
				40						+			+	-	-	
				60						+			O			
				80						O						
				100						-						
				120												
				140												

(Courtesy George Fischer Engineering Handbook)

Aggressive Media					Chemical Resistance											
Medium	Formula	Boiling point °C	Concentration	Temperature °C	PVC	CPVC	ABS	PE	PP-H	PVDF (SYGEF)		EPDM	FPM	NBR	CR	CSM
Ethylene diamine	$H_2N\text{-}CH_2\text{-}CH_2\text{-}NH_2$	117	technically pure	20	O	-	-	+	+	O		+	O	+	+	O
				40				+	+	O			O	O	O	O
				60				+	+	-			-	-	-	-
				80												
				100												
				120												
				140												
Ethylene glycol (SpRB)	$HO\text{-}CH_2\text{-}CH_2\text{-}OH$	198	technically pure	20	+	O	-	+	+	+		+	+	+	+	+
				40	+			+	+	+		+	+	+	+	+
				60	+			+	+	+		+	+	O	O	+
				80					+	+		+	O			O
				100					+	+						
				120						+						
				140												
Ethylene glycol	CH_2OHCH_2OH	198	technically pure	20	+		-	+	+	+		+	+	+	+	+
				40	+			+	+	+		+	+	+	+	+
				60	+			+	+	+		+	+	O	O	+
				80					+	+			O			O
				100						+						
				120												
				140												
Ethylene oxide	$CH_2\text{-}CH_2$	10	technically pure, moist	20	-	-	-	-	O	+		O	-	-	-	-
				40												
				60												
				80												
				100												
				120												
				140												
Ethylenediaminetetra-acetic acid (EDTA)				20				+	+	+		+				
				40												
				60												
				80												
				100												
				120												
				140												
Fatty acids $>C_6$ (SpRB)	R-COOH		technically pure	20	+	+	-	+	+	+		+	+	O	O	-
				40	+	+		+	+	+						
				60	+	+		O	+	+						
				80						+						
				100												
				120												
				140												
Fatty alcohol sulphonates (SpRB)			aqueous	20	+	+		+	+	+		+	+	+	+	+
				40	+	+		+	+	+		+	+	+	+	+
				60	O	O		+	O	+		+	+	+	+	+
				80						+						
				100						+						
				120												
				140												
Fertilizers			aqueous	20	+	+	O	+	+	+		+	+	+	+	+
				40	+	+		+	+	+		+	+	+	+	+
				60	O	+		+	+	+		+	+	+	+	+
				80		+				+			+			+
				100									+			
				120												
				140												

(Courtesy George Fischer Engineering Handbook)

Aggressive Media					Chemical Resistance											
Medium	Formula	Boiling point °C	Concentration	Temperature °C	PVC	CPVC	ABS	PE	PP-H	PVDF (SYGEF)		EPDM	FPM	NBR	CR	CSM
Fluorine	F_2		technically pure	20	-	-	-	-	-	-		-	-	-	-	-
				40												
				60												
				80												
				100												
				120												
				140												
Fluorosilicic acid (Q/E)	H_2SiF_6		32%, aqueous	20	+	+	+	+	+	+		+	O	O	O	+
				40	+	+	+	+		+				-	-	O
				60	+	+	+	+		+						-
				80						+						
				100						+						
				120												
				140												
Formaldehyde (SpRB)	HCHO		40%, aqueous	20	+	+	+	+	+	+		+	+	+	+	+
				40	+	+	+	+	+	+		+	+	+	+	+
				60			+	+		+		+	+	O	O	O
				80						+						
				100												
				120												
				140												
Formamide	$HCONH_2$	210	technically pure	20	-	-	-	+	+			+	O	+	+	
				40				+	+							
				60				+	+							
				80												
				100												
				120												
				140												
Formic acid (SpRB)	HCOOH		up to 50%, aqueous	20	+	-	O	+	+	+		+	+	-	+	+
				40	+			+	+	+		+	+		+	+
				60	O			+	O	+		O	O		O	+
				80						+			-			O
				100						+						
				120												
				140												
Formic acid (SpRB)	HCOOH	101	technically pure	20	+	-	-	+	+	+		+	+	-	+	+
				40	O			+	O	+		+			O	+
				60	-			+	-	+		+			-	+
				80						+		O				O
				100						+						
				120												
				140												
Formic acid (SpRB)			25%	20	+	+		+	+	+		+				
				40	+	+		+	+	+		+				
				60	+	+		+	+	+		+				
				80					+	+						
				100												
				120												
				140												
Freon 113	see trifluoro, trichlorethane	48														
Frigen 12 (D/P)	see Freon 12	-30	technically pure													

(Courtesy George Fischer Engineering Handbook)

Aggressive Media					Chemical Resistance											
Medium	Formula	Boiling point °C	Concentration	Temperature °C	PVC	CPVC	ABS	PE	PP-H	PVDF (SYGEF)		EPDM	FPM	NBR	CR	CSM
Fruit juices (SpRB)				20	+	+	+	+	+	+		+	+	+	+	+
				40	+	+	+	+	+	+		+	+	+	+	+
				60	+	+	+	+	+	+		+	+	+	+	+
				80		+			+	+		+	+	+	+	+
				100						+		+	+	+		+
				120						+			+			
				140												
Fruit pulp				20	+	+	+	+	+			+	+	+	+	+
				40			+	+	+							
				60				+	+							
				80												
				100												
				120												
				140												
Fuel oil				20	+	+		O	O	+		-	+	+	+	-
				40	O	+		-	-	+			+	+	+	
				60						+			+	+	O	
				80						+						
				100						+						
				120												
				140												
Furfuryl alcohol (SpRB)	$C_5H_6O_2$	171	technically pure	20	-	-	-	+	+	+		O	-	-	O	O
				40				+		+						
				60				+	O	O						
				80						-						
				100												
				120												
				140												
Gasoline (SpRB)	C_5H_{12} to $C_{12}H_{26}$	80-130	free of lead and aromatic compounds	20	+	+	-	+	O	+		-	+	+	-	O
				40	+	+		+		+			+	+		-
				60	+	+		O	-	+			+	+		
				80						+						
				100						+						
				120						+						
				140												
Gelatin			all, aqueous	20	+	+	+	+	+	+		+	+	+	+	+
				40	+	+	+	+	+	+		+	+	+	+	+
				60		+	+	+	+	+						
				80						+						
				100												
				120												
				140												
Glucose	$C_6H_{12}O_6$	Fp*., 148	all, aqueous	20	+	+	+	+	+	+		+	+	+	+	+
				40	+	+	+	+	+	+		+	+	+	+	+
				60	O	+	+	+	+	+		+	+	+	+	+
				80		+			+	+		+	+	+	+	+
				100						+			+			
				120												
				140												
Glycerol	HO-CH_2-CH(OH)-CH_2OH	290	technically pure	20	+	+	+	+	+	+		+	+	+	+	+
				40	+	+	+	+	+	+		O	+	+	+	+
				60	+	+		+	+	+		O	O	+	+	+
				80		+			+	+			-	O	+	+
				100					+	+					O	O
				120						+						
				140												

(Courtesy George Fischer Engineering Handbook)

Aggressive Media					Chemical Resistance											
Medium	Formula	Boiling point °C	Concentration	Temperature °C	PVC	CPVC	ABS	PE	PP-H	PVDF (SYGEF)		EPDM	FPM	NBR	CR	CSM
Glycocoll (SpRB)	NH_2-CH_2-COOH	Fp.* 233	10%, aqueous	20	+	+	+	+	+	+			+	+	+	+
				40	+	+	+	+	+	+			+	O	+	O
				60		+				+						
				80						+						
				100												
				120												
				140												
Glycol	see Ethylene glycol															
Glycolic acid	HO-CH_2-COOH	Fp.*, 80	37%, aqueous	20	+	-	+	+	+	+			+	+	+	+
				40			+	+		+						
				60				+		+						
				80						+						
				100						+						
				120												
				140												
Heptane (SpRB)	C_7H_{16}	98	technically pure	20	+	O	-	+	+	+		-	+	+	+	+
				40						+			+	+	+	O
				60				O	O	+			+	+	+	-
				80						+						
				100						+						
				120												
				140												
Hexane (SpRB)	C_6H_{14}	69	technically pure	20	+	O	-	+	+	+		-	+	+	+	+
				40						+			+	+	+	O
				60				O	O	+			+	+	+	-
				80						+						
				100						+						
				120												
				140												
Hydrazine hydrate (SpRB)	H_2N-NH_2 . H_2O	113	aqueous	20	+	-	-	+	+	-		+	O	-	-	+
				40				+	+							
				60				+	+							
				80												
				100												
				120												
				140												
Hydrobromic acid (SpRB)	HBr	124	aqueous, 50%	20	+	+	+	+	+	+		+	+	O	+	+
				40	+	+	+	+	+	+		+	+	-	+	+
				60	+	+		+	+	+		O	+		O	+
				80		O				+		-	O		-	O
				100						+			-			-
				120												
				140												
Hydrochloric acid (Q/E, D/P)	HCl		up to 38%	20	+	+	-	+	O	+		+	+	-	O	+
				40	+	+		+		+			+			
				60	+	+				+						
				80						+						
				100						+						
				120												
				140												
Hydrochloric acid (Q/E, D/P)	HCl		5%, aqueous	20	+		+	+	+	+		+	+	O	O	+
				40	+		+	+	+	+		+	+	-	-	O
				60	O			+	+	+		+	+			-
				80					O	+			+			
				100						+						
				120						+						
				140												

(Courtesy George Fischer Engineering Handbook)

Aggressive Media					Chemical Resistance											
Medium	Formula	Boiling point °C	Concentration	Temperature °C	PVC	CPVC	ABS	PE	PP-H	PVDF (SYGEF)		EPDM	FPM	NBR	CR	CSM
Hydrochloric acid (Q/E, D/P)	HCl		10%, aqueous	20	+	+	+	+	+	+		+	+	O	O	+
				40	+	+	+	+	+	+		+	+	-	-	O
				60	O	+		+	O	+		+	+			-
				80		+			O	+			+			
				100						+						
				120						+						
				140												
Hydrochloric acid (Q/E, D/P)	HCl		up to 30%, aqueous	20	+	+	O	+	+	+		+	+	-	-	+
				40	+	+	-	+	O	+		+	+			O
				60	O	+		+	O	+		O	O			-
				80		+			-	+						
				100						+						
				120												
				140												
Hydrochloric acid (Q/E, D/P)	HCl		36%, aqueous	20	+	+	-	+	+	+		O	+	-	-	O
				40	+	+		+	O	+		O	O			-
				60	O	O		+	-	+		-	-			
				80		O				+						
				100						+						
				120												
				140												
Hydrocyanic acid	HCN	26	technically pure	20	+	+	-	+	+	+		+	+	O	O	+
				40	+	+		+	+	+		O	O	-	-	O
				60	O	+		+	+	+						
				80						+						
				100												
				120												
				140												
Hydrofluoric acid	HF			20	+	-	-	+	+	+		-	+	-	-	+
				40	O			+	+	+			+			+
				60	O			O	+	+			O			O
				80						+						
				100						+						
				120												
				140												
Hydrogen	H_2	-253	technically pure	20	+	+	+	+	+	+		+	+	+	+	+
				40	+	+	+	+	+	+		+	+	+	+	+
				60	+	+	+	+	+	+		+	+	+	+	+
				80		+				+		+	+	+	+	+
				100					-	+		+	+	+		
				120												
				140												
Hydrogen chloride (Q/E)	HCl	-85	technically pure, gaseous	20	+	+	-	+	+	+		+	+	O	O	O
				40	+	+		+	+	+		+	+	-	-	O
				60	O	+		+	+	+		+	+			-
				80		O				+						
				100						+						
				120												
				140												
Hydrogen peroxide			70%	20	+	+	-	+	+	O		O	+			
				40						O						
				60												
				80												
				100												
				120												
				140												

(Courtesy George Fischer Engineering Handbook)

Aggressive Media					Chemical Resistance											
Medium	Formula	Boiling point °C	Concentration	Temperature °C	PVC	CPVC	ABS	PE	PP-H	PVDF (SYGEF)		EPDM	FPM	NBR	CR	CSM
Hydrogen peroxide (SpRB)	H_2O_2		50%, aqueous	20	+	+	-	+	+	O		O	+			
				40												
				60												
				80												
				100												
				120												
				140												
Hydrogen peroxide (SpRB)	H_2O_2		10%, aqueous	20	+	+	-	+	+	O		O	+	O	-	+
				40	+			+	+	O		O	O	-		+
				60	O			+	+	-		-	-			O
				80												-
				100												
				120												
				140												
Hydrogen peroxide (SpRB)	H_2O_2	139	90%, aqueous	20	+		-	+	-	O			O	-	-	O
				40												
				60				-								
				80												
				100												
				120												
				140												
Hydrogen peroxide (SpRB)	H_2O_2	105	30%, aqueous	20	+	+	-	+	+	O		O	+	-	-	+
				40												O
				60												-
				80												
				100												
				120												
				140												
Hydrogen sulphide	H_2S		technically pure	20	+	+	+	+	+	+		+	+	+	O	+
				40	+	+	+	+	+	+		-	+	O	-	O
				60	+	+		O	+	+			O	-		O
				80						+			-			-
				100						+						
				120						+						
				140												
Hydrogen sulphide	H_2S		saturated, aqueous	20	+	+	+	+	+	+		+	+	-	+	+
				40	+	+	+	+	+	+		-	+	-	-	+
				60	O	+		+	+$_x$	+			+			O
				80						+			O			-
				100						+						
				120						+						
				140												
Hydroquinone	$C_6H_4(OH)_2$		saturated	20	+	+		+	+			+				
				40	+	+		+	+							
				60				+	+							
				80					+							
				100												
				120												
				140												
Hydrosulphite	see Sodium dithione															
Hydroxylamine sulfate				20	+			+				+				
				40	+			+								
				60	+			+								
				80												
				100												
				120												
				140												

(Courtesy George Fischer Engineering Handbook)

Aggressive Media					Chemical Resistance											
Medium	Formula	Boiling point °C	Concentration	Temperature °C	PVC	CPVC	ABS	PE	PP-H	PVDF (SYGEF)		EPDM	FPM	NBR	CR	CSM
Hydroxylamine sulphate	$(NH_3OH)_2SO_4$		all, aqueous	20	+	+	-	+	+			+	+	+	O	+
				40	+	+		+	+				+	O		+
				60				+	+							
				80												
				100												
				120												
				140												
Iodine-potassium iodide solution (lugol's solution)				20	+	-	-			+			+			
				40												
				60												
				80												
				100												
				120												
				140												
Iodium	I_2	185	100%	20	-	-	-			+			+			
				40												
				60												
				80												
				100												
				120												
				140												
Iron (II) -chloride			saturated	20	+	+	+	+	+	+		+	+			
				40	+	+		+	+	+		+	+			
				60	+	+		+	+	+		+	+			
				80		+			+	+			+			
				100						+			+			
				120												
				140												
Iron (II) -chloride	$FeCl_2$		saturated	20	+	+	+	+	+	+		+	+			
				40	+	+		+	+	+		+	+			
				60	+	+		+	+	+		+	+			
				80		+			+	+		+	+			
				100						+			+			
				120												
				140												
Iron (II) -nitrate	$Fe(NO_3)_2$		saturated	20	+	+	+	+	+	+		+	+			
				40	+	+		+	+	+		+	+			
				60	+	+		+	+	+		+	+			
				80		+			+	+			+			
				100						+			+			
				120												
				140												
Iron (III) -chloride	$FeCl_3$		saturated	20	+	+	+	+	+	+		+	+			
				40	+	+		+	+	+		+	+			
				60	+	+		+	+	+		+	+			
				80		+			+	+		+	+			
				100						+			+			
				120												
				140												
Iron (III) -chloride			saturated	20	+	+	+	+	+	+		+	+			
				40	+	+		+	+	+		+	+			
				60	+	+		+	+	+		+	+			
				80		+			+	+		+	+			
				100						+			+			
				120												
				140												

(Courtesy George Fischer Engineering Handbook)

Aggressive Media					Chemical Resistance											
Medium	Formula	Boiling point °C	Concentration	Temperature °C	PVC	CPVC	ABS	PE	PP-H	PVDF (SYGEF)		EPDM	FPM	NBR	CR	CSM
Iron (III) -chloridsulfate			saturated	20	+	+	+	+	+	+		+	+			
				40	+	+		+	+	+		+	+			
				60	+	+		+	+	+		+	+			
				80		+			+	+		+	+			
				100						+			+			
				120												
				140												
Iron (III) -nitrate			saturated	20	+	+	+	+	+	+		+	+			
				40	+	+		+	+	+		+	+			
				60	+	+		+	+	+		+	+			
				80		+			+	+		+	+			
				100						+			+			
				120												
				140												
Iron (III) -nitrate	$Fe(NO_3)_3$		saturated	20	+	+	+	+	+	+		+	+			
				40	+	+		+	+	+		+	+			
				60	+	+		+	+	+		+	+			
				80		+			+	+		+	+			
				100						+			+			
				120												
				140												
Iron (III) -sulfate	$Fe_2(SO_4)_3$		saturated	20	+	+	+	+	+	+		+	+			
				40	+	+		+	+	+		+	+			
				60	+	+		+	+	+		+	+			
				80		+			+	+		+	+			
				100						+			+			
				120												
				140												
Iron (III) -sulfate			saturated	20	+	+	+	+	+	+		+	+			
				40	+	+		+	+	+		+	+			
				60	+	+		+	+	+		+	+			
				80		+			+	+		+	+			
				100						+			+			
				120												
				140												
Iron (III) -nitrate	$FE(NO_3)3$		saturated	20	+					+		+	+			
				40	+					+		+	+			
				60	+					+		+	+			
				80						+		+	+			
				100						+			+			
				120												
				140												
Iron (II) -sulfate	$FeSO_4$		saturated	20	+	+	+	+	+	+		+	+			
				40	+	+		+	+	+		+	+			
				60	+	+		+	+	+		+	+			
				80		+			+	+		+	+			
				100						+			+			
				120												
				140												
Iron (III) -sulfate			saturated	20						+						
				40						+						
				60						+						
				80						+						
				100						+						
				120												
				140												

(Courtesy George Fischer Engineering Handbook)

Aggressive Media					Chemical Resistance											
Medium	Formula	Boiling point °C	Concentration	Temperature °C	PVC	CPVC	ABS	PE	PP-H	PVDF (SYGEF)		EPDM	FPM	NBR	CR	CSM
Iron salts			all, aqueous	20	+	+	+	+	+	+		+	+	+	+	+
				40	+	+	+	+	+	+		+	+	+	+	+
				60	O	+		+	+	+		+	+	+	+	+
				80		+			+	+		+	+			+
				100						+			+			
				120						+						
				140												
Isooctane (SpRB)	$(CH_3)_3\text{-C-}CH_2\text{-CH-}(CH_3)_2$	99	technically pure	20	+		-	+	+	+			+	+	+	O
				40						+						
				60				O	O	+						
				80						+						
				100						+						
				120												
				140												
Isophorone (SpRB)	$C_9H_{14}O$		technically pure	20						-						
				40												
				60												
				80												
				100												
				120												
				140												
Isopropyl alcohol (SpRB)	$(CH_3)_2\text{-CH-OH}$	82	technically pure	20				+	+	+		+				
				40						+						
				60						+						
				80						O						
				100												
				120												
				140												
Isopropyl ether	$(CH_3)_2\text{-CH-O-CH-}(CH_3)_2$	68	technically pure	20	-	-	-	O	O	+		O	-	-	-	-
				40						+						
				60				-	-	+						
				80												
				100												
				120												
				140												
Isopropylbenzene				20	-	-	-									
				40												
				60												
				80												
				100												
				120												
				140												
Jam, Marmalade				20	+	+	+	+	+	+		+	+	+	+	+
				40	O	+	+	+	+	+		+	+	+	+	+
				60	O	+		+	+	+		+	+	+	+	+
				80					+	+		+	+			
				100					+	+						
				120						+						
				140												
Lactic acid (SpRB)	$CH_3CHOHCOOH$		10%, aqueous	20	+	+	+	+	+	+		O	+	-	-	O
				40	O	+	O	+	+	+		O	O			O
				60	-	+	-	+	+	O		O	O			O
				80		+			+	O		-	O			
				100					+	-						
				120												
				140												

(Courtesy George Fischer Engineering Handbook)

Aggressive Media					Chemical Resistance											
Medium	Formula	Boiling point °C	Concentration	Temperature °C	PVC	CPVC	ABS	PE	PP-H	PVDF (SYGEF)		EPDM	FPM	NBR	CR	CSM
Lanolin (SpRB)			technically pure	20	+	o	+	+	+	+			+	+	+	O
				40	O		+	+	+	+			+	+	O	
				60			+	+	+	+			+	+		
				80						+						
				100						+						
				120						+						
				140												
Lead acetate	$Pb(CH_3COO)_2$		aqueous, saturated	20	+	+	+	+	+	+		+	+	+	+	+
				40	+	+	+	+	+	+		+	+	+	+	+
				60	+	+	+	+	+	+		+	+	+	+	+
				80		+				+						
				100						+						
				120												
				140												
Lead salts	$PbCl_2$, $Pb(NO_3)_2$, $PbSO_4$		saturated	20		+										
				40		+										
				60		+										
				80		+										
				100												
				120												
				140												
Leadcarbonate				20	+	+		+	+	+		+				
				40						+						
				60						+						
				80												
				100												
				120												
				140												
Leadnitrate	$Pb(NO_3)2$			20		+										
				40		+										
				60		+										
				80		+										
				100												
				120												
				140												
Leadnitrate				20	+					+						
				40	+					+						
				60	+					+						
				80						+						
				100						+						
				120												
				140												
Leadtetrafluoroborate				20						+						
				40						+						
				60						+						
				80						+						
				100						+						
				120												
				140												
Linoleic acid				20						+						
				40						+						
				60						+						
				80						+						
				100						+						
				120												
				140												

(Courtesy George Fischer Engineering Handbook)

Aggressive Media					Chemical Resistance											
Medium	Formula	Boiling point °C	Concentration	Temperature °C	PVC	CPVC	ABS	PE	PP-H	PVDF (SYGEF)		EPDM	FPM	NBR	CR	CSM
Linseed oil (SpRB)			technically pure	20	+	+	+	+	+	+			+	+	O	+
				40	+	+	-	+	+	+			+	+	-	O
				60	O			+	+	+			+	+		-
				80					+	+						
				100					+	+						
				120						+						
				140												
Liqueurs				20	+			+	+	+		+	+	+	+	+
				40	+			+		+						
				60						+						
				80						+						
				100												
				120												
				140												
Liquid fertilizers				20				+	+			+				
				40				+	+			+				
				60				+	+			+				
				80					+							
				100												
				120												
				140												
Lithiumbromide	LiBr			20	+	+		+	+	+		+	+			
				40						+						
				60						+						
				80						+						
				100						+						
				120												
				140												
Lithiumsulfate				20	+	+		+	+	+		+	+			
				40						+						
				60						+						
				80												
				100												
				120												
				140												
Lubricating oils				20	+	O	-	+	O	+		-	+	+	+	+
				40	+			+		+			+	+	O	O
				60	+			O		+			+	O	-	-
				80						+			O			
				100						+			-			
				120						+						
				140												
Magnesium salts	$MgCl_2$, $MgCO_3$, $Mg(No3)_2$, $Mg(OH)_2$, $MgSO_4$		all, aqueous,saturated	20	+	+	+	+	+	+			+	+	+	+
				40	+	+	+	+	+	+			+	+	+	+
				60	O	+		+	+	+		+	+	+	+	+
				80		+			+	+		+	+			+
				100					+	+			+			
				120						+						
				140												
Magnesiumhydrogen-carbonate				20	+			+	+			+				
				40	+			+	+			+				
				60	+			+	+			+				
				80												
				100												
				120												
				140												

(Courtesy George Fischer Engineering Handbook)

Aggressive Media					Chemical Resistance											
Medium	Formula	Boiling point °C	Concentration	Temperature °C	PVC	CPVC	ABS	PE	PP-H	PVDF (SYGEF)		EPDM	FPM	NBR	CR	CSM
Maleic acid (SpR8)	$(CH-COOH)_2$	Fp. *131	cold saturated, aqueous	20	+	+	+	+	+	+			+	-	-	-
				40	+	+		+	+	+			+			
				60	O			+	+	+			+			
				80						+			-			
				100						+						
				120						+						
				140												
Media water or similar media				20	+	+	+	+	+	+						
				40	+	+	+	+	+	+						
				60	+	+	+	+	+	+						
				80		+			+	+						
				100					+	+						
				120						+						
				140						+						
Mercury	Hg	357	pure	20	+	+	+	+	+	+		+	+	+	+	+
				40	+			+	+	+		+	+	+	+	+
				60	+			+	+	+		+	+	+	+	+
				80						+			+			
				100						+						
				120						+						
				140												
Mercury (II) -chloride	$HgCl_2$			20	+	+	+	+	+	+		+	+	+	+	+
				40	+	+		+	+	+		+	+	+	+	+
				60	+	+		+	+	+		+	+	+	+	+
				80		+			+	+						
				100						+						
				120												
				140												
Mercury (II) -cyanide	Hg(CN)2			20	+	+	+	+	+	+		+	+	+	+	+
				40	+	+		+	+	+		+	+	+	+	+
				60	+	+		+	+	+		+	+	+	+	+
				80		+				+						
-				100						+						
				120												
				140												
Mercury (II) -cyanide	$Hg(NO_3)_2$			20	+	+		+	+	+		+	+	+	+	+
				40	+	+		+	+	+		+	+	+	+	+
				60	+	+		+	+	+		+	+	+	+	+
				80		+			+	+			+			
				100						+						
				120												
				140												
Mercury (II) -sulfate				20	+	+	+	+	+	+		+	+	+	+	+
				40	+	+		+	+	+		+	+	+	+	+
				60	+	+		+	+	+		+	+	+	+	+
				80		+			+	+			+			
				100						+						
				120												
				140												
Mercury salts	$HgNO_3$, $Hg Cl_2$, $Hg(CN)_2$		cold saturated, aqueous	20	+	+	+	+	+	+		+	+	O	O	O
				40	+	+		+	+	+		+	+	O	O	O
				60	O	+		+	+	+			+	-	-	-
				80						+						
				100						+						
				120						+						
				140												
Methane	see natural gas	-161	technically pure													

(Courtesy George Fischer Engineering Handbook)

Aggressive Media					Chemical Resistance											
Medium	Formula	Boiling point °C	Concentration	Temperature °C	PVC	CPVC	ABS	PE	PP-H	PVDF (SYGEF)		EPDM	FPM	NBR	CR	CSM
Methanol (SpRB)	CH_3OH	65	all	20	+	-	-	+	+	+		+	O	+	+	+
				40	+			+	+	O		+	O	+	+	+
				60	O			+	+	-		+	O	+	O	+
				80												
				100												
				120												
				140												
Methyl acetate	CH_3COOCH_3	56	technically pure	20	-	-	-	+	+	+			-	-	-	-
				40					+	O						
				60					O							
				80												
				100												
				120												
				140												
Methyl amine	CH_3NH_2	-6	32%, aqueous	20	O	-	-	+	+	O			+	-	+	+
				40												
				60												
				80												
				100												
				120												
				140												
Methyl bromide	CH_3Br	4	technically pure	20	-	-	-	O	-	+			O	-	-	O
				40						+						
				60						+						
				80												
				100												
				120												
				140												
Methyl chloride	CH_3Cl	-24	technically pure	20	-	-	-	O	-	+			-	-	-	-
				40						+						
				60						+						
				80												
				100												
				120												
				140												
Methyl ethyl ketone	$CH_3COC_2H_5$	80	technically pure	20	-	-	-	+	+	-			-	-	-	-
				40				O	O							
				60				-	O							
				80												
				100												
				120												
				140												
Methylene chloride	CH_2Cl_2	40	technically pure	20	-	-	-	O	O	+			O	-	-	-
				40						O						
				60						O						
				80												
				100												
				120												
				140												
Methylisobutylketone	$C_6H_{12}O$			20	-	-	-									
				40												
				60												
				80												
				100												
				120												
				140												

(Courtesy George Fischer Engineering Handbook)

Aggressive Media					Chemical Resistance											
Medium	Formula	Boiling point °C	Concentration	Temperature °C	PVC	CPVC	ABS	PE	PP-H	PVDF (SYGEF)		EPDM	FPM	NBR	CR	CSM
Methylmethacrylate	$C_5H_8O_2$			20	-	-	-									
				40												
				60												
				80												
				100												
				120												
				140												
Methylphenylketone (Acetophenon)	C_8H_8O			20	-	-	-									
				40												
				60												
				80												
				100												
				120												
				140												
Milk (SpRB)				20	+	+	+	+	+	+			+	+	+	+
				40	+	+	+	+	+	+						
				60	+	+	+	+	+	+						
				80		+			+	+						
				100					+	+						
				120						+						
				140												
Mineral oils, free of aromatics				20	+	+	-	+	+	+			+	+	O	O
				40	+			+	+	+			+	+	-	-
				60	+			O	O	+			+	+		
				80						+						
				100						+						
				120						+						
				140												
Mineral water				20	+	+	+	+	+	+		+	+	+	+	+
				40	+	+	+	+	+	+		+	+	+	+	+
				60	+	+	+	+	+	+		+	+	+	+	+
				80		+			+	+		+	+	+		+
				100					+	+		+	+			+
				120						+			+			
				140												
Mixed acids - nitric - hydrofluoric - sulphuric	15% HNO_3 15% HF 18% H_2SO_4		3 parts 1 part 2 parts	20	O	O	-	O	-	+			+	-	-	+
				40						+			O			O
				60						+						
				80												
				100												
				120												
				140												
Mixed acids - sulphuric - nitric - water	H_2SO_4 HNO_3 H_2O		48% 49% 43%	20	+	+	-	-	-	+			-	-	-	-
				40	O											
				60	-											
				80												
				100												
				120												
				140												
Mixed acids - sulphuric - nitric - water	H_2SO_4 HNO_3 H_2O		50% 50% 40%	20	O	O	-	-	-	+			-	-	-	-
				40	-											
				60												
				80												
				100												
				120												
				140												

(Courtesy George Fischer Engineering Handbook)

Aggressive Media					Chemical Resistance											
Medium	Formula	Boiling point °C	Concentration	Temperature °C	PVC	CPVC	ABS	PE	PP-H	PVDF (SYGEF)		EPDM	FPM	NBR	CR	CSM
Mixed acids - sulphuric - nitric - water	H_2SO_4 HNO_3 H_2O		10% 87% 43%	20	O	O	-	-	-	O			-	-	-	-
				40												
				60												
				80												
				100												
				120												
				140												
Mixed acids - sulphuric - nitric - water	H_2SO_4 HNO_3 H_2O		50% 33% 17%	20	+	+	-	-	-	+			+	-	-	O
				40	O											
				60												
				80												
				100												
				120												
				140												
Mixed acids - sulphuric - nitric - water	H_2SO_4 HNO_3 H_2O		10% 20% 70%	20	+	+	-	O	-	+			+	-	O	+
				40	+					+			+			O
				60						+			+			
				80						+						
				100												
				120												
				140												
Mixed acids - sulphuric - nitric - water	H_2SO_4 HNO_3 H_2O		50% 31% 19%	20	+		-	-	-	+			+	-	O	O
				40												
				60												
				80												
				100												
				120												
				140												
Mixed acids - sulphuric - phosphoric - phosphoric	H_2SO_4 H_3PO_4 H_2O		30% 60% 10%	20	+	+	-	+	+	+			+	-	+	+
				40	+	+		O	O	+			+		O	O
				60		+				+			+			
				80						+						
				100												
				120												
				140												
Molasses				20	+	+	+	+	+	+		+	+	+	+	+
				40	+	+	+	+	+	+		+	+	+	+	+
				60	O	+	+	+	+	+		+	+	+	+	+
				80		+				+		+	+	+	O	+
				100												
				120												
				140												
Molasses wort				20	+	+	+	+	+	+		+	+	+	+	+
				40	+	+	+	+	+	+		+	+	+	+	+
				60	+	+	+	+	+	+		+	+	+	+	+
				80		+				+						
				100												
				120												
				140												
Monochloroacetic acid ethyl ester	$ClCH_2COOC_2H_5$	144	technically pure	20	-	-	-	+	+	O			O	-	-	-
				40				+	+	-						
				60				+	+							
				80												
				100												
				120												
				140												

(Courtesy George Fischer Engineering Handbook)

Aggressive Media					Chemical Resistance											
Medium	Formula	Boiling point °C	Concentration	Temperature °C	PVC	CPVC	ABS	PE	PP-H	PVDF (SYGEF)		EPDM	FPM	NBR	CR	CSM
Morpholin	C_4H_9NO	129	technically pure	20	-	-	-	+	+	+			+	-	O	O
				40				+	+	+						
				60				+	+	O						
				80												
				100												
				120												
				140												
Mowilith D			usual commercial	20	+	+		+	+	+			+	+	+	+
				40												
				60												
				80												
				100												
				120												
				140												
Naphthalene		218	technically pure	20	-	-	-	+	+	+		-	+	+	-	O
				40						+			+	+		-
				60				O		O			+	+		
				80												
				100												
				120												
				140												
Natriumhydrogensulfite	$NaHSO_3$			20	+	+		+	+	+		+	+			
				40	+	+		+	+	+		+				
				60	+	+		+	+	+		+				
				80		+			+	+						
				100						+						
				120												
				140												
Natriumsulfate				20	+	+	+	+	+	+		+	+			
				40	+	+		+	+	+		+	+			
				60	+	+		+	+	+		+	+			
				80		+			+	+		+	+			
				100						+			+			
				120												
				140												
Natriumtetraborate (Borax)				20	+	+	+	+	+	+		+	+			
				40	+	+		+	+	+		+				
				60	+	+		+	+	+		+				
				80		+			+							
				100												
				120												
				140												
Nickel salts	$(CH_3COO)_2Ni$, $NiCl_2$, $Ni(NO_3)_2$, $Ni\,SO_4$		cold saturated, aqueous	20	+	+	+	+	+	+		+	+	+	+	+
				40	+	+	+	+	+	+		+	+	+	+	+
				60	O	+	+	+	+	+			+	+	+	+
				80						+			+			
				100						+			+			
				120						+						
				140												
Nitrating acid	H_2SO_4 HNO_3 H_2O		65% 20% 15%	20						+						
				40												
				60												
				80												
				100												
				120												
				140												

(Courtesy George Fischer Engineering Handbook)

Aggressive Media					Chemical Resistance											
Medium	Formula	Boiling point °C	Concentration	Temperature °C	PVC	CPVC	ABS	PE	PP-H	PVDF (SYGEF)		EPDM	FPM	NBR	CR	CSM
Nitric acid (SpRB)	HNO_3			20	+	+	-	+	O	+		+	+			
				40	+	+				+			+			
				60	+	+				+			+			
				80						+						
				100						+						
				120												
				140												
Nitric acid (SpRB)	HNO_3			20	+	+	-	+	+	+		+	+			
				40	+	+		+	O	+			+			
				60	+	+		+		+						
				80		+				+						
				100						+						
				120												
				140												
Nitric acid up to 55% (SpRB)				20	+	+	-	+	-	+			+			
				40	+	+				+						
				60						+						
				80												
				100												
				120												
				140												
Nitric acid (see note 2.3.1 on jointing) (SpRB)	see Salpetre		6,3%, aqueous													
Nitric acid (see note 2.3.1 on jointing) (SpRB)	see Salpetre		up to 40%, aqueous													
Nitric acid (see note 2.3.1 on jointing) (SpRB)	see Salpetre		65%, aqueous													
Nitric acid (see note 2.3.1 on jointing) (SpRB)	see Salpetre		100%													
Nitric acid (see note 2.3.1 on jointing) (SpRB)	see Salpetre		85%													
Nitric oxide	see Nitrous gases															
Nitrilotriacetic acid	$N(CH_2\text{-}COOH)_3$			20				+	+			+				
				40												
				60												
				80												
				100												
				120												
				140												
Nitrobenzene	$C_6H_5\text{-}NO_2$	209	technically pure	20	-	-	-	+	+	+		-	O	-	-	-
				40				O	+	O						
				60				O		-						
				80												
				100												
				120												
				140												

(Courtesy George Fischer Engineering Handbook)

Aggressive Media					Chemical Resistance											
Medium	Formula	Boiling point °C	Concentration	Temperature °C	PVC	CPVC	ABS	PE	PP-H	PVDF (SYGEF)		EPDM	FPM	NBR	CR	CSM
Nitrotoluene (o-, m-, p-)		222-238	technically pure	20	-	-	-	+	+	+		-	O	O	-	-
				40				O	O	+			-	-		
				60						+						
				80						+						
				100						O						
				120												
				140												
Nitrous acid	HNO_2			20	+	+	-	+	-	+		+	+			
				40	+	+				+						
				60						+						
				80												
				100												
				120												
				140												
Nitrous gases	see Nitric oxide		diluted, moist, anhydrous													
N-Methylpyrrolidon				20	-	-	-									
				40												
				60												
				80												
				100												
				120												
				140												
N,N-Dimethylaniline	$C_6H_5N(CH_3)_2$		technically pure	20	-	-	-	+	+			+				
				40												
				60												
				80												
				100												
				120												
				140												
n-Pentylacetate				20	-	-	-									
				40												
				60												
				80												
				100												
				120												
				140												
Oleic acid (SpRB)	$C_{17}H_{33}COOH$		technically pure	20	+	O	-	+	+	+		-	+	O	-	-
				40	+			+	+	+			O	-		
				60	+			O	O	+			-			
				80						+						
				100						+						
				120						+						
				140												
Oleum (SpRB)	$H_2SO_4+SO_3$		10% SO_3	20	-	-	-	-	-	-		-	-	-	-	-
				40												
				60												
				80												
				100												
				120												
				140												
Oleum vapours (SpRB)			traces	20	+	-	-	-	-	-		-	+	-	-	O
				40												
				60												
				80												
				100												
				120												
				140												

(Courtesy George Fischer Engineering Handbook)

Aggressive Media					Chemical Resistance											
Medium	Formula	Boiling point °C	Concentration	Temperature °C	PVC	CPVC	ABS	PE	PP-H	PVDF (SYGEF)		EPDM	FPM	NBR	CR	CSM
Olive oil (SpRB)				20	+	-	-	+	+	+		-	+	+	+	+
				40	+			+	+	+			+	+	+	+
				60	+			O	+	+			+	+	+	O
				80					+	+			+			-
				100												
				120												
				140												
Oxalic acid (SpRB)	$(COOH)_2$		cold saturated, aqueous	20	+	+	+	+	+	+		+	+	O	O	O
				40	+	+	+	+	+	+			+	-	-	O
				60	+	+		+	+	+			O			-
				80		O				+			-			
				100						+						
				120												
				140												
Oxygen	O_2		technically pure	20	+	+	+	+	+	+		+	+	+	+	+
				40	+		+	+	+	+		+	+		+	+
				60	+		+	O	O	+		+	+		+	+
				80						+			+		+	+
				100						O			+			+
				120						O			+			
				140												
Ozone (SpRB)	O_3		up to 2%, in air	20	+	+	-	O	O	O		O	+	-	O	+
				40				-	-							
				60												
				80												
				100												
				120												
				140												
Ozone (SpRB)	O_3		cold saturated, aqueous	20	+	+	-	O	O	O		-	+	-	O	+
				40	+			-	-				O		-	+
				60									-			O
				80												
				100												
				120												
				140												
Palm oil, palm nut oil (SpRB)				20	+	O	+	+	+	+		-	+	+	+	O
				40	-			+	+	+			+	+	O	-
				60				O	O	+			+	O	-	
				80						+						
				100						+						
				120												
				140												
Palmitic acid (SpRB)	$C_{15}H_{31}COOH$	390	technically pure	20	+	-	+	O	O	+		O	+	O	+	O
				40						+			O	-	-	-
				60					-	+			-			
				80						+						
				100						+						
				120						+						
				140												
Paraffin emulsions			usual commercial, aqueous	20	+	+	O	+	+	+		-	+	+	+	+
				40	+	+		+	+	+			+	+	O	-
				60				O	O	+			+	O	-	
				80						+			+			
				100						+						
				120												
				140												

(Courtesy George Fischer Engineering Handbook)

Aggressive Media					Chemical Resistance											
Medium	Formula	Boiling point °C	Concentration	Temperature °C	PVC	CPVC	ABS	PE	PP-H	PVDF (SYGEF)		EPDM	FPM	NBR	CR	CSM
Paraffin oil				20	+	+	O	+	+	+		-	+	+	+	O
				40	+			+	+	+			+	O	O	-
				60	O			+	O	+			+	O	-	
				80						+			O			
				100						+						
				120						+						
				140												
p-Dibromo benzene	$C_6H_5Br_2$		technically pure	20	-	-	-	O	O	+		-	+	-	-	-
				40						+						
				60						+						
				80						+						
				100						+						
				120												
				140												
Perchlorethylene (tetrachlorethylene)	$Cl_2C{=}CCl_2$	121	technically pure	20	-	-		O	O	+			+	O	-	-
				40						+			+	-		
				60						+			+			
				80						O						
				100						-						
				120												
				140												
Perchlorid acid (SpRB)	$HClO_4$		10%, aqueous	20	+	+	O	+	+	+		+	+	-	-	+
				40	+	+		+	+	+		O	+			+
				60	O	+		+	+	+			+			O
				80						+			O			-
				100						+						
				120												
				140												
Perchlorid acid (SpRB)			70%, aqueous	20	O	O	-	+	O	+		-	+	-	-	+
				40				O	-	+			+			+
				60				-		+			+			O
				80						+			O			
				100						+						
				120												
				140												
Petroleum			technically pure	20	+	-	-	+	+	+		-	+	+	O	-
				40				+	O	+			+	+	-	
				60				O	O	+			O	+		
				80						+						
				100						+						
				120						+						
				140												
Petroleum ether (SpRB)		40-70	technically pure	20	+	-	-	+	+	+		-	+	+	-	-
				40	+			O	O	+			+	O		
				60	+			O	O	+			O	-		
				80						+						
				100						+						
				120												
				140												
Phenol (SpRB)	$C_6H_5\text{-}OH$	182	up to 10%, aqueous	20	+	+	-	+	+	+			+	-	-	-
				40	O	+		+	+	+			+			
				60				O	+	+		+	+			
				80						+		O	O			
				100						+						
				120												
				140												

(Courtesy George Fischer Engineering Handbook)

Aggressive Media					Chemical Resistance											
Medium	Formula	Boiling point °C	Concentration	Temperature °C	PVC	CPVC	ABS	PE	PP-H	PVDF (SYGEF)		EPDM	FPM	NBR	CR	CSM
Phenol (SpRB)			up to 5%	20	+	+	-	+	+	+		+	+	-	-	
				40		+		+	+	+		O	+			
				60				+	+	+			+			
				80						+			O			
				100						O						
				120												
				140												
Phenol (SpRB)	C_6H_5-OH		up to 90%, aqueous	20	O	-	-	+	+	+		-	+	-	-	-
				40				+	+	+			O		O	
				60				O	+	O			-			
				80												
				100												
				120												
				140												
Phenylhydrazine	C_6H_5-NH-NH$_2$	243	technically pure	20	-	-	-	O	O	O		-	+	-	-	-
				40						-			+			
				60									O			
				80												
				100												
				120												
				140												
Phenylhydrazine hydrochloride	C_6H_5-NH-NH$_2$.HCl		aqueous	20	O	O	-		+	+			+	O	O	+
				40					O	+			+	-	-	+
				60					O	+		O	O			O
				80									-			-
				100												
				120												
				140												
Phosgene (SpRB)	$COCl_2$	8	liquid, technically pure	20	-	-	-	-	-	-		-	+	O	+	+
				40												
				60												
				80												
				100												
				120												
				140												
Phosgene (SpRB)			gaseous, technically pure	20	+	-	-	O	O	+		+	+	+	+	+
				40	O					+			+	+	O	O
				60	O								O	+	-	
				80												
				100												
				120												
				140												
Phosphate disodique	see d'isodiumphosphate		saturated													
Phosphoric acid	H_3PO_4		up to 30%, aqueous	20	+	+	+	+	+	+		+	+	O	+	+
				40	+	+	+	+	+	+		+	+	O	+	+
				60	O	+	O	+	+	+		O	+	-	+	+
				80		+			+	+			+		O	O
				100						+			+			
				120						+						
				140												
Phosphoric acid			50%, aqueous	20	+	+	+	+	+	+		+	+	O	+	+
				40	+	+	+	+	+	+		O	+	-	+	+
				60	+	+	O	+	+	+			+		O	+
				80		+			+	+			+			+
				100						+			O			O
				120						+						
				140												

(Courtesy George Fischer Engineering Handbook)

Aggressive Media					Chemical Resistance											
Medium	Formula	Boiling point °C	Concentration	Temperature °C	PVC	CPVC	ABS	PE	PP-H	PVDF (SYGEF)		EPDM	FPM	NBR	CR	CSM
Phosphoric acid			85%, aqueous	20	+	+	+	+	+	+		+	+	-	+	+
				40	+	+	+	+	+	+		+	+		+	O
				60	+	+	O	O	+	+		O	+		O	-
				80		+			+	+			+			
				100						+			O			
				120						+						
				140												
Phosphoric acid	H_3PO_4			20	+	+	-	+	+	+		O	+	-	-	-
				40	+	+		+	+	+			+			
				60		+				+			O			
				80						+						
				100												
				120												
				140												
Phosphoric acid	H_3PO_4			20	+	+	-	+	+	+			+			
				40	+	+		+	+	+			+			
				60	+	+			+	+			+			
				80		+			+	+			+			
				100						+			O			
				120												
				140												
Phosphoric acid tributyl ester	$(H_9C_4O)_3P=O$			20	-	-	-	+	+	-		+	-			
				40												
				60												
				80												
				100												
				120												
				140												
Phosphorous chlorides: - Phosphorous trichloride - Phosphorous pentachloride - Phosphorous oxichloride (SpRB)	PCl_3 PCl5 $POCl_3$	175 162 105	technically pure	20	-	-	-	+	O	-			+	-	-	+
				40												
				60				O	O							
				80												
				100												
				120												
				140												
Photographic developer (SpRB)			usual commercial	20	+	+	+	+	+	+		+	+	O	+	+
				40	+	+	+	+	+	+		+	+	O	+	+
				60	O	+	O	O		+						
				80		O										
				100												
				120												
				140												
Photographic emulsions (SpRB)				20	+	+	+	+	+	+		+	+	O	+	+
				40	+	+	+	+	+	+		+	+		+	+
				60		O				+						
				80												
				100												
				120												
				140												
Photographic fixer (SpRB)			usual commercial	20	+	+	+	+	+	+		+	+	+	+	+
				40	+	+	+	+	+	+		+	+	+	+	+
				60	O	+	O			+						
				80												
				100												
				120												
				140												

(Courtesy George Fischer Engineering Handbook)

Aggressive Media					Chemical Resistance											
Medium	Formula	Boiling point °C	Concentration	Temperature °C	PVC	CPVC	ABS	PE	PP-H	PVDF(SYGEF)		EPDM	FPM	NBR	CR	CSM
Phthalic acid (SpRB)	$C_6H_5(COOH)_2$	Fp.*, 208	saturated, aqueous	20	+	-	-	+	+	+		+	-	-	+	+
				40	O			+	+	+		O			+	+
				60	-			+	+	+					O	
				80						+						
				100						+						
				120												
				140												
Phthalic acid dioctayl ester	$C_{24}H_{38}O_4$			20	-	-	-	+	+	-		+	-	-		
				40												
				60												
				80												
				100												
				120												
				140												
Picric acid (SpRB)	$C_6H_3N_3O_7$	FP. 122	1%, aqueous	20	+	-	-	+	+	+		+	+	O	O	+
				40						+		+	+	-	-	O
				60						+		+	+			-
				80						+		+	+			
				100						+		+	+			
				120												
				140												
Potash	see potassium carbonate		cold saturated, aqueous													
Potash lye	KOH		50%	20	+	+		+	+	-		+				
				40	+	+		+	+			+				
				60	+	+		+	+			+				
				80												
				100												
				120												
				140												
Potassium (SpRB)	$KMnO_4$		cold saturated, aqueous	20	+	+		+	+	+		+	+	O	O	+
				40	+	+		+	+	+			+	-	-	+
				60	O			O		+			+			+
				80						+			+			
				100						+						
				120												
				140												
Potassium acetate (SpRB)	CH_3COOK		saturated	20	+	+	+	+	+	+		+	-			
				40	+	+		+	+	+		+				
				60	+	+		+	+	+		+				
				80		+			+	+		+				
				100						+						
				120												
				140												
Potassium bichromate (SpRB)	$K_2Cr_2O_7$	107	saturated, aqueous	20	+	+	+	+	+	+		+	+	+	O	+
				40	+	+	+	+	+	+			+	O	-	+
				60	O	+	+	+	+	+			+			+
				80					+	+						
				100					+	+						
				120						+						
				140												
Potassium borate	K_3BO_3		10%, aqueous	20	+	+	+	+	+	+		+	+	+	+	+
				40	+	+	+	+	+	+			+	+	+	+
				60	O	+	+	+	+	+			+	+	+	+
				80		+										
				100												
				120												
				140												

(Courtesy George Fischer Engineering Handbook)

Aggressive Media					Chemical Resistance											
Medium	Formula	Boiling point °C	Concentration	Temperature °C	PVC	CPVC	ABS	PE	PP-H	PVDF (SYGEF)		EPDM	FPM	NBR	CR	CSM
Potassium bromate	$KBrO_3$		cold saturated, aqueous	20	+	+	+	+	+	+		+	+	+	+	+
				40	+	+	+	+	+	+		+	+	+	+	+
				60	O	+	+	O	+	+		+	+	+	+	+
				80		+			+	+			+	+	O	+
				100					+	+				+	O	+
				120						+						
				140												
Potassium bromide	KBr		all, aqueous	20	+	+	+	+	+	+		+	+	+	+	+
				40	+	+	+	+	+	+		+	+	+	+	+
				60	O	+	+	+	+	+		+	+	+	+	+
				80		+				+			+	O	+	+
				100						+			+	O	O	+
				120						+						
				140												
Potassium carbonate (potash)				20	+	+	+	+	+	O		+				
				40	+	+		+	+			+				
				60	+	+		+	+			+				
				80		+			+							
				100												
				120												
				140												
Potassium chlorate (SpRB)	K ClO_3		cold saturated, aqueous	20	+	+	+	+	+	O		+	+	+	+	+
				40	+	+	+	+	+	-		+	+	O	O	+
				60	+	+	+	+	+				+			+
				80		+							+			O
				100									+			
				120												
				140												
Potassium chloride	KCl		all, aqueous	20	+	+	+	+	+	+		+	+	+	+	+
				40	+	+	+	+	+	+		+	+	+	+	+
				60	+	+	+	+	+	+		+	+	+	+	+
				80		+			+	+			+			+
				100					+	+			+			
				120						+						
				140												
Potassium chromate (SpRB)	K_2CrO_4		cold saturated, aqueous	20	+	+	+	+	+	+		+	+	+	+	+
				40	+	+	+		+	+			+	O	+	+
				60	+	+	+		+	+			+	-	O	O
				80						+						
				100						+						
				120												
				140												
Potassium cyanide	KCN		cold saturated, aqueous	20	+	+	+	+	+	+			+	+	+	+
				40	+	+	+	+	+	+			O	+	+	+
				60	+	+	+	+	+	O		+	-	+	O	+
				80		+			+			+		+	-	+
				100												
				120												
				140												
Potassium dichromate	$K_2Cr_2O_7$		saturated	20		+		+	+	+		+	+			
				40		+		+	+	+						
				60		+		+	+	+						
				80		+				+						
				100						+						
				120												
				140												

(Courtesy George Fischer Engineering Handbook)

Aggressive Media					Chemical Resistance											
Medium	Formula	Boiling point °C	Concentration	Temperature °C	PVC	CPVC	ABS	PE	PP-H	PVDF (SYGEF)		EPDM	FPM	NBR	CR	CSM
Potassium fluoride	KF		saturated	20	+	+		+	+	+			+			
				40	+	+		+	+	+						
				60	+	+		+	+	+						
				80		+			+	+						
				100						+						
				120												
				140												
Potassium Hexacyanoferrate -(II)	$K_4[Fe(CN)_6]\cdot 3H_2O$			20	+	+		+	+	+		+	+			
				40	+	+		+	+	+						
				60	+	+		+	+	+						
				80		+			+	+						
				100						+						
				120												
				140												
Potassium hydrogen carbonate	$KHCO_3$		saturated	20	+	+		+	+	+		+	+			
				40	+	+		+	+	+		+				
				60	+	+		+	+	+		+				
				80		+			+							
				100												
				120												
				140												
Potassium hydrogen sulphate	$KHSO_4$		saturated	20	+	+		+	+			+				
				40	+	+		+	+			+				
				60	+	+		+	+			+				
				80		+			+			+				
				100												
				120												
				140												
Potassium iodide	KJ		cold saturated, aqueous	20	+	+	+	+	+	+		+	+	+	+	+
				40	+	+	+	+	+	+			+	O	O	+
				60	+	+	+	+	+	+			+	·	-	+
				80		+				+			+			
				100						+						
				120												
				140												
Potassium nitrate	KNO_3		50%, aqueous	20	+	+	+	+	+	+		+	+	+	+	+
				40	+	+	+	+	+	+			+	+	+	+
				60	+	+	+	+	+	+			+	+	+	+
				80		+				+						
				100						+						
				120												
				140												
Potassium perchlorate (SpRB)	$KClO_4$		cold saturated, aqueous	20	+	+		+		+		+	+	+	+	+
				40	+	+				+			+	O	O	+
				60	O	+				+			+			+
				80		+				+			+			O
				100												
				120												
				140												
Potassium persulphate (SpRB)	$K_2S_2O_8$		all, aqueous	20	+	+	+	+	+	+		+	+	-	+	+
				40	+	+	+	+	+	+		+	+		+	+
				60	O	+	+	+	+	+			+		+	+
				80						+			+		O	O
				100									+			
				120												
				140												

(Courtesy George Fischer Engineering Handbook)

Aggressive Media					Chemical Resistance											
Medium	Formula	Boiling point °C	Concentration	Temperature °C	PVC	CPVC	ABS	PE	PP-H	PVDF (SYGEF)		EPDM	FPM	NBR	CR	CSM
Potassium sulphate	K_2SO_4		all, aqueous	20	+	+	+	+	+	+		+	+	+	+	+
				40	+	+	+	+	+	+		+	+	+	+	+
				60	O	+	+	+	+	+			+	+	+	+
				80		+				+			+			
				100						+			+			
				120												
				140												
Potassium sulphide	K_2S		saturated	20	+	+		+	+	O		+				
				40	+	+		+	+	O		+				
				60	+	+		+	+	O		+				
				80		+			+			+				
				100												
				120												
				140												
Potassium sulphite	K_2SO_3		saturated	20	+	+		+	+			+				
				40	+	+		+	+							
				60	+	+		+	+							
				80		+										
				100												
				120												
				140												
Potassium-aluminiumsulfate (alum)			50%	20	+	+		+	+	+		+				
				40	+	+		+	+	+		+				
				60	+	+		+	+	+		+				
				80		+			+	+		+				
				100						+						
				120												
				140												
Pottasium hexacyanoferrate -(III)	$K_3[Fe(CN)_6]$.			20	+	+		+	+	+		+	+			
				40	+	+		+	+	+						
				60	+	+		+	+	+						
				80		+			+	+						
				100						+						
				120												
				140												
Pottasium tartrat				20	+			+	+	+		+				
				40	+			+	+	+		+				
				60				+	+	+		+				
				80					+	+						
				100						+						
				120												
				140												
Pottasiumhydrogensulfite				20	+					+		+				
				40	+					+		+				
				60						+						
				80						+						
				100						+						
				120												
				140												
Pottasiumhypochlorite	KOCl			20	+	O		+	+	O		+	O			
				40												
				60												
				80												
				100												
				120												
				140												

(Courtesy George Fischer Engineering Handbook)

Aggressive Media					Chemical Resistance											
Medium	Formula	Boiling point °C	Concentration	Temperature °C	PVC	CPVC	ABS	PE	PP-H	PVDF (SYGEF)		EPDM	FPM	NBR	CR	CSM
Pottasiumperoxodisulfate	$K_2S_2O_8$		saturated	20	+	+										
				40	+	+										
				60	+	+										
				80		+										
				100												
				120												
				140												
Pottasiumphosphate	KH_2PO_4 und $K_2H\ PO_4$		all, aqueous	20	+	+	O	+	+	+		+	+	+	+	+
				40	+	+		+	+	+		+	+	O	O	+
				60	O	+		+	+	+			+	-	-	+
				80		+			+	+			+			O
				100									+			
				120												
				140												
Pottasiumphosphate				20	+				+							
				40	+				+							
				60	+				+							
				80					+							
				100												
				120												
				140												
Propane	C_3H_8	-42	technically pure, liquid	20	+	-	-	+	+	+		-	+	+	-	-
				40						+						
				60						+						
				80												
				100												
				120												
				140												
Propane			technically pure, gaseous	20	+	+	-	+	+	+		-	+	+	+	O
				40						+						
				60						+						
				80												
				100												
				120												
				140												
Propanol, n- and iso- (SpRB)	C_3H_7OH	97 bzw. 82	technically pure	20	+	-	-	+	+	+		+	+	+	+	+
				40	O			+	+	+		+	+	O	+	O
				60	O			+	+	+			+	-	+	O
				80						O						
				100												
				120												
				140												
Propargyl alcohol (SpRB)	$CH\equiv C$-CH_2-OH	114	7%, aqueous	20	+	-	-	+	+	+		+	+	+	+	+
				40	+			+	+	O		+	+	+	+	+
				60	+			+	+	O			+	+	O	O
				80												
				100												
				120												
				140												
Propionic acid (SpRB)	CH_3CH_2COOH	141	50%, aqueous	20	+	O	-	+	+	+		+	+	-	O	O
				40	+			+	+	+		+	+		-	-
				60	O			+	+	+			O			
				80												
				100												
				120												
				140												

(Courtesy George Fischer Engineering Handbook)

Aggressive Media					Chemical Resistance											
Medium	Formula	Boiling point °C	Concentration	Temperature °C	PVC	CPVC	ABS	PE	PP-H	PVDF (SYGEF)		EPDM	FPM	NBR	CR	CSM
Propionic acid (SpRB)		141	technically pure	20	+	O	-	+	+	+		+	+	-	-	-
				40	O			O	O	+		O	+			
				60				O	O	+			+			
				80									O			
				100												
				120												
				140												
Propylene glycol (SpRB)	$C_3H_8O_2$	188	technically pure	20	+	-	O	+	+	+		+	+	+	+	+
				40	+			+	+	+		+	+	O	+	+
				60	+			+	+	+			O	-		+
				80												
				100												
				120												
				140												
Propylene oxide	C_3H_6O	35	technically pure	20	O		-	+	+	+		O	-	-	-	-
				40						O						
				60												
				80												
				100												
				120												
				140												
Pyridine	C_5H_5N	115	technically pure	20	-	-	-	+	O	+		O	-	-	-	-
				40				O	O	-						
				60				O	O							
				80												
				100												
				120												
				140												
Pyrogallol	$C_6H_3(OH)_3$		100%	20						+			+			
				40						+						
				60												
				80												
				100												
				120												
				140												
Ramsit fabric waterproofing agents			usual commercial	20	+			+	+	+		+	+	+	+	+
				40	+					+						
				60	+					+						
				80												
				100												
				120												
				140												
Salicylic acid	$C_6H_4(OH)COOH$		saturated	20	+	+	O	+	+	+		+	+	+	+	+
				40	+			+	+	+		+				
				60				+	+	+		+				
				80						+						
				100												
				120												
				140												
Sea water	see Brine															
Silicic acid	$Si(OH)_4$			20	+	+	+	+	+			+				
				40	+	+		+	+			+				
				60	+	+		+	+			+				
				80					+							
				100												
				120												
				140												

(Courtesy George Fischer Engineering Handbook)

Aggressive Media					Chemical Resistance											
Medium	Formula	Boiling point °C	Concentration	Temperature °C	PVC	CPVC	ABS	PE	PP-H	PVDF (SYGEF)		EPDM	FPM	NBR	CR	CSM
Silicone oil				20	+	+	+	+	+	+		+	+	+	+	+
				40	O	+		+	+	+		+	+	+	+	+
				60	-			+	+	+		+	+	+	O	
				80					+	+						
				100						+						
				120												
				140												
Silver	AgCn		saturated	20	+	+	+	+	+	+		+	+	+	+	+
				40	+	+		+	+	+		+	+			
				60	+	+		+	+	+		+	+			
				80												
				100												
				120												
				140												
Silver salts	$AgNO_3$, AgCN, AgCl		cold saturated, aqueous	20	+	+	+	+	+	+		+	+	+	+	+
				40	+	+	+	+	+	+		+	+	+	+	+
				60	O	+	+	+	+	+		+	+	+	+	+
				80		+			+	+						
				100						+						
				120												
				140												
Silvercyanide				20	+	+	+	+	+	+		+	+	+	+	+
				40	+	+		+	+	+		+	+			
				60	+	+		+	+	+		+	+			
				80												
				100												
				120												
				140												
Soap solution (SpRB)			all, aqueous	20	+	+	+	+	+	+		+	+	+	+	+
				40	+	+	+	+	+	+		+	+	+	+	+
				60	O	+		+	+	+		+	+	+	+	+
				80						+						
				100						+						
				120												
				140												
Soda	see Sodium carbonate															
Sodium acetate	CH_3COONa		all, aqueous	20	+	+	+	+	+	+		+	-	+	+	O
				40	+	+		+	+	+		+		+	+	
				60	+	+		+	+	+		+				
				80		+			+	+						
				100					+	O						
				120												
				140												
Sodium aluminium sulfate				20	+			+	+							
				40	+			+	+							
				60	+			+	+							
				80					+							
				100												
				120												
				140												
Sodium arsenite	Na_3AsO_3		saturated	20	+	+		+	+			+				
				40	+	+		+	+			+				
				60	+	+		+	+			+				
				80		+			+							
				100												
				120												
				140												

(Courtesy George Fischer Engineering Handbook)

Aggressive Media					Chemical Resistance											
Medium	Formula	Boiling point °C	Concentration	Temperature °C	PVC	CPVC	ABS	PE	PP-H	PVDF (SYGEF)		EPDM	FPM	NBR	CR	CSM
Sodium benzoate	C_6H_5-COONa		cold saturated, aqueous	20	+	+	-	+	+	+		+	+	+	+	+
				40	+	+		+	+	+		O	+	+	+	+
				60	O	+		+	+	+			+			O
				80		+				+			O			
				100						O						
				120												
				140												
Sodium bicarbonate	$NaHCO_3$		cold saturated, aqueous	20	+	+	+	+	+	+		+	+	+	+	+
				40	+	+	+	+	+	+		+	+	+	+	+
				60	+	+	+	+	+	+		+	+	+	+	+
				80					+	+		+	+			
				100						+						
				120												
				140												
Sodium bisulphate	$NaHSO_4$		10%, aqueous	20	+	+	+	+	+	+		+	+	+	+	+
				40	+	+	+	+	+	+		O	+	O	+	+
				60	O	+	+	+	+	+			+	-	O	
				80						+			+			
				100						+			+			
				120						+						
				140												
Sodium bisulphite	$NaHSO_3$		all, aqueous	20	+	+		+	+	+		+	O	O	+	+
				40	O	+		+	+	+		O	-	-	+	+
				60	-	+		+	+	+		-			O	+
				80						+					-	O
				100						+						
				120												
				140												
Sodium borate	Na_3BO_3		saturated	20	+	+		+	+			+	+			
				40	+	+		+	+			+	+			
				60	+	+		+	+			+	+			
				80		+			+							
				100												
				120												
				140												
Sodium bromate	$NaBrO_3$		all, aqueous	20	+	+		+	+	+		+	+	+	+	+
				40	O	+		O	O	+			+	O	+	+
				60						+			+	-	O	+
				80						+						
				100						+						
				120												
				140												
Sodium bromide	NaBr		all, aqueous	20	+	+	+	+	+	+		+	+	+	+	+
				40	+	+	+	+	+	+			+	O	+	+
				60	O	+	+	+	+	+			+		O	O
				80		+			+	+			+			
				100						+						
				120						+						
				140												
Sodium carbonate	see soda		cold saturated, aqueous													
Sodium chlorate (SpRB)	$NaClO_3$		all, aqueous	20	+	+	+	+	+	O		+	+	+	+	+
				40	+	+	+	+	+			+	+	O	+	+
				60	O	+	+	+	+			+	+	-	O	+
				80		+						O	+		-	O
				100								-				
				120												
				140												

(Courtesy George Fischer Engineering Handbook)

Aggressive Media					Chemical Resistance										
Medium	Formula	Boiling point °C	Concentration	Temperature °C	PVC	CPVC	ABS	PE	PP-H	PVDF (SYGEF)	EPDM	FPM	NBR	CR	CSM
Sodium chlorite (SpRB)	$NaClO_2$		diluted, aqueous	20	O	+		+	+	+	+	+	-	O	+
				40		+		O	O	O	+	+		-	+
				60		+				O	+	+			+
				80		+									
				100											
				120											
				140											
Sodium chromate (SpRB)	Na_2CrO_4		diluted, aqueous	20	+	+	+	+	+	+	+	+	+	+	+
				40	+	+	+		+	+	+	+	O	+	+
				60	O		+			+	+	+	-	O	O
				80						+					
				100						+					
				120											
				140											
Sodium disulphite	$Na_2S_2O_5$		all, aqueous	20	+	+		+	+	+	+	+	O	+	+
				40	+	+				+	+	+	-	+	+
				60	O	+				+	+	+		+	O
				80						+					
				100						+					
				120											
				140											
Sodium dithionite	see hyposulphite		up to 10%, aqueous												
Sodium fluoride	NaF		cold saturated, aqueous	20	+	+	+	+	+	+	+	+	+	+	+
				40	+	+	+			+	+	+	+	+	+
				60	+	+	+			+	+	+	O	+	+
				80						+					
				100						+					
				120											
				140											
Sodium hydroxide (see Caustic soda)															
Sodium hypochlorite (SpRB)	NaOCl		12,5% active chlorine, aqueous	20	+			O	O	O	+	+	-	-	+
				40	+			-	-						
				60	O										
Sodium iodide	NaI		all, aqueous	20	+	+	+	+	+	+	+	+	+	+	+
				40	+	+	+			+		+	+	+	+
				60	O	+	+			+		+	O	+	O
				80		+				+					
				100						+					
				120											
				140											
Sodium nitrate	$NaNO_3$		cold saturated, aqueous	20	+	+	+	+	+	+	+	+	+	+	+
				40	+	+	+	+	+	+	+	+	+	+	+
				60	O	+		+	+	+	+	+	+	+	+
				80					+	+					
				100						+					
				120						+					
				140											
Sodium nitrite	$NaNO_2$		cold saturated, aqueous	20	+	+	+	+	+	+	+	+	+	+	+
				40	+	+	+	+	+	+		+	O	+	+
				60	+	+		+	+	+		+	-	+	+
				80		+			+	+					
				100						+					
				120						+					
				140											

(Courtesy George Fischer Engineering Handbook)

Aggressive Media					Chemical Resistance											
Medium	Formula	Boiling point °C	Concentration	Temperature °C	PVC	CPVC	ABS	PE	PP-H	PVDF (SYGEF)		EPDM	FPM	NBR	CR	CSM
Sodium oxalate	$Na_2C_2O_4$		cold saturated, aqueous	20	+	+	+	+	+	+			+	+	+	+
				40	+	+				+						
				60	O	+				O						
				80												
				100												
				120												
				140												
Sodium perborate	$NaBO_3 \cdot 4H_2O$		saturated	20	+	+		+	+	+		+	+			
				40	+	+				+						
				60	+	+				+						
				80		+										
				100												
				120												
				140												
Sodium perchlorate	$NaClO_4$		saturated	20	+	+		+	+			+	+			
				40	+	+										
				60	+	+										
				80		+										
				100												
				120												
				140												
Sodium persulphate (SpRB)	$Na_2S_2O_8$		cold saturated, aqueous	20	+			+	+	+		+	+	-	+	+
				40	+			+	+	+		+	+		+	+
				60	O			+	+	+			+		+	+
				80									+		O	O
				100									+			
				120												
				140												
Sodium phosphate	Na_3PO_4		cold saturated, aqueous	20	+	+	+	+	+	+		+	+	+	+	+
				40	+	+		+	+	+		+	+	+	+	+
				60	O	+		+	+	+		+	+	+	+	+
				80		+			+	O						
				100					+	-						
				120												
				140												
Sodium silicate	Na_2SiO_3		all, aqueous	20	+	+	+	+	+	+		+	+	+	+	+
				40	+	+	+	+	+	+		+	+	+	+	+
				60	O	+		+	+	O		+	+	+	+	+
				80					+	-						
				100												
				120												
				140												
Sodium Sulfide	Natriumsulfid															
Sodium sulphate	Na_2SO_4, $NaHSO_4$		cold saturated, aqueous	20	+	+	+	+	+	+		O	+	+	+	+
				40	+	+	+	+	+	+		O	+	+	+	+
				60	O	+	+	+	+	+		O	+	+	+	+
				80					+	+			+			
				100						+						
				120						+						
				140												
Sodium sulphide	Na_2S		cold saturated, aqueous	20	+	+	+	+	+	O		+	+	+	-	+
				40	+	+	+	+	+	O		+		+		+
				60	O	+	+	+	+	O		+		+		+
				80		+			+							
				100												
				120												
				140												

(Courtesy George Fischer Engineering Handbook)

Aggressive Media					Chemical Resistance											
Medium	Formula	Boiling point °C	Concentration	Temperature °C	PVC	CPVC	ABS	PE	PP-H	PVDF (SYGEF)		EPDM	FPM	NBR	CR	CSM
Sodium sulphite	Na_2SO_3		cold saturated, aqueous	20	+	+	+	+	+	+		+	+	+	+	+
				40	+	+		+	+	+		+	+	O	+	+
				60	O	+		+	+	+		+	+	-	O	+
				80		+			+	+						
				100						+						
				120												
				140												
Sodium thiosulphate	$Na_2S_2O_3$		cold saturated, aqueous	20	+	+	+	+	+	+		+	+	+	+	+
				40										O	+	+
				60										-	O	O
				80												
				100												
				120												
				140												
Sodiumchloride	$NaCl$		each, aqueous	20	+	+	+	+	+	+		+	+			
				40	+	+	+	+	+	+		+	+			
				60	+	+		+	+	+		+	+			
				80		+			+	+		+	+			
				100						+			+			
				120												
				140												
Sodiumcyanide	$NaCN$			20	+	+		+	+	+		+	+			
				40	+	+		+	+	+		+	+			
				60	+	+		+	+	+		+	+			
				80		+			+							
				100												
				120												
				140												
Sodiumdichromate	Na_2Cs2O_7			20	O	+		+	+			+	+			
				40		+		+				+	+			
				60		+							+			
				80		+										
				100												
				120												
				140												
Sodiumhydrogen-carbonate	$NaHCO_3$			20	+	+	+	+	+	+		+	+			
				40	+	+		+	+	+		+				
				60	+	+		+	+	+		+				
				80		+			+							
				100												
				120												
				140												
Sodiumhydrogensulfate	$NaHSO_4$			20	+	+	+	+	+	+		+	+			
				40	+	+		+	+	+		+	+			
				60	+	+		+	+	+		+	+			
				80		+			+	+						
				100						+						
				120												
				140												
Spindie oil				20	O	O	-	O	+	+		-	+	+	O	-
				40					O	+			O	+	-	O
				60				O	-	+			-	O		-
				80						+				-		
				100												
				120												
				140												

(Courtesy George Fischer Engineering Handbook)

Aggressive Media					Chemical Resistance											
Medium	Formula	Boiling point °C	Concentration	Temperature °C	PVC	CPVC	ABS	PE	PP-H	PVDF (SYGEF)		EPDM	FPM	NBR	CR	CSM
Spinning bath acids containing carbon disulphide (SpRB)			100 mg CS_2/l	20	+			+	+	+			+	-	-	O
				40	+					+						
				60												
				80												
				100												
				120												
				140												
Spinning bath acids containing carbon disulphide (SpRB)			200 mg CS_2/l	20	O			+	+	+		-	+	-	-	-
				40						+						
				60												
				80												
				100												
				120												
				140												
Spinning bath acids containing carbon disulphide (SpRB)			700 mg CS_2/l	20	-			+	+	+		-	+	-	-	-
				40						+						
				60												
				80												
				100												
				120												
				140												
Stannous chloride	see Tin II chloride		cold saturated, aqueous													
Stannous chloride - Tin IV chloride	$SnCl_4$		cold saturated, aqueous	20				+	+							
				40				+	+							
				60				+	+							
				80					+							
				100												
				120												
				140												
Starch solution	$(C_6H_{10}O_5)_n$		all, aqueous	20	+	+	+	+	+	+		+	+	+	+	+
				40	+	+	+	+	+	+		+	+	+	+	+
				60	+	+		+	+	+		+	+	+	+	+
				80		+				+						
				100						+						
				120												
				140												
Starch syrup			usual commercial	20	+	+	+	+	+	+		+	+	+	+	+
				40	+	+	+	+	+	+		+	+	+	+	+
				60	+	+		+	+	+		+	+	+	+	+
				80		+			+	+		+	+	+	+	+
				100						+		+	+	+	+	+
				120												
				140												
Stearic acid (SpRB)	$C_{17}H_{35}COOH$	Fp. 69	technically pure	20	+	O	+	+	+	+		+	+	+	+	O
				40	+		+			+		+	+	+	+	O
				60	+			O	O	+		O	O	O	O	-
				80						+						
				100						+						
				120						+						
				140												
Styrol				20	-	-	-			+			+			
				40												
				60												
				80												
				100												
				120												
				140												

(Courtesy George Fischer Engineering Handbook)

Aggressive Media					Chemical Resistance											
Medium	Formula	Boiling point °C	Concentration	Temperature °C	PVC	CPVC	ABS	PE	PP-H	PVDF (SYGEF)		EPDM	FPM	NBR	CR	CSM
Succinic acid	HOOC-CH_2-CH_2-COOH	Fp*., 185	aqueous, all	20	+	+	+	+	+	+		+	+	+	+	+
				40	+	+		+	+	+		+	+	+	+	+
				60	+	+		+	+	+		+	+	+	+	+
				80									+			
				100												
				120												
				140												
Sugar syrup			usual commercial	20	+	+	+	+	+	+		+	+	+	+	+
				40	+	+	O	+	+	+		+	+	+	+	+
				60	O	+		+	+	+		+	+	+	+	+
				80					+	+		+	+			+
				100					+	+						
				120						+						
				140												
Sulfur	S	Fp.*, 119	technically pure	20	O	O	-	+	+	+		+	+	-	+	+
				40	-			+	+	+			+			+
				60				+	+	+			+			+
				80					+	+			+			+
				100						+						
				120						+						
				140												
Sulfur dioxide	SO_2	-10	technically pure, anhydrous	20	+	+	-	+	+	O		+	+	-	-	O
				40	+	+		+	+	O		O	O			-
				60	+	+		+	+	-		-				
				80												
				100												
				120												
				140												
Sulfur dioxide	SO_2		technically pure, moist	20	-	-	-	-	-	-		-	O	-	-	O
				40												
				60												
				80												
				100												
				120												
				140												
Sulfur dioxide	SO_2		all, moist	20	+	+	-	+	+	+		+	+	-	-	O
				40	+	+		+	+	O		O	O			-
				60	O			+	+	-		-	-			
				80												
				100												
				120												
				140												
Sulfur trioxide	SO_3			20	-	-	-	-	-	-		-	-	-	-	-
				40												
				60												
				80												
				100												
				120												
				140												
Sulfuric acid saturated by Chlorine	H_2SO_4+Cl_2		60%	20						+						
				40						+						
				60						+						
				80						+						
				100						+						
				120												
				140												

(Courtesy George Fischer Engineering Handbook)

Aggressive Media					Chemical Resistance											
Medium	Formula	Boiling point °C	Concentration	Temperature °C	PVC	CPVC	ABS	PE	PP-H	PVDF (SYGEF)		EPDM	FPM	NBR	CR	CSM
Sulfuric acid (see note 2.3.1 on jointing)	H_2SO_4	120	up to 40%, aqueous	20	+	+	+	+	+	+		+	+	O	+	+
				40	+	+	O	+	+	+		+	+	-	O	+
				60	O	+		+	+	+		+	+			O
				80		+				+		O	O			O
				100						+		-	-			-
				120						+						
				140												
Sulfuric acid (see note 2.3.1 on jointing) (SpRB)	H_2SO_4	140	up to 60%, aqueous	20	+	+	-	+	+	+		+	+	-	-	+
				40	+	+		+	O	+		+	+			O
				60	+	+		+	-	+		O	+			O
				80		+				+		-	O			-
				100						+						
				120						+						
				140												
Sulfuric acid (see note 2.3.1 on jointing) (SpRB)	H_2SO_4	195	up to 80%, aqueous	20	+	+	-	+	+	+		O	+	-	-	+
				40	+	+		+	+	+		O	+			O
				60	+	+		O	O	+		-	O			-
				80		+				+			-			
				100						+						
				120						O						
				140												
Sulfuric acid (see note 2.3.1 on jointing) (SpRB)	H_2SO_4	250	90%, aqueous	20	+	+	-	O	O	+		-	+	-	-	-
				40	+	+				+			+			
				60		+				+						
				80						+						
				100						O						
				120						O						
				140												
Sulfuric acid (see note 2.3.1 on jointing) (SpRB)	H_2SO_4		96%, aqueous	20	+	+	-	-	-	+		-	+	-	-	-
				40	+	+				+			+			
				60	O	+				-						
				80												
				100												
				120												
				140												
Sulfuric acid (see note 2.3.1 on jointing) (SpRB)	H_2SO_4		97%	20	+	+	-	-	-	O		-	+	-	-	-
				40		+										
				60												
				80												
				100												
				120												
				140												
Sulfuric acid (see note 2.3.1 on jointing) (SpRB)	H_2SO_4	340	98%	20	+	+	-	-	-	-		-	O	-	-	-
				40	O	+										
				60		O										
				80												
				100												
				120												
				140												
Sulfurous acid	H_2SO_3		saturated, aqueous	20	+	+	O	+	+	+		+	+	-	-	O
				40	+	+	+	+	+	+		-	+			O
				60	O			+	+	+			O			-
				80						+			-			
				100						+						
				120												
				140												

(Courtesy George Fischer Engineering Handbook)

Aggressive Media					Chemical Resistance											
Medium	Formula	Boiling point °C	Concentration	Temperature °C	PVC	CPVC	ABS	PE	PP-H	PVDF (SYGEF)		EPDM	FPM	NBR	CR	CSM
Sulfuryl chloride	SO_2Cl_2	69	technically pure	20	-	-	-	-	-	O			+	-	O	+
				40												
				60												
				80												
				100												
				120												
				140												
Surfactants (SpRB)			up to 5%, aqueous	20	O	-	-	+	+	+		+	+	+	+	+
				40	O				O	O						
				60	O				O	O						
				80						O						
				100												
				120												
				140												
Surfactants (ESC)				20	O	O	O	O	O	O		O	O	O	O	
				40												
				60												
				80												
				100												
				120												
				140												
Tallow (SpRB)			technically pure	20	+	-	-	+	+	+		+	+	+	+	+
				40	+			+	+	+		+	+	+	+	+
				60	+			+	+	+		+	+	+	+	+
				80						+						
				100						+						
				120												
				140												
Tannic acid (SpRB)			all, aqueous	20	+	+	+	+	+				+	+	+	+
				40		+	+	+	+							
				60		+		+	+							
				80												
				100												
				120												
				140												
Tanning extracts form plants (SpRB)			usual commercial	20	+	+	+	+	+	+		+	+	+	+	+
				40		+	+									
				60												
				80												
				100												
				120												
				140												
Tartaric acid				20						+						
				40						+						
				60												
				80												
				100												
				120												
				140												
Tartaric acid	$HO_2C\text{-}CH(OH)\text{-}CH(OH)\text{-}CO_2H$		all, aqueous	20	+	+	+	+	+	+		+	+	+	+	+
				40	+		+	+	+	+		+	+	+	+	+
				60	O			+	+	+		+	+	O	+	+
				80						+						
				100						+						
				120						+						
				140												

(Courtesy George Fischer Engineering Handbook)

Aggressive Media					Chemical Resistance											
Medium	Formula	Boiling point °C	Concentration	Temperature °C	PVC	CPVC	ABS	PE	PP-H	PVDF (SYGEF)		EPDM	FPM	NBR	CR	CSM
Tartaric acid up to 10%				20						+						
				40						+						
				60						+						
				80												
				100												
				120												
				140												
Tetrachlorethylene				20	-	-	-	-	-	+		-	+			
				40												
				60												
				80												
				100												
				120												
				140												
Tetrachloroethane	$Cl_2CH\text{-}CHCl_2$	146	technically pure	20	-	-	-	O	O	+		-	O	-	-	-
				40						+						
				60						O						
				80												
				100												
				120												
				140												
Tetrachloroethylene	see Perchloroethylene	121														
Tetraetylene lead (SpRB)	$(C_2H_5)_4Pb$		technically pure	20	+	+	-	+	+	+		O	+	+	O	+
				40						+						
				60						+						
				80						+						
				100						+						
				120						+						
				140												
Tetrahydrofurane	C_4H_8O	66	technically pure	20	-	-	-	O	O	-		O	-	-	-	-
				40												
				60												
				80												
				100												
				120												
				140												
Tetrahydronaphthalene	Teralin	207	technically pure													
Thionyl chloride	$SOCl_2$	79	technically pure	20	-	-	-	-	-	-		O	+	-	-	-
				40												
				60												
				80												
				100												
				120												
				140												
Tin (IV) -chloride				20	+	+				+		+	+			
				40	+	+				+		+	+			
				60	+	+				+		+	+			
				80		+				+			+			
				100						+						
				120												
				140												

(Courtesy George Fischer Engineering Handbook)

Aggressive Media					Chemical Resistance											
Medium	Formula	Boiling point °C	Concentration	Temperature °C	PVC	CPVC	ABS	PE	PP-H	PVDF (SYGEF)		EPDM	FPM	NBR	CR	CSM
Tin-(II)-chloride	$SnCl_2$			20				+	+							
				40				+	+							
				60				+	+							
				80					+							
				100												
				120												
				140												
Toluene	C_6H_5-CH_3	111	technically pure	20	-	-	-	O	O	+		-	+	-	-	-
				40												
				60												
				80												
				100												
				120												
				140												
Triacetin (Glycerintriacetat)	$C_9H_{14}O_6$			20	-	-	-	+	+	+		+				
				40						+						
				60												
				80												
				100												
				120												
				140												
Tributylphosphate	$(C_4H_9)_3PO_4$	289	technically pure	20	-	-	-	+	+	+		+	-	-	-	-
				40				+	+							
				60				+	+							
				80												
				100												
				120												
				140												
Trichloroacetic acid	Cl_3C-COOH	196	technically pure	20	O	-	-	+	+	O		O	-	-	-	-
				40				O	+							
				60				-	O							
				80												
				100												
				120												
				140												
Trichloroacetic acid	Cl_3-C-COOH		50%, aqueous	20	+	-	-	+	+	+		O	-	-	-	-
				40	O			+	+	+						
				60				+	O	O						
				80						-						
				100												
				120												
				140												
Trichloroethane	Methylchloroform	74	technically pure													
Trichloroethylene	Cl_2C=CHCl	87	technically pure	20	-	-	-	-	O	+		-	+	-	-	-
				40						+						
				60						+						
				80						O						
				100												
				120												
				140												
Trichloromethane	Chloroform	61														

(Courtesy George Fischer Engineering Handbook)

Aggressive Media					Chemical Resistance											
Medium	Formula	Boiling point °C	Concentration	Temperature °C	PVC	CPVC	ABS	PE	PP-H	PVDF (SYGEF)		EPDM	FPM	NBR	CR	CSM
Tricresyl phosphate (SpRB)	$H_3C-C_6H_5-O)_3PO_4$		technically pure	20	-	-	-	+	+			+	-	O	-	-
				40				+						-		
				60				+	O							
				80												
				100												
				120												
				140												
Triethanolamine (SpRB)	$N(CH_2-CH_2-OH)_3$	Fp. *21	technically pure	20	O	-	-	+	+	+		O	-	O	-	-
				40						+						
				60												
				80												
				100												
				120												
				140												
Triethylamine (SpRB)	$N(CH_2-CH_3)3$	89	technically pure	20	-	-	-	+	+	O		-	-	-	-	-
				40						-						
				60												
				80												
				100												
				120												
				140												
Trifluoro acetic acid (SpRB)	$F_3C-COOH$		up to 50%	20	-	-	-	+	+	+		O	-	-	-	-
				40						O						
				60												
				80												
				100												
				120												
				140												
Trioctyl phosphate (SpRB)	$(C_8H_{17})_3PO_4$		technically pure	20	-	-	-	+	+	O		+	-	O	-	-
				40				+	O							
				60												
				80												
				100												
				120												
				140												
Turpentine oil (SpRB)			technically pure	20	+	-	-	O	-	+		-	+	O	-	-
				40	O			O					+			
				60									+			
				80												
				100												
				120												
				140												
Urea (SpRB)	$H_2N-CO-NH_2$	Fp.*, 133	up to 30%, aqueous	20	+	+	+	+	+	+		+	+	+	+	+
				40	+	+	+	+	+	+		+	+	+	+	+
				60	O	+		+	+	+		+	+	+	+	+
				80		O				+						
				100						O						
				120												
				140												
Urine				20	+	+	+	+	+	+		+	+	+	+	+
				40	+	+	+	+	+	+		+	+	+	+	+
				60	O	+		+	+	+		+	+	+	+	+
				80						+						
				100						+						
				120												
				140												

(Courtesy George Fischer Engineering Handbook)

Aggressive Media					Chemical Resistance											
Medium	Formula	Boiling point °C	Concentration	Temperature °C	PVC	CPVC	ABS	PE	PP-H	PVDF (SYGEF)		EPDM	FPM	NBR	CR	CSM
Vaseline			technically pure	20	O	O	-	+	O	+		-	+	+	-	-
				40	-					+			+	+		
				60				-	-	+			+	+		
				80						+			+	+		
				100						+			+	+		
				120						+			+			
				140												
Vegetable oils				20	O	-	-	+	+	+		-	+	+	O	O
				40						+						
				60						+						
				80												
				100												
				120												
				140												
Vegetable oils and fats (SpRB)				20	+	O	-	+	+	+		-	+	+	O	O
				40	O			O	+	+			+	+	O	O
				60					O	+			+	+	-	-
				80						+						
				100						+						
				120												
				140												
Vinegar	see wine vinegar															
Vinyl acetate	CH_2=CHOOCCH$_3$	73	technically pure	20	-	-	-	+	+	+		+	-	-	-	-
				40				+		-						
				60					O							
				80												
				100												
				120												
				140												
Vinyl chloride	CH_2=CHCl	-14	technically pure	20	-	-	-	-	-	+		-	+	-	-	
				40						+						
				60												
				80												
				100												
				120												
				140												
Viscose spinning solution				20	+	-	-	+	+	+			+	-	O	+
				40	+			+	+	+		+	+		O	+
				60	+			+	+	+		+	+		-	+
				80												
				100												
				120												
				140												
Waste gases containing - Alkaline				20	+	+		+	+	+		+	+	+	+	+
				40	+	+		+	+	O		+	+	+	+	+
				60	+	+		+	+	-		+	+	+	+	O
				80		+			+			+	O			-
				100									-			
				120												
				140												
Waste gases containing - Carbon oxides			all	20	+	+		+	+	+		+	+	+	+	+
				40	+	+		+	+	+		+	+	+	+	+
				60	+	+		+	+	+		+	+	+	+	+
				80		+			+	+		+	+			+
				100						+			+			
				120						+						
				140												

(Courtesy George Fischer Engineering Handbook)

Aggressive Media					Chemical Resistance											
Medium	Formula	Boiling point °C	Concentration	Temperature °C	PVC	CPVC	ABS	PE	PP-H	PVDF (SYGEF)		EPDM	FPM	NBR	CR	CSM
Waste gases containing - Hydrochloric acid			all	20	+	+		+	+	+		+	+	O	+	+
				40	+	+		+	+	+		+	+	-	+	+
				60	+	+		+	O	+		+	+		+	+
				80		+				+		O	+			+
				100						+			+			
				120						+						
				140												
Waste gases containing - Hydrogen fluoride (SpRB)			traces	20	+	+		+	+	+		+	+	+	+	+
				40	+	+		+	+	+		+	+	O	+	+
				60	+	+		+	+	+		O	+	-	O	+
				80		+				+			+			
				100						+						
				120												
				140												
Waste gases containing - Nitrous gases			traces	20	+	+		+	+	+		+	+	O	+	+
				40	+	+		+	+	+		+	+	-	+	+
				60	+	+		+	O	+		+	+		O	+
				80		+				+		O	+			O
				100						+			O			
				120												
				140												
Waste gases containing - Sulphur dioxide			traces	20	+	+		+	+	+		+	+	O	+	+
				40	+	+		+	+	+		+	+	-	+	+
				60	+	+		+	+	+		+	+		+	+
				80		+			+	+		+	+			+
				100						+			+			
				120						+						
				140												
Waste gases containing - Sulphur trioxide (SpRB)			traces	20	+	+		+	+	+		+	+	O	+	+
				40	+	+		+	+	+		+	+	-	+	+
				60	+	+		+	O	+		+	+		+	+
				80		+				+		O	+			
				100						+						
				120												
				140												
Waste gases containing - Sulphuric acid			all	20	+	+		+	+	+		+	+	O	+	+
				40	+	+		+	+	+		+	+	-	+	+
				60	+	+		+	+	+		+	+		+	+
				80		+			O	+		O	+			+
				100						+			+			
				120						+						
				140												
Water - distilled - deionised	H_2O	100		20	+	+	+	+	+	+			+	+	+	+
				40	+	+	+	+	+	+		+	+	+	+	+
				60	+	+	+	+	+	+		O	+	+	+	+
				80		+			+	+		-	+	+		+
				100					+	+			+	+		
				120						+			+			
				140												
Water, condensed				20	+	+	+	+	+	+			+	+	+	+
				40	+	+	+	+	+	+		+	+	+	+	+
				60	O	+	+	+	+	+		O	+	+	+	+
				80		+			+	+			+	O		+
				100						+						
				120						+						
				140												

(Courtesy George Fischer Engineering Handbook)

Aggressive Media					Chemical Resistance											
Medium	Formula	Boiling point °C	Concentration	Temperature °C	PVC	CPVC	ABS	PE	PP-H	PVDF (SYGEF)		EPDM	FPM	NBR	CR	CSM
Water, drinking, chlorinated				20	+	+	+	+	+	+			+	+	+	+
				40	+	+	+	+	+	+		+	+	+	+	+
				60	+	+	+	+	+	+		O	+	+	+	+
				80					+	+			+	O		+
				100					+	+			+			
				120						+						
				140												
Water, waste water without organic solvent and surfactants				20	+	+	+	+	+	+			+	+	+	+
				40	+	+	+	+	+	+		+	+	+	+	+
				60		+	+	+	+	+		O	+	+	+	+
				80		+			+	+			+	+		+
				100						+				O		
				120						+						
				140												
Wax alcohol (SpRB)	$C_{31}H_{63}OH$		technically pure	20	+	O	-	O	O	+		+	+	+	+	-
				40	+			-	-	+		+	+	+	+	
				60	+					+		+	+	+	+	
				80												
				100												
				120												
				140												
Wine vinegar (SpRB)			usual commercial	20	+	o	O	+	+	+		+	O	-	O	+
				40	+			+	+	+			-		-	O
				60	+			+	+	+						-
				80					+	+						
				100						+						
				120												
				140												
Wines, red and white			usual commercial	20	+	O	+	+	+	+		+	+	+	+	+
				40			+	+	+	+						
				60				+	+	+						
				80						+						
				100						+						
				120												
				140												
Xylene	$C_6H_4(CH_3)_2$	138?	technically pure	20	-	-	-	-	-	+		-	+	-	-	-
		144		40						+			O			
				60						O			-			
				80						-						
				100												
				120												
				140												
yeasts			all, aqueous	20	+	+	+	+	+	+		+	+	+	+	+
				40	+	+		+	+	+		+	+	+	+	+
				60		+		+	+	+						
				80		+				+						
				100												
				120												
				140												
Zinc salts	$ZnCl_2$, $ZnCO_3$, $Zn(NO_3)_2$, $ZnSO_4$		all, aqueous	20	+	+	+	+	+	+			+	+	+	+
				40	+	+	+	+	+	+		+	+	O	+	+
				60	O	+		+	+	+		+	+	-	+	+
				80						+						
				100						+						
				120						+						
				140												

(Courtesy George Fischer Engineering Handbook)

Aggressive Media					Chemical Resistance											
Medium	Formula	Boiling point °C	Concentration	Temperature °C	PVC	CPVC	ABS	PE	PP-H	PVDF (SYGEF)		EPDM	FPM	NBR	CR	CSM
Zinccarbonate				20	+	+	+	+	+	+		+	+			
				40	+	+		+	+	+		+	+			
				60	+	+		+	+	+		+	+			
				80		+			+	+		+	+			
				100						+						
				120												
				140												
Zincchloride			saturated	20	+	+	+	+	+	+		+	+			
				40	+	+		+	+	+		+	+			
				60	+	+		+	+	+		+	+			
				80		+			+	+			+			
				100						+						
				120												
				140												
Zincnitrate	$Zn(NO_3)_2$		saturated	20	+	+	+	+	+	+		+	+			
				40	+	+		+	+	+		+	+			
				60	+	+		+	+	+		+	+			
				80		+			+	+			+			
				100						+						
				120												
				140												
Zincoxide			Suspension	20						+						
				40						+						
				60						+						
				80						+						
				100						+						
				120												
				140												
Zincphosphate			saturated	20	+	+	O	+	+	+		+	+			
				40	+	+		+	+	+		+	+			
				60	+	+		+	+	+		+	+			
				80		+			+	+			+			
				100						+						
				120												
				140												
Zincstearate			Suspension	20	-	-	-	+	+	+		+	O			
				40				+	+	+		+				
				60				+	+	+		+				
				80					+	+						
				100						+						
				120												
				140												
Zincsulfate	$ZnSO_4$			20	+	+		+	+	+		+	+			
				40	+	+		+	+	+		+	+			
				60	+	+		+	+	+		+	+			
				80		+			+	+		+	+			
				100						+			+			
				120												
				140												
1-Chloropentan	$C_5H_{11}Cl$			20	-	-	-									
				40												
				60												
				80												
				100												
				120												
				140												

(Courtesy George Fischer Engineering Handbook)

Aggressive Media					Chemical Resistance											
Medium	Formula	Boiling point °C	Concentration	Temperature °C	PVC	CPVC	ABS	PE	PP-H	PVDF (SYGEF)		EPDM	FPM	NBR	CR	CSM
1,1,2-Trifluoro, 1,2,2-Trichloroethane (Freon 113) (SpRB)	$FCl_2C\text{-}CClF_2$	47	technically pure	20	+		-			+			+	+	+	+
				40	+											
				60												
				80												
				100												
				120												
				140												

(Courtesy George Fischer Engineering Handbook)

DRISCOPIPE

Engineering Characteristics

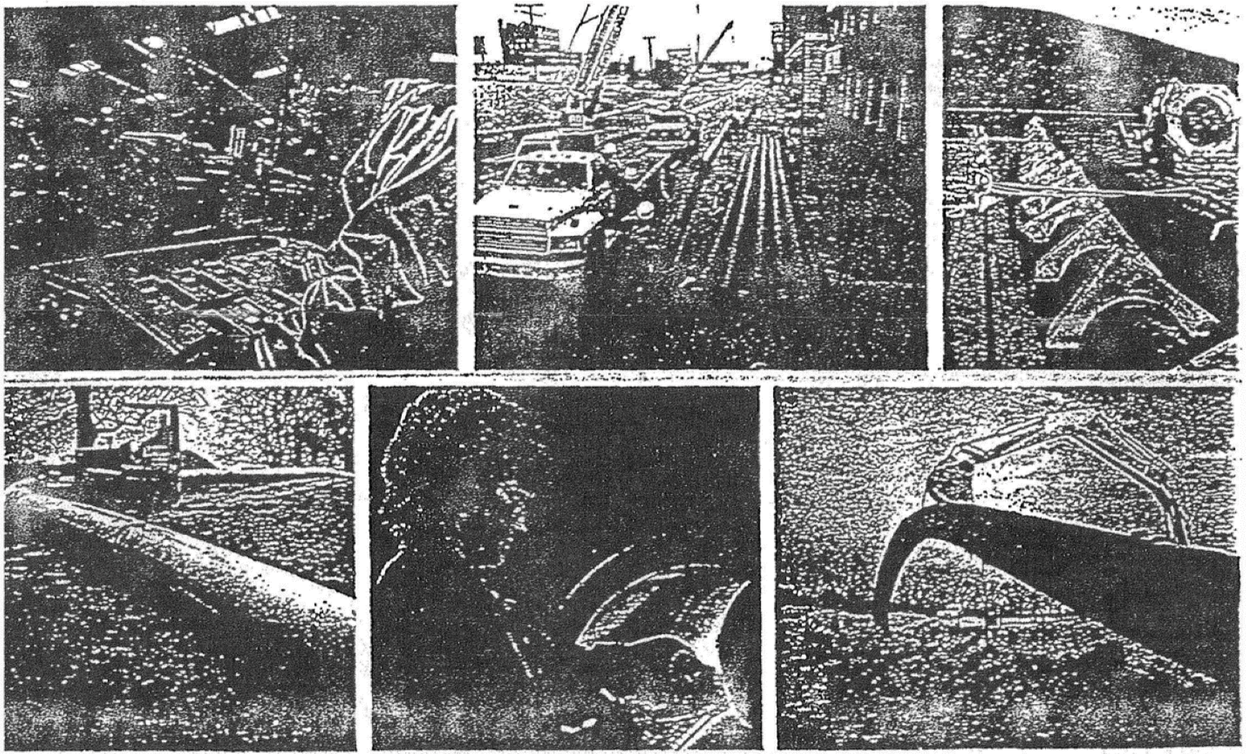

STOCKING DISTRIBUTORS OF FINE UTILITY PRODUCTS

iSCo

IRRIGATION SUPPLY CO., INC.
926 BAXTER AVE. P. O. BOX 4545
LOUISVILLE, KY. 40204
502 — 583-6591

PHILLIPS 66

Contents

Introduction 1
Physical Properties 1
Long Term Strength 1
Design Pressure Ratings 3
Flow Characteristics 4
Lightweight—Flexible 4
Toughness—"Ductile PE Pipe" 5
Environmental Stress Crack Resistance 7
Chemical Corrosion Resistance 8
Temperature Characteristics 11
Weatherability 14
Permeability 14
Abrasion Resistance 15
Heat Fusion Joining Method 16
Fatigue Resistance 17

Photographs shown are typical Driscopipe installations.

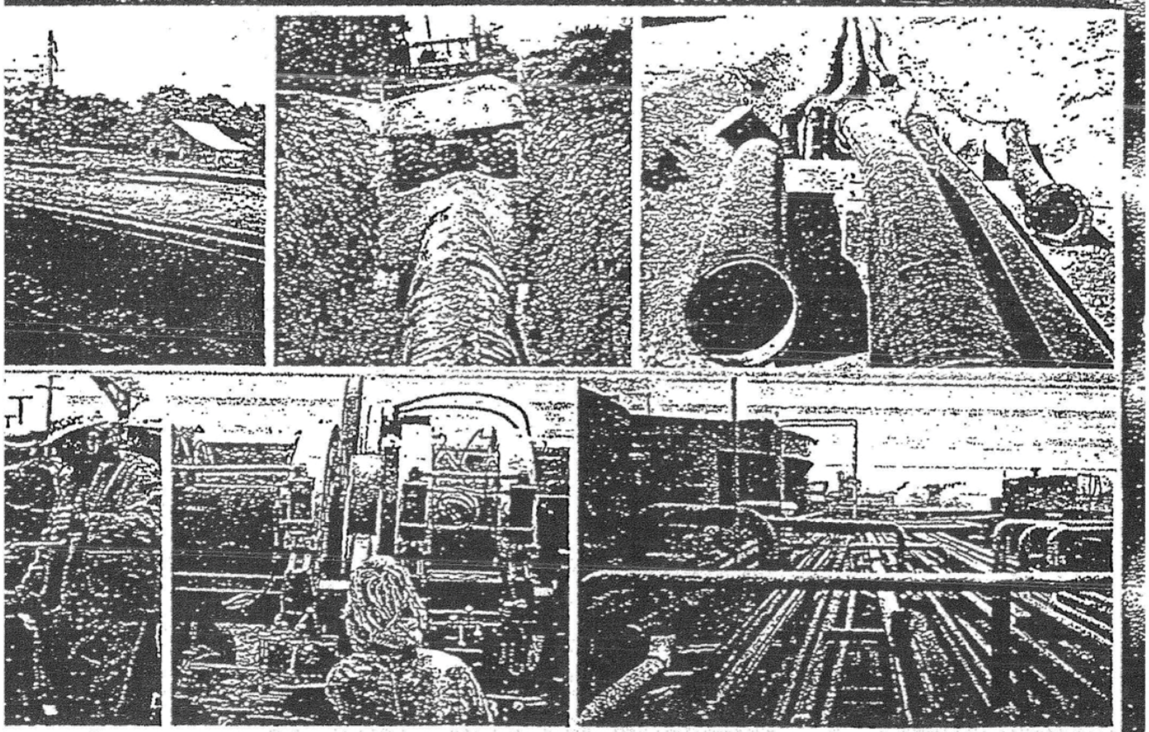

DRISCOPIPE

Driscopipe® Engineering Characteristics

Introduction

Driscopipe high density polyethylene piping systems offer the modern engineer the opportunity to take advantage of the unusual characteristics of these materials and use them to solve many old problems and to design systems for applications where traditional materials are either unsuitable or too expensive. When compared to the older traditional piping materials, Driscopipe polyethylene piping systems offer a new freedom in environmental design, extended service life, significant savings for installation labor and equipment costs, and reduced maintenance for pipeline systems where operating conditions are within the pressure and temperature capabilities of the material.

This brochure outlines the Engineering Characteristics of Driscopipe high density polyethylene pipe and fittings and points out many of the advantages and benefits to be realized through the use of these systems. The discussion is directed primarily toward the large diameter (3" through 54") Driscopipe 8600 and Driscopipe 1000 Industrial and Municipal product lines. However, these engineering characteristics are also typical of other Driscopipe polyethylene product lines.

Physical Properties

Driscopipe 8600 is manufactured from Marlex M-8000 very high molecular weight high density PE 3408 resin. Pipe and fittings made from Marlex M-8000 are extremely tough and durable, and possess exceptional long term strength. Marlex M-8000 is a proprietary product and is extruded only by Phillips Driscopipe, Inc.

Driscopipe 1000 is manufactured from Marlex TR-480, a PE 3408 polyethylene pipe resin in a molecular weight range which permits the pipe to be extruded by conventional methods. In this respect, Driscopipe 1000 is comparable to other extra high molecular weight, high density, PE 3408 polyethylene pipes commercially available in North America.

Sheets detailing typical physical properties for Driscopipe 1000 and Driscopipe 8600 are available upon request.

Long Term Hydrostatic Strength

One of the outstanding engineering characteristics of Driscopipe high density polyethylene pipe is its long term hydrostatic strength under various thermal and environmental conditions. Life expectancy is conservatively estimated to be in excess of 50 years using the standard design basis. This strength is determined by standardized methods and procedures which the plastic pipe industry has used for many years to evaluate the long term strength of all types of plastic pipe.

Pipe hoop stress versus time to failure plots of long term hydrostatic pressure data for thermoplastic pipe have been studied and analyzed for many years. The mathematical equations used to evaluate the test data and extrapolate values to longer periods of time were chosen after careful evaluation of more than 1,000 sets of long term test data representing more than 400 plastic pipe compounds. Continued testing on new compounds and extended testing of older compounds have proven the validity of these test methods. Actual data from more than 11½ years (100,000 hours) of continuous testing shows the industry methods to be slightly conservative in that actual values are slightly higher than those calculated by the industry-accepted ASTM method.

The reduction in strength which occurs with time, as indicated by the stress-life curves, does not represent a strength degradation of the material but is more in the nature of a relaxation effect. Plastic pipe samples which have been on test for periods up to 70,000 hours have been de-pressurized and checked for permanent reduction of strength by using the quick-burst test. No loss has been found when compared to samples previously quick-burst from the same test lot.

All evidence confirms that the methods used to predict the long term strength of plastic pipe are sound methods. Through the years, these policies and procedures, used to develop recommended hydrostatic design strengths, have influenced manufacturers to research and develop improved piping products such as Driscopipe 8600 and Driscopipe 1000.

Typical calculated long term strengths are shown below:

Long Term Strength @ 73.4°F(23°C)

Time	Hoop Stress, psi
100,000 hrs. (11.43 yrs.)	1635
438,000 hrs. (50 yrs.)	1604
500,000 hrs. (57 yrs.)	1601
1,000,000 hrs. (114 yrs.)	1586

The 114-year long term strength has been included to show more about the nature of the method used by the industry to evaluate the long term strength of plastic pipe and to illustrate the very slow reduction in strength as time progresses.

Long term hoop stresses for design purposes are normally selected at a level which is much lower than the long term strength of the materials. This ensures that the pipe is operating in a hoop stress range where creep (relaxation) of the materials is nil and assures service life in excess of 50 years. Design stress levels are discussed further in the next section.

The long term hydrostatic tests are conducted by using ASTM standard test procedures which may be applied to all types of plastic pipe (ASTM D 1598 Test for Time-to-Failure of Plastic Pipe Under Constant Internal Pressure). Stress-life tests are conducted by using numerous pipe samples which are filled with water (or other environmental fluids) and subjected to a controlled pressure at a controlled temperature.

Samples are held on test until they fail. The pressure, temperature and time-to-failure data from all samples are used to calculate and plot stress-life curves for the particular type pipe being tested (ASTM D 2837 Obtaining Hydrostatic Design Basis for Thermoplastic Pipe Materials). This data is then used to predict the probable safe life of the pipe at various stress levels (working pressures) and various temperatures. Because it is not practical to test at all temperature levels, these tests are generally conducted at temperatures of 73.4°F and one or more higher temperatures such as 100°F, 120°F and 140°F.

These stress-life curves give a relationship of the expected life span of the pipe when subjected to various internal stress levels (working pressures) at various temperatures. By comparing stress-life curves, one can compare relative long term performance ability of different plastic pipes. Stress-life curves for Driscopipe 8600 and Driscopipe 1000 are shown in Figure 1.

Figure 1

Stress-Life of Driscopipe® 8600 and Driscopipe® 1000

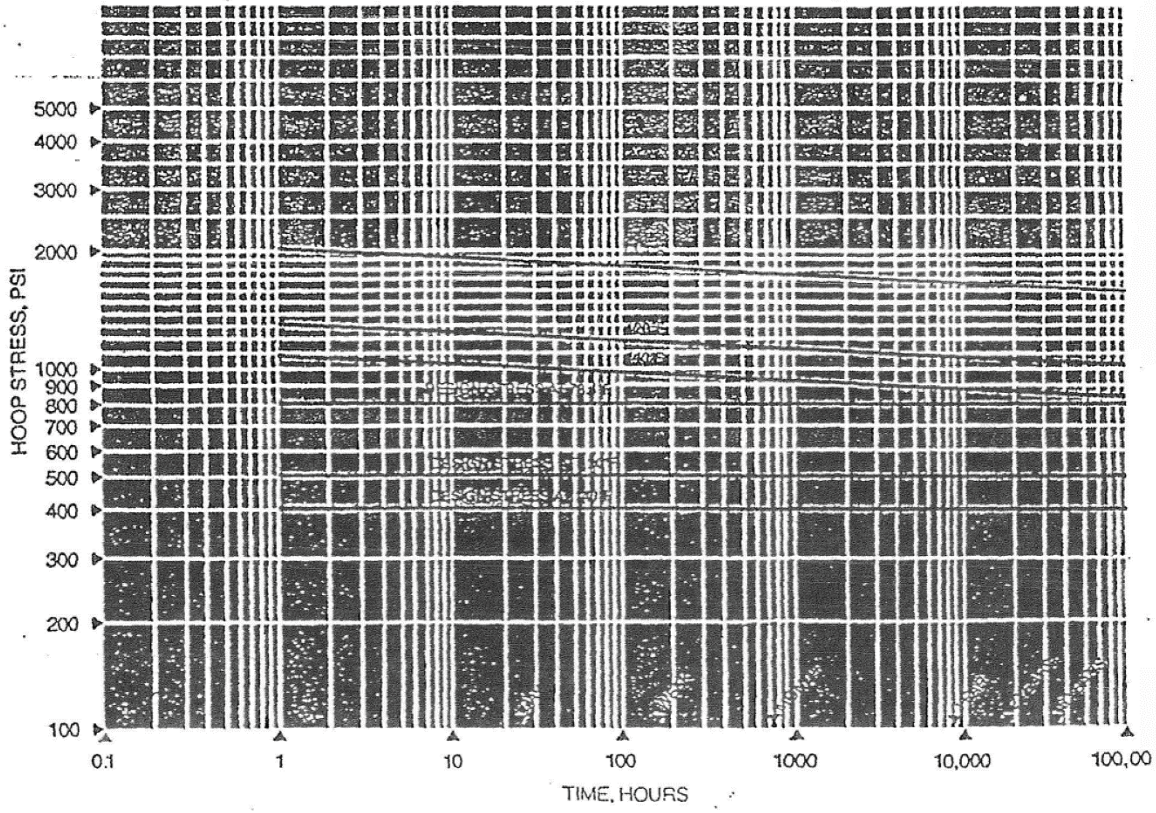

These stress-life curves were obtained using water as st medium. However, years of laboratory testing and field experience have shown that these same curves may be used to design Driscopipe systems for natural gas, salt water, sewage and hundreds of other industrial and municipal fluids, mixtures and effluents. The long term strength of Driscopipe indicated by these curves must be de-rated in some environmental circumstances, such as in the presence of liquid hydrocarbons or abrasive fluids, although the pipe is very suitable for use in these environments. An outstanding engineering advantage of Driscopipe is its exceptionally long term service life in the presence of internal and external corrosive service conditions.

Design Pressure Ratings

Since plastic pipe was introduced in the late 50s, the safety factor for design of water systems at standard temperature has been 2 to 1. The 2:1 design factor which was officially adopted by the plastic pipe industry in 1963, was based on allowances for many sources of variation. The guiding principle has always been to make the selection on a conservative basis but not to be unreasonably conservative.

The sources of variation for which allowances are made include ... variation in test methods and cedures among laboratories ... variation among s of the same compound ... variation of lots of pipe rom the compound in different plants and from different extruders ... variation in compounds of the same general class ... variations in handling and installation techniques ... variation in operating pressures (water hammer and surge) ... a strength-time allowance to give service life well beyond 50 years ... and, finally, the great unknown. Each of the factors was judged to reduce the 100,000 hour design strength by 5%-10% or 20% ... for a total of 100% ... or a design factor of 2:1. This is why polyethylene pipe, with a designated 100,000 hour strength of 1600 psi at 73.4°F, has a hydrostatic design strength of 800 psi hoop stress.

The design pressures for Driscopipe are determined by the following equation, adopted internationally by the industry for this purpose:

$$P = \frac{2S}{SDR-1} \times F \quad \text{or} \quad P = 2S\frac{t}{D-t} \times F$$

Where: D = Specified Outside Diameter, Inches
P = Design Pressure, psi
S = Long Term Hydrostatic Strength, psi, at the design temperature
t = Minimum Wall Thickness, Inches
F = Service Design Factor
SDR = Standard Dimension Ratio of D/t

The traditional Service Design Factor for water at standard temperature (73.4°F) is one-half (.5). The Service Design Factor for oil or liquid hydrocarbons is 0.25 @ 73°F. The service design factor may be adjusted by the design engineer to reflect the particular conditions anticipated for the application. The temperature selected for design should consider both internal and external conditions. The design temperature should be based on the temperature of the pipe itself. For practical purposes, it is safer to design to the highest temperature.

The design service factor for water may also be used for solutions of inorganic salts, alkaline fluids, non-oxidizing acids, low concentrations of oxidizing acids and many other solutions. See the discussion on chemical resistance for more information.

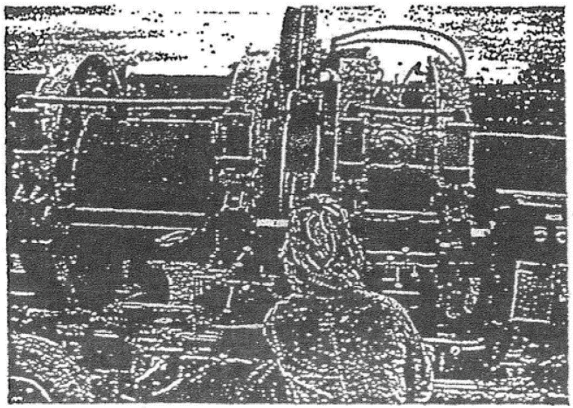

All standard design pressure ratings shown in Driscopipe literature are based on water at 73.4°F temperature; ie, a safety factor of 2:1 based on the long term hydrostatic strength of the material. Driscopipe is applicable at pressures from 0 to 265 psi and temperatures from below 32°F up to 180°F. Standard Dimension Ratios (SDR) are available from SDR 32.5 to SDR 7.0

Flow Characteristics

Driscopipe polyethylene has excellent flow characteristics as compared to traditional materials. An extremely smooth interior surface offers low resistance to flow. It maintains these excellent flow properties throughout its service life in most applications due to the inherent chemical and abrasion resistance of the material. Because of smooth walls and the non-wetting characteristic of polyethylene, higher flow capacity and less friction loss is possible with Driscopipe. In many cases this higher flow capacity may permit the use of smaller pipe at a lower cost.

A "C" factor of 155 is commonly used in the Hazen-Williams formula for calculating flow in pressure applications. For gravity flow, an "n" factor of .009 is used in Manning's formula.

Experimental test data regarding pumping and pressure drop through Driscopipe is available upon ~~request. This study compares the flow through 8"~~ Driscopipe with and without internal fusion beads using clear water. It also includes flow data for some clay-water slurries and clay-water-sand slurries. Velocities up to 20 fps are studied. Data includes determination of Hazen-Williams "C" factor, Reynolds number, boundry drag, relative roughness, sand grain roughness and friction loss at various velocities.

Lightweight – Flexible

The inherent light weight and flexibility of Driscopipe provides many cost saving benefits related to handling, storage, hauling, unloading, stringing, joining and installation. Because of its light weight, Driscopipe can be moved, handled and placed in the ditch with smaller and less expensive construction equipment. Usually, manpower requirements are also reduced.

Driscopipe weighs less than water; it has a specific gravity of .955-.957. Because it will float, it can be joined in long strings and easily towed into position on job sites where water is encountered. The combination of light weight and flexibility provides opportunity to fusion join the pipe in a convenient work area and pull it into position in difficult work areas where terrain or other obstacles present installation problems. The pipe can be joined above ground and rolled or lowered into the trench thus allowing the use of smaller trench widths and eliminating the necessity of placing men and equipment inside the trench. Such installation methods can dramatically reduce the time required for installation in many instances.

The flexibility of Driscopipe allows it to be curved over, under and around obstacles and to make elevation and directional changes, thus eliminating fittings and reducing installation costs. The pipe can be cold bent ~~as it is installed to a radius of 20-40 times the pipe~~ diameter. This flexibility and the butt fusion joining method make Driscopipe ideally suited for inserting it inside older piping systems to renew and renovate such systems at a much lower cost than would be possible otherwise.

Pipe flexibility and toughness also allow small diameter Driscopipe to be plowed-in or pulled-in with suitable equipment.

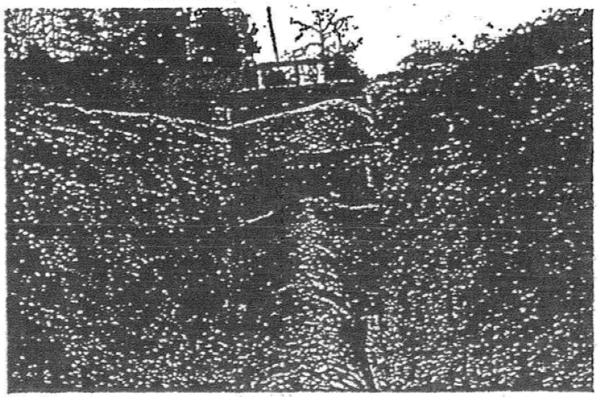

Toughness — "Ductile PE Pipe"

Overall "toughness" of Driscopipe is an important characteristic of the pipe which is derived from many of the chemical and physical properties of the material as well as the extrusion method. The pipe is ductile. It flexes, bends and absorbs impact loads over a wide temperature range of −180°F up to +180°F. This inherent resiliency and flexibility allow the pipe to absorb surge pressures, vibration and stresses caused by soil movement. Driscopipe can be deformed without permanent damage and with no adverse effect on long term service life. It is flexible for contouring to installation conditions. The toughness of Driscopipe is one of its outstanding engineering characteristics leading to innovative piping design.

Even though "toughness" has become generally recognized by the industry as a highly desirable characteristic ... there is no standard test which can be used to directly compare the "toughness" among polyethylenes ... as well as among the different plastic materials which are considered suitable for piping.

A "toughness" test has not been devised is simply because it is influenced by so many of the physical and chemical properties of the material. The extreme toughness of Driscopipe has been noted as one of its outstanding features since its introduction to the industry ... yet to explain "toughness", many properties are discussed and demonstrated. To obtain a complete evaluation of the toughness of a plastic material, it is necessary to see demonstrations of tests and to conduct some tests in person in order to compare it with materials which are more familiar, such as cast iron, steel, cement, copper, etc.

Toughness is related to ... Environmental Stress Crack Resistance (ESCR) ... Notch sensitivity ... Resistance to secondary stresses from external loading ... Impact strength ... Tear strength ... Flexibility ... Kink resistance ... Abrasion and scratch resistance ... Flexural strength ... Elongation ... Chemical resistance ... Tensile strength ... Ductility ... Creep resistance ... Temperature resistance ... Density ... Molecular weight ... and the thermoplastic nature of the material. Part of the toughness of any polyethylene material can be attributed to its flexibility, flexural strength and impact resistance as compared to the more rigid thermoplastic materials such as PVC. Polyethylene is ductile and will elongate many times more than PVC. Consequently, it will absorb more impact without damage or failure. PE will flex or elongate and stress relieve itself rather than rupture. Generally, impact strength is greater for the higher molecular weight PE resins. Impact resistance is also important from the standpoint of a piping system being able to absorb energy imposed on it by external forces.

The expansive force of water freezing inside Driscopipe will not damage it.

ESCR is one of the properties closely related to "toughness" and has been studied as a possible means to define and measure toughness. The exceptional resistance of Driscopipe 8600 to environmental stress cracking as compared to other PE materials is discussed further in the next section.

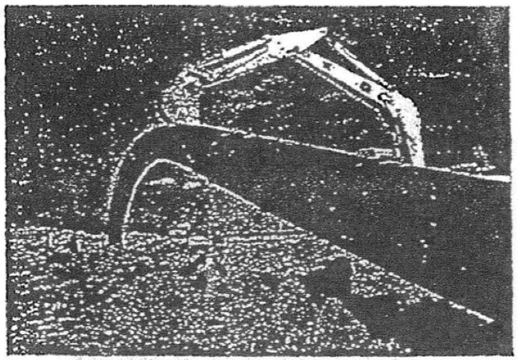

Driscopipe 8600 is unique and differs from Driscopipe 1000 and from all other polyethylene pipes. Driscopipe 8600 exhibits a superior toughness which gives the pipe the highest impact strength, highest tear strength and lowest notch sensitivity of any polyethylene pipe currently available. Driscopipe 8600 offers the highest resistance to cuts, scratches and abrasions which occur when handling and installing the pipe.

These properties are maintained throughout its temperature range without a loss of ductility or reduced resistance to notch sensitivity. Driscopipe has been successfully installed in numerous arctic applications. Some of these applications have included direct burial in the unstable arctic permafrost.

To learn more of the relative toughness of Driscopipe 8600, we encourage you to take a piece of pipe with a butt fusion joint and try to tear it up without using sharp tools. Pound it flat with a sledge hammer ... slam it against a corner of angle iron ... run over it with a truck ... then do the same with steel, copper, PVC, cast iron and the less rugged PEs. It's not very scientific ... but we believe you'll be convinced that Driscopipe 8600 has extremely high toughness. We have evaluated Driscopipe many times in laboratory and field test experiments to demonstrate and prove this toughness.

- One excellent indicator of the relative toughness of Driscopipe 8600, as compared to other polyethylene pipe materials, can be observed in the ASTM Standard Test for determination of flow rate of the thermoplastic materials.

  When Driscopipe 8600 is heated to 190°C (374°F) to measure the flow rate, it requires 432.5 pounds/sq. in. force, applied for 10 minutes, to flow 1½ grams of 8600 material through the orifice of the test unit! Other commercially available polyethylene pipe materials will flow 10 to 20 times this amount under the same conditions.
- When Driscopipe 8600 is heated to 475-500°F to melt it for fusion joining, it requires 150 pounds pressure per square inch of material to make the melted surfaces flow together. This is another indicator of toughness. Other commercially available polyethylene pipe materials require about one-half that amount of pressure and some competitive pipes require less than 25 psi!
- Driscopipe 8600 has been pressure tested for long periods at temperatures up to 140°F and performance requirements at these high temperatures can be used in purchase specifications to assure that the user is getting the highest performing polyethylene pipe.

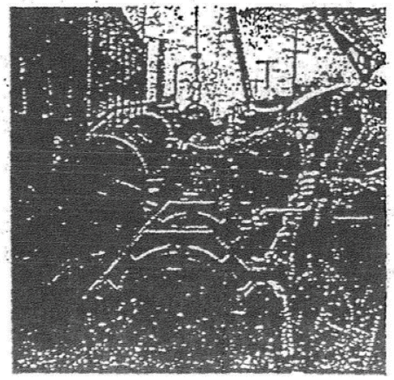

Environmental Stress Crack Resistance

The most recent ASTM specification written to identify polyethylene plastic pipe and fittings materials is ASTM D 3350, "Polyethylene Plastics Pipe and Fittings Materials", adopted in 1974. This specification uses six (6) properties to classify PE material ... one of these is ESCR.

ASTM D 3350 lists three cell limits for ESCR classification which use the ESCR test outlined in ASTM D 1693, Test Method for Environmental Stress Cracking of Ethylene Plastics. The cell limits are:

Cell Classification Limit	Test Condition ASTM D 1693	Test Duration Hours	Percent of Failures Allowed	Test Temp. °C
1	A	48	50	50°
2	B	24	50	50°
3	C	192	20	100°

Minimum Notch for A is .020"; for B and C is .012". Minimum Thickness for A is .120"; for B and C is .070". A and B use a diluted aqueous solution reagent, C uses full strength reagent.

This method of testing for ESCR was first written in 1959 and was developed primarily to evaluate polyethylene as a jacketing material for power and communications cable. Although the method requires the use of laboratory compression molded specimens rather than pipe, it became the generally accepted method for evaluating ESCR of PE materials used for piping. Its wide use was responsible for its inclusion in ASTM D 3550 to describe one of the six primary properties of a PE pipe material.

The test method, ASTM D-1693, is an accelerated test method to determine the resistance of a polyethylene material to environmental stress cracking. It is a measure of the ability of the polyethylene to withstand secondary stress loadings. These loadings are typically thought of as low-level, long-term, external stresses which may act upon the polyethylene pipe in field installations.

Under conditions of the test, high local multiaxial stresses are developed through the introduction of a controlled imperfection (notch). The notched sample is subjected to an elevated temperature bath of a surface active agent. Environmental stress cracking has been found to occur most readily under such conditions.

A note in the test specifications states that, generally, low density (Type I) polyethylenes are tested under Condition A, medium and high density (Type II and Type III) polyethylenes are generally tested under Condition B and high density resins with high melt viscosity, such as pipe grade P34, are tested under Condition C.

As pipe grade polyethylenes have improved, the testing requirements of ASTM D-1693 have become less stringent for P34 pipe grade polyethylenes such as Driscopipe 8600 and Driscopipe 1000. As a result, a more severe stress crack resistance test has been developed to evaluate high density polyethylene pipe. The ASTM F-1248 stress crack resistance test method was developed by a gas distribution company for quality control purposes and is often referred to as Ring ESCR since it tests actual produced pipe ring samples rather than molded specimens.

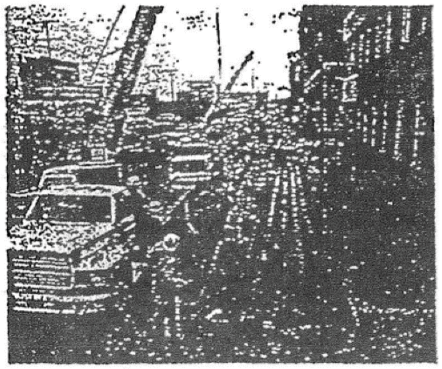

ASTM F-1248 utilizes rings cut from a pipe sample. The rings are notched on one side and compressed between parallel plates until the distance between the plates is three times the specified pipe minimum wall thickness. The compressed ring samples are subjected to an elevated temperature bath of a surface active agent and visibly inspected for crack formation or propagation.

The Ring ESCR test provides useful information regarding the different polyethylene pipe grade materials. Driscopipe 8600 shows no tendency for sample failures when tested in excess of 10,000 hours. This further reinforces the unique ability of Driscopipe 8600 to provide the highest degree of resistance to the external stresses inherent to a pipeline installation.

Driscopipe 1000, an extra high molecular weight HDPE pipe, will exhibit a ring ESCR of $F_{50} > 1000$ hours. Other lower molecular weight pipes may exhibit lower F_{50} values.

Chemical Corrosion Resistance

The outstanding resistance of Driscopipe to attack by most chemicals makes it suitable to transport these chemicals or to be installed in an environment where these chemicals are present. Factors which determine the suitability and service life of each particular application include the specific chemical and its concentration, pressure, temperature, period of contact and service conditions which may introduce stress concentrations in the pipe or fittings.

Driscopipe is, for all practical purposes, chemically inert within its temperature use range. This advantageous engineering characteristic is one of the primary reasons for the wide use of Driscopipe in industrial applications. It does not rot, rust, pit, corrode or lose wall thickness through chemical or electrical reaction with the surrounding soil, whether acid, alkaline, wet or dry. It neither supports the growth of, nor is affected by, algae, bacteria or fungi and is resistant to marine biological attack. It contains no ingredients which make it attractive to rodents, gophers, etc.

Information relative to the resistance of Driscopipe to a wide range of chemicals is shown in the following tables. This information is based on results of immersion tests (usually 3 months) at various temperatures. Changes in tensile strength and elongation are evaluated at a rapid strain rate to emphasize any strength decay in the material.

Most acids, bases and other chemicals can be transported by Driscopipe using the same design parameters as would apply to water, natural or manufactured gas and water solutions of inorganic salts. Strong oxidizing agents such as fuming sulfuric acid may adversely affect the pipe, depending upon concentration, temperature and period of contact. In many cases, such as gravity flow waste lines, these chemicals can be handled because of dilution and intermittent flow.

Some chemicals, such as all types of liquid hydrocarbons, will mechanically absorb into the wall of the pipe and cause a reduction in hoop stress but this does not degrade the material. This effect is temporary if exposure is intermittent. Where exposure is continuous, it is necessary to derate the pressure capability of the pipe for long term service. This includes such products as gasoline, ethyl alcohol, benzene, carbon tetrachloride, crude and refined oils, etc. Where 5-100% hydrocarbon liquids are continuously present in a pressure system, a service design factor of .25 should be used to calculate design pressures instead of the service design factor of .5 used with water.

$$P = \frac{2S}{SDR-1} \times F \quad \text{or} \quad P = 2S\frac{t}{D-t} \times F$$

Where: D = Outside Diameter, Inches
P = Design Pressure, psi
S = Long Term Hydrostatic Strength, psi, at the design temperature
t = Minimum Wall Thickness, Inches
F = Service Design Factor
SDR = Standard Dimension Ratio of D/t

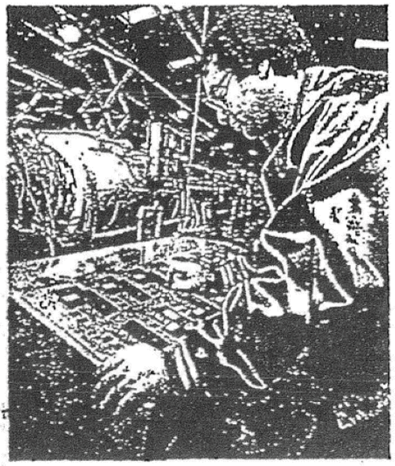

CHEMICAL RESISTANCE OF DRISCOPIPE

S – Satisfactory
U – Unsatisfactory
M – Marginal
N – Not known

All concentrations are 100% unless noted otherwise.

On reagents marked marginal, chemical attack will be recognized by a loss of physical properties of the pipe which may require a change in design factors.

Reagent	70°F (21°C)	140°F (60°C)
Acetic Acid 1-10%	S	S
Acetic Acid 10-60%	S	M
Acetic Acid 80-100%	S	M
Acetone	M	U
Acrylic Emulsions	S	S
Aluminum Chloride-Dilute	S	S
Aluminum Chloride Conc.	S	S
Aluminum Fluoride Conc.	S	S
Aluminum Sulfate Conc.	S	S
ums (All Types) Conc.	S	S
Ammonia 100% Dry Gas	S	S
Ammonium Carbonate	S	S
Ammonium Chloride Sat'd	S	S
Ammonium Fluoride 20%	S	S
Ammonium Hydroxide 0.88 S.G.	S	S
Ammonium Metaphosphate Sat'd	S	S
Ammonium Nitrate Sat'd	S	S
Ammonium Persulfate Sat'd	S	S
Ammonium Sulfate Sat'd	S	S
Ammonium Sulfide Sat'd	S	S
Ammonium Thiocyanate Sat'd	S	S
Amyl Acetate	M	U
Amyl Alcohol 100%	S	S
Amyl Chloride 100%	N	U
Aniline 100%	S	N
Antimony Chloride	S	S
Aqua Regia	U	U
Barium Carbonate Sat'd	S	S
Barium Chloride	S	S
Barium Hydroxide	S	S
Barium Sulfate Sat'd	S	S
Barium Sulfide Sat'd	S	S
Beer	S	S
Benzene	M	U
Benzene Sulfonic Acid	S	S
Bismuth Carbonate Sat'd	S	S
leach Lye 10%	S	S
Black Liquor	S	S
Borax Cold Sat'd	S	S
Boric Acid Dilute	S	S

Reagent	70°F (21°C)	140°F (60°C)
Boric Acid Conc.	S	S
Bromic Acid 10%	S	S
Bromine Liquid 100%	M	U
Butanediol 10%	S	S
Butanediol 60%	S	S
Butanediol 100%	S	S
Butyl Alcohol 100%	S	S
Calcium Bisulfide	S	S
Calcium Carbonate Sat'd	S	S
Calcium Chlorate Sat'd	S	S
Calcium Chloride Sat'd	S	S
Calcium Hydroxide	S	S
Calcium Hypochlorite BL'GH Sol.	S	S
Calcium Nitrate 50%	S	S
Calcium Sulfate	S	S
Camphor Oil	N	U
Carbon Dioxide 100% Dry	S	S
Carbon Dioxide 100% Wet	S	S
Carbon Dioxide Cold Sat'd	S	S
Carbon Disulfide	N	U
Carbon Monoxide	S	S
Carbon Tetrachloride	M	U
Carbonic Acid	S	S
Castor Oil Conc.	S	S
Chlorine Dry Gas 100%	S	M
Chlorine Moist Gas	M	U
Chlorine Liquid	M	U
Chlorobenzene	M	U
Chloroform	M	U
Chlorosulfonic Acid 100%	M	U
Chrome Alum Sat'd	S	S
Chromic Acid 20%	S	S
Chromic Acid Up to 50%	S	S
Chromic Acid and Sulfuric Acid	S	M
Cider	S	S
Citric Acid Sat'd	S	S
Coconut Oil Alcohols	S	S
Cola Concentrates	S	S
Copper Chloride Sat'd	S	S
Copper Cyanide Sat'd	S	S
Copper Fluoride 2%	S	S
Copper Nitrate Sat'd	S	S
Copper Sulfate Dilute	S	S
Copper Sulfate Sat'd	S	S
Cottonseed Oil	S	S
Crude Oil*	S	M
Cuprous Chloride Sat'd	S	S
Cychohexanol	S	S
Cyclohexanone	M	U
Detergents Synthetic	S	S
Developers, Photographic	S	S
Dextrin Sat'd	S	S
Dextrose Sat'd	S	S
Dibutylphthalate	S	M
Disodium Phosphate	S	S

Reagent	70°F (21°C)	140°F (60°C)
Diazo Salts	S	S
Diethylene Glycol	S	S
Diglycolic Acid	S	S
Dimethylamine	M	U
Emulsions, Photographic	S	S
Ethyl Acetate 100%	M	U
Ethyl Alcohol 100%	S	S
Ethyl Alcohol 35%	S	S
Ethyl Butyrate	M	U
Ethyl Chloride	M	U
Ethyl Ether	U	U
Ethylene Chloride	U	U
Ethylene Chlorohydrin	U	U
Ethylene Dichloride	M	U
Ethylene Glycol	S	S
Ferric Chloride Sat'd	S	S
Ferric Nitrate Sat'd	S	S
Ferrous Chloride Sat'd	S	S
Ferrous Sulfate	S	S
Fish Solubles	S	S
Fluoboric Acid	S	S
Fluorine	S	U
Fluosilicic Acid 32%	S	S
Fluosilicic Acid Conc.	S	S
Formaldehyde 40%	S	N
Formic Acid 0-20%	S	S
Formic Acid 20-50%	S	S
Formic Acid 100%	S	S
Fructose Sat'd	S	S
Fruit Pulp	S	S
Fuel Oil	S	U
Furfural 100%	M	U
Furfuryl Alcohol	M	U
Gallic Acid Sat'd	S	S
Gas Liquids*	S	M
Gasoline*	M	U
Gin	S	U
Glucose	S	S
Glycerine	S	S
Glycol	S	S
Glycolic Acid 30%	S	S
Grape Sugar Sat'd Aq.	S	S
Hexanol, Tert.	S	S
Hydrobromic Acid 50%	S	S
Hydrocyanic Acid Sat'd	S	S
Hydrochloric Acid 10%	S	S
Hydrochloric Acid 30%	S	S
Hydrochloric Acid 35%	S	S
Hydrochloric Acid Conc.	S	S
Hydrofluoric Acid 40%	S	S
Hydrofluoric Acid 60%	S	S
Hydrofluoric Acid 75%	S	S
Hydrogen 100%	S	S
Hydrogen Bromide 10%	S	S
Hydrogen Chloride Gas Dry	S	S

---

*HDPE Resin Service Design Factor for hydrocarbons per the formula on page 3 and 8 is F = 0.25 to compensate for hydrocarbon saturation effects on long term hydrostatic strength.

continued on page 10

continued from page 9

CHEMICAL RESISTANCE OF DRISCOPIPE

Reagent	70°F (21°C)	140°F (60°C)
Hydrogen Peroxide 30%	S	S
Hydrogen Peroxide 90%	S	M
Hydrogen Phosphide 100%	S	S
Hydroquinone	S	S
Hydrogen Sulfide	S	S
Hypochlorus Acid Conc.	S	S
Inks	S	S
Iodine (Alc. Sol.) Conc.	S	U
Lactic Acid 10%	S	S
Lactic Acid 90%	S	S
Latex	S	S
Lead Acetate Sat'd	S	S
Lube Oil*	S	M
Magnesium Carbonate Sat'd	S	S
Magnesium Chloride Sat'd	S	S
Magnesium Hydroxide Sat'd	S	S
Magnesium Nitrate Sat'd	S	S
Magnesium Sulfate Sat'd	S	S
Mercuric Chloride Sat'd	S	S
Mercuric Cyanide Sat'd	S	S
Mercurous Nitrate Sat'd	S	S
Mercury	S	S
Methyl Alcohol 100%	S	S
Methyl Bromide	M	U
Methyl Chloride	M	U
Methyl Ethyl Ketone 100%	M	U
Methylsulfuric Acid	S	S
Methylene Chloride 100%	M	U
Milk	S	S
Mineral Oils	S	U
Molasses Comm.	S	S
Nickel Chloride Sat'd	S	S
Nickel Nitrate Conc.	S	S
Nickel Sulfate Sat'd	S	S
Nicotine Dilute	S	S
Nicotinic Acid	S	S
Nitric Acid 0-30%	S	S
Nitric Acid 30-50%	S	M
Nitric Acid 70%	S	M
Nitric Acid 95-98%	U	U
Nitrobenzene 100%	U	U
Octyl Cresol	S	U
Oils and Fats*	S	M
Oleic Acid Conc.	S	U
Oleum Conc.	U	U
Orange Extract	S	S
Oxalic Acid Dilute	S	S
Oxalic Acid Sat'd	S	S
Ozone 100%	S	U
Perchloric Acid 10%	S	S
Petroleum Ether	U	U
Phenol 90%	U	U
Phosphoric Acid Up to 30%	S	S
Phosphoric Acid Over 30%	S	S
Phosphoric Acid 90%	S	S
Phosphorous (Yellow) 100%	S	N
Phosphorus Pentoxide 100%	S	N
Photographic Solutions	S	S
Pickling Baths		
Sulfuric Acid	S	S
Hydrochloric Acid	S	S
Sulfuric-Nitric	S	U
Plating Solutions		
Brass	S	S
Cadmium	S	S
Chromium	N	N
Copper	S	S
Gold	S	S
Indium	S	S
Lead	S	S
Nickel	S	S
Rhodium	S	S
Silver	S	S
Tin	S	S
Zinc	S	S
Potassium Bicarbonate Sat'd	S	S
Potassium Borate 1%	S	S
Potassium Bromate 10%	S	S
Potassium Bromide Sat'd	S	S
Potassium Carbonate	S	S
Potassium Chlorate Sat'd	S	S
Potassium Chloride Sat'd	S	S
Potassium Chromate 40%	S	S
Potassium Cyanide Sat'd	S	S
Potassium Dichromate 40%	S	S
Potassium Ferri/ Ferro Cyanide Sat'd	S	S
Potassium Fluoride	S	S
Potassium Hydroxide 20%	S	S
Potassium Hydroxide Conc.	S	S
Potassium Nitrate Sat'd	S	S
Potassium Perborate Sat'd	S	S
Potassium Perchlorate 10%	S	S
Potassium Sulfate Conc.	S	S
Potassium Sulfide Conc.	S	S
Potassium Sulfite Conc.	S	S
Potassium Persulfate Sat'd	S	S
Propargyl Alcohol	S	S
Propyl Alcohol	S	S
Propylene Dichloride 100%	U	U
Propylene Glycol	S	S
Rayon Coagulating Bath	S	S
Sea Water	S	S
Selenic Acid	S	S
Shortening	S	S
Silicic Acid	S	S
Silver Nitrate Sol.	S	S
Soap Solution Any Conc'n	S	S
Sodium Acetate Sat'd	S	S
Sodium Benzoate 35%	S	S
Sodium Bicarbonate Sat'd	S	S
Sodium Bisulfate Sat'd	S	S
Sodium Bisulfite Sat'd	S	S
Sodium Borate	S	S
Sodium Bromide Dilute Sol.	S	S
Sodium Carbonate Con.	S	S
Sodium Carbonate	S	S
Sodium Chlorate Sat'd.	S	S
Sodium Chloride Sat'd	S	S
Sodium Cyanide	S	S
Sodium Dichromate Sat'd	S	S
Sodium Ferricyanide	S	S
Sodium Ferrocyanide Sat'd	S	S
Sodium Fluoride Sat'd	S	S
Sodium Hydroxide Conc.	S	S
Sodium Hypochlorite	S	S
Sodium Nitrate	S	S
Sodium Sulfate	S	S
Sodium Sulfide 25%	S	S
Sodium Sulfide Sat'd Sol.	S	S
Sodium Sulfite Sat'd	S	S
Stannous Chloride Sat'd	S	S
Stannic Chloride Sat'd	S	S
Starch Solution Sat'd	S	S
Stearic Acid 100%	S	S
Sulfuric Acid 0-50%	S	S
Sulfuric Acid 70%	S	M
Sulfuric Acid 80%	S	U
Sulfuric Acid 96%	M	U
Sulfuric Acid 98%	M	U
Sulfuric Acid, Fuming	U	U
Sulfurous Acid	S	S
Tallow*	S	M
Tannic Acid 10%	S	S
Tanning Extracts Comm.	S	S
Tartaric Acid Sat'd	N	N
Tetrahydrofurane	N	U
Titanium Tetrachloride Sat'd	N	U
Toluene	M	U
Transformer Oil	S	M
Trisodium Phosphate Sat'd	S	S
Trichloroethylene	U	U
Urea Up to 30%	S	S
Urine	S	S
Vinegar Comm.	S	S
Vanilla Extract	S	S
Wetting Agents	S	S
Whiskey	S	N
Wines	S	S
Xylene	M	U
Yeast	S	S
Zinc Chloride Sat'd	S	S
Zinc Sulfate Sat'd	S	S

For additional chemical resistance listings, consult the P.P.I. technical report #TR 19/10-84, Table I and the ISO technical report #ISO/Data 8-1979, Tables I, II, III.

Temperature Characteristics

nce polyethylene is a thermoplastic material, many of its physical and chemical properties are dependent on temperature and will change as the temperature of the material is increased or decreased. However, the exposure of Driscopipe to temperature variations within the recommended operating range does not result in degradation of the material. As these temperature changes are reversed, the material properties also reverse to their original values.

You will note from the information on physical properties that Driscopipe has a brittleness temperature below −180°F and a softening temperature of +257°F. The recommended operating temperature is limited only on the higher temperature side to a range of 140-180°F, dependent upon the pressure of the application and other operating and installation considerations. On the lower temperature side, Driscopipe gains strength without becoming brittle and is ideal for use at sub-zero temperatures.

Driscopipe becomes molten at 400-500°F and temperatures in this range are used to fusion join the piping system. Pipe is extruded at about the same temperature. To protect the material against degradation at the higher temperature, it is chemically stabilized. This stabilizer protects the material against thermal degradation which might otherwise occur during manufacture, outside storage and installation.

Driscopipe has been tested for thousands of hours at elevated temperatures of 140°F and 180°F without thermal degradation. These long term pressure tests at the higher temperatures are used to obtain recommended design strengths for the pipe at these temperatures.

Since all thermoplastic piping materials are affected by temperature, it is a general practice to characterize these materials at ambient temperature of 23°C (73.4°F). Nearly all ASTM tests relating to physical, mechanical and chemical properties of thermoplastic materials are conducted at this temperature. If a test is conducted, or a property defined, at other than 73.4°F, it is always noted.

One example of the effect of temperature on Driscopipe is the change in long term strength of the material as shown on the stress-life curves. This type behavior is true for all thermoplastics but there are large differences between the performance of specific materials at the higher temperatures.

Knowledge of the long term strength of Driscopipe at the various temperatures allows selective design of a system. Accurate interpolations can be made for other temperatures between those which are known when data at three or more temperature levels is available.

Other properties of thermoplastic pipe which change with temperature and can affect system design and installation procedures include the following.

Burst strength – Short term (1 minute) burst tests on Driscopipe at various temperatures show these typical hoop stress values:

Temperature, °F	Hoop Stress, psi
73.4°	3250
32°	4300
0°	5290
−20°	5670
−40°	6385

Driscopipe will quick-burst at a pressure approximately four times greater than the rated operating pressure.

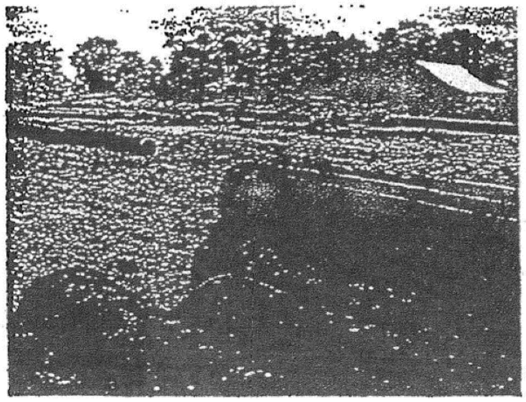

Chemical Resistance – The ability of most thermoplastics to resist degradation in the presence of corrosive chemicals is reduced as temperature increases. This is also true for Driscopipe but to a lesser extent because of its high density and high molecular weight. The effect of temperature on Driscopipe in the presence of various chemicals is shown in the chemical resistance tables.

Flexibility – As temperature is decreased, the flexibility of Driscopipe is also decreased. This has very little effect on installation except that at the lower winter temperatures, coiled pipe becomes more difficult, mechanically, to uncoil and stretch out in the ditch. Although Driscopipe becomes stiffer at low temperature, it can be bent, uncoiled or plowed in with sufficient mechanical power and no damage will occur to the pipe because of bending it at cold temperatures.

Other Physical Properties – There is a slight change with temperature of impact strength, notch sensitivity, flexural modulus, hardness and elongation ... but none are of such extent as to affect design parameters or installation procedures over the normal range of temperatures.

Modulus of Elasticity – Typical values for the variance in modulus of elasticity with temperature change is shown below.

Temperature °F	Modulus of Elasticity, psi
−20°	300,000
0°	260,000
32°	200,000
75°	130,000
100°	105,000
140°	60,000

Thermal Expansion and Contraction – Polyethylene, like other thermoplastics, has a coefficient of expansion higher than metals. This coefficient is usually determined by a standard test method which employs the use of molded specimens. Measurements are made with a quartz dilatometer while the test specimen is held at elevated temperature. Typical coefficient values by this method range from $.75 \times 10^{-4}$ for Driscopipe 8600 to $.83 \times 10^{-4}$ for Driscopipe 1000.

The coefficient of linear expansion may also be determined by measuring the change in length of unrestrained pipe samples at different temperatures. The calculated coefficient is somewhat higher on extruded pipe than on molded test specimens. This appears to be true for all polyethylene pipe. The average coefficient calculated from measurements made on Driscopipe in the temperature range 0°F to 140°F is 1.2×10^{-4} in/in/°F.

The circumferential coefficient of expansion and contraction for Driscopipe is approximately $.6 \times 10^{-4}$ in/in/°F in the range of 0° to 140°F ... or about ½ the linear coefficient. This circumferential change with temperature rarely presents any problems in system design. There may be need to consider this factor if compression fittings are used.

The expansion or contraction for Driscopipe can be stated in an easy rule of thumb ... the pipe will expand or contract approximately 1.4" per 100 feet for each 10°F change in temperature. Thus a 1000 foot unrestrained line which undergoes a 20°F increase in temperature change will increase in length 28 inches. The relatively large amount of expansion and contraction of plastic pipe generally presents no real problems in installation. The pipe has a relatively low elastic modulus and consequently there is less stress build-up. These stresses, caused by temperature change, are easily dissipated due to the thermoplastic nature of the material which relaxes and adjusts with time.

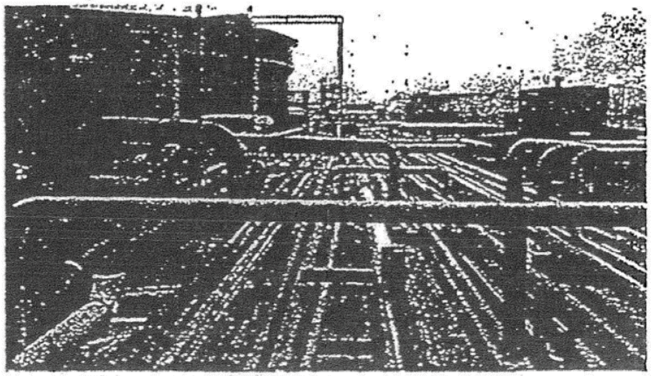

Tests have been conducted wherein the temperature re than 100 feet of unrestrained pipe was nged 130°F in a period of a few minutes. The total force created by contraction was measured and proved to be about (½) one-half the theoretical calculated value. Thermoplastic materials are unique in their ability to stress-relieve themselves. Actual changes in temperature in most applications take place slowly over an extended period of time. The total stresses imposed will vary but are generally much lower than the calculated values.

Direct buried pipe will generally have ample soil friction and interference to restrain movement of the pipe under normal application temperature changes. It is a good idea to make the final tie-ins on a system at a temperature which is as close to operating temperature as possible. This is particularly true for insert liner systems where there is no soil restraint.

Normal good direct burial installation practices which include snaking the pipe in the ditch, proper backfill and compaction, making the tie-in at the proper temperature, etc. should be used at all times and will substantially reduce the possibility of pull out at tie-in connections on such installations. However, planning the transition tie-in becomes more important when Driscopipe is used for insert renewal inside another pipe because there is no restraint from earth loading. contraction of the pipe due to reduction in perature is freely transmitted to the transition onnection and may result in pull-out if proper design precautions are not taken. In those cases, it may be necessary to provide additional anchoring at the terminations of the insert liner. Concrete anchors poured into undisturbed soil and cast around anchor projections in the Driscopipe line will restrict movement at the end of the line. Anchor projections on the Driscopipe liner can be made by fusing a blind tee into the line or by the use of two reducers, to the next larger size of pipe, fused together in the line.

Thermal Conductivity – This property of Driscopipe is lower than that for metals and can sometimes be exploited in the design of the system. It may eliminate or reduce the need for insulating pipe which carries water or other fluids through freezing temperatures. Thermal Conductivity of Driscopipe is 2.7 BTU per hour per sq. ft. per °F per inch of thickness. The slow heat transfer inhibits freezing and, if normal burial precautions are used, accidental freezing is usually eliminated. If the pipe does freeze, it does not fracture but fluid flow will be stopped. It will resume its function upon thawing. Direct application of intense heat should not be used to thaw a line. Antifreeze compounds such as methanol, isoproponol and ethylene glycol can be used without detrimental effect on the pipe.

Ignition Temperatures – The flash point for high density polyethylene using the Cleveland open cup method (ASTM D92) is 430°F. The flash ignition and self ignition temperatures using ASTM D1929 are 645°F and 660°F.

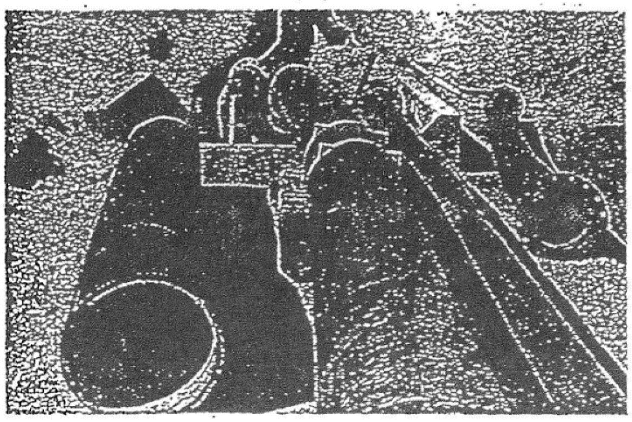

Weatherability

Two principal factors influence the weathering of plastic pipe in outside above ground applications ... temperature changes caused by seasonal variations and solar heating and solar radiation of ultraviolet rays. Effects of temperature variations on Driscopipe were discussed in the preceding section. Expansion and contraction of a line above ground, due to differential heating, will cause the line to move laterally, particularly if it is empty. This movement can easily be controlled within desired limits through the use of restraints.

Driscopipe is also protected against degradation caused by ultraviolet rays when exposed to direct sunlight. The material contains 2½% of finely divided carbon black which also accounts for the black color of Driscopipe. Carbon black is the most effective single additive capable of enhancing the weathering characteristic of plastic materials. The protection even relatively low levels of carbon black impart to the plastic is so great that it is not necessary to use other light stabilizers or UV absorbers.

Weatherability tests indicate that Driscopipe can be safely used outside in most climates for periods of many years without danger of loss of physical properties due to UV exposure. Phillips has done extensive testing of polyethylene compounds containing 2 to 3% carbon black and compared these to other UV stabilizers to determine their effectiveness for protection against UV degradation in outdoor exposure. Samples were aged in outdoor exposure in three geographical locations: Phoenix, Arizona, Bartlesville, Oklahoma (Phillips 66 headquarters) and Akron, Ohio. From these actual tests, it was determined that one year exposure in Arizona was equivalent to at least two years in Bartlesville and greater than three and one-half years in Akron.

Weather-Ometer tests were run under standard conditions as set out in ASTM D 1499-64 and compared with the actual test samples in the three locations described above. From this test work, it was determined, conservatively, that 5000 hours (approximately 7 months) in the Weather-Ometer compares to greater than 42 months exposure in Arizona. Samples containing 2 to 3% carbon black and thermal stabilizers as used in Driscopipe have been tested for greater than 25,000 hours (2.85 years) in the Weather-Ometer without any brittleness or loss of physical properties. This is equivalent to over 17 years in Arizona and over 60 years in Akron, Ohio.

Permeability

The permeability of gases, vapors or liquids through a plastic membrane is generally considered to be an activated diffusion process. That is, the gas, vapor or liquid dissolves in the membrane and then diffuses to a position of lower concentration. The permeation rate is determined by the functional groups of the permeating molecules and by the density of the plastic ... the higher the density, the lower the permeability. Listed below are typical permeability rates for HDPE.

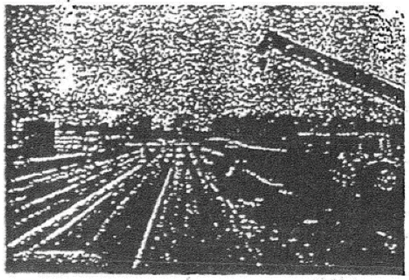

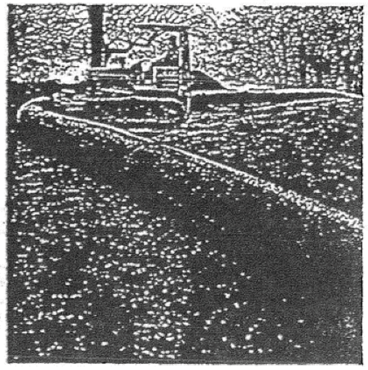

	Permeability Rate*
Carbon Dioxide	345
Hydrogen	321
Oxygen	111
Helium	247
Ethane	236
Natural Gas	113
Freon 12	95
Nitrogen	53

*Cubic centimeters per day per 100 sq. inches per mil thickness at atmospheric pressure differential.

These permeation rates are considered very low. They result in negligible loss of product and create no hazard. For example, polyethylene piping systems are the predominant material used to construct new gas distribution systems and to renew old deteriorated systems. The permeation rate will vary in direct proportion to the differential pressure applied.

If the internal operating pressure is 60 psi, for example, the permeability rate would be approximately 4 times that shown above but volume losses would still be extremely low. Calculated volume loss in one mile of SDR 11 pipe (any size) in one day, for natural gas, would be ¼ of one cubic foot. At 120 psi, it would be ½ cubic foot per day.

Abrasion Resistance

One of the many outstanding characteristics of Driscopipe polyethylene is its resistance to abrasion. The inherent resilience and toughness of Driscopipe allows the mining industry to use this pipe in numerous surface applications where more conventional materials would be unsatisfactory, either because of the terrain encountered or the abrasiveness of the slurry to be moved. Quite often, a Driscopipe system offers substantial economic advantage as a means of transport over more conventional transportation methods used in the mining industry. Some of the more common applications include tailings lines and the transport of gypsum, limestone, sand, slimes and coal.

Due to its unique toughness, as indicated by low melt flow values, Driscopipe 8600 provides improved abrasion resistance over all other polyethylene piping materials. Controlled pipe loop pumping tests have demonstrated that Driscopipe can outlast steel pipe by as much as 4 to 1. One such test, performed by Williams Brothers Engineering, Tulsa, Oklahoma, compared Driscopipe to steel in pumping a coarse particle size magnetite iron ore slurry. At 13½ ft/sec velocity, Driscopipe was better by a factor of 4:1 and at 17 ft/sec by a factor of 3:1.

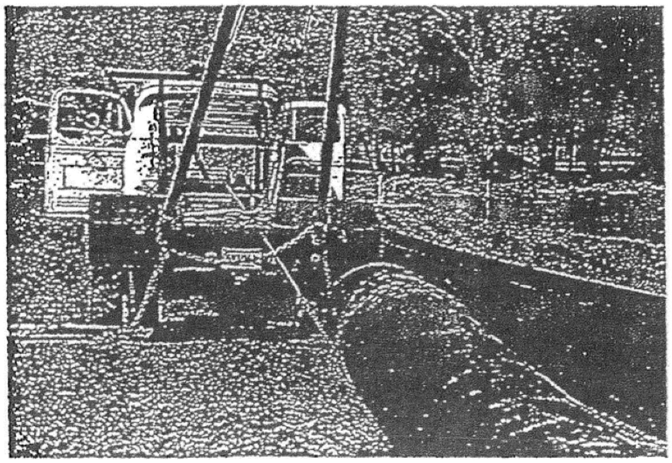

Heat Fusion Joining

The heat fusion joining technique has a long history of use for joining polyethylene pipe materials. The heat fusion method of joining PE pipe began shortly after the first commercial production of high density polyethylene in the early 1950s ... both developed by Phillips 66.

The integrity and superiority of heat fusion are now recognized universally. The modern day heat fusion joint is the same joint made in 1956 ... only the fusion equipment has evolved to gain efficiency, reliability and convenience. The principles learned on early equipment for making a successful joint are still in use today. Phillips designed, developed and built many models of heat fusion equipment from 1956 until the early 1970s. Since that time, Phillips has guided this development by others. The extensive line of high quality, efficient fusion equipment offered by McElroy Manufacturing, Inc., Tulsa, Oklahoma is one of the results of this long history of development. Phillips pioneered the idea and development of heat fusion and has used it exclusively in every high density polyethylene piping system sold by Phillips since 1956. There are millions of these joints in service today. In fact, 92% of all natural gas distribution pipe to homes, farms and factories is installed with polyethylene pipe and fittings. Heat fusion joints are industry accepted and field proven.

The heat fusion joining system has been so successful that it is the "standard" joining system for polyethylene. There are many reasons ... here are some.

Heat fusion joining ideally meets the requirements for a fast joining method to facilitate all phases of construction work in a safe and reliable manner.

The heat fusion joint is structurally superior to the socket fusion joint by configuration and, therefore, better meets the requirements of service. The heat joint configuration allows it to better disperse stresses initiated by pipe deflection and external loading. Stress concentration is minimized when the joint is placed in a strain and the joint is more "forgiving" when ground settlement occurs. In a socket joint, there is an extremely high ratio of "joint wall" to "pipe wall", resulting in stress intensification from external loading.

The Driscopipe heat fusion joining system is a simple, visual procedure with straight forward instructions. No "timing cycles" are necessary. The visual procedure allows the operator to concentrate on his work rather than a clock. Visually, he knows when the pipe ends have melted to the degree required to fuse them together. Visually, he observes and controls fusion pressure by observing the amount and configuration of the fusion bead as it is formed.

In the course of this work, the fusion operator is faced with a wide variety of job conditions. Changes in air temperature, material temperature, wind velocity, sun exposure, humidity, as well as condition of the terrain and the equipment all influence the joining requirements. Quality work under field conditions is more consistent with a simple, straight-forward, visual procedure.

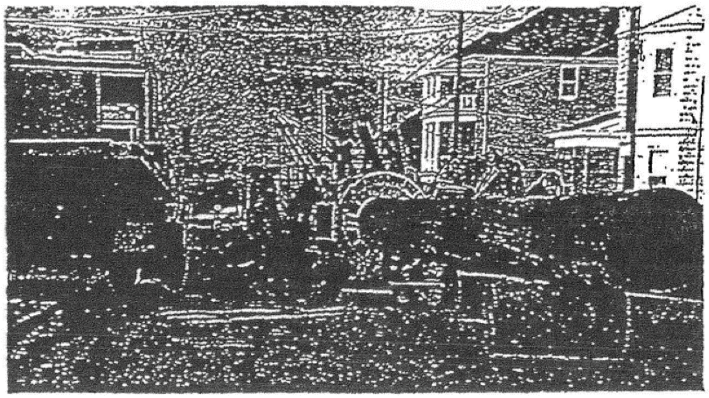

One heat fusion operator, with equipment, typically he whole operation himself, sometimes using a und person as a helper. Pipe tolerances, ovality and curvature are no problem and "melt" is easily controlled by the visual procedure.

Heat fusion joints offer a large advantage over socket coupled joints for plow-in installation and for insert renewal applications. Socket coupled pipe requires larger size plow chutes and bore holes. Heat fused pipe one size larger can usually be handled and installed through bore holes and plow chutes selected for socket coupled pipe. Larger sizes of heat fused pipe can be used inside old mains for insert renewal because it does not require the extra space for the coupling.

Heat fusion joints may easily be cut out and re-done. This fact has a bearing on the quantity and quality of training necessary and favorably affects operator attitude toward quality in the field. These joints can be easily cut out and destructively tested in the field to check joining proficiency and equipment condition and it's inexpensive. There is no coupling to destroy and throw away.

The heat fusion joining system is especially effective with Driscopipe 8600. The melt of this material is very viscous and tough. The operator can apply ample pressure to form the heat fusion joint with little danger rcing the molten material from between the two ds of the joint, as can be done with the softer, less viscous, high density materials.

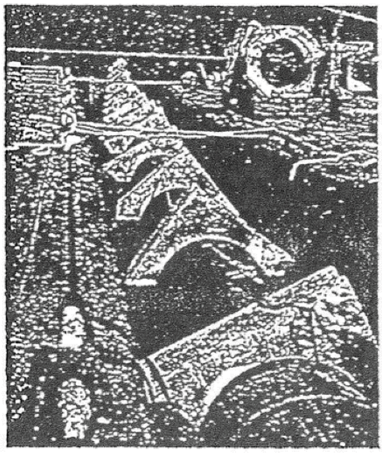

Driscopipe 8600 can be fusion joined to other polyethylene piping materials when necessary. Special joining techniques are required to achieve good joints. Phillips Driscopipe technical personnel are available to instruct and demonstrate the fusion joining procedure for joining Driscopipe to other polyethylene materials.

Fatigue Resistance

Driscopipe 8600 very high molecular weight, high density polyethylene has superior resistance to fatigue failure caused by cyclic loading. Independent laboratory tests were conducted to determine the suitability of Driscopipe 8600 for use as the cold water supply pipe and the barge mooring leg of the Mini-OTEC Project (Hawaii, 1979). In that application, 2150' of 24" 60 psi Driscopipe 8600 was deployed vertically in a deep ocean trench just offshore Keahole Point and was subject to cyclic distortion caused by wave action, current, and barge motion.

Cyclic tests showed that Driscopipe 8600 very high molecular weight PE could endure more than 100,000 cycles at a stress of 1800 psi without failure. Copies of this test report are avialable upon request.

Driscopipe 1000 offers good fatigue service life also, but not equal to 8600. Neither requires de-rating like PVC AWWA C-900 pipe. In fact, per AWWA C-906 for 4" to 63" HDPE pipe, no water hammer or fatigue de-rating factor need be applied to Driscopipe 8600 or Driscopipe 1000 ductile PE pipe.

The Driscopipe performance team offers you innovative solutions to your piping requirements. Contact your nearest Driscopipe Sales Representative. He'll give you personalized technical service, installation assistance and all the cost-savin advantages of a Driscopipe Piping System. Engineered for Performance!

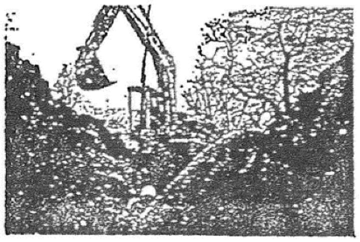

DRISCOPIPE

Phillips Driscopipe, Inc.
A Subsidiary of Phillips 66 Company

To Secure Product Information or Leave a Message for a Sales Engineer or Technical Service Representative:

Mail:
Attn: Customer Service Department
P.O. Box 83-3866
2929 North Central Expressway
Suite 100
Richardson, Texas 75083

Phone:
U.S. Domestic Toll Free (800) 527-0662

TWX:
910-867-4818

Fax:
214-783-2689

PLASTICS WITH POWER TO WIN.®

1774-90 A 01

butane may condense and liquefy in the pipe. Such liquefied fuel gasses are known to permeate polyethylene pipe, and result in unreliable heat fusion or electrofusion joints.

In potable water applications, permeating chemicals could affect the pipe or water in the pipe. ANSI/AWWA standards provide the following guidance for potable water applications:

> "The selection of materials is critical for water service and distribution piping where there is likelihood the pipe will be exposed to significant concentrations of pollutants comprised of low molecular weight petroleum products or organic solvents or their vapors. Research has documented that pipe materials such as polyethylene, polybutylene, polyvinyl chloride, and asbestos cement, and elastomers, such as used in jointing gaskets and packing glands, may be subject to permeation by lower molecular weight organic solvents or petroleum products. If water pipe must pass through such a contaminated area or an area subject to contamination, consult with the manufacturer regarding permeation of pipe walls, jointing materials, and so forth, *before* selecting materials for use in that area."[1]

Chemical Attack

A direct chemical attack on the polymer will result in permanent, irreversible polymer damage or chemical change by chain scission, cross-linking, oxidation, or substitution reactions. Such damage or change cannot be reversed by removing the chemical.

Chemical Resistance Information

The following chemical resistance guide, Table 5-1 (next page), presents immersion test chemical resistance data for a wide variety of chemicals.

☐ This data may be applicable to gravity flow and low stress applications.

☐ It may not be applicable when there is applied stress such as internal pressure, or applied stress at elevated temperature.

Unless stated otherwise, polyethylene was tested in the relatively pure, or concentrated chemical.

It is generally expected that dilute chemical solutions, lower temperatures, and the absence of stress have less potential to affect the material. At higher temperature, or where there is applied stress, resistance may be reduced, or polyethylene may be unsuitable for the application. Further, combinations of chemicals may have effects where individual chemicals may not.

Testing is recommended where information about suitability for use with chemicals or chemical combinations in a particular environment is not available. PLEXCO cannot provide chemical testing services.

---

[1] *ANSI/AWWA C906-90, Section 1.2; ANSI/AWWA C901-96, Section 4.1.*

Table 5-1 Chemical Resistance

Because the particular conditions of each application may vary, Table 5-1 information should be used only as a preliminary guide for PLEXCO and SPIROLITE polyethylene pipe materials. This information is offered in good faith, and is believed to be accurate at the time of publication, but it is offered without any warranty, expressed or implied. Additional information may be required, particularly in regard to unusual or special applications. Determinations of suitability for use in particular chemical or environmental conditions may require specialized laboratory testing.

Additional information on chemical compatibility may be found in PPI TR-19, *Thermoplastic Piping for the Transport of Chemicals.*

Chemical Resistance Key

Key†	*Meaning*
X	resistant (swelling <3% or weight loss <0.5%; elongation at break not substantially changed)
/	limited resistance (swelling 3 - 8% or weight loss 0.5 - 5%; elongation at break reduced by <50%)
—	not resistant (swelling > 8% or weight loss >5%; elongation at break reduced by >50%)
D	discoloration
*	aqueous solutions in all concentrations
**	only under low mechanical stress

† Where a key is not printed in the table, data is not available.

Medium	*73°F*	*140°F*
Acetaldehyde, gaseous	X	/
Acetic acid (10%)	X	X
Acetic acid (100%) (Glacial acetic acid)	X	/D
Acetic anhydride	X	/D
Acetone	X	X
Acetylene tetrabromide	**/ to —	—
Acids, aromatic	X	X
Acrylonitrile	X	X
Adipic acid	X	X
Allyl alcohol	X	X
Aluminum chloride, anhydrous	X	X
Aluminum sulphate	*X	X
Alums	X	X
Ammonia, liquid (100%)	X	X
Ammonium chloride	*X	X
Ammonium flouride, aqueous (up to 20%)	X	X
Ammonium nitrate	*X	X
Ammonium sulphate	*X	X
Ammonium sulfide	*X	X
Amyl acetate	X	X
Aniline, pure	X	X
Anisole	/	—
Antimony trichloride	X	X
Aqua regia	—	—
Barium chloride	*X	X
Barium hydroxide	*X	X

Medium	*73°F*	*140°F*
Beeswax	X	**/ to —
Benzene	/	/
Benezenesulphonic acid	X	X
Benzoic acid	*X	X
Benzyl alcohol	X	X to /
Borax, all concentrations	X	X
Boric acid	*X	X
Brine, saturated	X	X
Bromine	—	—
Bromine vapor	—	
Butanetriol	X	X
Butanol	X	X
Butoxyl	*X	/
Butyl acetate	X	/
Butyl glycol	X	X
Butyric acid	X	/
Calcium chloride	*X	X
Calcium hypochlorite	*X	X
Camphor	X	/
Carbon dioxide	X	X
Carbon disulphide	/	
Carbon tetrachloride	**/ to —	—
Caustic potash	X	X
Caustic soda	X	X
Chlorine, liquid	—	—
Chlorine bleaching solution (12% active chlorine)	/	—
Chlorine gas, dry	/	—
Chlorine gas, moist	/	—
Clorine water (disinfection of mains)	X	
Chloroacetic acid (mono)	X	X
Chlorobenzene	/	—
Chloroethanol	X	XD
Chloroform	**/ to —	—
Chlorosulphonic acid	—	—
Chromic acid (80%)	X	—D
Citric acid	X	X
Coconut oil	X	/
Copper salts	*X	X
Corn oil	X	/
Creosote	X	XD
Creosol	X	XD
Cyclohexane	X	X
Cyclohexanol	X	X
Cyclohexanone	X	X
Decahydronaphthalene	X	/
Desiccator grease	X	/
Detergents, synthetic	X	X
Dextrin, aqueous (18% saturated)	X	X
Dibutyl ether	X to /	—
Dibutyl phthalate	X	/
Dichloroacetic acid (100%)	X	/D
Dichloroacetic acid (50%)	X	X
Dicliloroacetic acid methyl ester	X	X
Dichlorbenzene	/	—
Diclolorethane	/	/
Dicloroethylene	—	—
Diesel oil	X	/
Diethyl ether	X to /	/
Diisobutyl ketone	X	/ to —
Dimethyl formamide (100%)	X	X to /
Dioxane	X	X
Emulsifiers	X	X
Esters, aliphatic	X	X to /
Ether	X to /	/
Ethyl acetate	/	—
Ethyl alcohol	X	X
Ethyl glycol	X	X
Ethyl hexanol	X	X
Ethylene chloride (dichlorothene)	/	/
Ethylene diamine	X	X
Fatty acids ($>C^6$)	X	/
Feric chloride*	X	X
Fluorine	—	—
Fluorocarbons	/	—
Fluorosilic acid, aqueous (up to 32%)	X	X
Formaldehyde (40%)	X	X
Formamide	X	X
Formic acid	X	
Fruit juices	X	X
Fruit pulp	X	X
Furfuryl alcohol	X	XD
Gelatine	X	X
Glucose	*X	X
Glycerol	X	X
Glycerol chlorohydrin	X	X
Glycol (conc.)	X	X

Medium	73°F	140°F
Glycolic acid (50%)	X	X
Glycolic acid (70%)	X	X
Halothane	/	/
Hydrazine hydrate	X	X
Hydrobromic acid (50%)	X	X
Hydrochloric acid (all concentrations)	X	X
Hydrocyanic acid	X	X
Hydrofluoric acid (40%)	X	/
Hydrofluoric acid (70%)	X	/
Hydrogen	X	X
Hydrogen chloride gas, moist and dry	X	X
Hydrogen peroxide (30%)	X	X
Hydrogen peroxide (100%)	X	
Hydrogen sulfide	X	X
Iodine, tincture of, DAB 7 (German Pharmacopoeia)	X	/D
Isooctane	X	/
Isopropanol	X	X
Isopropyl ether	X to /	—
Jam	X	X
Keotones	X	X to /
Lactic acid	X	X
Lead acetate	*X	X
Linseed oil	X	X
Magnesium chloride	*X	X
Magnesium sulphate	*X	X
Maleic acid	X	X
Malic acid	X	X
Menthol	X	/
Mercuric chloride (sublimate)	X	X
Mercury	X	X
Methanol	X	X
Methyl butanol	X	X
Methyl ethyl ketone	X	/ to —
Methyl glycol	X	X
Methylene chloride	/	/
Mineral oils	X	X to /
Molasses	X	X
Monochloroacetic acid	X	X
Monochloroacetic ethyl ester	X	X
Monochloroacetic methyl ester	X	X
Morpholine	X	X
Naptha	X	/
Naphthalene	X	/
Nickel salts	*X	X
Nitric acid (25%)	X	X
Nitric acid (50%)	/	—
Nitrobenzene	X	/
o-Nitrotoluene	X	/
Octyl cresol	/	—
Oils, ethereal	/	/
Oils, vegetable & animal	X	X to /
Oleic acid (conc.)	X	/
Oxalic acid (50%)	X	X
Ozone	/	—
Ozone, aqueous solution (Drinking water purification)	X	
Paraffin oil	X	X
Perchloric acid (20%)	X	X
Perchloric acid (50%)	X	/
Perchloric acid (70%)	X	—D
Petrol	X	X to /
Petroleum	X	/
Petroleum ether	X	/
Petroleum jelly	**X to /	/
Phenol	X	XD
Phosphates	*X	X
Phosphoric acid (25%)	X	X
Phosphoric acid (50%)	X	X
Phosphoric acid (95%)	X	/D
Phosphorus oxychloride	X	/D
Phosphorus pentoxide	X	X
Phosphorus trichloride	X	/
Photographic developers, commecial	X	X
Phthalic acid (50%)	X	X
Polyglycols	X	X
Potassium bichromate (40%)	X	X
Potassium borate, aqueous (1%)	X	X
Potassium bromate, aqueous (up to 10%)	X	X
Potassium bromide	*X	X
Potassium chloride	*X	X
Potassium chromate, aqueous (40%)	X	
Potassium cyanide	*X	X
Potassium hydroxide (30% solution)	X	X
Potassium nitrate	*X	X
Potassium permanganate	X	XD
Propanol	X	X
Propionic acid (50%)	X	X
Propionic acid (100%)	X	/

Medium	*73°F*	*140°F*
Propylene glycol	X	X
Pseudocumene	/	/
Pyridine	X	/
Seawater	X	X
Silicic acid	X	X
Silicone oil	X	X
Silver nitrate	X	X
Soduim benzoate	X	X
Sodium bisulphite, weak aqueous solutions	X	X
Sodium carbonate	*X	X
Sodium chloride	*X	X
Sodium chlorite (50%)	X	/
Sodium hydroxide (30% solution)	X	X
Sodium hypochlorite (12% active chlorine)	/	—
Sodium nitrate	*X	X
Sodium silicate	*X	X
Sodium sulfide	*X	X
Sodium thiosulphate	X	X
Spermaceti	X	/
Spindle oil	X to /	/
Starch	X	X
Steric acid	X	/
Succinc acid (50%)	X	X
Sugar syrup	X	X
Sulfates	*X	X
Sulfur	X	X
Sulfur dioxide, dry	X	X
Sulfur dioxide, moist	X	X
Sulfur trioxide	—	—
Sulfuric acid (10%)	X	X
Sulfuric acid (50%)	X	X
Sulfuric acid (98%)	/	—
Sulfuric acid, fuming	—	—
Sulfurous acid	X	X
Sulfuryl chloride	—	
Tallow	X	X
Tannic acid (10%)	X	X
Tartaric acid	X	X
Tetrachloroethane	**X to /	—
Tetrahydrofurane	**X to /	
Tetetrahydronapthalene	X	/
Thionyl chloride	—	—

Medium	*73°F*	*140°F*
Thiophene	/	/
Toluene	/	—
Transformer oil	X	/
Tributyl phosphate	X	X
Trichloroacetic acid (50%)	X	X
Trichloroacetic acid (100%)	X	/ to —
Trichloroethylene	**X to /	—
Triethanolamine	X	X
Turpentine, oil of	x to /	/
Tween 20 and 90 (Atlas Chemicals)	X	X
Urea	*X	X
Vinegar (commercial conc.)	X	X
Viscose spinning solutions	X	X
Waste gases containing		
carbon dioxide	X	X
carbon monoxide	X	X
hydrocloric acid (all conc.)	X	X
hydrogen fluoride (traces)	X	X
nitrous vitriol (traces)	X	X
sulfur dioxide (low conc.)	X	X
sulphuric acid, moist (all conc.)	X	X
Water gas	X	X
Xylene	—	—
Yeast, aqueous preparations	X	X
Zinc chloride	*X	X

Second Edition

Issued 12/98

TABLE OF CONTENTS

Section No.	Title	Page
1.0	INTRODUCTION	III.7-1
1.1	Site Location	III.7-1
1.2	Facility Description	III.7-1
2.0	DESIGN CRITERIA	III.7-2
3.0	FOUNDATION SOILS SETTLEMENT	III.7-2
4.0	WASTE SETTLEMENT CALCULATIONS	III.7-8
5.0	SOIL COVER SETTLEMENT CALCULATIONS	III.7-12
6.0	CONCLUSIONS	III.7-13

LIST OF FIGURES

Figure No.	Title	Page
III.7.1	SETTLEMENT POINTS	III.7-4

LIST OF TABLES

Table No.	Title	Page
III.7.1	SETTLEMENT AND ANGULAR DISTORTION OF FOUNDATION SOILS BETWEEN POINTS, NORTH-SOUTH CROSS-SECTION A	III.7-6
III.7.2	SETTLEMENT AND ANGULAR DISTORTION OF FOUNDATION SOILS BETWEEN POINTS, EAST-WEST CROSS-SECTION B	III.7-7
III.7.3	TOTAL SETTLEMENT AND ANGULAR DISTORTION BETWEEN POINTS, NORTH-SOUTH CROSS-SECTION A	III.7-10
III.7.4	TOTAL SETTLEMENT AND ANGULAR DISTORTION BETWEEN POINTS, EAST-WEST CROSS-SECTION B	III.7-11
III.7.5	TOTAL STTLEMENT AND ANGULAR DISTORTION BETWEEN POINTS, NORTH-SOUTH CROSS-SECTION A	III.7-14
III.7.6	TOTAL STTLEMENT AND ANGULAR DISTORTION BETWEEN POINTS, EAST-WEST CROSS-SECTION B	III.7-15

LIST OF ATTACHMENTS

Attachment No.	Title
III.7.A	QIAN, XUEDE; KOERNER, ROBERT M.; AND GRAY, DONALD H. 2002. GEOTECHNICAL ASPECTS OF LANDFILL DESIGN AND CONSTRUCTION. NEW YORK: PRENTICE HALL.
III.7.B	CODUTO, DONALD P. 1998. GEOTECHNICAL ENGINEERING PRINCIPLES AND PRACTICES. NEW JERSEY: PRENTICE HILL.
III.7.C	SHARMA, HARI .D. AND SANGEETA P. LEWIS. 1994. WASTE CONTAINMENT SYSTEMS, WASTE STABILIZATION AND LANDFILLS: DESIGN AND EVALUATION. NEW YORK: JOHN WILEY AND SONS.

1.0 INTRODUCTION

Lea Land LLC (the Facility) is an existing Surface Waste Management Facility (SWMF) providing oil field waste solids (OFWS) disposal services. The existing Lea Land SWMF is subject to regulation under the New Mexico Oil and Gas Rules, specifically 19.15.9.711 and 19.15.36 NMAC, administered by the Oil Conservation Division (OCD) of the NM Energy, Minerals, and Natural Resources Department (NMEMNRD). This document is a component of the “Application for Permit Modification” that proposes continued operations of the existing approved waste disposal unit; lateral and vertical expansion of the landfill via the construction of new double-lined cells; and the addition of waste processing capabilities. The proposed Facility is designed in compliance with 19.15.36 NMAC, and will be constructed and operated in compliance with a Surface Waste Management Facility Permit issued by the OCD. The Facility is owned by, and will be constructed and operated by, Lea Land LLC.

The Lea Land SWMF is one of the most recently designed facilities to meet the new more stringent standards that, for instance, mandate double liners and leak detection for land disposal. The new services that Lea Land will provide needed resources to fill an existing void in the market for technologies that exceed current OCD requirements.

1.1 Site Location

The Lea Land site is located approximately 27 miles northeast of Carlsbad, straddling US Highway 62-180 (Highway 62) in Lea County, NM. The Lea Land site is comprised of a 642-acre ± tract of land encompassing Section 32, Township 20 South, Range 32 East, Lea County, NM. Site access is currently provided on the south side of US Highway 62. The coordinates for the approximate center of the Lea Land site are Latitude 32°31’46.77” and Longitude -103°47’18.25”.

1.2 Facility Description

The Lea Land SWMF comprises approximately 463 acres ± of the 642-acre ± site, and will include two main components: an oil field waste Processing Area and an oil field waste solids Landfill, as well as related infrastructure (i.e., access, waste receiving, stormwater management, etc.). Oil field wastes are delivered to the Lea Land SWMF from oil and gas exploration and production operations in southeastern NM and west Texas. The Permit Plans (**Attachment III.1.A**) identify the locations of the Processing Area and Landfill Disposal facilities. The proposed facilities are detailed in **Table**

II.1.2 (**Volume II.1**), and are anticipated to be developed in four primary phases as described in **Table II.1.3** (**Volume II.1**).

2.0 DESIGN CRITERIA

The slope of the final cover, liner and leachate collection piping after settlement must be consistent with the performance specifications for leachate collection and stormwater control. That is, the final cover and leachate collection system must allow adequate stormwater to runoff to the management controls, and to convey generated leachate such that the head on the primary high-density polyethylene (HDPE) flexible membrane liner (FML) does not exceed 12 inches.

3.0 FOUNDATION SOILS SETTLEMENT

The methodology for estimating floor potential settlement involves selecting points on the landfill floor surface, computing the settlement at each point, and evaluating the resultant change in surface elevation. Points were conservatively selected from a cross-section where the waste and fill material is thickest. Qian et al. (2002), present a method to determine landfill foundation settlement that evaluates elastic, primary, and secondary settlement. Recent laboratory testing evaluated a mixture of clayey sands and sand-clay (i.e., USCS Classifications SC) in the primary excavation area. The laboratory testing results compiled from samples at applicable depths from geotechnical borings conducted on-site are provided in **Volume III.4**, **Attachments III.4.B** and **III.4.C**. Foundation soils consisting of clayey sands and sand-clay mixtures, elastic settlement is conservatively assumed for this calculation. The elastic settlement is estimated using equation 12.20 from **Attachment III.7.A, p. 469**.

$$Z_e = \left(\frac{\Delta\sigma}{M_S}\right) H_o$$

Where:

Z_e = elastic settlement of soil layer (ft)
H_o = initial thickness of soil layer (ft)
$\Delta\sigma$ = increment of vertical effective stress, lb/ft^2
M_S = constrained modulus of soil, lb/ft^2

The constrained modulus is provided in equation 12.21 from **Attachment III.7.A, p. 470**.

$$M_S = \frac{E_S(1 - v_S)}{(1 + v_S)(1 - 2^* v_S)}$$

Where:

M_S = constrained modulus of soil, lb/ft^2

E_s = elastic modulus of soil (lb/ft^2) **Attachment III.7.A, p. 310**
E_s was interpolated from the data from Table 9.5, p. 310 (**Attachment III.7.A**) for CL, MH, GC, SC soils between 85% and 95% standard Proctor dry density to determine E_s for 90% as specified in the subgrade soils. E_s= (800 psi +1,500 psi)/2 = 1,150 psi x144 in^2/ft^2 = 165,600 lb/ft^2.

v_s = Poisson's ratio for soil = 0.39, which was found using the same method to estimate the elastic modulus of soil.

Settlement is estimated at the select locations (East-West Stations 2+00 through 19+00, and North-South Stations 1+00 through 23+00 shown on the landfill cross-sections (**Figure III.7.1**). An example calculation is demonstrated at Station 10+00 on East-West Cross Section B, with a total overburden depth of 205 ft. (final cover + intermediate cover + waste + protective soil layer).

East-West Station 10+00

Elastic Foundation Soil Settlement

Thickness of Waste = 200 ft. (assume entire thickness of waste from intermediate cover to top of protective soil layer; this provides a conservative analysis)

Unit Weight of Soil = 101.8 *lb/ft^3* Dry Density

Unit Weight of Waste = 74 *lb/ft^3*

$\Delta\sigma$ = (waste effective stress) + (protective soil layer effective stress) + (intermediate cover effective stress) + (final cover effective stress)

$\Delta\sigma$ = (200 ft)(74 *lb/ft^3*)+(2ft)(101.8 *lb/ft^3*)+(1 ft)(101.8 *lb/ft^3*)+(3.0 ft)(101.8 *lb/ft^3*)=15,411 *lb/ft^2*

$$M_S = \frac{165{,}600\ lb/ft^2(1 - 0.39)}{(1 + 0.39)(1 - 2^* 0.39)} = 330{,}333.55\ lb/ft^2$$

H_o = 206 ft. the full thickness of the compressible CL, MH, GC, SC soils; the compressible soil is considered incompressible at the depth of 45 ft.

$$Z_e = \left(\frac{15{,}411}{330{,}333.55}\right) 45\ ft = 2.12\ ft$$

Settlement between East-West Stations 9+00 and 10+00 = 2.05 ft. – 2.12 ft. = **-** 0.071 ft.

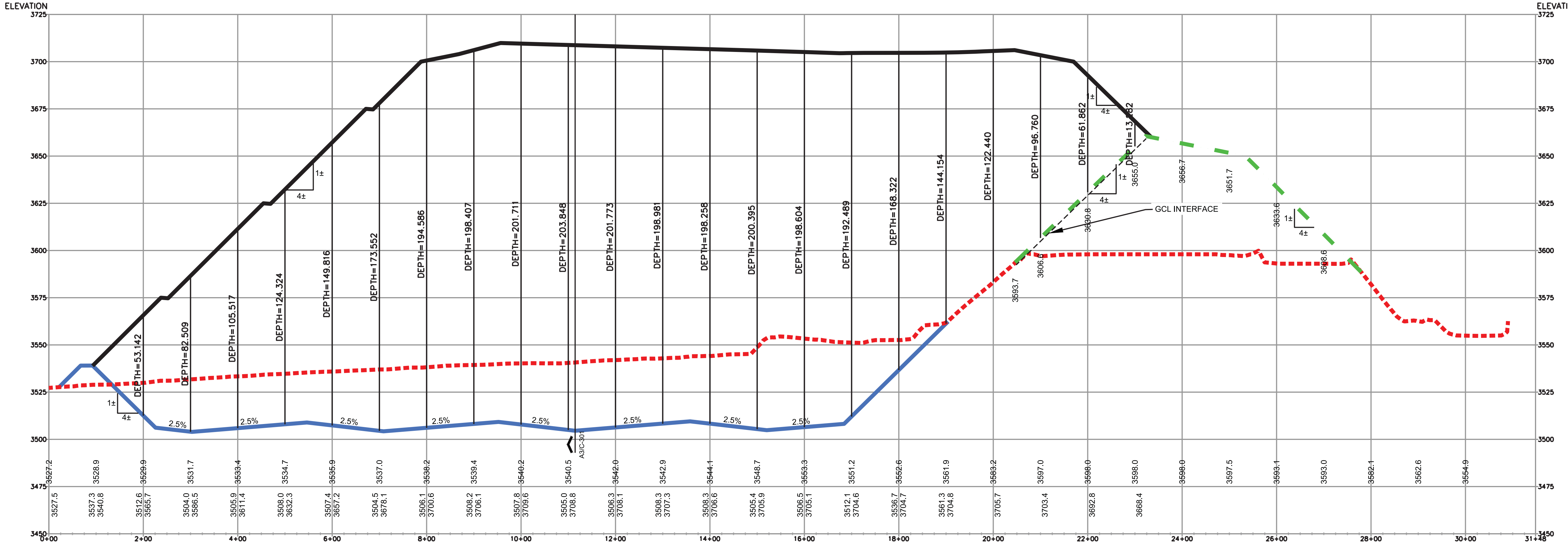

C3 NORTH-SOUTH SECTION ALONG CREST

1"=120' (Horiz.) 4:1 VERTICAL EXAGGERATION

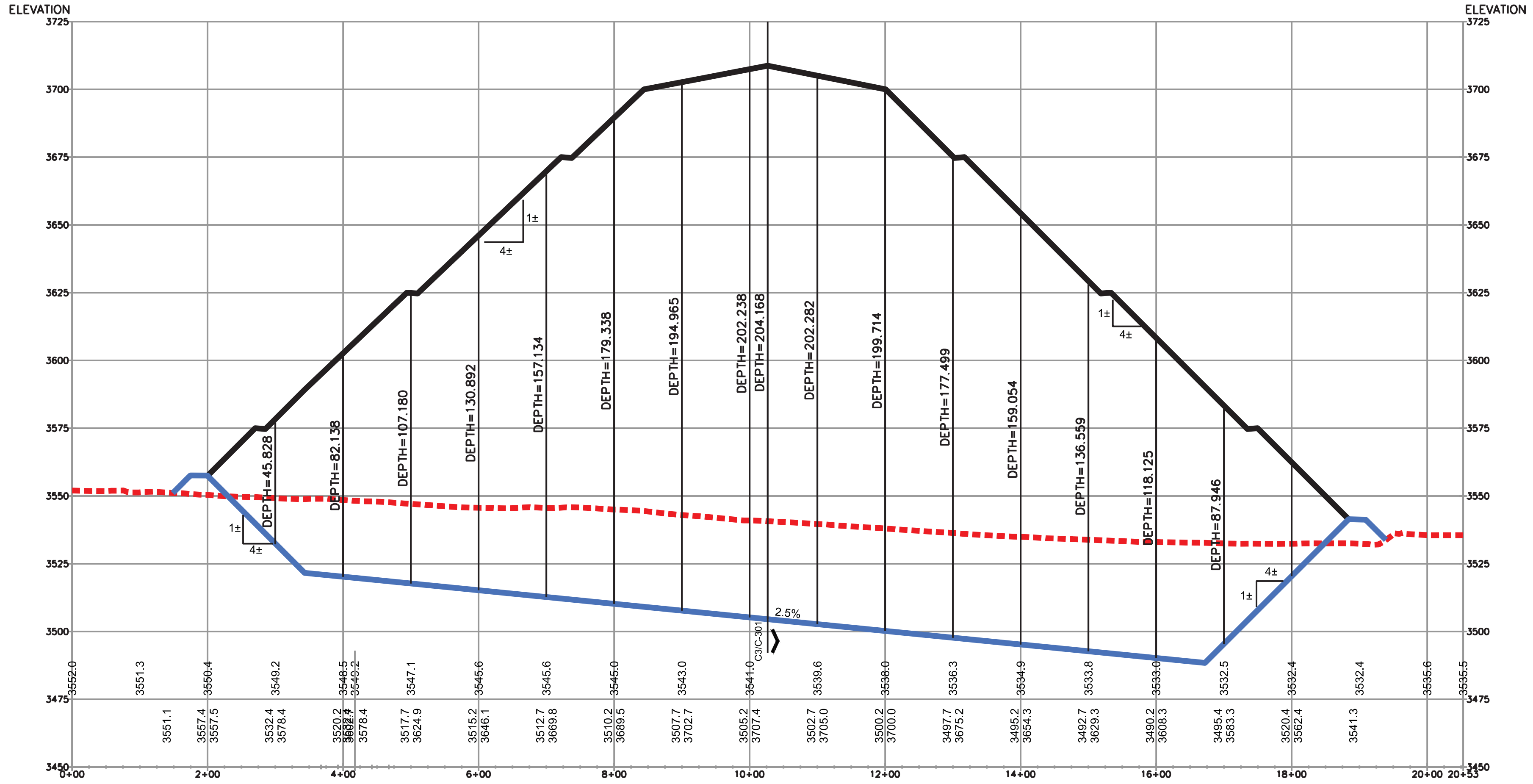

A3 EAST-WEST SECTION ALONG DEEPEST LEACHATE LINE

1"=120' (Horiz.) 4:1 VERTICAL EXAGGERATION

LEGEND

🟥 SECTION VIEW – EXISTING GRADES

🟩 SECTION VIEW – EXISTING PERMIT FINAL GRADES

🟦 SECTION VIEW – PROPOSED PERMIT BASE GRADES

⬛ SECTION VIEW – PROPOSED PERMIT FINAL GRADES

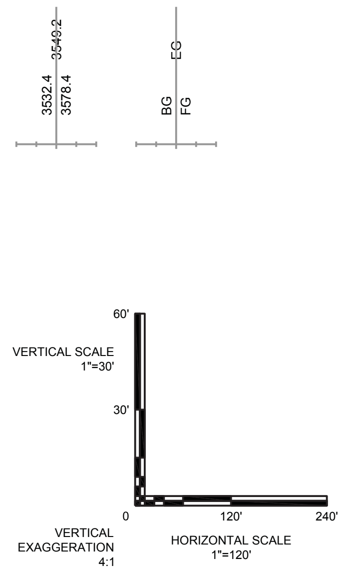

VERTICAL SCALE 1"=30'

VERTICAL EXAGGERATION 4:1

HORIZONTAL SCALE 1"=120'

GORDON PSC
ENVIRONMENTAL

NOT FOR CONSTRUCTION

THIS DOCUMENT IS RELEASED UNDER THE AUTHORITY OF CHARLES WALTER FIEDLER, P.E., NEW MEXICO LICENSE #19731 EXCLUSIVELY FOR THE PURPOSES CITED BELOW. IT IS NOT TO BE USED FOR ANY ADDITIONAL PURPOSES UNDER ANY CONDITION.

GORDON ENVIRONMENTAL | PSC

LEA LAND LLC
SURFACE WASTE MANAGEMENT FACILITY

PERMIT APPLICATION

LEA COUNTY, NEW MEXICO

KEY PLAN

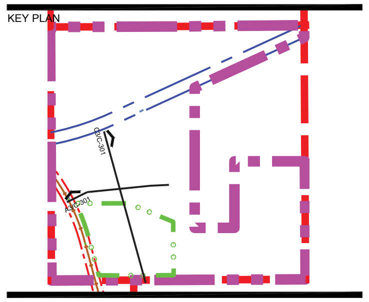

NO	DATE	DESCRIPTION
1	06/03/2019	REVISIONS PER OCD REVIEW
-	04/10/19	OCD PERMIT APPLICATION REVIEW

ISSUING OFFICE: RIO RANCHO PROJECT NO: 0416.18

SETTLEMENT
CROSS-SECTION

FIGURE III.7.1

Change in slope of base grade:

Elevation of base grade at East-West Station 10+00 = Approximately 3,505 ft.

Updated elevation of base grade at East-West Station 10+00 = 3,505 ft. – 2.12 ft. = 3,503 ft.

$$\text{Updated base grade slope} = \frac{(3{,}505.65\ ft - 3{,}503.08\ ft)}{100\ ft} \times 100 = 2.57\%$$

Change in base grade slope = 2.50% - 2.57% = -0.07%

The angular distortion between East-West Station 9+00 and 10+00 is determined as follows:

$$Distortion = \frac{(Settlement_{9+00} - Settlement_{10+00)}}{distance} x100$$

$$Distortion = \frac{(2.05\ ft - 2.12\ ft)}{100\ ft} x100 = 0.073\%$$

A summary of potential foundation soils settlement is provided in **Tables III.7.1** and **III.7.2.** The angular distortion between each point is calculated as above. The maximum angular distortion of the foundation soils on the floor (i.e., settlement points East-West Stations 4+00 to 16+00 and North-South Stations 3+00 to 16+00) of the landfill is 0.26% between Stations 5+00 and 6+00 on the North-South Cross-Section A. The minimum slope on the landfill floor; perpendicular to the leachate collection pipe is approximately 3.52% after settlement. Additionally, the minimum slope of the leachate collection pipe is 2.24% to the leachate collection sump. These slopes are adequate and will ensure that the design and performance standards for the leachate collection system will be met.

TABLE III.7.1 - Settlement and Angular Distortion of Foundation Soils Between Points
North-South Cross-Section A

Station	Total Settlement (feet)	Distance Between Points (feet)	Angular Distortion (%)	Distortion Direction	Design Base grade Elevation (feet)	Design Slope Between Point Locations (%)	Updated Base grade Elevation (feet)	Updated Slope Between Point Locations (%)
1+00	0.00				3537.30		3537.30	
		100	0.590	▼		24.70		25.29
2+00	0.59				3512.60		3512.01	
		100	0.296	▼		8.60		8.90
3+00	0.88				3504.00		3503.12	
		100	0.232	▼		1.90		1.67
4+00	1.12				3505.90		3504.78	
		100	0.190	▼		2.10		1.91
5+00	1.31				3508.00		3506.69	
		100	0.257	▼		0.60		0.86
6+00	1.56				3507.40		3505.84	
		100	0.240	▼		2.90		3.14
7+00	1.80				3504.50		3502.70	
		100	0.211	▼		1.60		1.39
8+00	2.01				3506.10		3504.09	
		100	0.034	▼		2.10		2.07
9+00	2.05				3508.20		3506.15	
		100	0.039	▼		0.40		0.44
10+00	2.09				3507.80		3505.71	
		100	0.020	▼		2.80		2.82
11+00	2.11				3505.00		3502.89	
		100	-0.020	▼		1.30		1.32
12+00	2.09				3506.30		3504.21	
		100	-0.028	▼		2.00		2.03
13+00	2.06				3508.30		3506.24	
		100	-0.007	▼		0.00		0.01
14+00	2.05				3508.30		3506.25	
		100	0.022	▼		2.90		2.92
15+00	2.07				3505.40		3503.33	
		100	-0.019	▲		1.10		1.12
16+00	2.05				3506.50		3504.45	
		100	-0.061	▲		5.60		5.66
17+00	1.99				3512.10		3510.11	
		100	-0.247	▲		24.60		24.85
18+00	1.75				3536.70		3534.95	
		100	-0.247	▲		24.60		24.85
19+00	1.50				3561.30		3559.80	
		100	-0.318	▲		32.40		32.72
20+00	1.18				3593.70		3592.52	
		100	-0.153	▲		12.90		13.05
21+00	1.03				3606.60		3605.57	
		100	-0.351	▲		24.20		24.55
22+00	0.68				3630.80		3630.12	
		100	-0.490	▲		24.20		24.69
23+00	0.19				3655.00		3654.81	

Notes:

Stations Correspond to Figure III.7.1
▲ *= potential upward distortion*
▼ *= potential downward distortion*
Elevations based on NM State Plan Coordinate System

TABLE III.7.2 - Settlement and Angular Distortion of Foundation Soils Between Points
East-West Cross-Section B

Station	Total Settlement (feet)	Distance Between Points (feet)	Angular Distortion (%)	Distortion Direction	Design Base grade Elevation (feet)	Design Slope Between Point Locations (%)	Updated Base grade Elevation (feet)	Updated Slope Between Point Locations (%)
2+00	0.00				3557.40		3557.40	
		100	0.547	▼		25.00		25.55
3+00	0.55				3532.40		3531.85	
		100	0.368	▼		12.20		12.57
4+00	0.91				3520.20		3519.29	
		100	0.249	▼		2.50		2.75
5+00	1.16				3517.70		3516.54	
		100	0.239	▼		2.50		2.74
6+00	1.40				3515.20		3513.80	
		100	0.264	▼		2.50		2.76
7+00	1.67				3512.70		3511.03	
		100	0.224	▼		2.50		2.72
8+00	1.89				3510.20		3508.31	
		100	0.158	▼		2.50		2.66
9+00	2.05				3507.70		3505.65	
		100	0.073	▼		2.50		2.57
10+00	2.12				3505.20		3503.08	
		100	0.001	▼		2.50		2.50
11+00	2.12				3502.70		3500.58	
		100	-0.025	▲		2.50		2.47
12+00	2.10				3500.20		3498.10	
		100	-0.225	▲		2.50		2.28
13+00	1.87				3497.70		3495.83	
		100	-0.185	▲		2.50		2.31
14+00	1.69				3495.20		3493.51	
		100	-0.227	▲		2.50		2.27
15+00	1.46				3492.70		3491.24	
		100	-0.186	▲		2.50		2.31
16+00	1.27				3490.20		3488.93	
		100	-0.304	▲		5.20		5.50
17+00	0.97				3495.40		3494.43	
		100	-0.463	▲		25.00		25.46
18+00	0.51				3520.40		3519.89	
		100	-0.423	▲		20.90		21.32
19+00	0.08				3541.30		3541.22	
		100	-0.083	▲		0.00		0.08
					3541.30		3541.30	

Notes:

Stations Correspond to Figure III.7.1

▲ *= potential upward distortion*

▼ *= potential downward distortion*

Elevations based on NM State Plan Coordinate System

4.0 WASTE SETTLEMENT CALCULATIONS

The methodology to estimate waste settlement involves selecting key points on the final cover surface, computing the settlement at each point, and evaluating the resultant change in surface elevation. Points were selected from North-South Cross-Section A and East-West Cross-Section B (**Figure III.7.1**). Qian et al. (2002; **Attachment III.7.A**) present a method developed by Sowers (1973) for determining settlement in landfills. This method is based on developed soils consolidation theory, which relates settlement to layer thickness and changes in void ratio.

The primary settlement is estimated using equation 12.4 (**Attachment III.7.A, p. 449**):

$$\Delta H_c = C_c \frac{H_o}{1+e_o} \log \frac{\sigma_i}{\sigma_o}$$

Where:

ΔH_c = primary settlement
$C_c/(1+e_o)$ = 0.006 (**Attachment III.7.B, p. 393, D_r = 80%**)
H_o = initial thickness of the waste layer before settlement (assume entire thickness of waste from intermediate cover to the top of protective soil layer; this provides a conservative analysis) [**Figure III.7.1**] = 200 ft.
σ_o = previously applied pressure in waste layer (assumed to equal the compaction pressure = 1,000 lbs/ft^2)
σ_i = total overburden pressure applied at the mid-level of the waste layer (lbs/ft^2)

Long-term secondary settlement is estimated by equation 12.10 (**Attachment III.7.A, p.451**):

$$\Delta H_s = C_\alpha \frac{H_o}{1+e_o} \log \frac{t_2}{t_1}$$

Where:

ΔH_s = secondary settlement
C_α = ⅓ [$C_c/(1+e_o)$] = 0.002 (**Attachment III.7.B, p. 393**)
H_o = waste thickness at start of secondary settlement = H-H_c (**Figure III.7.1**)
t_1 = starting time of secondary settlement (1 year)
t_2 = ending time of secondary settlement = Assume 30 years

Settlement is estimated at the key locations (North-South Stations 1+00 through 23+00 and East-West Stations 2+00 through 19+00) shown on the landfill North-South Cross-Section A and East-West Cross-Section B (**Figures III.7.1**). An example calculation is demonstrated at Station 11+00, the location of maximum waste depth for North-South Cross-Section A (i.e., 200 ft).

North-South Station 11+00

Primary Waste Settlement

Maximum Thickness of Waste = 200.8 ft.

$$\Delta H_c = C_c \frac{H_o}{1+e_o} \log \frac{\sigma_i}{\sigma_o}$$

Where:

$C_c/(1+e_o)$ = 0.006 (**Attachment III.7.B, p. 393, D_r = 80%**)
H_o = 200.8 ft.
σ_o = 1,000 lbs/ft^2
σ_i = 0.5[(200.8 ft.)(74 lbs/ft^3) + 4.0 ft. (101.8 lbs /ft^2)] = 7,633.2 lbs/ft^2

$$\Delta H_c = 0.006 \times 200.8 \times \log \frac{7{,}633 \frac{lbs}{ft}}{1{,}000 \frac{lbs}{ft^2}}$$

$$\Delta H_c = 1.06\, ft$$

Secondary Waste Settlement

$$H_o = 200.8\, ft - 1.06\, ft = 199.74\, ft$$

$$\Delta H_s = C_\alpha \frac{H_o}{1+e_o} \log \frac{t_2}{t_1}$$

$$\Delta H_s = 0.002 \times 200.8 \log \frac{30\, years}{1\, years} = 0.59\, ft$$

Total waste settlement = 1.06 ft. + 0.59 ft. = 1.65 ft.

The maximum final settlement of waste is the sum of primary and secondary settlement at North-South Station 11+00. The waste settlement is 1.06 ft. + 0.59 ft. = 1.65 ft, which has nominal impact on the corresponding calculations for landfill cap slope, runoff, etc. A summary of potential waste settlement is provided in **Tables III.7.3** and **III.7.4.**

TABLE III.7.3 - Total Settlement and Angular Distortion Between Points
North-South Cross-Section A

Station	Total Settlement (feet)	Distance Between Points (feet)	Angular Distortion (%)	Distortion Direction
1+00	0.00			
		100	0.24	▼
2+00	0.24			
		100	0.23	▼
3+00	0.47			
		100	0.20	▼
4+00	0.67			
		100	0.17	▼
5+00	0.85			
		100	0.25	▼
6+00	1.09			
		100	0.24	▼
7+00	1.33			
		100	0.22	▼
8+00	1.55			
		100	0.04	▼
9+00	1.59			
		100	0.04	▼
10+00	1.63			
		100	0.02	▼
11+00	1.65			
		100	-0.02	▲
12+00	1.63			
		100	-0.03	▲
13+00	1.60			
		100	-0.01	▲
14+00	1.59			
		100	0.02	▼
15+00	1.62			
		100	-0.02	▲
16+00	1.60			
		100	-0.06	▲
17+00	1.53			
		100	-0.26	▲
18+00	1.28			
		100	-0.25	▲
19+00	1.03			
		100	-0.30	▲
20+00	0.73			
		100	-0.14	▲
21+00	0.59			
		100	-0.29	▲
22+00	0.31			
		100	-0.29	▲
23+00	0.02			

Notes:

Stations Correspond to Figure III.7.1

▲ *= potential upward distortion*

▼ *= potential downward distortion*

Elevations based on NM State Plan Coordinate System

TABLE III.7.4 - Total Settlement and Angular Distortion Between Points
East-West Cross-Section B

Point Location	Total Settlement (feet)	Distance Between Points (feet)	Angular Distortion (%)	Distortion Direction
2+00	0.00			
		100	0.21	▼
3+00	0.21			
		100	0.28	▼
4+00	0.50			
		100	0.22	▼
5+00	0.71			
		100	0.22	▼
6+00	0.94			
		100	0.26	▼
7+00	1.20			
		100	0.23	▼
8+00	1.43			
		100	0.17	▼
9+00	1.59			
		100	0.08	▼
10+00	1.67			
		100	0.00	
11+00	1.67			
		100	-0.03	▲
12+00	1.64			
		100	-0.24	▲
13+00	1.41			
		100	-0.19	▲
14+00	1.22			
		100	-0.22	▲
15+00	0.99			
		100	-0.18	▲
16+00	0.82			
		100	-0.27	▲
17+00	0.54			
		100	-0.36	▲
18+00	0.19			
		100	-0.19	▲
19+00	0.00			

Notes:

Stations Correspond to Figure III.7.1
▲ *= potential upward distortion*
▼ *= potential downward distortion*
Elevations based on NM State Plan Coordinate System

5.0 SOIL COVER SETTLEMENT CALCULATIONS

The final cover soil layer consisting of vegetative, barrier, and intermediate cover layers will also experience nominal consolidation due to its own weight. The method for evaluating settlement of the soil cover and cushion layers is based on equation B.2 (**Attachment III.7.C, p. 569**).

Primary Soil Settlement

$$\Delta H_p = C_c \frac{H_p}{1+e_s} \log \frac{P_o + \Delta P}{P_o}$$

$C_c/(1+e_o)$ = 0.006 (**Attachment III.7.B, p. 393, D_r = 80%**)

Thickness of Soil = H = 3.0 feet of final cover +1 foot of intermediate cover soil + 2 feet of protective soil layer = 6 ft.

Unit Weight of Soil = 101.8 lb/ft^3 Dry Density

$$\Delta P = (3.0\,ft)(101.8\,lb/ft^3) + (1\,ft)(101.8\,lb/ft^3) + (2.0\,ft)(101.8\,lb/ft^3) = 610.8\ lb/ft^2$$

$$P_o = \frac{H}{2}(101.8\ lb/ft^3) = 3.0\,(101.8) = 305.4\ lb/ft^2$$

$$\Delta H_p = (0.006)(6.0\,ft)\log\left(\frac{305.4\ lbs/ft^2 + 610.8\ lbs/ft^2}{305.4\ lbs/ft^2}\right)$$

$$\Delta H_p = 0.017\,ft$$

Secondary Soil Cover Settlement

$$\Delta H_s = C_s \frac{H_o}{1+e_s} \log \frac{t_2}{t_1}$$

C_α = ⅓ [$C_c/(1+e_o)$] = 0.002 (**Attachment III.7.B, p. 393**)

H_o= 6.0 ft. – 0.017 ft. = 5.98 ft.

$$\Delta H_s = 0.002 \times 5.98 \log \frac{30\,years}{1\,years} = 0.018\,ft$$

The maximum settlement of the final cover is the sum of primary and secondary settlement at North-South Station 11+00. The soil final cover layer settlement is equal to 0.017 ft. + 0.018 ft. = 0.035 ft. The maximum angular distortion at the level of the top of final cover occurs between

North-South Stations 10+00 and 11+00 and equals 0.08%. Therefore, after conservative assumptions for settlement, the minimum slope of the final cover (5% grade) will be 5% - 0.08% = 4.92%, which has nominal impacts on the slope and runoff calculations (see Section 6.0).

6.0 CONCLUSIONS

Settlement projections have been calculated for the landfill foundation, the waste mass and for the landfill final soil cover. Settlement estimates include elastic deformation and both primary and secondary consolidation in the foundation soils, in the waste, and in the cover materials. The greatest value of projected settlement in both the foundation soils and in the waste occurs where the waste thickness is greatest.

The maximum final settlement of the landfill foundation, waste mass and landfill cover is the sum of primary and secondary settlement at North-South Station 11+00. The foundation soil settlement is equal to 2.11 ft, the waste settlement is equal to 1.65 ft, and the final cover layer settlement is calculated at 0.035 ft. Maximum total settlement that could occur on the final cover of the landfill is the sum of the foundation soil, waste, and cover settlement (i.e.: 2.11 ft + 1.65 ft + 0.035 ft = 3.8 ft). The methodology used to determine settlement at North-South Station 11+00 was used to find the settlement of Stations 1+00 through 23+00 for North-South Cross-Section A, and Stations 2+00 through 19+00 for East-West Cross-Section B. The total settlement for the stations on Cross-Sections A and B and the angular distortion between them, is provided on **Table III.7.5** through **Table III.7.6**.

The composite calculations demonstrate the slope of the final cover, liner and leachate collection piping following settlement does not compromise the design and performance specifications for the leachate collection system.

TABLE III.7.5 - Total Settlement and Angular Distortion Between Points
North-South Cross-Section A

Station	Total Settlement (feet)	Distance Between Points (feet)	Angular Distortion (%)	Distortion Direction	Design Final grade Elevation (feet)	Design Slope Between Point Locations (%)	Updated Final grade Elevation (feet)	Updated Slope Between Point Locations (%)
1+00	0.036				3541.90		3541.86	
		100	0.830	▼		26.80		25.97
2+00	0.865				3568.70		3567.83	
		100	0.526	▼		20.80		20.27
3+00	1.391				3589.50		3588.11	
		100	0.432	▼		24.90		24.47
4+00	1.823				3614.40		3612.58	
		100	0.363	▼		20.90		20.54
5+00	2.186				3635.30		3633.11	
		100	0.505	▼		24.90		24.40
6+00	2.691				3660.20		3657.51	
		100	0.482	▼		20.90		20.42
7+00	3.173				3681.10		3677.93	
		100	0.430	▼		22.50		22.07
8+00	3.603				3703.60		3700.00	
		100	0.071	▼		5.50		5.43
9+00	3.673				3709.10		3705.43	
		100	0.081	▼		3.50		3.42
10+00	3.754				3712.60		3708.85	
		100	0.042	▼		0.80		0.84
11+00	3.796				3711.80		3708.00	
		100	-0.042	▲		0.70		0.66
12+00	3.754				3711.10		3707.35	
		100	-0.058	▲		0.80		0.74
13+00	3.696				3710.30		3706.60	
		100	-0.015	▲		0.70		0.69
14+00	3.682				3709.60		3705.92	
		100	0.046	▲		0.70		0.75
15+00	3.727				3708.90		3705.17	
		100	-0.039	▲		0.80		0.76
16+00	3.688				3708.10		3704.41	
		100	-0.126	▲		0.50		0.37
17+00	3.561				3707.60		3704.04	
		100	-0.503	▲		0.10		0.60
18+00	3.059				3707.70		3704.64	
		100	-0.493	▲		0.10		0.59
19+00	2.565				3707.80		3705.23	
		100	-0.617	▲		0.90		1.52
20+00	1.948				3708.70		3706.75	
		100	-0.290	▲		2.30		2.01
21+00	1.658				3706.40		3704.74	
		100	-0.637	▲		10.60		9.96
22+00	1.021				3695.80		3694.78	
		100	-0.781	▲		24.40		23.62
23+00	0.239				3671.40		3671.16	

Notes:

Stations Correspond to Figure III.7.1
▲ = potential upward distortion
▼ = potential downward distortion
Elevations based on NM State Plan Coordinate System

TABLE III.7.6 - Total Settlement and Angular Distortion Between Points
East-West Cross-Section B

Station	Total Settlement (feet)	Distance Between Points (feet)	Angular Distortion (%)	Distortion Direction	Design Final grade Elevation (feet)	Design Slope Between Point Locations (%)	Updated Final grade Elevation (feet)	Updated Slope Between Point Locations (%)
3+00	0.035				3560.50		3560.46	
		100	0.760	▼		20.90		20.14
4+00	0.795				3581.40		3580.61	
		100	0.652	▼		24.30		23.65
5+00	1.447				3605.70		3604.25	
		100	0.467	▼		22.20		21.73
6+00	1.913				3627.90		3625.99	
		100	0.462	▼		21.20		20.74
7+00	2.375				3649.10		3646.72	
		100	0.523	▼		23.70		23.18
8+00	2.898				3672.80		3669.90	
		100	0.452	▼		19.70		19.25
9+00	3.351				3692.50		3689.15	
		100	0.324	▼		13.20		12.88
10+00	3.675				3705.70		3702.02	
		100	0.150	▼		4.70		4.55
11+00	3.825				3710.40		3706.57	
		100	0.002	▼		2.40		2.40
12+00	3.827				3708.00		3704.17	
		100	-0.052	▲		5.00		4.95
13+00	3.775				3703.00		3699.22	
		100	-0.461	▲		24.80		24.34
14+00	3.314				3678.20		3674.89	
		100	-0.375	▲		20.90		20.52
15+00	2.939				3657.30		3654.36	
		100	-0.451	▲		25.00		24.55
16+00	2.488				3632.30		3629.81	
		100	-0.364	▲		21.00		20.64
17+00	2.124				3611.30		3609.18	
		100	-0.577	▲		25.00		24.42
18+00	1.547				3586.30		3584.75	
		100	-0.820	▲		20.90		20.08
19+00	0.727				3565.40		3564.67	

Notes:

Points Correspond to Figure III.7.1
▲ *= potential upward distortion*
▼ *= potential downward distortion*
Elevations based on NM State Plan Coordinate System

ATTACHMENT III.7.A

QIAN, XUEDE; KOERNER, ROBERT M.; AND GRAY, DONALD H. 2002. GEOTECHNICAL ASPECTS OF LANDFILL DESIGN AND CONSTRUCTION.
NEW YORK: PRENTICE HALL.

GEOTECHNICAL ASPECTS OF LANDFILL DESIGN AND CONSTRUCTION

Xuede Qian
Geotechnical Engineering Specialist
Michigan Department of Environmental Quality

Robert M. Koerner
H. L. Bowman Professor of Civil Engineering, Drexel University
Director, Geosynthetic Research Institute

Donald H. Gray
Professor of Civil and Environmental Engineering
The University of Michigan

Prentice Hall

PRENTICE HALL
Upper Saddle River, New Jersey 07458

TABLE 6.5 Index Properties of Solid Waste

Source	Unit Weight		Volumetric Moisture Content	Porosity	Void Ratio
	lb/ft^3	kN/m^3			
Rovers and Farquhar (1973)	59	9.3	0.16	–	–
Fungaroli (1979)	63	9.9	0.05	–	–
Wigh (1979)	73	11.5	0.08	–	–
Walsh and Kinman (1979)	90	14.1	0.17	–	–
Walsh and Kinman (1981)	89	14.0	0.17	–	–
Schroeder et al. (1984a, b)	–	–	0.28	0.52	1.08
Oweis et al. (1990)	40 to 90	6.3 to 14.1	0.10 to 0.20	0.40 to 0.50	0.67 to 1.0
Schroeder et al. (1994a, b)	–	–	0.29	0.67	2.03
Zornberg et al. (1999)	64 to 95	10 to 15	0.30	0.49 to 0.62	1.02 to 1.65

Based on its constituent composition the average moisture content of the solid waste shown in Table 6.4 can be calculated as follows:

$$\begin{aligned} w_d &= [(60.0)(10.4) + (50.0)(19.1) + (20.0)(34.6) + (10.0)(6.0) + (15.0)(5.0) \\ &\quad + (15.0)(9.5) + (2.0)(4.0) + (2.0)(7.2) + (8.0)(2.8) + (3.0)(1.4)]/100 \\ &= (624 + 955 + 692 + 60 + 75 + 142.5 + 8 + 14.4 + 22.4 + 4.2)/100 \\ &= 2597.5/100 \\ &= \underline{26.0\%} \end{aligned}$$

Thus, the average dry gravimetric moisture content of the solid waste shown in Table 6.4 is 26.0%.

More information about the moisture content of solid waste can be found in Table 6.5. It should be noted that the values of moisture content listed in Table 6.5 are calculated on a volume basis and differ from those calculated on a weight basis, which is more common to geotechnical analyses.

6.4 POROSITY OF MUNICIPAL SOLID WASTE

Porosity is defined as the ratio of the volume of voids to the total volume occupied by a solid waste or soil. Void ratio is defined as the ratio of the volume of voids to the volume of solids. Porosity can be related to the void ratio by using the relationships

$$n = \frac{e}{1 + e} \tag{6.7}$$

and

$$e = \frac{n}{1 - n} \tag{6.8}$$

where n = porosity of solid waste; and
e = void ratio of solid waste.

The porosity of MSW varies typically from 0.40 to 0.67 depending on the compaction and composition of the waste. For comparison, a typical compacted clay liner material will have a porosity of about 0.40. Table 6.5 shows a summary of the index properties of municipal solid waste, which includes initial volumetric moisture content, initial porosity, initial void ratio and unit weight data.

6.5 HYDRAULIC CONDUCTIVITY OF MUNICIPAL SOLID WASTE

Proper assessment of the hydraulic conductivity of municipal solid waste is important in the design of leachate collection systems and in leachate recirculation planning particularly for bioreactor landfills (see Chapter 15). The hydraulic conductivity can be measured using a field leachate pumping test and a large-scale percolation test in test pits or by using large-diameter permeameters in the laboratory.

Hydraulic conductivity measured in test pits at several landfills in Canada by Landva and Clark (1990) is plotted against unit weight in Figure 6.3. The values shown are based on an intermediate stage of water level recession, after the flow had stabilized and before any debris could clog the voids. The measured coefficients of hydraulic conductivity (1.0×10^{-3} to 4.0×10^{-2} cm/sec) correspond to those associated with clean sand and gravel. Qian (1994) used three-year field data from an active landfill in the state of Michigan to develop a relationship between precipitation and leachate volume from a primary leachate collection system with time. With this information, the hydraulic conductivity of the waste can be calculated based on the water travel time, hydraulic gradient, and waste thickness. The hydraulic conductivity calculated in this way was estimated to be about 9.2×10^{-4} to 1.1×10^{-3} cm/sec. Table 6.6 summarizes the hydraulic conductivity of different types of MSW taken from the

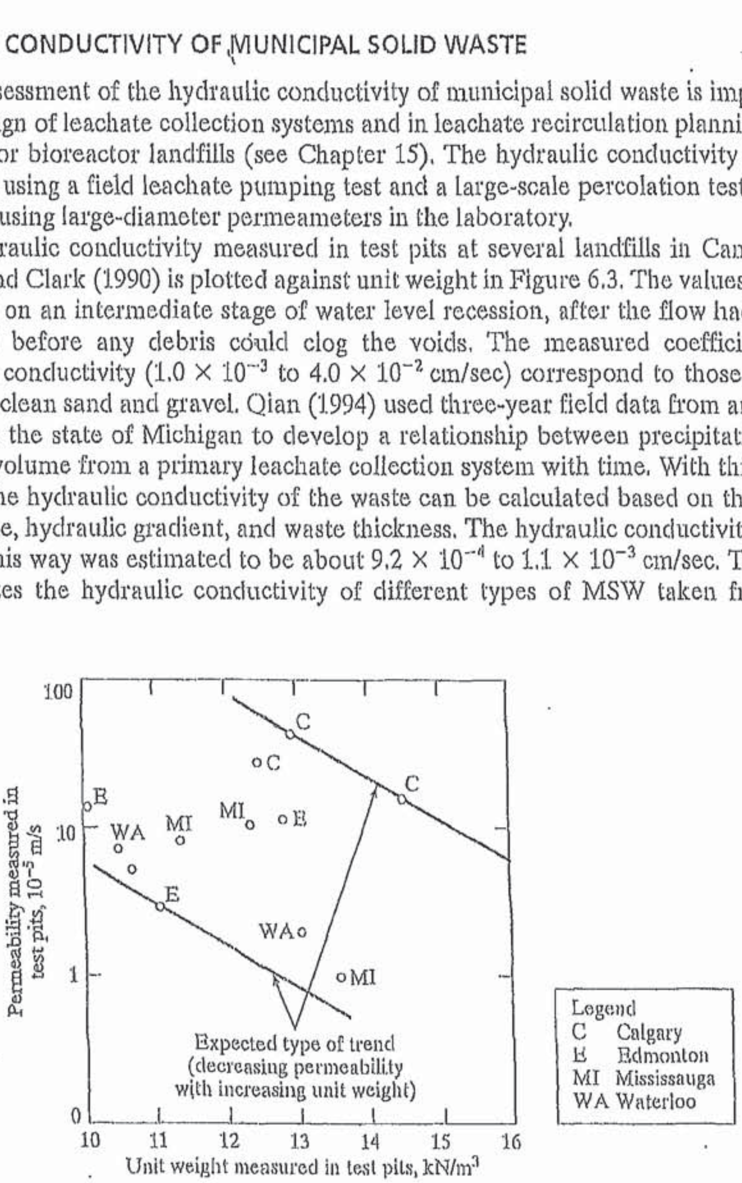

FIGURE 6.3 Unit Weight and Permeability (from Percolation) as Measured in Landfill Test Pits (Landva and Clark, 1990)

FIGURE 6.9 Compressive Strain versus Log Pressure for Various Landfills in Canada (Landva and Clark, 1990)

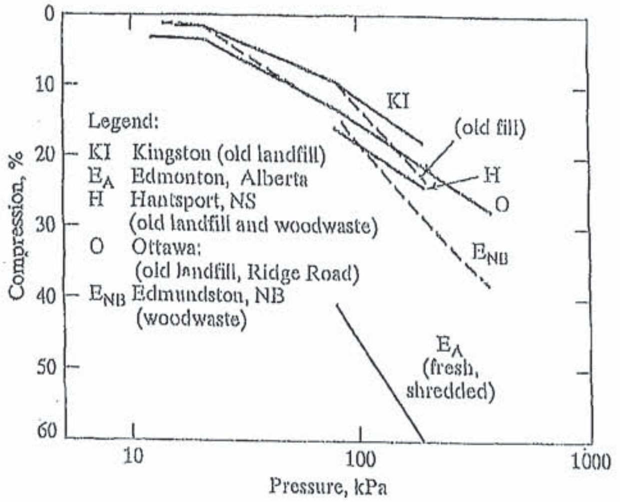

KI: $C_C' = 0.17$ ($p = 20 - 200$ kPa)
E_A: $C_C' = 0.35$ ($p = 80 - 200$ kPa)
H: $C_C' = 0.22$ ($p = 80 - 200$ kPa)
O: $C_C' = 0.21$ ($p = 100 - 400$ kPa)
E_{NB}: $C_C' = 0.36$ ($p = 100 - 400$ kPa)

cans; the lower values are for the less resilient materials. The maximum C_c for peat is about one-third greater than the maximum observed for waste fills.

Landva and Clark (1990) found that the coefficient of secondary consolidation, C_α, (the gradient of the compression versus log time relationship) was in the range 0.2 to 3.0 percent per log cycle time, depending on the type of waste involved. Field testing results using a settlement platform (Keene, 1977) showed that the coefficient of secondary consolidation, C_α, varies between 0.014 and 0.034. Too few tests have been carried out for any firm relationship to be established between the value of C_α and the type of waste, but it does appear that C_α increases with increasing organic content. Sowers (1973) pointed that the coefficient of secondary consolidation, C_α, is also a

FIGURE 6.10 Compressibility of MSW Landfills (Sowers, 1973)

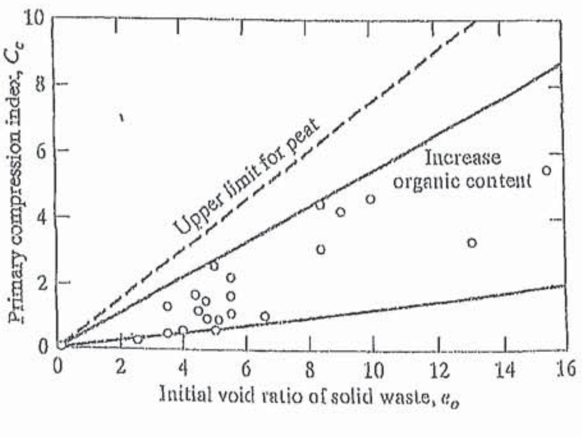

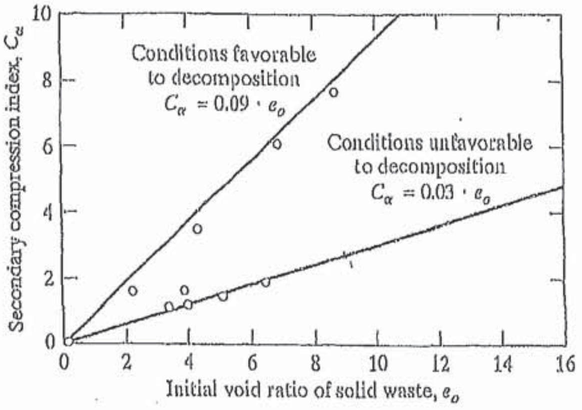

FIGURE 6.11 Secondary Compression of MSW Landfills (Sowers, 1973)

function of the void ratio, as shown in Figure 6.11. For any given void ratio, there is a large range in C_α, related to the potential for physico-chemical and bio-chemical decay. The value is high if the organic content subject to decay is large and the environment is favorable: namely, warm, moist, with fluctuating water table that pumps fresh air into the fill. The value is low for more inert materials and an unfavorable environment. More research and data are necessary before this relationship can be defined more closely.

The most widely reported compressibility parameter is the modified secondary compression index (C'_α). The reported values of C'_α range from 0.001 to 0.59. The lowest value represents the compressibility of a landfill that had been subjected to dynamic compaction. For typical landfills the lower limit of C'_α is generally around 0.01 to 0.03. This compares to 0.005 to 0.02 for common clays (Holtz and Kovacs, 1981). Fasset et al. (1994) observed that the typical upper limit of C'_α appears to be approximately 0.1.

According to Yen and Scanlon (1975), the settlement rate of waste increases with depth, hence larger values of C'_α should be associated with thicker fills. They observed that this effect leveled off at about 90 ft. and suggested that conditions within the landfill at great depths limit the biological activity to anaerobic decomposition, which is much slower than the aerobic decomposition believed to occur in shallower fills.

The values of C_α and C'_α, like C_c and C'_c, are dependent on the values used for e_0 or H_0. The value of C'_α is also dependent on stress level, time, and on how the origin of time is selected. The waste placement or filling period for landfills is often long and should be taken into consideration for settlement rate analyses (Yen and Scanlon, 1975). The zero time selection has a large impact on C'_α particularly during earlier phases of a landfill (Fassett et al., 1994)

An additional problem with determining C'_α is the fact that this parameter is generally not constant. Edgers (1992) presents settlement log-time data from 22 case histories (shown in Figure 6.12). The majority of the curves show a relatively flat slope (i.e. low C'_α values) at small times, but at larger times the slope greatly increases (Figure 6.13). They attributed the higher slopes in the later stages of compression to increasing decomposition, but it may simply be an artifact of the log-time scale. It is

d = diameter of perforated hole or width of perforated slot on the pipe, in or m; and
n = number of perforated holes or slots per row per foot of pipe.

Pipe stiffness is measured according to ASTM D2412 (Standard Test Method for External Loading Properties of Plastic Pipe by Parallel-Plate Loading). The elastic modulus of the pipe material depends on the type of resin and formulation being used. Three formulas that can be used to calculate pipe stiffness are

$$PS = \frac{E \cdot I}{0.149 \cdot r^3} \tag{9.24}$$

$$PS = 0.559 \cdot E \cdot (t/r)^3 \tag{9.25}$$

and

$$PS = 4.47 \cdot \frac{E}{(SDR - 1)^3} \tag{9.26}$$

where PS = pipe stiffness, lb/in^2 or kN/m^2;
E = elastic modulus of the pipe material, lb/in^2 or kN/m^2;
I = moment of inertia of the pipe wall per unit length,
$I = t^3/12$, in^4/in = in^3 or m^4/m = m^3;
r = mean radius of pipe, in or m;
t = wall thickness of pipe, in or m; and
SDR = standard dimension ratio, the same as the dimension ratio.

The allowable deflection ratios for a typical commercial polyethylene pipe are listed in Table 9.4.

Deflections of buried flexible pipe are commonly calculated using Equation 9.16 or 9.21. These equations use the soil reaction modulus, E', as a surrogate parameter for soil stiffness. It should be noted that the values of E' in Table 9.3 only apply for soil fills of less than 50 ft (15 m). However, megafills built over leachate collection pipes often exceed 150 ft (46 m) in height. The soil reaction modulus is not a directly measurable soil parameter; instead it must be determined by back-calculation using observed pipe deflections. Research by Selig (1990) showed that E' is a function of the bedding condition and overburden pressure. Selig's studies were carried out to seek a correlation between the soil reaction modulus and soil stiffness parameters such as

TABLE 9.4 Allowable Deflection Ratio of Polyethylene Pipe

SDR	Allowable Deflection Ratio
11	2.7%
13.5	3.4%
15.5	3.9%
17	4.2%
19	4.7%
21	5.2%
26	6.5%
32.5	8.1%

Young's modulus of soil, E_s, and the constrained modulus of soil, M_s, where E_s and D_s are related through Poisson's ratio of soil, υ_s, by

$$M_s = \frac{E_s \cdot (1 - \nu_s)}{(1 + \nu_s)(1 - 2 \cdot \nu_s)} \tag{9.27}$$

where M_s = constrained modulus of soil, lb/ft^2 or kN/m^2;
E_s = elastic modulus of soil, lb/ft^2 or kN/m^2; and
ν_s = Poisson's ratio of soil.

The studies and analyses by Neilson (1967), Allgood and Takahashi (1972), and Hartely and Duncan (1987) indicated that for

$$E' = k \cdot M_s \tag{9.28}$$

the value of k may vary from 0.7 to 2.3. Using $k = 1.5$ as a representative value and $\nu_s = 0.3$, in addition to combining Equations 9.27 and 9.28 yields the following relationship between the elastic modulus of the pipe and soil (Selig, 1990):

$$E' = 2 \cdot E_s \tag{9.29}$$

The values of elastic parameters, E_s and ν_s, can be found in Table 9.5 according to different percents of density from a standard Proctor compaction test (ASTM D698).

TABLE 9.5 Elastic Soil Parameters (Selig, 1990)

Soil Type	Stress Level		85% Standard Density			95% Standard Density		
			E_s			E_s		
	psi	kPa	psi	MPa	ν_s	psi	MPa	ν_s
SW, SP, GW, GP	1	7	1,300	9	0.26	1,600	11	0.40
	5	35	2,100	14	0.21	4,100	28	0.29
	10	70	2,600	18	0.19	6,000	41	0.24
	20	140	3,300	23	0.19	8,600	59	0.23
	40	280	4,100	28	0.23	13,000	90	0.25
	60	420	4,700	32	0.28	16,000	110	0.29
GM, SM, ML, and GC, SC with < 20% fines	1	7	600	4	0.25	1,800	12	0.34
	5	35	700	5	0.24	2,500	17	0.29
	10	70	800	6	0.23	2,900	20	0.27
	20	140	850	6	0.30	3,200	22	0.29
	40	280	900	6	0.38	3,700	25	0.32
	60	420	1,000	7	0.41	4,100	28	0.35
CL, MH, GC, SC	1	7	100	1	0.33	400	3	0.42
	5	35	250	2	0.29	800	6	0.35
	10	70	400	3	0.28	1,100	8	0.32
	20	140	600	4	0.25	1,300	9	0.30
	40	280	700	5	0.35	1,400	10	0.35
	60	420	800	6	0.40	1,500	10	0.38

Table 12.2 Comparison of Settlement and Construction Period (Yen and Scanlon, 1975)

Range of Fill Depth H_f, feet, (meter)	Average Construction Period, t_c (month)	Total Time Required for Construction and Settlement (months)	Approximate Time Required for Settlement to Complete (month)
40 to 80 (12 to 24)	12	113	101
40 to 80 (12 to 24)	72	324	252
80 to 100 (24 to 30)	12	245	233
80 to 100 (24 to 30)	72	310	238

Used with permission of ASCE.

12.4 ESTIMATION OF LANDFILL SETTLEMENT

The usual laboratory tests for soil consolidation testing are not well suited for obtaining accurate consolidation parameters for solid waste that has a heterogeneous composition and extremely large particle sizes. By analyzing the field settlement data from some large-scale pilot landfill cells, Sowers (1973) proposed an alternative method to estimate the amount of the landfill settlement. In recent years, this method has been revised and refined several times by other investigators.

The settlement of solid waste includes primary settlement and long-term secondary compression. The total amount of settlement is given by the expression

$$\Delta H = \Delta H_c + \Delta H_\alpha \tag{12.3}$$

where ΔH = total settlement of solid waste;
ΔH_c = primary settlement of solid waste;
ΔH_α = long-term secondary settlement of solid waste.

12.4.1 Settlement of New Solid Waste

Based on the procedure proposed by Sowers (1973), the equations that follow can be used to calculate the settlement for new landfilled solid waste. The *Initial primary settlement* is given by

$$\Delta H_c = C_c \cdot \frac{H_o}{1 + e_o} \cdot \log \frac{\sigma_i}{\sigma_o} \tag{12.4}$$

or

$$\Delta H_c = C_c' \cdot H_o \cdot \log \frac{\sigma_i}{\sigma_o} \tag{12.5}$$

where ΔH_c = primary settlement;
e_o = initial void ratio of the waste layer before settlement;
H_o = initial thickness of the waste layer before settlement;
C_c = primary compression index (recall Figure 6.10);
C_c' = modified primary compression index, $C_c' = 0.17 \sim 0.36$;
σ_o = previously applied pressure in the waste layer (assumed equal to the compaction pressure, $\sigma_o = 1{,}000$ lb/ft^2 or 48 kN/m^2);
σ_i = total overburden pressure applied at the mid level of the waste layer.

The previous compaction pressure applied on the solid waste layer during placement with compaction equipment is assumed to be 1,000 lb/ft^2 (48 kN/m^2) based on 1973 compaction efforts for municipal solid waste landfills. In other words, the waste that has been placed in the landfill is essentially incompressible at normal pressure below 1,000 lb/ft^2 (48 kN/m^2) due to the preconsolidation effect caused by previous compaction of the material. The value of the previously applied pressure, σ_o, should be changed during estimation of settlement if the compaction effort is much lower or higher than 1,000 lb/ft^2 (48 kN/m^2) for a specific landfill project. Indeed, current practices of using waste compactors in the 100 to 150 U.S. tons (900 to 1,300 kN) range will significantly increase the value of σ_o.

The *long-term secondary settlement* can be obtained from

$$\Delta H_\alpha = C_\alpha \cdot \frac{H_o}{1 + e_o} \cdot \log \frac{t_2}{t_1} \tag{12.6}$$

or

$$\Delta H_\alpha = C'_\alpha \cdot H_o \cdot \log \frac{t_2}{t_1} \tag{12.7}$$

where ΔH_α = long-term secondary settlement;
e_o = initial void ratio of the waste layer before settlement;
H_o = initial thickness of the waste layer before settlement;
C_α = secondary compression index (recall Figure 6.11);
C'_α = modified secondary compression index, $C'_\alpha = 0.03 \sim 0.1$;
t_1 = starting time of the time period for which long-term settlement of the layer is desired, $t_1 = 1$ month;
t_2 = ending time of the time period for which long-term settlement of the layer is desired.

Because a standard consolidation test method for solid waste has not yet been developed, the selection of waste compression indices are mainly based on experience and limited field data. The value of the primary compression index C_c can be selected from Figure 6.10 based on the initial void ratio and organic content of the solid waste. The value of the secondary compression index C_α can be selected from Figure 6.11 based on the initial void ratio of the waste and the decomposition conditions.

Generally, the initial void ratio of municipal solid waste placed in a landfill after compaction is quite difficult to determine, and hence the values of the primary compression index C_c and the secondary compression index C_α cannot be estimated readily for settlement analysis. Accordingly, an alternative approach has been used in engineering practice—namely, the use of a "modified" primary compression index C'_c and a "modified" secondary compression index C'_α. Based on experience, the value of the modified primary compression index C'_c varies from 0.17 to 0.36, and the value of the modified secondary compression index C'_α varies from 0.03 to 0.1 for municipal solid waste (depending on the initial compaction effort and composition of the solid waste). The value of the modified secondary compression index C'_α for common clay ranges from 0.005 to 0.02. Therefore, the secondary settlement for municipal solid waste is approximately five to six times that of common clay.

12.4.2 Settlement of Existing Solid Waste

The following equations can be used to calculate the settlement of an existing solid waste landfill caused by vertical expansion (Chapter 14) or other additional extra loading, such as a light structure on a raft foundation.

The *primary settlement* is obtained by

$$\Delta H_c = C_c \cdot \frac{H_o}{1 + e_o} \cdot \log \frac{\sigma_o + \Delta\sigma}{\sigma_o} \tag{12.8}$$

or

$$\Delta H_c = C_c' \cdot H_o \cdot \log \frac{\sigma_o + \Delta\sigma}{\sigma_o} \tag{12.9}$$

where ΔH_c = primary settlement;
e_o = initial void ratio of the waste layer before settlement;
H_o = initial thickness of the waste layer of the existing landfill;
C_c = primary compression index;
C_c' = modified primary compression index, $C_c' = 0.17 \sim 0.36$;
σ_o = existing overburden pressure acting at the mid level of the waste layer;
$\Delta\sigma$ = increment of overburden pressure due to vertical expansion or other extra load.

The *long-term secondary settlement* is given by

$$\Delta H_\alpha = C_\alpha \cdot \frac{H_o}{1 + e_o} \cdot \log \frac{t_2}{t_1} \tag{12.10}$$

or

$$\Delta H_\alpha = C_\alpha' \cdot H_o \cdot \log \frac{t_2}{t_1} \tag{12.11}$$

where ΔH_α = secondary settlement;
e_o = initial void ratio of the waste layer before starting secondary settlement;
H_o = initial thickness of the waste layer before starting secondary settlement;
C_α = secondary compression index;
C_α' = modified secondary compression index, $C_\alpha' = 0.03 \sim 0.1$;
t_1 = starting time of the secondary settlement. It is assumed to be equal to the age of the existing landfill for vertical expansion project;
t_2 = ending time of the secondary settlement.

(e.g., temperature within landfill and oxygen reaching the waste) still is not entirely clear. These functions should be used with caution in engineering practice and should be supported by additional testing data and research.

12.7 ESTIMATION OF LANDFILL FOUNDATION SETTLEMENT

If the landfill is underlain by a soil layer, particularly a thick layer of soft, fine-grained soil, consolidation settlements may be large. In these cases, design analyses should consider settlement of the foundation clay layer. Both primary consolidation and long-term secondary settlement should be considered. Calculations are performed using conventional equations from soil mechanics theory and a time frame at least equal to the active life and postclosure care period of the landfill.

Excessive settlement of an underlying foundation clay layer will affect the performance of a landfill liner and leachate collection system. The purposes of analyzing the settlement of a foundation clay layer and overlying landfill liner and leachate collection/removal system are as follows:

(i) Tensile strain induced in the liner system and leachate collection and removal system must be limited to a minimum allowable tensile strain for the components of these two systems. The compacted clay liner usually has the smallest allowable tensile strain value between 0.1% and 1.0% and an average allowable tensile strain of 0.5%.

(ii) Post-settlement grades of the landfill cell subbase and the leachate collection pipes must be sufficient to maintain leachate performance to prevent grade reversal and leachate ponding in accordance with the rule requirements.

12.7.1 Total Settlement of Landfill Foundation

The total settlement of landfill foundation soil can be divided into three portions: elastic settlement, primary consolidation settlement, and secondary consolidation settlement. The settlement of sandy soils includes only elastic settlement. The settlement of clayey soils includes all three types of settlements. The total settlement of clayey soil is equal to the sum of the elastic settlement and the primary and secondary settlements. Because the permeability of clay is quite low, it takes a long time to complete the whole process of consolidation settlement. The settlement of clayey soil is usually much larger than the settlement of sandy soils.

Because the settlement of sandy soils includes only elastic settlement, the settlement of sand layer can be calculated from the Elastic Settlement equation, which is

$$Z_e = (\Delta\sigma/M_s)H_0 \tag{12.20}$$

where Z_e = elastic settlement of soil layer, ft or m;

H_0 = initial thickness of soil layer, ft or m;

$\Delta\sigma$ = increment of vertical effective stress, lb/ft^2 or kN/m^2;

M_s = constrained modulus of soil, lb/ft^2 or kN/m^2.

The constrained modulus is given by

$$M_s = \frac{E_s \cdot (1 - v_s)}{(1 + v_s)(1 - 2 \cdot v_s)} \tag{12.21}$$

where M_s = constrained modulus of soil, lb/ft^2 or kN/m^2;
E_s = elastic modulus of soil, see Table 9.5, lb/ft^2 or kN/m^2;
v_s = Poisson's ratio of soil, see Table 9.5.

The *primary consolidation settlement* is given by

$$Z_c = C_r \cdot \frac{H_{oi}}{1 + e_{oi}} \cdot \log\frac{p_c}{\sigma_o} + C_c \cdot \frac{H_o}{1 + e_{oi}} \cdot \log\frac{\sigma_o + \Delta\sigma}{p_c} \tag{12.22}$$

where Z_c = primary consolidation settlement of clay layer, ft or m;
H_o = initial thickness of clay layer, ft or m; = 20'
e_{oi} = initial void ratio of clay layer;
C_r = recompression index;
C_c = primary compression index.
σ_o = initial vertical effective stress, lb/ft^2 or kN/m^2;
p_c = preconsolidation pressure, lb/ft^2 or kN/m^2;
$\Delta\sigma$ = increment of vertical effective stress, lb/ft^2 or kN/m^2.

The *secondary compression settlement* is given by

$$Z_\alpha = C_\alpha \cdot \frac{H_{os}}{1 + e_{os}} \cdot \log\frac{t_2}{t_1} \tag{12.23}$$

where Z_α = long-term secondary compression settlement, ft or m;
e_{os} = initial void ratio of clay layer before starting secondary consolidation settlement;
C_α = secondary consolidation compression index;
H_{os} = initial thickness of clay layer before starting secondary consolidation settlement, ft or m;
t_1 = starting time of the time period for which long-term settlement of the layer is desired;
t_2 = ending time of the time period for which long-term settlement of the layer is desired.

The total settlement of clay layer includes three portions: elastic settlement, primary consolidation settlement, and secondary consolidation settlement. These three types of settlement for clayey soil layers can be calculated from Equations 12.20, 12.22, and 12.23, respectively. The total settlement of clayey soil at point *i* can be determined from the equation

$$Z_i = (Z_e)_i + (Z_c)_i + (Z_\alpha)_i \tag{12.24}$$

where Z_i = total settlement of points *i*;
$(Z_e)_i$ = elastic settlement of point *i*;
$(Z_c)_i$ = primary consolidation settlement of point *i*;
$(Z_\alpha)_i$ = secondary consolidation settlement of point *i*.

ATTACHMENT III.7.B

CODUTO, DONALD P. 1998.
GEOTECHNICAL ENGINEERING PRINCIPLES AND PRACTICES.
NEW JERSEY: PRENTICE HALL.

Geotechnical Engineering

Principles and Practices

Donald P. Coduto

Professor of Civil Engineering
California State Polytechnic University, Pomona

PRENTICE HALL, Upper Saddle River, NJ 07458

where:

$(N_1)_{60}$ = corrected SPT N-value, as defined in Chapter 3

C_P = grain size correction factor

C_A = aging correction factor

C_{OCR} = overconsolidation correction factor

D_{50} = grain size at which 50 percent of the soil is finer (mm) as defined in Section 4.4

t = age of soil (time since deposition in years). If no age information data is available, use $t = 100$ yr.

OCR = overconsolidation ratio, as defined in Chapter 11. If no information is available to assess the OCR, use a value of 2.

q_c = cone resistance (kg/cm^2 or ton/ft^2), as defined in Chapter 3

Q_c = compressibility factor
= 0.91 for highly compressible sands
= 1.00 for moderately compressible sands
= 1.09 for slightly compressible sands
For purposes of solving this formula, a sand with a high fines content or a high mica content is "highly compressible," whereas a pure quartz sand is "slightly compressible."

σ_z' = vertical effective stress (lb/ft^2; kPa), as defined in Chapter 10

Many people confuse relative density with relative compaction. The latter is defined in Chapter 6. Although the names are similar, and they measure similar properties, these two parameters are numerically different. In addition, some people in other professions use the term "relative density" to describe what we call specific gravity! Geotechnical engineers should never use the term in this way.

Table 4.5 presents typical values of e_{min} and e_{max} for various sandy soils. These are not intended to be used in lieu of laboratory or in-situ tests, but could be used to check test results or for preliminary analyses.

TABLE 4.5 TYPICAL VALUES OF e_{min} AND e_{max} (Hough, 1969; Adapted by permission of John Wiley and Sons, Inc.)

Soil Description	e_{min} (dense)	e_{max} (loose)
Equal spheres (theoretical values)	0.35	0.92
Clean, poorly graded medium sand (Ottawa, Illinois)	0.50	0.80
Clean, fine-to-medium sand	0.40	1.0
Uniform inorganic silt	0.40	1.1
Silty sand	0.30	0.90
Clean fine-to-coarse sand	0.20	0.95
Micaceous sand	0.40	1.2
Silty sand and gravel	0.14	0.85

TABLE 11.3 TYPICAL CONSOLIDATION PROPERTIES OF SATURATED NORMALLY CONSOLIDATED SANDY SOILS AT VARIOUS RELATIVE DENSITIES (Adapted from Burmister, 1962)

Soil Type	$C_c / (1+e_0)$					
	$D_r = 0\%$	$D_r = 20\%$	$D_r = 40\%$	$D_r = 60\%$	$D_r = 80\%$	$D_r = 100\%$
Medium to coarse sand, some fine gravel (SW)		-	0.005	-		-
Medium to coarse sand (SW/SP)	0.010	0.008	0.006	0.005	0.003	0.002
Fine to coarse sand (SW)	0.011	0.009	0.007	0.005	0.003	0.002
Fine to medium sand (SW/SP)	0.013	0.010	0.008	0.006	0.004	0.003
Fine sand (SP)	0.015	0.013	0.010	0.008	0.005	0.003
Fine sand with trace fine to coarse silt (SP-SM)		-	0.011	-		-
Find sand with little fine to coarse silt (SM)	0.017	0.014	0.012	0.009	0.006	0.003
Fine sand with some fine to coarse silt (SM)		-	0.014	-		-

For saturated overconsolidated sands, $C_r / (1+e_0)$ is typically about one-third of the values listed in Table 11.3, which makes such soils nearly incompressible. Compacted fills can be considered to be overconsolidated, as can soils that have clear geologic evidence of preloading, such as glacial tills. Therefore, many settlement analyses simply consider the compressibility of such soils to be zero. If it is unclear whether a soil is normally consolidated or overconsolidated, it is conservative to assume it is normally consolidated.

Very few consolidation tests have been performed on gravelly soils, but the compressibility of these soils is probably equal to or less than those for sand, as listed in Table 11.3.

Another characteristic of sands and gravels is their high hydraulic conductivity, which means any excess pore water drains very quickly. Thus, the rate of consolidation is very fast, and typically occurs nearly as fast as the load is applied. Thus, if the load is due to a fill, the consolidation of these soils may have little practical significance.

However, there are at least two cases where consolidation of coarse-grained soils can be very important and needs more careful consideration:

1. Loose sandy soils subjected to dynamic loads, such as those from an earthquake. They can experience very large and irregular settlements that can cause serious damage. Kramer (1996) discusses methods of evaluating this problem.

ATTACHMENT III.7.C

SHARMA, HARI .D. AND SANGEETA P. LEWIS. 1994.
WASTE CONTAINMENT SYSTEMS, WASTE STABILIZATION
AND LANDFILLS: DESIGN AND EVALUATION.
NEW YORK: JOHN WILEY AND SONS.

WASTE CONTAINMENT SYSTEMS, WASTE STABILIZATION, AND LANDFILLS: DESIGN AND EVALUATION

HARI D. SHARMA, PH.D., P.E.
Chief Engineer and Director
EMCON Associates
San Jose, California

SANGEETA P. LEWIS, P.E.
Project Manager
CH_2M Hill
Oakland, California

A Wiley-Interscience Publication
JOHN WILEY & SONS, INC.
New York / Chichester / Toronto / Brisbane / Singapore

APPENDIX B

SETTLEMENT ANALYSES

Landfill settlement analyses include both foundation and refuse settlements. Foundation settlements are important in designing appropriately graded LCRSs, since these are typically gravity-flow systems. Refuse settlements are important in final cover design and estimating final landfill capacity. Estimating refuse settlements has also been critical in designing vertical landfill expansions and structures constructed on closed landfills.

Foundation settlement analyses for landfills follow the same principle as traditional geotechnical engineering settlement analyses. In this appendix we therefore focus on refuse settlements. For ease in reference, however, a brief discussion of foundation settlements is provided. The reader is referred to introductory geotechnical engineering textbooks if explanation is required on soil settlement and consolidation theories.

B.1 FOUNDATION SETTLEMENT

B.1.1 Mechanisms

For cohesive soils, settlement is characterized by the following three mechanisms:

- Immediate settlement following load application
- Consolidation settlements, which occur gradually as excess pore pressure caused by the applied loads are dissipated
- Secondary compression of the soil skeleton

Consolidation and secondary compression occur over several years and are theoretically never complete.

For granular soils, settlement is caused primarily by the compression of the soil skeleton as the particles rearrange due to the applied loads. Due to the relatively high permeability of granular soils, excess pore pressures induced by the applied load are assumed to dissipate in a very short period of time, and settlement is assumed to occur within a short period following load application; this is sometimes called immediate settlement.

B.1.2 Calculation of Settlement

For cohesive soils the total amount of consolidation settlement can be calculated using the following equation:

$$s=\Delta H=\frac{\Delta e}{1+e_0}H_t \tag{B.1}$$

where s = settlement
ΔH = change in height of layer
Δe = change in void ratio
e_0 = initial void ratio
H_t = layer thickness

Equation (B.1) can be modified as follows to suit the parameters obtained from a consolidation test:

$$s=\Delta H=\frac{C_c H_t}{1+e_0}\left(\log\frac{P_0+\Delta P}{P_0}\right) \tag{B.2}$$

where C_c = consolidation index or compression index
P_0 = initial stress
ΔP = change in stress

For an infinite layer of soil, the change in stress is relatively easy to calculate and is typically equal to the change in applied load or overburden. However, since most aboveground landfills may be considered embankment loads, the subsurface stress distribution may be calculated using the influence chart shown in Figure B.1 for embankments of infinite length (Osterberg, 1957; U.S. Dept. of the Navy, 1982).

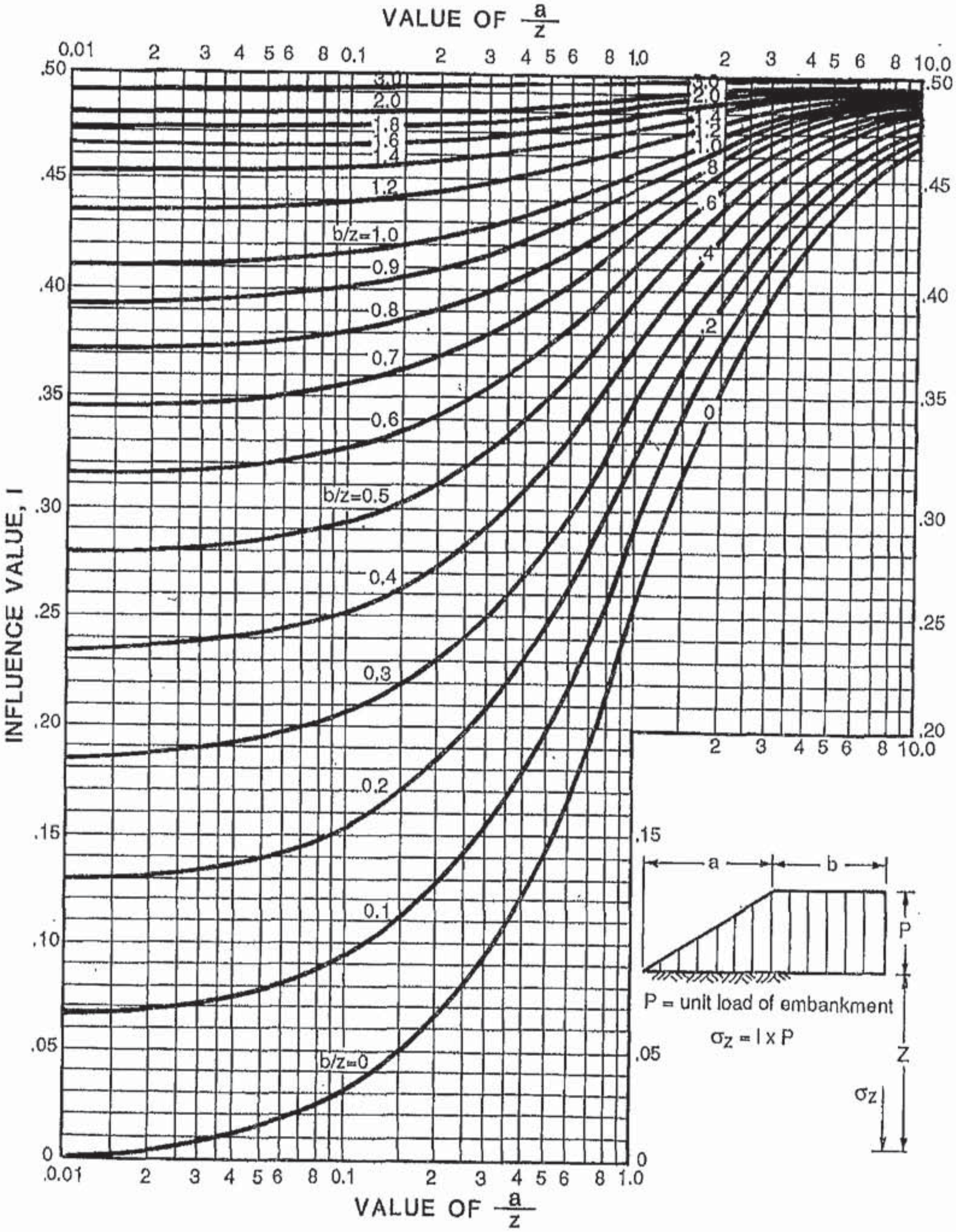

Figure B.1 Influence value for vertical stress under embankment load of infinite length. (From U.S. Dept. of the Navy, 1982.)

B.1.3 Liquefaction

B.1.3.1 Liquefaction Potential. In seismic regions, significant foundation settlements may also occur due to liquefaction of loose to medium-dense saturated cohesionless soils. Liquefaction is defined as a process where high shear deformations, typically induced by seismic activity, results in a progressive buildup of pore pressure. With limited drainage during the short period that the shear load is in-

TABLE OF CONTENTS

Section No. **Title** **Page**
1.0 INTRODUCTION III.8-1
  1.1 Facility Description III.8-1
2.0 DESIGN CRITERIA III.8-2
3.0 EVAPORATION POND DESIGN III.8-5
  3.1 Design Criteria III.8-5
  3.2 Design Concepts III.8-6
  3.3 Water Balance Modeling III.8-7
  3.4 Mechanical Evaporator Lateral Drift Analysis III.8-10
4.0 SUMMARY III.8-12

LIST OF FIGURES

Figure No. **Title** **Page**
III.8.1 WIND ROSE III.8-4
III.8.2 EVAPORATION POND WATER BALANCE FLOW DIAGRAM III.8-8
III.8.3 EVAPORATION POND MECHANICAL EVAPORATOR III.8-9
III.8.4 EFFECT OF HUMIDITY AND TEMPERATURE ON DRIFT III.8-14

LIST OF TABLES

Table No. **Title** **Page**
III.8.1 EVAPORATOR WATER BALANCE III.8-3
III.8.2 INFLUENCE OF DROPLET SIZE ON DRIFT DISTANCE III.8-11
III.8.3 LATERAL DRIFT AT VARIOUS WINDSPEEDS III.8-11
III.8.4 DRIFTSIM ANALYSIS RESULTS III.8-13

LIST OF ATTACHMENTS

Attachment No. **Title**
III.8.A EFFECTS OF MAJOR VARIABLES ON DRIFT DISTANCES OF SPRAY DROPLETS (OHIO STATE UNIVERSITY, 1998)
III.8.B DRIFTSIM®: PREDICTING DRIFT DISTANCE OF SPRAY DROPLETS AND RESULTING EVAPORATION

1.0 INTRODUCTION

Lea Land LLC (the Facility) is an existing Surface Waste Management Facility (SWMF) providing oil field waste solids (OFWS) disposal services. The existing Lea Land SWMF is subject to regulation under the New Mexico Oil and Gas Rules, specifically 19.15.9.711 and 19.15.36 NMAC, administered by the Oil Conservation Division (OCD) of the NM Energy, Minerals, and Natural Resources Department (NMEMNRD). This document is a component of the “Application for Permit Modification” that proposes continued operations of the existing approved waste disposal unit; lateral and vertical expansion of the landfill via the construction of new double-lined cells; and the addition of waste processing capabilities. The proposed Facility is designed in compliance with 19.15.36 NMAC, and will be constructed and operated in compliance with a Surface Waste Management Facility Permit issued by the OCD. The Facility is owned by, and will be constructed and operated by, Lea Land LLC.

The Lea Land SWMF is one of the most recently designed facilities to meet the new more stringent standards that, for instance, mandate double liners and leak detection for land disposal. The new services that Lea Land will provide needed resources to fill an existing void in the market for technologies that exceed current OCD requirements.

1.1 Site Location

The Lea Land site is located approximately 27 miles northeast of Carlsbad, straddling US Highway 62-180 (Highway 62) in Lea County, NM. The Lea Land site is comprised of a 642-acre ± tract of land encompassing Section 32, Township 20 South, Range 32 East, Lea County, NM. Site access is currently provided on the south side of US Highway 62. The coordinates for the approximate center of the Lea Land site are Latitude 32°31’46.77” and Longitude -103°47’18.25”.

1.2 Facility Description

The Lea Land SWMF comprises approximately 463 acres ± of the 642-acre ± site, and will include two main components: an oil field waste Processing Area and an oil field waste solids Landfill, as well as related infrastructure (i.e., access, waste receiving, stormwater management, etc.). Oil field wastes are delivered to the Lea Land SWMF from oil and gas exploration and production operations in southeastern NM and west Texas. The Permit Plans (**Attachment III.1.A**) identify the locations of the Processing Area and Landfill Disposal facilities. The proposed facilities are detailed in **Table**

II.1.2 (**Volume II.1**), and are anticipated to be developed in four primary phases as described in **Table II.1.3** (**Volume II.1**).

2.0 DESIGN CRITERIA

The Processing Area will include evaporation ponds for the disposal of Produced Water. The area and volume of the lined portion of each evaporation pond is 1.88 acres of water surface with a capacity of 9.5 acre-feet (ac-ft). Lea Land, LLC is considering the installation of approximately 12 ponds, which will provide a total of 18.80 surface acres for evaporation of 114 total acre-ft of pond capacity.

2.1 General Site Conditions

The site terrain is gently sloping toward the northwest with sparse vegetation. The macro-climate of the Lea Land, LLC area is classified by the Koppen Climate Classification System as a “BSk”, which indicates a semi-arid steppe with much of the characteristics of a desert. Meteorological climatic data was obtained from the Western Regional Climate Center for pan evaporation at Lake Avalon (north of Carlsbad) and precipitation at the Hobbs FAA Airport weather stations. The Hobbs climate summary provides a more conservative reporting point for this calculation than the Carlsbad weather station reported in other Parts of this Application.

The evaluation of climate data for these nearby weather stations indicates that they are relatively similar and will likely provide reasonable precipitation estimates for the site (**Table III.8.1**). Climatic data available for the Lake Avalon weather station includes pan evaporation for the years of record from 1914 through 1979. The Hobbs FAA Airport weather station includes precipitation for the years of record from 1942 through 2006. The Lake Avalon pan evaporation data was used to estimate monthly evaporation values at the Facility. The observed pan evaporation values were scaled by a factor of 0.7 to represent actual pond evaporation. The average monthly evaporation and precipitation data used for design of this Facility’s evaporation ponds is summarized in **Table III.8.1**. Considering this climatic data, the annual evaporation exceeds annual precipitation on average by over six times.

The predominant wind directions for the site are from the south/southeast, with an average annual wind speed of 11 miles per hour (mph). The maximum sustained wind speed conservatively used for facility design is 12 mph. **Figure III.8.1** is the Wind Rose from the Paduca weather station located approximately 24 miles south of the facility.

TABLE III.8.1 - Produced Water Evaporation Ponds - Evaporator Water Balance

All data in inches	January	February	March	April	May	June	July	August	September	October	November	December	Total
Rainfall	0.42	0.37	0.29	0.78	2.06	0.87	1.56	1.76	2.09	1.61	0.22	0.11	**12.14**
Pan Evaporation	4.49	5.33	9.42	12.36	14.31	15.16	14.14	12.33	9.25	7.26	4.68	4.2	**112.93**
Actual Evaporation	3.14	3.73	6.59	8.65	10.02	10.61	9.90	8.63	6.48	5.08	3.28	2.94	**79.05**
NET (Rainfall-Evaporation)	-2.72	-3.36	-6.30	-7.87	-7.96	-9.74	-8.34	-6.87	-4.39	-3.47	-3.06	-2.83	**-66.91**
Net Evaporation (bbl/pond)	3314	4090	7672	9580	9684	11856	10147	8362	5336	4225	3719	3444	81430

Mechanical Evaporation Analysis													
% Mech Evap Potential	30%	32%	44%	50%	50%	50%	50%	50%	44%	40%	35%	34%	
BBL/D@75GPM	386	411	566	643	643	643	643	643	566	514	450	437	
Assume 25% Mech Evap	25%	25%	25%	25%	25%	25%	25%	25%	25%	25%	25%	25%	
BBL/D@75GPM	321	321	321	321	321	321	321	321	321	321	321	321	
Evap Units Req:													
1000 bbl/Pond	3	3	3	3	3	3	3	3	3	3	3	3	
Phase I @3000 bbl	9	9	9	9	9	9	9	9	9	9	9	9	
Ultimate @9000 bbl	28	28	28	28	28	28	28	28	28	28	28	28	
bbl/day Factor of Safety (FS)	64	90	244	321	321	321	321	321	244	193	129	116	**224**
% FS	6%	9%	24%	32%	32%	32%	32%	32%	24%	19%	13%	12%	22%

Notes:

1. *Rainfall obtained from Hobbs FAA Airport and reports average monthly rainfall from 1942-2006.*
2. *Input is the maximum monthly Produced Water that can be introduces to Evaporation Ponds based on Water Balance.*
3. *Evaporation rates obtained from Lake Avalon, New Mexico from 1914 -1979.*
4. *Actual Evaporation rates represent 70% of reported Pan Evaporation rate.*
5. *% Mech Evap Potential is the expected mechanical evaporation rate (%) for the pan Evaporation Rate per TurboMist calculation criteria*
6. *Assume 25% Mech Evap is the mechanical evaporation rate (%) minimum expected from Resource West APEX 2.0 Evaporator*
7. *BBL/D@75GPM is the flow rate for the Resource West APEX 2.0 Evaporator (assumes 12HRS of operation/day)*
8. *1 BBL = 42 gallons (US, oil)*

STATION: PADUCA, NEW MEXICO
LATITUDE: 32° 10' 47" N
LONGITUDE: -103° 43' 18" W
ELEVATION: 3510 FT
ELEMENT: WIND SPEED

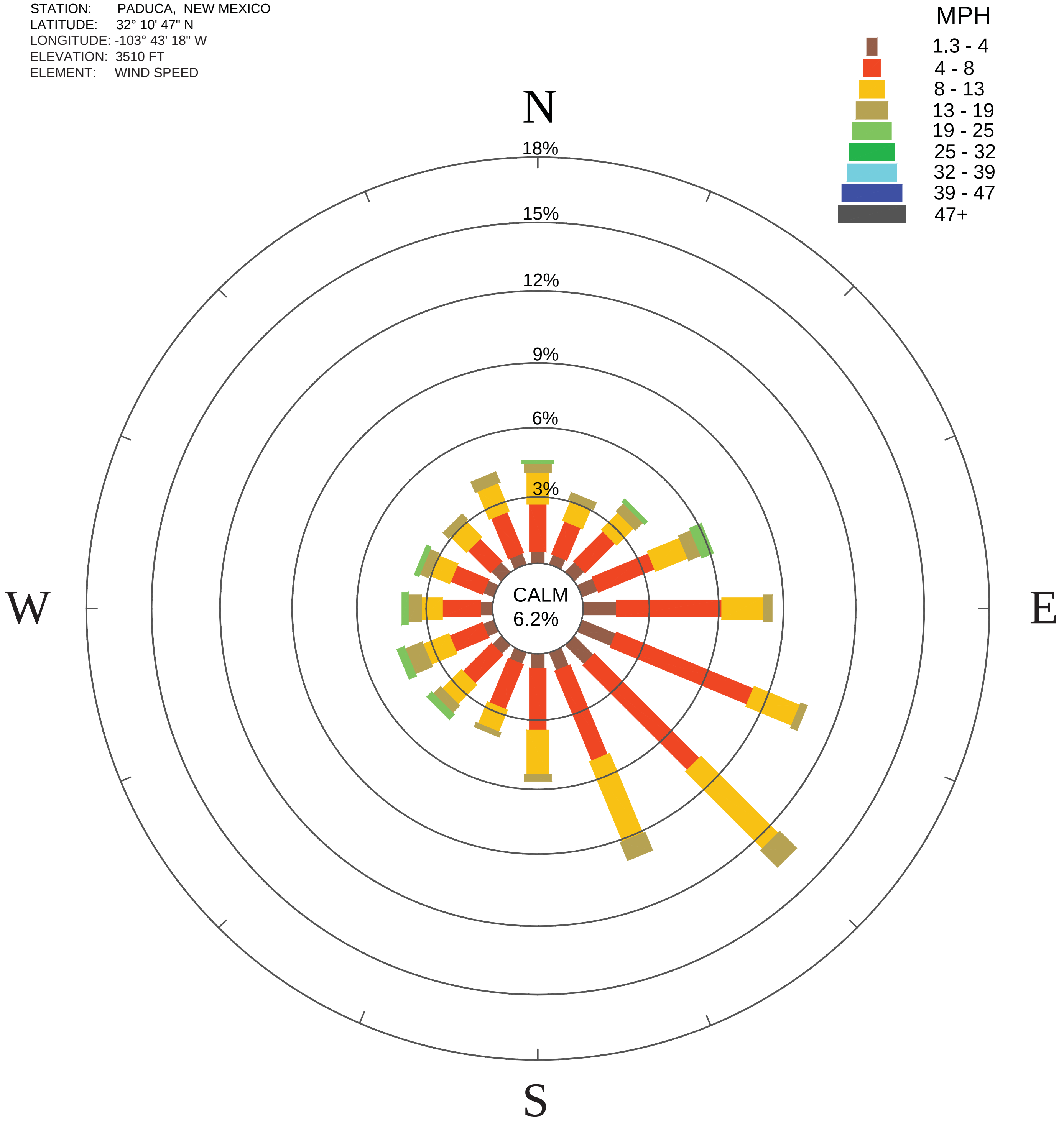

START DATE: DEC. 1, 2008
END DATE: DEC.31 2018
OF DAYS: 3683 OF 3683
OBS: Poss: 87196 of 88392
WESTERN REGIONAL CLIMATE CENTER

Drawing:X:\2018\0416.18\02_DSGN\02_DWG\050_CIVIL\02_CONTENT\PERMIT FIGURES\WINDROSE.dwg
Date/Time:Mar. 21, 2019-13:39:36 ; LAYOUT: A (P)

WIND ROSE

LEA LAND LLC SURFACE WASTE MANAGEMENT FACILITY
LEA COUNTY, NEW MEXICO

GORDON ENVIRONMENTAL PSC

333 Rio Rancho Blvd. NE
Rio Rancho, NM 87124
Phone: 505-867-6990
Fax: 505-867-6991

DATE: 03/14/2019	CAD: WINDROSE.dwg	PROJECT #: 0416.18
DRAWN BY: DMI	REVIEWED BY: CRK	FIGURE III.8.1
APPROVED BY: CWF	www.team-psc.com	

3.0 EVAPORATION POND DESIGN

This section provides the engineering analyses and technical details to support design of the evaporation ponds for the Lea Land SWMF with an average evaporation rate of 1,000 bbl per pond per day. The purpose of the design is to maintain potential drift (i.e., mist) within the pond boundary.

3.1 Design Criteria

3.1.1 Design Regulations

Regulations relevant to the design of the evaporation ponds presented here in Section 3.0 are summarized below.

Key Regulatory Agencies and Documents:

New Mexico Oil Conservation Division (OCD): Title 19 Natural Resources and Wildlife, Chapter 15 Oil and Gas, Part 36 Surface Waste Management Facilities, Section 17 Specific Requirements Applicable to Evaporation, Storage, Treatment and Skimmer Ponds, specifically B(12) which indicates that "*The maximum size of an evaporation or storage pond shall not exceed 10 acre-feet*".

New Mexico Office of the State Engineer (NMOSE): Title 19 Natural Resources and Wildlife, Chapter 25 Administration and Use of Water – General Provisions, Part 12 Dam Design, Construction and Dam Safety, Section 7 Definitions, D. (1) Dams, (a) Jurisdictional Dam which indicates that "*A dam 25 feet or greater in height, which impounds more than 15 acre-feet of water or a dam that impounds 50 acre-feet or more of water and is 6 feet or greater in height."* (b) Non-jurisdictional dam which indicates that *"Any dam not meeting the height and storage requirements of a jurisdictional dam."* exempting this facility's structures from this rule.

3.1.2 Project Design Criteria

Design criteria relevant to the analyses presented here in Section 3.0 are summarized below.

Geometry:

Process Operations: Design evaporation capacity of 1,000 barrels per day (bbl/d) of produced water per pond, with potential expansion capacity to 9,000 bbl/d.

Evaporation Pond Storage Capacity: Less than 10 acre-ft per pond, with potential expansion to 12 ponds. Developing an ultimate pond design configuration resulted in a 9.5 acre-foot pond capacity with a surface water area of 82,000 square feet (sq ft) and measuring 420 ft x 200 ft.

Maximum Evaporative Surface Area: for twelve ponds would be 984,000 square ft or 18.8 acres.

Process Design Life: 50 years.

Produced Water Properties:

Design Volumetric Flow Rate: 9,000 bbl/d or 263 gallons per minute (gpm).

System Requirements:

Evaporation Pond Liner System: Double layer liner system as follows (top to bottom): (1) upper (primary) 60 mil conductive smooth HDPE geomembrane liner; (2) leak detection system consisting of a 200 mil HDPE geonet; (3) lower (secondary) 60 mil smooth HDPE geomembrane liner; underlain by (4) a 6-inch thick density controlled compacted subgrade.

Leak Detection System: The leak detection system will meet the following requirements:(1) constructed with a bottom slope of at least two percent; (2) constructed with a 200 mil HDPE geonet with a transmissivity of $1x10^{-3}$ m^2/sec or greater; (3) constructed of materials that are chemically resistant to the waste and leachate; (4) designed and operated to minimize clogging during the active life; and (5) constructed with sumps and liquid removal methods (i.e., pumps).

3.2 Design Concepts

This section presents the general evaporation pond design concepts with the technical aspects discussed in detail in the following sections. The design of the Lea Land SWMF evaporation ponds shown on Figures and Permit Plans is preliminary; and construction plans and specifications for each major element will be submitted to OCD in advance of installation.

The Lea Land SWMF is designed for start-up operations at 3,000 bbl/d routinely, with a potential to expand to 9,000 bbl/d on average. The design produced water flows from the Produced Water Tanks will be discharged to the evaporation ponds. The average design flow rates associated with the start-up and ultimate production rates are 88 and 263 gallons per minute (gpm), respectively.

The evaporation pond system is designed for construction in phases. Phase I includes a single row of 3 ponds, each with a surface dimension of 420 ft by 200 ft (i.e. 1.88 acres), designed to evaporate the inflows associated with the average receipt of 3,000 bbl/d. Similarly, Future Phases will include an additional 9 ponds with the same dimensions designed to evaporate the flows associated with an additional 6,000 bbl/d of produced water received daily (for a total of 9,000 bbl/day). All ponds are designed and constructed to provide contingency storage with additional freeboard (above the required design capacities). Pond berms with a minimum crest width of 15 ft are designed between ponds to allow access to all sides of the ponds, as well as operation and maintenance of the evaporation equipment. Two leak detection system (LDS) sumps have been included in the design of each evaporation pond. Liquids collected in the LDS sumps will be pumped using a mobile pump. Upon sampling and if necessary, test of the LDS liquids, they will be returned to the evaporation ponds.

In order to improve performance of the evaporation pond system (i.e., enhance the evaporative capabilities), the design includes implementation of a mechanical evaporation system. The evaporators will be placed and sized to maximize evaporation and minimize the potential for wind-drift beyond the extents of the lined evaporation pond area.

3.3 Water Balance Modeling

A probabilistic water balance model was developed to assist in determining the evaporation potential of the pond system (i.e., required evaporative surface area). Water balance calculations were performed to compare precipitation vs. evaporation (See **Table III.8.1**).

The following water balance components were considered:

- the amount of Produced Water entering the pond system from the Produced Water Tanks
- water entering the pond system through meteoric precipitation
- the amount of water released to the atmosphere through evaporation

Precipitation values are likely to exhibit the largest variations, and were therefore treated as stochastic inputs (i.e., probabilistic), while the other parameters were treated as deterministic variables. **Figure III.8.2** presents the process flow diagram for the evaporation pond water balance.

Preliminary analyses revealed a prohibitively large evaporation area for extreme precipitation events when considering evaporation losses solely from the pond surface. To reduce the required evaporative area, subsequent analyses included a mechanical evaporation system resulting in enhanced evaporation losses. All evaporators will be located at points within the ponds (as depicted in **Figure III.8.3**) or as recommended by the equipment supplier to optimize evaporation, and operated to minimize the probability of wind-drift blowing the produced water beyond the lined evaporation pond area.

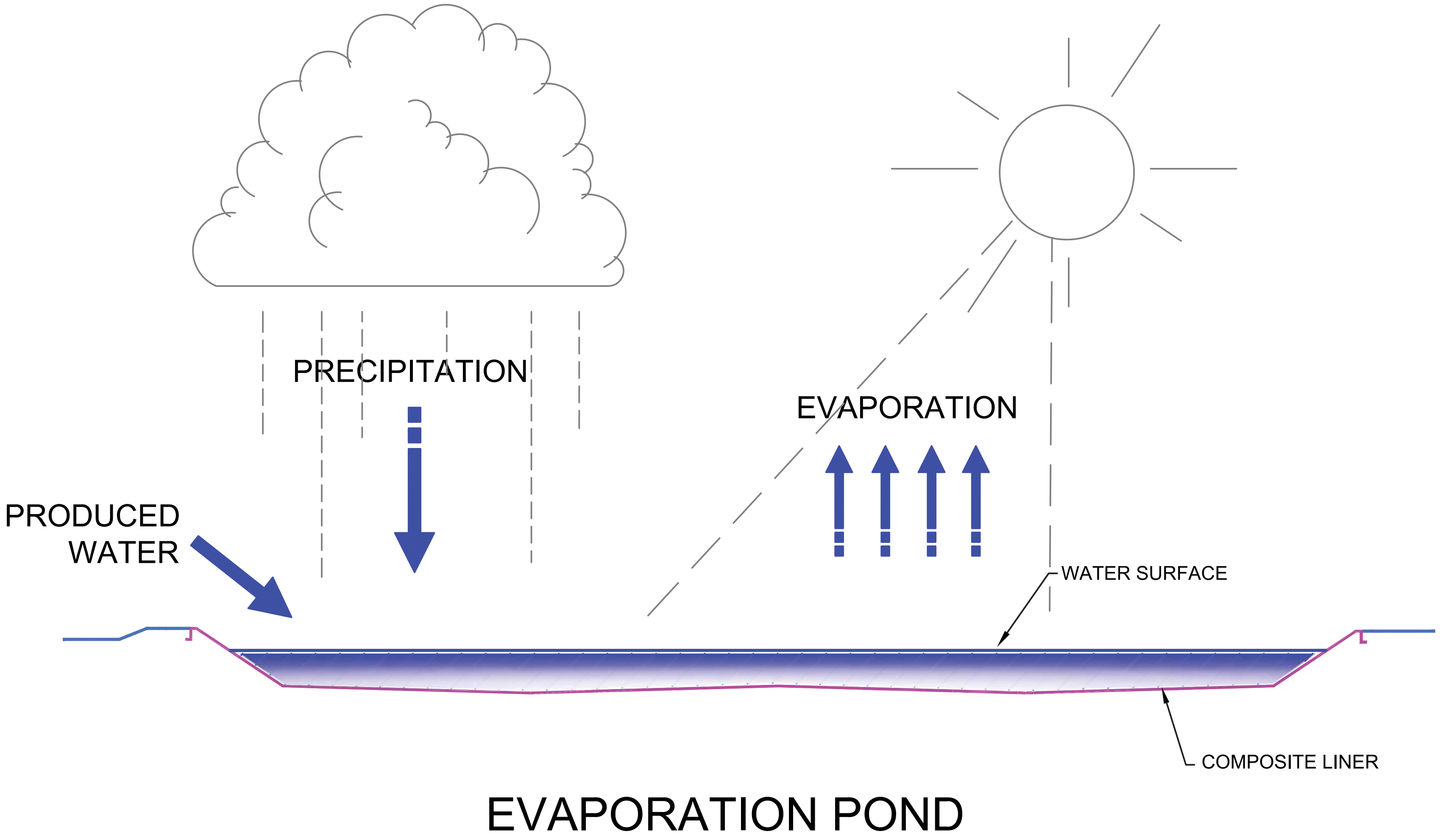

EVAPORATION POND WATER BALANCE FLOW DIAGRAM

LEA LAND LLC SURFACE WASTE MANAGEMENT FACILITY
LEA COUNTY, NEW MEXICO

GORDON ENVIRONMENTAL PSC

333 Rio Rancho Blvd. NE
Rio Rancho, NM 87124
Phone: 505-867-6990
Fax: 505-867-6991

DATE: 01/08/2019	CAD: EVAPORATION BAL.dwg	PROJECT #: 0416.18
DRAWN BY: DMI	REVIEWED BY: CRK	FIGURE III.8.2
APPROVED BY: CWF	www.team-psc.com	

Drawing:X:\2018\0416.18\02_DSGN\02_DWG\050_CIVIL\02_CONTENT\PERMIT FIGURES\EVAPORATION.dwg
Date/Time:Mar. 21, 2019-13:47:05 ; LAYOUT: A (LS)

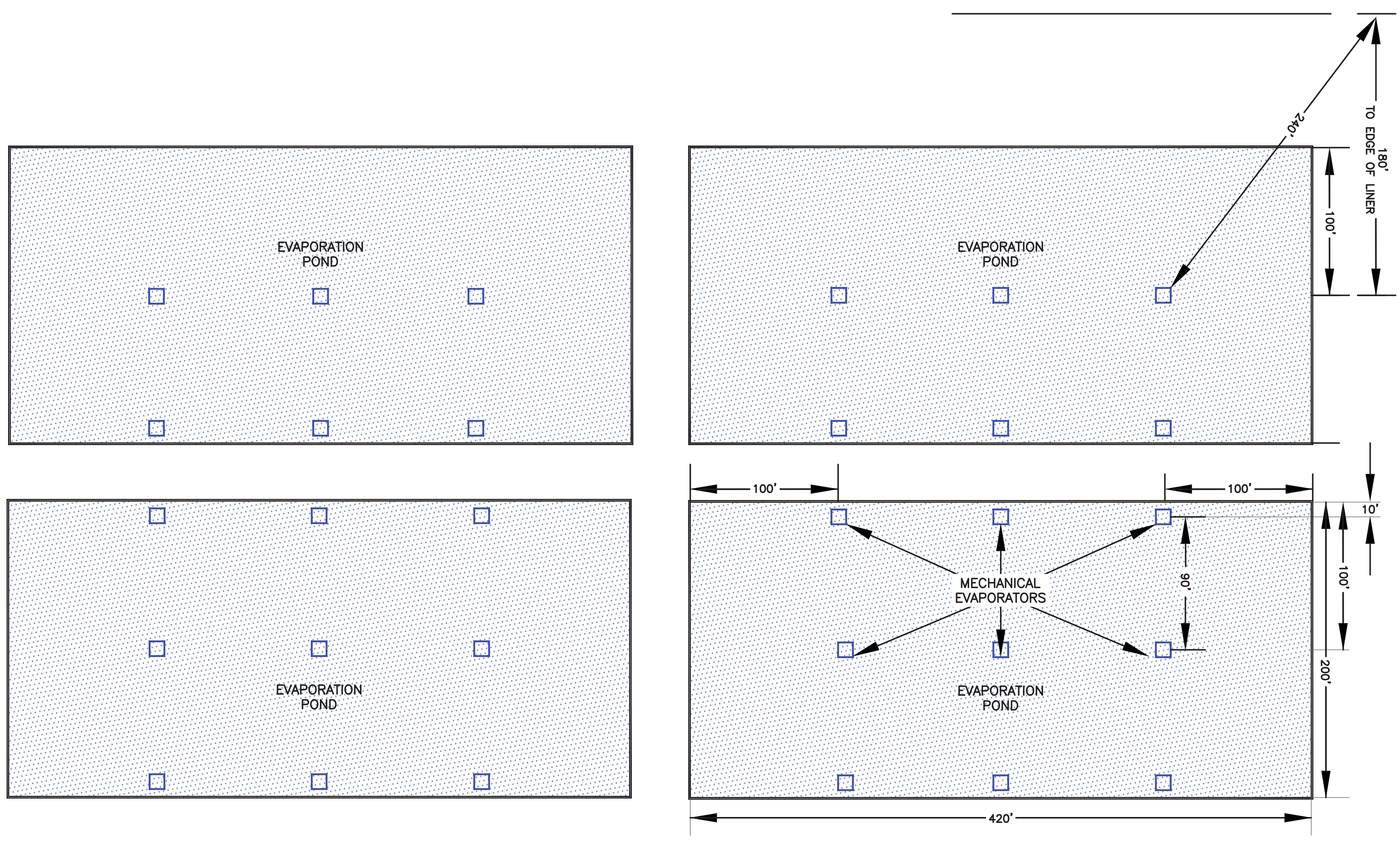

Drawing:X:\2018\0416.18\02_DSGN\02_DWG\050_CIVIL\02_CONTENT\PERMIT FIGURES\RAI1\EVAP POND MECH EVAPORATORS.dwg
Date/Time:Jun. 03, 2019-09:55:56

EVAPORATION POND
MECHANICAL EVAPORATORS

LEA LAND LLC SURFACE WASTE MANAGEMENT FACILITY
LEA COUNTY, NEW MEXICO

GORDON ENVIRONMENTAL PSC

333 Rio Rancho Blvd. NE
Rio Rancho, NM 87124
Phone: 505-867-6990
Fax: 505-867-6991

DATE: 01/08/2019	CAD: MECHANICAL EVAP.dwg	PROJECT #: 0416.18
DRAWN BY: DMI	REVIEWED BY: CRK	FIGURE III.8.3
APPROVED BY: CWF	www.team-psc.com	

The results of the water balance for each pond were calculated assuming the average annual rainfall and the percentage of an average day when the wind speed is under 12 mph. The mechanical evaporators will be operating; limiting the flow rate to 10 gpm flow rate through the evaporators (even though extensive experience with this equipment indicates a greater evaporative expectation); and an input of 1,000 bbl/d of Produced Water. Based on these assumptions, the required number of mechanical evaporators per pond to evaporate 1,000 bbl/d is estimated to be three. The conservative assumption was made to discount the surface evaporation potential from the pond due to the micro-climate created by the mechanical evaporators. **Table III.8.1** details the evaporation potential per pond and identifies the additional evaporation potential that may be available based on extensive industry experience with this technology.

The influence of dissolved solids in the process water flow to the evaporation ponds may affect pond evaporation. It will be important to collect field evaporation measurements during the early years of pond operations to confirm the adequacy of this initial design. These field measurements will assist in refining expansion design potential of the evaporation ponds for an increase to 9,000 bbl/d average.

3.4 Mechanical Evaporator Lateral Drift Analysis

The proposed mechanical evaporators were analyzed for drift potential to ensure that all of the mist generated in the evaporation process would remain within the area of the lined ponds. The objective of this analysis was to determine the distance that the suspended solids would fall out with a given wind speed, droplet diameter and known level of Total Suspended Solids (TDS).

The higher the TDS the less lateral distance traveled and time the water droplet spends suspended in the air. For this analysis an 8% total TDS saturation was assumed. The proposed mechanical evaporator makes water droplet particle sizes of approximately 150 microns. This analysis assumes a droplet particle size of 150 microns for the drift calculations. Based on **Table III.8.2** the distance required for a 150 micron particle size to fall 10 feet, is 10 seconds in a 3 mph wind and 39 feet from the evaporator discharge. Note that most newer evaporators use reverse air flow discharging the particles closer to the surface. To be conservative, the calculations assume upward discharge.

TABLE III.8.2 - Influence of Droplet Size on Potential Drift Distance

Droplet Diameter (Microns)	**Type of droplets**	**Time required to fall 10 feet**	**Lateral distance Droplets travel in falling 10 feet in a 3 mph wind**
5	Fog	66 minutes	3 miles
20	Very fine spray	4.2 minutes	1,100 feet
100	Fine spray	10 seconds	44 feet
150	**Evaporator Standard**	**9 seconds**	**39 feet**
240	Medium spray	6 seconds	28 feet
400	Course spray	2 seconds	8.5 feet
1,000	Fine rain	1 second	4.7 feet

Klingman, Glenn. 1961. Weed Control as a Science. John Wiley and Sons, New York, p. 67.

The proposed upward discharge mechanical evaporator propels the water droplets 15 feet in the air, resulting in a 15 feet anticipated fall height for the water droplet particles generated. In this 3 mph wind the water droplet could drift 39 ft before falling back into the pond. Drift particles can travel up to 17 feet per mph in a strong wind (<12 mph). **Table III.8.3** provides a summary of anticipated lateral drift at different wind speeds for 150 micron water droplets falling from a height of 15 feet.

TABLE III.8.3 - Lateral Drift at Various Windspeeds

Wind Speed MPH	**Lateral Drift**
2 MPH	39 ft
4 MPH	78 ft
6 MPH	117 ft
8 MPH	156 ft
10 MPH	195 ft
12 MPH	234 ft
14 MPH	273 ft

An analysis was performed with DRIFTSIM®, a computer modeling program (**Attachment III.8.B**) that predicts the drift distance of spray droplets. This program was developed by Ohio State University, Food Agriculture, and Biological Engineering Department in coordination with the United States Department of Agriculture, Agricultural Research Service. The results from this model, utilizing a low TDS liquid (assuming greater drift), a 12-mph maximum wind speed (maximum average sustained wind speed onsite) and variable humidity's at various temperatures confirmed that based on the anticipated 150 micron droplet size, all lateral drift will fall back into the lined pond area. **Table III.8.4** and **Figure III.8.4** provide a summary of the output from this analysis.

The majority of the strong winds at this location originate from the south/southeast direction (see **Figure III.8.1**). Given the layout of the evaporation ponds, the proposed mechanical evaporators could operate in wind conditions up to 14 mph before the automation would need to shut the machines down relative to concerns that drift might escape the lined pond area.

The mechanical evaporators will be controlled by a weather station with software designed to monitor wind speed; and to control (start and stop) the equipment to optimize evaporation hours and to minimize the potential for freezing during cold periods. This weather station will independently control each evaporator relative to wind speed and direction to minimize the potential for overspray and drift on windy days.

4.0 SUMMARY

The proposed evaporation ponds with mechanical evaporators will be able to evaporate the proposed volumes of Produced Waters that are anticipated for receipt in the various phases of this facility's development. The potential for drift can be managed to ensure that all materials remain within the lined area of the evaporation ponds. The phasing of evaporation pond installation will be based on the rates of Produced Water receipts, the characteristics of the material (e.g., TDS), and the observed efficacy of existing installations.

TABLE III.8.4 - DRIFTSIM Analysis Results (12 MPH Wind)

Temp	Drop Diameter	Humidity	Drift
50	150	10	84
50	150	20	79
50	150	30	79
50	150	40	78
50	150	50	77
50	150	60	77
50	150	70	77
50	150	80	75
50	150	90	75
50	150	100	74
60	150	10	85
60	150	20	82
60	150	30	82
60	150	40	81
60	150	50	80
60	150	60	79
60	150	70	79
60	150	80	77
60	150	90	76
60	150	100	75
70	150	10	86
70	150	20	84
70	150	30	84
70	150	40	83
70	150	50	82
70	150	60	80
70	150	70	80
70	150	80	78
70	150	90	76
70	150	100	75
80	150	10	94
80	150	20	92
80	150	30	92
80	150	40	90
80	150	50	88
80	150	60	86
80	150	70	84
80	150	80	82
80	150	90	79
80	150	100	76

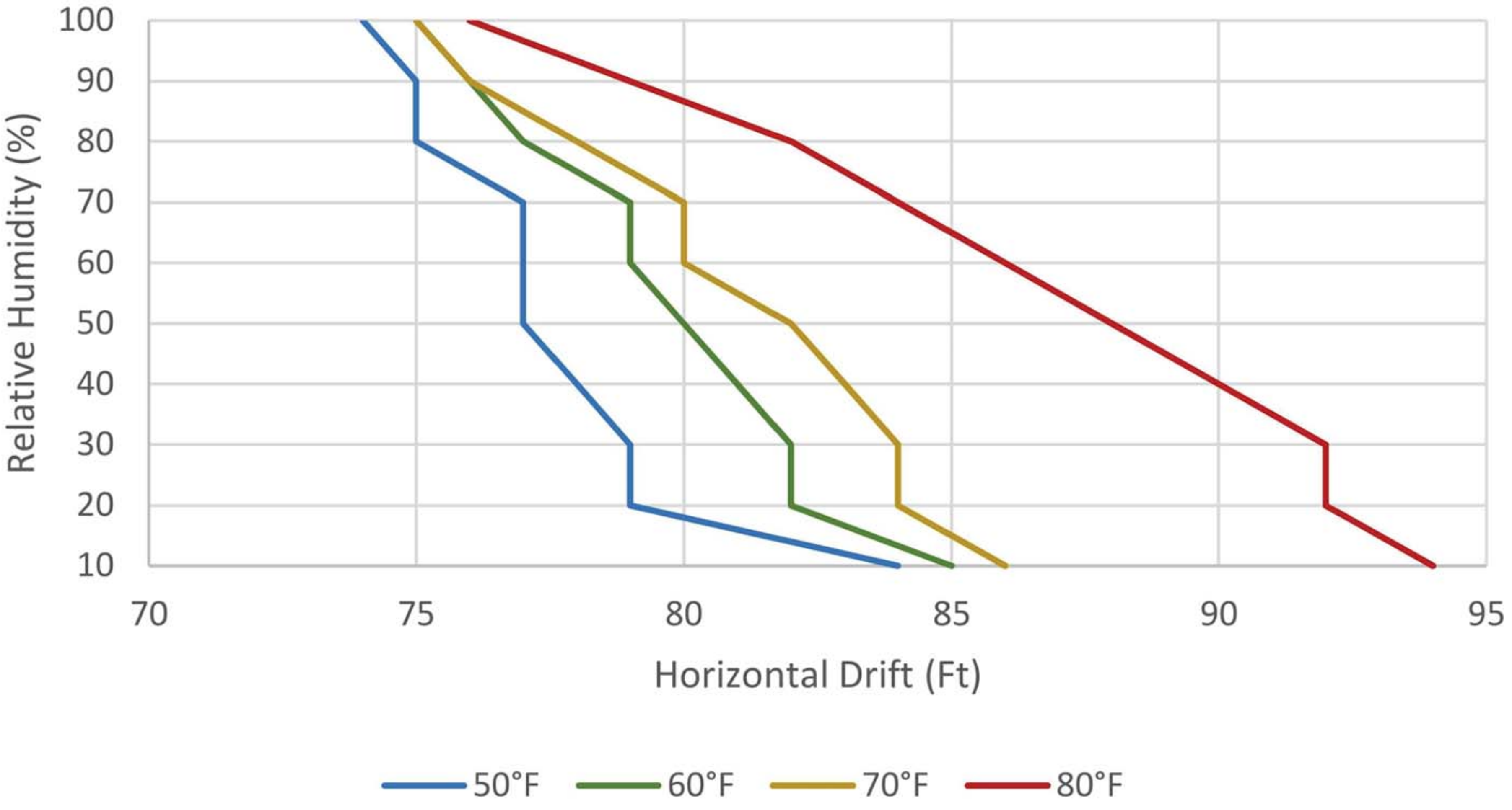

EFFECT OF HUMIDITY AND TEMPERATURE ON DRIFT

LEA LAND LLC SURFACE WASTE MANAGEMENT FACILITY
LEA COUNTY, NEW MEXICO

GORDON ENVIRONMENTAL PSC

333 Rio Rancho Blvd. NE
Rio Rancho, NM 87124
Phone: 505-867-6990
Fax: 505-867-6991

DATE: 01/08/2019	CAD: DRIFT GRAPH.dwg	PROJECT #: 0416.18
DRAWN BY: DMI	REVIEWED BY: CRK	FIGURE III.8.4
APPROVED BY: CWF	www.team-psc.com	

Drawing:X:\2018\0416.18\02_DSGN\02_DWG\050_CIVIL\02_CONTENT\PERMIT FIGURES\DRIFT GRAPH.dwg
Date/Time:Mar. 21, 2019-13:55:19

ATTACHMENT III.8.A

EFFECTS OF MAJOR VARIABLES ON DRIFT DISTANCES OF SPRAY DROPLETS (OHIO STATE UNIVERSITY, 1998)

ohioline.ag.ohio-state.edu -- your Link to Information, News, and Education

FactSheet Extension

Ohio State University Extension Fact Sheet

Food, Agricultural, and Biological Engineering

590 Woody Hayes Drive, Columbus, Ohio 43210

Effect of Major Variables on Drift Distances of Spray Droplets

AEX-525-98

Author

H. Erdal Ozkan
Professor
The Ohio State University
Food, Agricultural and Biological Engineering Department
590 Woody Hayes Drive
Columbus, OH 43210

Pesticide applications are required to ensure an adequate and high quality supply of many agricultural crops. Due to concerns for production costs, safety, and the environment, it is important to maximize the pesticide deposit on the target. One of the major problems challenging pesticide applicators is spray drift, which is defined as movement of pesticides by wind from the application site to an off-target site.

Spray drift occurs wherever liquid sprays are applied. Although complete elimination of spray drift is impossible, problems can be reduced significantly if the pesticide applicator is aware of major factors which influence drift, and takes precautions to minimize their influence on off-target movement of droplets.

Drift is influenced by many factors that usually may be grouped into one of the following categories: 1) Spray characteristics, 2) Equipment and application techniques used, 3) Weather, and 4) Operator care and skill. A general discussion of these factors can be found in another publication by Ozkan (1991). In this publication, you will find specific information on how much influence some of these major factors have on the drift distances of spray droplets.

The factors that significantly influence off-target movement of droplets are wind velocity and direction, droplet size and density, and distance from the atomizer to the target. Other factors that influence drift include droplet velocity and direction of discharge from the atomizer, volatility of the spray fluid, relative humidity, ambient temperature, and atmospheric turbulence intensity. Many scientists have conducted field tests to study influence of these variables on spray drift. Unfortunately, field tests have the limitation that weather conditions cannot be controlled and the variables that influence spray drift may interact and vary during a test. Computer simulations can allow determination of the effects of different values of variables such as droplet size and velocity, relative humidity, and wind velocity on spray drift. One such computer model was developed by Reichard et al.(1992a) in Ohio for modeling the effects of several variables on spray drift. Using the computer program, individual or mean droplet trajectories were determined for different values of several variables listed above. Experiments were also conducted to verify the accuracy of the computer model in predicting drift distances of water droplets in a wind tunnel. These tests revealed that the computer model can be used to accurately calculate spray drift distances for a wide range of spray droplet sizes and wind velocities (Reichard et. al., 1992b).

The major drift factors included in this publication are droplet size, wind velocity, relative humidity, ambient temperature, droplet discharge height, and initial droplet velocity. Although turbulence intensity is a major factor which influence drift, data related to this variable was not included in this publication because it is not something pesticide applicators can assess easily, and its magnitude can vary rapidly unlike the changes in other atmospheric conditions such as relative humidity and temperature. The affect of turbulence intensity on drift distances of droplets is discussed in the publication by Reichard et. al. (1992a). A turbulence intensity of 20% was assumed for all the computer simulation results reported in this publication,.

Although the accuracy of the drift data produced by computer simulation has been validated, one has to be cautious when drawing conclusions from the data presented in this publication. Due to the many variables that influence spray drift, it is extremely difficult to precisely predict drift distances of droplets for field conditions. Some of the variables that affect drift distances, such as wind turbulence, velocity and direction can vary considerably while a droplet is drifting. It is common for terrain and vegetation (size and density) to vary over the path of a drifting droplet and these influence local wind velocity and direction. The drift distance data presented in this publication are only valid for the constant conditions specified. The data presented are useful in comparing the relative effects of several factors on drift distances, but are not intended to precisely model variable field conditions.

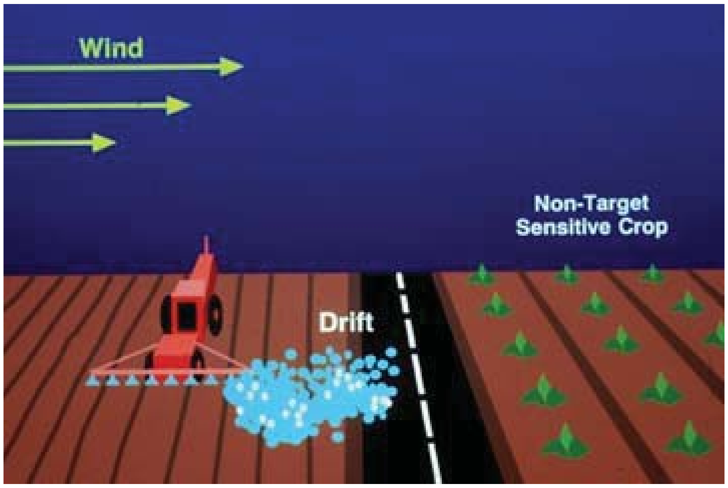

Spray drift is the reason for the discoloration of part of the wheat crop shown in this photograph. The size of the area affected by drift and its severity depend on how adverse the weather conditions are and poor decisions made by the operator of the sprayer.

Droplet Size, Wind Velocity and Relative Humidity

Droplet size and wind velocity are the two most influential factors affecting drift. Relative humidity influences the evaporation rate of a droplet and hence its size, flight time, velocity and drift distance. Table 1 and Figure 1 show the simulated mean drift distances for various sizes of water droplets (50-200 micron diameter), wind velocities (2-8 mph), relative humidities (20-80%), and 75 degrees F ambient temperature. (Additional data are included in Tables in the publication by Zhu et al., 1994). Unless otherwise indicated, all simulated drift distances discussed in this publication are for droplets discharged downward with 65 ft/second (45 mph) velocity toward a target 18 inches below the point of discharge.

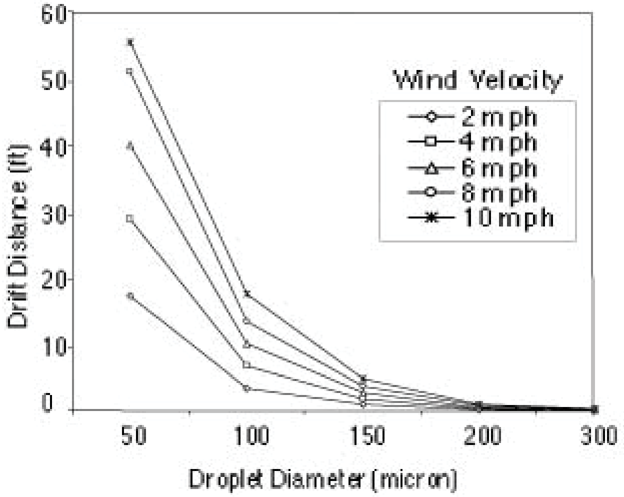

Figure 1. Effect of droplet diameter and wind velocity on drift distances of water droplets directed downward at 65 ft/second toward a target 18 inches below disharge point (Temperature = 75 degrees F; Relative Humidity = 60%).

Table 1. Effect of wind velocity and relative humidity on drift distances of droplets directed downward with initial velocity of 65 ft/second toward target 18 inches below discharge point. (Temperature = 75 degrees F; turbulence intensity = 20%)

Initial droplet size (microns)	Wind velocity (mph)	20	40	60	80
20	2	3.03*	3.72*	6.41*	15.29*
20	4	6.00*	6.47*	10.24*	21.45*
20	6	6.57*	7.66*	11.87*	23.23*
20	8	7.96*	8.97*	13.29*	26.42*
20	10	8.99*	10.58*	15.06*	30.10*
50	2	10.70*	12.10	17.20*	25.30*
50	4	18.70*	21.00*	28.80*	41.70*
50	6	26.50*	30.00*	40.00*	55.60*
50	8	34.30*	38.20*	50.90*	69.00*
50	10	37.60*	42.00*	55.32*	87.24*
100	2	3.44	3.41	3.37	3.30
100	4	6.87	6.81	6.71	6.58
100	6	10.30	10.20	10.05	9.85
100	8	13.72	13.61	13.39	13.14
100	10	17.94	17.77	17.48	17.05
150	2	0.92	0.92	0.92	0.91

150	4	1.83	1.82	1.82	1.82
150	6	2.74	2.74	2.73	2.71
150	8	3.67	3.66	3.62	3.60
150	10	4.78	4.78	4.75	4.77
200	2	0.20	0.20	0.20	0.20
200	4	0.38	0.38	0.38	0.38
200	6	0.55	0.55	0.55	0.55
200	8	0.75	0.75	0.75	0.75
200	10	0.96	0.96	0.96	0.96
300	2	0.05	0.05	0.05	0.05
300	4	0.10	0.10	0.10	0.10
300	6	0.15	0.15	0.15	0.15
300	8	0.21	0.21	0.21	0.21
300	10	0.26	0.26	0.26	0.26
* Droplet completely evaporated before deposition.					

Water droplets with 50 micron diameter and smaller are highly susceptible to drift. All droplets 50 micron diameter and smaller completely evaporated before they reached 18 inches below point of discharge for wind velocities between 2.0 and 10.0 mph and relative humidities (RH) between 20 and 80% (Table 1). The mean drift distances of small droplets increased rapidly with increased wind velocity. For example, with 60% RH, 50 micron diameter droplets were displaced 17.2, 28.8, 40.0, 50.9, and 55.3 ft before they completely evaporated when wind velocities were 2, 4, 6, 8, and 10 mph, respectively.

The mean drift distances of 50 micron diameter water droplets and smaller increased with increased relative humidity because high relative humidity increased the lifetimes of the volatile droplets. Although both evaporated completely before deposition, the mean drift distances of 50 micron diameter droplets were greater than for 20 micron diameter droplets with the same relative humidity and wind velocity. This occurs because 50 micron diameter droplets have 15.6 times more volume and hence longer life than 20 micron diameter droplets. With 10 mph wind velocity and 60% RH, 20 and 50 micron diameter droplets drifted 15.1 and 55.3 ft downwind from the discharge point, respectively.

Most nozzles used for applying pesticides produce a large portion of the spray volume in 100 micron diameter droplets and larger. For example, our measurements of spray droplets from an XR 8002 VS nozzle (Spraying Systems Co., Wheaton, IL 60189) with 0.2 gpm flow rate when operated at 40 psi indicated that about 75% of the total spray volume was in droplets 100 micron diameter and larger. Computer simulation results indicate that all 100 micron and larger diameter water droplets reached 18 in below point of discharge at wind velocities up to 10 mph regardless of the relative humidity. However, due to affecting the evaporation rate, and hence droplet size, relative humidity significantly influenced the drift distances of 50 micron diameter droplets before they evaporated. With wind velocity of 10 mph, the mean drift distances of 50 micron diameter water droplets increased from 37.6 to 87.2 ft as relative humidity increased from 20% to 80%.

Data in Table 1 indicate that drift distances of droplets 200 micron diameter and larger are much less than for 100 micron diameter. For example, with 10 mph wind velocity and 60% RH, the mean drift distance of 100 micron diameter droplets was about 18 times that of 200 micron diameter droplets (0.96 ft versus 17.48 ft). The mean drift distances of 200 micron diameter droplets were 0.20, 0.38, 0.55, 0.75, and 0.96 ft for wind velocities of 2, 4, 6, 8, and 10 mph, respectively. Relative humidity over a range of 20-80% had very little influence on the drift distances of 200 micron diameter droplets. The mean drift distances of all droplets 200 micron diameter and larger did not exceed 0.96 ft with wind velocities up to 10.0 mph.

Figure 1 illustrates the effect of water droplet size (50-300 micron diameter) on mean drift distance for wind velocities of 2.0, 4.0, 6.0, 8.0, and 10.0 mph, and 60% RH at 75 degrees F. All droplets 100 micron diameter or larger reached 18 in below point of discharge and deposited. The mean drift distances of the droplets increased with increased wind velocity but decreased as initial droplet size increased. The amount of droplet displacement that can be tolerated depends on several factors including the crop and surrounding area, and the pest control agent. If the target is a row crop that is sprayed from a nozzle centered over each row, then small amounts of droplet displacement by wind can result in large portions of the spray missing the target. It is also common for gusts with velocities two or more times the mean wind velocity to occur while spraying. Figure 1 indicates that drift is far less likely to be a problem when spraying with 200 micron diameter and larger droplets.

Figure 2 illustrates the simulated effect of wind velocities up to 10.0 mph on the mean drift distances for 100, 150, 200, and 300 micron diameter water droplets at 60% RH. Figure 2 and Table 1 both indicate that the influence of wind velocity on drift distance increases as droplet size decreases. Figure 2 shows that there is a nearly linear relationship between mean drift distance and wind velocity for each droplet size. The rate of change in drift distance with change in wind velocity was much greater for 100 than 200 micron diameter droplets. For example, over a range of 2 to 10 mph wind velocity the drift distances of 100 and 200 micron diameter droplets increased 1.8 and 0.01 ft per mph increase in wind velocity respectively.

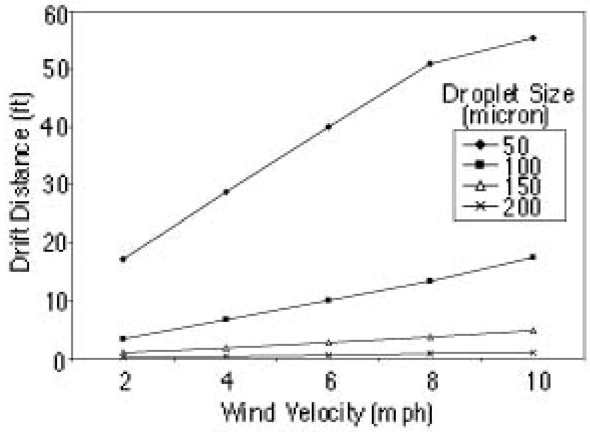

Figure 2. Effect of wind velocity and droplet diameter on drift distances of water droplets directed downward at 65ft/second toward a target 18 inches below discharge point (temperature = 75 degrees F; Relative Humidity = 60%).

Some spray carriers are oil or nonvolatile liquids. If the nonvolatile droplet density is close to the density of water, drift distances would be similar to drift distances in Table 1 for water droplets with 80% RH. Droplets 50 micron diameter or smaller can have very long drift distances with 100% RH. For example, the mean drift distances of 10 micron diameter droplets are beyond 650 ft with wind velocities of 5.5 mph and higher. For many pesticide applications, a small portion of the mixture is nonvolatile.

For small droplets that are still airborne when all of the water evaporates, there is potential for the small nonvolatile portion remaining to drift very long distances.

Temperature and Relative Humidity

Pesticides are applied over wide ranges of temperatures and relative humidities which influence the evaporation rates of droplets. Since evaporation of liquid from a droplet decreases its mass, it also influences the drift distance of the droplet. Table 2 shows the effects of temperatures (50, 68, and 86 degrees F) on droplet diameters at the end of droplet flights, and mean drift distances for water droplets with initial diameters ranging from 50 to 300 micron, wind velocities of 1 to 22 mph and 50% RH.

Table 2. Effect of temperature and wind velocity on droplet size at the end of flight of various size water droplets discharged downward at 65 ft/second toward a target 18 inches below point of discharge. (Relative humidity = 50%)

Initial Droplet size (micron)	Wind Velocity (mph)	Final Droplet Size (micron) and Drift Distance (ft)					
		Temperature (degrees F)					
		50		68		86	
		DS#	DD##	DS#	DD##	DS#	DD##
50	1.1	0.0	11.58*	0.0	9.84*	0.0	9.74*
50	5.6	0.0	53.14*	0.0	32.8*	0.0	23.52*
50	11.1	0.0	105.94*	0.0	61.34*	0.0	41.32*
50	22.4	0.0	208.61*	0.0	117.75*	0.0	75.76*
70	1.1	59.4	5.18	43.6	6.30	0.0	12.50*
70	5.6	59.2	26.14	42.7	32.14	0.0	38.70*
70	11.1	59.0	52.48	41.9	64.61	0.0	70.19*
70	22.4	58.8	105.94	40.4	132.18	0.0	132.51*
100	1.1	96.7	2.13	93.7	2.13	88.7	2.36
100	5.6	96.7	10.53	93.7	10.73	88.7	11.64
100	11.1	96.7	19.48	93.7	21.48	88.6	23.39
100	22.4	96.6	42.97	93.5	43.62	88.3	47.56
150	1.1	149	0.59	148	0.59	147	0.59
150	5.6	149	2.72	148	2.85	147	2.98
150	11.1	149	5.58	148	5.74	147	6.04
150	22.4	149	11.97	148	12.27	147	12.82
200	1.1	200	0.13	199	0.13	199	0.13
200	5.6	200	0.56	199	0.56	199	0.56
200	11.1	200	1.18	199	1.18	199	1.18
200	22.4	200	2.69	199	2.69	199	2.69
300	1.1	300	0.03	300	0.03	299	0.03
300	11.1	300	0.33	300	0.33	299	0.33

300	22.4	300	0.69	300	0.69	299	0.69

* Droplet completely evaporated before deposition.
\# DS - Droplet diameter (micron) at end of flight.
\## DD - drift distance (ft).

Table 2 indicates that ambient temperature had more influence on droplet sizes at end of flights for smaller droplets than larger droplets. For 70 micron diameter droplets, 5.6 mph wind velocity, and 50% RH, the mean droplet sizes at end of flights were 59.2, 42.7, and zero micron for ambient temperatures of 50, 68, and 86 degrees F, respectively. For 200 micron diameter droplets and the same conditions, the mean droplet sizes at times of deposition were 200, 199, and 199 micron. Over a temperature range of 50-86 degrees F, the volumes of 100 and 200 micron diameter water droplets changed about 20.9 and 1.5% respectively during flights when wind velocity was 1.1 m/s.

Table 2 also shows that wind velocities up to 22.4 mph had greater influence on droplet size change during flight on smaller than on larger droplets. For 70 micron diameter droplets at 68 degrees F and 50% RH, the droplet diameters at deposition were 43.6 and 40.4 micron with wind velocities of 1.1 and 22.4 mph, respectively. The 70 micron diameter water droplets lost 76 and 81% of their volume during flights with wind velocities of 1.1 and 22.4 mph, respectively. For 200 micron diameter droplets with the same conditions, the final droplet sizes at time of deposition were 199 micron for all wind velocities over a range of 1.1 to 22.4 mph.

Temperature can affect evaporation rate during flight and hence droplet size and drift distance. Because smaller droplets have greater surface area to volume ratios and longer flight times than larger droplets, temperature has greater influence on the drift distances of smaller droplets. With wind velocity of 5.6 mph and relative humidity of 50%, 50 micron diameter water droplets drifted 53.1 and 23.5 ft before completely evaporating at temperatures of 50 and 86 degrees F, respectively. With the same conditions, 100 micron diameter droplets drifted 10.5 and 11.6 ft before deposition at temperatures of 50 and 86 degrees F, respectively. Ambient temperatures within the range of 50 and 86 degrees F had very little influence on drift distances of 200 micron diameter and larger water droplets when wind velocity varied from 1.1 to 22.4 mph.

Figure 4 illustrates the simulated mean drift distances for 50, 100 and 200 micron diameter water droplets with 10 mph wind velocity, 50% RH and ambient temperatures of 55, 65, 75 , and 85 degrees F. The curve for 50 micron droplets shows that drift distance decreased as temperature increased. The 50 micron diameter droplets completely evaporated before deposition. Small droplets tend to travel at speed close to wind velocity. When temperature, and hence evaporation rate increases, their travel distance over their lifetime tends to decrease. The curve for 100 micron diameter droplets shows that drift distance before deposition increased with increased temperature. The drift distance tended to increase with increased temperature because increased temperature resulted in faster evaporation rate, smaller droplet size and increased travel distance before deposition. Temperature over the range of 50 to 86 degrees F had little influence on drift distances of 200 micron diameter droplets. The data used to produce the curves on Figure 3 are presented in Table 3.

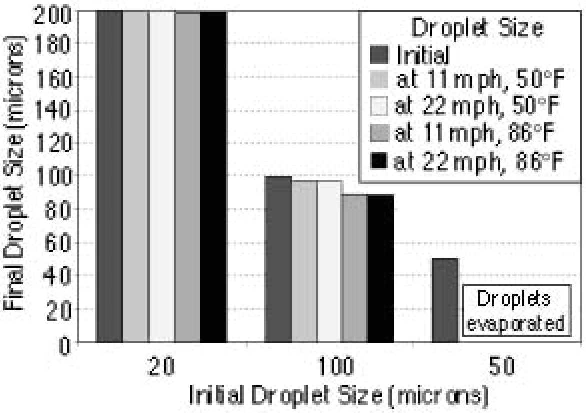

Figure 3. Effect of temperature and wind velocity on droplet sizes at the end of flight of 50, 100 and 200 micron diameter water droplets discharged down at 65 ft/second toward a target 18 inches below nozzle (RH=50%).

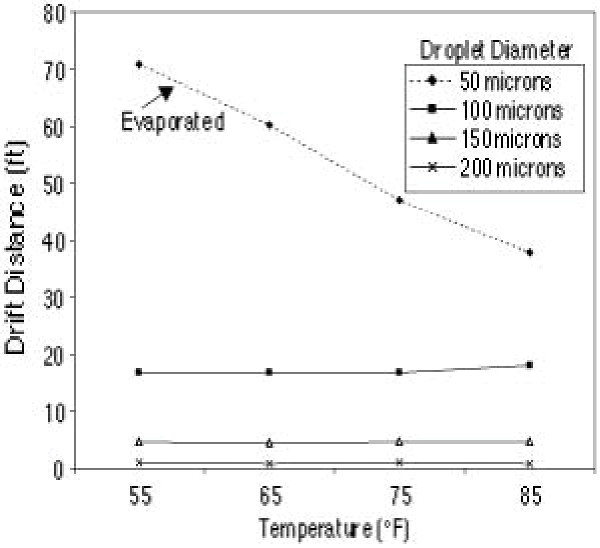

Figure 4. Mean drift distances for 50, 100 and 200 micron diameter water droplets with 10 mph wind velocity, 50% RH and ambient temperatures of 55, 65, 75 , and 85 degrees F.

Table 3. Effect of wind velocity and temperature on drift distances of droplets directed downward with initial velocity of 65 ft/second toward target 18 inches below discharge point. (Relative humidity = 50%; Turbulence intensity = 20%)

Initial Droplet size (micron)	Wind velocity (mph)	Drift Distance (ft)			
		Temperature (degrees F)			
		55	65	75	85
20	2	4.24*	4.47	4.64	4.79*
20	4	7.23*	7.33*	7.71*	7.79*

20	6	10.07*	9.20*	9.22*	9.07
20	8	12.82*	11.33*	10.42*	10.38*
20	10	15.55*	13.27*	11.92*	11.44
50	2	15.73*	14.97*	13.51*	12.60*
50	4	29.55*	26.39*	22.00*	18.82*
50	6	43.28*	37.87*	30.19*	25.18*
50	8	56.91*	49.21*	38.73*	31.79*
50	10	70.92*	60.31*	46.97*	37.90*
100	2	3.35	3.34	3.53	3.63
100	4	6.69	6.71	7.03	7.23
100	6	10.03	10.05	10.58	10.82
100	8	13.37	13.40	14.08	14.44
100	10	16.74	16.76	16.73	18.10
150	2	0.94	0.92	0.96	0.94
150	4	1.85	1.82	1.91	1.88
150	6	2.77	2.73	2.85	2.81
150	8	3.69	3.64	3.78	3.76
150	10	4.64	4.56	4.75	4.70
200	2	0.21	0.20	0.21	0.20
200	4	0.39	0.39	0.39	0.38
200	6	0.57	0.54	0.58	0.54
200	8	0.74	0.76	0.78	0.74
200	10	0.98	0.95	0.96	0.93

* Droplet completely evaporated before deposition.

Table 4 shows the mean drift distances for water droplets with initial diameters (25-300 micron), ambient temperatures (55-85 degrees F), relative humidities (20-100%), and 10 mph wind velocity. At low temperature (55 degrees F) and high relative humidity (80%), 50 micron diameter droplets were able to reach 18 in below their discharge point but traveled about 120 ft downwind before depositing. Table 4 indicates that relative humidity has little influence on drift distances of 150 micron diameter and larger droplets. This is because the flight times of these droplets are short. With wind velocity of 10 mph, 200 micron diameter droplets were only displaced over a range of less than 1 foot (0.93 to 0.98 ft) for the ranges of relative humidity and ambient temperature.

Table 4. Effect of relative humidity and ambient temperature on mean drift distances of various size water droplets directed downward at 65 ft/second toward a target 18 inches below point of discharge. (Wind velocity = 10 mph)

Droplet size (micron)	Ambient temp. (degrees F)	Drift distances (ft)				
		Relative humidity (%)				
		20	40	60	80	100

25	55	17.93*	20.37*	29.76*	56.43*	381.60
25	65	14.67*	16.63*	23.53*	43.18*	377.97
25	75	12.58*	14.41*	19.94*	37.95*	391.31
25	85	11.41*	12.77*	17.81*	33.25*	400.12
50	55	63.32*	60.87*	60.87*	119.73	76.78
50	65	48.21*	53.93*	63.82*	93.51*	76.05
50	75	37.58*	42.00*	55.32*	87.24*	78.82
50	85	30.81*	34.40*	44.81*	73.93*	80.34
100	55	16.90	16.82	16.63	16.43	16.20
100	65	16.97	16.88	16.64	16.36	15.99
100	75	17.94	17.77	17.48	17.05	16.46
100	85	18.55	18.28	17.88	17.34	16.55
150	55	4.65	4.64	4.62	4.62	4.59
150	65	4.58	4.57	4.56	4.54	4.50
150	75	4.78	4.78	4.72	4.72	4.66
150	85	4.76	4.73	4.70	4.64	4.58
200	55	0.98	0.98	0.95	0.95	0.95
200	65	0.95	0.95	0.94	0.94	0.94
200	75	0.96	0.96	0.96	0.96	0.96
200	85	0.93	0.93	0.93	0.93	0.93
300	55	0.98	0.98	0.95	0.95	0.95
300	65	0.95	0.95	0.94	0.94	0.94
300	75	0.96	0.96	0.96	0.96	0.96
300	85	0.93	0.93	0.93	0.93	0.93
* Droplet completely evaporated before deposition.						

Figure 5 illustrates the effect of relative humidity on mean drift distances of 25, 50, 100 and 200 micron size water droplets for 10 mph wind velocity. The ambient temperature was 65 degrees F for the simulations. The mean drift distances of 25 and 50 micron diameter water droplets, before complete evaporation, increased with increased relative humidity over the range of 20 to 80%. For the same conditions, but with 100% RH, 50 micron diameter droplets deposited 18 in below and 76 ft downwind from the point of discharge while 25 micron diameter droplets drifted beyond 378 ft. There was no change in drift distance of 200 micron diameter water droplets over the 10 to 80% range of relative humidity.

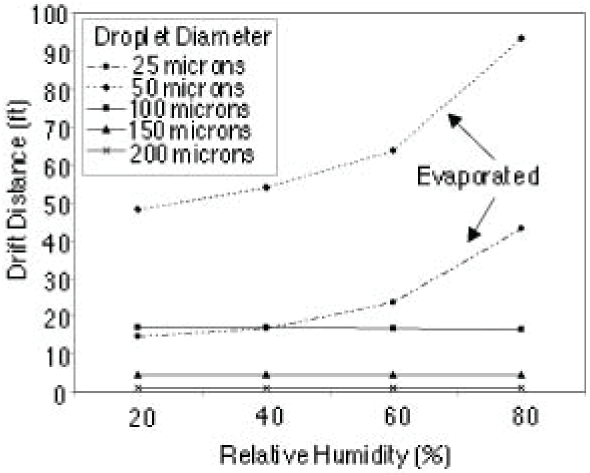

Figure 5. The effect of relative humidity on mean drift distances of 25, 50, 100 and 200 micron size water droplets for 10 mph wind velocity. (The ambient temperature= 65 degrees F).

Droplet Discharge Height

Agricultural pesticides are applied with a very wide range of nozzle heights above targets. Nozzle height depends on several factors including the sprayer setup, target and operating conditions. Table 5 shows the effects of discharge height (0.5-3.0 ft), droplet diameter (50-300 micron) and wind velocity (2.0-10.0 mph) on mean drift distances of water droplets directed downward with initial velocity of 65 ft/seconds. Relative humidity and ambient temperature were 50% and 70 degrees F, for all simulations. The mean drift distances of 50 micron diameter and smaller droplets were nearly constant with each wind velocity for the discharge height range of 0.5 to 3.0 ft. This occurs because these droplets have short life times and do not travel downward far enough to deposit before completely evaporating.

Table 5. Effect of droplet discharge height and wind velocity on drift distances of various size droplets discharged downward at 65 ft/second toward a target. (Temperature: 70 degrees F; Relative Humidity = 50%)

Initial Droplet size (micron)	Wind velocity (mph)	Drift distances (ft)					
		Nozzle height (ft)					
		0.5	1	1.5	2	2.5	3.0
50	2	0.43*	13.87*	14.02*	14.14*	14.22*	13.97*
50	4	14.28*	23.51*	23.72*	23.80*	23.83*	23.98*
50	6	19.96*	32.92*	33.41*	33.65*	33.78*	33.76*
50	8	25.61*	42.32*	43.18*	43.40*	43.39*	43.73*
50	10	31.20*	51.48*	52.29*	52.89*	53.37*	53.43*
100	2	0.50	1.50	3.37	5.40	7.51	9.85
100	4	0.99	2.99	6.76	10.82	15.02	19.72
100	6	1.48	4.47	10.15	16.23	22.54	29.62
100	8	1.98	5.97	13.51	21.63	30.05	39.51

100	10	2.49	7.47	16.91	27.06	37.59	49.40
150	2	0.04	0.29	0.92	1.80	2.77	3.76
150	4	0.07	0.57	1.82	3.57	5.50	7.49
150	6	0.11	0.86	2.73	5.34	8.25	11.23
150	8	0.16	1.15	3.63	7.12	11.01	14.99
150	10	0.19	1.43	4.55	8.92	13.78	18.75
200	2	0.02	0.07	0.20	0.61	1.13	1.76
200	4	0.03	0.14	0.38	1.19	2.24	3.51
200	6	0.05	0.20	0.55	1.76	3.34	5.23
200	8	0.06	0.27	0.75	2.37	4.48	7.01
200	10	0.08	0.34	0.93	2.98	5.63	8.79
300	2	0.00	0.01	0.05	0.11	0.20	0.38
300	4	0.02	0.05	0.10	0.24	0.41	0.79
300	6	0.02	0.07	0.15	0.35	0.62	1.17
300	8	0.02	0.08	0.21	0.46	0.80	1.56
300	10	0.04	0.12	0.26	1.04	1.04	1.97

* Droplet completely evaporated before deposition.

Increased discharge height resulted in increased drift distances for 100 micron diameter and larger water droplets (Table 5). For example, with 10 mph wind velocity and 65 ft/second initial droplet velocity, when discharge height increased from 0.5 to 3.0 ft, the mean drift distance of 200 and 300 micron diameter droplets increased from 2.49 to 49.40 ft and 0.08 to 8.79 ft, respectively. When the discharge height increased from 0.5 to 3.0 ft, the mean drift distance of 100 micron diameter droplets increased from 1.98 to 39.51 ft and kept increasing until the discharge height of 10 ft is reached. When the discharge height is increased beyond 10 ft, the drift distance remained constant (217 ft) because the 100 micron diameter water droplets completely evaporated before deposition.

When simulations for large size droplets were performed, results indicated that if the discharge height becomes too large, even the large droplets have tendency to drift under high wind velocity conditions. For example, the mean drift distance of 1000 micron diameter droplets was 5 ft for wind velocity and discharge height of 22 mph and 10 ft, respectively. Computer simulation also indicated that the mean drift distances of 1000 and 2000 micron diameter droplets were 57 and 19 ft, respectively, before impaction 13 ft below the point of discharge for 22 mph wind velocity, 50% relative humidity, and zero mph initial droplet velocity.

Figure 6 illustrates the effect of discharge height of droplets on the mean drift distances of 50, 100, 200, and 300 micron diameter water droplets for 10 mph wind velocity, 50% RH and 65 degrees F. The graph shows that increasing discharge height above 0.5 ft had no affect on the mean drift distance of 50 micron diameter droplets because they completely evaporated before depositing. However, increasing discharge height of 100 micron diameter and larger droplets affects their mean drift distances. Changes in discharge heights have less effect on mean drift distances as droplet size increases above 200 micron diameter.

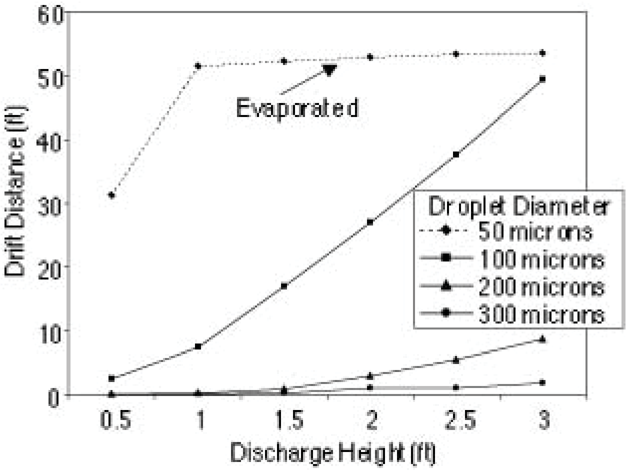

Figure 6. The effect of discharge height of droplets on drift distances of 50, 100, 200, and 300 micron diameter water droplets at 10 mph wind velocity (RH= 50%, T= 65 degrees F.)

Initial Droplet Velocity

Pesticides are applied with many different types of nozzles. The velocity of droplets delivered by nozzles depends on the configuration of the nozzle, and operating pressure. Table 6 shows the effects of initial droplet velocity (0-120 ft/second) and wind velocity (2.5-10.0 mph) on the mean drift distances of various size water droplets directed downward toward a target 1.5 ft below the point of discharge. Relative humidity and ambient temperature were 50% and 70 degrees F, for all simulations. The data indicate that increasing the initial downward droplet velocity can decrease the mean drift distances before deposition of 75 micron diameter and larger droplets. When spray is directed downward from a nozzle centered over a row of plants, for example, it is important to maximize spray deposition on the target. Even for 30 ft/second initial droplet velocities, the drift distances of 100 micron diameter and smaller water droplets would be excessive when spraying row crops if the droplets were exposed to crosswinds with velocities of only 1 mph. Also, for many applications where the spray is exposed to crosswinds, the drift distances of 200 micron diameter droplets would be excessive for droplets directed downward with slow velocities. For example, the mean drift distances of 200 micron diameter droplets in 2.5 mph crosswinds are 2.4 and 0.9 ft for droplets directed downward with 0 and 30 ft/sec velocities, respectively. When wind velocity was 10 mph, the mean drift distance of 200 micron diameter droplets decreased from 9.88 to 0.28 ft as the initial downward droplet velocity increased from 0 to 120 ft/s. Some applicators use large droplets to reduce spray drift potential. With no initial downward droplet velocity (zero ft/second) and 18 in discharge height, the mean drift distances of 1000 micron diameter droplets were 0.24, 0.63, 1.08, and 1.62 ft when wind velocities were 2.5, 5.0, 7.5, and 10.0 mph, respectively. With 60 ft/sec instead of 0 m/s initial velocity, the mean drift distance of the 1000 micron diameter drops was only 0.04 ft when wind velocity was 10 mph. Table 6 also illustrates that initial droplet velocities had no effect on drift distances of 50 micron diameter water droplets. None of the 50micron diameter and smaller droplets reached 18 in below the point of discharge before complete evaporation for a range of initial droplet velocities from zero to 120 ft/second and wind velocities from 2.5 to 10.0 mph.

Table 6. Effect of initial droplet velocity and wind velocity on drift distances of various size water droplets directed downward toward a target 18 inches below point of droplet discharge. (Temperature: 70 degrees F;

Relative Humidity = 50%)

Droplet size (micron)	Wind velocity (mph)	Drift Distances (ft)				
		Initial Droplet Velocity (ft/second)				
		0	30	60	90	120
50	2.5	16.50*	16.42*	16.40*	16.53*	16.50*
50	5.0	28.80*	28.74*	28.62*	28.67*	28.67
50	7.5	40.76*	40.73	40.74	40.70	40.54*
50	10.0	52.98*	52.70*	52.43*	52.48*	52.67*
75	2.5	17.86	13.05	11.35	10.29	9.09
75	5.0	33.83	25.82	22.19	20.03	18.31
75	7.5	49.58	38.64	33.03	29.74	27.17
75	10.0	65.28	52.26	44.00	39.49	36.01
100	2.5	5.39	5.39	4.37	3.64	3.06
100	5.0	14.51	10.79	8.75	7.26	6.10
100	7.5	21.84	16.25	13.11	10.88	9.12
100	10.0	29.25	21.75	17.51	14.48	12.15
150	2.5	3.64	2.05	1.26	0.73	0.39
150	5.0	7.34	4.10	2.49	1.45	0.76
150	7.5	11.07	6.19	3.73	2.15	1.12
150	10.0	14.83	8.34	5.00	2.87	1.49
200	2.5	2.36	0.89	0.31	0.13	0.07
200	5.0	4.82	1.79	0.58	0.25	0.15
200	7.5	7.34	2.72	0.89	0.82	0.20
200	10.0	9.88	3.72	1.20	0.52	0.28
300	2.5	1.39	0.24	0.08	0.04	0.03
300	5.0	2.91	0.49	0.15	0.08	0.5
300	7.5	4.56	0.76	0.22	0.12	0.07
300	10.0	6.23	1.06	0.31	0.17	0.11
500	2.5	0.67	0.08	0.03	0.01	0.00
500	5.0	1.52	0.16	0.05	0.03	0.03
500	7.5	2.49	0.25	0.09	0.05	0.03
500	10.0	3.58	0.34	0.11	0.06	0.04
1000	2.5	0.24	0.03	0.00	0.00	0.00
1000	5.0	0.63	0.05	0.03	0.01	0.00
1000	7.5	1.08	0.08	0.03	0.03	0.01
1000	10.0	1.62	0.11	0.04	0.03	0.03

* Droplet completely evaporated before deposition.

Figure 7 illustrates the influence of droplet size and initial downward velocity on drift distances of 50 to 300 micron diameter water droplets for 10 mph wind velocity. The relative humidity and ambient temperature were 50% and 70 degrees F for all simulations. As evident from the data presented on Figure 7, for 10 mph wind velocity, drift distances are greatly influenced by both droplet size and the initial downward velocity of the droplet. The drift distances of 100 micron diameter and larger droplets decreased with increased initial droplet velocity. Figure 7 also illustrates the large difference in drift distances between 100 and 200 micron diameter water droplets.

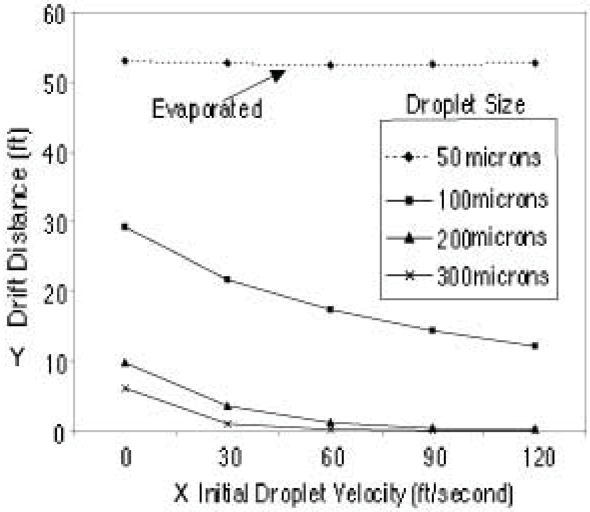

Figure 7. The influence of droplet size and initial downward velocity on drift distances of 50 to 300 micron diameter water droplets for 10 mph wind velocity (RH= 50%, T=70 degrees F).

Conclusions

The following conclusions are based on the computer simulations of mean drift distances of water droplets within the range of variables discussed in this publication.

1. 1. Changes in wind velocity, discharge height, ambient temperature and relative humidity had much greater influence on the drift distances of droplets 100 micron diameter or less than on 200 micron diameter and larger droplets. For droplets that did not evaporate before deposition, there was a nearly linear relationship between wind velocity and drift distance.
2. 2. With 100% RH, 10 micron diameter droplets drifted beyond 650 ft when wind velocity exceeded 5.5 mph.
3. 3. Droplets 50 micron diameter and smaller completely evaporated before reaching 18 inches below the discharge point, regardless of initial velocity, for relative humidities 60% and lower and temperatures between 55 and 85 degrees F. Also, the mean drift distances of these droplets increased with increased droplet size.
4. 4. Mean drift distances of 100 micron diameter and larger droplets increased with increased wind velocity and discharge height, but decreased with increased droplet size and discharge velocity.
5. 5. Drift distances of water droplets as large as 200 micron diameter were influenced by initial

droplet velocity and height of discharge.

6. 6. For 10 mph wind velocity, 20% turbulence intensity, 50% RH, 70 degrees F ambient temperature, 60 ft/second initial downward droplet velocity and 18 inches discharge height, the mean drift distances of 100, 200, and 500 micron diameter droplets were 17.5, 1.2, and 0.11 ft, respectively.
7. 7. The drift potential of 200 micron diameter droplets is considerably less than for 100 micron diameter droplets. Unless some means such as shields or air jets are used, drift reduction techniques should be directed toward reducing the portion of spray volume contained in droplets less than 200 micron diameter for applications where minimizing drift is important. For some applications, such as with high nozzles and slow initial downward velocity and high wind velocity, droplets larger than 200 micron diameter may be needed to satisfactorily reduce drift.

Acknowledgment

Most of the information presented in this publication was adapted from the following publication.

Zhu, H., D.L. Reichard, R.D. Fox, R.D. Brazee and H.E. Ozkan. 1994. Simulation of drift of discrete sizes of water droplets from field sprayers. Transactions of the ASAE 37(5):1401-1407.

References

Ozkan, H.E. 1991. Reducing spray drift. OSU Extension Bulletin 816. Ohio State University Extension, Columbus, Ohio.

Reichard, D.L., H. Zhu, R.D. Fox and R.D. Brazee. 1992a. Computer simulation of spray drift that influence spray drift. Transactions of the ASAE 35(5):1401-1407.

Reichard, D.L., H. Zhu, R.D. Fox and R.D. Brazee. 1992b. Wind tunnel evaluation of a computer program to model spray drift. Transactions of the ASAE 35(3):755-758.

Keith L. Smith, Associate Vice President for Ag. Adm. and Director, OSU Extension.

TDD No. 800-589-8292 (Ohio only) or 614-292-1868

ATTACHMENT III.8.B

DRIFTSIM$^{®}$: PREDICTING DRIFT DISTANCE OF SPRAY DROPLETS AND RESULTING EVAPORATION

Bulletin 923

DRIFTSIM—Predicting Drift Distances of Spray Droplets

Heping Zhu and Robert D. Fox
Agricultural Engineers
USDA-ARS
Application Technology Research Unit
Wooster, OH 44691

H. Erdal Ozkan
Professor and Extension Agricultural Engineer
Food, Agricultural, and Biological
Engineering Department
The Ohio State University
Columbus, OH 43210

Introduction

Spray drift, movement of pesticide droplets through air during or after application to a site other than the intended targets of application, is one of the most critical problems pesticide applicators have to deal with. For example, three-fourths of agriculture-related complaints investigated by the Ohio Department of Agriculture involved drift issues; two-thirds of the total complaints in a five-year period brought to the attention of Iowa Department of Agriculture were related to drift problems; about one-third of court cases due to spray misapplications reported by a major insurance company involved drift damages. Drift problems will become even more critical in the future when farmers use more genetically modified crops which restrict use of non-selective herbicides because even a small amount of these herbicides can cause serious damage to neighboring crops.

Although complete elimination of spray drift is impossible, problems can be minimized if chemicals are applied with the proper equipment and methods under favorable weather conditions. Increased awareness of environmental quality and better understanding of the causes of spray drift can help operators make reasonable judgments for safer, more efficient applications.

Factors that significantly influence off-target movement of droplets are wind velocity and direction, droplet size and density, and distance from the atomizer to the target. Other factors that influence drift include droplet velocity, and direction of discharge from the atomizer, volatility of the spray fluid, relative humidity, ambient temperature, and atmospheric turbulence intensity. Many scientists have conducted field tests to study influence of these variables on spray drift. Unfortunately, field tests have the limitation that weather conditions cannot be controlled and the variables that influence spray drift may interact and vary during a test.

Computer simulations can allow determination of effects of different variables such as droplet size and velocity, relative humidity, and wind velocity on spray drift. One such computer model or commercially available computational fluid dynamics (CFD) program was evaluated by Reichard et al. (1992) in Ohio for modeling the effects of several variables on spray drift. Experiments were conducted to verify the accuracy of the computer model in predicting drift distances of water droplets in a wind tunnel with a single size droplet generator. These tests revealed that the computer model could be used to accurately calculate spray drift distances for a wide range of spray droplet sizes and wind velocities. With the computer model, individual or mean droplet trajectories were determined for different values of several variables listed above (Zhu et al., 1994). However, the model is very expensive and requires special operator skills and a high-speed computer with a large memory space to operate. It also takes long time to calculate a drift distance even for a single simulation condition.

DRIFTSIM is a simplified and user-friendly version of a computer model developed with a visual BASIC language program to interpolate values from a large database of drift distances originally calculated from the CFD model evaluated by Reichard et al. (1992). Detailed information on DRIFTSIM is given in a publication by Zhu et al. (1995). DRIFTSIM can be used to determine effects of major drift-causing factors on the mean drift distances up to 656 feet from the release point for individual water droplets or classes of droplets. These factors or variables used in DRIFTSIM are listed in Table 1, with the limiting values acceptable to DRIFTSIM.

Table 1. Variables and their ranges used in DRIFTSIM program

Variable	Range			
	American Unit		Metric Unit	
Wind velocity	0-22	mph	0-10	m/s
Droplet size	10-2000	Micron (µm)	10-2000	µm
Droplet velocity	0-110	mph	0-50	m/s
Discharge height	0-6.5	ft	0-2.0	m
Temperature	50-86	°F	10-30	°C
Relative humidity	10-100	%	10-100	%

Turbulence intensity is another important factor indicating how much the wind velocity varies about the mean. It can vary considerably in field conditions, but based on the frequency of nearly 20% turbulence intensity observed in many of the field measurements conducted in Ohio, a constant value of 20% turbulence intensity was used in DRIFTSIM for all calculations.

For classes of droplets in this version of DRIFTSIM, the upper-limit log normal (ULLN) method (Goering and Smith, 1978) was used to calculate the drop-size distribution produced by a nozzle. The ULLN method used three size measurements, $D_{V.1}$, $D_{V.5}$, and $D_{V.9}$ to estimate the volume of spray in droplets less than a selected droplet size. The $D_{V.1}$, $D_{V.5}$, and $D_{V.9}$ for the droplet size spectra produced by a specific nozzle can be measured with most modern droplet sizing instruments. DRIFTSIM computes the drift distance for the average of lower and upper droplet size for each size class. It also computes the portion of spray in each size class.

Terms used in DRIFTSIM program

Single size droplets: For the program to calculate a mean drift distance of a given size droplets with other variables

Array of droplets (DVs): For the program to calculate drift distances with the portion of volume for many size classes of droplets by entering $D_{v.1}$, $D_{v.5}$ and $D_{v.9}$

$D_{v.1}$: Droplet diameter such that 10% of total liquid volume that is in droplets smaller than $D_{v.1}$ (micron or µm)

$D_{v.5}$: Droplet diameter such that 50% of total liquid volume that is in droplets smaller than $D_{v.5}$ (micron or µm)

$D_{v.9}$: Droplet diameter such that 90% of total liquid volume that is in droplets smaller than $D_{v.9}$ (micron or µm)

Array of droplets (nozzle): For the program to calculate drift distances with the portion of volume for many size classes of droplets by selecting nozzle type [**Note:** In DRIFTSIM, data is available for only a limited number of nozzles]

Temperature: Ambient air temperature during spray operation (°F in American unit or °C in Metric unit)

Relative humidity: Relative humidity of ambient air (%)

Wind velocity: Wind speed at nozzle level during the spray application (mph in American unit or m/s in Metric unit)

Discharge height: Nozzle orifice height above the ground (ft in American unit or m in Metric unit)

Droplet velocity: Velocity of droplets near the outlet of the nozzle orifice (mph in American unit or m/s in Metric unit)

Droplet diameter: Droplet diameter near the outlet of the nozzle orifice (micron or µm)

Operating pressure: Liquid pressure acting on the nozzle orifice (psi or kPa)

Operating DRIFTSIM

To operate DRIFTSIM, minimum requirements for a computer are Pentium PC with a CD drive, MS-Windows version 3.1 or later, 8 MB of memory, 30 MB free hard drive space, and a mouse.

DRIFTSIM is compact enough to fit on a CD. It can be operated from either a CD or a computer hard drive. DRIFTSIM automatically starts running when the CD containing DRIFTSIM is inserted in the CD drive of the computer. To operate the program from the computer hard drive, DRIFTSIM files and program should be first copied onto the hard drive, and then the user should execute DRIFTSIM.exe file to start the program. The program may run somewhat faster from a hard drive than a CD.

After the program starts, it gives three on-screen boxes for choosing units and droplet size types and entering values of simulation variables. A selection of units or droplet size types can be changed at any time during the operation without needing to exit the program. To change the value of any variable, simply click on the input area next to the variable, and enter a value that is within the acceptable range defined in Table 1. Only two screens appear during the whole calculation process: input and result screens.

Steps to run DRIFTSIM from a CD

(1) Insert CD in the computer.
(2) Introductory information for DRIFTSIM as shown in Figure 1 appears on the screen.

Figure 1

DRIFTSIM

Version 1.12.04

Created by

Dr. Heping Zhu and Dr. Robert D. Fox

Application Technology Research Unit
USDA-ARS

and Dr. H. Erdal Ozkan

Professor and Extension Agricultural Engineer

Food, Agriculture, and Biological Engineering Department
The Ohio State University

(3) Click on the *"Start Driftsim"* box. Three on-screen boxes for choosing and entering simulation conditions appear on the screen as shown in Figure 2. [**Note:** initial values for drift variables shown on the screen are built into DRIFTSIM. These values are only examples, not recommended values.]

Figure 2

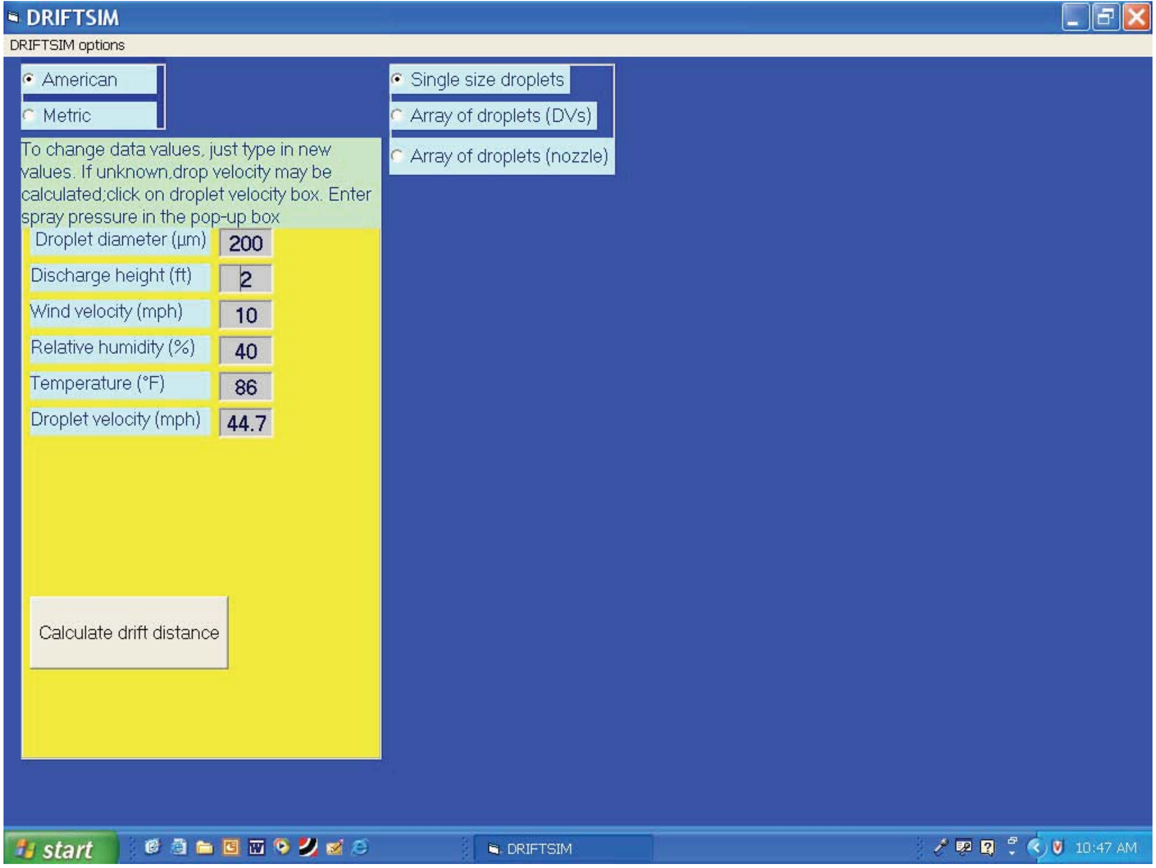

● American
○ Metric

● Single size droplets
○ Array of droplets (DVs)
○ Array of droplets (nozzle)

To change data values, just type in new values. If unknown,drop velocity may be calculated;click on droplet velocity box. Enter spray pressure in the pop-up box

Droplet diameter (μm) 200
Discharge height (ft) 2
Wind velocity (mph) 10
Relative humidity (%) 40
Temperature (°F) 86
Droplet velocity (mph) 44.7

(4) Select either *“American”* or *“Metric”* unit for calculation.

(5) Select one of the three choices as a type of input for the droplet size: “*Single size droplets”, “Array of droplets (DVs)”,* or *“Array of droplets (nozzle)”.*

(6) For “*Single size droplets*”, follow steps (7) to (11); for “*Array of droplets (DVs)*”, follow steps (12) to (17); for “*Array of droplets (nozzle)*”, follow steps (19) to (23).

[**Note:** Steps (7) to (11) are for *“Single size droplets”* only]

(7) Enter or change values for *“Droplet diameter”, “Wind velocity”, “Discharge height”, “Droplet velocity”, “Temperature”, “Relative humidity”* for inputs of variables. The value of *“Droplet velocity”* can be entered either by the user, or automatically by the program once the user enters a value for the operating pressure on the box which pops up on the screen as shown in Figure 3 after the user empties the “*Droplet velocity*” box. A red error message appears in the box under the variables if the value of an individual variable is outside the range defined in Table 1.

Figure 3

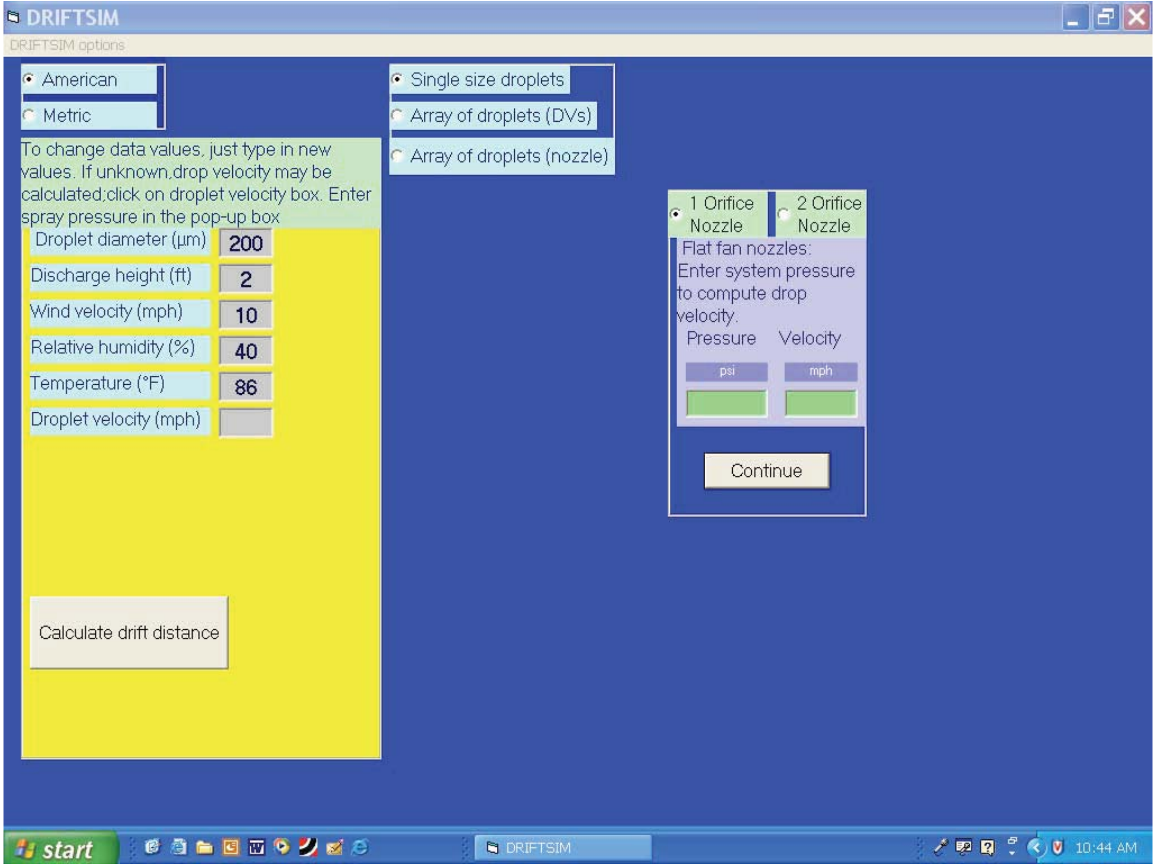

● American
○ Metric

● Single size droplets
○ Array of droplets (DVs)
○ Array of droplets (nozzle)

To change data values, just type in new values. If unknown,drop velocity may be calculated;click on droplet velocity box. Enter spray pressure in the pop-up box

Droplet diameter (µm)	200
Discharge height (ft)	2
Wind velocity (mph)	10
Relative humidity (%)	40
Temperature (°F)	86
Droplet velocity (mph)	

● 1 Orifice Nozzle
○ 2 Orifice Nozzle

Flat fan nozzles: Enter system pressure to compute drop velocity.

Pressure	Velocity
psi	mph

(8) Click on *"Compute drift distance"* to obtain the results on the screen as shown in Figure 4.

Figure 4

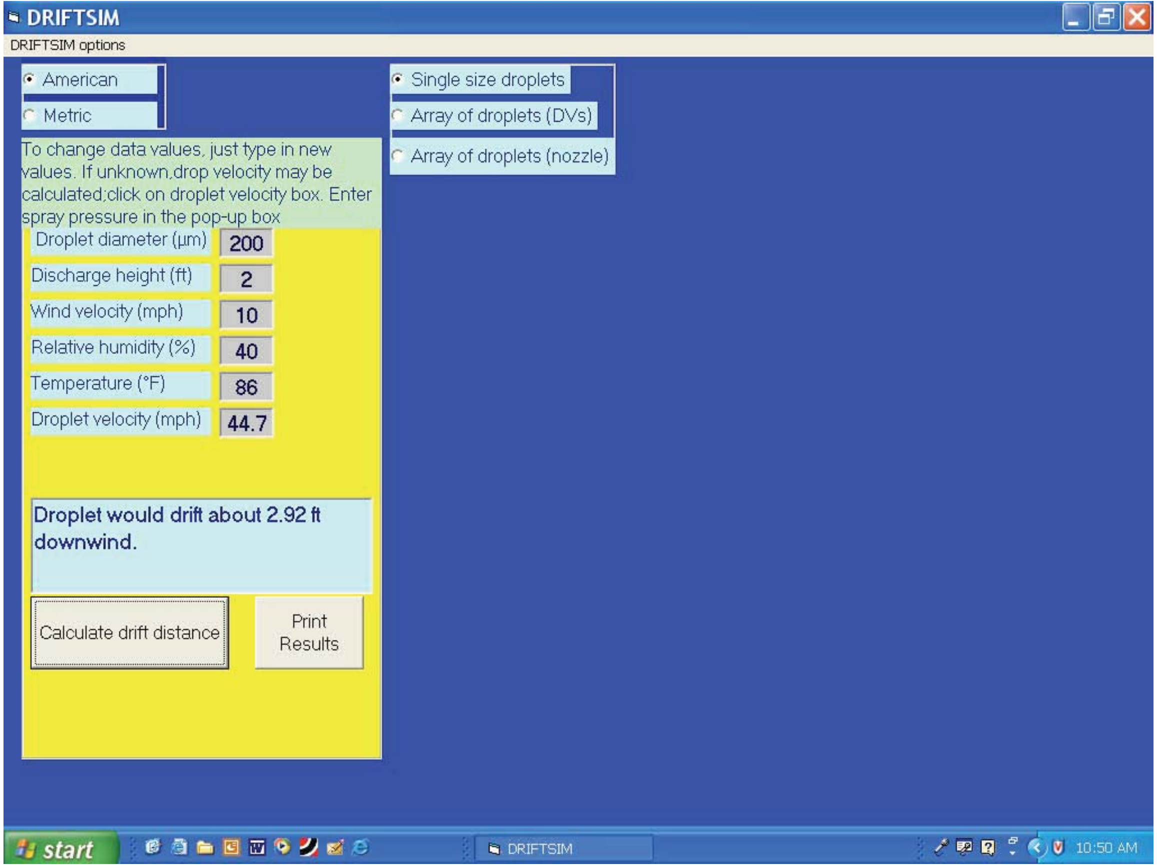

● American
○ Metric

● Single size droplets
○ Array of droplets (DVs)
○ Array of droplets (nozzle)

To change data values, just type in new values. If unknown,drop velocity may be calculated;click on droplet velocity box. Enter spray pressure in the pop-up box

Droplet diameter (μm)	200
Discharge height (ft)	2
Wind velocity (mph)	10
Relative humidity (%)	40
Temperature (°F)	86
Droplet velocity (mph)	44.7

Droplet would drift about 2.92 ft downwind.

(9) Click on *"Print results"* if you want to get a printout of input variables and the result.
(10) To continue running DRIFTSIM with a new or revised set of inputs for the "*single size droplet*", repeat steps (7) to (10).
(11) When you are done with all the simulations, exit DRIFTSIM by clicking on the **X** at the upper right corner of the window on the screen.

[**Note:** Steps (12) to (17) are for "*Array of droplets (DVs)*" only]
(12) After choosing "*Array of droplets (DVs)*", a new box for droplet size distribution appears on the screen as shown in Figure 5.

Figure 5

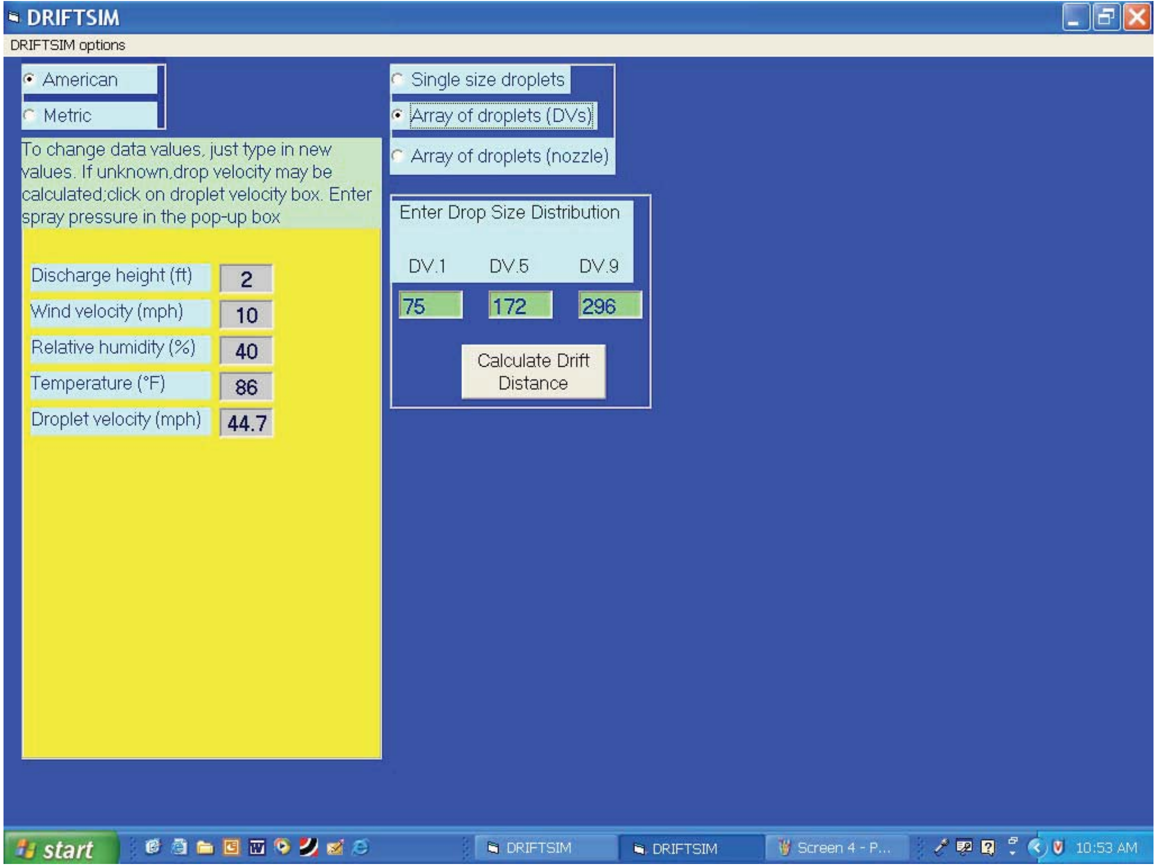

● American
○ Metric

○ Single size droplets
● Array of droplets (DVs)
○ Array of droplets (nozzle)

To change data values, just type in new values. If unknown,drop velocity may be calculated;click on droplet velocity box. Enter spray pressure in the pop-up box

Discharge height (ft)	2
Wind velocity (mph)	10
Relative humidity (%)	40
Temperature (°F)	86
Droplet velocity (mph)	44.7

Enter Drop Size Distribution

DV.1	DV.5	DV.9
75	172	296

(13) Enter “$D_{v.1}$”, “$D_{v.5}$“ and “$D_{v.9}$“ values in boxes.
(14) Enter or change values for “*Wind velocity*”, “*Discharge height*”, “*Droplet velocity*”, “*Temperature*” and “*Relative humidity*”.
(15) Click on “*Calculate Drift Distance*”. Drift distances of 9 size classes of droplets along with the portion of the spray volume corresponding to each size class appear on the screen as shown in Figure 6. Error message appears on this screen if “$D_{v.1}$”, “$D_{v.5}$“ and “$D_{v.9}$“ values are not reasonable.

Figure 6

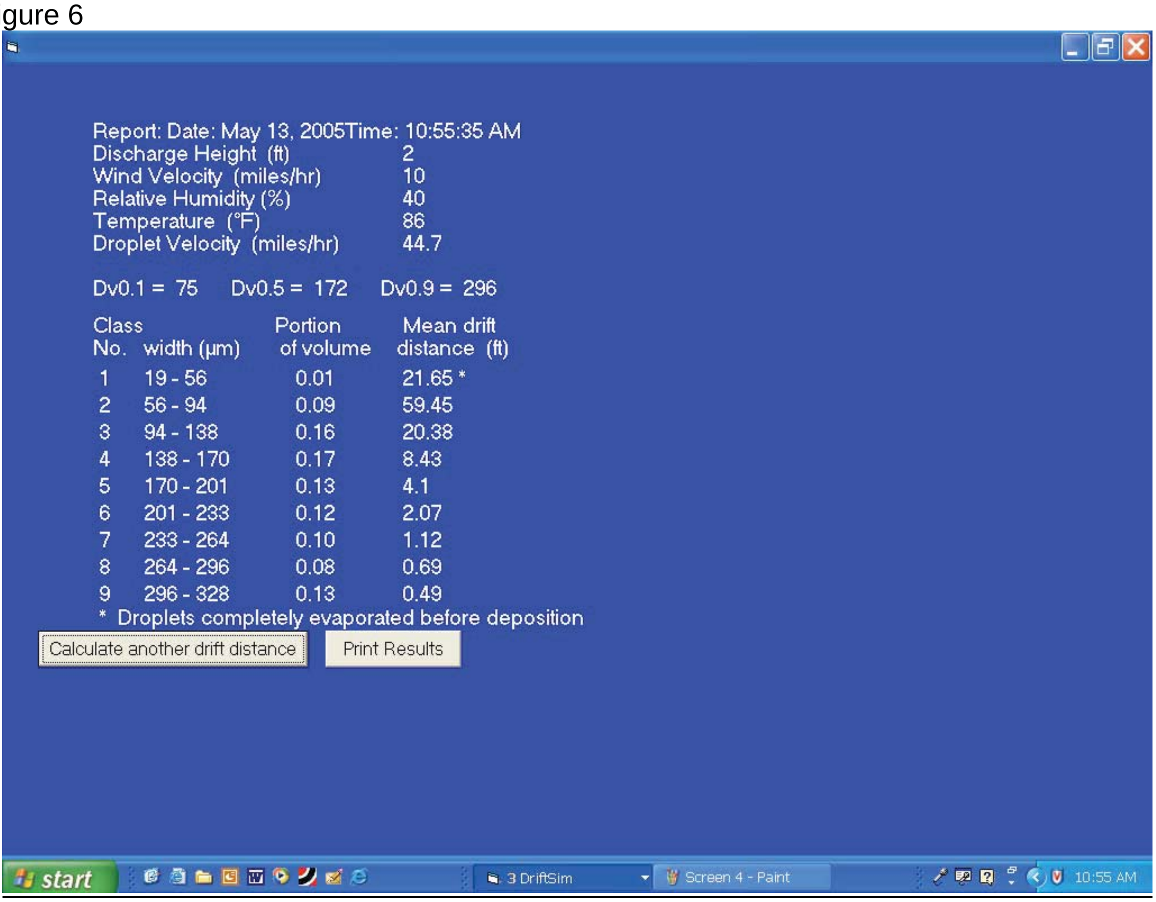

```
Report: Date: May 13, 2005Time: 10:55:35 AM
Discharge Height  (ft)              2
Wind Velocity  (miles/hr)           10
Relative Humidity (%)               40
Temperature  (°F)                   86
Droplet Velocity  (miles/hr)        44.7

Dv0.1 =  75     Dv0.5 =  172     Dv0.9 =  296

Class              Portion       Mean drift
No.   width (µm)   of volume     distance  (ft)
 1    19 - 56        0.01        21.65 *
 2    56 - 94        0.09        59.45
 3    94 - 138       0.16        20.38
 4    138 - 170      0.17        8.43
 5    170 - 201      0.13        4.1
 6    201 - 233      0.12        2.07
 7    233 - 264      0.10        1.12
 8    264 - 296      0.08        0.69
 9    296 - 328      0.13        0.49
 * Droplets completely evaporated before deposition
```

(16) Click on either “*Print Results*” to get a printout of the results, or “*Calculate another drift distance*” to repeat steps (13) to (16) for a revised or new set of inputs.

(17) When you are done with all the simulations, exit DRIFTSIM by clicking on the **X** at the upper right corner of the window on the screen.

[**Note:** Steps (18) to (23) are for *“Array of droplets (nozzle)”* only]

(18) After choosing “*Array of droplets (nozzle)*”, a new box with a list of several nozzles appears on the screen as shown in Figure 7.

Figure 7

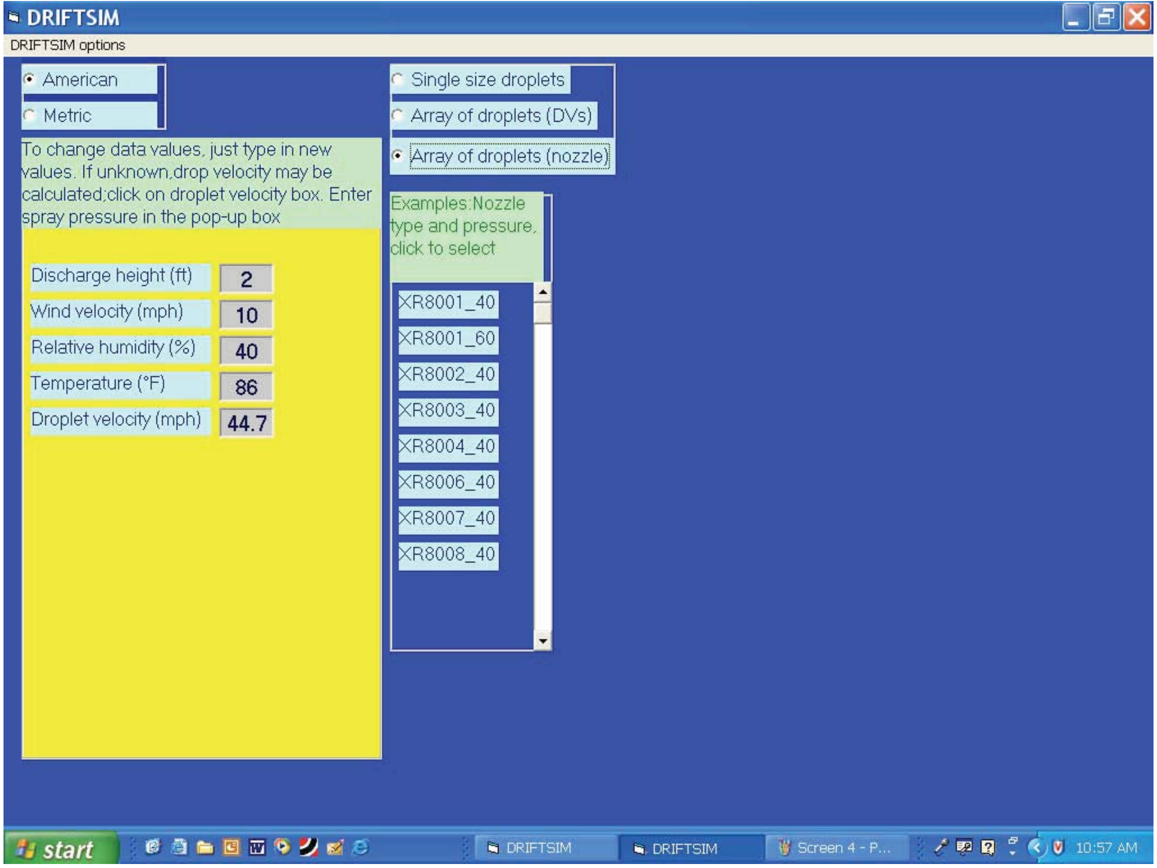

● American

○ Metric

To change data values, just type in new values. If unknown,drop velocity may be calculated;click on droplet velocity box. Enter spray pressure in the pop-up box

Discharge height (ft)	2
Wind velocity (mph)	10
Relative humidity (%)	40
Temperature (°F)	86
Droplet velocity (mph)	44.7

○ Single size droplets

○ Array of droplets (DVs)

● Array of droplets (nozzle)

Examples:Nozzle type and pressure, click to select

- XR8001_40
- XR8001_60
- XR8002_40
- XR8003_40
- XR8004_40
- XR8006_40
- XR8007_40
- XR8008_40

(19) Click on one of nozzle choices, then “$D_{v.1}$”, “$D_{v.5}$“ and “$D_{v.9}$“ values automatically appear in boxes for the nozzle chosen, as shown in Figure 8.

Figure 8

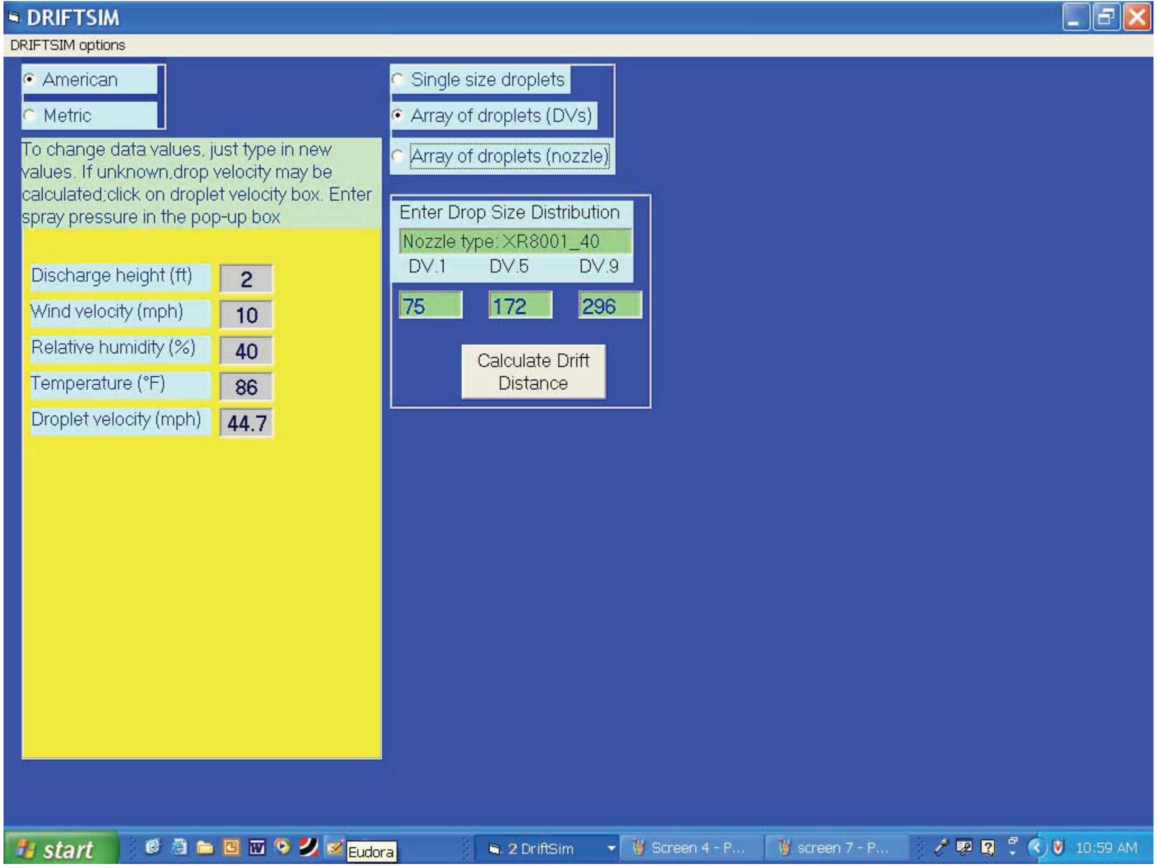

● American
○ Metric

To change data values, just type in new values. If unknown,drop velocity may be calculated;click on droplet velocity box. Enter spray pressure in the pop-up box

Discharge height (ft)	2
Wind velocity (mph)	10
Relative humidity (%)	40
Temperature (°F)	86
Droplet velocity (mph)	44.7

○ Single size droplets
● Array of droplets (DVs)
○ Array of droplets (nozzle)

Enter Drop Size Distribution

Nozzle type: XR8001_40

DV.1	DV.5	DV.9
75	172	296

(20) Enter or change values for "*Wind velocity*", "*Discharge height*", "*Droplet velocity*", "*Temperature*", and "*Relative humidity*".

(21) Click on "*Calculate Drift Distance*". Drift distances of 9 size classes of droplets along with the portion of the spray volume corresponding to each size class appear on the screen as the same as step (15). Error message appears on this screen if "$D_{v.1}$", "$D_{v.5}$" and "$D_{v.9}$" values are not reasonable.

(22) Click on either "*Print Results*" to get a printout of the results, or "*Calculate another drift distance*" to repeat steps (18) to (22) for a revised or new set of inputs.

(23) When you are done with all the simulations, exit DRIFTSIM by clicking on the **X** at the upper right corner of the window on the screen.

Steps to run DRIFTSIM from a computer hard drive

To operate DRIFTSIM from a hard drive, the user should copy both DRIFTSIM subdirectory and all contents in the subdirectory, except AUTORUN.INF and Browsercall.exe, from the CD to the hard drive [**Note:** the subdirectory name must be DRIFTSIM; otherwise, the program will not work]. After the copying process is completed, go to DRIFTSIM subdirectory in the hard drive and click on DriftSim.exe file. DRIFTSIM introductory page should appear on the screen. Then follow steps (3) to (23) above to run the program.

References

Goering, C.E. and D.B. Smith. 1978. Equations for droplet size distributions in sprays. Transactions of ASAE 21(2): 209-216.

Reichard, D.L., H. Zhu, R.D. Fox and R.D. Brazee. 1992. Wind tunnel evaluation of a computer program to model spray drift. Transactions of the ASAE 35(3):755-758.

Zhu, H., D.L. Reichard, R.D. Fox, R.D. Brazee and H.E. Ozkan. 1994. Simulation of drift of discrete sizes of water droplets from field sprayers. Transactions of the ASAE 37(5):1401-1407.

Zhu, H., D.L. Reichard, R.D. Fox, H.E. Ozkan and R.D. Brazee. 1995. DRIFTSIM, a program to estimate drift distances of spray droplets. Applied Engineering in Agriculture 11 (3): 365-369.

This manual, as well as other information on spray drift, is available at Ohio State University Extension’s web site “Ohioline” (**http://ohioline.osu.edu**) by clicking on “Search” and entering “DRIFTSIM” or "spray drift" in the search box.

Keith L. Smith, Associate Vice President for Agricultural Administration and Director, OSU Extension

TDD No. 800-589-8292 (Ohio only) or 614-292-1868

TABLE OF CONTENTS

Section No. **Title** **Page**
1.0 INTRODUCTION III.9-1
  1.1 Description III.9-1
2.0 DESIGN CRITERIA III.9-2
3.0 CALCULATION III.9-2
4.0 SUMMARY III.9-3

LIST OF ATTACHMENTS

Attachment No.	**Title**
III.9.A	LOW COST SHORE PROTECTION: A GUIDE FOR ENGINEERS AND CONTRACTORS (U.S. ARMY CORPS OF ENGINEERS 2004
III.9.B	WATER-RESOURCES ENGINEERING (LINSLEY & FRANZINI 1979)

1.0 INTRODUCTION

Lea Land LLC (the Facility) is an existing Surface Waste Management Facility (SWMF) providing oil field waste solids (OFWS) disposal services. The existing Lea Land SWMF is subject to regulation under the New Mexico Oil and Gas Rules, specifically 19.15.9.711 and 19.15.36 NMAC, administered by the Oil Conservation Division (OCD) of the NM Energy, Minerals, and Natural Resources Department (NMEMNRD). This document is a component of the “Application for Permit Modification” that proposes continued operations of the existing approved waste disposal unit; lateral and vertical expansion of the landfill via the construction of new double-lined cells; and the addition of waste processing capabilities. The proposed Facility is designed in compliance with 19.15.36 NMAC, and will be constructed and operated in compliance with a Surface Waste Management Facility Permit issued by the OCD. The Facility is owned by, and will be constructed and operated by, Lea Land LLC.

The Lea Land SWMF is one of the most recently designed facilities to meet the new more stringent standards that, for instance, mandate double liners and leak detection for land disposal. The new services that Lea Land will provide needed resources to fill an existing void in the market for technologies that exceed current OCD requirements.

1.1 Site Location

The Lea Land site is located approximately 27 miles northeast of Carlsbad, straddling US Highway 62-180 (Highway 62) in Lea County, NM. The Lea Land site is comprised of a 642-acre ± tract of land encompassing Section 32, Township 20 South, Range 32 East, Lea County, NM. Site access is currently provided on the south side of US Highway 62. The coordinates for the approximate center of the Lea Land site are Latitude 32°31’46.77” and Longitude -103°47’18.25”.

1.2 Facility Description

The Lea Land SWMF comprises approximately 463 acres ± of the 642-acre ± site, and will include two main components: an oil field waste Processing Area and an oil field waste solids Landfill, as well as related infrastructure (i.e., access, waste receiving, stormwater management, etc.). Oil field wastes are delivered to the Lea Land SWMF from oil and gas exploration and production operations in southeastern NM and west Texas. The Permit Plans (**Attachment III.1.A**) identify the locations of the Processing Area and Landfill Disposal facilities. The proposed facilities are detailed in **Table**

II.1.2 (**Volume II.1**), and are anticipated to be developed in four primary phases as described in **Table II.1.3** (**Volume II.1**).

2.0 DESIGN CRITERIA

The purpose of the Wave Action Calculations presented herein is to provide the wave height and run-up for the evaporation ponds proposed for the Lea Land Processing Area. The Lea Land Processing Area is planned to include up to 12 evaporation ponds, approximately 420 feet (ft) in length and 200 ft in width, each with a capacity of approximately 9.5 acre-ft. These calculations assume a pond length of 420 ft and a conservative wind speed of 75 miles per hour (mph). Wave height and run-up must be less than the 3.5 ft of freeboard provided in the pond design. The methodology applied for determining wave height and run-up in reservoirs for the Wave Action Calculations is provided in two documents, *Low Cost Shore Protection: A Guide for Engineers and Contractors* (U.S. Army Corps of Engineers 2004; (**Attachment III.9.A**); and *Water-Resources Engineering* (Linsley & Franzini 1979; **Attachment III.9.B**).

3.0 CALCULATION

The fastest mile wind speed for a 25-year return period was obtained from Figure 16, **Attachment III.9.A**. The fastest mile wind speed is approximately 75 mph for the Lea Land site vicinity.

Wave height in a pond is estimated using the following equation (i.e., page 166, Equation 7-4, **Attachment III.9.B)**:

$$Z_w = 0.034\ (V_w)^{1.06}\ F^{0.47}$$

Where:
Z_w = height of wave (feet)
V_w = wind speed (mph) = 75 mph
F = fetch length (miles) = 420 feet/5,280 feet/mile = 0.080 miles

Therefore:

$$Z_w = 0.034\ (75\ \text{mph})^{1.06}\ (0.080\ \text{miles})^{0.47}$$

$$Z_w = 0.034\ (97.2)\ (0.30)$$

$$Z_w = 0.99\ \text{feet} = \text{height of wave in pond due to a 75 mph wind}$$

The height of wave runup for a smooth (i.e., HDPE liner) surface can be obtained from Table 11, **Attachment III.9.A**. On Table 11, R = 1.75H for a 2.5H:1V smooth slope and R = 1.50H for a 4.0H:1V smooth slope. Interpolating between these two values a value of R = 1.68H is obtained for a 3.0H:1V smooth slope. Therefore:

Wave Runup = 1.68H = 1.68 (0.99 feet) = 1.66 feet for a 3H:1V smooth sideslope.

Total: Wave height + Wave run-up = 0.99 feet + 1.66 feet = 2.65 feet

4.0 SUMMARY

When considering a conservative 75 mph wind across the length of the pond, a wave height of 0.99 ft is calculated. This wave will run-up approximately 1.66 ft up the sideslope of the pond. The ponds have been designed with a minimum freeboard of 3.5 ft which will provide adequate protection against the combined potential impact of waves, wave run-up, and simultaneous rainfall event (i.e., 25-year, 24-hour rainfall = 4.48”) with a sufficient Factor of Safety (FS) of over 0.5 ft. In addition, the berm to be constructed around the entire pond area is lined to an additional height of at least 10 ft, providing additional potential drift protection (see **Permit Plans, Volume III.1**)

ATTACHMENT III.9.A

LOW COST SHORE PROTECTION: A GUIDE FOR ENGINEERS AND CONTRACTORS

(U.S. ARMY CORPS OF ENGINEERS 2004)

LOW COST SHORE PROTECTION

... a Guide for Engineers and Contractors

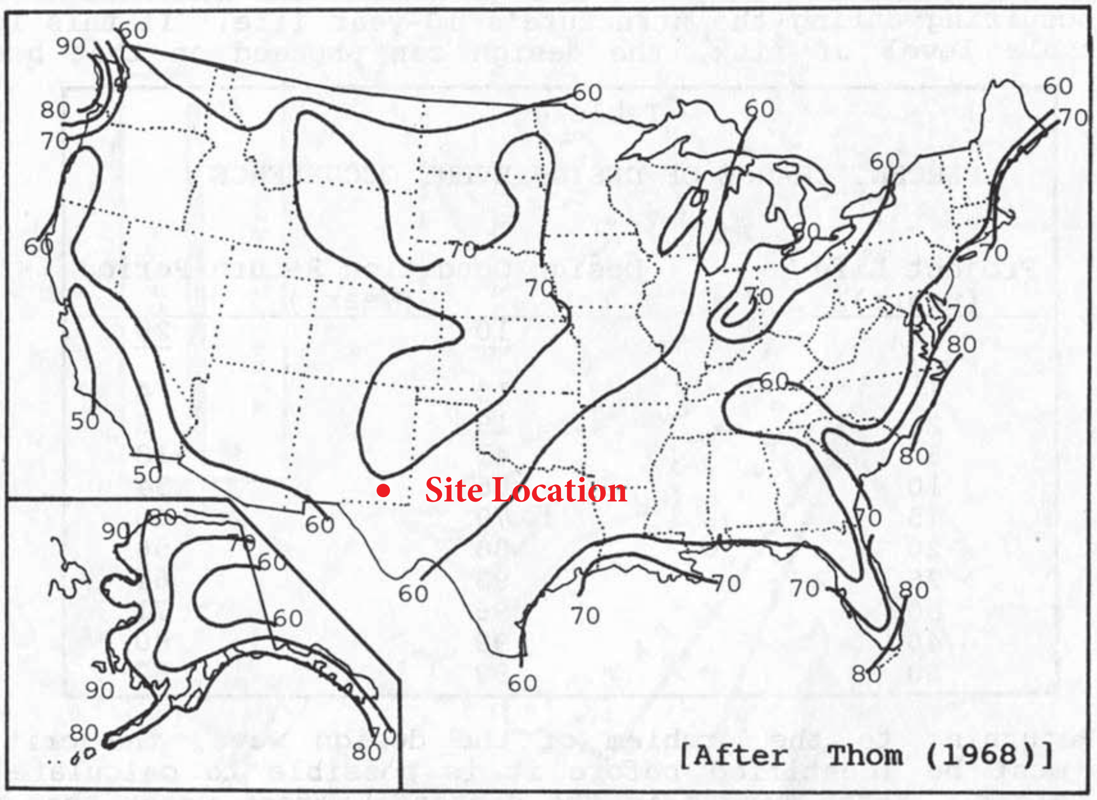

[After Thom (1968)]

Figure 15 Fastest-Mile Wind Speeds: 10-year Return Period

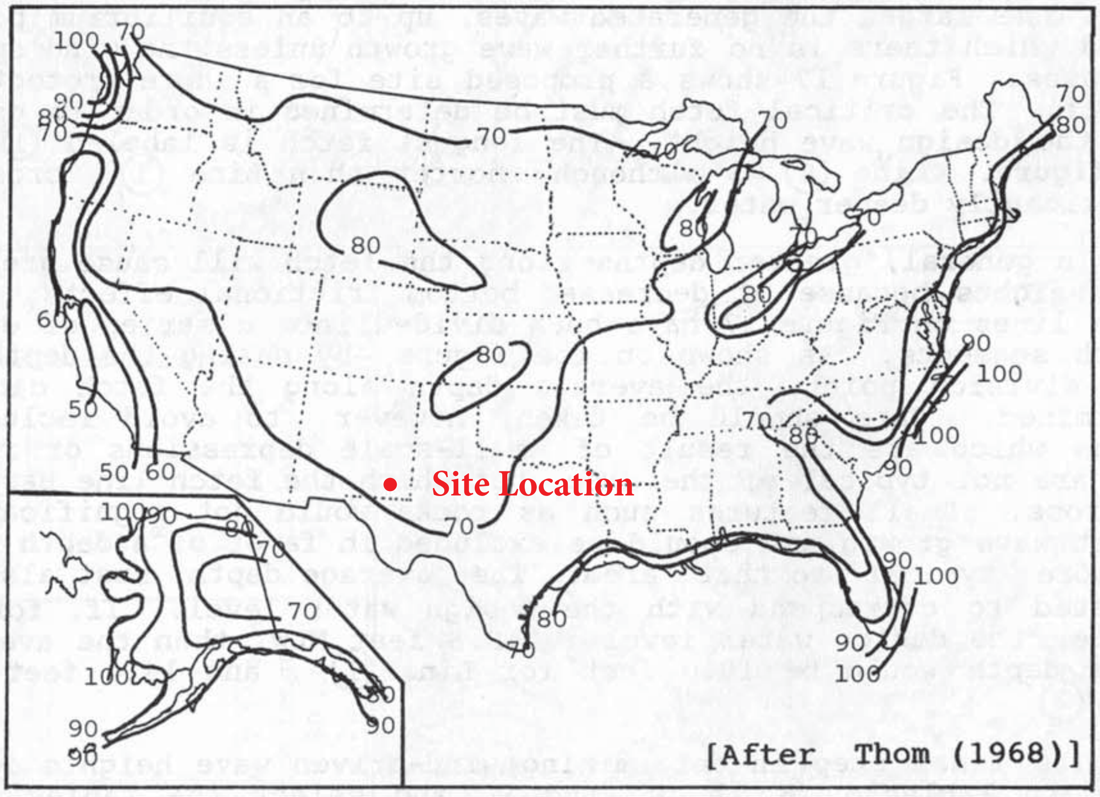

[After Thom (1968)]

Figure 16 Fastest-Mile Wind Speeds: 25-year Return Period

Structure Height

Waves breaking against an inclined structure will run up to an elevation higher than the Stillwater level depending on the roughness of the structure. Smooth concrete surfaces experience higher runup than rough stone slopes. Vertical structures also cause splashing and can experience overtopping. If possible, the structure should be built high enough to preclude severe overtopping. White spray does little damage, but solid jets of "green" water should be avoided. The required height of the structure will depend on the computed runup height based on the wave and structure characteristics. Detailed guidance is presented in Stoa (1978) and (1979). The runup height, R, can be found by a more approximate method as given below.

First, find the wavelength at the structure by using either Figure 26 or Equation (3) with the known depth at the structure and the design wave period. The definition sketch for runup is shown on Figure 27. For SMOOTH impermeable slopes, the runup, R, is given in Seelig (1980) by,

$$R=HC_1\,(0.12L/H)^\wedge(C_2\,(H/d_s)^{0.5}+C_3)$$

where: L = the local wavelength from Figure 26 or Eq. (3),
d_s = the depth at the structure (feet),
the approaching wave height (feet), and
C_1, C_2, C_3 = coefficients given below.

Structure Slope *	C_1	C_2	C_3
Vertical	0.96	0.23	+0.06
1 on 1.0	1.47	0.35	-0.11
1 on 1.5	1.99	0.50	-0.19
1 on 2.25	1.81	0.47	-0.08
1 on 3.0	1.37	0.51	+0.04

*Interpolate linearly between these values for other slopes.

For ROUGH slopes, Seelig (1980) gives the runup as,

$$R = (0.69\xi/1+0.5\xi)H \qquad (14)$$

$$\xi = \tan\theta/(H/L_o)^{0.5} \qquad (15)$$

$$L_o = 5.12\,T^2 \qquad (16)$$

θ = structure of the slope (e. g., $\tan\theta = 0.25$ for a slope of 1V on 4H

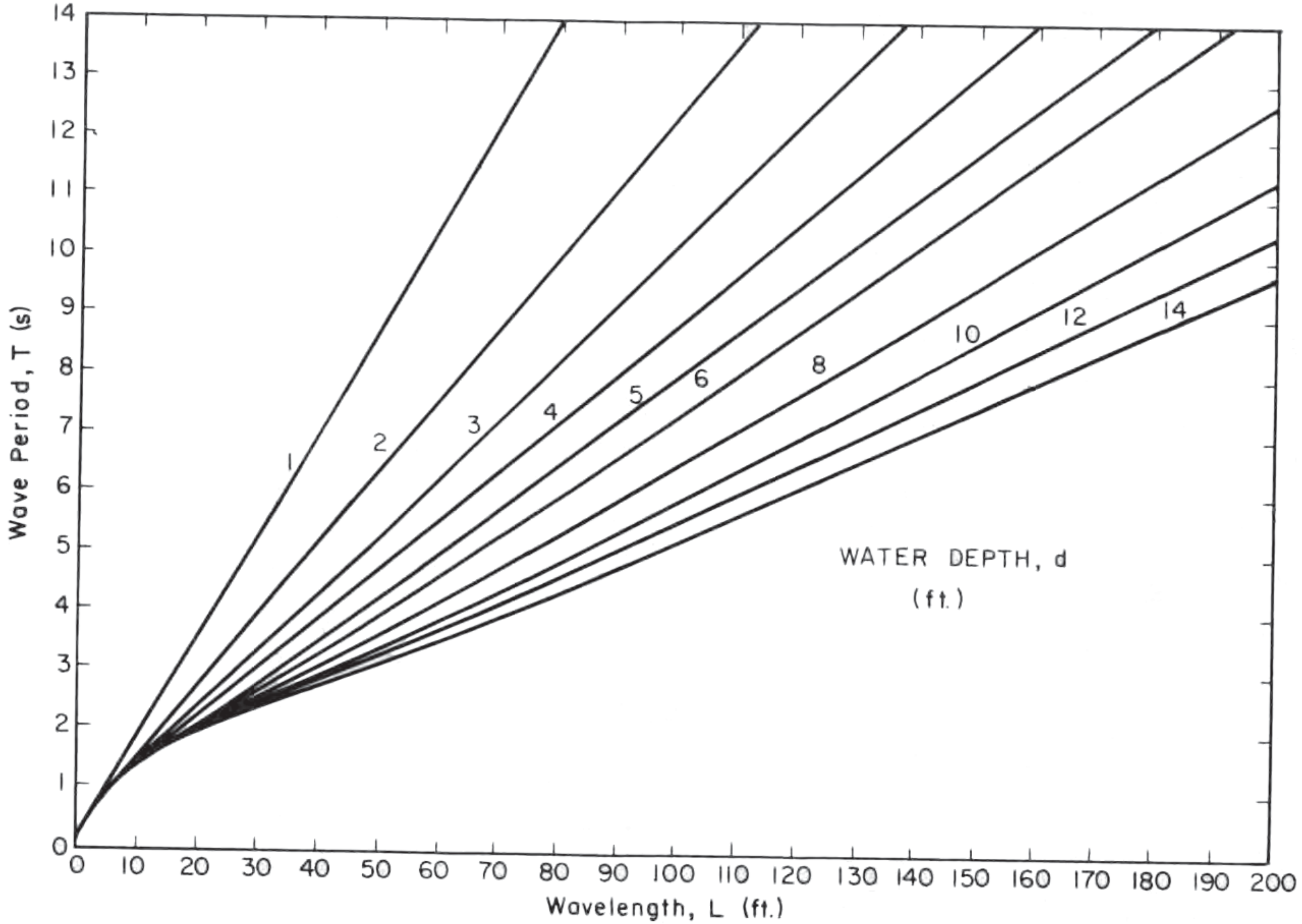

Figure 26 Local Wavelength Given Depth and Period
[After Giles and Eckert (1979)]

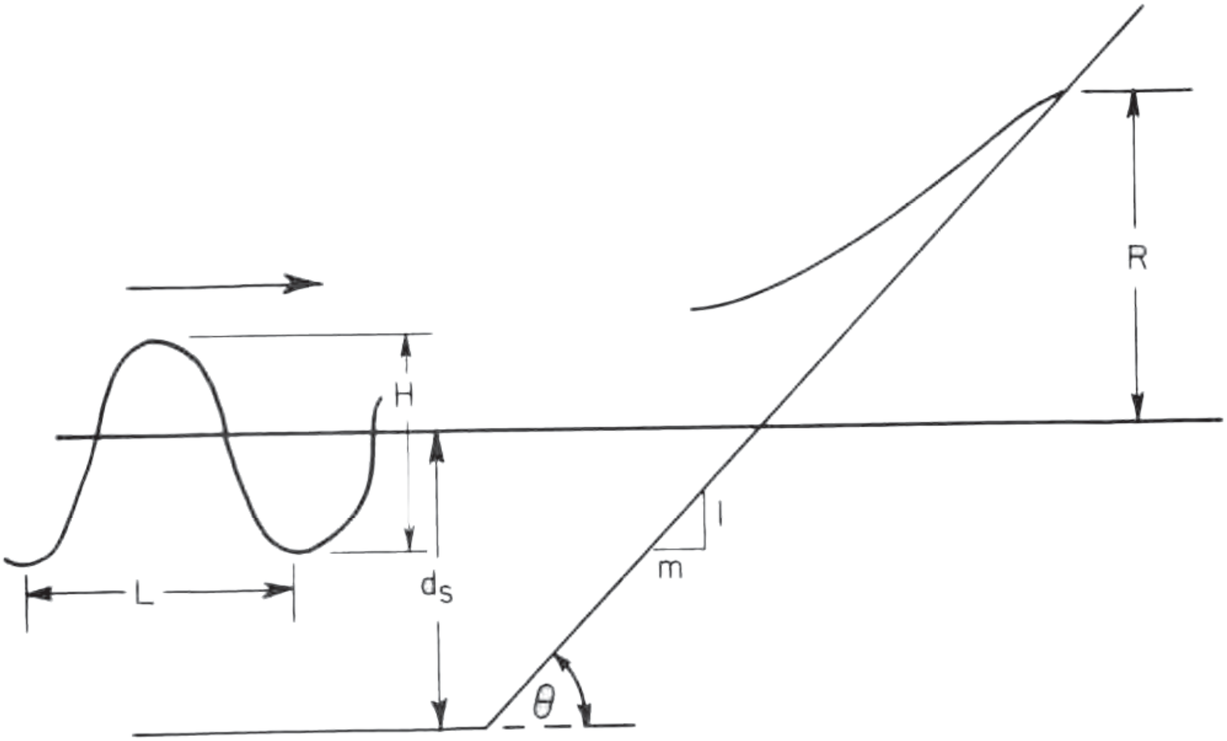

Figure 27 Wave Runup Definition Sketch

For STEPPED slopes, Stoa (1979) recommends using 70 to 75 percent of the smooth slope runup if the risers are vertical, and 86 percent if the edges are rounded.

A rough approximation of the runup height can be obtained from Table 11. However, the values in the table tend to represent the upper bound of the available data and may result in over design. Equations (13) and (14) or the methods given in Stoa (1978) and (1979) are recommended.

If it is impossible or undesirable to build a structure to the recommended height, a splash apron should be provided at the top of the structure. These are generally constructed of rock and they prevent the ground at the top from being eroded and undermining that portion of the structure.

Environmental Factors

Many different materials can be used to construct shore protection structures, including rock, concrete, timber, metal and plastics. The choice often depends on the desired permanence of the protection. Durable materials usually cost considerably more than shorter-lived materials used for temporary protection. The choice of materials is important because the coastal environment is a harsh testing ground for all man-made structures. Aside from wave forces, which are formidable in and of themselves, a host of chemical, biological and other factors can degrade structural materials. A brief review of these follows.

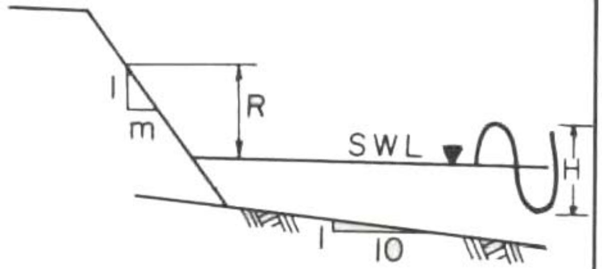 SMOOTH FACE	m 1.5 2.5 4.0	R 2.25H 1.75H 1.50H
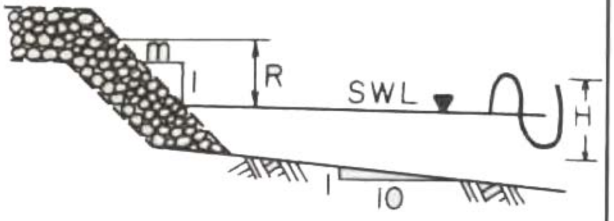 ROUGH FACE	m 1.5 2.5 4.0	R 1.25H 1.00H 0.75H
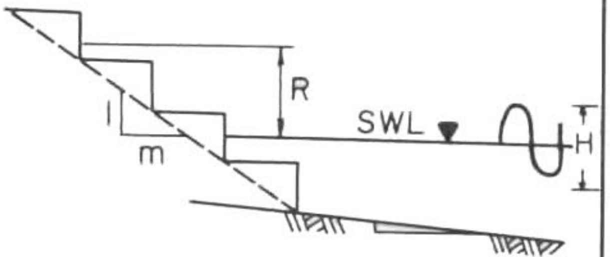 STEPPED FACE	m 1.5	R 2.00H
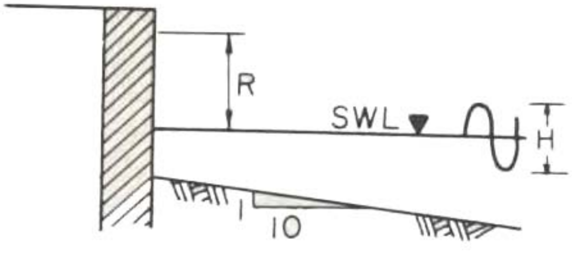 VERTICAL FACE	m —	R 2.00H

Table 11 Wave Runup Heights

ATTACHMENT III.9.B
WATER-RESOURCES ENGINEERING
(LINSLEY & FRANZINI 1979)

WATER-RESOURCES ENGINEERING

THIRD EDITION

Ray K. Linsley
Professor Emeritus of Hydraulic Engineering
Stanford University
Partner, Linsley, Kraeger Associates

Joseph B. Franzini
Professor of Civil Engineering
Associate Chairman, Department of Civil Engineering
Stanford University

McGraw-Hill Book Company

New York St. Louis San Francisco Auckland Bogotá Düsseldorf
Johannesburg London Madrid Mexico Montreal New Delhi Panama
Paris São Paulo Singapore Sydney Tokyo Toronto

by ordinary earth-moving methods would be expensive unless the excavated sediment has some sales value.

7-9 Wind setup and waves in reservoirs Earth dams must have sufficient freeboard above maximum pool level so that waves cannot wash over the top of the dam. Waves in reservoirs may also damage shoreline structures and embankments adjacent to the water and interfere with navigation. Part of the design of any reservoir is an estimate of wind setup and wave height.

Wind setup is the tilting of the reservoir water surface caused by the movement of the surface water toward the leeward shore under the action of the wind. This current of surface water is a result of tangential stresses between the wind and the water and of differences in atmospheric pressure over the reservoir. The latter, however, is, typically, a smaller effect. As a consequence of wind setup, the reservoir water surface is above normal still-water level on the leeward side and below the still-water level on the windward side. This results in hydrostatic unbalance, and a return flow at some depth must occur. The water-surface slope which results is that necessary to sustain the return flow under conditions of bottom roughness and cross-sectional area of flow which exist. Wind setup is generally larger in shallow reservoirs with rough bottoms.

Wind setup may be estimated from

$$Z_s = \frac{V_w^2 F}{1400d} \tag{7-3}$$

where Z_s is the rise in feet (meters) above still-water level, V_w is the wind speed in miles (kilometers) per hour, F is the *fetch* or length of water surface over which the wind blows in miles (kilometers), and d is the average depth of the lake along the fetch in feet (meters). In SI metric units, the constant in the denominator becomes 63,200.

Equation (7-3) is modified[1] from the original equation developed by Dutch engineers on the Zuider Zee. Additional information and techniques are given in other references.[2] Wind-setup effects may be transferred around bends in a reservoir and the value of F used may be somewhat longer than the straight-line fetch.

When wind begins to blow over a smooth surface, small waves, called capillary waves, appear in response to the turbulent eddies in the wind stream. These waves grow in size and length as a result of the continuing push of the wind on the back of the waves and of the shearing or tangential force between the wind and the water. As the waves grow in size and length, their speed increases until they move at speeds approaching the speed of the wind. Because growth of a wave depends in part upon the difference between wind speed and wave speed, the growth rate approaches zero as the wave speed approaches the wind speed.

---

[1] T. Saville, Jr., E. W. McClendon, and A. L. Cochran, Freeboard Allowances for Waves in Inland Reservoirs, *J. Waterways and Harbors Div., ASCE*, pp. 93–124, May, 1962.

[2] Shore Protection, Planning and Design, *Tech. Rept.* 3, 3d ed., U.S. Army Coastal Engineering Research Center, June, 1966.

The duration of the wind and the time and direction from which it blows are important factors in the ultimate height of a wave. The variability of the wind and the amazingly complex and yet to be fully understood response of the water surface to the wind lead to a wave pattern that is a superposition of many waves. The pattern is often described by its energy distribution or spectrum. The growth of wind waves as a function of fetch, wind speed, and duration can be calculated from knowledge of the mechanism of wave generation and use of collected empirical results.[1] The duration of the wind and the fetch play an important role because a wave may not reach its ultimate height if the wave passes out of the region of high wind or strikes a shore during the growth process. The depth of water also plays a key role, tending to yield smaller and shorter waves in deep water.

Wave-height data gathered at two major reservoirs[2] confirm the theoretical and experimental data for ocean waves if a modified value of fetch is used. The derived equation is

$$z_w = 0.034 V_w^{1.06} F^{0.47} \tag{7-4}$$

---

[1] W. J. Pierson, Jr., and R. W. James, Practical Methods for Observing and Forecasting Ocean Waves, *U.S. Navy Hydrographic Office Pub.* 603, 1955 (reprinted 1960).

[2] T. Saville, Jr., E. W. McClendon, and A. L. Cochran, Freeboard Allowances for Waves in Inland Reservoirs, *J. Waterways and Harbors Div., ASCE*, pp. 93–124, May, 1962.

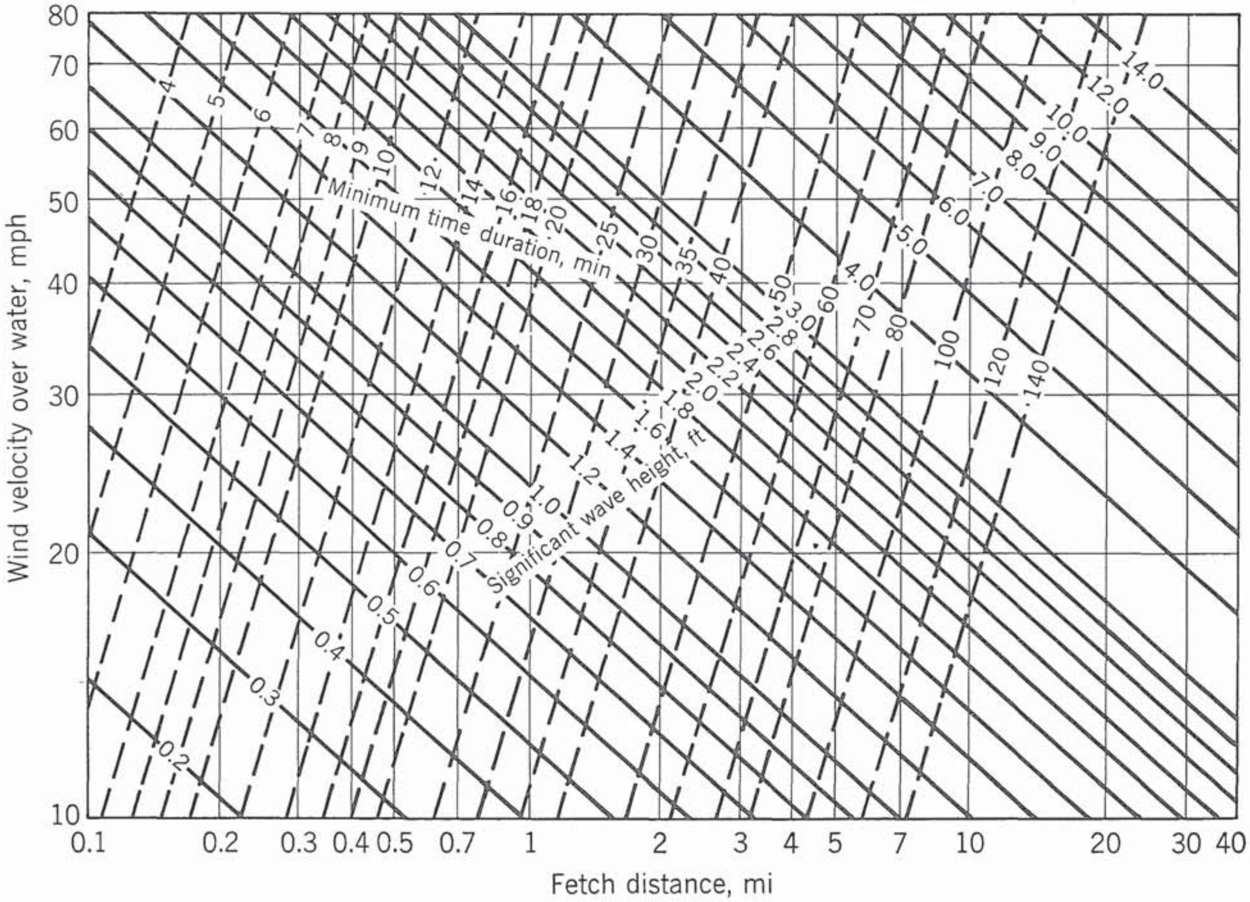

Figure 7-14 Significant wave heights and minimum wind durations (*from Saville, McClendon, and Cochran*). For metric version see Appendix B.

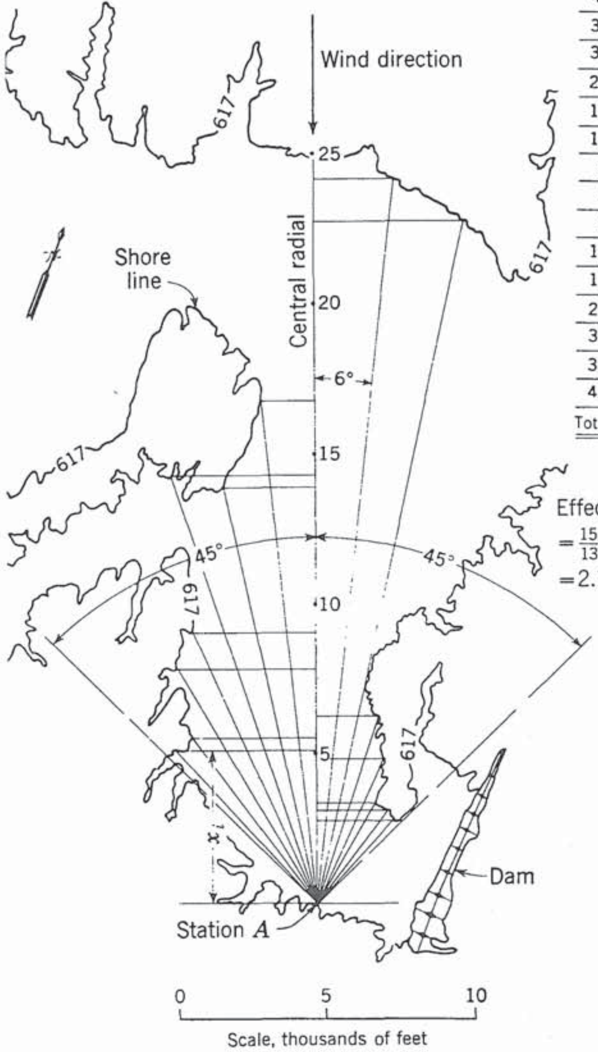

θ	cos θ	x_i	x_i cos θ
42	0.743	5.1	3.79
36	0.809	5.5	4.45
30	0.866	7.8	6.75
24	0.914	9.0	8.23
18	0.951	14.2	13.50
12	0.978	13.8	13.50
6	0.995	16.7	16.62
0	1.000	24.7	24.70
6	0.995	24.1	23.98
12	0.978	22.7	22.20
18	0.951	6.2	5.90
24	0.914	4.8	4.39
30	0.866	3.3	2.86
36	0.809	3.1	2.51
42	0.743	2.8	2.08
Total	13.512		155.46

Effective fetch

$$= \frac{155.46}{13.512} \times 10^3 = 11{,}510 \text{ ft}$$

$$= 2.18 \text{ mi}$$

igure 7-15 Computation of effective fetch. (*Modified from Saville, McClendon, and Cochran*)

vhere z_w is the average height in feet (meters) of the highest one-third of the waves nd is called the *significant wave height*, V_w is the wind velocity in miles (kilmeters) per hour about 25 ft (7.6 m) above the water surface, and F is the fetch in niles (kilometers). In SI metric units the coefficient becomes 0.005. The equation s shown graphically in Fig. 7-14[1] together with lines showing the minimum duraion of wind required to develop the indicated wave height. Figure 7-15 shows the nethod of computing the effective fetch for a narrow reservoir.

Since the design must be made before the reservoir is complete, wind data ver land must generally be used. Table 7-2 gives ratios of wind speed over land to hose over water and may be used to correct observed wind to reservoir condiions. Waves are critical only when the reservoir is near maximum levels. Thus in electing the critical wind speed for reservoirs subject to seasonal fluctuations,

---

[1] A graph for the solution of Eq. (7-4) in SI metric units is given in Appendix B-1.

Table 7-2 Relationship between wind over land and that over water. (After Saville, McClendon, and Cochran)

Fetch, mi (km)	0.5 (0.8)	1 (1.6)	2 (3.2)	4 (6.5)	6 (9.7)	8 (12.9)
$V_{\text{water}}/V_{\text{land}}$	1.08	1.13	1.21	1.28	1.31	1.31

only winds which can occur during the season of maximum pool levels should be considered. The direction of the wind and the adopted fetch must also be the same.

The height of the significant wave is exceeded about 13 percent of the time. If a more conservative design is indicated, a higher wave height may be chosen. Table 7-3 gives ratios of z'/z_w for waves of lower exceedance.

When a wave strikes a land slope, it will *run up* the slope to a height above its open-water height. The amount of run-up depends on the surface. Figure 7-16 shows the results of small-scale experiments[1] on smooth slopes and rubble mounds. Height of run-up z_r is shown as a ratio z_r/z_w and is dependent on the ratio of wave height to wavelength (wave steepness). Wavelength λ for deep-water waves may be computed from

$$\lambda = 5.12 t_w^2 \text{ ft} \qquad \text{or} \qquad \lambda = 1.56 t_w^2 \text{ m} \tag{7-5}$$

where the wave period t_w is given by

$$t_w = 0.46 V_w^{0.44} F^{0.28} \tag{7-6}$$

For shallow-water waves other length relations are appropriate.[2] In metric units the coefficient of Eq. (7-6) becomes 0.32. The curves for rubble mounds represent extremely permeable construction, and for more typical riprap on earth embankments the run-up may be somewhat higher, depending on both the permeability and the relative smoothness of the surface.

---

[1] T. Saville, Jr., Wave Run-up on Shore Structures, *Trans. ASCE*, Vol. 123, pp. 139–158, 1958; R. Y. Hudson, Laboratory Investigation of Rubble-mound Breakwaters, *Trans. ASCE*, Vol. 126, Part IV, pp. 492–541, 1962.

[2] Shore Protection, Planning and Design, *Tech. Rept.* 3, 3d ed., U.S. Army Coastal Engineering Research Center, June, 1966.

Table 7-3 Percentage of waves exceeding various wave heights greater than z_w. (After Saville, McClendon, and Cochran)

z'/z_w	1.67	1.40	1.27	1.12	1.07	1.02	1.00
Percentage of waves > z'	0.4	2	4	8	10	12	13

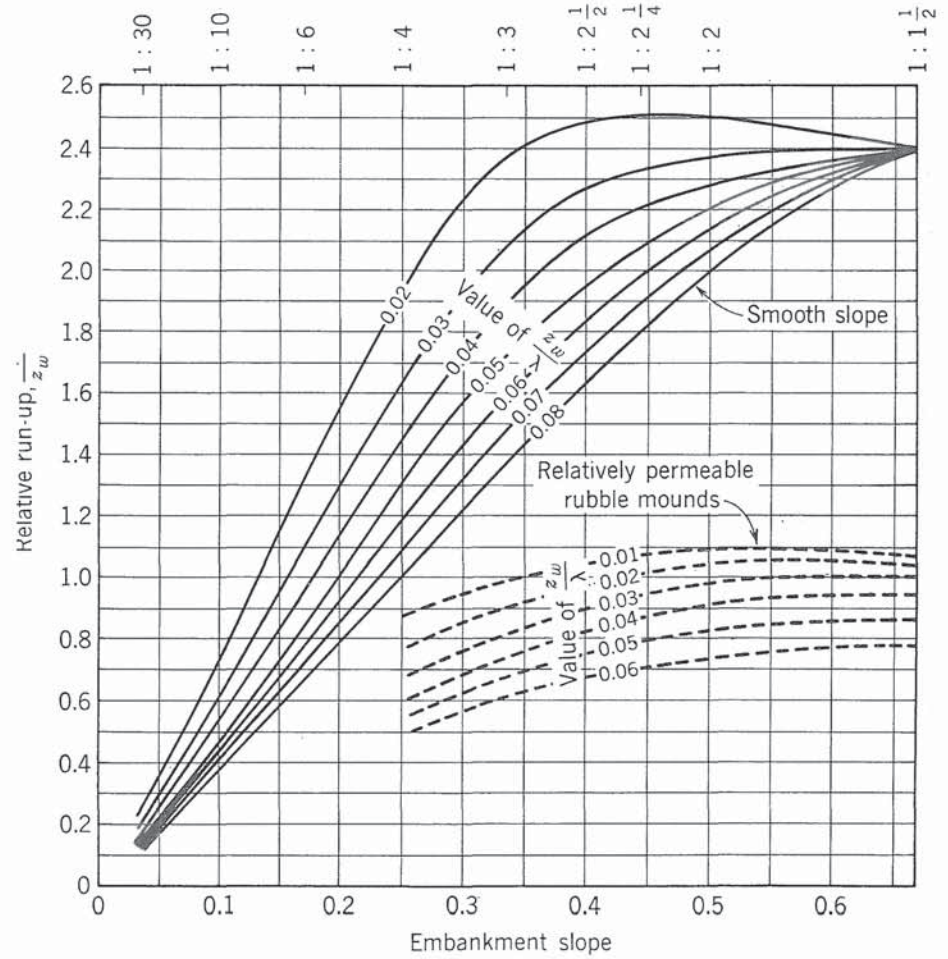

Figure 7-16 Wave run-up ratios versus wave steepness and embankment slopes. (*From Saville, McClendon, and Cochran*)

TABLE OF CONTENTS

1.0 INTRODUCTION III.10-1
  1.1 Site Location III.10-1
  1.2 Facility Description III.10-1
2.0 DESIGN CRITERIA III.10-2
3.0 REFERENCES III.10-2
4.0 FACTOR OF SAFTEY AGAINST PUNCTURE OF THE 10 OZ/YD^2 NONWOVEN GEOTEXTILE III.10-2
5.0 10 OZ/YD2 NONWOVEN GEOTEXTILE RETENTION, PERMEABILITY, PERMITTIVITY AND POROSITY III.10-4
  5.1 Protective Soil Layer Properties III.10-4
  5.2 AASHTO Requirements III.10-5
  5.3 Landfilldesign.com Geotextile Filter – Design Calculator Requirements III.10-5
5.3.1 Retention Requirement (Maximum AOS) Under Steady State Flow III.10-5
5.3.2 Permeability III.10-5
5.3.3 Clogging (Porosity Criteria) III.10-6
6.0 200-MIL GEOCOMPOSITE AND GEONET III.10-7
7.0 PROPOSED PROJECT SPECIFICATIONS III.10-9
  7.1 Nonwoven Geotextile III.10-9
  7.2 Geocomposite/Geonet III.10-9

LIST OF TABLES

Table No.	Title	Page
III.10.1	LANDFILL STATIC LOAD PARAMETERS	III.10-3
III.10.2	RECOMMENDED GEOTEXTILE FILTER CRITERIA (AASHTO M288-96)	III.10-5
III.10.3	PROPOSED NONWOVEN GEOTEXTILE SPECIFICATIONS	III.10-10

LIST OF ATTACHMENTS

Attachment No.	**Title**
III.10.A	KOERNER, ROBERT M. 2005. CHAPTER 2.5.4, "PUNCTURE RESISTANCE" IN DESIGNING WITH GEOSYNTHETICS, FIFTH EDITION, PAGES 171-173. NEW JERSEY: PEARSON PRENTICE HALL.
III.10.B	"GSE LINING TECHNOLOGY, INC.", NONWOVEN GEOTEXTILE PRODUCT DATA SHEET 2007
III.10.C	ADVANCED GEOTECH SYSTEMS. GEOTEXTILE FILTER CALCULATOR.LANDFILLDESIGN.COM. HTTP://WWW.LANDFILL DESIGN.COM/DESIGN/CALCULATORS/GEOFIL.ASPX (2013).
III.10.D	KOERNER, ROBERT M. 2005. "POROSITY" IN CHAPTER 2.3.4, "HYDRAULIC PROPERTIES" IN DESIGNING WITH GEOSYNTHETICS, FIFTH EDITION, PAGE 128. NEW JERSEY: PEARSON PRENTICE HALL.
III.10.E	GSE PRODUCT DATA SHEET FOR GSE BIODRAIN LP GEOCOMPOSITE (DOUBLE-SIDED)
III 10.F	GEOSYNTHETIC RESEARCH INSTITUTE; GRI STANDARD GC8 - DETERMINATION OF THE ALLOWABLE FLOW RATE OF A DRAINAGE GEOCOMPOSITE
III.10.G	GFR ARTICLE; LANDFILL DRAINAGE LAYERS: PART 3 OF 4, APRIL 2005

1.0 INTRODUCTION

Lea Land LLC (the Facility) is an existing Surface Waste Management Facility (SWMF) providing oil field waste solids (OFWS) disposal services. The existing Lea Land SWMF is subject to regulation under the New Mexico Oil and Gas Rules, specifically 19.15.9.711 and 19.15.36 NMAC, administered by the Oil Conservation Division (OCD) of the NM Energy, Minerals, and Natural Resources Department (NMEMNRD). This document is a component of the "Application for Permit Modification" that proposes continued operations of the existing approved waste disposal unit; lateral and vertical expansion of the landfill via the construction of new double-lined cells; and the addition of waste processing capabilities. The proposed Facility is designed in compliance with 19.15.36 NMAC and will be constructed and operated in compliance with a Surface Waste Management Facility Permit issued by the OCD. The Facility is owned by, and will be constructed and operated by, Lea Land LLC.

The Lea Land SWMF is one of the most recently designed facilities to meet the new more stringent standards that, for instance, mandate double liners and leak detection for land disposal. The new services that Lea Land will provide needed resources to fill an existing void in the market for technologies that exceed current OCD requirements.

1.1 Site Location

The Lea Land site is located approximately 27 miles northeast of Carlsbad, straddling US Highway 62-180 (Highway 62) in Lea County, NM. The Lea Land site is comprised of a 642-acre ± tract of land encompassing Section 32, Township 20 South, Range 32 East, Lea County, NM. Site access is currently provided on the south side of US Highway 62. The coordinates for the approximate center of the Lea Land site are Latitude 32°31'46.77" and Longitude -103°47'18.25".

1.2 Facility Description

The Lea Land SWMF comprises approximately 463 acres ± of the 642-acre ± site and will include two main components: an oil field waste Processing Area and an oil field waste solids Landfill, as well as related infrastructure (i.e., access, waste receiving, stormwater management, etc.). Oil field wastes are delivered to the Lea Land SWMF from oil and gas exploration and production operations in southeastern NM and west Texas. The Permit Plans (**Attachment III.1.A**) identify the locations of the Processing Area and Landfill Disposal facilities. The proposed facilities are detailed in **Table II.1.2** (**Volume II.1**) and are anticipated to be developed in four primary phases as described in **Table II.1.3** (**Volume II.1**).

2.0 DESIGN CRITERIA

The purpose of these calculations is to evaluate that:

- The proposed 10 ounces per square yard (oz./yd^2) nonwoven cushion geotextile provides adequate puncture resistance as to prevent damage the underlying 60-mil high-density polyethylene (HDPE) flexible membrane liner (FML) from the ¾ to 2-inch select aggregate in the leachate collection system.
- The proposed 10 ounces per square yard (oz./yd^2) nonwoven geotextile, as integral components of the geocomposites, meets specific retention, permeability, permittivity and porosity criteria based on the geotechnical characteristics of the proposed protective soil layer material to be used in the Lea Land landfill.
- The proposed 200-mil geonet as an integral component of the leak detection system, meets specific lateral flow, and porosity characteristics based on compressive loading.

3.0 REFERENCES

The following references were used to confirm the adequacy of a 10 oz./yd^2 nonwoven geotextile for use in the select aggregate leachate collection system and protective drainage layer system:

1. Koerner, Robert M. 2005. Chapter 2.5.4, “Puncture Resistance” In *Designing With Geosynthetics, Fifth Edition,* Pages 171-173. New Jersey: Pearson Prentice Hall.
2. Advanced Geotech Systems. Geotextile Filter Calculator. Landfilldesign.com. http://www.landfilldesign.com/design/calculators/geofil.aspx (2013).
3. Geotextile Criteria for Subsurface Drainage”, AASHTO M288-96
4. Geosynthetic Research Institute; GRI Standard GC8 – Determination of the Allowable Flow Rate of a Drainage Geocomposite
5. GFR Article; Landfill Drainage Layers: Part 3 of 4, April 2005

4.0 FACTOR OF SAFTEY AGAINST PUNCTURE OF THE 10 OZ/YD^2 NONWOVEN GEOTEXTILE

A 10 oz./yd^2 nonwoven geotextile is to be installed to provide a cushion between the ¾ to 2-inch select aggregate in the leachate collection system and the underlying 60-mil HDPE upper liner. The purpose of the nonwoven geotextile is to provide adequate puncture resistance so that the underlying HDPE upper liner is not damaged by the select aggregate; and to act as a filter to prevent soil fines from infiltrating into the geocomposite system.

The load on the 10 oz./yd^2 nonwoven geotextile is based on the maximum depth of the landfill components. For the Lea Land landfill, this occurs at a point in Unit III; A3 East-West Section as identified in the Pipe Loading Calculations (**Volume III.5**). In the same Section, it was shown that dynamic equipment loading was significantly less than the static load due to the over lying landfill components. The static load is calculated using the thickness of each layer and assigned unit weights taken from **Table III.5.2** and restated below. This static load will be used to determine the puncture resistance of the 10 oz./yd^2 nonwoven geotextile to protect the underlying 60-mil HDPE FML. The required vertical puncturing force is summarized in **Table III.10.1.**

TABLE III.10.1
Landfill Static Load Parameters

Layer	**Thickness (feet)**	**Unit Weight (pcf)**	**Actual Load (psf)**
Vegetative (Erosion) Layer	2.5	102.5	256.25
Barrier (Infiltration) Layer	0.5	102.5	51.25
Intermediate Cover Soils	1	102.5	102.5
Waste	205	74	15,170.0
Protective Soil Layer	2	102.5	205.0
Select Aggregate above the 10 oz/yd^2 nonwoven geotextile in the leachate collection trench	1	130	130.0
Design Load (P’)		**TOTAL:**	**15,915.0 psf (110.5 psi)**

The vertical puncturing force of the 10 oz/yd^2 nonwoven geotextile to protect the underlying 60-mil HDPE upper liner is calculated using the following equation (**Attachment III.10.A, Pages 171, 172,** and **173**):

$$F_{required} = (p')(d_a)^2(S_1)(S_2)(S_3)$$

Where:

$F_{required}$ = required vertical puncturing force to be resisted
p' = pressure exerted on the 10 oz./yd^2 geotextile = 110.5 psi
d_a = average diameter of puncturing aggregate = 1.375 inches
S_1 = protrusion factor of puncturing aggregate = 0.7
S_2 = scale factor to adjust the ASTM D4833 puncture test value that uses an 8.0 mm diameter puncture probe to the actual puncturing object= 0.6
S_3 = shape factor to adjust the ASTM D4833 flat puncture probe to the actual shape of the puncturing object=0.6

Note: Values used for S_1, S_2 and S_3 assumes the puncturing object is sub rounded and relatively large.

$$F_{required} = (110.5\ \text{psi})(1.375\ \text{inches})^2(0.7)(0.6)(0.6)$$

$$F_{required} = 52.65\ \text{lbs}$$

Assuming a Factor of Safety of 2.0, $F_{required}$ **=** 2.0 (52.65 lbs.) = 105.29 lbs. The puncture strength for a 10 oz./yd^2 nonwoven geotextile is established at 165 lbs (**Attachment III.9.B**). Therefore, the 10 oz./yd^2 nonwoven geotextile will provide adequate puncture resistance to a ¾ to 2-inch aggregate; and the underlying 60-mil HDPE FML will not be damaged by the select aggregate in the leachate collection system.

5.0 10 OZ/YD2 NONWOVEN GEOTEXTILE RETENTION, PERMEABILITY, PERMITTIVITY AND POROSITY

One function of the 10 oz./yd^2 nonwoven geotextile filter within the leachate collection system is the retain soils fines while allowing fluids to flow freely. To achieve this objective, the 10 oz./yd^2 nonwoven geotextile filter must meet certain retention, permeability, permittivity, maximum AOS size, and porosity criteria. These criteria were evaluated using the “Geotextile Filter – Design Calculator” listed on the landfilldesign.com website; and the requirements of AASHTO M288-96 (**Attachment III.10.C**).

5.1 Protective Soil Layer Properties

Attachments III.4.B and **C** provides laboratory geotechnical data for Lea Land landfill soils and are not repeated in this section. Based upon the geotechnical data, New Mexico Oil and Gas Rules, 19.15.36 NMAC, administered by the OCD, and standard landfill industry practices; Lea Land is proposing a protective drainage layer (i.e., protective soil layer, PSL) that meets the following properties:

- ≤ 10% passing the No. 200 sieve by weight
- Uniformity coefficient ≤ 30
- Hydraulic conductivity ≥ 2.0 x 10 $^{-4}$ cm/sec

The on-site soils encountered from the surface to the proposed depth of excavation consist primarily of clayey sand, sand-clay mixture that meet the criteria for SC material per the Unified Soil Classification System (USCS). As excavation proceeds, Lea Land will segregate potentially suitable soils for testing and use as the protective drainage layer as further described in **Volume III.4**. Proposed PSL materials will be pre-qualified as described in the Lea Land CQA Plan (**Volume II.7**).

5.2 AASHTO Requirements

The American Association of State Highway and Transportation Officials (AASHTO) recommends that the minimum hydraulic requirements shown in **Table III.10.2** be used for a nonwoven geotextile subsurface filter.

TABLE III.10.2
Recommended Geotextile Filter Criteria (AASHTO M288-96)

Nonwoven Geotextile Filter Criteria	Percent of Soil Passing the No. 200 Sieve By Weight		
	<15%	15% to 50%	>50%
Minimum Permittivity (ASTM D4491)	0.5 sec^{-1}	0.2 sec^{-1}	0.1 sec^{-1}
Maximum AOS (ASTM D4751)	0.43 mm	0.25 mm	0.22 mm

Based on the criteria in **Table III.10.2**, the nonwoven geotextile filter should have a minimum permittivity of 0.5 sec^{-1} and a maximum AOS size of 0.43 millimeters (mm).

5.3 Landfilldesign.com Geotextile Filter – Design Calculator Requirements

5.3.1 Retention Requirement (Maximum AOS) Under Steady State Flow

The particle size distribution of the soils was input into the Geotextile Filter – Design Calculator (**Attachment III.9.C**) and the resulting maximum AOS size was computed to be 1.18 mm, which is greater than the maximum AOS size recommended by AASHTO; therefore, an AOS size of 0.43 mm was used.

5.3.2 Permeability

The principle of the permeability (k) criteria is that, as long as the permittivity (Ψ) of the nonwoven geotextile is greater than the permeability of the soil, leachate will flow freely at the soil/geotextile interface. Given the importance of long-term function of the protective soil layer and geotextile, industry standards recommend a minimum Factor of Safety of 10 for the nonwoven geotextile permittivity:

$k_{geotextile} > 10\ k_{soil}$ where the permeability of the protective soil layer is $\geq 2.0 \times 10^{-4}$ cm/sec
$k_{geotextile} > 10\ (2.0 \times 10^{-4}$ cm/sec)
$k_{geotextile} > 2.0 \times 10^{-3}$ cm/sec

A typical 10 oz./yd^2 nonwoven geotextile product has a minimum permeability of 3 x 10^{-1} cm/sec (**Attachment III.10.B**); therefore, the selected nonwoven geotextile meets the permeability criteria.

5.3.3 Clogging (Porosity Criteria)

The nonwoven geotextile must remain at a high porosity to prevent clogging of the leachate collection system. Per Landfilldesign.com (**Attachment III.10.C.**), the porosity of the nonwoven geotextile is sufficient if it is greater than 30%. A GSE 10 oz./yd^2 nonwoven geotextile is selected for use in the leachate collection system for the Lea Land Landfill. Porosity is calculated using the following equation (**Attachment III.10.D, Page 128**):

$n_{geotextile} = 1 – [\mu / ((\rho)(t))]$

Where:

$n_{geotextile}$ = porosity of the GSE 10 oz./yd^2 nonwoven geotextile filter (dimensionless)
μ = mass per unit area of the GSE 10 oz./yd^2 nonwoven geotextile filter (0.0335 g/cm^2)
ρ = density of polymeric compound = 0.94 g/cm^3 for Polypropylene
t = thickness of the GSE 10 oz./yd^2 nonwoven geotextile filter = 100 mil (0.254 cm)

The design nonwoven geotextile filter has a weight of 10 oz./yd^2. Properties of the proposed 10 oz./yd^2 nonwoven geotextile filter are listed in **Attachment III.10.B.**

Therefore:

$n_{geotextile} = 1 – [\mu / ((\rho)(t))]$

$n_{geotextile} = 1 – [0.0335 \text{ g/cm}^2 / ((0.94 \text{ g/cm}^3) (0.254 \text{ cm}))]$

$n_{geotextile} = 1 – [0.0335 \text{ g/cm}^2 / 0.2388 \text{ g/cm}^2]$

$n_{geotextile} = 1 – [0.1403]$

$n_{geotextile} = 0.8597$

Since the porosity of the GSE 10 oz./yd^2 nonwoven geotextile is greater than 0.3, the selected nonwoven geotextile meets the required porosity criteria.

6.0 200-MIL GEOCOMPOSITE AND GEONET

The primary function of geocomposites is to convey or transmit fluid within the planar direction of a drainage layer. Transmissivity is defined as the flow rate of water transmitted through a unit width of the product under a specific hydraulic gradient as measured in a laboratory test. Solmax/GSE Environmental BioDrain LP Double-Sided Geocomposite (**Attachment III.4.D**), has a transmissivity of 0.48 gal/min/ft or (1 X 10^{-4} m^2/sec) and was evaluated using Solmax/GSE Environmental Online Drainage Design Manual; Landfill Leachate Collection and Removal System Design module; and Geosynthetic Research Institute (GRI) Standard GC8 – Determination of Allowable Flow Rate of a Drainage Geocomposite (**Attachment III.10.F**).

The supporting calculations utilize the average annual leakage rate through the performance-based alternative final cover system taken the HELP Model output Simulation #9. Of the 17.66 inches of precipitation the site receives annually, based on the five wettest consecutive years of historical weather data, evapotranspiration and runoff account for approximately 13 inches with the balance percolating through various cover layers. The HELP Model estimates that approximately 3.31 inches of moisture leak through the bottom layer and must be eventually be drawn back to the cover system to be evaporated; absorbed and contained in the oil field waste; or handled by the leachate collection and removal system component of the liner system. In the case of the proposed geonet serving as a drainage layer between the upper (primary) FML layer and the bottom (secondary) FML layer, the same model predicts zero moisture for the leak detection geonet to convey. Nevertheless, to be conservative, the same assumptions were used for both the geocomposite layer and the geonet leak detection layer. The geocomposite component is a part of the overall collection and removal system and is supported by a protective soil layer, leachate collection piping system, and potentially a chimney drain system. For simplicity as well as conservative design approach, Gordon/PSC limited the evaluation to the geocomposite performance only. The design approach is based on the determining the design transmissivity, adjusted for performance creep over time and other environmental factors, to make a comparison of the documented performance of the geocomposite and to determine the design factor of safety (FS).

The calculations utilize three equations (**Attachment III.4.F**). The first determines the required transmissivity as follows:

$$\theta_{design} = \frac{\vartheta i \times L}{sin\beta}$$

Where,

- θ_{design} = calculated design transmissivity (m^3/s per m width);
- ϑi = liquid impingement rate (m/s), i.e., leakage rate;

[from HELP Model, percolation through layer 2 is (3.3199 inches/year) x (1 year/365 days) = (9.096 x 10^{-3} inches/day) = (2.674 x 10^{-7} cm/s)]

- L = horizontal length of slope (m); [longest leachate path to sump, 278f =84.73m]
- β = slope angle (degrees) [floor cross slope is 3.78% = 2.166^0]

$$\theta_{design} = \frac{2.674\ x\ 10^{-9}\ ms\ x\ 84.73m}{\sin 2.166^0}$$

$$\theta_{design} = \frac{2.265\ x\ 10^{-7}\ m2/s}{0.03779}$$

θ_design = (〖5.995 x 10〗^(−7) m2/s)

The second equation determines the allowable transmissivity by multiplying the design transmissivity by an overall factor of safety. Per the referenced attachment, a factor of safety of 2.0 was chosen as the waste loading is at its maximum when considering the final cover crown.

$$\emptyset_{allowable} = \emptyset_{design} \times FS_D$$

$$\emptyset_{allowable} = \frac{5.995\ \times\ 10^{-7}m^2}{sec} \times 2.0$$

$$\emptyset_{allowable} = \frac{1.199\ \times\ 10^{-5}m^2}{sec}$$

The third equation determines the specified transmissivity by applying a long-term creep factor RF$_{CR}$; a chemical clogging factor RF$_{CC}$; and a biological clogging factor RF$_{BC}$ as specified:

- RF$_{CR}$ = 2.0
- RF$_{CC}$ = 1.0
- RF$_{BC}$ = 1.1

The equation is:

$$\emptyset_{specified} = \emptyset_{allowable} \times RF_{CR} \times RF_{CC} \times RF_{BC}$$

$$\emptyset_{specified} = \frac{1.199 \times 10^{-5}\, m^2}{sec} \times 2.0 \times 1.0 \times 1.1$$

$$\emptyset_{specified} = \frac{2.63 \times 10^{-5}\, m^2}{sec}$$

The GSE BioDrain HP Geocomposite has a Transmissivity of:

$$\emptyset_{GSE\ geocomposite} = \frac{1.0 \times 10^{-4}\, m^2}{sec}$$

The ratio of the geocomposite transmissivity and the specified transmissivity is:

$$\frac{\emptyset_{GSE\ geocomposite}}{\emptyset_{specified}} = 3.8 \text{ which is } > 1.0 \text{ and is therefore acceptable}$$

Note: The factor of safety and reduction factors have already been incorporated throughout the calculations and accumulatively represent 4.7. The acceptable transmissivity value is established by literature review.

7.0 PROPOSED PROJECT SPECIFICATIONS

7.1 Nonwoven Geotextile

The proposed 10 oz./yd^2 nonwoven geotextile for use in the Lea Land leachate collection system must meet the product properties calculated above. The 10 oz./yd^2 nonwoven geotextile product properties are specified on the data sheet published by GSE Lining Technology, Inc. (**Attachment III.10.B)**. The product properties specified for the 10 oz./yd^2 nonwoven geotextile are summarized in **Table III.10.3**.

7.2 Geocomposite/Geonet

The proposed 10 oz./yd^2 / 200-mil / 10 oz./yd^2 geocomposite and 200-mil geonet for use in the Lea Land leachate collection system and leak detection system must meet the product properties calculated above. The geocomposite product properties are specified on the data sheet published by GSE Lining Technology, Inc. (**Attachment III.10.E**).

TABLE III.10.3
Proposed Nonwoven Geotextile Specifications

Property	Calculated/Recommended Value	Product Specification
Puncture	44.08 lbs	165 lbs
Minimum Permittivity	0.5 sec^{-1}	1.20 sec^{-1}
Maximum AOS	0.43 mm	0.15 mm
Permeability	> 1.13×10^{-3} cm/sec	0.30 cm/sec
Porosity	> 0.30	0.86

ATTACHMENT III.10.A

KOERNER, ROBERT M. 2005. CHAPTER 2.5.4, "PUNCTURE RESISTANCE" IN DESIGNING WITH GEOSYNTHETICS, FIFTH EDITION, PAGES 171-173. NEW JERSEY: PEARSON PRENTICE HALL.

DESIGNING WITH GEOSYNTHETICS

FIFTH EDITION

ROBERT M. KOERNER

b = width of stone void, and

y = deformation into stone void.

Example 2.9

Given a truck with 700 kPa tire inflation pressure on a stone base course consisting of 50 mm maximum-sized stone with a geotextile beneath it, calculate (**a**) the required grab tensile stress on the geotextile, and (**b**) the factor of safety for a geotextile whose maximum grab strength is 500 N with cumulative reduction factors of 2.5. Use a value of $f(\epsilon) = 0.52$.

Solution: **(a)** Using an empirical relationship that $d_v = 0.33\, d_a$ and the value of $f(\epsilon) = 0.52$, the required grab tensile strength is as follows:

$$\begin{aligned} T_{\text{reqd}} &= p'(d_v)^2(0.52) \\ &= p'(0.33\, d_a)^2(0.52) \\ &= 0.057 p' d_a^2 \\ &= 0.057(700)(1000)(0.050)^2 \\ T_{\text{reqd}} &= 100\ N \end{aligned}$$

(b) The factor of safety on a 500 N maximum grab tensile geotextile with reduction factors of 2.5, is as follows:

$$\begin{aligned} \text{FS} &= \frac{T_{\text{allow}}}{T_{\text{reqd}}} \\ &= \frac{500/2.5}{100} \\ \text{FS} &= 2.0, \text{ which is acceptable.} \end{aligned}$$

2.5.4 Puncture Resistance

The geotextile must always survive the installation process. This is not just related to the roadway separation function; indeed, fabric survivability is critical in all types of applications; without it the best of designs are futile (recall Figure 2.20). In this regard, sharp stones, tree stumps, roots, miscellaneous debris, and other items, either on the ground surface beneath the geotextile or placed above it, could puncture through the geotextile during backfilling and when traffic loads are imposed. The design method suggested for this situation is shown schematically in Figure 2.32. For these conditions, the vertical force exerted on the geotextile (which is gradually tightening around the protruding object) is as follows:

$$F_{\text{reqd}} = p' d_a^2 S_1 S_2 S_3 \tag{2.30}$$

where

F_{reqd} = required vertical puncturing force to be resisted,

d_a = average diameter of the puncturing aggregate or sharp object,

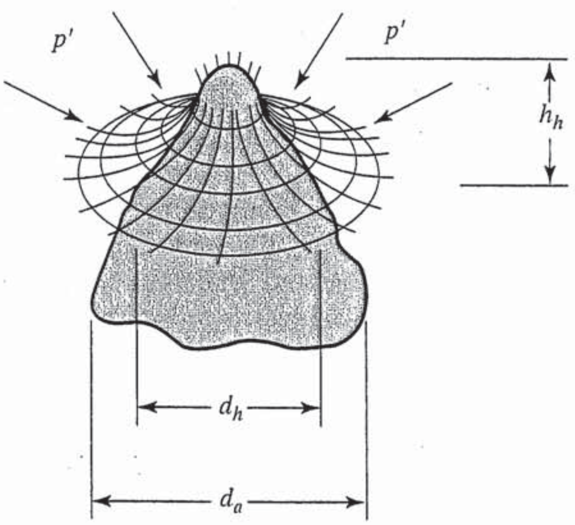

Figure 2.32 Visualization of a stone puncturing a geotextile as pressure is applied from above.

p' = pressure exerted on the geotextile (approximately 100% of tire inflation pressure at the ground surface for thin covering thicknesses),
S_1 = protrusion factor of the puncturing object (see Table 2.13),
S_2 = scale factor to adjust the ASTM D4833 puncture test value that uses a 8.0 mm diameter puncture probe to the actual puncturing object (see Table 2.13), and
S_3 = shape factor to adjust the ASTM D4833 flat puncture probe to the actual shape of the puncturing object (see Table 2.13).

Example 2.10

What is the factor of safety against puncture of a geotextile from a subrounded 25 mm diameter stone on the ground surface mobilized by a loaded truck with tire inflation pressure of 550 kPa traveling on the surface of the base course? The geotextile has an ultimate puncture strength of 300 N according to ASTM D4833.

TABLE 2.13 RECOMMENDED VALUES FOR FACTORS USED IN PUNCTURE ANALYSIS (DIMENSIONLESS)

Puncturing Object	S_1	S_2	S_3
Angular and relatively large	0.9	0.8	0.9
Angular and relatively small	0.6	0.6	0.7
Subrounded and relatively large	0.7	0.6	0.6
Subrounded and relatively small	0.4	0.4	0.5
Rounded and relatively large	0.5	0.4	0.4
Rounded and relatively small	0.2	0.2	0.3

S_1 = protrusion factor
S_2 = scale factor
S_3 = shape factor
} see equation (2.30)

Solution: Using the full stress on the geotextile of 550 kPa and factors from Table 2.13 of 0.55, 0.50, and 0.55 for S_1, S_2, and S_3 respectively, we see that

$$\begin{aligned} F_{\text{reqd}} &= p' d_a^2 S_1 S_2 S_3 \\ &= (550)(1000)(25 \times 0.001)^2(0.55)(0.50)(0.55) \\ F_{\text{reqd}} &= 52\text{ N} \end{aligned}$$

Assuming that the cumulative reduction factors are 2.0, the factor of safety is as follows:

$$\begin{aligned} \text{FS} &= \frac{F_{\text{allow}}}{F_{\text{reqd}}} \\ &= \frac{300/2.0}{52} \\ \text{FS} &= 2.9\text{, which is acceptable} \end{aligned}$$

2.5.5 Impact (Tear) Resistance

As with the puncture requirement just described, the resistance of a geotextile to impact is as much a survivability criterion as it is a separation function. Yet in many instances of separation the geotextile must resist the impact of various objects. The most obvious one is that of a rock falling on it, but there are also situations in which construction equipment and materials can cause or contribute to impact damage on geotextiles.

The problem addresses the energy mobilized by a free-falling object of known weight and height of drop. Rarely will an object be intentionally impelled onto an exposed geotextile with additional force, so only gravitational energy will be assumed.

To develop a design procedure, we assume a free-falling rock of specific gravity of 2.60, varying in diameter from 25 to 600 mm and falling from heights of 0.5 to 5 m. Using this data, the design curves in Figure 2.33 are developed. The relationship used is as follows:

$$\begin{aligned} E &= mgh \\ &= (V \times \rho)gh \\ &= [V \times (\rho_w G_s)]gh \\ &= \left(\frac{\pi(d_a/1000)^3}{6}\right)\left(\frac{1000\,kg}{m^3}\right)(2.6)(9.81)h \\ E &= 13.35 \times 10^{-6}\, d_a{}^3 h \end{aligned} \tag{2.31}$$

where

E = energy developed (Joules),
m = mass of the falling object (kg),
g = acceleration due to gravity (m/sec^2),

ATTACHMENT III.10.B

“GSE LINING TECHNOLOGY, INC.”, NONWOVEN GEOTEXTILE PRODUCT DATA SHEET

Product Data Sheet

GSE Nonwoven Geotextiles

GSE Nonwoven Geotextiles is a family of polypropylene, staple fiber, nonwoven, needlepunched geotextiles. Manufactured using an advanced manufacturing and quality system, these products are the most uniform and consistent nonwoven, needlepunched geotextile currently available in the industry. GSE combines a fiber selection and approval system with in-line quality control and a state-of-the-art laboratory to ensure that every roll shipped meets customer specifications. The company has performed extensive performance testing to evaluate suitability of its nonwovens for various applications. GSE Nonwoven Geotextiles are available in a range of weights to meet your specific project needs. *These product specifications meet or exceed GRI GT12, GRI GT13 and AASHTO M288.*

Product Specifications

TESTED PROPERTY	TEST METHOD	FREQUENCY	NW4	NW6	NW8	NW10	NW12	NW16
Product Code			GEO 0408002	GEO 0608002	GEO 0808002	GEO 1008002	GEO 1208002	GEO 1608002
AASHTO M288 Class			3	2	1	>1	>>1	>>>1
Mass per Unit Area, oz/yd² (g/m²)	ASTM D 5261	90,000 ft²	4 (135)	6 (200)	8 (270)	10 (335)	12 (405)	16 (540)
Grab Tensile Strength, lb (N)	ASTM D 4632	90,000 ft²	120 (530)	170 (755)	220 (975)	260 (1,155)	320 (1,420)	390 (1,735)
Grab Elongation, %	ASTM D 4632	90,000 ft²	50	50	50	50	50	50
Puncture Strength, lb (N)	ASTM D 4833	90,000 ft²	60 (265)	90 (395)	120 (525)	165 (725)	190 (835)	240 (1,055)
Trapezoidal Tear Strength, lb (N)	ASTM D 4533	90,000 ft²	50 (220)	70 (310)	95 (420)	100 (445)	125 (555)	150 (665)
Apparent Opening Size, Sieve No. (mm)	ASTM D 4751	540,000 ft²	70 (0.212)	70 (0.212)	80 (0.180)	100 (0.150)	100 (0.150)	100 (0.150)
Permittivity, sec⁻¹	ASTM D 4491	540,000 ft²	1.50	1.50	1.50	1.20	0.80	0.70
Permeability, cm/sec	ASTM D 4491	540,000 ft²	0.22	0.30	0.30	0.30	0.29	0.27
Water Flow Rate, gpm/ft² (l/min/m²)	ASTM D 4491	540,000 ft²	120 (4,885)	110 (4,480)	110 (4,480)	85 (3,460)	60 (2,440)	50 (2,035)
UV Resistance (% retained after 500 hours)	ASTM D 4355	per formulation	70	70	70	70	70	70
Roll Length[1], ft (m)			600 (182)	600 (182)	600 (182)	300 (91)	300 (91)	300 (91)
Roll Width[1], ft (m)			15 (4.6)	15 (4.6)	15 (4.6)	15 (4.6)	15 (4.6)	15 (4.6)
Roll Area, ft² (m²)			9,000 (836)	9,000 (836)	9,000 (836)	4,500 (418)	4,500 (418)	4,500 (418)

NOTES:

- The property values listed are in weaker principal direction. All values listed are Minimum Average Roll Values (MARV) except apparent opening size in mm and UV resistance. Apparent opening size (mm) is a Maximum Average Roll Value. UV is a typical value.
- [1]Roll lengths and widths have a tolerance of ±1%.

North America	GSE Lining Technology, Inc.	Houston, Texas	800.435.2008	281.443.8564	Fax: 281.230.6739
South America	GSE Lining Technology Chile S.A.	Santiago, Chile		56.2.595.4200	Fax: 56.2.595.4290
Asia Pacific	GSE Lining Technology Company Limited	Bangkok, Thailand		66.2.937.0091	Fax: 66.2.937.0097
Europe & Africa	GSE Lining Technology GmbH	Hamburg, Germany		49.40.767420	Fax: 49.40.7674234
Middle East	GSE Lining Technology-Egypt	The 6th of October City, Egypt		20.2.828.8888	Fax: 20.2.828.8889

www.gseworld.com

ATTACHMENT III.10.C

ADVANCED GEOTECH SYSTEMS. GEOTEXTILE FILTER CALCULATOR. LANDFILLDESIGN.COM. HTTP://WWW.LANDFILL DESIGN.COM/DESIGN/CALCULATORS/GEOFIL.ASPX

landfilldesign.com

Design Calculator

Geotextile Filter

Problem Statement

The function of a geotextile filter is to retain the soil while allowing the liquid to flow as freely as possible. In order to achieve this objective, a geotextile filter needs to meet: (1) **Retention criterion**: the filter opening size must be sufficiently small to retain soil particles. (2) **Permeability criterion**: the filter must be sufficiently permeable to ensure that the liquid flow is as free as possible, and (3) **Porosity criterion**: the filter should remain a high porosity so the probability for clogging is small.

Giroud's filter criteria is used in the calculation. It is recommended that AASHTO M288-96 minimum hydraulic requirements as shown in the table below be also considered in the selection of a geotextiles filter.

Table 1 - **Geotextile Criteria for Subsurface Drainage**
(after AASHTO M288-96)

Filter Criteria	PercentSoil Passing No. 200 (0.075mm) Sieve		
	<15	15 - 50	>50
Minimum Permittivity, ASTM D-4491	0.5 sec^{-1}	0.2 sec^{-1}	0.1 sec^{-1}
Maximum AOS, ASTM D-4751	0.43 mm	0.25 mm	0.22 mm

Retention Criterion

Giroud (2000) uses a linearization of the particle distribution curve that, when plotted with the classical log scale horizontal axis, is as close as possible to the actual particle distribution curve (Figure 1). A least variance approach was used to determine the best linearization of the central portion (Equation 1 & 2). It should be noted in Figure 1 that there is greater uncertainty on the two extremities (d_0 and d_{100}) of the actual particle size distribution. This justifies the use of the linear particle size distribution curve. The result obtained using Giroud's retention criterion is not affected by the truncation of the particle size distribution curve. A coefficient of determination (R2) is calculated to indicate the effectiveness of the linearization (Equation 3).

$m=\frac{n(\Sigma xy)-(\Sigma x)(\Sigma y)}{n(\Sigma(x^2))-(\Sigma x)^2}$	$b=\frac{(\Sigma y)(\Sigma(x^2))-(\Sigma x)(\Sigma xy)}{(\Sigma(x^2))-(\Sigma x)^2}$	$R^2=\frac{n(\Sigma xy)-(\Sigma x)(\Sigma y)}{\sqrt{[n\Sigma x^2-(\Sigma x)^2][n\Sigma y^2-(\Sigma y)^2]}}$
Eq. 1 - Slope determination by the method of the least squares	Eq. 2 - Intercept determination by the method of the least squares	Eq. 3 - The r-squared value can be interpreted as the proportion of the variance in y attributable, to the variance in x

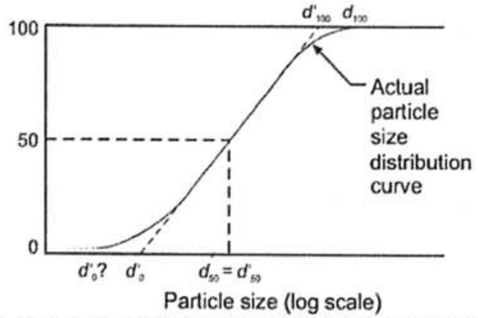

Figure 1 - Linearization of Particle Size Distribution Curve (after Giroud, 2000)

Table 2 - **Retention Criterion for the Hyperstable Case**
(C'_{cu} = 3) expressed using d'_{85S}

Soil Density	**Density Index (Relative Density) I_D**	**Relative Compaction (R_C)**	**Linear coefficient of uniformity of the soil, C'_u**	
			$1 \leq C'_u \leq 3$	**$C'_u \geq 3$**
loose	$I_D \leq 35\%$	$R_C \leq 86\%$	$O_F \leq (C'_u)^{0.3} d'_{85S}$	$O_F \leq (9/C'^{1.7}_u) d'_{85S}$
medium dense	$35\% < I_D \leq 65\%$	$86\% < R_C \leq 92\%$	$O_F \leq 1.5 (C'_u)^{0.3} d'_{85S}$	$O_F \leq (13.5/C'^{1.7}_u) d'_{85S}$
dense	$I_D > 65\%$	$R_C > 92\%$	$O_F \leq 2 (C'_u)^{0.3} d'_{85S}$	$O_F \leq (18/C'^{1.7}_u) d'_{85S}$

Table 3 - **Retention Criterion for the Hyperstable Case**
(C'_{cu} = 3) expressed using d'_{50S}

Soil Density	**Density Index (Relative Density) I_D**	**Relative Compaction (R_C)**	**Linear coefficient of uniformity of the soil, C'_u**	
			$1 \leq C'_u \leq 3$	**$C'_u \geq 3$**
loose	$I_D \leq 35\%$	$R_C \leq 86\%$	$O_F \leq (C'_u) d'_{50S}$	$O_F \leq (9/C'_u) d'_{50S}$
	$35\% < I_D \leq 65\%$	$86\% < R_C \leq 92\%$	$O_F \leq 1.5 (C'_u) d'_{50S}$	$O_F \leq (13.5/C'_u) d'_{50S}$

medium dense				
dense	$I_D > 65\%$	$R_C > 92\%$	$O_F \leq 2\,(C'_u)\,d'_{50S}$	$O_F \leq (18/C'_u)\,d'_{50S}$

where:

	C'_u	linear coefficient of uniformity of the soil $= d'_{60S} / d'_{10S}$
	I_D	relative density or density index of the soil
	d'_{ms}	the particle size such that m% (on the linear particle size distribution curve) of the linear soil particles by mass are smaller than d'_{ms}
	R_C	relative compaction
	O_F	maximum filter opening size

Permeability Criteria

	$k_f \geq k_s * I_s$	-> against excessive pore water pressure
	$k_f \geq k_s$	-> against excessive reduction of flow rate

where:

k_f - Hydraulic conductivity of the geotextile filter

k_s - Hydraulic conductivity of the soil

I_s - Hydraulic gradient in the soil (typical values presented in Table 4)

Table 4 - **Typical Hydraulic Gradients in the Soil in the Vicinity of the Filter**

Application	Typical hydraulic gradient
Ordinary dewatering trench	1
Vertical wall drain	1.5
Pavement edge drain	1
Landfill leachate collection/detection removal system	1
Landfill closure surface water collection removal system	1
Dam toe drains	2
Dam clay cores	3 to 10
Island channel protection	1
Shoreline protection	10
Liquid impoundment with clay liners	>10

Porosity Criteria

$$N_{GTX} > 0.3$$

where N_{GTX} is the porosity of geotextile filter.

There are two mechanisms that are known to cause progressive clogging in a filter: (1) Chemical, biological and biochemical clogging. (2) Accumulation of soil particles on or in the filter.

Input Values

Particle Size Distribution

d_{10}	.095	mm
d_{20}	.194	mm
d_{50}	1.010	mm
d_{60}	1.593	mm
d_{85}	10.41	mm

w factor 2

w Factor

loose	medium dense	dense
1	1.5	2

Calculate

Solution

Input data

Actual Particle Distribution Curve

d_{10}	0.095 mm
d_{20}	0.194 mm
d_{50}	1.010 mm
d_{60}	1.520 mm
d_{85}	6.500 mm

Output Data

Values of the Linear Particle Distribution Curve

d'_0	0.066 mm
d'_{10}	0.104 mm
d'_{20}	0.163 mm
d'_{50}	0.643 mm
d'_{60}	1.015 mm
d'_{85}	3.177 mm
d'_{100}	6.300 mm

Coefficient of Determination (R^2) **1.0844**

Indicates how acurate the linearization is

Coefficient of Uniformity **16.0000**

If greater than 1 and smaller than 5, it is said to be uniformly graded.
If greater than 20, it is said to be broadly graded.

Linear Coefficient of Uniformity **9.80**

Maximum Filter Opening Size **1.1802 mm**

Assistance

References

Giroud, J.P., 2000, "Filter Criteria", in Jubilee Volume 75th Anniversary of K. Terzaghi's Erdbaumechanik (Soil Mechanics), Technical University, Vienna, Austria, Vol 5/2000, Brandl, H., editor.

Giroud, J. P., 1994, "Quantification of Geosynthetics Behavior", Special Lecture, Proceedings of the Fifth International Conference on Geotextiles, Geomembranes and Related Products, Singapore, September 1994, Vol. 4, pp. 1249-1273.

Giroud, J. P., 1988, "Review of Geotextile Filter Criteria", Proceedings of the First Indian Geotextiles Conference, Bombay, India, December 1998, pp. 1-6.

Giroud, J. P., 1982, "Filter Criteria for Geotextiles", Proceedings of the Second International Conference of Geotextiles, Vol. 1, Las Vegas, Nevada, USA, August 1982, pp. 103-108.

ATTACHMENT III.10.D

KOERNER, ROBERT M. 2005. "POROSITY" IN CHAPTER 2.3.4, "HYDRAULIC PROPERTIES" IN DESIGNING WITH GEOSYNTHETICS, FIFTH EDITION, PAGE 128. NEW JERSEY: PEARSON PRENTICE HALL.

DESIGNING WITH GEOSYNTHETICS

FIFTH EDITION

ROBERT M. KOERNER

Since the test greatly resembles a direct shear test, albeit with stationary soil on both sides of the tensioned geotextile, a possible design strategy is to take direct shear test results (for both sides of the geotextile) and use these values for pullout design purposes. However, this may not be a conservative practice.

Test results by Collios et al. [36] show a relationship of pullout test results to shear test results with some notable exceptions. For pullout testing, if the soil particles are smaller than the geotextile openings, efficiencies are high; if not, they can be low. In all cases, however, pullout test resistances are less than the sum of the direct shear test resistances. This is due to the fact that the geotextile is taut in the pullout test and exhibits large deformations. This in turn causes the soil particles to reorient themselves into a reduced shear strength mode at the soil-to-geotextile interfaces, resulting in lower pullout resistance. The stress state mobilized in this test is both interesting and complex as evidenced by a large number of technical references on this topic.

2.3.4 Hydraulic Properties

Unlike the physical and mechanical properties just discussed, traditional tests on textile materials rarely have hydraulic applications; that is, the garment and industrial fabrics industry obviously does not test for liquid flow. As a result, hydraulic testing of geotextiles has required completely new and original test concepts, methods, devices, interpretation, and databases. Both geotextile tests in-isolation and with soil will be described in this section.

Porosity. As conventionally defined with soils in geotechnical engineering, the porosity of a geotextile is the ratio of void volume to total volume. It is related to the ability of liquid to flow through or within the geotextile but is rarely measured directly. Instead, it is calculated from other properties of the geotextile:

$$n = 1 - \frac{m}{\rho t} \tag{2.15}$$

where

n = porosity (dimensionless),
m = mass per unit area, i.e., weight, (g/m^2),
ρ = density (g/m^3), and
t = thickness (m).

It is seen in equation (2.15) that for a given geotextile's weight and density, the porosity is directly related to thickness. Thickness in turn is related to the applied normal stress (see again Figure 2.6).

Pore size can be measured by careful sieving with controlled-size glass beads (see the AOS test later in this section), by the use of image analyzers [37], or by the use of

ATTACHMENT III.10.E

GSE PRODUCT DATA SHEET FOR GSE BIODRAIN LP GEOCOMPOSITE (DOUBLE-SIDED)

PRODUCT DATA SHEET

GSE BioDrain LP Geocomposite (Double-Sided)

GSE BioDrain LP consists of a GSE HyperNet geonet heat-laminated with a nonwoven geotextile on one side and with a low permittivity (LP) woven geotextile on the other side. The geotextiles serve as filters and separators, while the geonet core provides liquid flow medium. The type of geotextile and thickness of the core can be varied depending on requirements of a project.

Product Specifications

Tested Property	Test Method	Frequency	Minimum Average Roll Value(1)
Geocomposite			
Transmissivity(2), gal/min/ft (m^2/sec)	ASTM D 4716	1/540,000 ft^2	0.48 (1×10^{-4})
Geonet Core(1,3)-HyperNet 200			
Geonet Core Thickness, mil	ASTM D 5199	1/50,000 ft^2	200
Density, g/cm^3	ASTM D 1505	1/50,000 ft^2	0.94
Tensile Strength (MD), lb/in	ASTM D 7179	1/50,000 ft^2	45
Carbon Black Content, %	ASTM D 4218	1/50,000 ft^2	2.0
Geotextile(1,3) - 6 oz/yd^2			
Mass per Unit Area, oz/yd^2	ASTM D 5261	1/90,000 ft^2	6
Grab Tensile Strength, lb	ASTM D 4632	1/90,000 ft^2	160
Grab Elongation	ASTM D 4632	1/90,000 ft^2	50%
CBR Puncture Strength, lb	ASTM D 6241	1/540,000 ft^2	435
Trapezoidal Tear Strength, lb	ASTM D 4533	1/90,000 ft^2	65
AOS, US sieve (mm)	ASTM D 4751	1/540,000 ft^2	70 (0.212)
Permittivity, sec^{-1}	ASTM D 4491	1/540,000 ft^2	1.5
Water Flow Rate, gpm/ft^2	ASTM D 4491	1/540,000 ft^2	110
UV Resistance, % retained	ASTM D 4355 (after 500 hours)	per formulation	70
Geotextile(1,3) - LP			
Grab Tensile Strength, lb	ASTM D 4632	1/540,000 ft^2	150
Puncture Strength, lb	ASTM D 4833	1/180,000 ft^2	100
AOS, US sieve (mm)	ASTM D 4751	1/180,000 ft^2	70 US Sieve (0.212)
Permittivity, sec^{-1}	ASTM D 4491	1/180,000 ft^2	0.2
Water Flow Rate, gpm/ft^2	ASTM D 4491	1/180,000 ft^2	12
UV Resistance, % retained	ASTM D 4355 (after 500 hours)	per formulation	85
NOMINAL ROLL DIMENSIONS(4)			
Roll Width, ft			14.5
Roll Length, ft			230
Roll Area, ft^2			3,335

NOTES:

- (1)All geotextile properties are minimum average roll values except AOS which is maximum average roll value and UV resistance is typical value. Geonet core thickness is nominal value.
- (2)This is an index transmissivity value measured at stress = 10,000 psf, water at 70 F gradient = 0.1; between steel plates for 15 minutes. Contact GSE for performance transmissivity value for use in design.
- (3)Component properties prior to lamination.
- (4)Roll widths and lengths have a tolerance of ±1%.

[*]

AT THE CORE:

BioDrain is used as a leachate distribution layer to disperse leachate uniformly over the waste system.

BioDrain LP can also be used for applications with extended UV exposure enviroment.

GSE is a leading manufacturer and marketer of geosynthetic lining products and services. We've built a reputation of reliability through our dedication to providing consistency of product, price and protection to our global customers.

Our commitment to innovation, our focus on quality and our industry expertise allow us the flexibility to collaborate with our clients to develop a custom, purpose-fit solution.

[DURABILITY RUNS DEEP]

For more information on this product and others, please visit us at GSEworld.com, call 800.435.2008 or contact your local sales office.

GSE ENVIRONMENTAL™

ATTACHMENT III.10.F

GEOSYNTHETIC RESEARCH INSTITUTE; GRI STANDARD GC8 – DETERMINATION OF THE ALLOWABLE FLOW RATE OF A DRAINAGE GEOCOMPOSITE

Geosynthetic Institute
475 Kedron Avenue
Folsom, PA 19033-1208 USA
TEL (610) 522-8440
FAX (610) 522-8441

Original: April 17, 2001
Rev. 1: January 9, 2013-Editorial

GRI Standard GC8*

Standard Guide for

Determination of the Allowable Flow Rate of a Drainage Geocomposite

1. Scope

1.1 This guide presents a methodology for determining the allowable flow rate of a candidate drainage geocomposite. The resulting value can be used directly in a hydraulics-related design to arrive at a site-specific factor of safety.
1.2 The procedure is to first determine the candidate drainage composite's flow rate for 100-hours under site-specific conditions, and then modify this value by means of creep reduction and clogging reduction factors.
1.3 For aggressive liquids, a "go-no go" chemical resistance procedure is suggested. This is a product-specific verification test for both drainage core and geotextile covering.
1.4 The type of drainage geocomposites under consideration necessarily consists of a drainage core whose purpose it is to convey liquid within its manufactured plane. The drainage core can be a geonet, 3-D mesh, built-up columns, single or double cuspations, etc.
1.5 The drainage core usually consists of a geotextile on its upper and/or lower surface. In some cases, the drainage core is used by itself. The guide addresses all of these variations.
1.6 The guide is also applicable to thick nonwoven geotextiles when they are utilized for their drainage capability.

---

*This GRI standard is developed by the Geosynthetic Research Institute through consultation and review by the member organizations. This specification will be reviewed at least every 2-years, or on an as-required basis. In this regard it is subject to change at any time. The most recent revision date is the effective version.

1.7 All types of polymers are under consideration in this guide.

1.8 The guide does not address the required (or design) flow rate to which a comparison is made for the final factor of safety value. This is clearly a site-specific issue.

2. Referenced Documents

2.1 ASTM Standards

D1987 – “Test Method for Biological Clogging of Geotextile or Soil/Geotextile Filters”

D2240 – “The Method for Rubber Property – Durometer Hardness”

D4716 – “Test Method for Constant Head Hydraulic Transmissivity (In Plane Flow) of Geotextiles and Geotextile Related Products”

D5322 – “Standard Practice for Immersion Procedures for Evaluating the Chemical Resistance of Geosynthetics to Liquids”

D6364 – “Test Method for Determining the Short-Term Compression Behavior of Geosynthetics”

D6388 – “Standard Practice for Tests to Evaluate the Chemical Resistance of Geonets to Liquids”

D6389 – “Standard Practice for Tests to Evaluate the Chemical Resistance of Geotextiles to Liquids”

2.2 GRI Standards

GS4 – Test Method for Time Dependent (Creep) Deformation Under Normal Pressure

2.3 Literature

Giroud, J.-P., Zhao, A. and Richardson, G. N. (2000), “Effect of Thickness Reduction on Geosynthetic Hydraulic Transmissivity,” Geosynthetics International, Vol. 7, Nos. 4-6, pp. 433-452.

Koerner, R. M. (2012), Designing with Geosynthetics, 6th Edition, Xlibris Publishing Co., 914 pgs.

3. Summary of Guide

3.1 This guide presents the necessary procedure to be used in obtaining an allowable flow rate of a candidate drainage geocomposite. The resulting value is then compared to a required (or design) flow rate for a product-specific and site-specific factor of safety. The guide does not address the required (or design) flow rate value, nor the subsequent factor of safety value.

3.2 The procedures recommended in this guide use either ASTM or GRI test methods.

3.3 The guide is applicable to all types of drainage geocomposites regardless of their core configuration or geotextile type. It can also be used to evaluate thick nonwoven geotextiles.

4. Significance and Use

4.1 The guide is meant to establish uniform test methods and procedures in order for a designer to determine the allowable flow rate of a candidate drainage geocomposite for site-specific conditions.

4.2 The guide requires communication between the designer, testing organization and manufacturer in setting site-specific control variables such as product orientation, stress level, stress duration, type of permeating liquid and materials below/above the geocomposite test specimen.

4.3 The guide is useful to testing laboratories in that a prescribed guide is at hand to provide appropriate data for both designer and manufacturer clients.

5. Structure of the Guide

5.1 Basic Formulation – This guide is focused on determination of a "q_{allow}" value using the following formula:

$$q_{\text{allow}} = q_{100}\left[\frac{1}{RF_{CR} \times RF_{CC} \times RF_{BC}}\right] \tag{1}$$

where

q_{allow} = allowable flow rate
q_{100} = initial flow rate determined under simulated conditions for 100-hour duration
RF_{CR} = reduction factor for creep to account for long-term behavior
RF_{CC} = reduction factor for chemical clogging
RF_{BC} = reduction factor for biological clogging

Note 1: By simulating site-specific conditions (except for load duration beyond 100 hours and chemical/biological clogging), additional reduction factors such as intrusion need not be explicitly accounted for.

Note 2: The value of q_{allow} is typically used to determine the product-specific and site-specific flow rate factor of safety as follows:

$$FS = \frac{q_{\text{allow}}}{q_{\text{reqd}}} \tag{2}$$

The value of "q_{reqd}" is a design issue and is not addressed in this guide. Likewise, the numeric value of the factor-of-safety is not addressed in this guide. Suffice it to say that, depending on the duration and criticality of the situation, FS-values should be conservative unless experience allows otherwise.

5.2 Upon selecting the candidate drainage geocomposite product, one must obtain the 100-hour duration flow rate according to the ASTM D4716 transmissivity test. This establishes the base value to which drainage core creep beyond 100-hours and clogging from chemicals and biological matter must be accounted for.

> Note 3: It is recognized that the default duration listed in ASTM D4716 is 15-minutes. This guide purposely requires that the test conditions be maintained for 100-hours.

5.3 Reduction Factor for Creep – This is a long-term (typically 10,000 hours) compressive load test focused on the stability and/or deformation of the drainage core without the covering geotextiles. Stress orientation can be perpendicular or at an angle to the test specimen depending upon site-specific conditions.

5.4 Chemical and/or Biological Clogging – The issue of long term reduction factors to account for clogging within the core space is a site-specific issue. The issue is essentially impractical to simulate in the laboratory, hence a table is provided for consideration by the designer.

5.5 Chemical Resistance/Durability – This procedure results in a "go-no go" decision as to potential chemical reactions between the permeating liquid and the polymers comprising the drainage core and geotextiles. The issue will be addressed in this guide but is not a reduction factor, per se.

6. Determination of the Base Line Flow Rate (q_{100})

6.1 Using the ASTM D4716 transmissivity test with the conditions stated below (unless otherwise agreed upon by the parties involved), determine the 100-hour flow rate of the drainage geocomposite under consideration.

6.1.1 The test specimen shall be the entire geocomposite. If geotextiles are bonded to the drainage core, they shall not be removed and the entire geocomposite shall be tested as a unit. A minimum of three replicate samples in the site-specific orientation shall be tested and the results averaged for the reported value.

6.1.2 Specimen size shall be 300 × 300 mm (12 × 12 in.) within the stressed area.

6.1.3 The specimen orientation is to be agreed upon by the designer, testing laboratory and manufacturer. In this regard, it should be recognized that the specimen orientation during testing has to match the proposed installation orientation. Thus the site-specific design governs both the testing orientation and subsequent field installation orientation.

6.1.4 Specimen substratum shall be one of the following four options. The decision of which is made by the project designer, testing organization and manufacturer. The options are (i) rigid platen, (ii) foam, (iii) sand or (iv) site-specific soil or other material.

6.1.4.1 If a rigid platen is used the choices are usually wood, plastic or metal. The testing laboratory must identify the specifics of the material used.

6.1.4.2 If closed cell foam is used, it shall be 12 mm (0.5 in.) thick and a maximum durometer of 2.0 as measured in ASTM D2240, Type D.

6.1.4.3 If sand is used it shall be Ottawa test sand at a relative density of 85%, water content of 10% and compacted thickness of 25 mm (1.0 in.).

6.1.4.4 If site-specific soil or other material is used it must be carefully considered and agreed upon between the parties involved. Size, gradation, moisture content, density, etc., are all important considerations.

6.1.5 Specimen superstratum shall also be one of the four same options as mentioned in § 6.1.3 above. It need not be the same as the substratum.

6.1.6 The applied stress level is at the discretion of the designer, testing organization and manufacturer. Unless stated otherwise, the orientation shall be normal to the test specimen.

6.1.7 The duration of the loading shall be for 100 hours. A single site-specific data point is obtained at that time, i.e., it is not necessary to perform intermediate flow rate testing, unless otherwise specified by the various parties involved.

6.1.8 The hydraulic gradient at which the above data point is taken (or a range of hydraulic gradients) is at the discretion of the designer, testing organization and manufacturer.

6.1.9 The permeating liquid is to be tap water, unless agreed upon otherwise by the designer, testing organization, and manufacturer.

6.1.10 Calculations

$$Q = kiA \tag{3}$$

$$Q = ki(Wt)$$

$$Q / W = \theta i \tag{4}$$

$$q = \theta i \tag{5}$$

where

Q = flow rate per unit time (m^3/sec)
k = permeability (m/sec)
i = hydraulic gradient (= H/L)
H = head loss across specimen (m)
L = length of specimen (m)
A = cross sectional area of specimen (m^2)
W = width of specimen (m)
t = thickness of specimen (m)
θ = transmissivity (m^3/sec-m or m^2/sec)
q = flow rate per unit width (m^2/sec)

The results can be presented as flow rate per unit width (Q/W), or as transmissivity (θ), as agreed upon by the parties involved.

7. Reduction Factor for Creep

7.1 Using the GRI GS4 test method or ASTM D6364 (mod.) for time dependent (creep) deformation, the candidate drainage core is placed under compressive stress and its decrease in thickness (deformation) is monitored over time.

> Note 4: This is not a flow rate test, although the test specimen can be immersed in a liquid to be agreed upon by the designer, testing organization, and manufacturer. However, it is usually a test conducted without liquid.

7.1.1 The test specimen shall be the drainage core only. If geotextiles are bonded to the drainage core they should be carefully removed. Alternatively, a sample of the drainage core can be obtained from the manufacturer before the geotextiles are attached. A minimum of three replicate tests shall be performed and the results averaged for the reported value.

7.1.2 Specimen size should be 150 × 150 mm (6.0 × 6.0 in.) and placed in a rigid box made from a steel base and sides. The steel load plate above the test specimen shall be used to transmit a constant stress over time. Deformation of the upper plate is measured by at least two dial gauges and the results averaged accordingly.

> Note 5: For high stress conditions requiring a large size and number of weights with respect to laboratory testing and safety, the specimen size can be reduced to 100 × 100 mm (4.0 × 4.0 in.).

7.1.3 Specimen substratum and superstratum shall be rigid platens. Alternatively, a 1.5 mm (60 mil) thick HDPE geomembrane can be placed against the drainage core with the steel plates as back-ups.

7.1.4 The test specimen shall be dry unless water or a simulated or site-specific leachate is agreed upon by the parties involved.

7.1.5 The normal stress magnitude(s) shall be the same as applied in the transmissivity test described in Section 6.0. Alternatively, it can be as agreed upon by the designer, testing organization, and manufacturer.

7.1.6 The load inclination shall be normal to the test specimen. If there exists a tendency for the core structure to deform laterally, separate tests at the agreed upon load inclinations shall also be performed at the discretion of the parties involved.

7.1.7 The dwell time shall be 10,000 hours. If, however, this is a confirmation test (or if a substantial data base exists on similar products of the same type), the dwell time can be reduced to 1000 hours. This decision must be made with agreement between the designer, testing organization, and manufacturer.

> Note 6: Alternative procedures to arrive at an acceptable value for the creep reduction factor based on shorter test times (e.g., the use of time-temperature superposition or stepped isothermal method) may be acceptable if agreed upon by the various parties involved.

7.1.8 The above process results in a set of creep curves similar to Figure 1(a). The curves are to be interpreted as shown in Figure 1(b). The reduction factor for creep of the core is interpreted according to the following formulas, after Giroud, Zhao and Richardson (2000).

$$RF_{CR} = \left[\frac{(t_{CO} / t_{original}) - (1 - n_{original})}{(t_{CR} / t_{original}) - (1 - n_{original})} \right]^3 \tag{6}$$

where

RF_{CR} = reduction factor for creep
$t_{original}$ = original thickness (m)
t_{CO} = thickness at 100-hours (m)
t_{CR} = thickness at >>100-hours, e.g., at 10,000 hours (m)
$n_{original}$ = original porosity (see Equation 7)

$$n_{original} = 1 - \frac{\mu}{\rho t_{original}} \tag{7}$$

where

μ = mass per unit area (kg/m^2)
ρ = density of the formulation (kg/m^3)

7.1.9 The above illustrated numeric procedure is <u>not applicable</u> to drainage geocomposites which include geotextiles. It is for the drainage core only.

<u>Example</u>: A HDPE geonet has the following properties: mass per unit area μ = 1216 g/m^2 (or 1.216 kg/m^2); density ρ = 950 kg/m^2 and original thickness of 8.55 mm.

Test specimens were evaluated according to ASTM D4716 for 100 hours and the average thickness decreased to 7.14 mm. A 10,000 hour creep test was then performed on a representative specimen according to GRI-GS4 and the resulting thickness further decreased to 6.30 mm. Thus Δy in Figure 1(b) is 7.14 – 6.30 = 0.84 mm. Determine the creep reduction factor "RF_{CR}".

<u>Solution</u>: The porosity n, is calculated according to Eq. (7) as follows

$$
\begin{aligned}
n_{original} &= 1 - \frac{\mu}{\rho t_{original}} \\
&= 1 - \frac{1.216}{(950)(0.00855)} \\
&= 1 - 0.150 \\
n_{original} &= 0.850
\end{aligned}
$$

The reduction factor for creep is calculated according to Eq. (6) as follows:

$$
\begin{aligned}
RF_{CR} &= \left[\frac{(t_{CO} / t_{original}) - (1 - n_{original})}{(t_{CR} / t_{original}) - (1 - n_{original})}\right]^3 \\
&= \left[\frac{(7.14 / 8.55) - (1 - 0.850)}{(6.30 / 8.55) - (1 - 0.850)}\right]^3 \\
&= \left[\frac{0.835 - 0.150}{0.737 - 0.150}\right]^3 \\
&= \left[\frac{0.685}{0.587}\right]^3 \\
RF_{CR} &= 1.59
\end{aligned}
$$

Note 7: Other calculation methods to arrive at the above numeric value of creep reduction factor may be considered if agreed upon by the various parties involved.

8. Reduction Factors for Core Clogging

There are two general types of core clogging that might occur over a long time period. They are chemical clogging and biological clogging. Both are site-specific and both are essentially impractical to simulate in the laboratory.

8.1 Chemical clogging within the drainage core space can occur with precipitates deposited from high alkalinity soils, typically calcium and magnesium. Other precipitates can also be envisioned such as fines from turbid liquids although this is less likely since the turbid liquid must typically pass through a geotextile filter. It is obviously a site-specific situation.

8.2 Biological clogging within the drainage core space can occur by the growth of biological organisms or by roots growing through the overlying soil and extending downward, through the geotextile filter, and into the drainage core. It is a site-specific situation and depends on the local, or anticipated, vegetation, cover soil, hydrology, etc.

8.3 Default tables for the above two potential clogging mechanisms (chemical and biological) are very subjective and by necessity broad in their upper and lower limits. The following table is offered as a guide.

Range of Clogging Reduction Factors (modified from Koerner, 1998)

Application	Chemical Clogging (RF_{CC})	Biological Clogging (RF_{BC})
Sport fields	1.0 to 1.2	1.1 to 1.3
Capillary breaks	1.0 to 1.2	1.1 to 1.3
Roof and plaza decks	1.0 to 1.2	1.1 to 1.3
Retaining walls, seeping rock and soil slopes	1.1 to 1.5	1.0 to 1.2
Drainage blankets	1.0 to 1.2	1.0 to 1.2
Landfill caps	1.0 to 1.2	1.2 to 3.5
Landfill leak detection	1.1 to 1.5	1.1 to 1.3
Landfill leachate collection	1.5 to 2.0	1.1 to 1.3

9. Polymer Degradation

9.1 Degradation of the materials from which the drainage geocomposite are made, with respect to the site-specific liquid being transmitted, is a polymer issue. Most geocomposite drainage cores are made from polyethylene, polypropylene, polyamide or polystyrene. Most geotextile filter/separators covering the drainage cores are made from polypropylene, polyester or polyethylene.

Note 8: It is completely inappropriate to strip the factory bonded geotextile off of the drainage core and then test one or the other component. The properties of both the geotextile and drainage core will be altered in the lamination process from their original values.

9.2 If polymer degradation testing is recommended, the drainage core and the geotextile should be tested separately in their as-received condition before lamination and bonding.

9.3 The incubation of the drainage cores and/or geotextile coupons is to be done according to the ASTM D5322 immersion procedure.

9.4 The testing of the incubated drainage cores is to be done according to ASTM D6388 which stipulates various test methods for evaluation of incubated geonets.

Note 9: For drainage cores other than geonets, e.g., columnar, cuspated, meshes, etc., it may be necessary to conduct additional tests than appear in ASTM D6388. These tests, and their procedures, should be discussed and agreed upon by the project designer, testing organization, and manufacturer.

9.5 The testing of the incubated geotextiles is to be done according to ASTM D6389 which stipulates various test methods for evaluation of incubated geotextiles.

Note 10: The information obtained in testing the drainage core (Section 9.4) and the geotextile (Section 9.5) result in a "go-no go" situation and not in a reduction factor, per se. If an adverse chemical reaction is indicated, one must select a different type of geocomposite material (drainage core and/or geotextile).

10. Summary

10.1 For a candidate drainage geocomposite, the 100-hour flow rate behavior under the site-specific set of variables, e.g., specimen orientation, stress level, hydraulic gradient, and permeating liquid is to be obtained per ASTM D4716 following procedures of Section 6.0.

10.2 A reduction factor for long term creep of the drainage core following Section 7.0 per GRI GS4 or ASTM D6364 (mod.) is then obtained. The result is usually a unique value for a given set of conditions.

10.3 A reduction factor for chemical and/or biological clogging, as discussed in Section 8.0 can be included. It is very much a site-specific situation at the discretion of the parties involved.

10.4 Polymer degradation to aggressive liquids is covered in separate immersion and test protocols, e.g., ASTM D5322 (immersion), ASTM D6388 (geonets) and ASTM D6389 (geotextiles) as discussed in Section 9.0. The procedure does not result in a reduction factor, rather in a "go-no go" decision with the product under consideration.

10.5 Other possible flow rate reductions and/or concerns such as flow in overlap regions, effect of high or low temperatures, etc., are site-specific and cannot readily be generalized in a guide such as this.

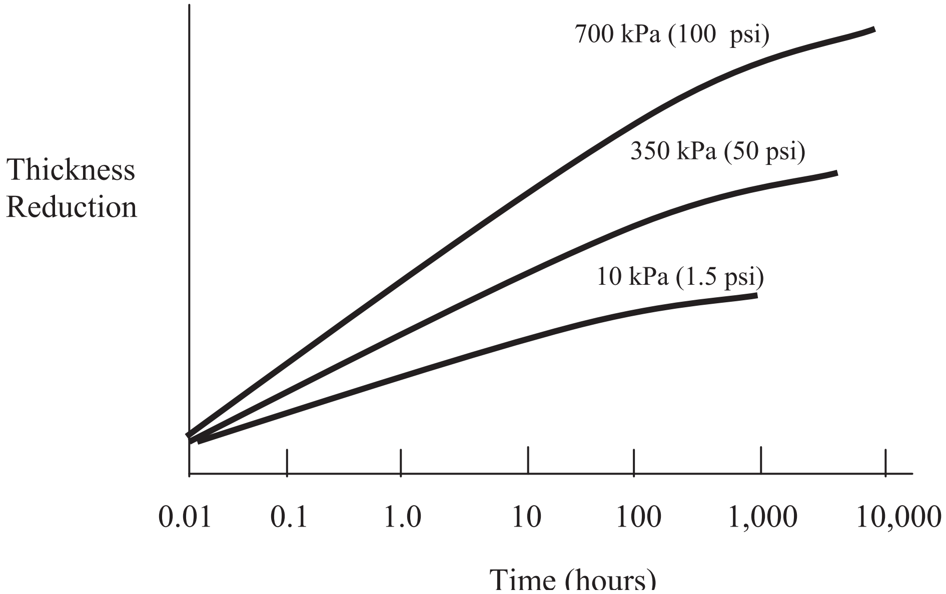

(a) Hypothetical data from creep testing illustrating effect of normal load magnitude

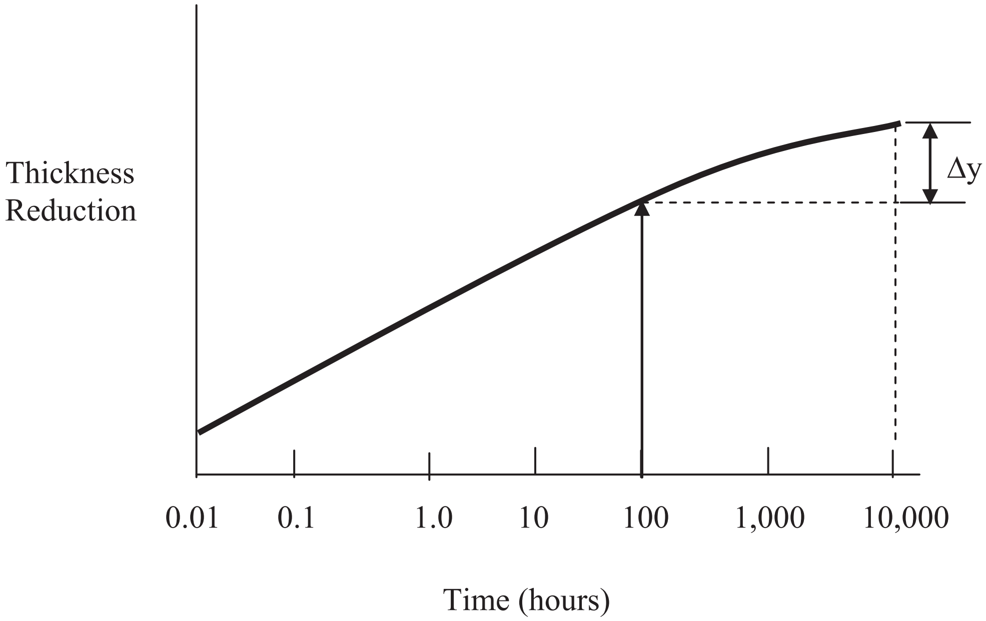

(b) Interpretation of project specific normal load curve to obtain creep reduction factor

Figure 1 – Hypothetical example of creep test data and data interpretation to obtain creep reduction factor

ATTACHMENT III.4.G

GFR ARTICLE; LANDFILL DRAINAGE LAYERS: PART 3 OR 4, APRIL 2005

By Richard Thiel, Dhani Narejo, and Gregory N. Richardson

Landfill drainage layers: Part 3 of 4

Previous *GFR* articles have described the methodology for designing a geocomposite for use in a landfill leachate collection system (LCS). (See Part 1 of this series—January/February 2005 for a complete *GFR* bibliography of geocomposite-related articles since 1998.) This article updates the magazine's series regarding this aspect of designing with geocomposites by expanding the documented design methodology to account for the different stages of a landfill life during operations and post-closure.

Also, the article will review the basic design equation for head buildup, which for geocomposites is often referred to as the "Giroud Equation." It will be seen that a key input parameter to this equation, which is the leachate impingement rate, typically decreases over the landfill life. At the same time, the reduction factors typically increase over the landfill life due to aging, creep, chemical precipitation and the like. These two considerations tend to offset each other. A logical design can take these factors into account so that an overly conservative design does not result. The proposed design concept is illustrated through the use of a design example.

Background on "design" transmissivity

The calculation procedure for the design of geocomposites used in leachate collection systems can be performed using Giroud's method (Giroud et. al. 2000). The "design" transmissivity (θ_{design})—also referred to in the literature as "required" transmissivity ($\theta_{required}$)—of relatively low-thickness layers such as with geonets and geocomposites can be calculated as:

Equation 1

$$\theta_{design} = \frac{q_i \bullet L}{\sin\beta}$$

where θ_{design} = calculated design transmissivity for geocomposites (m^3/s per m width); q_i = liquid impingement rate (m/s); L = horizontal length of slope (m); and β = slope angle (degrees). Leachate impingement into the leachate collection layer is buffered to lesser and greater degrees due to the thickness of overlying waste and soil material. A commonly used computer model that is available for performing water balance analyses is the HELP Model (Schroeder, et al. 1994). Landfill leachate collection system (LCS) impingement rates depend on the operational stage of a landfill, which can be conveniently broken down as follows: (i) initial operation stage; (ii) active operation stage; and (iii) post-closure stage. Early in the landfill operation, surface water control may not be well established, and relatively thin layers of soil and waste may allow for a relatively large portion of the surface water to infiltrate into the LCS. As filling progresses, the use of protective soil and surface grading can reduce the amount of infiltration into the waste; thus, decreasing the LCS flow rate. In the post-closure period, the application of the final cover system greatly reduces the amount of infiltration into the waste, and thus greatly reduces the amount of leachate entering the LCS.

Photo 1. Author Richard Thiel holding 35 mm rounded gravel cemented by leachate chemical precipitation.

Pressure kPa (psf)	Creep Reduction Factor (RF_{CR})
48 (1000)	1.1
240 (5000)	1.2
478 (10,000)	1.3
718 (15,000)	1.6

Table 1. Creep reduction factors (RF_{CR}) for one manufacturer's biplanar geonet product line (Narejo and Allen 2004).

It is possible to model the landfill leachate generation in several operational stages (as few as three and as many as six) with varying geometry, waste thickness, cover slopes and cover materials. Separate HELP analyses can be performed for each operational stage modeled. An example of what a designer might consider when modeling a landfill broken into four stages is presented below (Bachus, et. al 2004):

- *Initial operation stage*—Model leachate flow into the LCS based on a "fluff" layer of waste being placed in the landfill cell. A typical waste thickness might be on the order of 10 ft. The slope might be fairly flat (~2%) with a 6 inch daily cover layer.
- *Active operation stage I*—Model leachate flow into the LCS based on the landfill at a representative point in time in the landfill's developmental phasing plan. The waste thickness might be on the order of half of the final thickness of the waste. The slope might be fairly flat, with an intermediate cover.
- *Active operation stage II*—Model leachate flow into the LCS based on the landfill at final grades with an intermediate cover in place and fair vegetation.
- *Post-closure stage*—Model leachate flow into the LCS based on the final closure conditions. The landfill will be at final grades with a permanent cover in place. Often this condition is modeled in HELP as simply the amount of infiltration through the final cover system.

Allowable and specified transmissivity

The next step in the design process is to define an allowable transmissivity (θ_{allow}), which is related to the design transmissivity (θ_{design}), by multiplying the design transmissivity by an overall factor of safety, FS_D.

Equation 2

$$\theta_{allow} = \theta_{design} \bullet FS_D$$

The overall drainage factor of safety should be applied to take into account possible uncertainties in the selection and determination of the design parameters. Recommended values of FS_D are typically between 2.0 and 3.0 or greater (Giroud, et al. 2000). For bottom liner LCS systems, a lower FS would be acceptable in the early stages of the project, but a higher FS may be desirable for long-term conditions. The authors will demonstrate that taking into account the various stages of landfill development and leachate generation can work to the advantage of many designs accounting for appropriate factors of safety.

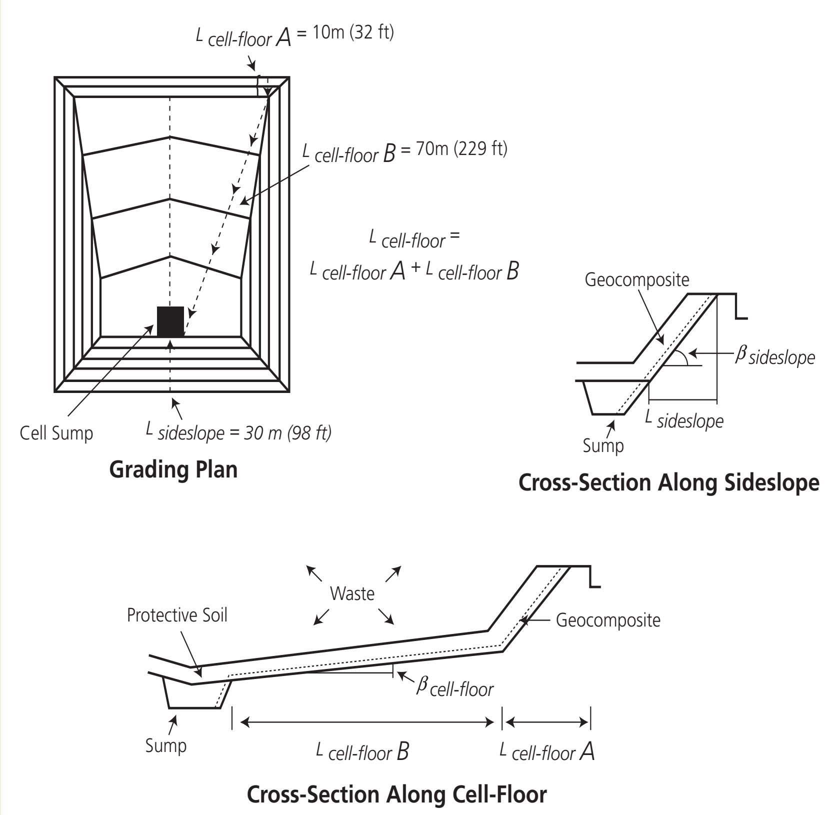

Figure 1. Simplified schematic of design geometry for example problem.

Finally, the *specified* (also referred to as *maximum* or *ultimate* in the literature) transmissivity (θ_{spec}), which is the value that appears in the specifications, is obtained by multiplying the allowable transmissivity by appropriate *reduction factors*. These reduction factors take into account environmental factors such as biological clogging, chemical clogging and long-term creep of the geocomposite drainage layer that will decrease the in-place capacity of the geocomposite over time. The magnitude of each reduction factor (which should be equal to or greater than 1) should reflect a correction that provides a best estimate of the anticipated reduction. The reduction factors should not be inflated to a larger value to account for uncertainty, since this is accounted for in the overall factor of safety, FS. The *specified* transmissivity is shown in **Equation 3** (see also, test standard GRI-GC8 [2001]):

Equation 3

$$\theta_{spec} = \theta_{allow} \bullet RF_{CR} \bullet RF_{CC} \bullet RF_{BC}$$

where:

θ_{spec} = specified value of transmissivity for geocomposites or geonet (m^2/s), as tested in accordance with GRI-GC8 and ASTM D4716;

θ_{allow} = minimum allowable transmissivity of geocomposites or geonet (m^2/s);

RF_{CR} = partial reduction factor for long-term creep (dimensionless);

RF_{CC} = partial reduction factor for chemical clogging (dimensionless); and

RF_{BC} = partial reduction factor for biological clogging (dimensionless).

Additional reduction factors, such as for particulate clogging, can be incorporated by the designer if deemed applicable to a given situation. The specified transmissivity (θ_{spec}) in **Equation 3** should be compared with the

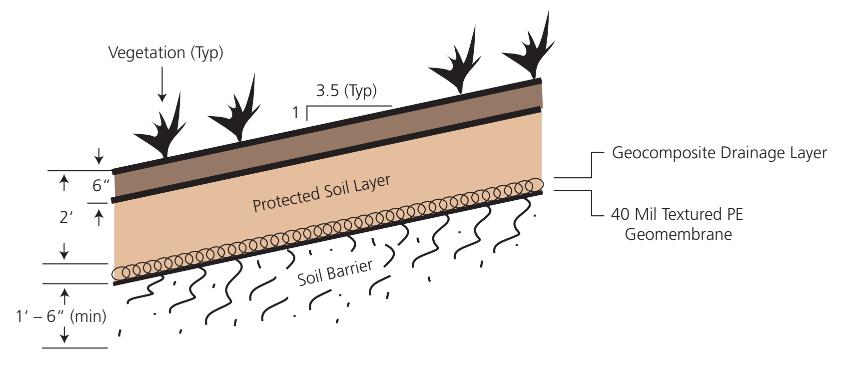

Figure 2. Design of final cover system.

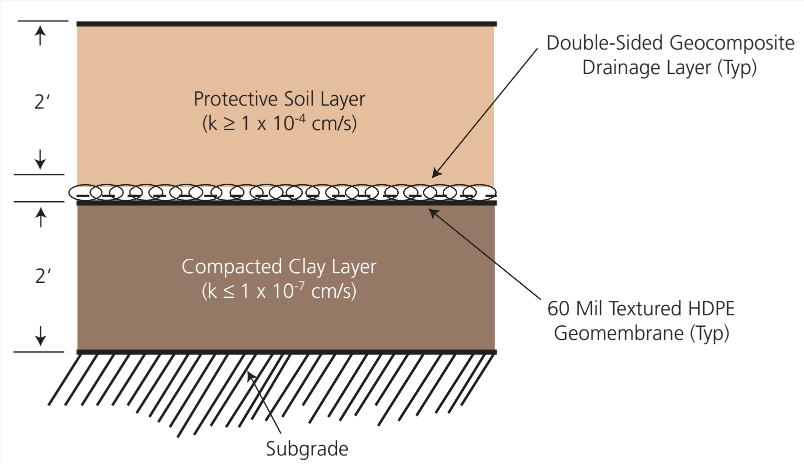

Figure 3. Design of bottom liner system.

100-hour transmissivity value obtained from a laboratory test. The 100-hour transmissivity test value should be equal to or higher than the specified value of θ_{spec}. A description of typical values of reduction factors for bottom liner LCSs is given in the following paragraphs.

Chemical clogging reduction factor, RF_{CC}

The designer should evaluate the soils she anticipates using in the protective layer of the liner system and the materials anticipated in the overlying waste, in order to judge the risk of chemical clogging. GRI-GC8 recommends using values in the range of 1.5 to 2.0 for chemical clogging in the leachate collection system. A greater reduction factor might be appropriate for "bioreactor" landfills based on observations of significant leachate collection gravel clogging (**Figure 1**). The design example presented in this paper illustrates how a properly designed system can accommodate such a large reduction.

Biological clogging reduction factor, RF_{BC}

The biological clogging reduction factor accounts for the reduction of flow in the geonet due to the growth of biological organisms such as fungi or algae, or root penetration through the overlying soil. GRI-GC8 recommends using values in the range of 1.1 to 1.3 for biological clogging in the leachate collection system. In the authors' experience, and as suggested in other field literature (e.g., Rowe et al. 1997), the reduction factor for biological clogging in leachate collection systems can either be maintained fairly low or be lumped in with the reduction factor for chemical precipitation.

Creep reduction factors, RF_{CR}

Performance transmissivity tests are typically conducted for up to 100 hours, as required by GRI test procedure GC8. The decrease in transmissivity with time asymptotically approaches a stable value within 100 hours, and usually much sooner than that, indicating that much of the initial compression (and geotextile intrusion) has already taken place. The reduction factor for creep, RF_{CR}, accounts for the decrease in transmissivity beyond the first 100 hours experienced in the transmissivity test. The quality of the geonet core, including its structure, thickness, mass and density can have a significant influence on creep reduction factors. **Table 1** presents creep reduction factors for one manufacturer's biplanar geonet. Products from other manufacturers can have creep factors different from those given here.

Creep reduction factors should be selected on the basis of the expected normal stress in the LCS if one is to follow the staged design concept presented in this paper. A much lower creep reduction factor should be used at the initial stage of landfill operation as overlying waste thickness is small. A conservative value of creep reduction factors may be 2 for the final (closure) stage of landfill liner systems with overburden stresses up to 15,000 pounds per square foot (psf).

LCS geocomposite design example

The purpose of this design example is to demonstrate how the different stages of a landfill life can be taken into account when designing a geocomposite for a leachate collection system. The particular case of a "bioreactor" landfill, which is especially aggressive on drainage systems, is used. The design process involves the following steps:

Step 1. Choose appropriate values for site specific design parameters (geometry and soil properties).

Step 2. Establish design input flow rate (i.e., impingement rate, q_i) for each stage of landfill life.

Step 3. Solve for the needed design transmissivity, θ_{design}, at different stages of the

Stage	Description	Peak LCS in-flow—q_i
I	Initial operation—10 ft. (3 m) waste	0.571 in./day = 1.68×10^{-5} cm/s
II	Active operation—80 ft. (24 m) waste	0.064 in./day = 1.88×10^{-6} cm/s
III	Intermediate cover—140 ft. (43 m) waste	0.030 in./day = 8.80×10^{-7} cm/s
IV	Post closure—140 ft. (43 m) waste	1.09×10^{-5} in./day = 3.20×10^{-10} cm/s

Table 2. HELP analysis results for LCS design example.

landfill life.

Step 4. Establish a specified transmissivity, θ_{spec}, for each of the stages by selecting an appropriate global factor of safety and appropriate reduction factors. For this design example, several specified transmissivities would be calculated, one for each stage of the landfill life. The maximum required transmissivity would be specified in the contract documents.

Step 5. Develop specifications describing laboratory testing conditions and acceptance criteria.

Step 1—Establish input parameters

Several of the input parameters are derived from the geometry of the design. For this example, **Figure 1** shows a simplified design that will be used in selecting these geometric input parameters. **Figure 2** shows the schematic cross section of the liner and leachate collection system.

The inputs used in this example are presented below:

- Slope of cell floor = 4.5% = 2.57 degrees
- Drainage length on cell floor = 262 ft. (229 ft. + 33 ft. [70 m + 10 m])
- Side slope angle = 18.43 degrees (ΔS sideslope = 0.333)
- Drainage length on sideslope = 98 ft. (30 m)
- Unit weight of waste = 75 pcf (11.8 kN/m^3) (typically ranges from 60 to 90 pcf)
- Thickness of waste = varies depending on operating stage

Cover soil properties (daily cover, interim cover, final cover):

Daily cover

- Permeability of daily cover = 5 x 10^{-3} cm/s (based on type of soil used for interim cover)
- Thickness of daily cover = 0.5 ft. (15 cm) (based on anticipated/required operating procedures)

Interim cover

- Permeability of interim cover = 1 x 10^{-4} cm/s (based on type of soil used for interim cover)
- Thickness of interim cover = 1 ft. (30 cm) (based on anticipated/required operating procedures)

Step 2—Establish design impingement rates

Select the impingement rates, q_i, to include in the various stages of operational life and for the final cover design. It is recommended that the designer model the impingement rate for key stages in the operating life of the landfill. The number of key stages will vary depending on site-specific landfill conditions such as: (i) interim staging and sequencing; (ii) runoff/run-on control practices; (iii) use of daily, interim and final cover materials; and (iv) thickness of waste and other overlying materials. For most sites it will likely take 3–6 stages to adequately define the operation stages.

For the leachate collector design example, it will be assumed that four stages will provide an adequate modeling of the landfill life. The results for the impingement rate for various operational stages for the design example have been obtained using HELP and are shown for each stage in **Table 2**. A more reliable indicator of stage impingement rates can generally be obtained from past operational records of the landfill itself or neighboring facilities. With over a decade of national lined landfill experience on file with most state regulators, good regional data on leachate generation rates is readily available.

Step 3—Solve for design transmissivity

Solve for θ_{design} for cell floor and side slope for each Stage (I–IV). For this example, the results of the θ_{design} solution are:

Stage IA (cell-floor)

$$\theta_{design} = \frac{1.68 \text{ x } 10^{-7} \text{ m/sec x } 30 \text{ m}}{\sin 18.435°} = 1.59 \text{ x } 10^{-5} \text{ m}^2\text{/sec}$$

Stage IB (side slope)

$$\theta_{design} = \frac{1.68 \text{ x } 10^{-7} \text{ m/sec x } 80 \text{ m}}{\sin 2.577°} = 2.99 \text{ x } 10^{-4} \text{ m}^2\text{/sec}$$

Results of similar calculations for other cases are summarized in **Table 3**.

Step 4—Establish specified transmissivity values

The specified transmissivity, θ_{spec}, is increased above the design transmissivity to account for uncertainties (in the form of an overall factor of safety) and the long-term reduction of the transmissivity of the geocomposite due to anticipated environmental factors (in the form of reduction factors).

- FS_D = The global factor of safety is a somewhat arbitrary value selected by the designer based on the level of uncertainty and relative risk associated with failure. Typical values suggested for design with geocomposites range from 2.0 to 3.0 (Narejo and Richardson 2003). Given the higher levels of uncertainty associated with long-term performance of bioreactor systems, and the relative importance of having leachate collection systems that operate well into the future, somewhat higher factors of safety may be warranted for the different life stages. For this design example we have chosen values of FS_D = 2.0, 3.0, 4.0 and 5.0 for Stages I–IV, respectively, as shown in **Table 3**. These values reflect advancing degrees of uncertainty as time goes forward.
- RF_{CC} = The suggested range for the reduction factor for chemical clogging from GRI-GC8 is from 1.5 to 2.0 for most leachate collection systems based on the chemical makeup of leachate and the length of time exposure. While these values might be typical for "standard average" landfill conditions, a more rigorous and expansive interpretation might be appropriate over the lifetime of a "bioreactor" landfill. For a very short exposure time, as in Stage I, a low value would be appropriate. As exposure time increases, the recommended reduction factor would be increased. We have chosen values of 1.2, 1.5, 2.0, and 4.0 for Stages I-IV, respectively, as shown on **Table 3**. This suggests that up to half of the flow capacity could be lost due to biological clogging during the active life of the cell, and 75% of the flow capacity could be lost to chemical precipitation during the long-term post-closure period.
- RF_{BC} = The suggested range for the reduction factor for biological clogging from GRI-GC8 is from 1.1 to 1.3 for leachate collection systems. We believe this range is appropriate even for bioreactor landfills because the most serious clogging condition is probably from chemical precipitation rather than a biological mechanism.
- RF_{CR} = The creep reduction factor varies with stress and is product-specific. For this design example, **Table 1** provides data for a particular bi-planar product from one manufacturer.

Based on the selected reduction factors and global factors of safety, the specified transmissivities, θ_{spec}, can be calculated as follows:

Case	Description	q_i (cm/sec)	θ_{design} (m²/sec)	σ_{100} (psf)	RF_{cc}	RF_{bc}	FS_d	RF_{cr}	θ_{spec} (m²/sec)	θ_{100} (m²/sec)	Ratio $\theta_{100}/\theta_{req}$	Acceptable
IA	Initial Operation	1.68E-05	2.99E-04	750 psf	1.2	1.1	2.0	1.10	8.7E-04	9.0E-04	1.0	Yes
IB	Initial Operation	1.68E-05	1.59E-05	750 psf	1.2	1.1	2.0	1.10	4.6E-05	5.0E-04	11	Yes
IIA	Active Operation	1.88E-06	3.34E-05	6,000 psf	1.5	1.2	3.0	1.25	2.2E-04	4.0E-04	1.8	Yes
IIB	Active Operation	1.88E-06	1.78E-06	6,000 psf	1.5	1.2	3.0	1.25	1.2E-05	3.0E-04	25	Yes
IIIA	Intermediate Cover	8.80E-07	1.56E-05	10,000 psf	2.0	1.3	4.0	1.30	2.1E-04	2.0E-04	0.95	No
IIIB	Intermediate Cover	8.80E-07	8.35E-07	10,000 psf	2.0	1.3	4.0	1.30	1.1E-05	1.5E-04	13	Yes
IVA	Post-Closure	3.20E-10	5.69E-09	10,500 psf	4.0	1.3	5.0	1.40	2.1E-07	2.0E-04	966	Yes
IVB	Post-Closure	3.20E-10	3.04E-10	10,500 psf	4.0	1.3	5.0	1.40	1.1E-08	1.5E-04	13,565	Yes

Table 3. Results of calculations for the design example.

Stage IA (floor)

$$\theta_{spec} = 2.99 \times 10^{-4}\ m^2/s \bullet 2 \bullet 1.2 \bullet 1.1 \bullet 1.1 = 8.6 \times 10^{-4}\ m^2/s$$

Stage IB (side slope)

$$\theta_{spec} = 1.59 \times 10^{-5}\ m^2/s \bullet 2 \bullet 1.2 \bullet 1.1 \bullet 1.1 = 4.6 \times 10^{-5}\ m^2/s$$

Results of similar computations for all stages of the design case are shown in **Table 3**.

Step 5—Specification development

The specifications should clearly define the conditions of the laboratory testing and the criteria that define the product's acceptability.

The required laboratory testing conditions include: (i) applied stress; (ii) hydraulic gradient; (iii) boundary conditions; and (iv) seating time.

(i) Applied stress—The applied stress used in testing should be equal to the maximum applied stress anticipated in field conditions.

For the design example:

$$\sigma_{100} = t_{waste} \bullet \gamma_{waste}$$

Stage I: σ_{100} = 10 ft. • 75 pcf
= 750 psf (36 kPa)

Stage II: σ_{100} = 80 ft. • 75 pcf
= 6000 psf (287 kPa)

Stages III and IV: σ_{100} = 140 ft. • 75 pcf
= 10,500 psf (503 kPa)

(ii) Hydraulic gradient—The hydraulic gradient is equal to the sine of the slope angle in units of length/length.

For the design example:

Stages A (cell floor)
Slope angle = 2.57 deg.
—> Gradient = 0.045

Stages B (cell side slope)
Slope angle = 18.43 deg. _
—> Gradient = 0.32

(iii) Boundary conditions—The term "boundary conditions" refers to the makeup of the overlying and underlying materials during testing of the geocomposite. The testing procedure should follow the guidelines of GRI-GC8, which requires that the boundary conditions mimic field conditions. This means that site-specific materials shall be used wherever possible. This example assumes that the on-site soil anticipated to be used as protective soil between the waste and the geocomposite will be used above the geocomposite, and that a textured geomembrane will be used below the geocomposite. Both materials to be used in testing should be provided to the laboratory by the engineer or contractor.

(iv) Seating time—Seating time affects the amount of creep and intrusion that the geocomposite undergoes prior to transmissivity testing, which in turn affects the measured transmissivity of the product. The laboratory testing should follow the guidelines of GRI-GC8, which requires a seating time of at least 100 hours for testing the transmissivity of the geocomposite. A greater seating time is acceptable; however, this may incur greater testing expense and is usually not necessary. As required by GRI-GC8, a seating time of 100 hours is used in this design example.

An acceptable product should possess a creep reduction factor lower than that used in the design, and a 100-hour transmissivity value higher than the specified value (θ_{spec}) for each of the design stages as presented in **Table 3**.

Discussion of results, conclusions

This third part to the Designer's Forum series demonstrates how the different stages of a landfill life can be taken into account when designing for a leachate collection system with geocomposites. **Table 3** summarizes the results for the design example. The following observations can be drawn from this exercise:

- For this design example, the critical stages in the design of the geocomposite appear to occur right at the beginning of cell operations, and towards the end of the active cell life. This is probably a typical situation for many landfills.
- If the most conservative parameters had been used for the reduction factors for all stages, even with a modest factor of safety of only 2.0, the selected geocomposite would have failed the criteria by a very large margin.
- The condition on the floor is typically more critical than on the side slope. This is because the smaller gradient on the floor requires more head build-up to pass a certain amount of flow.
- **Table 3** indicates that the sample product that was tested for this design passes all the criteria, except for the condition of Stage III of the landfill life on the floor. It only fails that stage just barely, however, and the designer could either re-visit the arbitrary factor of safety for that design stage (a FS_D value of 4.0 is fairly high, whereas a value of 3.8 would result in a passing criteria), or could require a thicker or more robust geocomposite product that has a higher transmissivity.

The most significant conclusion demonstrated by this exercise is that the use of unique reduction factors, and a unique factor of safety, for each stage of a landfill's life can reduce the conservatism inherent in a single calculation. This design approach allows the critical points in a landfill's life to be identified with regard to performance of the geocomposite, and focused laboratory testing can be performed to address those critical conditions.

References

Bachus, R., Narejo, D., Thiel, R. and Soong, T. 2004. *The GSE Drainage Design Manual*. GSE Lining Technologies, Houston.

Giroud, J.P., Zornberg, J.G., and Zhao, A. 2000. "Hydraulic Design of Geosynthetic and Granular Liquid Collection Layers." *Geosynthetics International*, vol. 7, nos. 4–6, pp. 285–380.

GRI-GC8. 2001. *Determination of the Allowable Flow Rate of a Drainage Geocomposite*. Geosynthetic Research Institute, Folsom, Pa.

Narejo, D. and Allen, S. 2004. "Using the Stepped Isothermal Method for Geonet Creep Evaluation." *Proceedings of EuroGeo3, Third European Geosynthetics Conference*, Munich, pp. 539–544.

Narejo, D. and Richardson, G. 2003. "Designing with GRI Standard GC8." *GFR*, vol. 21, no. 6, pp. 20–23. (Note: Errata on this article's presentation were published in vol. 21., no. 8. The full, correct version is published online in the August 2003 issue. Visit www.gfrmagazine.info.)

Rowe, R.K., Fleming, I.R., Armstrong, M.D., Cooke, A.J., Cullimore, D.R., Rittmann, B.E., Bennett, P., and Longstaffe, F.J. 1997. "Recent Advances in Understanding the Clogging of Leachate Collection Systems." *Proceedings of the Sixth International Landfill Symposium*, Sardinia '97, CISA, Cagliari, Italy, V. III, pp. 383–390.

Schroeder, P.R., Dozier, T.S., Zappi, P.A., McEnroe, B.M., Sjostrom, J.W. and Peyton, R.L. 1994. "The Hydrologic Evaluation of Landfill Performance (HELP) Model: Engineering Documentation for Version 3." EPA/600/R-94/168b. U.S. Environmental Protection Agency, Risk Reduction Engineering Laboratory, Cincinnati.

Richard Thiel is president of Thiel Engineering, Oregon House, Calif., www.rthiel.com, and vice president of engineering for Vector Engineering, Grass Valley, Calif., www.vectoreng.com.

Dhani Narejo is the drainage product manager for GSE Lining Technologies, Houston, www.gseworld.com.

Gregory N. Richardson is president of G.N. Richardson & Associates, Raleigh, N.C., www.gnra.com.